frontiers | Research Topics

Legume root diseases, 2nd edition

Edited by
Marie-Laure Pilet-Nayel, Clarice Coyne J.,
Christophe Le May and Sabine Banniza

Published in
Frontiers in Plant Science

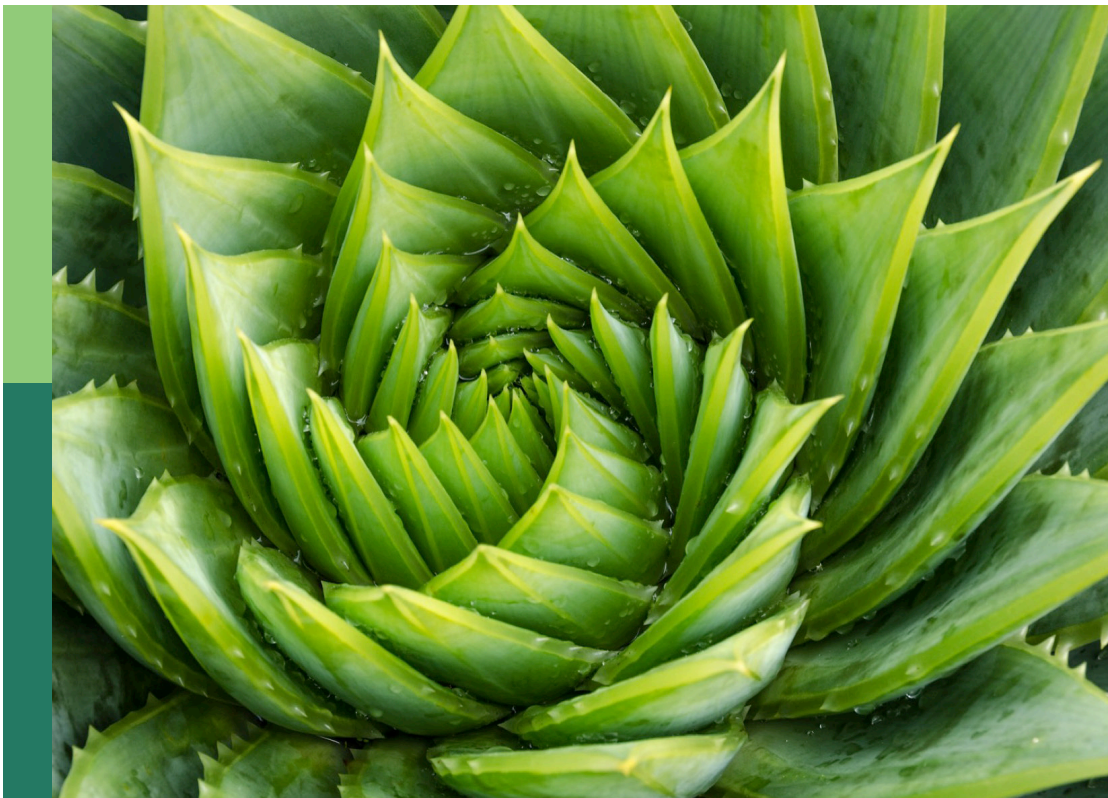

ISSN 1664-8714
ISBN 978-2-8325-4835-6
DOI 10.3389/978-2-8325-4835-6

About Frontiers

Frontiers is more than just an open access publisher of scholarly articles: it is a pioneering approach to the world of academia, radically improving the way scholarly research is managed. The grand vision of Frontiers is a world where all people have an equal opportunity to seek, share and generate knowledge. Frontiers provides immediate and permanent online open access to all its publications, but this alone is not enough to realize our grand goals.

Frontiers journal series

The Frontiers journal series is a multi-tier and interdisciplinary set of open-access, online journals, promising a paradigm shift from the current review, selection and dissemination processes in academic publishing. All Frontiers journals are driven by researchers for researchers; therefore, they constitute a service to the scholarly community. At the same time, the *Frontiers journal series* operates on a revolutionary invention, the tiered publishing system, initially addressing specific communities of scholars, and gradually climbing up to broader public understanding, thus serving the interests of the lay society, too.

Dedication to quality

Each Frontiers article is a landmark of the highest quality, thanks to genuinely collaborative interactions between authors and review editors, who include some of the world's best academicians. Research must be certified by peers before entering a stream of knowledge that may eventually reach the public - and shape society; therefore, Frontiers only applies the most rigorous and unbiased reviews. Frontiers revolutionizes research publishing by freely delivering the most outstanding research, evaluated with no bias from both the academic and social point of view. By applying the most advanced information technologies, Frontiers is catapulting scholarly publishing into a new generation.

What are Frontiers Research Topics?

Frontiers Research Topics are very popular trademarks of the *Frontiers journals series*: they are collections of at least ten articles, all centered on a particular subject. With their unique mix of varied contributions from Original Research to Review Articles, Frontiers Research Topics unify the most influential researchers, the latest key findings and historical advances in a hot research area.

Find out more on how to host your own Frontiers Research Topic or contribute to one as an author by contacting the Frontiers editorial office: frontiersin.org/about/contact

Legume root diseases, 2nd edition

Topic editors

Marie-Laure Pilet-Nayel — Institut de Génétique, Environnement et Protection des Plantes (IGEPP), France

Clarice Coyne J. — United States Department of Agriculture (USDA), United States

Christophe Le May — Institut Agro Rennes-Angers, France

Sabine Banniza — University of Saskatchewan, Canada

Citation

Pilet-Nayel, M.-L., Coyne J. C., Le May, C., Banniza, S., eds. (2024). *Legume root diseases, 2nd edition*. Lausanne: Frontiers Media SA. doi: 10.3389/978-2-8325-4835-6

Publisher's note: In this 2nd edition, the following article has been added: Moussart A, Lavaud C, Onfroy C, Leprévost T, Pilet-Nayel M-L and Le May C (2024) Pathotype characterization of *Aphanomyces euteiches* isolates collected from pea breeding nurseries. *Front. Plant Sci*. 15:1332976. doi: 10.3389/fpls.2024.1332976

Table of contents

frontiers | Frontiers in Plant Science

TYPE Editorial
PUBLISHED 20 March 2024
DOI 10.3389/fpls.2024.1393326

OPEN ACCESS

EDITED AND REVIEWED BY
Brigitte Mauch-Mani,
Université de Neuchâtel, Switzerland

*CORRESPONDENCE
Marie-Laure Pilet-Nayel
marie-laure.pilet-nayel@inrae.fr

RECEIVED 28 February 2024
ACCEPTED 12 March 2024
PUBLISHED 20 March 2024

CITATION
Pilet-Nayel M-L, Coyne CJ, Le May C and Banniza S (2024) Editorial: Legume root diseases.
Front. Plant Sci. 15:1393326.
doi: 10.3389/fpls.2024.1393326

Editorial: Legume root diseases

Marie-Laure Pilet-Nayel[1]*, Clarice J. Coyne[2], Christophe Le May[3] and Sabine Banniza[4]

[1]IGEPP, INRAE, Institut Agro, Univ Rennes, Le Rheu, France, [2]USDA-ARS Plant Germplasm Introduction & Testing Research, Pullman, WA, United States, [3]IGEPP, INRAE, Institut Agro, Univ Rennes, Rennes, France, [4]Crop Development Centre/Department of Plant Sciences, University of Saskatchewan, Saskatoon, SK, Canada

KEYWORDS

soil-borne pathogens, root rot complex, disease resistance and breeding, plant-pathogen-microbe interaction, integrated disease management

Editorial on the Research Topic
Legume root diseases

Legume crop development is a major challenge worldwide for sustainable agriculture and food security. In particular, legume root diseases are economically important, affecting large areas of crop production in many countries worldwide. Root rots, caused by *Aphanomyces euteiches, Rhizoctonia solani, Fusarium* species, and wilts, caused by several formae speciales of *Fusarium oxysporum*, are some of the most destructive soil-borne diseases of cultivated legumes including pea, chickpea, lentil, soybean, bean, faba bean, lupin, and alfalfa. A number of control strategies have been developed including resistance breeding, cultural practices and chemical control. However, root diseases management remains challenging, especially due to difficult accessibility to the soil horizon and implementation of most control methods has been hard to achieve or resulted in incomplete protection. Collaborative and multidisciplinary research is needed to develop effective integrated control strategies against these diseases.

International Workshop meetings were initiated on legume root diseases, with the first held in 2002 in Rennes, France. As the community interest in this topic has grown, the meetings have performed an important role in the international promotion and discussion of results on the research and scientific achievements in this field. They have also been important in supporting the scientific community and helping breeders and stakeholders with funding applications and partnerships. The eighth International Legume Root Diseases (ILRD8) workshop was held online on August 23-26, 2022 (https://workshop.inrae.fr/ilrd8/) and gathered nearly 100 scientists from different continents of the world. The workshop provided the opportunity to develop this Frontiers Research Topic bringing together a collection of the latest quality articles that report on recent advances in research on legume root diseases. Manuscripts of this Research Topic address the various areas of legume root diseases research, including disease survey, pathogen identification and diversity (four articles), disease resistance and breeding (four articles), plant-pathogen-microbe interactions (three articles) and integrated disease management (five articles).

Root disease survey, pathogen identification and diversity were reported on faba bean, chickpea and pea. In China, Long et al. first reported black root rot on faba bean caused by *Berkeleyomyces rouxiae*. These authors confirmed and expanded the broad host range of *B. rouxiae* in legumes and identified moderately resistant faba bean cultivars. In a survey

undertaken across Germany from 2016-2019, Šišić et al. identified significantly higher frequencies of *Fusarium redolens* and *Didymella pinodella* in roots of faba bean from organic fields compared with conventional fields, and lower frequencies of *F. avenaceum*, *F. tricinctum* and *F. culmorum*. These differences in frequency of isolation of several species were linked to the presence of legumes in organic field rotations compared to their absence in conventional fields. In a two year-survey in Saskatchewan, Canada, Armstrong-Cho et al. identified prevalence of *Fusarium* species, including *F. redolens*, *F. solani* and *F. avenaceum* obtained by root isolations and molecular tests, associated with root rot of chickpea. Isolates of *F. avenaceum* were the most aggressive of the *Fusarium* isolates identified on chickpea. In France and in the United States, Moussart et al. characterized pathotypes of pea-infecting isolates of *Aphanomyces euteiches* recovered from pea breeding nurseries. The authors identified a reduced virulence diversity and a higher vs. lower aggressiveness on pea vs. *Medicago truncatula* of French isolates compared to American isolates, suggesting the role of legume crop history as a driver of pathogen population evolution.

Studies on disease resistance and breeding for root diseases were addressed on chickpea, pea and *Medicago* spp. Bithell et al. showed that *Phytophthora medicaginis* soil DNA concentrations, as a parameter for quantifying pathogen proliferation, was correlated to disease severity and yield loss and thus could be used to screen for partial resistance in chickpea. In pea, Kälin et al. analyzed the level of partial resistance to *Aphanomyces euteiches* from the landrace PI 180693 in back-crossed pea breeding lines. They identified variability in pea responses to *Aphanomyces euteiches* isolates in controlled condition tests, that depended on their virulence levels. They reported that partial resistance could to be less effective towards root rot caused by *Phytophthora pisi* in field assays. Leprévost et al. provided a meta-analysis of the diversity of Quantitative Trait Loci (QTL) for resistance to *Aphanomyces euteiches* in different sources of resistance in pea, by integrating a novel QTL mapping study in two advanced backcross populations with previous QTL analyses and genome-wide association study (GWAS). The authors identified ten consistent genetic regions and a diversity of resistance haplotypes in new sources of resistance which will be helpful to support breeding efforts for resistant pea varieties. In a *Medicago truncatula* collection, Fartash et al. identified by GWAS new genetic loci associated with resistance towards an Iranian strain of *Verticillium alfalfae* adapted to higher temperature (25°C), compared to loci identified previously with another strain adapted to lower temperature (20°C). The authors suggested that a simple shift in temperature combined with a new pathogen strain could change the architecture of genetic control of resistance to the pathogen.

Research advances on plant-pathogen-microbe interactions were also reported in this Research Topic with a special application to legume-*Aphanomyces euteiches* interactions. Fortier et al. reviewed the role of the root border cells in plant root defense against soilborne pathogens, with a focus on root rot disease caused by *Aphanomyces euteiches*. The root extracellular trap, a thick mucilage layer at the interface between the soil and the root, was reported to be enriched in antimicrobial compounds including defense-related proteins, secondary metabolites and glycan-containing molecules. *In vitro* assays showed that arabinogalactan proteins isolated from pea root cap and border cells were able to attract zoospores of *Aphanomyces euteiches* and inhibit subsequent cyst germination. Kiselev et al. identified 35 active extracellular microbial proteases using Activity Based Protein Profiling and mass spectrometry (ABPP-MS) on apoplastic fluids isolated from pea roots infected by *Aphanomyces euteiches*. These novel active modular extracellular eukaryotic proteases are relevant targets as potential pathogenicity factors in the *Aphanomyces* genus. Hashemi et al. reported that *Pythium oligandrum*, a soilborne oomycete used as a biological control agent, promoted plant growth in pea and *Medicago truncatula* and protected them against infection by *Aphanomyces euteiches*. *P. oligandrum* also activated plant immunity in *M. truncatula* roots, notably upregulating genes involved in the biosynthesis of antimicrobial compounds and enhancing the production of phytoalexins, medicarpin and formononetin, but it did not impair symbiotic interactions.

Integrated root disease management was reported in several studies on pea, lentil, faba bean, bean and lucerne. For prophylactic management, Chatterton et al. developed molecular methods for quantifying soil inoculum to assess the risk of pea root rot in field soil samples. A significant linear relationship was determined between DNA concentrations of *Aphanomyces euteiches* measured in soil by digital droplet PCR and quantitative PCR and oospore inoculum concentration, although it was dependent on soil types and other pathogens. For biological management, Hubbard et al. examined the impacts of nitrogen fertilization and a commercial arbuscular mycorrhizal fungal (AMF) inoculant on pea and lentil plant health and production in three fields in Canada. The authors identified no impact of the AMF on pea and lentil *Aphanomyces* and *Fusarium* root rot severity. Nitrogen fertilization showed variable effects on root rot for pea and lentil crops, depending on field trial sites. Pisarčik et al. reported that application of the mycoparasitic oomycete *Pythium oligandrum* as a biocontrol agent, in both the autumn and intensive schedules in the field, showed no effect on lucerne root disease score when attacked by *Fusarium* and *Verticillium*. All these authors suggested that both environmental and soil characteristics can affect biological treatment efficacy substantially. For integrated disease management, Yu et al. reviewed disease management methods for root rots on faba bean in China, caused by multiple pathogens among which *Fusarium* spp. were the most prevalent. These methods include intercropping with non-host crops, the most widely utilized control method, applying rational nitrogen, and treating seeds with chemical or bio-seed treatments. Naseri and Kakhki evaluated and modeled the effect of different cultivars, planting dates and weed control methods on progression of common bean growth, *Rhizoctonia* root rot and weed development in a two-year trial in Iran. The authors showed that late planting restricted *Rhizoctonia* root rot progress, thus improving bean yield, and identified model parameters for monitoring bean-disease-weed development and predicting bean productivity.

All of these research results clearly illustrate the need and opportunities to both deepen knowledge in targeted disciplines and integrate them into a more comprehensive, multidisciplinary

system, so that they translate into impactful plant protection innovations in the field. Further communications within the scientific community through international legume root disease workshops, such as the ILRD9 hosted on September 18, 2023 in Granada, Spain, and the upcoming ILRD10, will be very useful in accelerating progress towards the development of integrated, effective, sustainable and environment-friendly management methods for legume root diseases worldwide.

Author contributions

M-LP-N: Writing – original draft. CC: Writing – review & editing. CM: Writing – review & editing. SB: Writing – review & editing.

Funding

The author(s) declare financial support was received for the research, authorship, and/or publication of this article. We thank Institut National de Recherche pour l'Agriculture, l'alimentation et l'Environnement. (INRAE, France), Institut Agro Rennes-Angers (France), United States Department of Agriculture ARIS Project #2090-21000-037-00D (USDA, USA) and University of Saskatchewan (Canada) for supporting our research. We are thankful to INRAE, Departments of Biology and Plant Breeding and Plant Health and Environment (France), as well as the Brittany region (France), for financial support of the ILRD8 workshop.

Acknowledgments

We thank all the authors who have contributed to this Research Topic and the reviewer who have provided valuable feedback to enhance the quality of the articles. We also thank the Frontiers teams for their support.

Conflict of interest

The authors declare that the research was conducted in the absence of any commercial or financial relationships that could be construed as a potential conflict of interest.

Publisher's note

frontiers | Frontiers in Plant Science

TYPE Original Research
PUBLISHED 30 November 2022
DOI 10.3389/fpls.2022.1038538

OPEN ACCESS

EDITED BY
Christophe Le May,
Institut Agro Rennes-Angers, France

REVIEWED BY
Cheryl Armstrong-Cho,
University of Saskatchewan, Canada
Edwison Alberto Rojas-Triviño,
National University of Colombia,
Palmira, Colombia

*CORRESPONDENCE
Bita Naseri
bitanaseri@yahoo.com;
b.naseri@areeo.ac.ir

SPECIALTY SECTION
This article was submitted to Plant Pathogen Interactions, a section of the journal Frontiers in Plant Science

RECEIVED 07 September 2022
ACCEPTED 17 November 2022
PUBLISHED 30 November 2022

CITATION
Naseri B and Nazer Kakhki SH (2022) Predicting common bean (*Phaseolus vulgaris*) productivity according to *Rhizoctonia* root and stem rot and weed development at field plot scale. *Front. Plant Sci.* 13:1038538. doi: 10.3389/fpls.2022.1038538

Predicting common bean (*Phaseolus vulgaris*) productivity according to *Rhizoctonia* root and stem rot and weed development at field plot scale

Bita Naseri[1]* and Seyed Hossein Nazer Kakhki[2]

[1]Plant Protection Research Department, Kermanshah Agricultural and Natural Resources Research and Education Center, AREEO, Kermanshah, Iran, [2]Plant Protection Research Department, Zanjan Agricultural and Natural Resources Research and Education Center, AREEO, Zanjan, Iran

Introduction: A two-year research trial was conducted to evaluate progression of common bean (Phaseolus vulgaris) growth, Rhizoctonia root rot and weed development in association with productivity when treated with different cultivars, planting dates and weed control methods in north-western part of Iran.

Methods: To determine the best descriptors, six standard curves were examined to model development of bean dry matter, Rhizoctonia root rot incidence, and weed density during two growing seasons across 256 field plots. Exponential and linear-by-linear models were fitted to bean-disease-weed progression data, and then model parameters representing over-season progress curve elements were used in multivariate regression analyses to estimate bean production.

Results and discussion: Furthermore, using herbicides (Imazethapyr and Trifluralin) restricted weed density by 28% in early (mid-spring) and 42% in late (late spring to early summer) plantings. Late plantings of two bean cultivars decreased disease progress up to 36% for herbicide use, hand-weeding and control. Although bean dry matter, pod and seed production for herbicide use and hand-weeding treatments were 6-17% greater than control, late planting improved productivity in control by 10-24%. Findings suggested that late planting of bean improved efficiency of herbicides to control weeds. Late planting also restricted Rhizoctonia root rot progress and thus, improved bean yield. There were significant correlations between bean-disease-weed development descriptors. According to principal component analysis, bean-disease-productivity-weed variables accounted for 80% of total data variance. Such information extends our understanding of bean-disease-weed progress in interaction with planting date to develop more effective and sustainable integrated Rhizoctonia management programs.

KEYWORDS

crop management, legumes, root canker, dry bean, yield

Introduction

Knowing *Rhizoctonia* root rot and weed development as damaging agents in common bean (*Phaseolus vulgaris* L.) cultivation worldwide (Naseri, 2019b; Oveisi et al., 2021), an improved understanding of bean production affected by the agrosystem-disease-weed interaction leads to develop more influential integrated crop management programs. A large number of *Rhizoctonia* root rot and weed control strategies in the forms of agronomic practices (Naseri and Veisi, 2019), bean resistance, biological and chemical management methods (Dehghani et al., 2018; Tabande and Naseri, 2020) have been reported previously. However, the estimation of bean production according to the progression of *Rhizoctonia* root rot in conjunction with the development of bean and weeds across experimental plots differing in bean cultivars, sowing dates and weed management treatments is still lacking.

Rhizoctonia root rot caused by *Rhizoctonia solani* has been known as a destructive disease in bean growing lands around the world as reviewed by Naseri and Younesi (2021). A number of agro-ecological factors restricted *Rhizoctonia* root rot spread and thus, improved productivity in commercial bean cropping systems surveyed by Naseri and Moradi (2015) as follows: manure application, sprinkler irrigation, growing beans following potato and tomato, the lack of urea application, proper planting density, shallow sowing, avoiding furrow irrigation, manual cultivation, planting Red beans, adequate soil organic matter, irrigating at 6–9 days intervals, increasing rhizobial nodulation, and growing beans in soils with 15–30% silt content. Further to management of bean root rot, it is essential to optimize the integrated management of diseases in conjunction with weeds for sustainable bean production. Chemical weed control is widely used by Iranian bean farmers. Although herbicide use can effectively restrict crop losses to weeds, they increase bean farming expenses, weed resistance to herbicide, environmental pollutants and human health risks (Oveisi et al., 2021). Therefore, it is highly desired to minimize herbicides usage with the assistance of effective agricultural practices for sustainable bean production. For instance, bean competitiveness and herbicide efficiency improved following the application of herbicides when combined with the mixed-cropping (Oveisi et al., 2021). A large number of reports on agricultural, biological and chemical control of either *Rhizoctonia* root rot or weeds in bean farming systems are available (Stagnari and Pisante, 2011; Esmaeilzadeh and Aminpanah, 2015; Byiringiro et al., 2017). However, more reliable yield estimates according to the disease and weed development under influential sustainable crop management programs consisting a well-timed planting deserves much more attention. Therefore, an advanced understanding of the best descriptors of *Rhizoctonia* root rot progress in conjunction with weed development under different planting date and weed control treatments at field plot scale is still needed to predict crop damage more accurately. Previous plot- and large-scale (Naseri, 2013a; Naseri, 2013b) findings in Iran indicated that later (early summer) sowing of bean crops restricted *Rhizoctonia* root rot and weed development (Kakhki et al., 2022), and improved seed production. To extend such benefits of later bean sowings, an experimental plot scale study was conducted to examine the interrelationships among descriptors of bean dry matter, pod and seed production, *Rhizoctonia* root rot and weed density development in two commercial cultivars (COS16 and Talash) planted under various sowing date and weed control treatments during two growing seasons.

Materials and methods

Experimental design

In 2015 and 2016 years, bean dry matter, *Rhizoctonia* root rot, and weed density were examined across experimental plots naturally infested with *R. solani* and weed populations, confirmed by the pre-test of soil (clay-loamy, mixed, mesic, Typic Haploxerepts) samples collected from the experimental plots. The experiments were performed at Kheirabad Research Site (latitude 36°31′ N, longitude 48°47′ E; 1,770 m a.s.l; 284.5 mm annual rainfall, 142 annual frost days). The experiment was a split-split-plot designed as follows: planting date as the main plots which consisted of four dates of 10-15 May, 26-31 May, 10-15 June, and 25-30 June, and weed-control practices as the subplots: Imazethapyr application, Trifluralin application, hand-weeding and control, and two commercial common bean cultivars as the sub-subplots: Talash (climbing bean) and COS16 (bush bean). The two chemical weed control treatments involved the pre-emergence use of Imazethapyr (Pursuit™ 10% SL) at 1 l ha^{-1}, and pre-planting Trifluralin (Treflan™ 48% EC) at 2.5 l ha^{-1}. In this two-year research, each experimental plot was replicated four times. Each experimental plot was consisted of six 5-m-length rows spaced by 0.30 m with plant spacing of 0.075 m resulting in an approximate density of 40 plant/m^2. To avoid herbicide-mixing, plots were spaced by 5 m.

For each plot, weed density was determined as the number of weeds in a 0.6 × 0.6 m quadrat (three quadrats per plot) at seedling (with one and three leaflets or cotyledon leaves opened), 50% flowering, podding and physiological maturity stages of bean plants per plot. To detect *Rhizoctonia* root rot incidence, five bean plants per quadrat were dug up randomly to assess red-brown cankers on the root (Naseri, 2013b). The percentage of plants having *Rhizoctonia* root cankers in five examined plants per quadrat (the same quadrats tested for weed density) was recorded as disease incidence. Then, the isolation and confirmation of the pathogen was performed in the laboratory (Kakhki et al., 2022). The disease incidence was assessed at one-leaflet seedling, three-leaflet seedling, flowering, podding and

maturity stages. In the next step, 10 bean plants, which were assessed for the disease incidence at each of five assessment times, were used to measure bean plant dry matter per plot. The number of pods per plant and seeds per pod were counted for 10 randomly assessed plants per plot at maturity stage.

Statistical analysis

A total of 256 (128 in 2015 and 128 in 2016) experimental plots were examined for bean dry matter, *Rhizoctonia* root rot, and weed density progress based on the parameters estimated by the best model fitted to the disease, bean and weed development datasets. To improve the degrees of freedom, the datasets for the two study years were pooled. To fit the best regression model, the seasonal measurements of the development of either variable for the two bean cultivars grown under diverse sowing-date and weed-control treatments were examined using the six following standard models: exponential, logistic, Gompertz, linear-by-linear, quadratic-by-linear, and Gaussian (Table 1). All the statistical analyses were performed using the GENSTAT (VSN International, Oxford, UK), which fitted standard curves according to maximum likelihood. The best model was fitted considering the following criteria: the co-efficient of determination (R^2), Fisher's test, and associations of fitted values with observed values (Brusco and Stahl, 2005; Tabande and Naseri, 2020).

The Kruskal-Wallis test is a nonparametric (distribution free) test, and is used when the assumptions of one-way ANOVA (data normality, homogeneity and independency) are not met. The normality of data variance was determined using kurtosis and skew tests. However, a high heterogeneity in datasets was required to improve predictive values of variables involved in the regression model (Kranz, 2003). Thus, the heterogeneous bean-disease-weed datasets were subjected to the Kruskal-Wallis one-way ANOVA to rank different levels of planting date and weed control treatments. The levels of planting date factor were defined as follows: early level involving two dates of 10-15 May and 26-31 May, and late level involving two dates of 10-15 June and 25-30 June. The weed control practices were classified as follows: herbicide use class applying either Imazethapyr or Trifluralin, hand-weeding class without weeds, and not treated class or control plots. Experimental data for the two bean cultivars, Talash and COS16, were pooled due to slight differences across treated plots. Then, simple correlations between the continuous variables of bean dry matter, *Rhizoctonia* root rot, and weed density descriptors were examined. Loading values indicating the associations of variables with the principal component (with an eigenvalue or proportion of data variance ≥ 1.0), were regarded significant if they were ≥ 0.35 (Kranz, 2003).

Considering the interrelationships among the predictors obtained from the PCA (Tabande and Naseri, 2020), a descriptive regression of bean production was modeled. Principal components with significant contributions into the bean-*Rhizoctonia*-weed interaction were involved in the regression model. Stepwise process used the two criteria of adjusted coefficient of determination (R^2) and Mallows Cp to fit the best predictors (Brusco and Stahl, 2005). Further to minimizing collinearity among variables by using principal components as predictors of a regression model (Tabande and Naseri, 2020), different principal components were considered independent. Therefore, such bean-*Rhizoctonia*-weed predictors and their two-way interactions were selected to be used in the

TABLE 1 Standard regression models to characterize development of bean dry matter, *Rhizoctonia* root rot, and weed density in two bean cultivars grown under different planting date and weed control treatments.

Models	Year	Dry matter		*Rhizoctonia* root rot		Weed density	
		R^2	*F* prob.	R^2	*F* prob.	R^2	*F* prob.
Exponential	2015	0.99	< 0.001	0.80	0.198	0.91	< 0.001
	2016	0.96	< 0.001	0.87	0.005	0.74	0.560
Logistic	2015	0.99	nd[a]	0.83	nd	0.82	nd
	2016	0.99	nd	0.86	nd	0.58	nd
Gompertz	2015	0.99	nd	0.88	nd	0.73	nd
	2016	0.99	nd	0.87	nd	0.49	nd
Linear-by-linear	2015	0.99	< 0.001	0.79	0.225	0.98	< 0.001
	2016	0.96	< 0.001	0.88	0.003	0.95	< 0.001
Linear-by-quadratic	2015	0.99	nd	0.99	nd	1.00	nd
	2016	1.00	nd	1.00	nd	1.00	nd
Gaussian	2015	0.99	nd	0.99	nd	0.90	nd
	2016	0.99	nd	0.97	nd	0.94	nd

[a]nd = Not detected by statistical procedure.

multivariate regression. Then, the graphical appraisal of normally distributed residuals, F-test and R^2 were checked for the best model fitness (Tabande and Naseri, 2020).

Results

Model fitting

Due to the lack of significant effect of study year, bean-disease-weed datasets for the two years of current study were pooled. This study examined six types of standard regressions to model the development of bean dry matter, *Rhizoctonia* root rot, and weed density across 256 experimental plots during the two growing seasons (Table 1). Among the standards models studied, an exponential model or asymptotic regression curve provided the best fit to bean-dry-matter data collected from bean cultivars grown under different planting date and weed control treatments over the two growing seasons. For the exponential model ($a + b^*(r^{**}x)$), a refers to the constant term, b to the bean-dry-matter increase factor, r to the rate of bean-dry-matter increase, and x is the time intervals (day) between assessments. This function represents a slow increase of bean dry matter at first, followed by a more rapid increase without bound when r is greater than 1.

The linear-by-linear regression model ($a + b/(1 + d^*x)$) was fitted to *Rhizoctonia* root rot incidence data as the best curve. This model with a bimodal distribution described a as the constant term, b as the disease increase factor, d as the strength of regression model (disease progress rate), and x as the time (day) between measurements. The linear-by-linear model represents a rapid initial increase/decline of *Rhizoctonia* root rot incidence, and then a subsequently slow decline/recovery to an approximate equilibrium.

The linear-by-linear model ($a + b/(1 + d^*x)$) was also fitted to weed density data as the best weed development curve. In this model, a is the constant term, b is the weed density increase factor, d is the strength of regression (density progress rate), and x is the time intervals. This regression curve indicates a rapid initial increase/decline of weed density followed by a slow decline/recovery.

The exponential (a, b and r) and linear-by-linear (a, b and d) parameters were estimated for each field plot based on the bean-disease-weed datasets. These model fitted parameters were considered as predictors to estimate bean dry matter, *Rhizoctonia* root rot, and weed density development over the growing season for each field plot. The average, standard deviation, minimum and maximum values were provided for the three exponential parameters of bean dry matter and three linear-by-linear parameters of disease incidence and weed density estimators in two cultivars of bean planted at different dates (Table 2). Greater standard deviations than the average values obtained for these variables showed diverse ranges of data variations.

Kruscal-Wallis one-way ANOVA

According to the results of Kurtosis and skew tests, the distributions of bean dry matter, disease incidence and weed density datasets were normal. According to the Kruscal-Wallis one-way ANOVA results, the exponential parameter r estimated for the development of bean dry matter was affected (H adjusted = 1.8; *Chi* prob. = 0.053) by planting date and weed control factors (Table 3). Experimental plots neither treated with herbicides nor hand-weeded indicated the lowest rankings of bean dry matter increase rate (the exponential parameter r) at both of the early and late plantings. Hand-weeding classes defined for both levels of the planting date factor showed greater rankings of dry matter increase rate when compared with the herbicide use classes. The constant term of *Rhizoctonia* root rot development (the linear-by-linear parameter a) was also affected by the planting date and weed control factors (H adjusted = 7.5; *Chi* prob. = 0.048). This suggested lower initial disease rankings for either herbicide use or hand-weeding classes than the class of not treated plots (control) planted at early and

TABLE 2 Average, standard deviation, and range values obtained for metric variables of bean dry matter, *Rhizoctonia* root rot incidence, and weed density development in bean cultivars grown under different planting dates and weed control treatments.

Descriptors		Average	Standard deviation	Range
Bean dry matter	Exponential parameter *a*	-139	628	-3845.00 to 449.00
	Exponential parameter *b*	125	617	-474.00 to 3765.00
	Exponential parameter *r*	4.4	7.91	0.69 to 39.40
Rhizoctonia root rot	Linear-by-Linear parameter *a*	30	190.7	-354.00 to 1033.00
	Linear-by-Linear parameter *b*	-31.3	201.5	-1063.00 to 334.00
	Linear-by-Linear parameter *d*	-0.254	1.26	-7.00 to 3.50
Weed density	Linear-by-Linear parameter *a*	60.8	73.3	0.00 to 310.00
	Linear-by-Linear parameter *b*	-50.3	310.2	-2395.00 to 219.00
	Linear-by-Linear parameter *d*	-0.28	3.22	-8.00 to 23.00

TABLE 3 Analysis of development of bean dry matter, *Rhizoctonia* root rot incidence, and weed density using Kruskal-Wallis one-way ANOVA for bean cultivars grown under different planting date and weed control treatments.

Planting date levels	Weed control treatments	Bean dry matter			*Rhizoctonia* root rot			Weed density			Yield	
		Exp.a	Exp.b	Exp.r	Ll.a	Ll.b	Ll.d	Ll.a	Ll.b	Ll.d	Pod	Seed
Early	Herbicide use	30.3	34.8	34.0	35.8	35.1	30.1	38.3	26.1	32.1	39.1	40.7
	Hand-weeding	29.8	33.3	37.5	38.4	24.9	33.3	8.5	47.5	53.5	45.1	48.7
	Not treated	35.3	31.3	26.8	39.9	26.8	37.6	53.4	11.0	29.0	16.6	21.8
Late	Herbicide use	33.4	31.4	31.8	24.4	38.2	34.0	30.4	37.2	20.6	35.9	28.9
	Hand-weeding	28.3	35.5	34.8	24.6	36.1	28.5	8.5	47.5	53.5	27.8	32.8
	Not treated	39.5	27.5	29.5	36.7	25.5	32.5	52.3	27.4	18.8	20.5	17.6
Mean adjusted *H*		2.2	1.1	1.8	7.5	5.3	1.4	48.1	24.9	32.1	15.8	17.5
Ranking *Chi* prob.		ns	ns	0.053	0.048	ns	ns	0.001	0.001	0.001	0.007	0.004

Exp, Exponential parameter; Ll, linear-by-linear parameter; ns, Not significant; Pod, pod number per plant; Seed, seed number per pod.

late dates. Furthermore, late plantings indicated lower initial disease rankings than early plantings at each class of the weed control factor. The planting date and weed control factors affected all the three weed density development descriptors, linear-by-linear parameters *a*, *b* and *d*. The initial weed density or the constant term of the linear-by-linear model of weed density development over the growing seasons had the lowest and highest rankings for the hand-weeding and not treated classes, respectively, at both early and late planting dates. Due to negative estimations of linear-by-linear parameters *b* and *d* by the weed density development model, the lowest and highest rankings were detected for not treated and hand-weeding classes, respectively, at both planting date levels. For pod and seed production, planting date and weed control factors affected pod number per plant (H adjusted = 15.8; *Chi* prob. = 0.007) and seed number per pod (H adjusted = 17.5; *Chi* prob. = 0.004). Lower and higher pod and seed production rankings at each planting date were obtained for not treated and hand-weeding classes of the weed control factor, respectively. In addition, herbicide use and hand-weeding classes indicated a greater pod and seed productivity in early plantings than late plantings (Table 3). Whereas, the class of not treated plots showed higher productivity rankings in late planted beans in comparison with early planted beans.

Correlation analysis

Based on the correlation analysis results, there was a significantly negative relationship ($P \leq 0.05$) between the exponential parameters *a* and *b* estimated for the development of bean dry matter (Table 4). For *Rhizoctonia* root rot development over the two growing seasons studied, the linear-by-linear parameter *b* was negatively linked ($P \leq 0.05$) to the exponential parameters *a* and *d*. From the weed density progression variables, only linear-by-linear parameter *b* negatively corresponded ($P \leq 0.05$) with linear-by-linear parameter *d*. The seed number per pod variable was negatively

TABLE 4 Correlations between descriptors of plant production, *Rhizoctonia* root rot, and weed development in bean cultivars planted under different dates and weed control treatments.

Descriptors		BDM*a*[a]	BDM*b*	BDM*r*	RRR*a*	RRR*b*	RRR*d*	WD*a*	WD*b*	WD*d*	PP	SP
Bean dry matter	Exponential parameter *a*	1.00										
(BDM)	Exponential parameter *b*	-0.99[b]	1.00									
	Exponential parameter *r*	0.11	-0.08	1.00								
Rhizoctonia root rot	Linear-by-Linear parameter *a*	0.03	-0.03	-0.05	1.00							
(RRR)	Linear-by-Linear parameter *b*	-0.03	0.03	0.05	**-0.97**	1.00						
	Linear-by-Linear parameter *d*	-0.01	0.01	-0.00	0.04	**-0.28**	1.00					
Weed density	Linear-by-Linear parameter *a*	0.19	-0.21	-0.19	0.01	-0.21	0.06	1.00				
(WD)	Linear-by-Linear parameter *b*	-0.05	0.04	0.06	-0.05	0.08	-0.09	-0.10	1.00			
	Linear-by-Linear parameter *d*	0.01	-0.01	-0.16	0.07	-0.11	0.11	0.03	**-0.96**	1.00		
Pod no./Plant (PP)		-0.17	0.16	-0.08	-0.05	0.05	0.07	-0.17	-0.08	0.11	1.00	
Seed no./Pod (SP)		0.07	-0.06	-0.03	0.09	-0.09	0.03	**-0.26**	0.08	-0.02	**0.31**	1.00

[a]Italic letters following abbreviations refer to model parameters.
[b]Bold numbers refer to significance at 0.05 probability level.

correlated ($P \leq 0.05$) with the linear-by-linear parameter *a* estimated for the weed density progress variable. There was a significantly positive correlation between the pod number per bean plant and the seed number per pod (Table 4).

Principal component analysis

The PCA using a correlation matrix indicated associations of relevant bean-disease-weed development, pod-seed production indicators with principal components estimating linear combinations of the variables. From the PCA, the five principal components accounted for 79.5% of the variation in bean dry matter, *Rhizoctonia* root rot, and weed density development data obtained from two commercial bean cultivars planted at different planting dates and weed control treatments during the two seasons as shown in Table 5. The first principal component justified 20.5% of the total data variance. This factor provided the positively moderate loadings for the correspondence of the exponential parameter *a* of bean dry matter, linear-by-linear parameter *a* and *d* estimated for *Rhizoctonia* root rot and weed density, respectively. The linear-by-linear parameter *b* estimated for either *Rhizoctonia* root rot and weed density were negatively associated with the first principal component. Thus, this factor of PCA test determined the indirect association of linear-by-linear parameter *b* with the linear-by-linear parameters *a* and *d* significantly contributed. This suggested the association of a lower linear-by-linear parameter *b* (more effective *Rhizoctonia* root rot or weed increase factor) with greater linear-by-linear parameter *a* (initially more intense *Rhizoctonia* root rot) and *d* (weed density progress rate).

The second principal component, accounting for 19.2% of the total bean-disease-weed data variance, demonstrated the moderately significant contributions of the initial bean dry matter (constant term or exponential parameter *a*) and the dry matter increase factor (exponential parameter *b*) to characterize a diverse range of bean-disease-weed development curves developed during two growth seasons (Table 5). This factor detected the association of a lower parameter *b* of exponential (less effective bean dry matter increase factor) models with a higher exponential parameter *a* (greater initial bean dry matter).

The third principal component justified 16.9% of the total bean-disease-weed data variance (Table 5). This factor provided the significantly positive contributions of the initial *Rhizoctonia* root rot (linear-by-linear parameter *a*) and weed density increase factor (linear-by-linear parameter *b*), and negative contributions of the disease increase factor (linear-by-linear parameter *b*) and weed density increase rate (linear-by-linear parameter *d*). This suggested the indirect association of parameter *b* (*Rhizoctonia* root rot or weed density increase factor) with the parameters *a* (the initial disease) and *d* (weed density increase rate) of linear-by-linear models.

The forth principal component justified 13.0% of the total dataset variance, detecting significant associations of the two bean productivity variables, pod number per plant and seed number per pod, and the initial weed density (linear-by-linear parameter *a*; Table 5). This demonstrated the correspondence of the initially less dense weed populations with greater pod numbers per plant and seed numbers per pod produced by the two bean cultivars studied. The

TABLE 5 Principal component analysis of plant production, *Rhizoctonia* root rot, and weed development in bean cultivars planted at different dates and weed control treatments.

Variables		Principal components				
		1	2	3	4	5
Bean dry matter	Exponential parameter *a*	0.35[a]	**-0.55**	-0.05	0.22	-0.03
	Exponential parameter *b*	-0.34	**0.55**	0.05	-0.20	0.06
	Exponential parameter *r*	-0.09	-0.16	0.08	0.15	**0.78**
Rhizoctonia root rot	Linear-by-Linear parameter *a*	**0.42**	0.19	**0.50**	-0.09	0.06
	Linear-by-Linear parameter *b*	**-0.45**	-0.21	**-0.49**	0.09	-0.04
	Linear-by-Linear parameter *d*	0.18	0.13	0.07	0.03	-0.10
Weed density	Linear-by-Linear parameter *a*	0.18	-0.18	-0.13	**-0.45**	**-0.44**
	Linear-by-Linear parameter *b*	**-0.40**	-0.26	**0.49**	-0.03	-0.18
	Linear-by-Linear parameter *d*	**0.40**	0.31	**-0.47**	0.07	0.12
Pod no./Plant		-0.07	0.26	-0.06	**0.50**	-0.31
Seed no./Pod		0.02	0.07	0.17	**0.65**	-0.22
Eigenvalues		2.3	2.1	1.9	1.4	1.1
Variation (%)		20.5	19.2	16.9	13.0	9.9
Accumulated variation (%)		20.5	39.7	56.6	69.6	79.5

[a]A bold number indicates a significant loading value ≥ 0.35.

fifth principal factor explained 9.9% of the data variance and received a highly significant contribution from the exponential parameter *r* (the bean dry matter increase rate) and a moderately significant contribution from linear-by-linear parameter *a* estimated for weed density. This suggested the correspondence of the initially less dense weed populations with a greater bean dry matter increase rate (exponential parameter *a*; Table 5). This PCA identified not only the significant indicators estimating the progression of bean dry matter, *Rhizoctonia* root rot and weed density, but also the joint associations between the crop production, disease and weed development.

Multivariate regression analysis

The multivariate regression analyses (F probability = 0.001; R^2 = 0.49) demonstrated that 49% of variations in pod and seed production in bean cultivars treated with different planting dates and weed control methods across 256 experimental plots were explained according to the bean dry matter, *Rhizoctonia* root rot and weed density development descriptors (Table 6). Singular and two-way interactions of bean dry matter exponential parameter *a*, *b* and *r*, and linear-by-linear parameters *a* and *b* estimated for *Rhizoctonia* root rot and weed density development corresponded significantly with the number of pod/plant and seed/pod in the bean crops studied during the two growing seasons. There was no significant difference between the observed and fitted values of pod and seed regression models developed based on the bean growth, disease and weed parameters. Therefore, bean pod and seed production was estimated using the predictors described for over-season development of bean growth, disease and weed examined at field-plot scale (Table 6).

Discussion

Sustainable bean production strictly requires the development of an integrated environmental friendly crop management program (Naseri, 2019a). To meet this requirement, it was attempted in the current research to study over-season fluctuations in plant growth, *Rhizoctonia* root and stem rot, and weed density in two bean cultivars (with different habits) treated with different planting dates and weed control practices across experimental field plots. Hence, we firstly needed to determine the best indicators of plant dry matter, *Rhizoctonia* root rot, and weed density development in bean cultivars treated with diverse planting dates and weed control methods. This experimental design provided a diverse range of variations in the bean-disease-weed progression over time due to treating field plots with different planting dates and weed control practices. Such a noticeable variability in data helps to increase the predictive value of a disease progress curve element (Kranz, 2003; Naseri and Veisi, 2019). The current findings suggested exponential and linear-by-linear parameters as the best predictors of plant dry matter, *Rhizoctonia* root rot, and weed density progress in early to very late-planted bean cultivars under gone different weed control practices studied during the two growing seasons. With the best of our knowledge, the current field-scale findings demonstrated the notable predictive values of bean-disease-weed development variables to improve the accuracy of future estimation of bean production, *Rhizoctonia* root rot, and weed to develop more effective crop management programs and higher yield levels.

In China, Tan et al. (2007) developed Gompertz and logistic models to simulate rice sheath blight progress dynamics according to disease severity ratings. Campbell et al. (1980) described the final disease severity and first-difference regression linear coefficient as predictors of bean root rot progress curves to

TABLE 6 Multivariate regression analysis of pod and seed production based on principal component analysis of bean growth, *Rhizoctonia* root rot, and weed descriptors in two cultivars sown under different dates and weed control treatments.

Variables	Model	Parameter estimate	Standard error	*t*-probability
Bean dry matter EXP*b* × *Rhizoctonia* root rot LL*a*	Pod no./Plant	-0.00007	0.00009	0.431
	Seed no./Pod	-0.00004	0.00004	0.340
Rhizoctonia root rot LL*a* × *Rhizoctonia* root rot LL*b*	Pod no./Plant	-0.00001	0.00001	0.123
	Seed no./Pod	-0.00001	0.00001	0.100
Rhizoctonia root rot LL*b* × Weed density LL*b*	Pod no./Plant	0.00030	0.00025	0.246
	Seed no./Pod	0.00011	0.00010	0.288
Bean dry matter EXP*a* × Bean dry matter EXP*b*	Pod no./Plant	-0.00001	0.00000	0.024
	Seed no./Pod	-0.00001	0.00000	0.046
Rhizoctonia root rot LL*a* × Weed density LL*b*	Pod no./Plant	0.00042	0.00036	0.257
	Seed no./Pod	0.00015	0.00014	0.288
Weed density LL*a*	Pod no./Plant	0.04400	0.01170	<0.001
	Seed no./Pod	0.01747	0.00465	<0.001
Bean dry matter EXP*r* × Weed density LL*a*	Pod no./Plant	0.00895	0.00396	0.028
	Seed no./Pod	0.00378	0.00158	0.020

[a]EXPa, Exponential parameter a; EXPb, exponential parameter b; EXPr, exponential parameter r; LLa, Linear-by-Linear parameter a; LLb, Linear-by-Linear parameter b.

improve accuracy of epidemiological findings. In Nigeria, Chikoye et al. (2006) estimated the efficiency of a new formulation of Atrazine herbicide to manage weed populations in maize fields using an exponential model. However, none of previous studies simulated the progression of bean growth, *Rhizoctonia* root rot, and weed according to the best indicators fitted to field-scale datasets. Therefore, the present findings on interrelationships among the crop productivity, *Rhizoctonia* root and stem rot, and weed development using the three exponential and three linear-by-linear parameters as the best indicators of bean dry matter, disease, and weed dynamics in bean cultivars appears to be the first report. Such information must add a further value to future estimations of bean production in farming systems infested by root rots and weeds.

According to the Kruskal-Wallis one-way ANOVA results, the use of herbicides in early planted plots restricted the development of weed density during the growing season by 28%. Whereas, late planting improved the weed control efficiency of herbicides by reducing weed density by 42% based on the linear-by-linear parameter *a* estimates for herbicide use and not treated classes of weed control factor. For the over-season progression of *Rhizoctonia* root rot, late plantings of bean cultivars decreased the disease development by 8-36% according to the linear-by-linear parameter *a* estimates for the three weed control treatments. Although the dry matter, pod and seed production of bean cultivars for the herbicide use and hand-weeding treatments were greater than not treated control plots, late planting improved bean dry matter and pod production in plots neither treated with herbicides nor hand-weeded by 10-24%. To the best of our knowledge, such new information on significant effects of planting date on the current bean dry matter and productivity, *Rhizoctonia* root rot and weed density datasets collected from experimental field plots treated with various planting dates and weed control practices may emphasize on the necessity of proper planting date to be considered as an sustainable disease and weed management method into future bean cultivation programs.

Associations of bean production with agronomic practices and soil conditions (Naseri and Veisi, 2019), bean growth (Manschadi et al., 1998), *Rhizoctonia* root rot (Campbell et al., 1980), weed populations (Ghamari and Ahmadvand, 2012) had been reported earlier. The treatments of Clethodim herbicide and *Trichoderma* spp. reduced weeds and *Rhizoctonia* root rot and improved plant growth and yield parameters in two faba bean (*Vicia faba* L.) cultivars grown in naturally infested field soils (El-Dabaa et al., 2019). However, none of the previous studies reported the best indicators of bean growth, disease and weed dynamics over the growing season in association with the pod and seed production. As far as we know, the associations of pod and seed production in beans with the best indicators of plant dry matter, *Rhizoctonia* root rot, and weed density development at the scale of an experimental field is reported for the first time. This multivariate analysis demonstrated that the independent principal components explained 80% of total variance in bean-disease-weed datasets obtained during the two growing seasons at plot scale.

It could be concluded that a main (80%) part of variations in the crop growth and production, disease and weed development in bean cultivars grown under different planting dates and weed control treatments was explained according to the eleven bean-disease-weed descriptors in the current study. In addition to the above-mentioned findings, the present study determined the similar descriptive values for bean dry matter, *Rhizoctonia* root rot, and weed density indicators. The PCA results demonstrated the significant contribution of bean dry matter, disease and weed development into the first principal component explaining 21% of total data variance, suggesting the noticeable interrelationships among these bean-disease-weed variables. Furthermore, the multivariate regression models developed for pod and seed production explained a considerable part (49%) of variations in the bean-disease-weed datasets. This suggested that those model parameters estimated in the current research were responsible for about half of the variability in bean growth, *Rhizoctonia* root rot and weed density during the two growing season. Such information may assists with more accurately monitoring bean-disease-weed development and predicting bean productivity for sustainable crop management programs in future.

Data availability statement

The raw data supporting the conclusions of this article will be made available by the authors, without undue reservation.

Author contributions

SN: Designing and performing the work, and BN: interpreting the data and writing the paper. All authors contributed to the article and approved the submitted version.

Funding

This study was funded by the Iranian Agricultural Research, Education & Extension Organization, projects 4-47-16-88113 and 4-47-16-90070.

Acknowledgments

Authors appreciate the technical assistance in the field.

Conflict of interest

The authors declare that the research was conducted in the absence of any commercial or financial relationships that could be construed as a potential conflict of interest.

Publisher's note

References

Brusco, M. J., and Stahl, S. (2005). *Branch-and-bound applications in combinatorial data analysis* (New York: Statistics and Computing. Springer).

Byiringiro, B., Birungi, S., Musoni, A., and Mashingaidze, A. B. (2017). The effect of planting date on weed density, biomass and seed yield in common bean (*Phaseolus vulgaris* l.) in the semi-arid region of nyagatare, Rwanda. *Trop. Agric. (Trinidad)* 94, 335–345. doi: 0041-3216/2017/040335-11

Campbell, C. L., Madden, L. V., and Pennypacker, S. P. (1980). Structural characterization of bean root rot epidemics. *Phytopathology* 70, 152–155. doi: 10.1094/Phyto-70-152

Chikoye, D., Udensi, U. E., and Lum, A. F. (2006). Performance of a new formulation of atrazine for weed control in maize in Nigeria. *J. Food Agric. Environ.* 4, 1–4.

Dehghani, A., Panjehkeh, N., Asadi Rahmani, H., Salari, M., and Darvishnia, M. (2018). Effectiveness of simultaneous application of indigenous rhizobium and arbuscular mycorrhiza on root rot disease and yield of red bean (*Phaseolus vulgaris* l.) in lorestan province. *Biocontrol Plant Prot.* 6, 43–58. doi: 10.22092/BCPP.2018.119375

El-Dabaa, M. A. T., Abd-El-Khair, H., and El-Nagdi, W. M. A. (2019). Field application of clethodim herbicide combined with trichoderma spp. for controlling weeds, root knot nematodes and *Rhizoctonia* root rot disease in two faba bean cultivars. *J. Plant Prot. Res.* 59, 255–264. doi: 10.24425/jppr.2019.129287

Esmaeilzadeh, S., and Aminpanah, H. (2015). Effects of planting date and spatial arrangement on common bean (*Phaseolus vulgaris*) yield under weed-free and weedy conditions. *Planta Daninha* 33, 425–432. doi: 10.1590/S0100-83582015000300005

Ghamari, H., and Ahmadvand, G. (2012). Weed interference affects dry bean yield and growth. *Notulae Scientia Biologicae* 4, 70–75. doi: 10.15835/nsb437810

Kakhki, S. H. N., Taghaddosi, M. V., Moini, M. R., Veisi, M., and Naseri, B. (2022). How bean fly, rhizoctonia root rot, weed and productivity are affected by cultivar, herbicide application and planting date. *All Life* 15, 706–717. doi: 10.1080/26895293.2022.2087106

Kranz, J. (2003). "Comparison of temporal aspects of epidemics: The disease progress curves," in *Comparative epidemiology of plant diseases* (Berlin, Heidelberg: Springer).

Manschadi, A. M., Sauerborn Stutzel, J. H., Gobel, W., and Saxena, M. C. (1998). Simulation of faba bean (*Vicia faba* l.) growth and development under Mediterranean conditions: model adaptation and evaluation. *Eur. J. Agron.* 9, 273–293. doi: 10.1016/S1161-0301(98)00045-8

Naseri, B. (2013a). Interpretation of variety × sowing date × sowing depth interaction for bean–Fusarium–Rhizoctonia pathosystem. *Arch. Phytopathol. Plant Prot.* 46, 2244–2252. doi: 10.1080/03235408.2013.792535

Naseri, B. (2013b). Linkages of farmers' operations with rhizoctonia root rot spread in bean crops on a regional basis. *J. Phytopathol.* 161, 814–822. doi: 10.1111/jph.12140

Naseri, B. (2019a). "Legume root rot control through soil management for sustainable agriculture," in *Sustainable management of soil and environment*. Eds. R. S. Meena, S. Kumar, J. Singh and M. Lal (Woodhead Publishing: Springer).

Naseri, B. (2019b). "The potential of agro-ecological properties in fulfilling the promise of organic farming: a case study of bean root rots and yields in Iran," in *Organic farming*. Eds. M. R. Unni, C. Sarathchandran Veloormadom and S. Thomas (Singapore: Elsevier).

Naseri, B., and Moradi, P. (2015). Farm management strategies and the prevalence of rhizoctonia root rot in bean. *J. Plant Dis. Prot.* 5, 238–243. doi: 10.1007/BF03356558

Naseri, B., and Veisi, M. (2019). How variable characteristics of bean cropping systems affect fusarium and rhizoctonia root rot epidemics? *Arch. Phytopathol. Plant Prot.* 52, 30–44. doi: 10.1080/03235408.2018.1564226

Naseri, B., and Younesi, H. (2021). Beneficial microbes in biocontrol of root rots in bean crops: A meta-analysis, (1990-2020). *Phsiol Molecu Plant Pathol.* 116, 101712. doi: 10.1016/j.pmpp.2021.101712

Oveisi, M., Pourmorad Kaleibar, B., Rahimian Mashhadi, H., Müller-Schärer, H., Bagheri, A., Amani, M., et al. (2021). Bean cultivar mixture allows reduced herbicide dose while maintaining high yield: A step towards more eco-friendly weed management. *Eur. J. Agron.* 122, 126173. doi: 10.1016/j.eja.2020.126173

Stagnari, F., and Pisante, M. (2011). The critical period for weed competition in French bean (*Phaseolus vulgaris* l.) in Mediterranean areas. *Crop Prot.* 30, 179–184. doi: 10.1016/j.cropro.2010.11.003

Tabande, L., and Naseri, B. (2020). How strongly rhizobial nodulation is associated with bean cropping system? *J. Plant Prot. Res.* 60, 176–184. doi: 10.24425/jppr.2020.133307

Tan, W. Z., Zhang, W., Ou, Z. Q., Li, C. W., Zhou, G. J. , Wang, Z. K., et al. (2007). Analyses of the temporal development and yield losses due to sheath blight of rice (*Rhizoctonia solani* AG1.1a). *Agric. Sci. China* 6, 1074–1081. doi: 10.1016/S1671-2927(07)60149-7

frontiers | Frontiers in Plant Science

TYPE Original Research
PUBLISHED 06 December 2022
DOI 10.3389/fpls.2022.1045225

OPEN ACCESS

EDITED BY
Sabine Banniza,
University of Saskatchewan,
Canada

REVIEWED BY
Ram B. Khadka,
Nepal Agricultural Research
Council, Nepal
Amitava Rakshit,
Banaras Hindu University, India

*CORRESPONDENCE
Martin Pisarčik
pisarcik@af.czu.cz

SPECIALTY SECTION
This article was submitted to
Plant Pathogen Interactions,
a section of the journal
Frontiers in Plant Science

RECEIVED 15 September 2022
ACCEPTED 21 November 2022
PUBLISHED 06 December 2022

CITATION
Pisarčik M, Hakl J, Szabó O and
Nerušil P (2022) Efficacy of *Pythium
oligandrum* on improvement of
lucerne yield, root development and
disease score under field conditions.
Front. Plant Sci. 13:1045225.
doi: 10.3389/fpls.2022.1045225

Efficacy of *Pythium oligandrum* on improvement of lucerne yield, root development and disease score under field conditions

Martin Pisarčik[1]*, Josef Hakl[1], Ondřej Szabó[1] and Pavel Nerušil[2]

[1]Department of Agroecology and Crop Production, Czech University of Life Sciences Prague, Prague, Czechia, [2]Research Station of Grassland Ecosystems Jevíčko, Crop Research Institute, Jevíčko, Czechia

Introduction: Biological control of root diseases of lucerne (Medicago sativa L.) has potential benefits for stand performance but this remains unsupported by evidence from practical field studies.

Methods: In field experiments at three sites our objectives were to determine the effect of Pythium oligandrum, as spring, autumn and intensive regime treatments on (i) lucerne plant density and root traits development, and (ii) forage yield and forage traits. Lucerne stands were managed under two or three treatments: non-treated control and P. oligandrum applied at two intensities of application under four-cut utilization.

Results and discussion: Under relatively dry conditions (annual mean 10°C and <500 mm precipitation) lucerne dry matter yield was significantly reduced by 6%, which could be related to mechanisms of inappropriate stimulation and disturbance of the balance between auxins and ethylene. Under annual precipitation of >500 mm, positive impacts on stand height or fine root mass were observed for the autumn and intensive treatments where positive root response was visible only in alluvial soil. However, these changes did not result in higher yield and probably more applications per year will be needed for significant forage yield improvement. This study highlights the limits of field-scale biological control in which the potential of P. oligandrum for lucerne productivity improvement was realised only under a humid environment or deep alluvial soils, where higher root disease infestation may also be expected.

KEYWORDS

alfalfa, Medicago sativa, plant growth promotion, Polyversum, dry conditions

Introduction

Biological control of pests and diseases of field crops has become of increasing importance in recent years in line with the current emphasis on improved sustainability of crop production and reduced use of chemical pesticides in agriculture. Increasing implementation of biological approaches, including biological control, biopesticides, biostimulants and pheromones, is a high priority for sustainable agriculture leaders and farmers (Baker et al., 2020). Among potential biological control agents, beneficial fungi have received significant attention worldwide due to their remarkable antagonistic properties against plant pathogens and numerous successful applications have been reported (Ghorbanpour et al., 2018). Several studies on the use of fungi as biological control agents have identified multiple mechanisms by which fungal agents, such as *Pythium* (Gerbore et al., 2014) or *Trichoderma* (Ghorbanpour et al., 2018) may protect plants from pathogens, as well as showing the limits for their effective utilization in affecting soil-borne diseases (Campbell, 1994). Understanding the mechanisms for fungal control of pathogens is crucial for the development of effective biocontrol strategies against plant diseases, and there are further requirements affecting their use such as the ability to produce liquid cultures for easy application and ensuring an adequate persistence of the fungal agent in the environment (O'Brien, 2017). In addition to the biocontrol properties of *Trichoderma*, as highlighted by Ghorbanpour et al. (2018), *Pythium oligandrum* has been investigated for its potential as a biological protection agent for several crops over the last two decades (Gerbore et al., 2014), either alone or in combination with bacterial strains (Ouhaibi-Ben et al., 2021). Benhamou et al. (2012) summarized that *P. oligandrum* is a mycoparasitic oomycete, and has the ability to colonize the rhizosphere and root systems of many crop plants, directly attacking soil-borne fungal pathogens, promoting plant growth, and increasing crop protection against fungal disease *via* the activation of the plant's immune system. Examples of the efficacy of *P. oligandrum* against the plant pathogens have been reported for *P. ultimum, P. aphanidermatum, Fusarium oxysporum*, *Verticillium albo-atrum, Rhizoctonia solani* and *Physperma solani* (Benhamou et al., 1999, 2012). Bělonožníková et al. (2020) described differences among 12 diverse strains of *P. oligandrum* with regard to their properties and effect on plants, and identified strain M1 with positive influence on plant fitness.

Forage legumes such as lucerne (*Medicago sativa* L.) or red clover (*Trifolium pratense* L.) comprise an important group of field crops that are susceptible to root diseases which can seriously limit their survival and yield through reduction of plant density and productivity over successive years (Sedman et al., 2007). Although a number of studies have been conducted over several decades, no effective fungicidal control of these root diseases has yet been established or approved. This is partly because fungicidal control by chemical fungicides is thought to be ineffective in providing complete disease control (McKenna et al., 2018) and several studies have reported reduced crop growth efficiency, especially in terms of forage yield improvement (Larkin et al., 1996; Hwang et al., 2002; Gray and Koch, 2004). Although some studies have demonstrated positive effects of fungicides on disease protection of forage legumes (Leath et al., 1973; Larkin et al., 1995), this was usually followed by negative effects on crop growth (Jenkyn, 1975; Nan et al., 1991) and/or adverse effects on non-target microorganisms such as mycorrhizal fungi (Yang et al., 2011) and N fixation, where inhibition of molecular signalling between rhizobia and the host legume plants has been observed (Ahemad and Khan, 2013). Abbas et al. (2022) suggested also suitable combinations of fungicide with biological control agents reducing environment pollution. The absence of an approved fungicide protection treatment has meant that plant breeding for disease resistance (Riday, 2010) and/or suitable cultivation management (Gray and Koch, 2004) remain as the key disease-control strategy for lucerne or red clover producers (2020; Pisarčik et al., 2019).

Among biological control methods, some positive effects for lucerne were reported after *Streptomyces* (Jones and Samac, 1996; Xiao et al., 2002) or *Bacillus cereus* application (Handelsman et al., 1990), both of which reduced lucerne seedling damping-off during stand establishment. Morsy et al. (2011) observed a positive response of lucerne to application of *Bacillus megatherium* or *Trichoderma album*, although neither was as effective as abiotic agents in their study. Öhberg and Bang (2010) confirmed there was a positive yield effect of application of *Conithirium minitans* prior to seeding, when red clover plants were infected with *Sclerotinium trifoliorum*. Despite some positive examples of biological control, Pisarčik et al. (2019) found that biological control under field conditions may not always give beneficial outcomes, in contrast to the results of laboratory or greenhouse experiments, because of complicated interactions between plant, organism/preparation, and environment resulting in general unstable controllling effects from year to year. Although there has been intensive research in biological protection of diseases under controlled conditions, there still remains a lack of field-based studies to provide evidence supporting the economic efficiency of biological control for particular crops, especially for the successive harvest years of perennial forage crops. Among the *Fabaceae* crops, the effectiveness of *P. oligandrum* has been documented mostly for grain legumes such as soybean (You et al., 2019) or pea (Nikolova et al., 2015) and only a few studies have been reported for forage legumes. The *Fusarium* and *Verticilium* generally represent the main root pathogens of lucerne

(Miller-Garvin and Viands, 1994) and were also identified as the key genera of lucerne root pathogens in central Europe (Hakl et al., 2017). Efficacy of *P. oligandrum* (strain M1) against *Fusarium* (*F. avenaceum*, *F. oxysporum*, *F. culmorum*, and *F. solani*) in red clover stands has been presented (2021; Pisarčik et al., 2020)

Positive effects on forage yield have been reported in two independent experiments with red clover under treatments with intensive application of *P. oligandrum* but this improved yield was associated more with plant growth stimulation than from a direct protection against *Fusarium* (2021; Pisarčik et al., 2020). In lucerne, spring application of *P. oligandrum* was found to provide zero effect on yield and it even increased the proportion of infected plants in the last year of the field experiment (Pisarčik et al., 2019). For vetch (*Vicia sativa* L.), significantly lower effects of biological control than with conventional chemical control have been reported (Georgieva et al., 2020). Previous research has also shown a significant relationship between lucerne root morphology and infection of root diseases (Larkin et al., 1995; Hakl et al., 2017) and therefore there is a need for evaluation of disease score together with root traits and forage yield.

Optimization of the number of applications and dates of application is needed to ensure economic practice in crop protection (Pisarčik et al., 2021). This is especially difficult for perennial forage crops that are utilized over multiple-year growing seasons covering the seeding year and two or three subsequent harvest years. The results with a single spring application of *P. oligandrum* in lucerne have not provided positive yield response at the one location investigated so far (Pisarčik et al., 2019). For red clover some benefits under an intensive or autumn application regime, in contrast to spring application, have been reported in terms of improved red clover yield and/or root traits (Pisarčik et al., 2021). These previous outcomes for red clover highlights potential of *P. oligandrum* for forage legumes and gives further encouragement to extend the biological control research with treatments including variable timing of applications to lucerne. Testing effective lucerne protection would have an innovative benefit as no such practical method has yet been recommended for field conditions. Therefore, in the work reported here, we have combined results obtained from three field experiments that investigated different timing and intensity of lucerne biological control of root diseases. Our aims were to investigate the effect of spring, autumn and intensive regimes of *P. oligandrum* application to lucerne on (i) plant density and root traits development, and (ii) on forage yield and forage traits in a four-year field experiment on different sites. An additional aim was to evaluate the relationship between lucerne fine root mass, other root morphology traits and plant root disease score. These comprehensive evaluations from different locations could be valuable for better understanding of the simultaneous effects of tested treatments on the improvement of lucerne stand performance and provided outcomes can be practically applied in the similar field conditions.

Materials and methods

Field experiments

Field plot experiments with lucerne were conducted at three sites in the Czech Republic during 2016 - 2020. Site 1 (Červený Újezd, elevation 410 m a.s.l.) is characterized by clay-loam Haplic Luvisol with a shallow soil profile, long-term mean annual temperature of 8.4°C and cumulative annual rainfall of 502 mm. Site 2 (Jevíčko, elevation 350 m a.s.l.) is located on a river floodplain with a deep loam Haplic Luvisol and high soil humidity. Site 3 (Drválovice, elevation 460 m a.s.l.) is characterized by loamy-sandy Cambisol. Sites 2 and 3 are close to each other and share data from the same meteorological station: long-term mean annual temperature of 7.4°C and cumulative annual rainfall of 545 mm. All characteristics of sites are summarized in Table 1.In all three experiments, lucerne varieties Oslava (at Sites 1 and 2) and Pálava (at Site 3) were established in spring as monocultures with a sowing rate of 700 viable seeds m^{-2} and row seeding at a between-row distance of 12.5 cm. Each experiment consisted of a non-treated control and one or two Polyversum treatments, and was arranged in a completely randomized block design with four replicate blocks. Plot size was 7.2 × 2.5 m with a harvested area of 10 m^2. The preparation of Polyversum (Biopreparáty spol. s r.o., Czech Republic) contained 1 000 000 active oospores of *Pythium oligandrum* M1 per gram. The Polyversum was applied once each year (in spring or autumn) with additional applications per year for the intensive treatment. In the seeding year, Polyversum treatments were applied one to three times (6 weeks after stand establishment, after an initial mowing of the new sward at 5 cm for which the cut herbage mass was not recorded), and also after an autumn cut, depending on intensity of application. Timing of Polyversum applications in post-seeding years corresponded with a four-cut schedule where the number of applications for the intensive treatment varied from two at Site 2 (after first and autumn cut) to five at Site 1 (in spring and after each cut). The single applications of Polyversum were made after first cut (spring treatment) or after the autumn cut (autumn treatment). The timing of all applications across years and experiments is described in Table 2. Polyversum was always activated one hour before application, and the rate was 100 g ha^{-1} applied in 300 litres of water, using a backpack sprayer (Cooper Pegler 15 EVO) with a working pressure of 3 bar, always in humid weather without intensive sunshine.

TABLE 1 Description of localities, annual temperature mean and cumulated precipitation.

Locality		Červený Újezd (Site 1)	Jevíčko (Site 2)	Drválovice (Site 3)
Elevation (m a.s.l.)		410	350	460
GPS coordinate		50.07207 N 14.17136 E	49.62904 N 16.72815 E	49.56745 N 16.65041E
Soil texture and type		clay-loam Haplic Luvisol	deep loam Haplic Luvisol	loamy-sandy Cambisol
Temperature (°C)	2016	9.6 (+1.2)*	–	
	2017	9.5 (+1.1)	8.4 (+1.0)	
	2018	10.4 (+2.0)	9.6 (+2.2)	
	2019	10.4 (+2.0)	9.4 (+1.8)	
	2020	–	9.1 (+1.5)	
Precipitation (mm)	2016	475 (-27)*	–	
	2017	492 (-10)	539 (-6)	
	2018	334 (-168)	401 (-144)	
	2019	479 (-23)	574 (+30)	
	2020	–	722 (+178)	

*difference to long-term mean (1981 - 2010).

Lucerne root morphology and root disease score

In each plot of all three of the experimental sites, lucerne plants were dug each autumn to a depth of about 20 - 25 cm. The sampling area was increased over time to provide a similar number of plants under the natural decrease of plant density. Sampling dates and size of the root sampling areas are presented in Table 2. Lucerne plant density (PD, plants m^{-2}) was calculated from the number of plants per sample and size of the root sampling area. For each plant, the tap-root diameter below the crown (TD, mm) and lateral root number per plant tap-root (LRN, when diameter larger than 1 mm) were measured. Presence of fine root mass (FRM, when less than 1 mm) was estimated subjectively on a scale of 1 to 5 with scores of 1, 3, and 5 indicating none, moderate and many fine roots, respectively. Washed root samples were oven-dried at 60°C for 48 h and total root dry matter (RDM, g m^{-2}) was calculated based on the size of the sampling area. Plant root disease score (PRDS) was determined subjectively and based on discoloration on a cross-cut of the tap-root. The disease scoring followed Hakl et al. (2017): 0 = healthy plant, no discoloration in the root; living plants with root discoloration were scored from 1 to 6 with a score of 1 = 1 to 5%, 2 = 5 - 20%, 3 = 20 - 40%, 4 = 40 - 60%, 5 = 60 - 80%, 6 = 80 - 95% of the area of the tap-root cross-cut; 7 = dead plant. Ratio of infected plants (IP) was calculated from proportion of healthy plants and PRDS is reported as mean of infected plants between treatments or years. At stand level, the percentage of branch-rooted plants (root system with lateral roots developing from the tap root; RB) was calculated per sample. The root potential index (RPI) integrating TD and plant density was calculated according to equation proposed by Hakl et al. (2017). For precise detection of root pathogens, root samples (2 x 5 plants per plot) were taken in the autumn of the final year of the experiments. Taproots of five plants were combined, frozen and lyophilized. Quantitative real-time PCR (qPCR) were used for detection of key pathogens in the given environment, i.e. *Fusarium oxysporum*, *F. avenaceum* and *Verticillium albo-atrum*, separately in each sample. Primers were based on known sequences for *F. avenaceum* (Waalwijk et al., 2004), *F. oxysporum* (Haegi et al., 2013) and *Verticillium albo-atrum* (Maurer et al., 2013). All qPCR reactions were set in the Hard-Shell® 96-Well PCR plates (BioRad) in a total volume of 10 µl by mixing 5 µl of gb Easy PCR Master Mix (twofold concentrated, Generi Biotech, Hradec Králové, Czech Republic), 1 µl of each of the qPCR assay mixture (tenfold concentrated), and 3 µl of the target DNA. PCR plate was placed into the heating block of the CFX Connect Real-Time PCR Detection System (BioRad) operated using CFX ManagerTM Software (ver. 3.0, BioRad). The cycling parameters were: 95°C for 3 min (initial denaturation) followed by 50 cycles of 95°C for 10 s (denaturation), and 50°C for 30 s (annealing plus extension). Fluorescence of FAM (λex = 495 nm, λem = 520 nm) and HEX (λex = 535 nm, λem = 556 nm) was monitored during every PCR cycle, after the extension step. The absolute DNA concentration was calculated using the linearized cloned target sequence standards (Generi Biotech, Hradec Králové, Czech Republic).

Harvest management, sampling and measurement of forage structure traits and yield

In the seeding year, 2016, an initial unrecorded cut made in mid-summer was followed by an autumn harvest (at Sites 1 and

10.3389/fpls.2022.1045225

TABLE 2 Description of treatments, application dates of Polyversum at a dose rate of 100 g ha^{-1} in Polyversum treatments together with root sampling area and sampling dates, and forage harvest dates for all treatments in the years of the study.

Locality	Treatments	2016	2017	2018	2019	2020
		Application, sampling and harvest dates				
Červený Újezd (Site 1)	Autumn	6 Jun, 28 Oct	26 Oct	9 Oct	9 Oct	–
	Nr. of app.	2	1	1	1	–
	Intensive	6 Jun, 27 July, 28 Oct	11 Apr, 29 May, 7 Jul, 28 Aug, 26 Oct	13 Apr, 17 May, 21 Jun, 14 Aug, 9 Oct	12 Apr, 24 May, 9 Jul, 27 Aug, 9 Oct	–
	Nr. of app.	3	5	5	5	–
	Root sampling Area (cm)	2 Nov 25 x 12.5	14 Nov 50 x 12.5	16 Oct 50 x 12.5	29 Oct 50 x 12.5	–
	Forage harvest dates	20 Oct	18 May, 28 Jun, 17 Aug, 19 Oct	10 May, 14 Jun, 31 Jul, 9 Oct	16 May, 27 Jun, 12 Aug, 3 Oct	–
Jevíčko (Site 2)	Spring	–	3 Jun	25 May	11 Jun	–
	Nr. of app.	–	1	1	1	–
	Intensive	–	3 Jun 3 Nov	25 May, 15 Oct	11 Jun, 15 Oct	–
	Nr. of app.	–	2	2	2	–
	Root sampling Area (cm)	–	10 Nov 25 x 12.5	1 Nov 50 x 12.5	1 Nov 50 x 12.5	–
	Forage harvest dates		20 Jun, 31 Jul, 19 Sep	4 May, 11 Jun, 19 Jul, 20 Sep	17 May, 24 Jun, 9 Aug, 24 Sep	–
Drválovice (Site 3)	Spring/Autumn	–	23 May	15 May	15 Oct	12 Oct
	Nr. of app.	–	1	1	1	1
	Root sampling Area (cm)	–	14 Nov 50 x 12.5	1 Nov 50 x 12.5	12 Nov 50 x 12.5	18 Nov 100 x12.5
	Forage harvest dates	–	11 May, 16 Jun, 19Jul, 24 Aug, 11 Oct	4 May, 1 Jun, 19 Jul, 29 Aug, 9 Oct	16 May, 25 Jun, 12 Aug, 24 Sep	18 May, 22 Jun, 14 Aug, 25 Sep

3) whilst three cuts were taken at Site 2. In the post-seeding years a four-cut management was applied at Sites 1 and 2, but at Site 3 there were five cuts per year taken in the first two years (2017 and 2018) and a four-cut schedule in 2019 and 2020. All dates of cutting are summarized in Table 2. Before each harvest in the post-seeding years, the compressed stand height (CH, cm) was measured using a metal rising plate meter with disc diameter 0.3 m, area 0.07 m^2 and weight 0.2 kg, and six measurements per plot were taken according to Hakl et al. (2012). Fresh matter yield was assessed by harvesting 10 m^2 in the centre of each plot, to a residual height of 5 cm, using a mower (MF-70, Agrostroj Jičín, Czech Republic) with a working width of 1.4 m. Fresh forage samples of 400-500 g per plot were oven-dried at 103°C for 24 h to determine dry matter content and thus the dry matter yield per m^2.

Statistical analysis

Due to different Polyversum treatments, timing of applications and harvests, analyses were done separately within each location. As results from the first two years for Drválovice (Site 3) have been already published (Pisarčik et al., 2019), only the data for years 2019 and 2020 were analysed in the study reported here. The root morphology traits and annual forage yield were analysed by general mixed model (GLM) including effects of treatment, year, block, and treatment × year interaction where plant density was used as a covariate for some analyses. Tap-root diameter was analysed as mean of all individual plants per treatment whereas LRN was averaged only for branch-rooted plants. Data on the proportion of branch-rooted plants and infected plants expressed as percentage were arcsin-transformed, and back-transformed mean

values are presented in the results. Plant root disease score calculated at plant level did not meet the assumption of normality (except for Site 3) and was analysed by Kruskal-Wallis ANOVA for treatment and year, followed by multiple comparisons of mean ranks. The compressed stand height values were evaluated by four-way GLM (treatment, year, block, cut) with treatment × year interaction. In all analyses, effect of block was considered as random whereas other factors were considered as fixed. Significant differences between means were reported using the Tukey HSD test at $\alpha = 0.05$. Correlation between LRN or FRM class and selected root traits at individual plants across sites was quantified using Pearson linear correlation. All these analyses were carried out using the STATISTICA program (StatSoft, Inc, 2012).

Results

Annual temperature mean and sum of precipitation for the experimental locations over the evaluated years are presented in Table 1. The monthly precipitation totals and mean temperatures during the growing seasons of 2016 - 2020 are shown in Figure 1. At Site 1, all evaluated years were warmer and drier than the long-term mean values for the locality, but the most severe drought stress was observed in 2018 when the growth period from April to October was not only the warmest (16.8°C) but also driest (210 mm). The driest months in this year were April (14 mm) and July (12 mm). For Sites 2 and 3, all evaluated years were also warmer than the long term mean for the locality, with drought stress in 2018. Precipitation was close to the long-term average in 2017 and 2019, with above-average rainfall in 2020.

Development of root morphology and disease score

For root morphology, a total of 1958 lucerne plants were evaluated, of which 903 were visually detected by root discoloration and 1284 were branch-rooted. The effect of *P. oligandrum* treatment and year on root traits within the locations of the experiments are shown in Tables 3–5. For

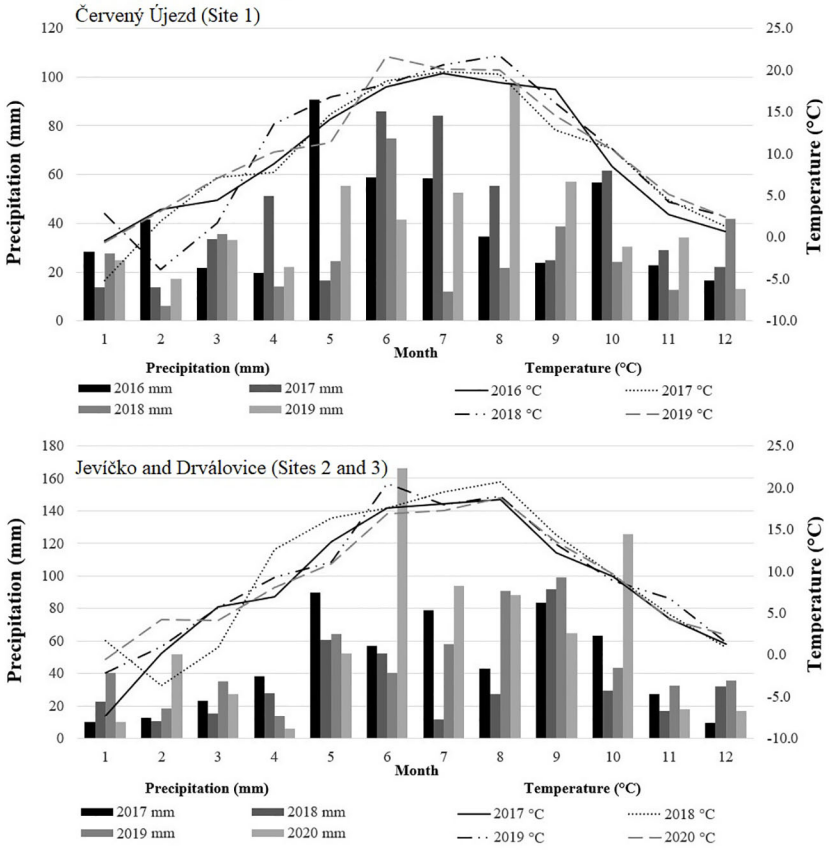

FIGURE 1
The monthly sums of precipitation and temperature means during the experimental years, from the meteorological station Červený Újezd (Site 1) and Jevíčko (Site 2 and 3), Czech Republic.

TABLE 3 Effect of treatment and year for Site 1 (Červený Újezd) on lucerne plant density (PD, plant m^{-2}), root potential index (RPI), ratio of infected plants (IP, as %), ratio of branch-rooted plants (RB, as %), total root dry matter (RDM, g m^{-2}), tap root diameter (TD, mm), fine root mass score (FRM), plant root disease score of infected plants (PRDS), lateral root number at branch-rooted plants (LRN, pcs $plant^{-1}$), dry matter yield (DMY, t ha^{-1}) and compressed stand height (CH, cm).

		PD	RPI	IP	RB	RDM	n	TD	FRM	n	PRDS	n	LRN	n	DMY	CH
	Control	291	84	33.7	59.3	366	16	5.80	3.14	293	2.18	100	2.17	170	12.6^{b}	34.9^{b}
Treatment	Autumn	334	93	33.1	65.9	391	16	5.96	3.07	309	2.07	102	2.07	191	11.8^{a}	33.4^{a}
	Intensive	299	90	28.1	63.2	364	16	5.90	2.95	307	2.05	94	2.06	187	11.9^{a}	33.4^{a}
	P	0.476	0.449	0.383	0.628	0.539		0.705	0.107		0.545*		0.759		**0.021**	**<0.001**
	2016	348	44^{a}	12.2^{a}	62.8^{ab}	361	12	3.16^{a}	2.76^{ab}	149	1.71^{a}	14	1.42^{a}	84	–	–
	2017	303	97^{bc}	39.6^{b}	73.7^{b}	369	12	6.74^{b}	3.18^{b}	261	1.74^{a}	100	2.65^{b}	181	13.4^{b}	38.5^{c}
Year	2018	296	88^{b}	30.8^{b}	44.8^{a}	374	12	6.33^{b}	2.82^{ab}	254	2.67^{b}	77	2.19^{ab}	117	9.6^{a}	29.6^{a}
	2019	286	114^{c}	43.9^{b}	67.8^{b}	390	12	7.31^{d}	3.45^{c}	245	2.28^{ab}	105	2.15^{ab}	166	13.3^{b}	33.6^{b}
	P	0.497	**<0.001**	**<0.001**	**<0.001**	0.228		**<0.001**	**<0.001**		**0.006***		**<0.001**		**<0.001**	**<0.001**
Cut		-	-	-	-	-		-	-		-		-		-	**<0.001**
Year × treatment	*P*	**0.048**	0.946	0.373	0.360	0.181		0.996	0.071		-		0.339		0.522	0.514
Density (covariate)		-	-	-	**0.001**	–		**<0.001**	**0.016**		-		**<0.001**		-	-

P: F - test probability of three-way (year, treatment, block) or four-way (year, treatment, block, cut) GLM including year × treatment interaction (significant values are in bold), different letters indicate statistical differences between treatments or years according to Tukey HSD test at $p < 0.05$.
* Kruskal - Wallis ANOVA with differences according to multiple comparisons of mean ranks.

Sites 1 and 3, no significant influence of treatments on root traits were observed across the years, but at Site 2 a positive response in the fine root mass was detected for the intensive treatment. At Sites 1 and 2, there was significant year × treatment interaction showing the highest value for plant density in the spring (Site 2) or autumn (Site 3) treatment, relative to the non-treated control, in the seeding year, but there was no impact on forage yield or other root traits, and this effect disappeared in subsequent years (data not shown). For Site 3, the significant interaction showed a higher ratio of branch-rooted plants in the control than in the autumn treatment, but this was associated with higher plant density after Polyversum application in the last year of the experiment.

Effect of year on root traits was generally manifested in a decrease in plant density over time followed by increase of tap-root diameter, root potential index, proportion of infected plants, and plant root disease score along with increasing plant age. Branch-rooted plants percentage and fine root mass varied between years but did not show any consistent trends. In contrast to the general pattern for traits development over

TABLE 4 Effect of treatment and year for Site 2 (Jevíčko) on lucerne plant density (PD, plant m^{-2}), root potential index (RPI), ratio of infected plants (IP, as %), ratio of branch-rooted plants (RB, as %), total root dry matter (RDM, g m^{-2}), tap root diameter (TD, mm), fine root mass score (FRM), plant root disease score of infected plants (PRDS), lateral root number at branch-rooted plants (LRN, pcs $plant^{-1}$), dry matter yield (DMY, t ha^{-1}) and compressed stand height (CH, cm).

		PD	RPI	IP	RB	RDM	n	TD	FRM	n	PRDS	n	LRN	n	DMY	CH
	Control	259	81	52.1	70.4	215	12	6.47	3.32^{a}	172	2.24	88	2.79	118	10.3	42.0^{a}
Treatment	Spring	329	94	51.5	64.6	208	12	6.38	3.60^{ab}	224	1.74	109	2.69	140	10.9	42.4^{a}
	Intensive	282	89	54.3	67.8	214	12	6.40	3.64^{b}	188	1.98	102	2.99	125	11.0	44.7^{b}
	P	0.170	0.528	0.880	0.994	0.970		0.919	**0.008**		0.105*		0.549		0.366	**<0.001**
Year	2017	441^{c}	101	19.3^{a}	66.8	263^{b}	12	5.73	3.45^{b}	188	1.49a	34	3.35	119	–	–
	2018	266^{b}	85	65.4^{b}	70.0	224^{ab}	12	6.09	3.82^{c}	234	1.90a	146	2.83	157	11.4^{b}	44.7^{b}
	2019	163^{a}	77	73.2^{b}	66.0	148^{a}	12	7.44	3.29^{a}	162	2.57b	119	2.29	107	10.1^{a}	41.4^{a}
P		**<0.001**	0.108	**<0.001**	0.151	**0.003**		0.205	**<0.001**		**<0.001***		0.098		**0.006**	**<0.001**
Cut		-	-	-	-	-		-	-		-		-		-	**<0.001**
Year × treatment		**0.043**	0.303	0.694	0.715	0.996		**0.011**	0.942		-		0.666		0.866	0.986
Density (covariate)		-	–	–	**0.038**	-		**0.163**	0.007		-		**0.026**			

P: F - test probability of three-way (year, treatment, block) or four-way (year, treatment, block, cut) GLM including year × treatment interaction (significant values are in bold), different letters indicate statistical differences between treatments or years according to Tukey HSD test at $p < 0.05$.
* Kruskal - Wallis ANOVA with differences according to multiple comparisons of mean ranks.

TABLE 5 Effect of treatment and third and fourth harvest year for Site 3 (Drválovice) on lucerne plant density (PD, plant m^{-2}), root potential index (RPI), ratio of infected plants (IP, as %), ratio of branch-rooted plants (RB, as %), total root dry matter (RDM, g m^{-2}), tap root diameter (TD, mm), fine root mass score (FRM), plant root disease score of infected plants (PRDS), lateral root number at branch-rooted plants (LRN, pcs $plant^{-1}$), dry matter yield (DMY, t ha^{-1}) and compressed stand height (CH, cm).

		PD	RPI	IP	RB	RDM	n	TD	FRM	n	PRDS	n	LRN	n	DMY	CH
	Control	156	126	73.2	82.1	349	8	10.71	3.25	117	2.26	84	2.71	94	10.5	64.3^{a}
Treatment	Autumn	157	135	65.4	75.2	370	8	10.58	3.08	128	2.71	78	2.63	91	10.4	65.0^{b}
	P	0.973	0.509	0.469	0.113	0.608		0.795	0.331		0.051		0.731		0.937	**0.015**
Year	2019	196^{b}	134	67.0	77.6	351	8	10.15	3.30	112	2.05^{a}	74	3.08	86	11.1^{b}	58.9^{a}
	2020	116^{a}	127	71.6	79.7	369	8	10.36	3.03	133	2.91^{b}	88	2.05	99	9.8^{a}	70.4^{b}
Year		**0.011**	0.589	0.660	0.242	0.685		0.990	0.532		**<0.001**		0.072		**<0.001**	**<0.001**
Cut		–	–	–	–	–		–	–		–	–	–		–	**<0.001**
Year × treatment		0.182	0.529	0.196	**0.004**	0.647		0.168	0.265		-		0.155		0.855	0.447
Density (covariate)		-	–	–	0.055	–		**<0.001**	0.494		-		**0.008**		-	-

P: F - test probability of three-way (year, treatment, block) or four-way (year, treatment, block, cut) GLM including year × treatment interaction (significant values are in bold), different letters indicate statistical differences between treatments or years according to Tukey HSD test at $p < 0.05$.

years, there were some differences among locations. At Site 1 there was no significant decrease in plant density and this site had the lowest proportion of infected plants (average 30%). For the other two sites, tap root diameter increased over time but changes were not significant. The proportion of infected plants associated with root disease score reached values of around 70% in the last two years.

Results of qPCR detected the pathogens *Fusarium avenaceum*, *F. oxysporum*, and *Verticillium albo-atrum* in all sites and the average percentages of positive detections across sites within each treatment were 39, 19 and 13% for non-treated control, autumn and intensive treatment, respectively.

Relationships between root-branching classes, fine root score, tap root diameter, lateral root number, ratio of infected plants and plant disease score are presented in Table 6. Increasing the number of plant lateral roots simultaneously increased tap-root diameter, fine root mass, and proportion of infected plants. Higher fine root score resulted in linear increases in tap-root diameter whereas plant root disease score was improved for plants with fine roots.

Forage yield and canopy traits

In the seeding year, annual forage yield ranged from 2 t ha^{-1} for one-cut regime (at Sites 1 and 3) to 6.4 t ha^{-1} for three-cut regime (at Site 2) although no significant differences between treatments were detected (data not shown). Therefore, Tables 4–6 present only the stand height and yield results from the different harvest years. At Site 1 the forage yield averaged across harvest years was significantly reduced under both of the Polyversum treatments in comparison with the non-treated control. The results for forage yield also corresponded with differences in compressed stand height, with significantly lower values for both Polyversum treatments. In the driest year of the evaluation period (2018) values for forage yield and stand height

TABLE 6 Effect of root branching (RBC) and fine root mass (FRM) class on taproot diameter (TD), fine root mass score (FRM), ratio of infected plants (IP, as %), plant root disease score (PRDS) and lateral root number (LRN) measured as individual plants averaged across all locations and years.

RBC	LRN	TD	FRM	IP	n	PRDS	n	FRM class	TD	IP	n	PRDS	n
0	0	5.87^{a}	2.86^{a}	37.18^{a}	676	2.42^{b}	259	1	5.96^{a}	46.36	144	3.39^{b}	77
1	1 - 2	7.08^{b}	3.20^{b}	43.53^{b}	797	1.90^{a}	367	2	6.90^{ab}	43.77	336	2.27^{a}	150
2	3 - 4	8.63^{c}	3.35^{b}	49.78^{b}	325	2.17^{ab}	167	3	7.03^{a}	44.86	707	2.04^{a}	308
3	≥5	10.91^{d}	3.81^{c}	63.74^{c}	160	2.13^{ab}	110	4	7.40^{b}	41.59	455	1.94^{a}	201
								5	8.52^{c}	44.41	316	1.89^{a}	167
	P	**<0.001**	**<0.001**	**<0.001**		**<0.001***			**<0.001**	0.783		**<0.001***	
Year	*P*	**<0.001**	**<0.001**	**<0.001**		**<0.001***			**<0.001**	**<0.001**		**<0.001***	
Linear effects		**0.43**	**0.19**	**0.16**		**0.09**			**0.19**	0.01		**-0.11**	

Linear effects represent Pearson correlation coefficients between LRN or FRM class and root traits with values significant at $p < 0.05$ in bold.
P: F – test probability; two-way ANOVA (year, branching class); different letters indicate statistical differences between classes.
* Kruskal - Wallis ANOVA with differences according to multiple comparisons of mean ranks.

were lower than in other years. For Sites 2 and 3 no differences in forage yield were detected but the intensive Polyversum treatment at Site 2 and the autumn treatment at Site 3 provided significantly higher values for lucerne stand height.

Discussion

Development of root traits in relation to biological control, year, and fine root score

Application of *P. oligandrum*, when applied in both the autumn and intensive schedules in the present study, showed no effects on lucerne root disease score when attacked by *Fusarium* and *Verticillium*. In several other studies, positive responses to *P. oligandrum* in terms of root health of crops were observed (Pharand et al., 2002; Gerbore et al., 2014; Ouhaibi-Ben et al., 2021). Among other root traits, only the fine root-mass score was improved under the intensive treatment at Site 2, Jevíčko. These results are in contrast to those for application of *P. oligandrum* to red clover, where the same treatments were found to support root branching and reduce the plant disease score in the second harvest year (Pisarčik et al., 2020) or they resulted in increased total root dry mass and root potential index across years with drought stress, and with simultaneous improvement of plant disease score in the case of autumn treatment (Pisarčik et al., 2021). The different responses of red clover and lucerne may be explained, at least partly, by differences in the aridity of the climate at the experimental sites. The total annual precipitation for the location of the red clover site of Pisarčik et al. (2021) (at Větrov, Czechia) was always over 530 mm (range 538 - 701 mm), despite some drought periods, and the annual temperature range was 8.2 - 9.4°C. In the present study, the location of Site 1 (Červený Újezd) had annual precipitation below 500 mm in all years of evaluation (334 - 492 mm) with annual mean temperatures in the range 9.5 - 10.4°C. At the more humid location of Jevíčko (Site 2) with alluvial soil and rainfall over 500 mm (except in 2018) there was a positive effect of *P. oligandrum* on the fine-root score under the intensive treatment. In Drválovice (Site 3 in the present study) with loamy-sandy soil, Pisarčik et al. (2019) observed at this same location an increased proportion of infected lucerne plants after spring *P. oligandrum* application, but only for the relatively dry year of 2018 (401 mm and 9.6°C). In two subsequent years rainfall was 574 and 722 mm and no negative effects were observed. These results suggest that responses to *P. oligandrum* application depend on the combined environmental effects of soil and weather, rather than on differences in the responses by lucerne and red clover.

Root development over successive years of the experiments followed general patterns observed previously, including increase in tap-root diameter or root branching with plant age (Lamb et al., 1999). The negative effect of drought on root development was visible especially for Site 1, at the driest location of Červený Újezd, where tap-root increase was strongly reduced with a final value of around 7 mm. This contrasts with the 12 mm reported by Hakl et al. (2017) for comparable plant age at the same location. Effect of the dry year 2018 on tap-root diameter was also obvious at Jevíčko and Drválovice (Sites 2 and 3) (Pisarčik et al., 2019). It demonstrates that the severe drought stress that occurred during this experiment could be considered as a significant factor in not only reducing forage yield and the potential for a biological control effect, but also in terms of its impact on development of root traits and their subsequent agronomic stand performance, in line with Hakl et al. (2021).

The positive impact of higher fine-root score on root disease resistance, as presented in Table 6, generally supports a pattern about existing relationships between root traits and disease infection. Similar positive effects of fine-root mass on root disease score were observed for red clover by Pisarčik et al. (2020), and Lamb et al. (2000) reported improved Fusarium wilt resistance for a lucerne population selected for fibrous root mass, together with increased forage yield. According to Hakl et al. (2017), a higher value for lateral root number was positively correlated with higher disease score of lucerne plants, although results from the present study show that this phenomenon is related more to an increasing proportion of infected plants than to a higher root disease score of the infected plants. It seems that the presence of fine roots has a positive role here, which was associated mainly with improved disease score of infected plants. However, it should be remembered that although this trait could be effective for selection (Lamb et al., 2000), fine root mass and lateral root number are correlated with each other (Lamb et al., 1999) and there are also a number of seasonal patterns affecting the presence of fine roots, such as soil temperature and carbohydrate supply (Luo et al., 1995).

Effect of *Pythium oligandrum* on forage yield in association with root morphology

Across the three experiments with lucerne reported here, our results showed that application of *P. oligandrum* did not provide a positive yield response, and that at the warmest and driest location the forage yield was even slightly reduced (by 6%) together with reduced stand height. In more humid environments, a positive effect of either the intensive or autumn application on stand height was observed but this advantage was not realised in any significant forage yield improvement. The positive effect is consistent with the beneficial effects of root colonization by *P. oligandrum* on crop growth promotion as described by Benhamou et al. (2012) or Gerbore et al. (2014). In line with Pisarčik et al. (2021), the

greater stand height could not be attributed fully to the improved root traits at Site 2 (Jevíčko), because greater stand height was observed also at Site 3 (Drválovice) where there was no effect on roots. We may conclude, therefore, that the observed positive effect of *P. oligandrum* on lucerne forage growth was not related to root traits. The efficacy of *P. oligandrum* was driven by environmental conditions, in which colder and more humid conditions promote a positive response when recorded in the field. This further emphasises the importance of temperature and other aspects of weather during the growing season on the activity and efficiency of *P. oligandrum* (Boček et al., 2012; Baturo-Cieśniewska et al., 2018).

Apart from the effect of humidity on *P. oligandrum* activity, some negative effects of biological control on crop biomass accumulation in early stages of growth have been reported (McGehee et al., 2019), in which there was a negative effect on crop roots and aboveground biomass especially when the pathogen was not inoculated along with biological control. This could also be relevant in the present study, where there was a negative effect of *P. oligandrum* at the location with the lowest ratio of infected plants, whereas some positive effects (on fine root mass score, stand height) were observed in both locations with the proportion of infected plants around 70%. In previous work, a positive response of red clover was also reported under high pressure of root diseases, where about 90% of plants were positively scored for root discoloration in the last year of the field experiments (2021; Pisarčik et al., 2020). However, the effect of higher plant infection cannot be easily separated from the temperature-precipitation relationship. Nevertheless, we can speculate that reduced attack by soil pathogens could also have some association with the observed negative effects on lucerne stand height and yield performance.

Results of two independent field experiments with red clover suggest that the stimulation effect of *P. oligandrum* on stand height played a more important role in increased vegetative biomass yield than through a direct protection against fungal diseases or root traits improvement (2021; Pisarčik et al., 2020). The results for lucerne reported here are in line with those previous findings, as autumn or spring + autumn applications of *P. oligandrum* per year were associated with increased stand height without any response in the ratio of infected plants and root disease score. However, either a single autumn, or two applications, were not sufficient for significant yield enhancement, and the single spring application did not provide any significant effect, in line with the suggestion of Pisarčik et al. (2021) about the need to optimize the application timing over the second half of the growing season. An important result here could be a negative lucerne yield response on this potential stimulation under the relatively dry environment. Pisarčik et al. (2021) considered that the stimulation of red clover is related to the ability of *P. oligandrum* to synthesize tryptamine in direct interaction with plant roots, and root absorption of this newly formed auxin-compound in appropriate concentrations has been associated with enhancement of plant growth, in line with Le Floch et al. (2003) or Binyamin et al. (2019). Although auxins stimulate plant growth and also could be beneficial for plant defence to drought stress (Zhang et al., 2012; Liu et al., 2014; Korver et al., 2018) it must be remembered that sustaining growth under unfavourable conditions could be detrimental (Dubois et al., 2018). *Pythium oligandrum* also activates the plant defence system through production of oligandrin and the cell-wall protein fraction which appear to be closely involved in activation of the jasmonic acid and ethylene dependent signalling pathways (Benhamou et al., 2012). Ethylene has an important role in regulation of organ growth and yield under abiotic stress (Dubois et al., 2018) therefore its imbalance could be also responsible for reduced lucerne growth and yield. This field-based study clearly demonstrated that application of *P. oligandrum* under drought stress did not support lucerne root development and it may even affect forage production negatively, probably due to the imbalance between auxins and ethylene.

These relationships between the legume plant and *P. oligandrum* can also be largely influenced by the total plant microbiome, where plant–microbiome interactions are significant determinant for plant growth, fitness and productivity (Gupta et al., 2021). Understanding the plant microbiome interactions within the microbial community can contribute to hypotheses about why biological control is inconsistent in promoting or reducing crop growth (Berendsen et al., 2012) Understanding the mechanisms linked to the positive effects of beneficial fungi is also essential for achieving favourable outcomes and development of novel strategies (Ghorbanpour et al., 2018). In field conditions, these relationships are further complicated by interactions with environment, where results of biological control of crop diseases are more variable in comparison with the controlled conditions of glasshouse or laboratory studies (Boček et al., 2012; Pisarčik et al., 2019).

It can be summarized that under the relatively dry climate with mean temperature close 10°C and annual total precipitation below 500 mm, there was reduced potential of *P. oligandrum* for improvement of lucerne root traits, disease score or forage yield and where even a negative effect on crop growth has been observed. This negative response could be probably associated with inappropriate stimulation or disturbance of the balance between auxins and ethylene, and which seems to be mitigated on deep, more humid soils. Under conditions with annual precipitation over 500 mm, the positive impact on fine root

mass score and stand height was observed for the autumn and intensive treatments but this advantage was not realised in significantly increased yield. Therefore, we conclude that although there is some potential for *P. oligandrum* for lucerne productivity improvement, this is most likely to be realised only under conditions of relatively humid environments or under irrigation, where higher root disease infestation by *Fusarium* or *Verticilium* may also be expected, and as found previously for red clover, more applications per year will be needed for forage yield improvement. Further research is also needed in plant-microbiome interactions in association with biological control agents which could be essential for development of effective strategies of crop biological control.

Data availability statement

The raw data supporting the conclusions of this article will be made available by the authors, without undue reservation.

Author contributions

MP: writing-original draft, data analysis, preparation, writing-review and editing. JH: conceptualization, investigation, writing-original draft, supervising, editing OS: investigation, writing-review PN: editing. All authors contributed to the article and approved the submitted version.

Funding

This research was supported by project TJ01000150 of Technology Agency of the Czech Republic and the Ministry of Agriculture of the Czech Republic CZE MZe RO 0418. The completion of the paper was supported by "S" grant of MŠMT ČR.

Acknowledgments

We sincerely thank Pavel Cihlář and Jaroslav Tomášek for field assistance.

Conflict of interest

The authors declare that the research was conducted in the absence of any commercial or financial relationships that could be construed as a potential conflict of interest.

Publisher's note

References

Öhberg, H., and Bang, U. (2010). Biological control of clover rot on red clover by *Coniothyrium minitans* under natural and controlled climatic conditions. *Biocontrol Sci. Technol.* 20 (1), 25–36. doi: 10.1080/09583150903337805

Abbas, A., Mubeen, M., Sohail, M. A., Solanki, M. K., Hussain, B., Nosheen, S., et al. (2022). Root rot a silent alfalfa killer in China: Distribution, fungal, and oomycete pathogens, impact of climatic factors and its management. *Front. Microbiol.* 13, 961794. doi: 10.3389/fmicb.2022.961794

Ahemad, M., and Khan, M. S. (2013). Pesticides as antagonists of rhizobia and the legume-rhizobium symbiosis: a paradigmatic and mechanistic outlook. *Biochem. Mol. Biol.* 1, 63–75. doi: 10.12966/bmb.12.02.2013

Baker, B. P., Green, T. A., and Loker, A. J. (2020). Biological control and integrated pest management in organic and conventional systems. *Biol. Control* 140, 104095. doi: 10.1016/j.biocontrol.2019.104095

Baturo-Cieśniewska, A., Łukanowski, A., Koczwara, K., and Lenc, L. (2018). Development of sclerotinia sclerotiorum (Lib.) de bary on stored carrot treated with pythium oligandrum drechsler determined by qPCR assay. *Acta Sci. Pol. Hortorum Cultus* 17 (5), 111–121. doi: 10.24326/asphc.2018.5.10

Bělonožníková, K., Vaverová, K., Vaněk, T., Kolařík, M., Hýsková, V., Vaňková, R., et al. (2020). Novel insights into the effect of pythium strains on rapeseed metabolism. *Microorganisms* 8 (10), 1472. doi: 10.3390/microorganisms8101472

Benhamou, N., Rey, P., Picard, K., and Tirilly, Y. (1999). Ultrastructural and cytochemical aspects of the interaction between the mycoparasite Pythium oligandrum and soilborne plant pathogens. *Phytopathology* 89 (6), 506–517.

Benhamou, N., leFloch, G., Vallance, J., Gerbore, J., Grizard, D., and Rey, P. (2012). *Pythium oligandrum*: an example of opportunistic access. *Microbiology* 158 (11), 2679–2694. doi: 10.1099/mic.0.061457-0

Berendsen, R. L., Pieterse, C. M., and Bakker, P. A. (2012). The rhizosphere microbiome and plant health. *Trends Plant Sci.* 17 (8), 478–486. doi: 10.1016/j.tplants.2012.04.001

Binyamin, R., Nadeem, S. M., Akhtar, S., Khan, M. Y., and Anjum, R. (2019). Beneficial and pathogenic plant-microbe interactions: A review. *Soil Environ.* 38 (2), 11–33. doi: 10.25252/SE/19/71659

Boček, S., Salaš, P., Sasková, H., and Mokričková, J. (2012). Effect of alginure (seaweed extract), myco-sin VIN (sulfuric clay) and polyversum (*Pythium oligandrum* drechs.) on yield and disease control in organic strawberries. *Acta Univ. Agric. Silviculturae Mendelianae Brunensis* 8, 19–28. doi: 10.11118/actaun201260080019

Campbell, R. (1994). Biological control of soil-borne diseases: some present problems and different approaches. *Crop Prot.* 13 (1), 4–13. doi: 10.1016/0261-2194(94)90129-5

Dubois, M., Van den Broeck, L., and Inzé, D. (2018). The pivotal role of ethylene in plant growth. *Trends Plant Sci.* 23 (4), 311–323. doi: 10.1016/j.tplants.2018.01.003

Georgieva, N., Nikolova, I., and Delchev, G. (2020). Response of spring vetch (Vicia sativa l.) to organic production conditions. *Bulg. J. Agric. Sci.* 26 (3), 520–526.

Gerbore, J., Benhamou, N., Vallance, J., leFloch, G., Grizard, D., Regnault-Roger, C., et al. (2014). Biological control of plant pathogens: Advantages and limitations seen through the case study of *Pythium oligandrum*. *Environ. Sci. pollut. Res.* 21 (7), 4847–4860. doi: 10.1007/s11356-013-1807-6

Ghorbanpour, M., Omidvari, M., Abbaszadeh-Dahaji, P., Omidvar, R., and Kariman, K. (2018). Mechanisms underlying the protective effects of beneficial

fungi against plant diseases. *Biol. Control* 117, 147–157. doi: 10.1016/j.biocontrol.2017.11.006

Gray, F. A., and Koch, D. W. (2004). Influence of late season harvesting, fall grazing, and fungicide treatment on verticillium wilt incidence, plant density, and forage yield of alfalfa. *Plant Dis.* 88 (8), 811–816. doi: 10.1094/PDIS.2004.88.8.811

Gupta, R., Anand, G., Gaur, R., and Yadav, D. (2021). Plant–microbiome interactions for sustainable agriculture: a review. *Physiol. Mol. Biol. Plants* 27 (1), 165–179. doi: 10.1007/s12298-021-00927-1

Haegi, A., Catalano, V., Luongo, L., Vitale, S., Scotton, M., Ficcadenti, N., et al. (2013). A newly developed real-time PCR assay for detection and quantification of fusarium oxysporum and its use in compatible and incompatible interactions with grafted melon genotypes. *Phytopathology* 103 (8), 802–810. doi: 10.1094/PHYTO-11-12-0293-R

Hakl, J., Hrevušová, Z., Hejcman, M., and Fuksa, P. (2012). The use of a rising plate meter to evaluate lucerne (*Medicago sativa* l.) height as an important agronomic trait enabling yield estimation. *Grass Forage Sci.* 67 (4), 589–596. doi: 10.1111/j.1365-2494.2012.00886.x

Hakl, J., Pisarčik, M., Fuksa, P., and Šantrůček, J. (2021). Potential of lucerne sowing rate to influence root development and its implications for field stand productivity. *Grass Forage Sci.* 76 (3), 378–389. doi: 10.1111/gfs.12546

Hakl, J., Pisarčik, M., Hrevušová, Z., and Šantrůček, J. (2017). In-field lucerne root morphology traits over time in relation to forage yield, plant density, and root disease under two cutting managements. *Field Crops Res.* 213, 109–117. doi: 10.1016/j.fcr.2017.07.017

Handelsman, J., Raffel, S., Mester, E. H., Wunderlich, L., and Grau, C. R. (1990). Biological control of damping-off of alfalfa seedlings with bacillus cereus UW85. *Appl. Environ. Microbiol.* 56 (3), 713–718. doi: 10.1128/aem.56.3.713-718.1990

Hwang, S. F., Gossen, B. D., Turnbull, G. D., Chang, K. F., and Howard, R. J. (2002). Seedbed preparation, timing of seeding, fertility and root pathogens affect establishment and yield of alfalfa. *Can. J. Plant Sci.* 82 (2), 371–381. doi: 10.4141/P01-121

Jenkyn, J. F. (1975). The effect of benomyl sprays on sclerotinia trifoliorum and yield of red clover. *Ann. Appl. Biol.* 81 (3), 419–423. doi: 10.1111/j.1744-7348.1975.tb01660.x

Jones, C. R., and Samac, D. A. (1996). Biological control of fungi causing alfalfa seedling damping off with a disease-suppressive strain of streptomyces. *Biol. Control* 7 (2), 196–204. doi: 10.1006/bcon.1996.0084

Korver, R. A., Koevoets, I. T., and Testerink, C. (2018). Out of shape during stress: a key role for auxin. *Trends Plant Sci.* 23 (9), 783–793. doi: 10.1016/j.tplants.2018.05.011

Lamb, J. F. S., Barnes, D. K., and Henjum, K. I. (1999). Gain from two cycles of divergent selection for root morphology in alfalfa. *Crop Sci.* 39 (4), 1026–1035. doi: 10.2135/cropsci1999.0011183X003900040011x

Lamb, J. F. S., Samac, N. A., Barnes, D. K., and Henjum, K. I. (2000). Increased herbage yield in alfalfa associated with selection fibrous and lateral roots. *Crop Sci.* 40 (3), 693–699. doi: 10.2135/cropsci2000.403693x

Larkin, R. P., English, J. T., and Mihail, J. D. (1995). Effects of infection by pythium spp. on root system morphology of alfalfa seedlings. *Phytopathology* 85 (4), 430–435. doi: 10.1094/Phyto-85-430

Larkin, R. R., English, J. T., and Mihail, J. D. (1996). The relationship of infection by pythium spp. to root system morphology of alfalfa seedlings in the field. *Plant Dis.* 80, 281–285. doi: 10.1094/PD-80-0281

Leath, K. T., Zeiders, K. E., and Byers, R. A. (1973). Increased yield and persistence of red clover after a soil drench application of benomyl 1. *Agron. J.* 65 (6), 1008–1010. doi: 10.2134/agronj1973.00021962006500060052x

Le Floch, G., Rey, P., Benizri, E., Benhamou, N., and Tirilly, Y. (2003). Impact of auxin-compounds produced by the antagonistic fungus *Pythium oligandrum* or the minor pathogen pythium group f on plant growth. *Plant Soil* 257 (2), 459–470. doi: 10.1023/A:1027330024834

Liu, L., Guo, G., Wang, Z., Ji, H., Mu, F., and Li, X. (2014). "Auxin in plant growth and stress responses," in *Phytohormones: A window to metabolism, signaling and biotechnological applications*. (New York, NY: Springer). 1–35.

Luo, Y., Meyerhoff, P. A., and Loomis, R. S. (1995). Seasonal patterns and vertical distributions of fine roots of alfalfa (*Medicago sativa* l.). *Field Crops Res.* 40 (2), 119–127. doi: 10.1016/0378-4290(94)00090-Y

Maurer, K. A., Radišek, S., Berg, G., and Seefelder, S. (2013). Real-time PCR assay to detect verticillium albo-atrum and v. dahliae in hops: development and comparison with a standard PCR method. *J. Plant Dis. Prot.* 120 (3), 105–114. doi: 10.1007/BF03356461

McGehee, C. S., Raudales, R. E., Elmer, W. H., and McAvoy, R. J. (2019). Efficacy of biofungicides against root rot and damping-off of microgreens caused by pythium spp. *Crop Prot.* 121, 96–102. doi: 10.1016/j.cropro.2018.12.007

McKenna, P., Cannon, N., and Conway, J. (2018). Soil mineral nitrogen availability predicted by herbage yield and disease resistance in red clover (Trifolium pratense) cropping. *Nutr. Cycl. Agroecosys.* 112 (3), 303–315. doi: 10.1007/s10705-018-9947-1

Miller-Garvin, J. E., and Viands, D. R. (1994). Selection for resistance to fusarium root rot, and associations among resistances to six diseases in alfalfa. *Crop Sci.* 34 (6), 1461–1465. doi: 10.2135/cropsci1994.0011183X003400060008x

Morsy, K. M., Abdel-Monaim, M. F., and Mazen, M. M. (2011). Use of abiotic and biotic inducers for controlling fungal diseases and improving growth of alfalfa. *World J. Agric. Sci.* 7 (5), 566–576.

Nan, Z. B., Skipp, R. A., and Long, P. G. (1991). Use of fungicides to assess the effects of root disease: effects of prochloraz on red clover and microbial populations in soil and roots. *Soil Biol. Biochem.* 23 (8), 743–750. doi: 10.1016/0038-0717(91)90144-9

Nikolova, I., Georgieva, N., and Naydenova, Y. (2015). Forage quality in *Pisum sativum*, treated by biological and synthetic active compounds. *Plant Sci.* 52 (5), 94–98.

O'Brien, P. A. (2017). Biological control of plant diseases. *Australas. Plant Pathol.* 46 (4), 293–304. doi: 10.1007/s13313-017-0481-4

Ouhaibi-Ben, A. N., Vallance, J., Gerbore, J., Yacoub, A., Daami-Remadi, M., and Rey, P. (2021). Combining potential oomycete and bacterial biocontrol agents as a tool to fight tomato rhizoctonia root rot. *Biol. Control* 155, 104521. doi: 10.1016/j.biocontrol.2020.104521

Pharand, B., Carisse, O., and Benhamou, N. (2002). Cytological aspects of compost-mediated induced resistance against fusarium crown and root rot in tomato. *Phytopathology* 92 (4), 424–438. doi: 10.1094/PHYTO.2002.92.4.424

Pisarčik, M., Hakl, J., and Hrevušová, Z. (2020). Effect of *Pythium oligandrum* and poly-beta-hydroxy butyric acid application on root growth, forage yield and root diseases of red clover under field conditions. *Crop Prot.* 127, 104968. doi: 10.1016/j.cropro.2019.104968

Pisarčik, M., Hakl, J., Menšík, L., Szábo, O., and Nerušil, P. (2019). Biological control in lucerne crops can negatively affect the development of root morphology, forage yield and quality. *Plant Soil Environ.* 65 (10), 477–482. doi: 10.17221/398/2019-PSE

Pisarčik, M., Hakl, J., Szabó, O., and Hrevušová, Z. (2021). Efficacy of variable timing of pythium oligandrum applications on red clover grown under field conditions. *Crop Prot.* 149, 105780. doi: 10.1016/j.cropro.2021.105780

Riday, H. (2010). Progress made in improving red clover (*Trifolium pratense* l.) through breeding. *Int. J. Plant Breed.* 4 (1), 22–29.

Sedman, J. N., Bastian, C. T., Held, L. J., Gray, F. A., and Koch, D. W. (2007). An economic analysis of alfalfa harvest methods when infested with verticillium wilt. *Agron. J.* 99 (6), 1635–1639. doi: 10.2134/agronj2007.0010

StatSoft, Inc (2012). *Statistica for windows* (Tulsa, USA: StatSoft).

Waalwijk, C., Heide, R. V. D., Vries, I. D., Lee, T. V. D., Schoen, C., Corainville, G. C. D., et al. (2004). "Quantitative detection of fusarium species in wheat using TaqMan," in *Molecular diversity and PCR-detection of toxigenic fusarium species and ochratoxigenic fungi* (Dordrecht: Springer), 481–494.

Xiao, K., Kinkel, L. L., and Samac, D. A. (2002). Biological control of phytophthora root rots on alfalfa and soybean with streptomyces. *Biol. Control* 23 (3), 285–295. doi: 10.1006/bcon.2001.1015

Yang, C., Hamel, C., Vujanovic, V., and Gan, Y. (2011). Fungicide: modes of action and possible impact on nontarget microorganisms. *Int. Sch. Res. Not.* 2011, 1–8. doi: 10.5402/2011/130289

You, X., Barraud, J., and Tojo, M. (2019). Suppressive effects of *Pythium oligandrum* on soybean damping off caused by *P. aphanidermatum* and *P. myriotylum*. *Annu. Rep. Kansai Plant Prot. Soc.* 61, 9–13. doi: 10.4165/kapps.61.9

Zhang, Q., Li, J., Zhang, W., Yan, S., Wang, R., Zhao, J., et al. (2012). The putative auxin efflux carrier OsPIN3t is involved in the drought stress response and drought tolerance. *Plant J.* 72 (5), 805–816. doi: 10.1111/j.1365-313X.2012.05121.x

frontiers | Frontiers in Plant Science

TYPE Original Research
PUBLISHED 08 December 2022
DOI 10.3389/fpls.2022.989517

OPEN ACCESS

EDITED BY
Marie-Laure Pilet-Nayel,
INRAE Bretagne Normandie, France

REVIEWED BY
Sabine Banniza,
University of Saskatchewan, Canada
Syama Chatterton,
Agriculture and Agri-Food Canada (AAFC), Canada

*CORRESPONDENCE
Suli Sun
sunsuli@caas.cn
Zhendong Zhu
zhuzhendong@caas.cn

†These authors have contributed equally to this work

SPECIALTY SECTION
This article was submitted to Plant Pathogen Interactions, a section of the journal Frontiers in Plant Science

RECEIVED 08 July 2022
ACCEPTED 09 November 2022
PUBLISHED 08 December 2022

CITATION
Long JC, Wu WQ, Sun SL, Shao Y, Duan CX, Guo YP and Zhu ZD (2022) *Berkeleyomyces rouxiae* is a causal agent of root rot complex on faba bean (*Vicia faba L.*). *Front. Plant Sci.* 13:989517. doi: 10.3389/fpls.2022.989517

Berkeleyomyces rouxiae is a causal agent of root rot complex on faba bean (*Vicia faba L.*)

Juechen Long[1,2†], Wenqi Wu[1†], Suli Sun[1*], Yang Shao[3], Canxing Duan[1], Yanping Guo[3] and Zhendong Zhu[1*]

[1]Institute of Crop Sciences, Chinese Academy of Agricultural Sciences, Beijing, China, [2]Institute of Specialty Crop, Chongqing Academy of Agricultural Sciences, Chongqing, China, [3]Linxia Institute of Agricultural Sciences, Linxia, Gansu, China

Faba bean (*Vicia faba* L.) is an important food and feed legume crop in the world. The root rot complex caused by various pathogens is a main constraint in faba bean production. In April 2021, a severe disease of faba bean with symptoms of black necrosis on roots occurred in experimental fields at the Linxia Institute of Agricultural Sciences, Gansu Province, China. This study aimed to identify the pathogen and evaluate the resistance of faba bean cultivars. The pathogen was isolated from infected soils, and five representative isolates were identified as *Berkeleyomyces rouxiae* based on morphological characteristics, pathogenicity, and molecular phylogenetic analyses. A host range test showed that chickpea, common bean, cowpea, mung bean, rice bean, lentil, and hyacinth bean were susceptible hosts of the faba bean isolate, whereas adzuki bean, pea, and soybean were non-susceptible hosts, and maize and wheat were non-hosts. Identification of resistance among 36 faba bean cultivars was carried out, and six cultivars were found to be moderately resistant to *B. rouxiae*. In this study, we first reported black root rot on faba bean caused by *B. rouxiae*, confirmed and expanded the host range of *B. rouxiae*, and identified resistant faba bean cultivars.

KEYWORDS

***Vicia faba* L., black root rot, *Thielaviopsis basicola*, host range, phylogenetic analysis**

Introduction

Faba bean (*Vicia faba* L.) is one of the earliest legumes to have been domesticated and ranks fourth in terms of cultivation area among the cool-season food legumes after pea, chickpea, and lentil in this world (Kaur et al., 2014). Faba bean seeds have a high protein content, are a good source of mineral nutrients, and also contain some bioactive

compounds (Etemadi et al., 2019). The fresh and dry seeds of the faba bean are used for human consumption, and the dry seeds and straw are also used in livestock feed (Karkanis et al., 2018). Faba bean contributes to the sustainability of cropping systems by fixing atmospheric nitrogen to improve soil fertility, which is often incorporated into various multi-crop and intercropping systems (Jensen et al., 2010; Li et al., 2017). China is a leading faba bean producer with an average planting area of 1.1 million ha and also is one of the largest consumers of faba bean (Ji et al., 2022). In China, the faba bean is mainly grown in the southwest region, Yangtze River basin, and northwest region (Li et al., 2017).

The productivity and quality of faba beans are often significantly reduced by biotic and abiotic stresses. Abiotic factors include frost, heat, waterlogging, and soil salinity and acidity, while biotic factors include diseases, insect pests, and weeds (Stoddard et al., 2010; Maalouf et al., 2018). More than 100 diseases of faba bean have been documented in the world (Yu, 1979; Kumari and Makkouk, 2007), and the number continues to increase (Afshari and Hemmati, 2017; Al-Shahwan et al., 2017; You et al., 2021). Among the diseases of faba bean, the root rot complex has been widely reported worldwide (Sillero et al., 2010). Many fungal and oomycete pathogens have been reported to cause root rot on faba beans, and major pathogens include *Aphanomyces euteiches*, *Fusarium* spp., *Macrophomina phaseolina*, *Pythium* spp., *Rhizoctonia solani* (Kraft et al., 1988; Rubiales and Khazaei, 2022).

Thielaviopsis basicola is a cosmopolitan soilborne plant pathogen that attacks more than 230 plant species and causes the disease known as black root rot, and the number of new hosts is increasing (Pereg, 2013; Nakane et al., 2019; Le et al., 2022; Rahnama et al., 2022). The disease is characterized by black necrosis on various parts of the host roots, which leads to stunting, reduced vigor, wilt, and yield loss (Noshad et al., 2006; Coumans et al., 2011). *T. basicola* has a complex taxonomic history and has been assigned different species names. Recently, Nel et al. (2018) performed a phylogenetic analysis using DNA sequence data of six different gene regions and showed that the isolates of *T. basicola* represent two distinct fungal species in the newly described genus *Berkeleyomyces*, *B. basicola* and *B. rouxiae*, which are morphologically indistinguishable but can be distinguished by molecular characterization (Crous et al., 2021; Cavalcante et al., 2022).

Severe root rot on faba bean has occurred in faba bean experimental fields for many years at the Linxia Institute of Agricultural Sciences, Gansu Province, China (35.62 N 103.199 E), which caused stunting, yellowing, premature defoliation, and plant death. However, the pathogens inciting root rot were unclear. In June 2021, several faba bean roots with a symptom of black necrotic lesions were collected from a faba bean field at this Institute. We examined some diseased root epidermal tissues under a microscope and found dark-colored and muriform chlamydospores similar to those of *T. basicola*. The objective of the current study was to confirm the identity of the pathogen causing black root rot on the faba bean using morphological characterization, pathogenicity test, and molecular phylogenetic analysis. In addition, we evaluated the resistance of faba bean cultivars by artificial inoculation.

Materials and methods

Isolation of pathogen

In June 2021, soil samples were collected from three experimental plots for faba bean breeding where severe root rot had occurred, and this field has been used for faba bean breeding for 3 years and in rotation with wheat. Three bulk soil samples (2 kg of soil at 5–20 cm depth) were taken from the root zone of plants with root rot. A greenhouse bioassay was used to bait the root rot pathogens from soils. The faba bean cultivar Qinghai 13 which was highly susceptible to root rot in the field was selected for the bioassay. The soil samples were passed through a 10-mesh sieve and filled into 500 mL paper cups with holes at the bottom to about 3/4 of the cup height. For each soil sample, three replicate cups were prepared. Each cup was sown with 5 seeds and watered to saturation. The seeds were also sown in rough vermiculite as controls. The planted cups were kept on a rack in a glasshouse at 22-25°C with natural sunlight and watered as needed. Four weeks after sowing, plants were removed and roots were carefully washed free of soil. Epidermal tissues of black necrotic roots were examined under a microscope, and the diseased root tissues with chlamydospores typical for *T. basicola* were used for pathogen isolation using carrot discs (Nel et al., 2019). The diseased lateral roots were excised into 0.5 cm segments and placed on fresh carrot discs in Petri dishes with three layers of moistened filter paper, which were sealed with parafilm and incubated at 25°C. After 7 days, endoconidia were picked from diseased carrot discs with a sterile scalpel for confirmation using a microscope and then diluted to 50 spores/ml in sterile water. Then, 100 µl spore suspension was evenly spread on the 90 mm potato-dextrose agar (PDA; AoBoXing, Biotech, Beijing, China) plates with 25 ug/ml chloramphenicol. The plates were incubated at 25°C for two days, and single colonies were individually transferred to the new PDA plates. Pure single-spore isolates were stored at -80°C on PDA for future use.

Morphological identification

Five representative isolates (LXBR1 to LXBR5) were selected to determine their identity. The isolates were grown on PDA plates to assess colony characteristics at 25°C. Seven days after incubation, endoconidia, chlamydospores, and phialides were

observed and measured under a microscope (Olympus CX 31). Fifty arbitrarily selected structures were measured.

Pathogenicity and host range tests

The pathogenicity of five representative isolates was tested on the faba bean cultivar Qinghai 13. The inoculum of each isolate was prepared by placing several mycelial plugs (5 mm in diameter) into 100 mL potato dextrose broth, which was incubated for 4 days in an incubation shaker (100 rpm) at 25° C in darkness. The endoconidia suspension was then filtered and adjusted to a final concentration of 1.0×10^7 spores/mL to inoculate faba bean seedlings.

Five seeds were planted in each paper cup (500 mL) filled with fresh vermiculite. The planted cups were placed in the greenhouse for 3 weeks at 22–25°C. The seedlings were uprooted and the roots were washed thoroughly under running tap water, then the roots were soaked in the conidia suspension for 10 minutes, and finally, the seedlings were transplanted into a new cup. There were three replications per isolate, each replicate consisted of three cups, each cup containing three plants, arranged in a completely randomized design (CRD). Plants soaked in sterile water served as the control. The inoculated plants and controls were maintained in a greenhouse at 22–25°C with natural sunlight. The symptoms were investigated 2 weeks after inoculation. The chlamydospores were observed in inoculated roots under the microscope. The pathogen was re-isolated, and the morphology and molecular characteristics of pathogens were identified. The test was repeated twice.

The crops in the host range test included ten legume and two grass crops, namely common bean (*Phaseolus vulgaris* cvs. Biyun 6, Longyundou 29), pea (*Pisum sativum* cvs. Longwan7, Zhongqin 1), chickpea (*Cicer arietinum* cvs. Xinying 1, Xinying 2), cowpea (*Vigna unguiculata* cvs. Liaojiang1, Guijiang 18-11), mung bean (*Vigna radiata* cvs. Elv 1, Zhenglv 8), adzuki bean (*Vigna angularis*; cvs. Jinxiaodou 5, Yuhong 2), rice bean (*Vigna umbellata* cvs. Fandou 1, Hongfandou), lentil (*Lens culinaris* cvs. Yingguozhonglv, Faguo), hyacinth bean (*Lablab purpureus*; cvs. Jiaoda yanhong, Biandou 1), soybean (*Glycine max* cvs. Williams, Zhonghuang13), wheat (*Triticum aestivum* cvs. 197, 198), and maize (*Zea mays* cvs. Zhongdan 1168, Dongdan 6688). LXBR1 was used in this experiment, and the inoculation procedure was the same as in the pathogenicity test. The host range test was arranged in a randomized complete block design (RCBD) with 3 replicate blocks and 3 plants were inoculated in each replicate. The pathogenicity of the isolate was evaluated by investigating the crop symptoms and chlamydospore production on the roots 2 weeks post-inoculation. Typical symptoms and chlamydospores were observed in all three replicates, denoted by "+", otherwise by "-". The test was performed twice.

Molecular phylogenetic analyses

Genomic DNA from the five isolates was extracted from mycelium using the Fungi Genomic DNA Extraction Kit (Solarbio, Beijing, China) following the manufacturer's instructions. The partial sequence of the internal transcribed spacers (ITS), the ribosomal large subunit (LSU), the minichromosome maintenance complex component 7 (*MCM7*), and the 60S ribosomal protein RPL10 (60S) genes were amplified with primer pairs ITS1/ITS4 (White et al., 1990), LR0R/LR5 (Vilgalys and Hester, 1990), MCM7-for/MCM7-rev de Beer et al., 2014), and 60S-506F/60S-908R (Stielow et al., 2015), respectively. PCR was performed in a final volume of 25 µl containing 9.5 µl water, 1 µl DNA template, 1 µl each primer, and 12.5 µl GoTaq Master Mix PCR (Promega). The amplification cycles were performed by initial denaturation at 94°C for 5 min, followed by 35 cycles of denaturation at 94°C for 30 s, annealing at 56°C (ITS), 53°C (LSU), 58°C (*MCM7*) or 54°C (60S) for 45 s and extension at 72°C for 2 min; and a final extension at 72°C for 7 min. The amplified PCR products were purified and sent to Sangon Biotech (Shanghai) Co., Ltd. for sequencing, using the aforementioned primers.

The resulting sequences were blasted in the National Center for Biotechnology Information (NCBI) Database (http://www.ncbi.nlm.nih.gov) after splicing. The sequences of *B. rouxiae* strains and some related species (Nakane et al., 2019; Le et al., 2022) were obtained from the GenBank. The phylogenetic trees for tandem sequences of ITS, LSU, *MCM7*, 60S and a phylogenetic tree for *MCM7* were constructed using the Maximum likelihood method and the Tamura-Nei distance model in MEGA 11 with 1000 bootstrap repeats (Kumar et al., 2016).

Evaluation of faba bean cultivars for resistance

Thirty-six faba bean cultivars were evaluated for resistance by inoculating with isolate LXBR1. The inoculation procedure was the same as for the pathogenicity test. The experiment was arranged in a RCBD with three replicate blocks, one plastic tray was considered as a block. and each cultivar was randomly assigned to a cup within each plastic tray. The disease severity of each cultivar was investigated 2 weeks after inoculation, and evaluated with a 0 to 5 scale using the criterion of Bodker et al. (1993) as follows: 0 = no symptoms; 1 = 1-10% root or epicotyl area with disease symptoms; 2 = 11-30%; 3 = 31-60%; 4 = 61-90%; and 5 = 91-100%. The disease index (DI) was used to evaluate the resistance of each cultivar. DI was calculated using the following formula: $(DI) = (\sum (n \times s)/(N \times 5)) \times 100$, where s is the score of the disease severity, n is the number of plants at that score, and N is the total number of plants tested. The resistance was classified based on DI: highly resistant (HR, 0 <

DI ≤ 15), resistant (R, 15 < DI ≤ 35), moderately resistant (MR, 35 < DI ≤ 55), susceptible (S, 55 < DI ≤ 75), and highly susceptible (HS, 75 < DI).

The repeated trials were combined for analysis after homogeneity test for variance, and blocks nested within trials were considered as a random component in the mixed model. Square root transformation was carried out for data normalization. Data were used for analyzed using the General Linear Model procedure in SPSS 22.0, Fisher's least significant difference (LSD) was used for the means comparison. The Anaylsis of Variance (ANOVA) was used to determine any difference in resistance to *B. rouxiae* between cultivars.

Result

Isolation and morphological identification

Four weeks after faba bean seeds were sown in soil samples, the faba bean seedlings were dwarfed compared to the controls, and severe black necrosis occurred on the roots, while the controls remained healthy (Figure 1A). Abundant chlamydospores typical of *T. basicola* were observed in the epidermal tissues under the microscope (Figure 1B). Seven days after inoculating disease root segments on the carrot discs, many gray hyphae were growing on the discs (Figure 1C), and abundant endoconidia were observed under the microscope (Figure 1D). Single-spore isolates were obtained by the spore-dilution technique. The colonies of isolates on PDA were initially white, and later the center turned olive green to black following the development of chlamydospores (Figure 2A). The average growth rate of isolates on PDA at 25°C was 4 mm/day. Two types of asexual spores, chlamydospores and endoconidia, were produced by the isolates. The chlamydospores were produced in chains containing 3-5 cells (Figures 2C, D), dark brown, and 5.6-10.2 µm × 8.6-12.9 µm in size. The endoconidia were hyaline, cylindrical in shape, and produced from phialides, which measured 10.49-25.10 µm × 4.41-6.10 µm in size, and the phialide were measured 5.8-8.2 µm × 112.3-226.7 µm in size (Figures 2B, E). The colony characteristics, chlamydospores, and endoconidia size of the isolates were similar to those of *B. rouxiae* (Nakane et al., 2019; Le et al., 2022).

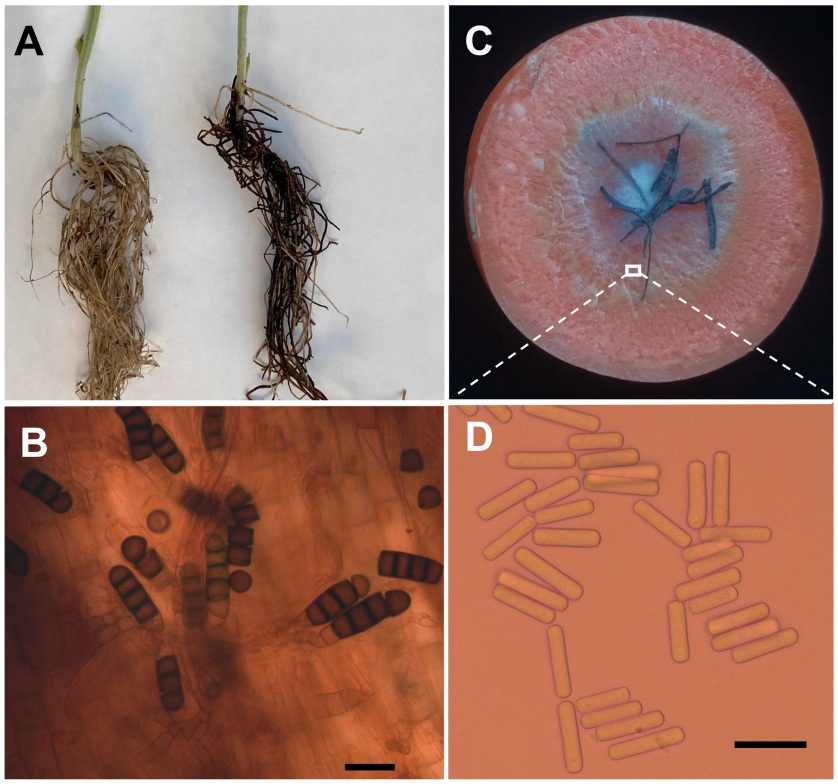

FIGURE 1
Bioassay of infected soils and isolation of pathogen causing black root on faba bean. **(A)** Seedlings of faba bean from control (left) and infected soils (right). **(B)** Chlamydospores of *Berkeleyomyces rouxiae* produced in faba bean diseased root. **(C)** Carrot slice infected by *Berkeleyomyces rouxiae* on faba bean diseased root. **(D)** Endoconidia of *B rouxiae* produced on carrot slice. (bar = 20µm).

Pathogenicity and host range tests

Two weeks after inoculation, all five isolates were able to cause stunting of "Qinghai 13" plants and reduced plant vigor, and black necrosis was also observed on the stem base of some plants. Typical black necrotic lesions on plant roots were observed, and chlamydospores were also discovered on the black necrotic lesions under a microscope, while there were no symptoms on the control plants. The results indicated all five isolates were pathogenic to faba bean. The five isolates were also re-isolated from symptomatic lesions to confirm Koch's postulates. The results of the two experiments were similar.

The results of the host range test revealed that isolate LXBR1 was able to infect all the ten tested legume crops, but was not pathogenic on wheat and maize. Isolate LXBR1 had strong pathogenicity on common bean, chickpea, cowpea, mung bean, rice bean, lentil, and hyacinth bean, where it caused typical black necrosis on roots and produced abundant chlamydospores in the necrotic tissues. However, the isolate did not cause symptoms in soybean, adzuki bean, and pea, and only a few chlamydospores were produced on roots (Table 1). The experiment was performed two times, and similar results were obtained.

Sequence alignment and phylogenetic analyses

Partial sequences of the ITS region, 60S, LSU, and *MCM7* genes from the five isolates were sequenced and submitted to NCBI to obtain GenBank accessions (ON679637- ON679641 for ITS; ON679600- ON679604 for LSU; ON711031- ON711035 for 60S; ON711036-ON711040 for *MCM7*). The BLASTn analysis of these sequences showed that the five isolates had high similarity (99 to 100%) with other *B. rouxiae* isolates including the type isolate CMW7625. The maximum likelihood (ML) trees based on tandem sequences of ITS, LSU, *MCM7* and 60S, and *MCM7* of the five isolates from faba bean and related fungal species were constructed respectively (Figures 3, 4), and the five isolates were identified as *B. rouxiae* based on their phylogenetic position.

Evaluation of faba bean cultivars for resistance

Thirty-six cultivars were identified for resistance to root rot by inoculating with LXBR1 at the seedling stage. Significant differences in resistance were found among the cultivars

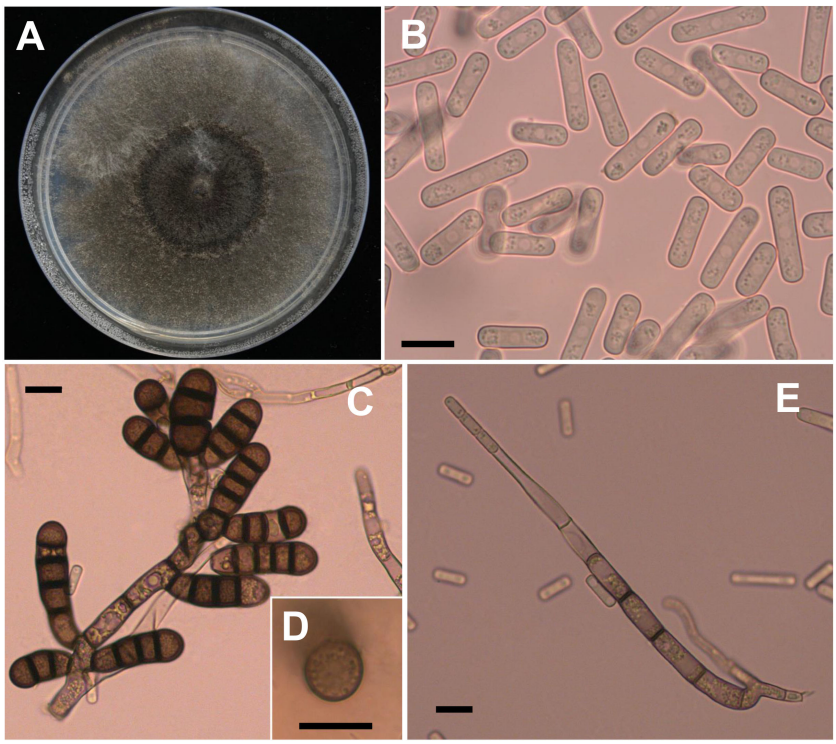

FIGURE 2
Morphological characteristics of *Berkeleyomyces rouxiae*. **(A)** Colony of *B rouxiae* isolates on PDA after 20 days at 25 °C. **(B)** Endoconidia of *B rouxiae* produced on PDA. **(C, D)** Chlamydospores of *B rouxiae* produced on PDA. **(E)** Phialide of *B rouxiae*. (Bar = 10μm).

(P<0.01) (Table 2). Resistance levels in these cultivars showed a very broad range of DI ranging from 33.3 to 88.9. Cultivar T18501 with a DI of 33.3 was classified as resistant, and five cultivars T20604, T20605, Edou3203, Edou1103, and Jingdou701 were moderately resistant reactions. The remaining cultivars were susceptible or highly susceptible (Table 3).

Discussion

Recently, the taxonomic status of the fungus *T. basicola* was revised based on molecular phylogenetic analysis, and the isolates from different hosts were classified into two species under a newly described genus *Berkeleyomyces*, namely *B. basicola* and *B. rouxiae* (Nel et al., 2018). In this study, we identified the agent causing black root rot of faba beans in experimental field plots in Gansu Province, China. Combining morphological, pathogenic, and molecular characteristics, the faba bean isolates were identified as *B. rouxiae* (Nakane et al., 2019; Le et al., 2022). Based on molecular phylogenetic analysis, Nel et al. (2018) classified the pathogens causing black root rot from *Ipomoea batatas* and *P. sativum* as *B. rouxiae* (Nel et al., 2018). Our results confirmed *B. rouxiae* as a pathogen causing black root rot on the faba bean.

Black root rot caused by *T. basicola* has been reported on more than 230 plant species (Pereg, 2013). Reclassification based on molecular phylogenetic analysis has also classified *T. basicola* (= *Thielavia basicola*, *Trichocladium basicola*) isolates from *Arachis hypogaea*, *Chamaecytisus* cult. Aura, *Cichorium intybus*, *Citrus* sp., *Daucus carota*, *Euphorbia pulcherrima*, *Eucalyptus regnans*, *E. globulus*, *E. globulus*, *E. nitens*, *Lathyrus odoratus*, *Nicotiana tabacum*, and *Phaseolus vulgaris* as *B. rouxiae* (Nel et al., 2018). New hosts of *B. rouxiae* including *Cannabis sativa* (Rahnama et al., 2022), *Cucumis melo* (Wang et al., 2019), *Gossypium hirsutum* (Le et al., 2022), and *Lactuca sativa* (Nakane et al., 2019) were found or confirmed since 2018. In this study, our results showed that *B. rouxiae* isolate LXBR1 from faba bean was pathogenic to chickpea, common bean, cowpea, hyacinth bean, lentil, mung bean, and rice bean, and infective to adzuki bean, pea, and soybean, whereas it could not infect wheat and maize. Previous studies revealed infection of chickpea, common bean, cowpea, faba bean, hyacinth bean,

TABLE 1 Host range test of *Berkeleyomyces rouxiae* isolate from faba bean.

Crop	Cultivar	Infectibility to *B. rouxiae*[a]	
		black necrosis on root	Sporulationon root
Common bean (*Phaseolus vulgaris*)	Biyun 6	+	+
	Longyundou 29	+	+
Pea (*Pisum sativum*)	Longwan 7	-	+
	Zhongqin 1	-	+
Chickpea (*Cicer arietinum*)	Xinying 1	+	+
	Xinying 2	+	+
Cowpea (*Vignaun unguiculata*)	Liaojiang1	+	+
	Guijiang 18-11	+	+
Mung bean (*Vigna radiata*)	Elv 1	+	+
	Zhenglv 8	+	+
Adzuki bean (*Vigna angularis*)	Jinxiaodou 5	-	+
	Yuhong 2	-	+
Rice bean (*Vigna umbellata*)	Fandou 1	+	+
	Hongfandou	+	+
Lentil (*Lens culinaris*)	Yingguozhonglv	+	+
	Faguo	+	+
Hyacinth bean (*Lablab purpureus*)	Jiaodayanhong	+	+
	Biandou 1	+	+
Soybean (*Glycine max*)	Williams	-	+
	Zhonghuang13	-	+
Wheat (*Triticum aestivum*)	197	-	-
	198	-	-
Maize (*Zea mays* L.)	Zhongdan 1168	-	-
	Dongdan 6688	-	-

a, "+": positive results, "-": negative results

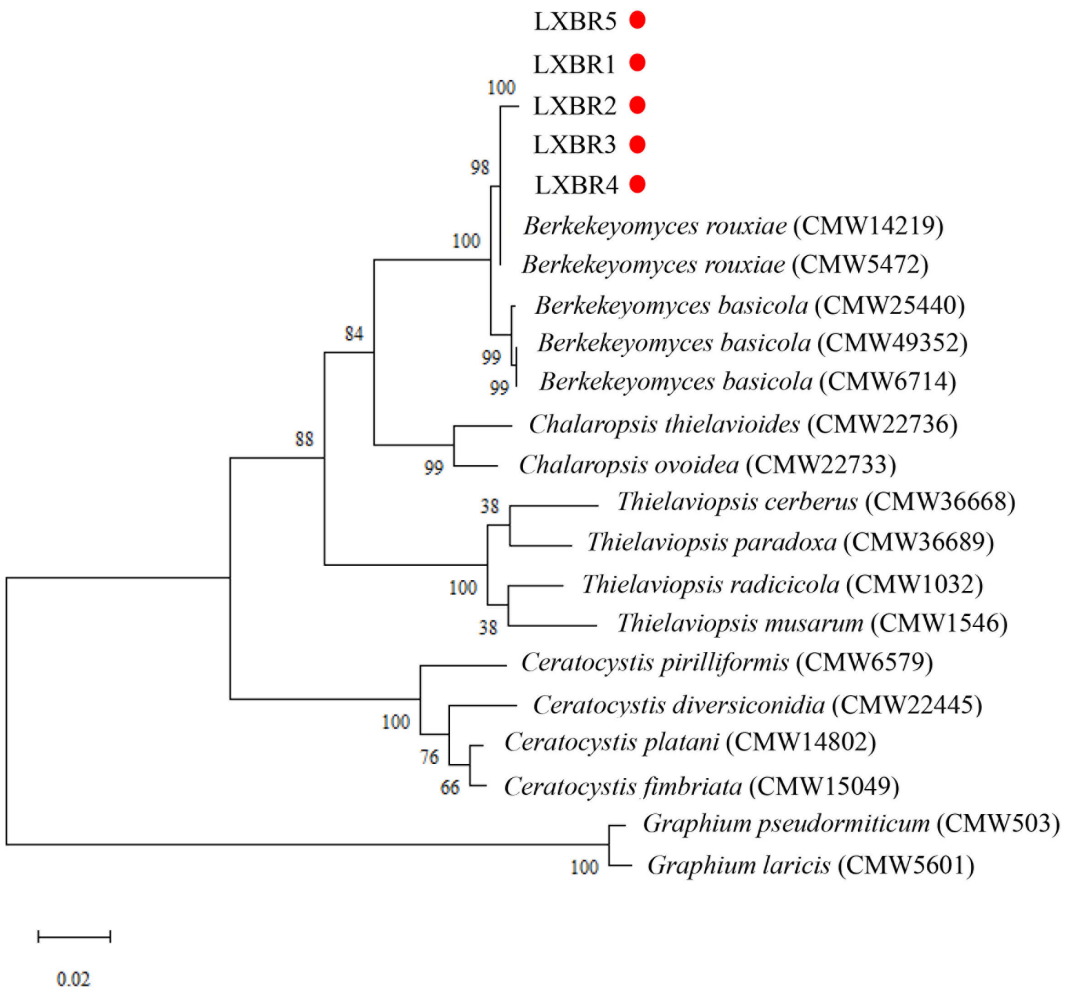

FIGURE 3
Combined phylogenetic tree based on the ITS, LSU, 60S, and *MCM7* sequences of the *Berkeleyomyces rouxiae* isolates by Maximum-Likelihood method in the MEGA11with bootstrap values estimated by 1000 replicates. Bootstrap support values are indicated in the nodes.

lentil, pea, soybean, and wheat with *T. basicola* (= *Thielavia basicola*, *Trichocladium basicola*) (Johnson, 1916; Gayed 1972; Bowden et al., 1985; Monfort et al., 2010; Pereg, 2011), while maize was not infected by *T. basicola* (= *Thielavia basicola*) after natural or artificial inoculations (Johnson, 1916; Gayed 1972). Pereg (2011) found that *T. basicola* exhibits three modes of interaction with plants: infects roots and causes the disease; infects roots but does not cause disease; and does not infect roots. Based on these three modes, plants could be divided into susceptible hosts, non-susceptible hosts, and non-hosts of *T. basicola*. Non-susceptible hosts are those in which chlamydospores of *T. basicola* were detected on healthy-looking roots of the plants. In this study, we found that inoculated adzuki bean, pea, and soybean did not develop symptoms on the roots, but chlamydospores were present, suggesting these crops are non-susceptible hosts of *B. rouxiae* from faba bean. Our results confirmed that the 11 legume crops tested were hosts of *B. rouxiae*, and the infection of adzuki bean, mung bean, and rice bean by *B. rouxiae* was recorded for the first time.

T. basicola from common bean (= *Thielavia basicola*) and pea (= *Trichocladium basicola*) was renamed as *B. rouxiae* by Nel et al. (2018), our results showed that the common bean was a host of *B. rouxiae*, but pea was a non-susceptible host of *B. rouxiae*. Previous studies had shown differences in the host range of *T. basicola* isolates from different hosts, suggesting that *T. basicola* may exhibit host specificity and preference for different species (Pereg, 2011; Nel et al., 2018). For example,

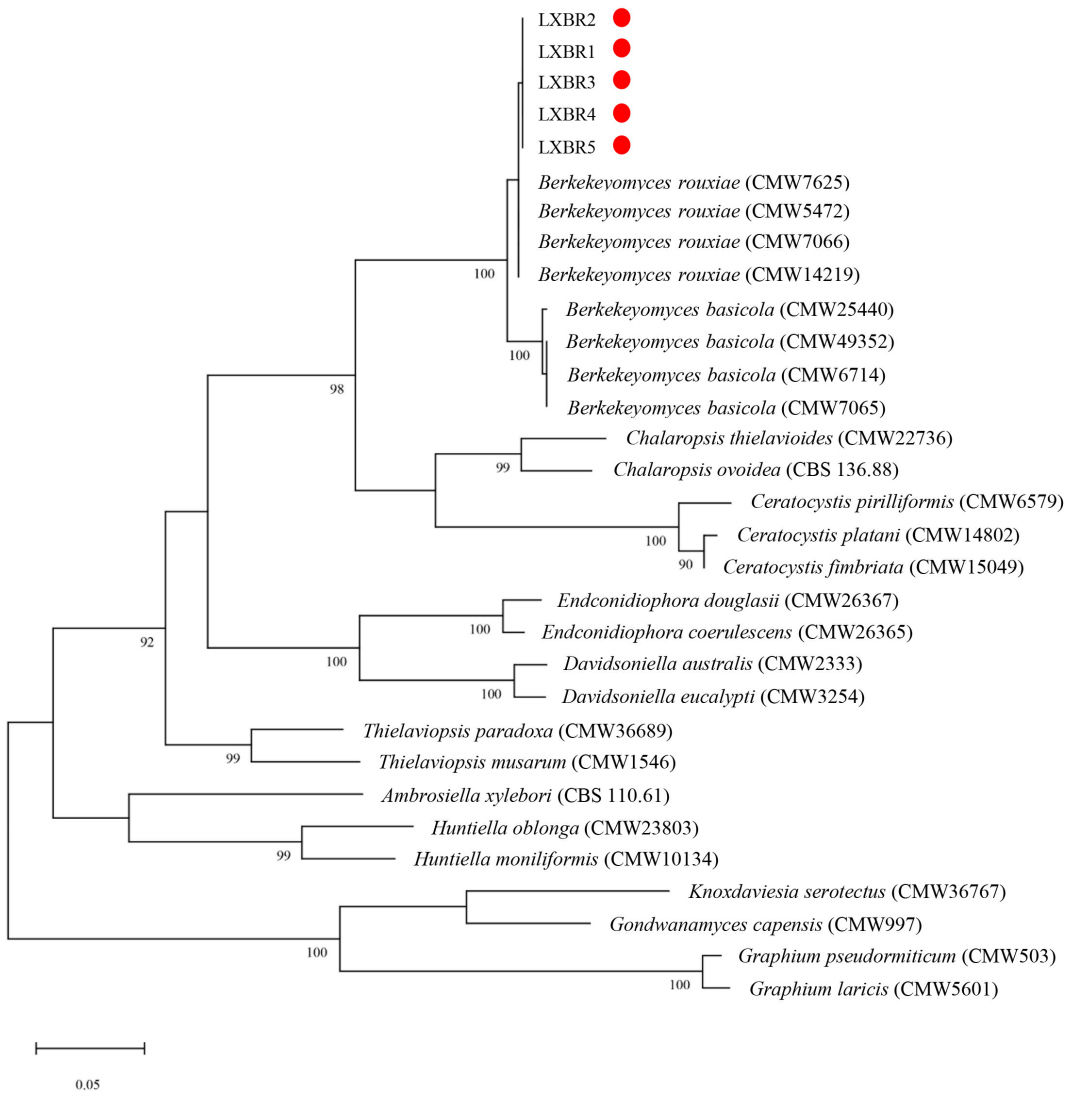

FIGURE 4
Phylogenetic tree based on the *MCM7* sequences of the *Berkeleyomyces rouxiae* isolates by Maximum-Likelihood method in the MEGA11 with bootstrap values estimated by 1000 replicates. Bootstrap support values are indicated in the nodes.

O'Brien and Davis (1994) found that two *T. basicola* (= *Chalara elegans*) isolates from lettuce were not pathogenic to cotton. Recently *T. basicola* isolates from cotton and lettuce had been re-identified as *B. rouxiae* (Nakane et al., 2019; Le et al., 2022). These results suggest that *B. rouxiae* could have host specificity and preference, but this should be confirmed by host range tests of *B. rouxiae* from different host plants in the future.

TABLE 2 Anaylsis of Variance (ANOVA) used to evaluate the significance differences in 36 cultivars resistance to the *Berkeleyomyces rouxiae*.

Variance	SS	df	MS	F	P-value
cultivars	20751.44	35	592.72	13.59	0.0000
Blocks	187.14	2	93.57	2.22	0.116
Error	2949.51	70	42.13		
Total	23888.09	107			

TABLE 3 Resistance identification of thirty-six faba bean cultivars to *Berkeleyomyces rouxiae*.

Cultivar	Source	Disease Index	Resistance
TC3	Jiangsu	82.2	HS
15-147	Jiangsu	68.9	S
Tongqing1	Jiangsu	80.0	HS
T20601	Jiangsu	73.3	S
T20602	Jiangsu	77.8	HS
T20603	Jiangsu	66.7	S
T18501	Jiangsu	33.3	R
T20604	Jiangsu	51.1	MR
T20606	Jiangsu	62.2	S
T20605	Jiangsu	42.2	MR
T09-110-1	Jiangsu	75.6	HS
T16028	Jiangsu	73.3	S
Sucan6	Jiangsu	73.3	S
Chenghu201010-1-1	Sichuan	88.9	HS
Cehnghu25	Sichuan	88.9	HS
Yucan3	Chongqing	84.4	HS
Yucan4	Chongqing	84.4	HS
Zhongcan202	Beijing	73.3	S
Zhongcan201	Beijing	80.0	HS
Haiqing1	Qinghai	82.2	HS
Wancan1	Anhui	66.7	S
1103	Hubei	73.3	S
TC15	Hubei	64.4	S
Edou3203	Hubei	37.8	MR
Edou1103	Hubei	46.7	MR
Yundou1299	Yunnan	80.0	HS
Yundou2883	Yunnan	86.7	HS
Yundou147	Yunnan	73.3	S
Fengdou35	Yunnan	57.8	S
Fengdou36	Yunnan	73.3	S
Jingdou622	Yunnan	57.8	S
Jingdou651	Yunnan	71.1	S
Jingdou650	Yunnan	71.1	S
Jingdou701	Yunnan	53.3	MR
Jingdou614	Yunnan	66.7	S
Jingdou215	Yunnan	68.9	S

Previous studies revealed that resistance levels to *T. basicola* were different in several crops such as chickpea (Bhatti and Kraft, 1992), cotton (Wheeler et al., 2000), soybean (Maduewesi and Lockwood, 1976), and tobacco (Miki and Katsuya, 1998). In this study, we evaluated the resistance of 36 faba bean cultivars to *B. rouxiae* by artificial inoculation at the seedling stage. Although none were completely resistant to *B. rouxiae*, one cultivar showed resistance and five were moderately resistant. The cultivation of these resistant cultivars could be an effective means to manage the black root rot of faba bean by contributing to a decrease in disease severity. To our knowledge, this is the first report of *B. rouxiae* causing root rot on faba beans in China and this disease should be paid sufficient attention to due to the serious risk of *B. rouxiae* in faba beans.

Data availability statement

The datasets presented in this study can be found in online repositories. The names of the repository/repositories and accession number(s) can be found in the article.

Author contributions

ZZ planned and designed the experiments. JL and WW performed the experiments and wrote the manuscript. YS and YG provided the diseased soil samples for this study. SS, WW, and CD revised the manuscript. All authors contributed to the article and approved the submitted version.

Funding

This study was supported by the China Agriculture Research System of MOF and MARA (CARS-08), and the Scientific Innovation Program of the Chinese Academy of Agricultural Sciences.

Conflict of interest

The authors declare that the research was conducted in the absence of any commercial or financial relationships that could be construed as a potential conflict of interest.

Publisher's note

All claims expressed in this article are solely those of the authors and do not necessarily represent those of their affiliated organizations, or those of the publisher, the editors and the reviewers. Any product that may be evaluated in this article, or claim that may be made by its manufacturer, is not guaranteed or endorsed by the publisher.

References

Afshari, N., and Hemmati, R. (2017). First report of the occurrence and pathogenicity of *Clonostachys rosea* on faba bean. *Australas. Plant Path.* 46, 231–234. doi: 10.1007/s13313-017-0482-3

Al-Shahwan, I. M., Abdalla, O. A., Al-Saleh, M. A., and Amer, M. A. (2017). Detection of new viruses in alfalfa, weeds and cultivated plants growing adjacent to alfalfa fields in Saudi Arabia. *Saudi J. Biol. Sci.* 24, 1336–1343. doi: 10.1016/j.sjbs.2016.02.022

Bhatti, M. A., and Kraft, J. M. (1992). Reaction of selected chickpea lines to Fusarium Thielaviopsis root rots. *Plant disease* 76 (1), 54–56. doi: 10.1094/PD-76-0054.

Bodker, L., Leroul, N., and Smedegaard- Petersen, V. (1993). The occurrence in Denmark of black root rot of pea caused by *Thielaviopsis basicola*. *Plant Pathol.* 42, 820–823. doi: 10.1111/j.1365-3059.1993.tb01572.x

Bowden, R. L., Wiese, M.V., Crock, J. E., and Auld, D.L (1985). Root rot of chickpeas lentils caused by *Thielaviopsis basicola*. *Plant Dis.* 69 (12), 1089–1091.

Cavalcante, S. V., Josiene, M., Alexandre Marcos, C., and Marcos, C. G. (2022). Prevalence of Berkeleyomyces basicola infections in black rot affected carrot determined using the *MCM7* gene region. *Plant Pathol.* 71, 1185–1194. doi: 71.10.1111/ppa.13552

Coumans, J. V. F., Harvey, J., Backhouse, D., Poljak, A., Raftery, M. J., Nehl, D., et al. (2011). Proteomic assessment of host-associated microevolution in the fungus *Thielaviopsis basicola*. *Environ. Microbiol.* 13, 576–588. doi: 10.1111/j.1462-2920.2010.02358.x

Crous, P. W., Rossman, A. Y., Aime, M. C., Allen, W. C., Burgess, T., Groenewald, J. Z., et al. (2021). Names of phytopathogenic fungi: a practical guide. *Phytopathology* 111(9), 1500–1508. doi: 10.1094/PHYTO-11-20-0512-PER

de Beer, Z. W., Duong, T. A., Barnes, I., Wingfield, B. D., and Wingfield, M. J. (2014). Redefning *Ceratocystis* and allied genera. *Stud. Mycol.* 79, 187–219. doi: 10.1016/j.simyco.2014.10.001

Etemadi, F., Hashemi, M., Barker, A. V., Zandvakili, O. R., and Liu, X. (2019). Agronomy, nutritional value, and medicinal application of faba bean (*Vicia faba* l.). *Can J Plant Sci* 52 (6), 869–873. doi: 10.1016/j.hpj.2019.04.004

Gayed, S. K. (1972). Host range persistence of *Thielaviopsis basicola* in tobacco soil. *Can J Plant Sci* 52 (6), 869–73. doi: 10.4141/cjps72-150

Jensen, E. S., Peoples, M. B., and Hauggaard-Nielsen, H. (2010). Faba bean in cropping systems. *Field. Crops Res.* 115, 203–216. doi: 10.1016/j.fcr.2009.10.008

Ji, Y., Chen, Z., Cheng, Q., Liu, R., Li, M., Yan, X., et al. (2022). Estimation of plant height and yield based on UAV imagery in faba bean (*Vicia faba* l.). *Plant Methods* 18, 26. doi: 10.1186/s13007-022-00861-7

Johnson, J. (1916). Host plants of *Thielavia basicola*. *J. Agric. Sci.* 7, 289–300. Available at: https://naldc.nal.usda.gov/download/IND43965746/PDF.

Karkanis, A., Ntatsi, G., Lepse, L., Fernandez, J. A., Vagen, I. M., Rewald, B., et al. (2018). Faba bean cultivation-revealing novel managing practices for more sustainable and competitive European cropping systems. *Front. Plant Sci.* 9. doi: 10.3389/fpls.2018.01115

Kaur, S., Kimber, R. B., Cogan, N. O., Mateme, M., Foster, J. W., and Paull, J. G. (2014). SNP discovery and high-density genetic mapping in faba bean (*Vicia faba* l.) permits identification of QTLs for ascochyta blight resistance. *Plant Sci.* 217-218, 47–55. doi: 10.1016/j.plantsci.2013.11.014

Kraft, J. M., Haware, M. P., and Hussein, M. M. (1988). *Root rot and wilt diseases of food legumes. world crops: Cool season food legumes* (Dordrecht: Springer), 565–575. doi: 10.1007/978-94-009-2764-3_47

Kumari, S. G., and Makkouk, K. M. (2007). Virus diseases of faba bean (*Vicia faba* l.) in Asia and Africa. *Plant Viruses* 1 (1), 93–105. Available at : https://www.researchgate.net/profile/Safaa-Kumari/publication/298158358_Virus_Diseases_of_Faba_Bean_Vicia_faba_L_in_Asia_and_Africa/links/56e6797b08ae68afa1137fb3/Virus-Diseases-of-Faba-Bean-Vicia-faba-L-in-Asia-and-Africa.pdf.

Kumar, S., Stecher, G., and Tamura, K. (2016). MEGA7: molecular evolutionary genetics analysis version 7.0 for bigger datasets. *Mol. Biol. Evol.* 33, 1870–1874. doi: 10.1093/molbev/msw054

Le, D. P., Gregson, A., and Jackson, R. (2022). Identification of *Berkeleyomyces rouxiae* causing black root rot disease on cotton seedlings in new south Wales, Australia. *J. Gen. Plant Pathol.* 88, 155–159. doi: 10.1007/s10327-021-01047-0

Li, L., Yang, T., Liu, R., Redden, B., Maalouf, F., and Zong, X. (2017). Food legume production in China. *Crop J.* 5, 115–126. doi: 10.1016/j.cj.2016.06.001

Maalouf, F., Hu, J., O'Sullivan, D. M., Zong, X., Hamwieh, A., Kumar, S., et al. (2018). Breeding and genomics status in faba bean (*Vicia faba*). *Plant Breed* 138, 465–473. doi: 10.1111/pbr.12644

Maduewesi, J. N. C., and Lockwood, J. L. (1976). Test tube method of bioassay for Thielaviopsis basicola root rot of soybean. *Phytopathology* 66 (6), 81.

Miki, J. I., and Katsuya, S. (1998). Virulence of *Thielaviopsis basicola* isolated from tobacco fields in Japan. *J Phytopathol* 64 (5), 471–473. doi: 10.3186/jjphytopath.64.471

Monfort, W. S., Carroll, A. G., Emerson, M. J., Fortner, J., and Rothrock, C. S. (2010). First report of black root rot caused by *Thielaviopsis* basicola on soybean (Glycine max) in Arkansas. *Plant Dis.* 94 (9), 1168. doi: 10.1094/PDIS-94-9-1168A

Nakane, R., Miki, S., Ikeda, K., Sakai, H., Hayashi, K., and Usami, T. (2019). First report of black root rot of lettuce in Japan caused by *Berkeleyomyces rouxiae*. *J. Gen. Plant Pathol.* 85, 436–439. doi: 10.1007/s10327-019-00860-y

Nel, W. J., Duong, T. A., Beer, Z. W., and Wingfield, M. J. (2019). Black root rot: a long known but little understood disease. *Plant Pathol.* 68, 834–842. doi: 10.1111/ppa.13011

Nel, W. J., Duong, T. A., Wingfield, B. D., Wingfield, M. J., and de Beer, Z. W. (2018). A new genus and species for the globally important, multihost root pathogen *Thielaviopsis basicola*. *Plant Pathol.* 67, 871–882. doi: 10.1111/ppa.12803

Noshad, D., Riseman, A., and Punja, Z. K. (2006). First report of Thielaviopsis basicola on Daphne cneorum. *Canadian Journal of Plant Pathology* 28 (2), 310–312. doi: 10.1080/07060660609507300

O'Brien, R. G., and Davis, R. D. (1994). Lettuce black root rot-a disease caused by *Chalara elegans*. *Australas. Plant Pathol.* 23, 106–111. doi: 10.1071/APP9940106

Pereg, L. L. (2013). Black root rot of cotton in Australia: The host, the pathogen and disease management. *Crop Pasture Sci.* 64, 1112–1126. doi: 10.1071/CP13231

Pereg, L. L. (2011). Molecular factors determining Thielaviopsis basicola-cotton interactions leading to black root rot disease. Full Final Report to the Cotton Catchment Communities CRC, Narrabri, NSW. Available at: www.cottoncrc.org.au/general/Research/Projects/1_01_21.

Rahnama, M., Szarka, D., Boyadjieva, L., and Ward Gauthier, N. A. (2022). First report of black root rot (*Berkeleyomyces rouxiae*) on greenhouse hemp (*Cannabis sativa*) in Kentucky. *Plant Dis.* 106 (9), 2534. doi: 10.1094/PDIS-10-21-2146-PDN

Rubiales, D., and Khazaei, H. (2022). Advances in disease and pest resistance in faba bean. *Theor. Appl. Genet.* 19, 1–22. doi: 10.1007/s00122-021-04022-7

Sillero, J. C., Villegas-Fernandez, A. M., Thomas, J., Rojas-Molina, M. M., Emerand, M. M., Fernández-Apariciob, M., et al (2010). Faba bean breeding for disease resistance. *Field Crops Res.* 115 (3), 297–307. doi: 10.1016/J.FCR.2009.09.012

Stoddard, F. L., Nicholas, A. H., Rubiales, D., Thomas, J., and Villegas-Fernandez, A. M. (2010). Integrated pest management in faba bean. *Field Crops Res.* 115, 308–318. doi: 10.1016/j.fcr.2009.07.002

Stielow, J.B., Lévesque, C.A., Seifert, K.A., Meyer, W., Irinyi, L., Smits, D., et al (2015). One fungus, which genes Development and assessment of universal primers for potential secondary fungal DNA barcodes. *Persoonia* 35, 242. doi: 10.3767/003158515x689135

Vilgalys, R., and Hester, M. (1990). One fungus, which genes Development assessment of universal primers for potential secondary fungal DNA barcodes. *Persoonia* 35, 242. doi: 10.3767/003158515x689135

Wang, F., Zhang, W., Yuan, X., and Liu, D. W. (2019). First report of black root rot on *Cucumis melo* caused by *Berkeleyomyces rouxiae* in heilongjiang province of China. *Plant Dis.* 103, 2675. doi: 10.1094/PDIS-11-18-2007-PDN

Wheeler, T. A., Hake, K. D., and Dever, J. K. (2000). Survey of Meloidogyne incognita Thielaviopsis basicola: their impact on cotton fruiting producers' management choices in infested fields. *J Nematol* 32 (4S), 576.

White, T. J., Bruns, T., Lee, S., and Taylor, J. (1990). Amplification and direct sequencing of fungal ribosomal RNA genes for phylogenetics. *Pcr Protocols: guide to Methods Appl.* 38, 315–322. doi: 10.1016/B978-0-12-372180-8.50042-1

You, M. P., Eshete, B. B., Kemal, S. A., Leur, J., and Barbetti, M. J. (2021). *Physoderma*, not *Olpidiu*m, is the true cause of faba bean gall disease of *Vicia faba* in Ethiopia. *Plant Pathol.* 70, 1180–1194. doi: 10.1111/ppa.13359

Yu, T. F. (1979). *Faba bean diseases* (Beijing, China: Science Press).

frontiers | Frontiers in Plant Science

TYPE Original Research
PUBLISHED 21 December 2022
DOI 10.3389/fpls.2022.1009906

OPEN ACCESS

EDITED BY
Sabine Banniza,
University of Saskatchewan, Canada

REVIEWED BY
Bita Naseri,
Education and Extension Organization (AREEO), Iran
Bruce D. Gossen,
Agriculture and Agri-Food Canada (AAFC), Canada

*CORRESPONDENCE
Adnan Šišić
adnan_sisic@uni-kassel.de

SPECIALTY SECTION
This article was submitted to Plant Pathogen Interactions, a section of the journal Frontiers in Plant Science

RECEIVED 02 August 2022
ACCEPTED 29 November 2022
PUBLISHED 21 December 2022

CITATION
Šišić A, Baćanović-Šišić J, Schmidt H and Finckh MR (2022) Farming system effects on root rot pathogen complex and yield of faba bean (*vicia faba*) in Germany.
Front. Plant Sci. 13:1009906.
doi: 10.3389/fpls.2022.1009906

Farming system effects on root rot pathogen complex and yield of faba bean (*vicia faba*) in Germany

Adnan Šišić[1]*, Jelena Baćanović-Šišić[2], Harald Schmidt[3] and Maria R. Finckh[1]

[1]Department of Ecological Plant Protection, University of Kassel, Witzenhausen, Germany, [2]Section of Organic Plant Breeding and Agrobiodiversity, University of Kassel, Witzenhausen, Germany, [3]Foundation Ecology & Agriculture (SOEL), Ahrweiler, Germany

A survey across Germany was undertaken from 2016-2019 to evaluate effects of management system (organic vs conventional), pedo-climatic conditions and crop rotation history on faba bean root health status, diversity of major root rot pathogens and yield. Root rot incidence was generally low and there was no effect of the management system on the spectrum of pathogens isolated. Among the most common fungal species identified, frequencies of *Fusarium redolens* and *Didymella pinodella* were significantly higher in roots from organic fields compared with conventional and lower was observed for *F. avenaceum*, *F. tricinctum* and *F. culmorum*. Faba bean roots were colonized at similar rates by *F. equiseti* and the members of the *F. oxysporum* (FOSC) and *F. solani* (FSSC) species complexes in both management systems. Almost no legumes had been grown in the 5-11 years preceding the conventional faba beans surveyed while legumes had almost always been present during this period in the organic fields. This difference in rotational histories between the farming systems led to apparent cropping systems effects on the isolation frequencies of several species. For example, *D. pinodella* was ubiquitous in organic fields with a high frequency of legumes in the rotations but much rarer and often absent in conventional fields. Pedo-climatic conditions, particularly cool conditions at sowing and plant emergence and/or during the vegetative season favored most of the most prevalent *Fusarium* species identified in this study. In organic systems, yields correlated negatively with *D. pinodella* and *F. redolens* frequencies whereas higher levels of *F. tricintum* in faba bean roots had a positive correlation with yield. In conventional systems, faba bean yields depended more on the total precipitation before sowing and during the main growing season but were also negatively correlated with the frequencies of FOSC and *F. culmorum*.

Phylogenetic analysis based on the *TEF1 alpha* locus indicated that the FSSC isolates mainly belonged to the *F. pisi* lineage. In contrast, the FOSC isolates were placed in 9 different lineages, with a conspicuous dominance of *F. libertatis* that has until now not been associated with any leguminous host.

KEYWORDS

fusarium, didymella, root rot, faba bean, grain legumes, organic agriculture, conventional agriculture

Introduction

Foot and root rots, caused by a complex of soil-borne pathogens are among the most widespread and important grain legume diseases and one of the major constrains in grain legume production worldwide (Wille et al., 2019). Several *Fusarium* species, *Aphanomyces euteiches* and the *Ascochyta* complex pathogens, *Didymella pinodella* and *D. pinodes*, are the most commonly associated pathogens with the disease complex (Baćanović-Šišić et al., 2018; Wille et al., 2019). Plants under field conditions are usually colonized by multiple pathogens simultaneously, and the importance of each species varies depending on the geographical region, pedo-climatic conditions and the crop management strategy (Esmaeili Taheri et al., 2016; Naseri and Ansari Hamadani, 2017; Baćanović-Šišić et al., 2018; Chatterton et al., 2019; Williamson-Benavides and Dhingra, 2021). In northern USA and Canada for example, *F. avenaceum* together with *Aphanomyces eutheiches* is a major threat to pea and lentil production (Chittem et al., 2015; Chatterton et al., 2019), whereas in France and northern European countries including Denmark and Sweden, in addition to *A. euteiches* and *F. avenaceum*, *F. solani*, *F. redolens* and *Didymella pinodella* (syn. *Phoma medicaginis* var. *pinodella*) play an important role in pea growing areas (Persson et al., 1997; Hossain et al., 2012; Gibert et al., 2022). Other pathogens such as, *Rhizoctonia solani*, *Pythium* spp., *Thielaviopsis basicola* and *Macrophomina phaseolina* have also been implicated as important parts of the grain legume root rot complex (Naseri and Mousavi, 2015; Wille et al., 2019; Williamson-Benavides and Dhingra, 2021; Wohor et al., 2022).

In the past 15 years, two large root rot surveys have been conducted on grain legumes in Germany. The first (2005-2007) focused on root health assessments of conventional peas, including detailed identification of the pathogens involved based on morphology (Pflughöft et al., 2012). This survey indicated declining importance of *F. solani* and *F. oxysporum* while *D. pinodella* together with *F. redolens* and *F. avenaceum* were identified as the primary pathogens in the pea root rot complex in Germany. The second survey (2008-2012) was conducted in four regions of Germany and, in addition to pea, also included faba beans but covered organic fields only (Wilbois et al., 2013). This survey focused solely on rating of the plants in the fields and, besides pointing to the importance of *Fusarium* spp. did not identify the major *Fusarium* species involved in the root rot complex of organic pea and faba bean. Although faba bean usually appeared healthier than pea they frequently harbored the same pathogens as peas (Pflughöft et al., 2012; Wilbois et al., 2013). No information is available on pathogens associated with conventional faba bean in Germany. Since the pathogen complex as a whole has a wide host range among legumes and, in addition, especially *Fusarium* spp. often affect cereals (Bainard et al., 2017; Walder et al., 2017), farmers are forced to grow pulses in wide rotations in order to avoid disease problems.

As a result of the new protein crop strategy adopted in 2012 by the German Federal Ministry of Food and Agriculture, and the EU Common Agricultural Policy (CAP) greening measures in 2015, faba bean production area in Germany has quadrupled since 2014 to about 60.000 ha in 2020. To avoid inoculum build-up and maintain or increase the area grown to faba bean and pulses in general, there is a need to evaluate current pathological risks in order to plan rotations. The overall objective of this study was to determine the root health status of organic and conventional faba beans in Germany and to characterize diversity and frequency of root associated pathogens as affected by farming system, pedo-climatic conditions and crop rotation management. We further report on the effects of root health status and root infections with major fungal species on faba bean yield and provide insights into the genetic variability of the *F. oxysporum* and *F. solani* isolates recovered.

Material and methods

Weather data, cropping history and site characteristics

Between 2016 and 2019, a total of 110 faba bean fields were sampled throughout Germany (Figure 1). Of these, 53 surveyed fields were managed organically according to the European

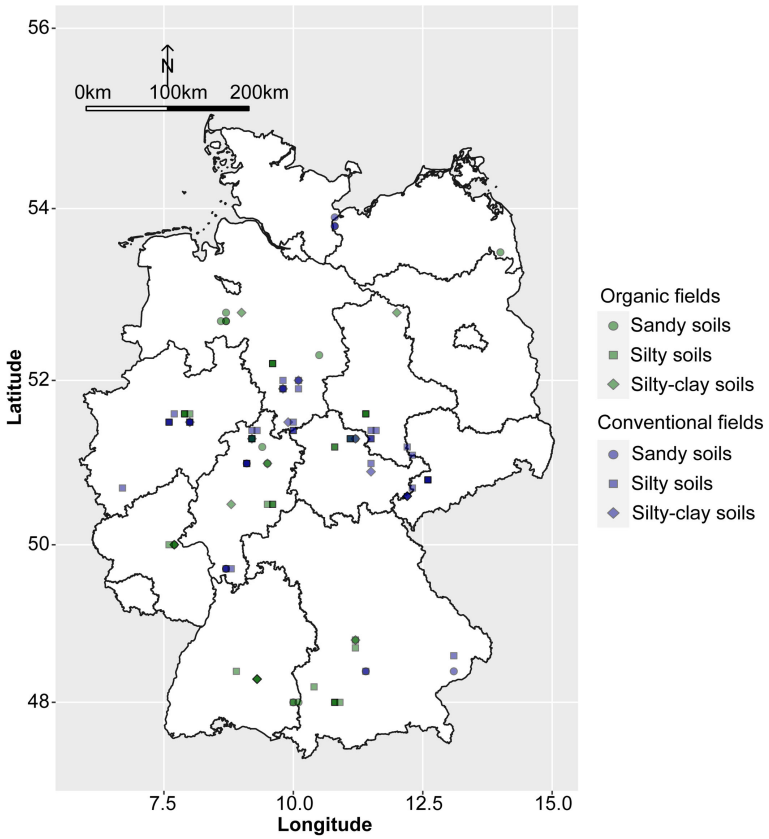

FIGURE 1
Map of Germany showing locations and the soil types of the surveyed organic and conventional faba bean fields.

Union and national standards and 57 fields conventionally. The meteorological data were obtained from the closest weather stations (<10 km) to the fields. Sand, silt, clay, and soil organic matter content as well as pH were determined in accordance with the standard DIN EN ISO/IEC 17025:2018-03. Data on cropping history were obtained from the farmers directly. These included the number of years fields were planted to different leguminous species (i.e. clover species and alfalfa, pea, faba bean, lentil, lupin, soybean, vetch and the unspecified group of 'other grain' or 'small seeded legumes') and the number of years of cereals (bulked data for all cereal crops) for a 5- and 11-year period prior to the sampling of faba bean. The complete data set is given in Supplementary Table 1.

Sampling, disease assessments, morphological characterization of the isolates and yield estimation

Thirty-six to 40 faba bean plants were uprooted at full flowering from two areas per field, each 5 m^2 in size with the distance between the two areas of 10 to 20 meters, depending on the field. Half of the roots were immediately washed to remove adhering soil and individual plants were evaluated for the severity of root rot symptoms using a visual 1-9 score (1=healthy, 9=dying plant) based on external root tissue discoloration levels (Figure 2) according to Pflughöft et al. (2012). The remaining half of the sampled roots were shipped to the University of Kassel and stored at -18°C until fungal isolations were performed as described previously (Šišić et al., 2018b). Isolations were targeted at the species belonging to the genus *Fusarium* and those sharing *Didymella* (*Phoma*) like morphology as these had been identified previously as the most common pathogens associated with field peas and faba beans in Germany (Pflughöft et al., 2012; Wilbois et al., 2013; Baćanović-Šišić et al., 2018). Briefly, roots were thoroughly washed under running tap water, surface sterilized with 3% sodium hypochlorite for 10 s, rinsed in distilled water and placed on filter paper under a laminar flow hood for ≥1 h. Three approximately 1-cm-long pieces per plant, representing root, crown, and the transition zone, were placed on COONs (Coons, 1916) media and incubated at 20°C under 12 h cycles of UV light and dark. Roots included both lateral and tap roots up to the point of seed attachment, the crown was considered as the point

FIGURE 2
Varying root discoloration levels and the assigned root rot disease severity ratings (1=healthy plant, 9=dying plant). Plants with disease severity ratings of 8 and 9 (i.e. severe rots) were not observed during the survey.

of seed attachment up to ca. 0.5 cm below the soil surface and the transition zone covered about 1.5 cm between crown and stem.

After 1 to 2 weeks incubation, fungal colonies developing from the root pieces were sub-cultured separately in Petri dishes containing half-strength potato dextrose agar (19 g/l Difco PDA and 10 g/l agar). Pure cultures were generated either through hyphal tipping (*Fusarium* morphology) or transfer of single pycnida (*Didymella* morphology). Each isolate was examined microscopically and identified to the species level based on cultural appearance (colony color and pigmentation) and morphology of conidiogenous cells following the protocols of Leslie and Summerell (2006) for *Fusarium* spp. and Boerema et al. (2004) for *Didymella* spp.

Grain yield was estimated by hand harvesting the plants in five 0.5 m^2 plots within each of the 5 m^2 area used for root collection. The yield was adjusted to 86% dry matter.

Molecular confirmation of fungal species identity and phylogenetic analyses

The identity of 120 *Fusarium* and 8 *Didymella* randomly selected isolates obtained in this study representing 11 different fungal species (Supplementary Table 2) was confirmed by sequencing the portion of the translation elongation factor 1 (*TEF1*) alpha for *Fusarium* spp. (O'Donnell et al., 1998) and the beta tubulin gene region for *Didymella* spp. (Chen et al., 2015). DNA extraction, PCR amplification, sequencing and raw sequence data analysis were performed as described previously (Šišić et al., 2018a). Briefly, genomic DNA was extracted from pure cultures growing on half strength PDA agar plates (*Fusarium* spp; ½ strength PDA; 19 g/l Difco PDA and 10 g/l agar) or Coons (*Didymella* spp.; Coons, 1916) medium using the protocol described by Doyle and Doyle, (1987). A portion of the translation-elongation factor 1 alpha (*tef1*) gene was amplified using primer pairs EF1 and EF2 (O'Donnell et al., 1998). The β tubulin (tub2) gene region was amplified with the primers Btub2Fd and Btub4Rd (Chen et al., 2015). Amplicons were visualized *via* electrophoresis on a 1% agarose gel and purified using the DNA Clean & Concentrator kit (Zymo Research, Freiburg, Germany) according to the manufacturer's instructions. Sanger sequencing in both directions was performed by Macrogen Europe Laboratories (Amsterdam, Netherlands). Obtained row sequence data were assembled and errors identified and corrected manually in SeqMan Lasergene software (DNAStar, Madison, WI, U.S.A.). To confirm the taxonomic identity of the isolates, these sequences were used as queries for the *Fusarium*-ID v. 1.0 (Geiser et al., 2004) and NCBI (Madden, 2002) databases.

Phylogenetic analyses

Single locus phylogenetic analyses based on the *TEF1 alpha* gene sequences were performed for the 35 *Fusarium oxysporum* species complex (FOSC) and 33 *Fusarium solani* species complex (FSSC) isolates. Reference sequences for the analysis were selected based on the previously published phylogenetic relationship within the FOSC (O'Donnell et al., 2009; Lombard et al., 2018) and the FSSC (O'Donnell et al., 2020; Geiser et al., 2021) (Supplementary Tables 3 and 4). The sequence alignments were generated using MAFFT v.7 (Katoh and Standley, 2013) and further adjusted manually with MEGA v6 (Tamura et al., 2013). A bootstrapped Maximum-Likelihood (ML) analysis was

performed using the RAxML-VI-HPC v. 7.0.3 with non-parametric bootstrapping and 1000 replicates implemented on the Cipres portal (Stamatakis et al., 2008). For the FOSC we first performed the phylogenetic analysis on the data set which included 174 representative isolates from the study of O'Donnel et al. (2009) and 91 isolates from Lombard et al. (2018). The resulting *TEF1 alpha* tree topology revealed several isolates which belonged to the same forma specialis, shared identical or had similar *TEF1 alpha* gene sequences. These were excluded from subsequent analysis resulting in a data set which comprised 181 FOSC sequences. The FSSC data set consisted of 96 *TEF1* sequences (Supplementary Tables 2–4). For outgroup purposes, *F. udum* (CBS 177.31) and *F. thapsinum* (H05-557S-1 DCPA) were used to generate the phylogenetic trees.

Statistical analyses

All statistical analyses were performed in R (R Core Team, 2013). Prior to the analysis, the abundance of individual fungal species was used to calculate isolation frequencies (i.e., percent colonized roots) by dividing the number of roots in which the species occurred by the total number of roots processed. The fields were further scored as positive or negative for presence of a particular fungal species and these data were used to calculate the prevalence for each pathogen in each management system (organic and conventional) by dividing the number of fields in which each species was present by the total number of fields sampled. In addition, the root rot incidence for each management system was calculated as the percentage of fields with mean disease severity score greater than 3 i.e., roots with clearly visible symptoms (Figure 2).

In the analysis of the isolation frequencies of individual fungal species associated with faba bean roots, rare species (i.e., <2% of total isolations) were not considered. To determine if the isolation frequencies were affected by the management system or sampling year, a generalized linear mixed model analysis was performed on proportional data with a binomial distribution and logit link function (Brooks et al., 2017). Fields were used as random effects, and to account for the two sampling areas within each field, sampling replicates were nested within. In data analyzed across sampling years, year was also used as random effect. Prevalence of fungal species and root rot incidence (the proportion of fields with mean disease severity ratings > 3; Chatterton et al., 2019) were treated as binary data (presence/absence) and were analyzed with Bayesian generalized linear model and logit link function (package 'arm', Su et al., 2018). The goodness of fit of the models was assessed using Pearson chi-square residual tests and further verified by the Kolmogorov–Smirnov test of normality and by checking if the data contain potentially significant outliers (package 'DHARMa', Hartig, 2021). Data were also visually inspected for normality by plotting the Pearson residuals against the expected values (package 'ggplot2', Wickham, 2016). The significance of the main effects in generalized linear models was assessed using an ANOVA function with the type III margin sum of squares (package 'arm'). If significant treatment effects were observed, comparisons of least squares means with Tukey's correction across the effect levels were performed ($P < 0.05$) (package 'lsmeans', Lenth, 2016).

Root rot severity data were analyzed with the non-parametric ranking procedure of the Kruskal-Wallis test (Conover, 1999) using the package 'agricolae' (Mendiburu, 2014). Management system and/or year were included as main explanatory variables. If significant treatment effects were observed ($P<0.05$), mean rank values were separated with the Kruskal multiple comparison test. For both, Kruskal-Wallis test and Kruskal multiple comparison test, the Benjamini and Hochberg (Benjamini and Hochberg, 1995) stepwise adjustment of P-values was used to control false discovery rate (FDR) and reduce type I errors.

The relationship between frequencies of individual fungal species and root rot incidence data including pedo-climatic, crop rotation and yield effects were examined using path analysis (package 'lavaan', Rosseel, 2012). Prior to the analysis, highly correlated environmental variables (Pearson $r \geq \pm 0.7$) were removed. Data were then subjected to the stepwise forward selection procedure (package 'stats', R Core Team, 2013) and only significant variables were retained in the path analysis. In addition, distinct soil clusters of the sampled fields were used as entries clustered based on their similarities in soil abiotic properties (sand, silt, clay, soil organic matter content and pH) employing the hierarchical clustering on principle components (HCPC) (package 'FactoMineR', Lê et al., 2008).

Results

Environmental conditions of the fields sampled

The 110 organic and conventional faba bean fields sampled represented a wide range of environments with respect to soil and climatic conditions (Table 1). Organic and conventional fields were placed in soil types ranging from sandy to loamy; large variation in soil organic matter (SOM) contents and moderate ranges in pH were present in organic and conventional fields.

Sowing conditions ranged from very wet (up to 59 mm of rain in the 2 weeks before sowing) to no rain during the same period and, from very cold soils (minimal mean temperature two weeks before sowing -3.8°C) to very warm (maximal mean temperature before sowing 13.8°C). The driest conditions were observed in the year 2018 with a field receiving as little as 21 mm, the wettest in 2016 with a field that received 517 mm of rain between sowing and sampling (Table 1 and Supplementary Table 1).

10.3389/fpls.2022.1009906

TABLE 1 Range of pedo-climatic conditions for the faba bean fields sampled from 2016-2019.

	Organic (N=53)[a]			Conventional (N=57)		
Parameter	**Minimum**	**Maximum**	**Median**	**Minimum**	**Maximum**	**Median**
% sand	0.15	78.0	21.3	3.5	61.0	16.3
% silt	16.8	76.9	53.7	28.6	75.2	59.7
% clay	3.8	48.0	21.65	10.4	54.4	19
pH	5.1	7.3	6.55	5.9	7.3	6.7
Soil organic matter content (SOM)	1.5	4.9	2.6	1.8	4.8	2.6
Precipitation mm (14 days prior to sowing)	0	59	13.5	0	44	15
Precipitation mm (sowing-sampling)	21	517	167.6	48	327	174.6
Average temp. °C (01. Jan-sowing)	-0.4	5.5	2.3	0.0	4.8	2.3
Number of days <0° in March	0	10	0	0	11	0
Average temp. °C (14 days prior to sowing)	-3.8	9.7	6.4	-2.0	13.6	6.2
Average temp. °C (sowing-sowing + 14 days)	3.2	14.8	7.9	1.6	14.7	8.2
Average temp. °C (sowing-sampling)	7.1	16.8	13.3	10.1	17.3	12.8
Temp. sum °C (sowing-sampling)	902	1788	1316.2	959	1567	1309.7
Cereals (5 year history)[b]	1	5	3	0	5	3
Grain legumes (5 year history)[c]	0	2	0	0	1	0
Distance (grain legume crop)[d]	1	≥11	3	2	≥11	11

[a] N=Number of fields.
[b] Number of cereals grown during the 5 years preceding the sampling.
[c] Number of times grain legumes were grown during the five years preceding the sampling.
[d] Number of years since a grain legume crop was grown in the field prior to the sampling. No data beyond 11 years were available.

The hierarchical clustering of faba bean fields on principal components (HCPC) based on their similarities in soil parameters *i.e.* soil pH, sand, silt, clay and organic matter content (SOM) grouped the 110 faba bean fields into three clusters (cluster I, II and III) (Figure 3). The first two dimensions of the PCA summarized 77% of the variability in the data. Dimension 1 explained 50.6% of the variance and separated fields in cluster I from fields in clusters II and III based on their differences in soil pH values, sand and silt content. Dimension 2 explained 26.8% of the variance and separated the clusters mainly based on their differences in SOM content, which was also positively correlated with the soil clay content (e.g. cluster III) (Figure 3 and Table 2). The PCA dimension 3 explained an additional 14.9% of the variability in the data and was most strongly related to the pH (not shown).

Cluster 1 included 12 organic and 8 conventional fields classified as sandy loam and characterized by lower pH (around 6.0) compared with the clusters II and III (around 6.7), and

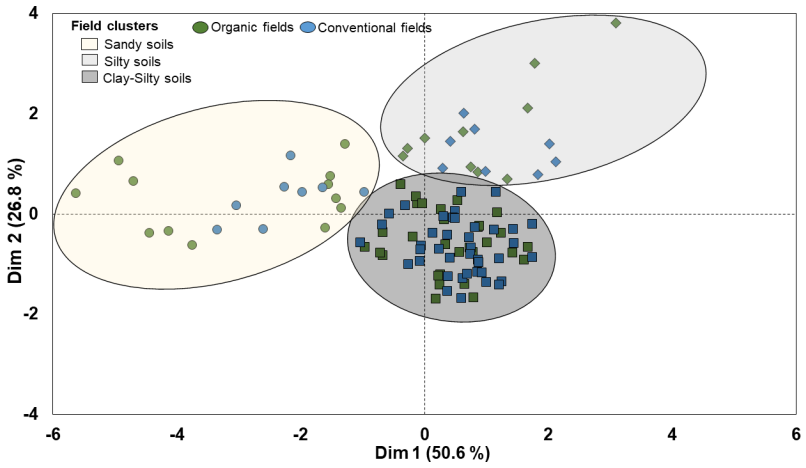

FIGURE 3
Cluster analysis for 110 organic and conventional faba bean fields based on their similarities in soil abiotic properties.

10.3389/fpls.2022.1009906

TABLE 2 The number of organic and conventional fields in each year, grouped by their similarities according to soil abiotic properties.

System	Cluster	Year[a]				N[b]	N[c]	SOM (%)[d]	pH	Clay (%)	Sand (%)	Silt (%)
		2016	2017	2018	2019							
Organic	I	4	4	2	2	12	218	2.3	6.0	12.1	55.6	32.3
	II	5	7	9	9	30	508	2.4	6.7	21.1	17.5	61.4
	III	3	3	5	0	11	220	3.7	6.4	31.4	18.2	50.4
Conventional	I	1	3	2	2	8	140	2.4	6.2	15.9	48.0	36.1
	II	10	10	8	12	40	675	2.6	6.8	18.8	16.2	65.0
	III	3	2	4	0	9	178	3.6	6.8	32.7	14.4	53.0

[a] Number of fields sampled in 2016, 2017, 2018 and 2019.
[b] N= Total number of fields.
[c] n=Number of roots evaluated.
[d] Mean value of soil organic matter content.

mean SOM content of 2.3% and 2.4% in organic and conventional fields, respectively (Figure 3 and Table 2). Cluster II included 30 organic and 40 conventional fields associated with silty soils with higher pH (around 6.7) but similar SOM content as cluster I (Figure 3 and Table 2). Cluster III included 11 organic and 9 conventional fields. It included silty clay soils but with higher clay and SOM (around 3.6%) contents than cluster II (SOM ca. 2.4%) (Figure 3 and Table 2).

Cropping histories

Across all fields for the 5-year period prior to the faba bean sampling, approximately 26% of the crops in rotations under organic management were legumes. Of these, approximately 70% were clover and alfalfa and about 30% grain legumes (mainly peas and faba beans - see below; hereafter grain legumes). In contrast, legumes in conventional fields constituted only about 5% of the crops in the 5-year rotation plan. The ratio of cereals in organic and conventional crops rotations was similar and accounted for 57% (organic) and 68% (conventional) of all crops. Overall frequencies of legumes and cereals for the 11-year period in both management systems was similar to the 5 year rotation plan (Supplementary Table 5).

In the organic fields, 37 out of the 52 (71%) fields for which data were available had been cropped with legumes either as main or cover crops during the past five years (Figure 4A). Clover and alfalfa had been grown in 32 (62%) fields usually for one to two years and grain legumes in 17 (32%) fields for one or two seasons. Also, cereals were part of the rotation during the preceding 5-years usually for two to three seasons (73% of the organic fields; Supplementary Table 6). In contrast, 43 (75%) of the conventional fields had not been planted to any legume in the preceding 5 years (Figure 4A). Twelve of the remaining 14 fields (25%) had been planted once with faba bean, one with pea during that period and one with small seeded legumes. Most

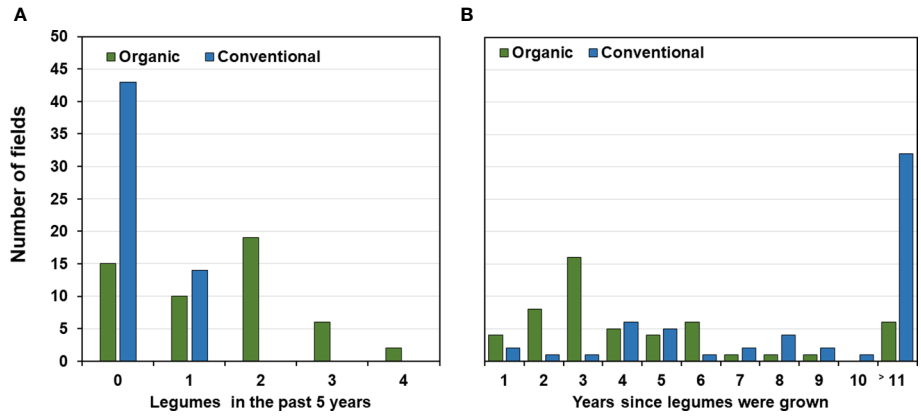

FIGURE 4
Ratio of legumes in organic and conventional crop rotations. **(A)** Number of fields and years since legumes were grown before the faba bean sampling. No information available for 11 or more years. **(B)** Number of fields depending on the frequency of legumes planted for the five-year period preceding the faba bean sampling.

rotations (48 out of 57 fields; 84%) included three or four years of cereals and five fields even 5 years while one conventional field had not been grown to cereals (Figure 4B and Supplementary Table 6). When considering the past 11 years prior to faba bean sampling, almost all organic farmers had grown legumes at least once while 32 of the 57 conventional farmers had not grown legumes during the least 11 years or longer (Figure 4B).

Root rot incidence and root health status

Overall disease severity ratings (DSR) did not significantly differ between management systems (mean DSR of 2.6 and 2.0 for organic and conventional system, respectively) or among years (P≥0.28). However, there was a difference in the proportion of organic and conventional fields with clearly visible symptoms of root rot (i.e. root rot incidence, mean DSR>3). Faba bean plants from 18 out of 53 organic fields (34%) had mean DSR>3, significantly (P=0.03) more than in the conventional fields (9/57, 16%) with some variation among years (Table 3). Nevertheless, even in the organic fields, mean root rot severity was usually just above the threshold level of 3 with no significant difference in overall root rot symptom severity between the management systems (fields with mean DSR>3; Table 3).

Among the years, the highest root rot incidence in both management systems was recorded in 2016 (58% organic and 36% conventional fields), followed by 2018 (50% organic and 29% conventional fields). In 2017, all roots collected from conventional fields showed no visible symptoms of rot (mean DSR<3) whereas roots collected from 21% of the organic fields were symptomatic (mean DSR>3). In 2019, all roots collected from both management systems appeared healthy (mean DSR<3).

Fungal species associated with root infections

Out of a total of 2175 roots analyzed over the four years, 1939 yielded fungal isolates. A total of 4213 *Fusarium* and 490 *Didymella*- like isolates were obtained from the 110 fields. Of these, 49.7% (n=2093) of the *Fusarium* and 91.8% (n=450) of the *Didymella* isolates originated from organically managed fields (N = 53 fields; n = 946 roots), whereas the remaining 50.3% (n=2093) *Fusarium* and 8.2% (n=40) *Didymella* isolates were obtained from conventional fields (N=57; n=993).

Combined over years and management systems, members of the *Fusarium oxysporum* species complex (FOSC; 36% colonized roots), *F. redolens* (34%), members of the *F. solani* species complex (FSSC; 27%) and *F. avenaceum* (23%) were the most frequent. Together, they constituted 74% of all isolates recovered, and occurred in 82 to 94% of the fields. The next most frequent *Fusarium* species were *F. tricinctum*, *F. culmorum* and *F. equiseti* which were isolated from 6% (*F. equiseti*) to 11% (*F. tricinctum*) of the roots. *Didymella pinodella* was recovered from 17% of all roots, but occurred mainly in organic fields with overall isolation frequency of 31%. The latter four species together represented 23% of all isolates recovered and were found in 44 to 54% of the fields over the years. Species isolated at frequencies ≤ 2% included seven *Fusarium* and one *Didymella* spp.: *F. acuminatum, F. graminearum, F. crookwalance, F. torulosum, F. sporotrichioides, F. sambucinum, F. flocciferum* (Šišić et al., 2020) and *D. eupyrena (*syn. *Juxtiphoma eupyrena).*

Across years, frequencies of *F. redolens* and *D. pinodella* were significantly higher in roots from organic fields than from conventional fields. In contrast, *F. avenaceum*, *F. tricinctum* and *F. culmorum* more frequently colonized roots in conventionally managed fields (for all comparisons P < 0.01). Overall mean isolation frequencies of the species within the *F. oxysporum* and the *F. solani* species complexes and the mean isolation frequencies of *F. equiseti* did not differ significantly between the management systems (Figure 5A).

With few exceptions, the trends observed over the years were similar within years (Table 4). For example, during 2016-2018, *F. redolens* was more common in organically grown faba beans roots (31 to 66%) compared with conventionally grown faba beans (17 to 44%) while in 2019, the species occurred only rarely in either management system. *Didymella pinodella* varied

TABLE 3 Mean root rot incidence (%) and root rot severity ratings (DSR) of faba bean fields in Germany, 2016-2019.

	Organic				Conventional				Overall	
Sampling year	**2016**	**2017**	**2018**	**2019**	**2016**	**2017**	**2018**	**2019**	**Organic**	**Conventional**
Root rot incidence (%)	58 a	21 bcd	50 ab	0 d	36 abc	0 d	29 abcd	0 d	34 a	16 b
Root rot severity[a]	3.9 ns	3.7	3.9	-[d]	3.6	–	3.6	–	3.9 ns	3.6
N[b]	12	14	16	11	14	15	14	14	53	57
n[c]	236	274	320	220	273	293	279	280	1050	1125

[a]Mean root rot severity for fields which that had DSR > 3.
[b]N, total number of sampled fields.
[c]n, total number of roots evaluated for severity of root rot symptoms.
Among years, means in a row followed by different letters do not significantly differ (Tukey-adjusted LSMeans comparisons for incidence data; Kruskal post hoc test for disease severity data (P < 0.05)).
[d]All roots sampled in organic fields 2019 and conventional fields in 2017 and 2019 appeared healthy (DSR < 3).

10.3389/fpls.2022.1009906

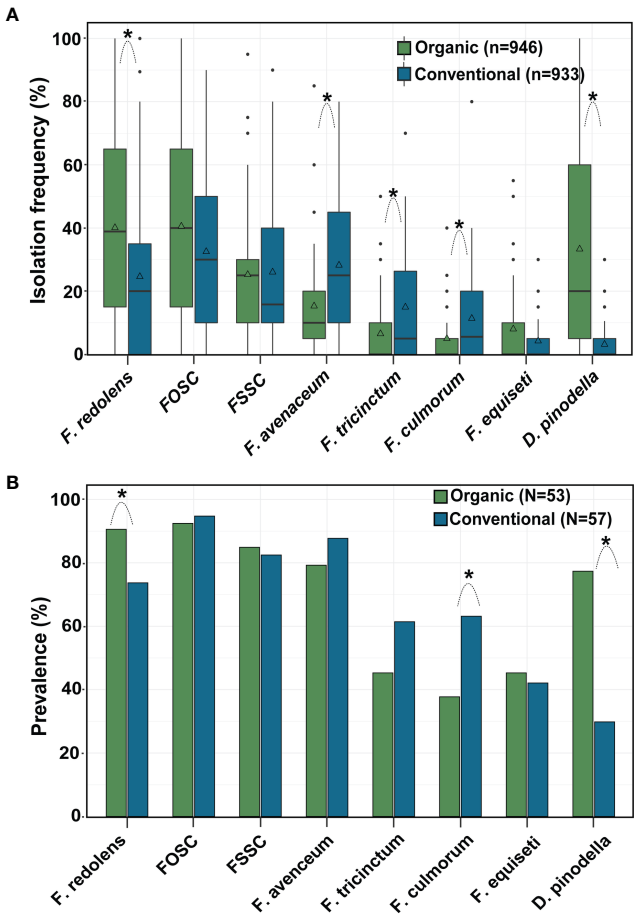

FIGURE 5
Effect of management system on **(A)** isolation frequency (%) and **(B)** prevalence (% fields yielding a given species) of the eight most common fungal species recovered from faba bean roots. Asterisks indicate significant differences ($P < 0.05$) between organic and conventional fields for each fungal species separately (Tukey-adjusted pairwise LSMeans comparisons). n = number of roots, N = number of fields evaluated. The horizontal line in the boxplot shows the median value, the bottom and tops of the box the 25th and 75th percentiles and the vertical lines the minimum and maximum values, outliers as single points. Mean values are marked with triangles.

considerably in frequency among organic fields depending on the year (15 to 51%) but was consistently low in conventional fields (≤ 6%) (Table 4).

Fusarium avenaceum, *F. tricinctum* and *F. culmorum* isolation frequencies varied greatly among years with the latter two species occurring generally less frequently in both management systems (11 to 37% for *F. avenaceum* vs 2 to 21% for *F. tricintum*, and 2 to 16% colonized roots for *F. culmorum*). *Fusarium equiseti* was recovered at low frequencies in both growing systems (2-16%) (Table 4) while members of the FOSC and the FSSC were common in isolation frequencies among years and between management systems (Table 4).

Pathogen prevalence, *i.e.* the percentage of fields in which the pathogens occurred, followed a similar pattern to the isolation frequencies (Figure 5B). Across years, *F. redolens* and *D. pinodella* were more prevalent (P=0.0018) in organic fields (91% for *F. redolens* and 77% for *D. pinodella*) compared with conventional fields (74% for *F. redolens* and 30% for *D. pinodella*) (Figure 5B and Table 5). Presence of *F. redolens* was considerably lower in conventional fields in 2016 and 2019, while in 2017 and 2018, the prevalence rates of *F. redolens* in organic and conventional fields were more similar (Table 5). The prevalence patterns of *D. pinodella* were more variable. Predominantly occurring in organic systems, this species showed moderate to high prevalence rates over the years ranging from 63% (2018) to 93% (2017). In conventional systems, the highest *D. pinodella* prevalence rate was observed in 2017 (47%), the lowest also in 2018 (14%) (Table 5).

Although isolated more frequently from roots collected from conventional fields, the overall prevalence rates of *F. avenaceum* and *F. tricinctum* did not differ significantly between the management systems (Figure 5B). The prevalence of

10.3389/fpls.2022.1009906

TABLE 4 Variation in isolation frequencies (%) of the eight most common fungal species recovered from faba bean roots separated based on sampling year and management system.

System	Year	N[a]	n[b]	*F. redolens*	*F. oxysporum*	*F. solani*	*F. avenaceum*	*F. tricinctum*	*F. culmorum*	*F. equiseti*	*D. pinodella*
Organic	2016	12	240	41.3 ab	40.4 ns	30 ab	20.0 ab	5.0 ab	7.9 ab	16.3 a	15.0 abc
	2017	14	279	30.8 bc	35.1	21.1 ab	17.2 ab	14.0 a	3.6 ab	8.2 ab	40.9 a
	2018	16	317	65.6 a	44.5	32.8 ab	11.4 b	1.9 b	1.9 b	2.2 b	28.7 ab
	2019	11	110	13.6 d	41.8	14.5 ab	13.6 ab	5.5 ab	8.2 ab	7.3 ab	50.9 a
Conventional	2016	14	280	17.1 c	29.6	31.1 ab	37.1 a	21.4 a	9.3 ab	5.0 ab	2.5 cd
	2017	15	298	20.5 bc	28.9	19.1 ab	26.8 ab	11.7 ab	10.4 ab	3.7 ab	2.7 cd
	2018	14	275	44.0 ab	32.0	42.2 a	28.7 ab	7.6 ab	9.5 ab	3.3 ab	1.8 d
	2019	14	140	17.1 bc	40.0	12.1 b	20.7 ab	19.3 a	16.4 a	5.0 ab	5.7 bcd
Overall % colonized roots				34.1	35.8	27.2	22.6	10.6	7.7	6.1	16.8

[a]Number of fields.
[b]Number of roots evaluated.
Means within column (for each species across the years) followed by different letters indicate significant differences ($P < 0.05$) in single species isolation frequencies across management systems and years (Tukey-adjusted multiple LSMeans comparisons). ns = Non-significant.

F.culmorum was significantly higher in conventional fields (63%) than in organic (38%) as observed for isolation frequencies.

For the members of the FOSC and FSSC, some variability in the proportion of positive fields was observed similar to the isolation frequencies, but these differences were not significant between the management systems over the years (Figure 5B) or during any single year (Table 5). Members of the FOSC were consistently found in more than 80% of the fields. The proportion of FSSC positive fields ranged from 64 to 93%. *Fusarium equiseti* prevalence rates varied between 19 and 75% depending on year and growing system (Table 5).

Phylogeny

Phylogenetic analyses inferred from the *TEF1 alpha* gene sequences resolved the phylogenetic positions of the 35 FOSC and 33 FSSC isolates studied in relation to currently recognized species in both species complexes (Figures 6, 7). Both the members of the FOSC and the FSSC varied greatly in morphology, which was reflected in high genetic variability, particularly for the members of the FOSC. Based on the single locus phylogeny, the 35 FOSC isolates were distributed throughout the FOSC clade and belonged to 9 different lineages. The most abundant group comprising 17 isolates was placed in the *F. libertatis* lineage. The second most abundant group, represented by 6 isolates, did not cluster clearly with any of the recently described species within the FOSC. These were most closely related to the previously assigned *F. oxysporum* special form *conglutinans* (NRRL 36364). The results of the *TEF1 alpha* tree topology further revealed 4 isolates matching recently erected epitype specimen (Lombard et al., 2018) and 3 isolates were placed in *F. odoratissimum* linages. In addition, single isolates were placed in the *F. nirenbergie, F. hodiae, F. fabacearum/F. calistephi, F. curvatum* and *F. commune* lineages (Figure 6).

TABLE 5 Variation in prevalence (% of fields) of the eight most common fungal species recovered from faba bean roots separated based on sampling year and management system.

System	Year	N[a]	n[b]	*F. redolens*	*F. oxysporum*	*F. solani*	*F. avenaceum*	*F. tricinctum*	*F. culmorum*	*F. equiseti*	*D. pinodella*
Organic	2016	12	240	100 a	92 ns	92 ns	100 a	42 ab	58 ab	75 a	75 ab
	2017	14	279	86 ab	93	86	79 ab	79 a	50 abc	57 ab	93 a
	2018	16	317	100 a	88	94	63 b	25 b	19 c	19 c	63 abc
	2019	11	110	73 abc	100	64	82 ab	36 b	27 bc	36 abc	82 ab
Conventional	2016	14	280	57 bc	100	86	93 a	86 a	64 ab	57 ab	29 cd
	2017	15	298	87 ab	80	80	93 ab	53 ab	80 a	40 abc	47 bcd
	2018	14	275	100 a	100	93	93 ab	50 ab	43 bc	43 abc	14 d
	2019	14	140	50 c	100	71	71 ab	57 ab	64 ab	29 bc	29 cd

[a]Number of fields.
[b]Number of roots evaluated.
Means within column (for each species across the years) followed by different letters indicate significant differences ($P < 0.05$) in single species prevalence rates across management systems and years (Tukey-adjusted multiple LSMeans comparisons). ns = Non-significant.

10.3389/fpls.2022.1009906

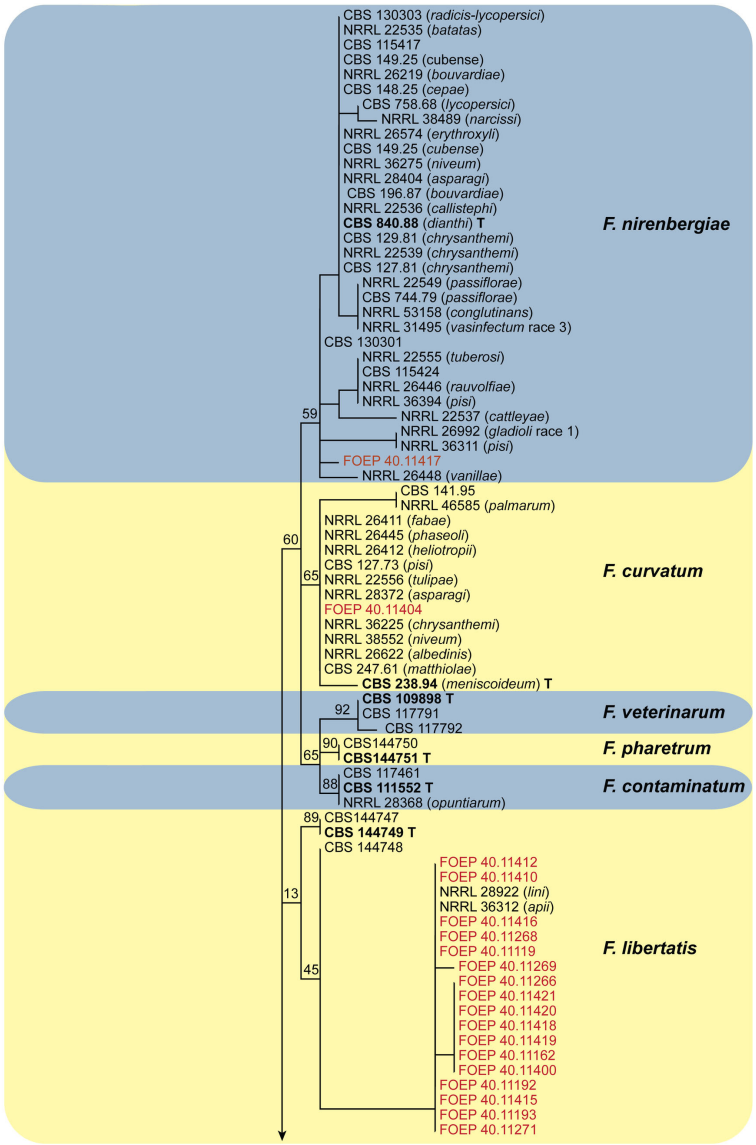

FIGURE 6 (Continued)

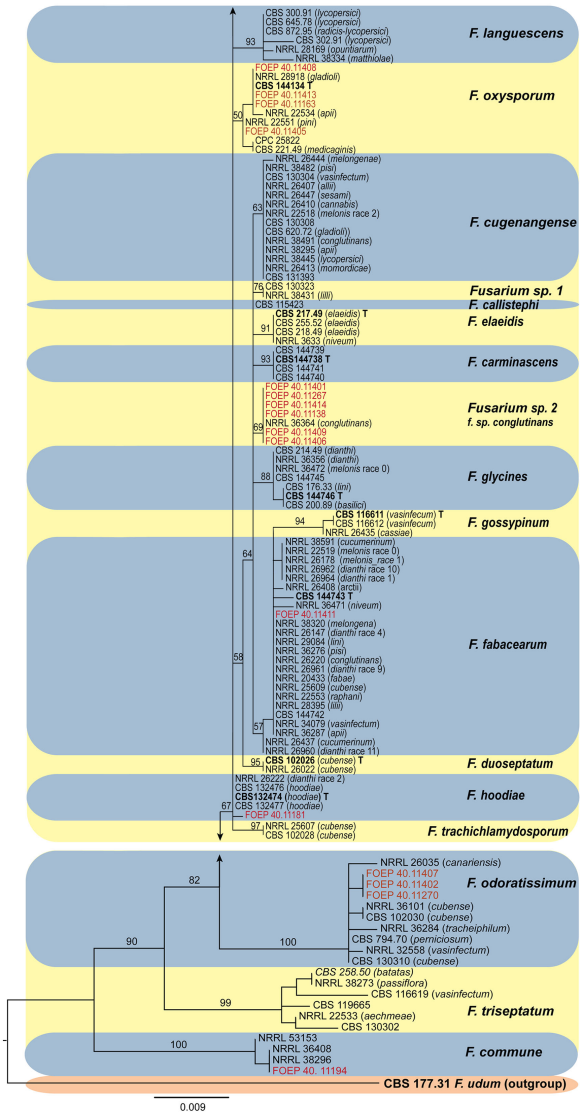

FIGURE 6 (Continued)
The maximum likelihood (RAxML) tree inferred from the partial *TEF1 alpha* gene sequence alignments of the *Fusarium oxysporum* species complex isolates (FOSC) used in this study. Isolates (i.e. FOEP) are indicated in red. Epi- and ex-type strains are indicated in bold and superscript 'T' (Lombard et al., 2018). The scale bar indicates 0.009 expected changes per site. The tree is rooted to *F. udum* (CBS 177.31).

The 33 FSSC isolates were placed into three different lineages, all nested within clade 3. Most isolates (n=29) matched *F. pisi* (syn. *F. solani* f. sp *pisi*), the lineage recently renamed to *Fusarium vanettenii* (Geiser et al., 2021). A group of 3 isolates were placed in the *Fusarium solani* sensu stricto lineage, and one isolate matched *F. breviconum* (Figure 7).

Major factors influencing pathogen frequency and faba bean yield

The overall path model from stepwise regression showed a good fit with the data for both organic and conventional fields (Supplementary Table 8). In organic fields, yield correlated negatively with *D. pinodella* (β = -0.42) and *F. redolens* (β = -0.40) frequencies and positively with *F. tricintum* in faba bean roots (β = 0.33). In conventional fields, weak but significant negative correlations between yield and FOSC (β = -0.20) and *F. culmorum* (β = -0.21) were found. Additionally, yield correlated positively with the total precipitation before sowing (β = 0.27) and in particular the total precipitation from sowing to root sampling (β = 0.48) for conventional faba bean. Overall, these variables accounted for approximately 40% of the yield variation in both management systems (Supplementary Table 7).

The frequencies of *F. redolens* in both management systems were positively correlated with the number of days below zero in March (i.e. colder conditions at sowing and plant emergence: path coefficients for organic/conventional system, β = 0.44/0.50) and the average temperature measured for the period from sowing to root sampling (β = 0.62/0.42). Following this pattern, in organic fields *F. redolens* frequencies was correlated negatively with the average

10.3389/fpls.2022.1009906

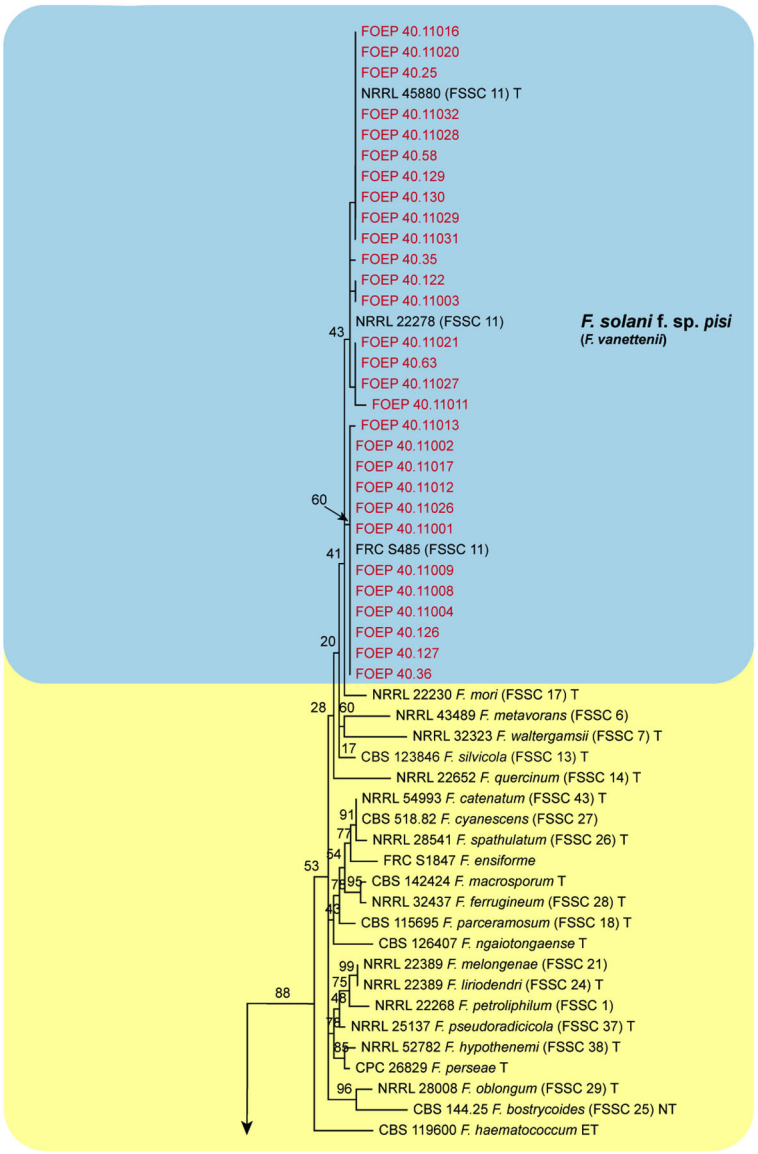

FIGURE 7 (Continued)

temperature two weeks before sowing (β = -0.30). In addition, the frequency of cereals in the preceding five years before sampling (β = 0.24) and silty soils (β = 0.22) was associated with this pathogen. Cumulatively, these variables explained 55% and 25% of variation in *F. redolens* frequencies in organic and conventional systems, respectively (Table 6 and Supplementary Table 7).

The FOSC in both management systems was positively correlated with sandy, slightly acidic soils (β = 0.52/0.43). In organic fields, FOSC frequencies correlated positively with the number of days below 5°C two weeks after sowing (β = 0.46), the total precipitation from sowing to two weeks after (β = 0.21) and the average temperature from sowing to root sampling (β = 0.24). Thus, wet and colder conditions up to plant emergence followed by higher temperatures during the main growing season favored this pathogen complex in organic fields similar to what was observed for *F. redolens*. In conventional fields, in

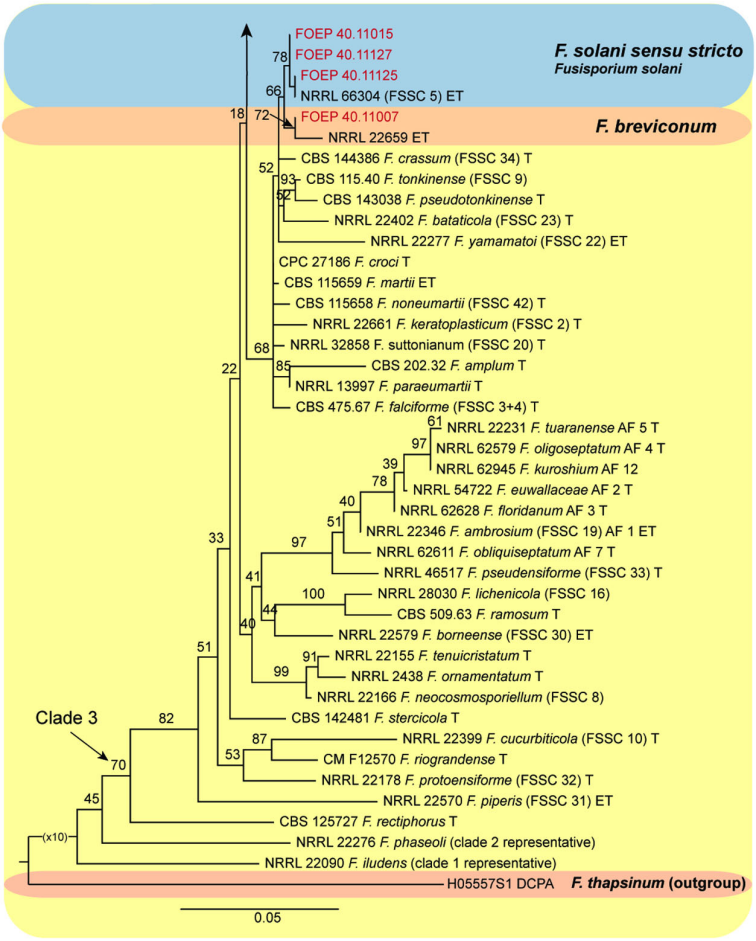

FIGURE 7 (Continued)
The maximum likelihood (RAxML) tree inferred from the partial *TEF1 alpha* gene sequence alignments of the *Fusarium solani* species complex isolates (FSSC) used in this study. Isolates (i.e. FOEP) are indicated in red. Epi- and ex-type strains are indicated in bold and superscript 'T' (O'Donnell et al., 2020; Geiser et al., 2021). The scale bar indicates 0.05 expected changes per site. The tree is rooted to *F. thapsinum* (H05557S1 DCPA).

addition to the observed correlation with sandy soils, the FOSC frequencies were favored by higher temperatures early in the year (January to sowing; β = 0.30). Together, these variables explained 46% and 26% of the FOSC total variance in organic and conventional fields, respectively (Table 6 and Supplementary Table 7).

Similar to *F. redolens* and to the FOSC in organic systems, colder conditions at sowing and/or plant emergence correlated positively with the FSSC frequencies (in conventional system: positive correlation with the number of days below zero in March, β = 0.32; in organic system: negative correlation with the average temperatures from January to sowing, β = -0.32). The analysis also indicated that low precipitation in the period of plant emergence (from sowing to 2 weeks after; β = -0.28) and growing faba bean in clay soils (β = 0.31) enhanced FSSC root colonization rates in conventional but not organic fields. Together, these variables explained 10% and 34% of the FSSC total variance in organic and conventional fields, respectively (Table 6 and Supplementary Table 7).

For *F. tricinctum*, 11% of the variance in organic fields was explained by the negative correlation with number of days below 5°C two weeks before sowing (β = -0.33), i.e. warmer conditions before sowing favored it. In conventional systems this effect was opposite (β = 0.34). In addition, the lower precipitation two weeks before sowing (β = 0.23) explained 20% variation in the species root colonization rates data (Table 6 and Supplementary Table 7).

The frequencies of *F. culmorum* in both management systems correlated negatively correlated with the average temperature measured for the period from sowing to root sampling (β = -0.28/-0.49). In conventional fields only, there was also a negative correlation of *F. culmorum* frequencies with the total precipitation 4 weeks prior to sowing (β = -0.27) and from sowing to root sampling (β = -0.38) i.e. colder and drier conditions favored this pathogen. Together, these variables explained 11% and 18% of the *F. culmorum* total variance in organic and conventional fields, respectively (Table 6 and Supplementary Table 7).

10.3389/fpls.2022.1009906

TABLE 6 Summary of the path analysis results showing the main environmental and cropping history factors affecting abundance (isolation frequencies) of major fungal species in roots of organically (Org.) and conventionally (Conv.) grown faba beans.

	Temperature		Precipitation		Crop rotation		Soil		% variance explained	
	Org.	Conv.	Org.	Conv.	Org.	Conv.	Org.	Conv.	Org.	Conv.
F. redolens	+ early cold[1] + warm season[2]				+ cereals		+ silty soils		55	25
FOSC	+ early cold + warm season	- early cold	+ early wet[3]				+ sandy soils		46	26
FSSC	+ early cold			- early wet				+ clay soils	10	34
F. tricinctum	- early cold	+ early cold		- early wet					11	20
F. culmorum	+ cool season[2]			- early wet + dry season[4]					11	18
F. avenaceum	+ cool season								9	
F. equiseti	+ cool season		+ early wet		+ cereals				18	
D. pinodella	- early cold			+ early wet + dry season	+ legumes	- cereals			33	37

[1]+/- early cold: positive (+) or negative (-) correlation with Average temp. °C (Jan-sowing) and/or, Number of days < 5°C (14 days prior to sowing-sowing) and/or, Number of days <0° in March and/or, Average temp. °C (14 days prior to sowing-sowing) and/or, Number of days < 5°C (sowing-14 days after).
[2]+ warm season: positive correlation with Average temp. °C (sowing-root sampling); +cool season: negative correlation with Average temp. °C (sowing-root sampling).
[3]+/- early wet: positive (+) or negative (-) correlation with Precipitation sum (mm) (28 days prior to sowing-sowing) and/or, Precipitation sum (mm) (14 days prior to sowing-sowing) and/or, Precipitation sum (mm) (sowing-14 days after).
[4]+dry season: negative correlation with Precipitation sum (mm) (sowing-root sampling).
Positive correlations are indicated with '+' and indicate increase in isolation frequencies of a fungal species. Negative correlations are indicated with '–'. The original output of the path analysis with standardized path coefficients are given in Supplementary Table 7.

The frequencies of *F. avenaceum* and *F. equiseti* could not be related to any of the environmental factors or the cropping history in conventional systems. In organic systems, isolation frequencies of both species correlated negatively with total temperature between sowing and root sampling (*F. avenaceum/F. equiseti*; β = -0.31/-0.27). In addition, *F. equiseti* was correlated negatively with the total precipitation two weeks after sowing (β = -0.27; as the FSSC) and positively with the frequency of cereals in the preceding five years (β = 0.30) similar to *F. redolens*. These variables together explained 9% and 18% of the variation in the *F. avenaceum* and *F. equiseti* data, respectively (Table 6 and Supplementary Table 7).

Didymella pinodella in organic fields was positively correlated with frequencies of cool season grain and small seeded legumes in the preceding five years before sampling (β = 0.47) and clover and alfalfa for the same period (β = 0.31). Conversely, in conventional systems, the frequencies of cereals in the preceding five years before sampling negatively affected *D. pinodella* root colonization rates (β = -0.45). Also, *D. pinodella* frequencies were negatively associated with the number of days below zero in March (conventional system: β = -0.47) and the number of days below zero 2 weeks prior to sowing (organic system: β = -0.27) i.e. opposite to *F. redolens* and FOSC. In conventional systems, *D. pinodella* frequencies were also positively correlated with the total precipitation during the 14 days after sowing (β = 0.44) but negatively with the total precipitation from sowing to root sampling (β = -0.42) i.e. warmer and wetter conditions at sowing/plant emergence followed by drier growing seasons favored this pathogen in conventional fields. The model explained 33% and 37% of the species variation in organic and conventional system, respectively (Table 6 and Supplementary Table 7).

Discussion

Root rot incidence was generally low in both management systems especially in 2017 and 2019 when precipitation prior to sowing was low followed by dry growing seasons. Among the 14 *Fusarium* and two *Didymella* species identified, the *F. oxysporum* (FOSC) and *F. solani* (FSSC) species complexes, *F. redolens*, and *F. avenaceum* were present in 82 to 94% of the fields and were most abundant, accounting for 74% of all isolates recovered. Less frequently found *Fusarium* spp. included *F. tricinctum*, *F. culmorum* and *F. equiseti*. The species *D. pinodella* occurred in moderate abundance in organic fields but was much less frequent in conventional fields. *Fusarium redolens* was also more common in roots from organic fields compared with conventional fields. In contrast, *F. avenaceum*, *F. tricinctum* and *F. culmorum* occurred more frequently in conventionally managed fields. Faba bean roots were colonized at similar rates by FOSC, FSSC and *F. equiseti* in both management systems.

There was no difference in the composition nor the frequencies (% colonized roots) of the fungal species in symptomatic and asymptomatic faba bean roots. There were also no effects of the management system (organic vs conventional) on the spectrum of pathogens isolated.

Cropping system effects were intricately connected with differences in cropping histories as conventional systems had been devoid of legumes for at least five years in most cases. Cropping history affected the isolation frequencies of a number of species.

The low levels of root rot symptoms observed in some fields may have been due to other factors not assessed in this study. This could have included the presence of other pathogens such as *Pythium* or *Rhizoctonia* spp. (Esmaeili Taheri et al., 2017; Chatterton et al., 2019; Wille et al., 2019) and/or adverse abiotic soil properties such as elevated levels of Fe and Mn contents in the soil which are contributing factors in development of root rot disease (Nayyar et al., 2009). Soil-borne pathogens need to reach a threshold population within the root before causing visible disease symptoms (Gu et al., 2022) and cultural methods fail to reflect pathogen densities in roots. Also, a given root is often colonized by multiple fungal species simultaneously and competitive interactions may have played a role in the generally low symptom expression. For example, we have previously shown that co-occurrence of *F. equiseti* and highly aggressive strains of *F. avenacem* and *D. pinodella* in pea roots can almost completely neutralize detrimental effects of these pathogens (Šišić et al., 2017). Similarly, other beneficial members of root associated microbial communities such as arbuscular mycorrhizal fungi are also known for their ability to reduce biotic stresses (Wille et al., 2019). It is unknown to what extent such interactions played a role in symptom expression. This could be evaluated using, for example, quantitative real-time PCR (qPCR). While qPCR assays targeting all major *Fusarium* species identified in this study including the qPCR for detection and quantification of *D. pinodella* have been developed recently (Zitnick-Anderson et al., 2018; Šišić et al., 2022), these assays were not available when this study was initiated. This study provides solid foundation to further analyze the nature of interactions among the major fungal species isolated as the success of qPCR depends on prior knowledge of the pathogen population targeted. Despite the limitations resulting from the culture based identifications used in our study, taken together, our results indicate a generally high tolerance of faba beans to major root rot pathogens of grain legumes which are a common part of the root microflora of this crop.

Yield effects

The lack of a clear association between root rot incidence and the major pathogens identified in this study and between root rot incidence and faba bean yield is in line with previous reports pointing to the ability of legume associated *D. pinodella* and *Fusarium* spp. (Rodriguez et al., 2009; Šišić et al., 2018b; Šišić et al., 2022) to infect various hosts without causing visible root rot disease symptoms. Nevertheless, path analysis indicated significant negative correlations of *D. pinodella* and *F. redolens* with yield in organic systems, and significant negative yield effects of FOSC and *F. culmorum* in conventional systems. These results are in line with the hypothesis that there are rarely neutral biological interactions (Schulz and Boyle, 2005). Thus, asymptomatic plant infections likely result from mutually balanced antagonisms between a plants defense system and pathogen virulence factors (Schulz and Boyle, 2005). The positive association of pathogen frequencies with yield reductions in this study could reflect a need for higher investment of the faba bean to maintain a balanced antagonism with the aforementioned pathogens (i.e. absence to low levels of root rot), resulting in lower yields. We have recently demonstrated that *D. pinodella* is highly aggressive on pea causing symptoms and biomass reductions. In contrast, it can colonize wheat roots without causing visible disease symptoms while reducing wheat biomass (Šišić et al., 2022). This is the first instance where predominantly asymptomatic root infections by this pathogen appear to be negatively associated with faba bean yield. The fact that this negative correlation occurred only in organic systems is a result of the differences in rotational history between the management systems as this pathogen was inseparably connected with the frequency of legumes in rotation which constituted only about 5% of the crops in conventional fields compared to 26% of the crops in organic fields (Figure 4 and Supplementary Table 5).

Fusarium redolens is commonly isolated from diseased roots of different grain legumes, however its role in the root rot complex is not fully understood. For example, Booth (1971) reported that this pathogen was wide spread in temperate regions causing damping-off, wilts and cortical rots on a variety of non-legume and legume crops including pea and faba bean. A more recent study established *F. redolens* as an important and very aggressive root rot pathogen of pea in northern France causing similar damage as *F. solani* f. sp. *pisi* (Gibert et al., 2022). In contrast, Persson et al. (1997) and more recently Safarieskandari et al. (2020) found *F. redolens* to be a generally weak root rot pathogen based on the *in vitro* pathogenicity assays despite its frequent isolation from symptomatic field pea and lentil roots (Chatterton et al., 2019). In our study, it is possible, however, that asymptomatic infections with *F. redolens* could have affected yields opportunistically when the plants were stressed by cold conditions in early crop growth stages followed by warm and dry conditions. There is a need to more precisely characterize the interactions of this pathogen, faba bean yield and environmental variables including other fungal species. This may be particularly important as *F. redolens* is also pathogenic on cereals (Esmaeili Taheri et al., 2011; Yegin et al., 2017; Gebremariam et al., 2018) which are common part of crop rotations.

In contrast to negative yield effects of *D. pinodella* and *F. redolens*, higher abundance of *F. tricintum* in faba bean roots was positively associated with faba bean yield in organic systems. Although frequently isolated from legume crops (Šišić et al.,

2018b; Chatterton et al., 2019), *F. tricinctum* is mainly associated with the Fusarium Head Blight (FHB) complex of small grain cereals in Europe and North America (Uhlig et al., 2007). Our previous research (Šišić et al., 2018b) indicated that this species was only a weak pathogen on pea where root colonization even resulted in increased pea biomass. In contrast, Yan and Nelson (2020) recently reported that *F. tricinctum* is an important soybean root rot pathogen. Due to apparent positive yield effects observed, however, further studies are recommended to better understand the role of this species in the faba bean root rot complex.

In contrast to organic systems, higher abundance of FOSC and *F. culmorum* in faba bean roots led to yield depressions in conventional fields, possibly reflecting cropping system-driven differences in overall soil properties. *Fusarium* root rot of faba bean caused by multiple *Fusarium* species including *F. culmorum*, and *Fusarium* wilt in particular caused by *F. oxysporum*, are among the most destructive diseases of this crop worldwide (Sillero et al., 2010; Lv et al., 2020). However, it is important to note that, in contrast to organic systems, faba bean yields in conventional systems were less affected by the pathogens and depended more on the total precipitation.

Cropping history effects on main root associated fungal species

Almost no legumes had been grown in the 5-11 years preceding the conventional faba beans surveyed in this study while grain legumes (mostly pea and faba bean) and also clover and alfalfa had almost always been present during this period in the organic fields sampled. This difference in rotational histories was strongly correlated with the occurrence of *D. pinodella*, which was ubiquitous in organic fields but much rarer or even absent in conventional fields. (Bainard et al., 2017) reported similar results with pea intensified rotations leading to substantial increase in abundance of this pathogen in soil and pea roots.

It is likely that the higher frequencies of legumes in organic rotations also contributed to higher abundance of *F. redolens* in organic systems compared to conventional as abundance of this pathogen in soil has been shown previously to increase substantially following intensified grain legume rotations (Bainard et al., 2017). The positive correlation of this pathogen with the frequency of cereals in organic systems is not surprising, however, as *F. redolens* is also a wheat (Esmaeili Taheri et al., 2011; Gebremariam et al., 2018) and barley (Yegin et al., 2017) pathogen.

The higher relative abundance of *F. avenaceum*, *F. tricinctum* and *F. culmorum* in conventionally grown faba beans is likely related to the generally higher ratio of cereals in conventional rotations despite the absence of clear correlations. In most conventional fields, cereals were grown three to five times in the five years preceding faba beans. The three species are major small grain cereal and maize pathogens frequently associated with ear, stem and root rots and responsible for pre-harvest mycotoxin contaminations (Bottalico and Perrone, 2002; Pfordt et al., 2020). Among the three species, *F. avenaceum* is the most important and wide-spread. It is an opportunistic pathogen especially in the absence of organic matter (Baćanović-Šišić et al., 2018) and the major causal agents of pea and lentil root rot in Canada (Esmaeili Taheri et al., 2016; Chatterton et al., 2019) and pea root rot in the USA (Chittem et al., 2015) in the past 20 years. In Europe, *F. avenacem* is frequently isolated from diseased pea roots but usually at moderate frequencies (Persson et al., 1997; Pflughöft et al., 2012; Baćanović-Šišić et al., 2018; Šišić et al., 2019).

Effects of environmental conditions on major fungal species identified

Pedo-climatic conditions appeared to be the main drivers for the occurrence of most of the *Fusarium* species identified in this study. Cold conditions at sowing and plant emergence and/or during the vegetative season in particular were found to favor most of the dominant *Fusarium* species identified in this study. These conditions were associated with increased root colonization rates by *F. redolens, F. solani* and *F. culmorum* in both management systems, and the FOSC and *F. equiseti* in organic systems. Sowing into cold soils prolongs seedling emergence favoring early plant infections by these pathogens (Naseri and Marefat, 2011). Although *Fusarium* spp. can infect their hosts at all growth stages, previous research has shown that the timing of infection plays a crucial role in the extent of root rot severity and yield reduction (Papavizas, 1974; Šišić et al., 2017; Navas-Cortés et al., 2020). For example, Šišić et al. (2017) showed that the detrimental effect of *F. avenaceum* on pea root health and biomass depended strongly on the timing of pathogen inoculation. When inoculated at sowing, *F. avenaceum* caused severe wilting resulting in 83% pea biomass loss compared to a non-inoculated control. In contrast, inoculation five days after pea sowing resulted in moderate root rot disease severity with greatly reduced negative effects on pea biomass (-14%). Therefore, vigorous seeds are likely to rapidly outgrow the highly susceptible seedling growth stage, reducing the overall risks of *Fusarium* damage. But also higher temperatures e.g. hot weather following sowing and/or in the period from sowing to root sampling can favor root infections e.g. by *F. redolens* which was more severe in both management systems in hot and dry seasons. The opposite was observed for *F. culmorum* in both management systems and *F. avenaceum* and *F. equiseti* in organic systems. Their root colonization rates were favored by cooler growing season. The precipitation effects were highly variable and mostly management system and *Fusarium* species specific. While *Fusarium* spp. are able to adapt to various

ranges of environmental conditions, the competitive advantage of each species in the faba bean root rot complex will vary depending on the site specific pedo-climatic conditions (Yergeau et al., 2009). Furthermore, abiotic plant stress (i.e. the crop defense response) seems to have an important impact on the susceptibility of faba beans to *Fusarium* infections.

In contrast to *Fusarium* spp., warmer conditions at sowing/plant emergence favored *D. pinodella* in both management systems. In addition, although this species occurred rarely in conventional systems, *D. pinodella* frequencies were positively correlated with warmer and wetter conditions at sowing/plant emergence followed by drier growing seasons. The positive effect of drier conditions on *D. pinodella* root colonization rates and especially the high incidence of this pathogen in 2019, the driest sampling year in this study, are in contrast with what has been reported in the *D. pinodella*-pea system where infections are primarily favored by wet and humid conditions during the main growing season (Bretag et al., 2006; Esmaeili Taheri et al., 2016). These results suggest that short periods of wet conditions are sufficient for infections by this pathogen and also point to its opportunistic nature where abiotic plant stress (e.g. lack of precipitations) can enhance colonization process once the primary infections occur.

Our observations that the frequency of the FOSC was correlated positively with sandy soils characterized by lower pH supports previous reports that sandy soils and lower pH are more conducive for this pathogen and contribute to increased root rot and wilt incidence in a range of different crops, including chickpea, banana, flax, carnations, watermelon, tomato and marigold (Scher and Baker, 1980; Amir and Alabouvette, 1993; Singh et al., 2017; Orr and Nelson, 2018; Saeedi and Jamali, 2021). Some of these studies also showed that silty and clay soils and/or increasing soil pH were often suppressive to *Fusarium* wilt development. We also found a weak but statistically significant association of *F. redolens* with organic silty soils in this study. (Saeedi and Jamali, 2021) recently reported that *F. redolens* is a very aggressive pathogen of chickpea in Iran where *F. oxysporum* dominated on sandy soils while *F. redolens* was highly correlated with low sand and organic matter among others. In addition, the positive correlation between the FSSC frequencies in conventional system and silty-clay soils with generally high SOM content (*i.e.* fields in soil cluster 3) suggest that the FSSC members are highly competitive saprophytes.

Genetic diversity among *F. oxysporum* and *F. solani* isolates

The observation that the members of the FOSC and the FSSC are important components of the faba bean root rot complex both in organic and conventional fields is consistent with many previous findings (Chittem et al., 2015; Esmaeili Taheri et al., 2016; Šišić et al., 2018a; Šišić et al., 2018b; Chatterton et al., 2019). The wide-spread occurrence of the FOSC and FSSC over a range of soil and environmental conditions observed in this study indicates a high adaptability of both species complexes to a range of pedo-climatic and environmental conditions, which may in turn indicate high genetic diversity. The high genetic variability among the 35 F. *oxysporum* isolates from a single host observed in this study came as a surprise, however. With the exception of *F. curvatum, F. nirenbergie, F. oxysporum* and *F. fabacearum* lineages which have been previously associated either with faba bean or other legumes, the remaining five lineages including the most abundant *F. libertatis* (17/35 isolates) have not been associated with any legume host previously. Further analysis is required to determine their role in the faba bean root rot complex.

In contrast to FOSC, 29 of the 33 FSSC isolates analyzed matched *F. pisi* (syn. *F. solani* f. sp. *pisi*; *Fusarium vanettenii*), and a group of 3 isolates were placed in *Fusarium solani sensu stricto* lineage, and one isolate matched *F. breviconum*. These results confirm the common association of *F. pisi* with various legumes and its ability to occupy diverse ecological niches (Šišić et al., 2018a). More recently, Safarieskandari et al. (2020) demonstrated a high level of aggressiveness of *F. pisi* to faba beans. It is also important to note that, while the phylogenetic analysis generally confirmed a good resolution power of the *TEF1 alpha* locus in *Fusarium*, poor bootstrap support for some lineages within the FOSC was observed. These results were expected however, due to the single locus analysis and were consistent with the results of the *TEF1 alpha* tree topology reported for the FOSC (Lombard et al., 2018) and for the FSSC (Šišić et al., 2018a; Geiser et al., 2021). Work is on-going to obtain additional sequence data from more loci and also aggressiveness tests to better understand genetic variation and the role of the collected isolates in the faba bean root rot complex.

Conclusions

This four-year survey provides the first comparative documentation on the prevalence and frequency of *Fusarium* and *Didymella* species associated with faba bean roots in organic and conventional fields in Germany. By covering a wide range of pedoclimatic and field history conditions under conventional and organic production systems, it was possible to develop inferences about the main drivers currently influencing the pathobiome community on faba beans. Pedoclimatic conditions were the main drivers of the *Fusarium* communities, whereas *D. pinodella* was primarily influenced by the presence of grain legumes in the recent cropping history. This led to the dominance of this pathogen in organic systems, almost certainly because of the higher frequency of legumes in organic rotations. The role of *F. libertatis* and the other FOSC

members identified that had not previously been associated with root rot of grain legumes needs to be examined. This study indicated that several major root rot pathogens of grain legumes may asymptomatically colonize faba bean roots as had been reported previously for other crops (Šišić et al., 2018b; Šišić et al., 2022). The study indicated that faba bean yields in organic systems apparently were affected by asymptomatic root infections by *D. pinodella* and *F. redolens* whereas yields in conventional systems depended more on the total precipitation during the main growing season. As described in the introduction, the new protein strategy of the EU has encouraged many conventional farmers to adopt grain legumes since 2012 and our survey shows that most conventionally grown faba beans were grown for the first time in many years. An overall increase of grain legume production under conventional conditions will likely change their health status, however, as has already been observed in Canada (Bainard et al., 2017; Niu et al., 2018).

Data availability statement

The original contributions presented in the study are included in the article/Supplementary Files. Further inquiries can be directed to the corresponding author.

Author contributions

AŠ, HS, JŠ, MF study design/methodology/investigation. AŠ data analysis/drafted the manuscript. AŠ, MF resources/funding acquisition. All authors contributed to the article and approved the submitted version.

Funding

This work was carried out within the framework of the research projects PATHO-ID (2814EPS40) and APSOLU (2814EPS035), funded by the Federal Ministry of Food and Agriculture within the framework of the BMEL protein plant strategy, in cooperation with the German Demonstration network Pea/Bean.

Conflict of interest

The authors declare that the research was conducted in the absence of any commercial or financial relationships that could be construed as a potential conflict of interest.

Publisher's note

All claims expressed in this article are solely those of the authors and do not necessarily represent those of their affiliated organizations, or those of the publisher, the editors and the reviewers. Any product that may be evaluated in this article, or claim that may be made by its manufacturer, is not guaranteed or endorsed by the publisher.

Supplementary material

The Supplementary Material for this article can be found online at: https://www.frontiersin.org/articles/10.3389/fpls.2022.1009906/full#supplementary-material

References

Amir, H., and Alabouvette, C. (1993). Involvement of soil abiotic factors in the mechanisms of soil suppressiveness to *Fusarium* wilts. *Soil Biol. Biochem.* 25, 157–164. doi: 10.1016/0038-0717(93)90022-4

Baćanović-Šišić, J., Šišić, A., Schmidt, J. H., and Finckh, M. R. (2018). Identification and characterization of pathogens associated with root rot of winter peas grown under organic management in Germany. *Eur. J. Plant Pathol.* 151, 745–755. doi: 10.1007/s10658-017-1409-0

Bainard, L. D., Navarro-Borrell, A., Hamel, C., Braun, K., Hanson, K., and Gan, Y. (2017). Increasing the frequency of pulses in crop rotations reduces soil fungal diversity and increases the proportion of fungal pathotrophs in a semiarid agroecosystem. *Agricult. Ecosyst. Environ.* 240, 206–214. doi: 10.1016/j.agee.2017.02.020

Benjamini, Y., and Hochberg, Y. (1995). Controlling the false discovery rate: A practical and powerful approach to multiple testing. *J. R. Stat. Soc.* 57, 289–300. doi: 0035-9246/95/57289

Boerema, G. H., Gruyter, J., Noordeloos, M. E., and Hamers, M. E. C. (2004). *Phoma identification manual: Differentiation of specific and infra-specific taxa in culture* (Wallingford, Oxfordshire, UK: CABI publishing).

Booth, C. (1971). *The genus fusarium* (Kew, Surrey, England: Commonwealth Mycological Institute).

Bottalico, A., and Perrone, G. (2002). Toxigenic *Fusarium* species and mycotoxins associated with head blight in small-grain cereals in Europe. *Eur. J. Plant Pathol.* 108, 611–624. doi: 10.1023/A:1020635214971

Bretag, T. W., Keane, P. J., and Price, T. V. (2006). The epidemiology and control of ascochyta blight in field peas: A review. *Aust. J. Agric. Res.* 57, 883. doi: 10.1071/AR05222

Brooks, M. E., Kristensen, K., Benthem, K. J., Magnusson, A., Berg, C. W., Nielsen, A., et al. (2017). glmmTMB balances speed and flexibility among packages for zero-inflated generalized linear mixed modeling. *R J.* 9, 378–400. doi: 10.32614/RJ-2017-066

Chatterton, S., Harding, M. W., Bowness, R., Mclaren, D. L., Banniza, S., and Gossen, B. D. (2019). Importance and causal agents of root rot on field pea and lentil on the Canadian prairies 2014–2017. *Can. J. Plant Pathol.* 41, 98–114. doi: 10.1080/07060661.2018.1547792

Chen, Q., Jiang, J. R., Zhang, G. Z., Cai, L., and Crous, P. W. (2015). Resolving the *Phoma* enigma. *Stud. Mycology* 82, 137–217. doi: 10.1016/j.simyco.2015.10.003

Chittem, K., Mathew, F. M., Gregoire, M., Lamppa, R. S., Chang, Y. W., Markell, S. G., et al. (2015). Identification and characterization of fusarium spp. associated with root rots of field pea in north Dakota. *Eur. J. Plant Pathol.* 143, 641–649. doi: 10.1007/s10658-015-0714-8

Conover, W. J. (1999). *Practical nonparametric statistics. 3rd ed* (New York, USA: John Wiley & Sons, Inc).

Coons, G. H. (1916). Factors involved in the growth and the pycnidium formation of *Plenodomus fuscomaculans*. *J. Agric. Res.* 5, 713–769.

Doyle, J. J., and Doyle, J. L. (1987). A rapid DNA isolation procedure for small quantities of fresh leaf tissue. *Phytochemical Bull.* 19, 11–15.

Esmaeili Taheri, A., Chatterton, S., Foroud, N. A., Gossen, B. D., and McLaren, D. L. (2016). Identification and community dynamics of fungi associated with root, crown, and foot rot of field pea in western Canada. *Eur. J. Plant Pathol.* 147, 489–500. doi: 10.1007/s10658-016-1017-4

Esmaeili Taheri, A., Chatterton, S., Gossen, B. D., and McLaren, D. L. (2017). Metagenomic analysis of oomycete communities from the rhizosphere of field pea on the Canadian prairies. *Can. J. Microbiol.* 63, 758–768. doi: 10.1139/cjm-2017-0099

Esmaeili Taheri, A., Hamel, C., Gan, Y., and Vujanovic, V. (2011). First report of *Fusarium redolens* from Saskatchewan and its comparative pathogenicity. *Can. J. Plant Pathol.* 33, 559–564. doi: 10.1080/07060661.2011.620631

Gebremariam, E. S., Sharma-Poudyal, D., Paulitz, T. C., Erginbas-Orakci, G., Karakaya, A., and Dababat, A. A. (2018). Identity and pathogenicity of *Fusarium* species associated with crown rot on wheat (*Triticum* spp.) in Turkey. *Eur. J. Plant Pathol.* 150, 387–399. doi: 10.1007/s10658-017-1285-7

Geiser, D. M., Al-Hatmi, A. M. S., Aoki, T., Arie, T., Balmas, V., Barnes, I., et al. (2021). Phylogenomic analysis of a 55.1-kb 19-gene dataset resolves a monophyletic *Fusarium* that includes the *Fusarium solani* species complex. *Phytopathology* 111, 1064–1079. doi: 10.1094/PHYTO-08-20-0330-LE

Geiser, D. M., Jiménez-Gasco, M. M. D., Kang, S., Makalowska, I., Veeraraghavan, N., Ward, T. J., et al. (2004). FUSARIUM-ID v. 1.0: A DNA sequence database for identifying *Fusarium*. *Eur. J. Plant Pathol.* 110, 473–479. doi: 10.1007/978-1-4020-2285-2_2

Gibert, S., Edel-Hermann, V., Gautheron, E., Gautheron, N., Bernaud, E., Sol, J. M., et al. (2022). Identification, pathogenicity and community dynamics of fungi and oomycetes associated with pea root rot in northern France. *Plant Pathol.* 71, 1550–1569. doi: 10.1111/ppa.13583

Gu, Y., Banerjee, S., Dini-Andreote, F., Xu, Y., Shen, Q., Jousset, A., et al. (2022). Small changes in rhizosphere microbiome composition predict disease outcomes earlier than pathogen density variations. *ISME J.* 14, 2448–2456. doi: 10.1038/s41396-022-01290-z

Hartig, F. (2021) *DHARMa: Residual diagnostics for hierarchical (multi-level / mixed) regression models*. Available at: http://florianhartig.github.io/DHARMa/.

Hossain, S., Bergkvist, G., Berglund, K., Mårtensson, A., and Persson, P. (2012). *Aphanomyces* pea root rot disease and control with special reference to impact of brassicaceae cover crops. *Acta Agriculturae Scandinavica Section B - Soil Plant Sci.* 62, 1–11. doi: 10.1080/09064710.2012.668218

Katoh, K., and Standley, D. M. (2013). MAFFT multiple sequence alignment software version 7: improvements in performance and usability. *Mol. Biol. Evol.* 30, 772–780. doi: 10.1093/molbev/mst010

Lê, S., Josse, J., and Husson, F. (2008). FactoMineR: An R package for multivariate analysis. *J. Stat. Software* 25, 1–18. doi: 10.18637/jss.v025.i01

Lenth, R. V. (2016). Least-squares means: The R package lsmeans. *J. Stat. Soft.* 69, 1–33. doi: 10.18637/jss.v069.i01

Leslie, J. F., and Summerell, B. A. (2006). *The fusarium laboratory manual. 1st ed* (Ames, Iowa, USA: Blackwell publishing).

Lombard, L., Sandoval-Denis, M., Lamprecht, S. C., and Crous, P. W. (2018). Epitypification of fusarium oxysporum – clearing the taxonomic chaos. *persoonia*. 43, 1–47. doi: 10.3767/persoonia.2019.43.01

Lv, J., Dong, Y., Dong, K., Zhao, Q., Yang, Z., and Chen, L. (2020). Intercropping with wheat suppressed fusarium wilt in faba bean and modulated the composition of root exudates. *Plant Soil* 448, 153–164. doi: 10.1007/s11104-019-04413-2

Madden, T. (2002). "Chapter 16 "The BLAST sequence analysis tool," in *The NCBI handbook*. Eds. J. McEntyre and J. Ostell (Bethesda (MD: National Center for Biotechnology Information (US) 2002). Available at: http://www.ncbi.nlm.nih.gov/books/NBK21097/.

Mendiburu, D. F. (2014). Agricolae: Statistical procedures for agricultural research 1, 2. R package version.

Naseri, B., and Ansari Hamadani, S. (2017). Characteristic agro-ecological features of soil populations of bean root rot pathogens. *Rhizosphere* 3, 203–208. doi: 10.1016/j.rhisph.2017.05.005

Naseri, B., and Marefat, A. (2011). Large-Scale assessment of agricultural practices affecting fusarium root rot and common bean yield. *Eur. J. Plant Pathol.* 131, 179–195. doi: 10.1007/s10658-011-9798-y

Naseri, B., and Mousavi, S. S. (2015). Root rot pathogens in field soil, roots and seeds in relation to common bean (*Phaseolus vulgaris*), disease and seed production. *Int. J. Pest Manage.* 61, 60–67. doi: 10.1080/09670874.2014.993001

Navas-Cortés, J. A., Hau, B., and iménez-Díaz, R. M. (2020). Yield loss in chickpeas in relation to development of *Fusarium* wilt epidemics. *Phytopathology* 11, 1269–1278. doi: 10.1094/PHYTO.2000.90.11.1269

Nayyar, A., Hamel, C., Lafond, G., Gossen, B. D., Hanson, K., and Germida, J. (2009). Soil microbial quality associated with yield reduction in continuous-pea. *Appl. Soil Ecol.* 43, 115–121. doi: 10.1016/j.apsoil.2009.06.008

Niu, Y., Bainard, L. D., May, W. E., Hossain, Z., Hamel, C., and Gan, Y. (2018). Intensified pulse rotations buildup pea rhizosphere pathogens in cereal and pulse based cropping systems. *Front. Microbiol.* 9. doi: 10.3389/fmicb.2018.01909

O'Donnell, K., Al-Hatmi, A. M. S., Aoki, T., Brankovics, B., Cano-Lira, J. F., Coleman, J. J., et al. (2020). No to *Neocosmospora*: phylogenomic and practical reasons for continued inclusion of the *Fusarium solani* species complex in the genus. *Fusarium* 5, 7. doi: 10.1128/mSphere.00810-20

O'Donnell, K., Gueidan, C., Sink, S., Johnston, P. R., Crous, P. W., Glenn, A., et al. (2009). A two-locus DNA sequence database for typing plant and human pathogens within the fusarium oxysporum species complex. *Fungal Genet. Biol.* 46, 936–948. doi: 10.1016/j.fgb.2009.08.006

O'Donnell, K., Kistler, H. C., Cigelnik, E., and Ploetz, R. C. (1998). Multiple evolutionary origins of the fungus causing Panama disease of banana: Concordant evidence from nuclear and mitochondrial gene genealogies. *Proc. Natl. Acad. Sci.* 95, 2044–2049. doi: 10.1073/pnas.95.5.2044

Orr, R., and Nelson, P. N. (2018). Impacts of soil abiotic attributes on *Fusarium* wilt, focusing on bananas. *Appl. Soil Ecol.* 132, 20–33. doi: 10.1016/j.apsoil.2018.06.019

Papavizas, G. C. (1974). *Aphanomyces species and their root diseases in pea and sugarbeet: A review* (US Department of Agriculture: Agricultural Research Service).

Persson, L., Bødker, L., and Larsson-Wikström, M. (1997). Prevalence and pathogenicity of foot and root rot pathogens of pea in southern Scandinavia. *Plant Dis.* 81, 171–174. doi: 10.1094/PDIS.1997.81.2.171

Pflughöft, O., Merker, C., von Tiedemann, A., and Schäfer, B. C. (2012). Zur verbreitung und bedeutung von pilzkrankheiten in körnerfuttererbsen (*Pisum sativum* l.) in deutschland. *Gesunde Pflanzen* 64, 39–48. doi: 10.1007/s10343-011-0270-x

Pfordt, A., Ramos Romero, L., Schiwek, S., Karlovsky, P., and von Tiedemann, A. (2020). Impact of environmental conditions and agronomic practices on the prevalence of *Fusarium* species associated with ear- and stalk rot in maize. *Pathogens* 9, 236. doi: 10.3390/pathogens9030236

R Core Team (2013). *R: A language and environment for statistical computing* (Vienna, Austria: R Foundation for Statistical Computing). Available at: http://www.R-project.org/.

Rodriguez, R. J., White, J. F.Jr., Arnold, A. E., and Redman, R. S. (2009). Fungal endophytes: diversity and functional roles. *New Phytol.* 182, 314–330. doi: 10.1111/j.1469-8137.2009.02773.x

Rosseel, Y. (2012). Lavaan: An R package for structural equation modeling. *J. Stat. Software* 48, 1–36. doi: 10.18637/jss.v048.i02

Saeedi, S., and Jamali, S. (2021). Mol. characterization distribution Fusarium isolates uncultivated soils chickpea Plants Iran special reference to Fusarium redolens. *J. Plant Pathol.* 103, 167–183. doi: 10.1007/s42161-020-00698-w

Safarieskandari, S., Chatterton, S., and Hall, L. M. (2020). Pathogenicity and host range of *Fusarium* species associated with pea root rot in Alberta, Canada. *Can. J. Plant Pathol.* 43, 162–171. doi: 10.1080/07060661.2020.1730442

Scher, F. M., and Baker, R. (1980). Mechanism of biological control in a *Fusarium*-suppressive soil. *Phytopathology* 70, 412–417. doi: 10.1094/Phyto-70-412

Schulz, B., and Boyle, C. (2005). The endophytic continuum. *Mycological Res.* 109, 661–686. doi: 10.1017/S095375620500273X

Sillero, J. C., Villegas-Fernández, A. M., Thomas, J., Rojas-Molina, M. M., Emeran, A. A., Fernández-Aparicio, M., et al. (2010). Faba bean breeding for disease resistance. *Field Crops Res.* 115, 297–307. doi: 10.1016/j.fcr.2009.09.012

Singh, B., Singh, V., Srivastava, S., Pandey, A., and Shukla, D. (2017). Influence of soil properties on wilt incidence of water melon, tomato and marigold. *ARRB* 19, 1–6. doi: 10.9734/ARRB/2017/34350

Šišić, A., Baćanović, J., and Finckh, M. R. (2017). Endophytic *Fusarium equiseti* stimulates plant growth and reduces root rot disease of pea (*Pisum sativum* l.) caused by *Fusarium avenaceum* and *Peyronellaea pinodella*. *Eur. J. Plant Pathol.* 148, 271–282. doi: 10.1007/s10658-016-1086-4

Šišić, A., Baćanović-Šišić, J., Al-Hatmi, A. M. S., Karlovsky, P., Ahmed, S. A., Maier, W., et al. (2018a). The 'forma specialis' issue in *Fusarium*: A case study in *Fusarium solani* f. sp. *pisi*. *Sci. Rep.* 8, 1252. doi: 10.1038/s41598-018-19779-z

Šišić, A., Baćanović-Šišić, J., Karlovsky, P., Wittwer, R., Walder, F., Campiglia, E., et al. (2018b). Roots of symptom-free leguminous cover crop and living mulch species harbor diverse *Fusarium* communities that show highly variable aggressiveness on pea (*Pisum sativum*). *PloS One* 13, e0191969. doi: 10.1371/journal.pone.0191969

Šišić, A., Baćanović-Šišić, J., Schmidt, H., and Finckh, M. R. (2019). *Root pathogens occurring on pea (Pisum sativum) and faba bean (Vicia faba) in Germany* (Sarajevo: Springer International Publishing). Sept. 26-27, 2019.

Šišić, A., Baćanović-Šišić, J., Schmidt, H., and Finckh, M. R. (2020). First report of *Fusarium flocciferum* causing root rot of pea (*Pisum sativum*) and faba bean (*Vicia faba*) in Germany. *Plant Dis.* 104, 283–283. doi: 10.1094/PDIS-06-19-1302-PDN

Šišić, A., Oberhänsli, T., Baćanović-Šišić, J., Hohmann, P., and Finckh, M. R. (2022). A novel real time PCR method for the detection and quantification of *Didymella pinodella* in symptomatic and asymptomatic plant hosts. *J. Fungi* 8, 41. doi: 10.3390/jof8010041

Stamatakis, A., Hoover, P., and Rougemont, J. (2008). A rapid bootstrap algorithm for the RAxML web servers. *Systematic Biol.* 57, 758–771. doi: 10.1080/10635150802429642

Su, Y. S., Yajima, M., Hill, J., Pittau, M. G., Kerman, J., Zheng, T., et al. (2018) *Package a'rm': Data analysis using regression and multilevel/hierarchical models*. Available at: https://cran.r-project.org/web/packages/car/car.pdf (Accessed February 17, 2020).

Tamura, K., Stecher, G., Peterson, D., Filipski, A., and Kumar, S. (2013). MEGA6: Molecular evolutionary genetics analysis version 6.0. *Mol. Biol. Evol.* 30, 2725–2729. doi: 10.1093/molbev/mst197

Uhlig, S., Jestoi, M., and Parikka, P. (2007). *Fusarium* avenaceum — the north European situation. *Int. J. Food Microbiol.* 119, 17–24. doi: 10.1016/j.ijfoodmicro.2007.07.021

Walder, F., Schlaeppi, K., Wittwer, R., Held, A. Y., Vogelgsang, S., and van der Heijden, M. G. A. (2017). Community profiling of *Fusarium* in combination with other plant-associated fungi in different crop species using SMRT sequencing. *Front. Plant Sci.* 8. doi: 10.3389/fpls.2017.02019

Wickham, H. (2016). *ggplot2: Elegant graphics for data analysis. 2nd ed* (New York: Springer International Publishing). Available at: https://ggplot2.tidyverse.org.

Wilbois, K. P., Böhm, H., Bohne, B., Brandhuber, R., Bruns, C., Demmel, M., et al. (2013). "Steigerung der wertschöpfung ökologisch angebauter marktfrüchte durch optimierung des managements der bodenfruchtbarkeit," in *Gesamtprojekt abschlussbericht*. Available at: www.orgprints.org/28973.

Wille, L., Messmer, M. M., Studer, B., and Hohmann, P. (2019). Insights to plant–microbe interactions provide opportunities to improve resistance breeding against root diseases in grain legumes. *Plant Cell Environ.* 42, 20–40. doi: 10.1111/pce.13214

Williamson-Benavides, B. A., and Dhingra, A. (2021). Understanding root rot disease in agricultural crops. *Horticulturae* 7, 33. doi: 10.3390/horticulturae7020033

Wohor, O. Z., Rispail, N., Ojiewo, C. O., and Rubiales, D. (2022). Pea breeding for resistance to rhizospheric pathogens. *Plants* 11, 2664. doi: 10.3390/plants11192664

Yan, H., and Nelson, B. (2020). Effect of temperature on *Fusarium solani* and *F. tricinctum* growth and disease development in soybean. *Can. J. Plant Pathol.* 42, 527–537. doi: 10.1080/07060661.2020.1745893

Yegin, N. Z., Ünal, F., Tekiner, N., and Dolar, F. S. (2017). First report of *Fusarium redolens* causing root and crown rot of barley (*Hordeum vulgare*) in Turkey. *J. Turkish Phytopathol.* 46, 101–105.

Yergeau, E., Labour, K., Hamel, C., Vujanovic, V., Nakano-Hylander, A., Jeannotte, R., et al. (2009). Patterns offusarium community structure and abundance in relation to spatial, abiotic and biotic factors in soil. *FEMS Microbiol. Ecol.* 71, 34–42. doi: 10.1111/j.1574-6941.2009.00777.x

Zitnick-Anderson, K., Simons, K., and Pasche, J. S. (2018). Detection and qPCR quantification of seven *Fusarium* species associated with the root rot complex in field pea. *Can. J. Plant Pathol.* 40, 261–271. doi: 10.1080/07060661.2018.1429494

frontiers | Frontiers in Plant Science

TYPE Original Research
PUBLISHED 06 February 2023
DOI 10.3389/fpls.2023.1117788

OPEN ACCESS

EDITED BY
Rachid Lahlali,
Ecole Nationale d'Agriculture de Meknès, Morocco

REVIEWED BY
Malkhan Singh Gurjar,
Indian Agricultural Research Institute (ICAR), India
Magnus Karlsson,
Swedish University of Agricultural Sciences, Sweden

*CORRESPONDENCE
Cheryl Armstrong-Cho
cheryl.cho@usask.ca

†These authors have contributed equally to this work and share first authorship

SPECIALTY SECTION
This article was submitted to Plant Pathogen Interactions, a section of the journal Frontiers in Plant Science

RECEIVED 06 December 2022
ACCEPTED 23 January 2023
PUBLISHED 06 February 2023

CITATION
Armstrong-Cho C, Sivachandra Kumar NT, Kaur R and Banniza S (2023) The chickpea root rot complex in Saskatchewan, Canada- detection of emerging pathogens and their relative pathogenicity. *Front. Plant Sci.* 14:1117788. doi: 10.3389/fpls.2023.1117788

The chickpea root rot complex in Saskatchewan, Canada- detection of emerging pathogens and their relative pathogenicity

Cheryl Armstrong-Cho*†, Nimllash Thangam Sivachandra Kumar†, Ramanpreet Kaur and Sabine Banniza

Crop Development Centre, University of Saskatchewan, Saskatoon, SK, Canada

Chickpea fields in Saskatchewan, one of the three Canadian prairie provinces, have suffered from major health issues since 2019, but no definitive cause has been determined. Field surveys were conducted in Saskatchewan in 2020 and 2021 in order to develop a better understanding of root rot pathogens associated with chickpea. Root samples were analyzed for the presence of 11 potential chickpea root rot pathogens using end-point PCR. *Fusarium redolens*, *F. solani* and *F. avenaceum* were the most prevalent pathogen species detected in both survey years. The cause of Fusarium wilt in chickpea, *F. oxysporum* f. sp. *ciceris*, was not detected in either year, nor were *Phytophthora* spp. and *Verticillium albo-atrum*. *Berkeleyomyces* sp. was detected in one field in each year, and *Verticillium dahliae* was detected in several fields sampled in 2021. These two pathogens have not been reported previously on chickpea in Saskatchewan. The prevalence of *Fusarium* species obtained from 2021 root isolations was similar to that determined by molecular tests, with frequent isolation of *F. redolens*, *F. oxysporum*, *F. avenaceum* and *F. solani*. A series of indoor pathogenicity testing compared root disease severity caused by a selection of 16 isolates of six *Fusarium* species and single isolates of *V. dahliae*, *Berkeleyomyces* sp. and *Macrophomina phaseolina*. Results showed that select isolates of *F. avenaceum* were the most aggressive of the *Fusarium* isolates on chickpea. Despite relatively low inoculum density, a highly aggressive isolate of *F. avenaceum* caused severe stunting and more root rot symptoms than single isolates of *V. dahliae*, *Berkeleyomyces* sp. and *M. phaseolina* under the test conditions.

KEYWORDS

disease survey, fusarium avenaceum, fusarium redolens, verticillium dahliae, berkeleyomyces (thielaviopsis) basicola

Introduction

Chickpea (*Cicer arietinum* L.) is an important pulse crop grown in Saskatchewan, one of the three Canadian prairie provinces, accounting for 78% of Canadian chickpea production in 2021 (Government of Saskatchewan, 2021). The majority of chickpeas grown in Saskatchewan are the kabuli type, which have a thin, colorless seed coat, making them susceptible to attack by

a variety of soil-borne pathogens. Seed treatment with fungicide, particularly to control damping off caused by *Pythium* spp., is a routine part of disease management programs in this region. In addition to *Pythium* and *Rhizoctonia* spp., several *Fusarium* spp. can cause economically damaging root rot to chickpea worldwide (Haware, 1998; Infantino et al., 2006; Chen et al., 2011). The intensification of pulse production on the prairies has resulted in increased prominence of root rots, including those caused by *Fusarium* spp. The wide-spread occurrence of Aphanomyces root rot in this region makes chickpea an attractive alternative to lentil and pea in crop rotations due to their high partial resistance (Moussart et al., 2008). However, it has been suspected that root rots caused by other pathogens have been increasing. To date, the spectrum of root-rot pathogens prevalent in the chickpea cropping system, particularly *Fusarium* spp. and their potential for causing significant disease, are unknown, while this has been well studied in pea and lentil during the last decade.

Fusarium avenaceum (Fr.) Sacc. and *F. solani* (Mart.) Sacc. (syn. *Neocosmospora solani* (Mart.) L. Lombard & Crous) are the predominant *Fusarium* species in the root rot complex attacking pea and lentil (Esmaeili Taheri et al., 2017, Chatterton et al., 2019). Both of these species are known to impact emergence and cause moderate to severe symptoms on chickpea roots (Kraft, 1969; Westerlund et al., 1974; Safarieskandari et al., 2021). Besides root rot, *F. avenaceum* also contributes to the development of Fusarium head blight in cereal crops (Tekauz et al., 2000; Xue et al., 2004, Tekauz et al., 2004). In a recent study, isolates of *Fusarium redolens* Wollenw., *F. culmorum* (Wm.G. Sm.) Sacc., *F. sporotrichioides* Sherb. (now *Fusarium chlamydosporum Wollenw. & Reinking*), *F. oxysporum* Schltdl. and *F. equiseti* (Corda) Sacc. obtained from diseased chickpea samples were all confirmed to be pathogenic on chickpea (Zhou et al., 2021). The most aggressive isolates on chickpea were of *F. culmorum* and *F. chlamydosporum*, but there were also isolates of these species with low aggressiveness. In addition to root rot, Fusarium wilt of chickpea, caused by *F. oxysporum* f. sp. *ciceris* Matuo & K. Sato, can cause devastating losses in many chickpea growing areas, including most of those found in Asia, Africa, southern Europe, and the Americas (Jiménez-Díaz et al., 2015; Jha et al., 2020). This pathogen has not been reported in Canada.

In addition to *Fusarium* spp., several other chickpea root pathogens have been reported around the globe. *Berkeleyomyces basicola* (Berk. & Broome) W.J. Nel, Z.W. de Beer, T.A. Duong & M.J. Wingf (formerly *Thielaviopsis basicola* Berk. & Broome) which causes black streak root rot, was reported from chickpea roots in eastern Washington in 1985 (Bowden et al., 1985). *Macrophomina phaseolina* (Tassi) Goid. (dry root rot) and *Verticillium albo-atrum* Reinke & Berthold (Verticillium wilt) have been reported in California (Erwin, 1958; Westerlund et al., 1974). These three pathogens have not been reported from chickpea grown in the North American Prairies. Verticillium wilt of canola caused by *V. dahliae* Kleb. was recently reported on the prairies (Hwang et al., 2017) but has not been observed in Canadian chickpea (Chen et al., 2011). Similarly, although *Phytophthora medicaginis* E.M. Hansen & D.P. Maxwell, (Phytophthora root rot) is a pathogen of alfalfa fields in North America, Phytophthora root rot is not common in alfalfa in Saskatchewan (Bill Biligetu, Crop Development Centre/Dept. of Plant Sciences, University of Saskatchewan, personal communication) and it has not been recorded from chickpea crops in the USA or Canada.

Materials and methods

Field survey

Commercial chickpea fields in Saskatchewan were surveyed in June and July of 2020 and 2021. The scope of the survey included 41 rural municipalities with 42 commercial chickpea fields and one research location with chickpea breeder plots in 2020. Rural municipalities where chickpea root rot symptoms were most prevalent in 2020 were chosen for sampling in 2021, which included 19 commercial chickpea fields in 14 rural municipalities. Above-ground disease symptoms were recorded for five plants at each of ten locations in each field in 2020, and for five plants each at five locations in each field in 2021. Disease scoring was performed according to a 1-5 qualitative scale adapted from Infantino et al. (2006), in which 1 = no symptoms, 2 = slight yellowing of lower leaves, 3 = yellowing of the lower leaves up to the 3rd or 4th node and some stunting, 4 = necrosis of at least half or more of the plant with some stunting, 5 = entire plant dead or nearly so. Roots were collected at five locations in each field and submitted to the University of Saskatchewan Pulse Crop Pathology Laboratory for further analysis. Due to laboratory access restrictions during the COVID-19 pandemic, roots submitted in 2020 were immediately frozen and not assessed for visual root symptoms. In 2021, root rot symptoms were rated on dry root samples using the 1-7 scale described by Safarieskandari et al. (2021): 1 = no symptoms, 2 = 0.1–0.2 cm, small reddish brown lesions at seed attachment area, 3 = coalescing of localized tap root lesions approximately 180° around the tap root with lesions from 0.5 to 1 cm, 4 = lesions extending and completely encircling the tap root (1–2 cm), 5 = increasingly discoloured and extended tap root lesions (2–4 cm), 6 = lesions encircling the tap root extending over 4 cm and 7 = tap root completely brown/black.

Molecular detection of potential root pathogens

A total of 208 root samples collected in 2020 and 93 samples collected in 2021 were freeze-dried (FreeZone 6, Labconco Corp., Kansas City MO USA) and ground for DNA extraction. Grinding was performed using custom designed tubes (high strength polycarbonate, Metalshapes Manufacturing, Saskatoon) containing a 1.7 cm diameter stainless steel ball placed in a homogenizer (2010 Geno/GrinderTM, SPEX Sample Prep, Metuchen, NJ USA) at 1400 rpm for 5 min (2020) or at 1000 rpm for 2 min (2021). Ground tissue (approx. 10 mg) was transferred to microcentrifuge tubes along with a 0.6 cm diameter ceramic bead for a second grinding step (1400 rpm for 1 min). Extraction of DNA from ground tissue was conducted using a DNeasy Plant Mini Kit (Qiagen, Hilden, Germany) according to the manufacturer's instructions, with elution volume reduced to 60 µL. Concentration and quality of DNA (260/280 nm and 260/230 nm ratios) were assessed using a NanoDrop spectrophotometer (Thermo Scientific, Waltham MA, USA), and DNA concentration was diluted to 20 ng μL^{-1}.

For molecular detection of pathogens, primer sets specific to various root rot pathogens were selected based on their prior use in the scientific literature and successful amplification of DNA of their particular target. Cross-reaction of primers with other closely related pathogens of relevance to the project was evaluated to determine the

possibility of false positive results. The primers chosen for pathogen detection and their respective positive controls are listed in Table 1. Of the 12 primer sets, five were originally designed with a central TaqMan probe, but were used as conventional primers without the probe. The IPC primer set, which detects ascomycete fungi (Kulik, 2011), was redesigned using Primer 3 Plus software (Untergasser et al., 2012) and renamed IPC9 (Table 1). This primer set combines part of the probe with the reverse primer and uses an upstream forward primer.

Detection of pathogens was accomplished through end-point PCR of 20 µL reactions consisting of 1X buffer, 2.5 mM $MgCl_2$, 125 µM dNTP mixture, 0.1 µM of each primer, 1 U of Taq DNA Polymerase (Invitrogen recombinant), and 40 ng of genomic DNA. In order to avoid non-specific bands with primers designed for *F. culmorum*, the $MgCl_2$ concentration was reduced to 2 mM. Cycler conditions were 95°C for 4 min, followed by 34 cycles of 95°C for 30 s, 60°C for 30 s and 72°C for 30 s, finished with a final extension at 72°C for 7 min. Amplicons were run on 1.5% agarose gel containing GelRed® (Biotium, Freemont CA USA) for 1 h at 120 v and visualized using a ChemiDoc (Bio-Rad, Hercules CA USA).

Detection of previously unreported pathogens by PCR (*Berkeleyomyces basicola, Verticillium dahliae* and *Macrophomina phaseolina*) was confirmed by sequencing the band produced by their respective species-specific primers (Table 1). DNA from excised bands was extracted using a monarch gel extraction kit (New England Biolabs, Ipswich MA USA) and samples were sent for sequencing (Eurofins Genomics, Louisville KY USA). Sequence data were used to construct a trimmed consensus contig (DNA Baser, Heracle Biosoft, Arges, Romania) which was compared with sequences in the NCBI Genbank database (Altschul et al., 1990).

Pathogen isolation and identification

Frozen tissues in 2020 and air-dried root tissues in 2021 were used for pathogen isolation. Root segments were surface sterilized for 2 min in 10% bleach solution, rinsed in sterile deionized water and placed on potato dextrose agar (PDA) medium for 7-10 days. Fungal colonies were selected based on colony morphology to exclude common saprophytes. Colonies were purified by transferring single germinated conidia to fresh medium. Culture plugs were stored in milk-glycerol solution at -80°C.

Mycelia were produced for DNA extraction by growing purified isolates in liquid medium (1 g $NH_4H_2PO_4$ [Millipore Sigma], 0.2 g KCl [Fisher Chemical], 0.2 g $MgSO_4$ x 7 H_2O [Millipore Sigma], 10 g D-glucose [Fisher Chemical], 5 g yeast extract [Fisher Chemical], 0.01 g $ZnSO_4$ x 7 H_2O [Millipore Sigma], 0.005 g $CuSO_4$ x 5 H_2O [Millipore Sigma], 1 L distilled water) on a rotary shaker for 2-4 days, filtered to remove media and freeze dried. Freeze-dried tissues were pulverized inside microcentrifuge tubes containing a 0.6 cm diameter ceramic bead using a custom-made paint can shaker at full speed for 1 min. Extraction, quantification and dilution of DNA were conducted as described above.

Soil was collected from the research field from which *Berkeleyomyces* sp. had been detected by PCR in 2020. Desi

TABLE 1 Primers used for pathogen detection in DNA samples derived from chickpea roots collected in Saskatchewan in 2020 and 2021.

Target species	Forward Primer	Reverse Primer	Target Locus	Reference	Positive Control
General ascomycete fungi	IPC9f ACTTTTAACAACGGATCTCTTGGT	IPC9r CAATGTGCGTTCAAAGATTCGATG	5.8S rDNA	modified from Kulik, 2011	F56**
Fusarium redolens	RedF*	RedR*	EF1a	Willsey et al., 2018	FR05**
Fusarium solani	SolF*	SolR*	EF1a	Willsey et al., 2018	DAOMC 193418
Fusarium avenaceum	AveF*	AveR*	EF1a	Willsey et al., 2018	F56**
Fusarium chlamydosporum	AF330109CF	AF330109CR	TRI13	Demeke et al., 2005	F47**
Fusarium culmorum	Fc01F	Fc01R	RAPD derived	Nicholson et al., 1998	C1 (S. Chatterton)
Fusarium oxysporum f. sp. *ciceris*	Foc0-12f	Foc0-12r	SCAR marker	Jiménez-Gasco and Jiménez-Díaz, 2003	SB12 (W. Chen)
Verticillium dahliae	Df	Dr	ITS	Inderbitzin et al., 2013	DAOMC 250722
Verticillium albo-atrum	Aaf	AaTr	ACT	Inderbitzin et al., 2013	DAOMC 216604
Phytophthora spp.	18Ph2F	5.8S-1R	ITS1	Scibetta et al., 2012	DAOMC BR 610
Berkeleyomyces sp.	Tb1*	Tb2*	ITS	Huang and Kang, 2010	DAOMC 187829
Macrophomina phaseolina	MpKFI*	MpKRI*	ITS	Babu et al., 2007	CBS 205.47

*primers were used without the aid of TaqMan probes.
**identification done in-house based on Ef1a sequence identity with sequences in Fusarium ID and NCBI databases.

chickpea seedlings were grown in this field soil and the root tissue was used for pathogen isolation as described above. Examination of endoconidia and chlamydospore morphology (Nel et al., 2018) was used to select *Berkeleyomyces*-like colonies. Identification of a *Berkeleyomyces sp*. isolate was confirmed with species-specific primers (Huang and Kang, 2010), and sequence data was generated and analyzed as described above.

Since morphological identification of *Fusarium* species is often unreliable, species-specific primers were also used to identify isolates of common *Fusarium* species by end-point PCR (Table 1). Reactions were processed as described above, except that 1.5 mM $MgCl_2$ and 1 ng μL^{-1} of genomic DNA were used. For *Fusarium* isolates with inconclusive identification using selective primers, the TEF1 locus was sequenced after amplification with primers EF1 and EF2 (Geiser et al., 2004). Extraction of PCR amplicons, sequencing and data analysis were performed as described above. In addition to using the NCBI database, results were submitted to the online Fusarium identification tool (fusarium.mycobank.org, CBS-KNAW Fungal Biodiversity Centre).

Pathogenicity testing

A series of three pathogenicity tests were conducted for comparisons among isolates obtained from field surveys and those obtained from culture collections. All experiments were conducted in controlled environment chambers (Conviron model GR-48, Winnipeg, Canada) with 25°C daytime, 10°C night temperature and a 16 h photoperiod. Plants were grown in 10 cm diameter pots of peat-based medium (Sunshine mix #4, Sun Gro Horticulture, Agawam, MA USA or ProMix-BX-general purpose soil mix, Premier Tech Horticulture, Rivière-du-Loup, QC Canada). Cultures were grown on PDA for 5 to 7 days under incandescent lighting at room temperature. To prepare spore suspension of *F. culmorum*, PDA cultures were rinsed with deionized water and filtered through miracloth (Calbiochem, San Diego, CA USA). For spore production of all other *Fusarium* species, two plugs cut from the growing edge of the colony on PDA were added to a 250 mL flask containing 100 mL of carboxymethyl cellulose (CMC) medium and incubated under light for 4-5 days at 23°C on a shaker at 150 rpm (Foroud et al., 2012). After filtering through miracloth, conidia in liquid cultures were harvested by centrifugation for 5 min at 3400 rpm, followed by two washes with deionized water. Following re-suspension in deionized water, the resulting suspension was adjusted to 1 x 10^4 spores mL^{-1}. This suspension was added to moist growth medium at a rate of 3 x 10^6 conidia per kg (300 mL of 1 x 10^4 conidia mL^{-1}) prior to planting. Ten days after seeding, fresh conidia suspensions were prepared as described above and adjusted to 1 x 10^3 conidia mL^{-1}. Aliquots of 5 mL were pipetted to the base of each seedling, henceforth referred to as drenching. Water was pipetted to the base of seedlings in non-inoculated controls. Seedling emergence was recorded 10 days after planting. Root rot severity was assessed 3 weeks after planting by assessing disease development on the hypocotyl. All experiments had four replicates arranged in a randomized complete block design and were conducted twice.

Experiment 1 included three chickpea survey isolates each of *F. redolens* (FR06, FR08, FR10) and *F. solani* (FSL01, FSL03, FSL04) as well as one isolate of *F. avenaceum* (Fav7). Two additional local isolates of *F. avenaceum*, Fav3 from pea and Fav 5 from lentil, which had previously been used for germplasm screening of various other pulse crops, were included. Seeds of CDC Orkney (kabuli) and CDC Sunset (desi) were surface sterilized in 10% bleach for 2 min and rinsed twice with deionized water prior to seeding in inoculated potting mix and further processed as described above. Disease severity was assessed on a 0-5 scale (modified from Coyne et al., 2019), where 0 indicated no disease symptoms, 1 indicated small hypocotyl lesions, 2 indicated lesions coalescing around epicotyls and hypocotyls, 3 indicated lesions starting to spread into the root system with some root tips infected, 4 indicated epicotyl, hypocotyl and root system almost completely infected and 5 indicated a completely infected root and dead plant.

Experiment 2 compared the most aggressive *F. avenaceum* (Fav3, Fav5), *F. solani* (FSL04) and *F. redolens* (FR06) isolates evaluated in the first experiment to an isolate of *F. oxysporum* f. sp. *ciceris* from Washington state (race 1 isolate SB12, W. Chen, USDA ARS, Dept. of Crop and Soil Sciences, and Plant Pathology, Washington State University) and 6 other local *Fusarium* isolates. These included four *F. culmorum* from chickpea (FC04, FC05, FC06, FC07), one *F. inflexum* from chickpea (Fi01) and one *F. inflexum* from lentil (Fi02). Inoculation of soil at planting and 10 days later was performed as described above. Seeds of kabuli chickpea cultivar CDC Leader were planted as described above, but without surface sterilization. Plant height was measured on 3-week-old plants prior to removing plants from pots for disease assessment. Disease assessment was performed using a 0-10 incremental scale (0 = no symptoms, 1 = 1 to 10% of root tissue affected, 2 = 11 to 20% of root tissues affected, and so on, to 10 = 91 to 100% of root tissues affected) to indicate the degree of damage to the hypocotyl region.

In Experiment 3, disease severity caused by a local, highly aggressive *F. avenaceum* (Fav5) was compared to disease caused by single isolates of *V. dahliae* (DAOMC 250722, from soil, Ontario), *M. phaseolina* (CBS 205.47, from common bean, Italy), and a local isolate of *Berkeleyomyces* sp. from chickpea (TB02). The kabuli cultivar CDC Leader was planted after seeds were surface sterilized as described above. For *F. avenaceum*, *Berkeleyomyces* sp. and *M. phaseolina*, soil incorporation of inoculum was followed by drenching 10 days after seeding as previously described, with method modifications to suit the biology of each pathogen, including inoculum preparation, concentration, and, for *V. dahliae*, delivery method. Inoculum preparation and concentrations for *F. avenaceum* followed the standard protocol described above. Cultures of *Berkeleyomyces* sp. were grown on PDA and incubated for 10 days at room temperature under continuous incandescent lighting. Chlamydospores and endoconidia (which were the majority of spores) were harvested by flooding the Petri dishes with sterile tap water, scraping with a sterile glass slide, and filtering the suspension through miracloth. Based on prior research, the spore suspension was adjusted to 1 x 10^4 spores mL^{-1} for soil incorporation and drenching (Tabachnik et al., 1979). Cultures of *M. phaseolina* were grown on oatmeal agar medium incubated at room temperature for 10 days under continuous incandescent lighting. Mycelia were harvested by flooding the Petri dishes with sterile distilled water and scraping the culture surface with a sterile glass slide. The mycelia were homogenized in a blender and adjusted to 3 x 10^4 mycelia fragments per mL for soil incorporation and for drenching (modified from Cota-Barreras et al., 2022). Cultures of *V. dahliae* were prepared on PDA and in CMC medium for spore production as described above.

Based on prior research, spore suspensions were adjusted to 3 x 10^7 spores mL^{-1}, and a seedling root soaking method was used for inoculation (Jiménez-Fernández et al., 2016). Seedlings were grown in medium horticultural vermiculite (Perlite Canada Inc., Lachine QC Canada) and removed from their pots 7 days after seeding. Seedlings were soaked in spore suspension for 15 min and transplanted into non-inoculated ProMix-BX-general purpose soil mix (Premier Tech Horticulture, Rivière-du-Loup, QC Canada). Spore suspension of 3 x 10^7 spores mL^{-1} was used for drenching 10 days after transplanting. Non-inoculated controls were maintained for each isolate (species) treatment in order to capture any effect of seedling dipping and transplanting or the soil incorporation method to help determine relative differences in disease severity. Plant height was measured prior to removing plants from pots for disease assessment. Disease assessment was performed using the 0-10 incremental scale to indicate the degree of damage to the hypocotyl region.

Statistical analysis

All analyses were conducted using SAS software version 9.4 (SAS Institute, Cary NC, USA). Pooling of experimental runs was performed after ensuring that there was no statistical effect of experimental run. Analysis of ordinal disease rating data from pathogenicity experiment 1 was performed following conversion to rank using the rank procedure. The mid-ranks (r), the default in the rank procedure, were then used in the mixed procedure to calculate the nonparametric test statistics and their significance levels (P-values). Genotype, treatment and genotype by treatment were considered fixed effects. The Wald-type statistic (WTS) was computed using the Chi-squared test. The anovaf option in the mixed procedure was used to generate the calculation of the ANOVA-type statistic (ATS), and the repeated statement was used to specify properties of the variances within experimental units (Shah and Madden, 2004).

For pathogenicity experiments 2 and 3 that had percentage disease data, normality of errors were evaluated with the Shapiro–Wilk test and homogeneity of variance with the Levene's test before being modelled with the mixed model procedure. Replicate nested in experimental runs and experimental run were considered random effects whereas isolates were considered fixed effects. Heterogeneous variances were modeled with the repeated statement as required. Means were separated based on Fisher's least significant difference at P = 0.05.

Results

Field survey

Spring moisture was adequate in the chickpea growing area of Saskatchewan in 2020, but moisture was limited in spring 2021. Summer conditions in both years were characterized by below average rainfall along with hot temperatures and drying winds. Mean disease severity assessments of above-ground symptoms (yellowing, stunting, necrosis) on a 1 to 5 rating scale ranged from 1.1 to 4.1 in 2020 and from 2.2 to 4.4 in 2021 when averaged for each field (Tables S1, S2). The median score for all fields assessed was 1.8 in 2020, indicating slight yellowing on above-ground plant parts in many fields at most assessment locations in each field. It is noteworthy that even in those fields with low average disease scores, 39 of the 43 fields had locations that were rated with scores of 3 and 4, indicating the possibility of serious root rot foci in the majority of fields. Fields in 15 rural municipalities had average ratings of 3 and higher indicating moderate to severe yellowing and stunting, and in four RMs, dead plants were observed (rating score of 5). Rural municipalities where the most severe root rot symptoms were observed in 2020 were selected for sampling in 2021. Of the 19 fields surveyed in 2021, 16 fields had maximum ratings of 4 or 5, indicating that severe symptoms and/or dead plants were observed in most fields. Heat and drought stress likely contributed to these symptoms, as may have other unknown factors.

Assessment of root rot severity in 2021 was performed on dry roots, which made fine features of lesions more difficult to observe. Mean severity of root rot symptoms ranged from 1.6, indicating only very small lesions, to 6.0, indicating extensive lesion development on the taproot. The overall mean root rot severity for the 19 fields was 2.9, which demonstrates that root rot damage was significant despite dry growing conditions. Severe root rot (rating of 4 to 7) was observed in root samples from seven of the 19 fields (Table S2).

Molecular detection of potential root pathogens

Primer testing demonstrated that cross-reactions among the species involved in this study were only observed for *F. culmorum* primers Fc01F/R (Nicholson et al., 1998). This primer set resulted in cross reaction with several other species at 2.5 mM $MgCl_2$, including *V. albo-atrum*, *F. avenaceum*, *F. solani*, *F. redolens*, and *F. chlamydosporum*. Reduction of $MgCl_2$ to 2 mM eliminated most cross-reactions so that only a faint band persisted with *F. redolens*. Although this primer set has been cited extensively in the literature, it has only been used in the context of cereal pathology, and thus its specificity was not tested against a full spectrum of *Fusarium* species and other fungi.

In both survey years, *Fusarium solani* and *F. redolens* were the most prevalent pathogens detected in root samples, but *F. solani* was the most frequently detected pathogen in 2020 samples, whereas *F. redolens* was most frequent in 2021 samples. *Fusarium avenaceum* was also frequently detected in 2021 samples (73%), whereas it was only present in 33% of samples in 2020. *Fusarium chlamydosporum* was also detected in both years at relatively low frequency. *Fusarium culmorum* was not detected in any of the 2020 samples, and at a relatively low frequency (9%) in 2021 samples (Figure 1).

Amplicons of the expected size were obtained with primers designed for detection of *Macrophomina phaseolina* in 5% of 2020 and 14% of 2021 samples, but attempts to sequence these bands were unsuccessful, suggesting that amplification was non-specific. *Berkeleyomyces basicola* was detected in two 2020 samples originating from the University of Saskatchewan research farm in Saskatoon, and from 1 sample from a commercial farm in 2021.

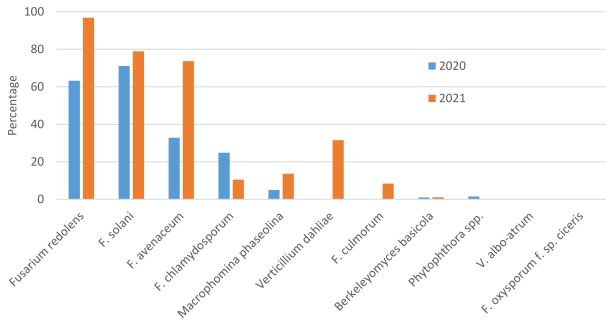

FIGURE 1
Percentage of chickpea root samples collected in Saskatchewan in 2020 and 2021 in which potential chickpea root pathogens were detected by end-point PCR.

Although not detected in 2020 samples, *Verticillium dahliae* was detected in 33% of 2021 samples (Figure 1). Bands amplified with the *Berkeleyomyces* sp. and *V. dahliae*-specific primers (Table 1) were sequenced to confirm species identity. A 312 bp consensus sequence generated from the *Berkeleyomyces* sp. band (OQ183437) had 100% coverage and 100% identity with NCBI sequences for a reference strain of *B. basicola* (MF952429) and the type strain of *B. rouxiae* (MF952412.1). Identity with both of these reference strains at an rDNA locus is not surprising, as these organisms were only recently split into two species, *B. basicola* and *B. rouxiae* W.J. Nel, Z.W. de Beer, T.A. Duong & M.J. Wingf. (Nel et al., 2018). Bands obtained from two root samples using the *V. dahliae* primers generated 498 bp (OQ183438) and 508 bp (OQ183439) sequences, which had 99.48% and 97.22% identity with NCBI sequences for the type specimen of *V. dahliae* (NR_126124.1) with 77% coverage. Higher coverage (99%) was observed for *V. dahliae* accession HE972025.1, with 99.6% identity for the 498 bp contig and 98.02% identity for the 508 bp contig. Both *Berkeleyomyces* sp. and *V. dahliae* have not been reported previously from chickpea in Saskatchewan.

Fusarium oxysporum f. sp. *ciceris* and *V. albo-atrum* were not detected in any samples. Detection of members of the *Phytophthora* genus were rare, with 1% of samples in 2020 but zero in 2021 (Figure 1).

Pathogen isolation and identification

Pathogen isolation from chickpea root tissues resulted in the purification of 7 *Fusarium* spp. isolates in 2020, and 52 *Fusarium* spp. isolates in 2021. Of the 59 *Fusarium* spp. isolates, 58 were identified using a combination of species-specific primers and sequencing at the Ef1a locus. Sequencing was performed for 20 *Fusarium* spp. isolates, including all putative *F. oxysporum* (OQ181356 to OQ181375). Seventeen isolates were *Fusarium redolens*, 13 F. *oxysporum*, ten *F. avenaceum*, seven *F. solani*, five *F. culmorum*, three *F. caucasicum* Letov, one *F. incarnatum-equiseti* complex, one *F. acuminatum* or *F. tricinctum* complex and one *F. toxicum* L. Lombard & J.W. Xia. The identity of one isolate remained undetermined. No *F. oxysporum* f. sp. *ciceris* isolates were obtained.

One *Berkeleyomyces* isolate was obtained from chickpea seedlings grown in field soil collected from a research site in 2020. The amplicon obtained for DNA of this isolate using species-specific primers (Huang and Kang, 2010) was of expected size and matched the amplicon size obtained with a culture collection isolate (DAOMC 187829). A 318 bp consensus sequence generated from the band had 100% coverage and 100% identity with NCBI sequences for a reference strain *of B. basicola* (MF952429.1) and the type strain of *B. rouxiae* (MF952412.1). Due changes in fungal taxonomy that occurred after the publication of the primer set and inability to resolve species based on the ITS sequence, we refer to this isolate as *Berkeleyomyces* sp.

Pathogenicity testing

In growth chamber tests comparing three isolates each of *F. redolens*, *F. avenaceum* and *F. solani* (Experiment 1), chickpea cultivars and isolates both had significant effects on root rot severity ($P \leq 0.014$), but their interaction was not significant ($P = 0.18$). Disease severity was highest for two isolates of *F. avenaceum* (Fav 3, Fav5) on both the desi and kabuli cultivar tested. The remaining isolates caused only limited disease, with mean ratings of less than 1 on both cultivars (Figure 2). The two most aggressive isolates of *F. avenaceum* (Fav 3, Fav5) originating from pea and lentil caused a 16 to 22% reduction in emergence of the kabuli cultivar (data not shown). These isolates, as well as *F. redolens* (FR06) and *F. solani* (FSL04), were chosen to be included in Experiment 2.

Experiment 2 included nine selected isolates of six different *Fusarium* species. None of the isolates had a significant effect on emergence of kabuli cultivar CDC Leader ($P = 0.075$) but isolate significantly impacted plant height and root rot severity ($P<0.0001$ for both). Single isolates of *F. solani*, *F. culmorum*, *F. redolens* and both *F. inflexum* isolates caused low disease severity (<24%, Figure 3). Disease severity observed for the Fav3 isolate of *F. avenaceum* and an isolate of *F. oxysporum* f. sp. *ciceris* did not differ from that observed in the non-inoculated controls. This result was not unexpected for *F. oxysporum* f. sp. *ciceris*, given that this organism causes vascular wilting rather than root rot symptoms, but this isolate also failed to cause any height reduction of CDC Leader within the 21-day time frame of the experiment (Figure 4). Three of the *F. culmorum* isolates caused moderate to severe root rot symptoms, ranging from 57% to 82% severity. This was significantly less than the 94% disease severity

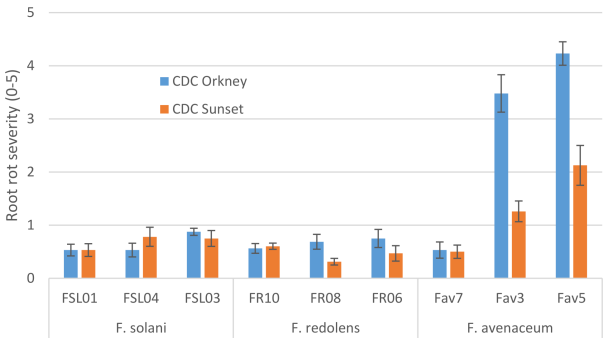

FIGURE 2
Root rot severity (0-5 scale) caused by three isolates each of three *Fusarium* species on 3-week-old plants of CDC Orkney kabuli chickpea and CDC Sunset desi chickpea under controlled conditions. Inoculum was incorporated into soil at planting and applied by soil drenching 10 days after planting.

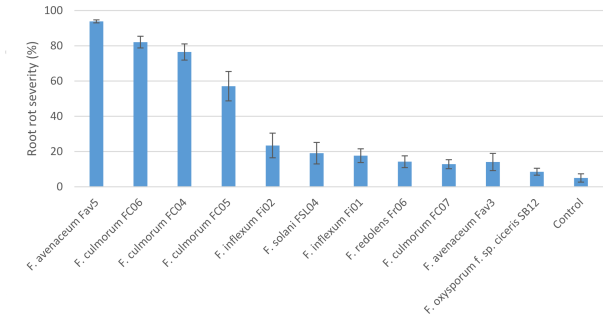

FIGURE 3
Root rot severity (%) caused by nine isolates of six *Fusarium* species on 3-week-old plants of CDC Leader kabuli chickpea under controlled conditions. Inoculum was incorporated into soil at planting and applied by soil drenching 10 days after planting.

caused by *F. avenaceum* isolate Fav5 (Figure 3). These same four isolates (*F. culmorum* FC04, FC05, FC06, and *F. avenaceum* Fav5) were the only ones that caused a significant height reduction relative to non-inoculated CDC Leader plants (Figure 4).

Comparison of pathogenicity of single isolates of *M. phaseolina*, *Berkeleyomyces* sp., and *V. dahliae* to a local, highly aggressive isolate of *F. avenaceum* (Fav5) used in the two prior experiments in Experiment 3, revealed no significant effect of the isolates on emergence ($P = 0.84$), but isolate impacted height ($P < 0.0001$) and root rot severity ($P < 0.0001$). Plants in the non-inoculated controls accompanying soil-incorporated inoculum treatments showed no root rot, and non-inoculated plants that had been removed from their pots and dipped in deionized water showed only trace root discoloration (<2%, Figure 5). In the combined data analysis, the only isolate to significantly impact plant height was *F. avenaceum* Fav5, which resulted in 79% height reduction relative to non-inoculated control plants (data not shown). *Verticillium dahliae* significantly reduced plant height in one of the two experimental runs, but this effect was not statistically supported by means comparisons with combined data. Disease severity differed significantly for the single

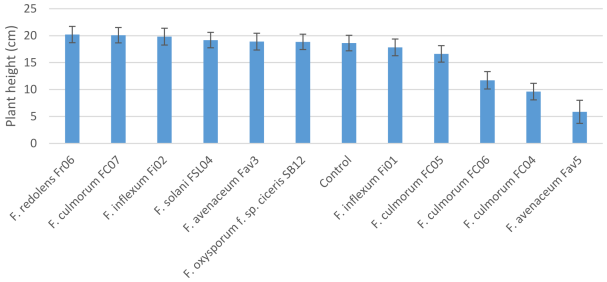

FIGURE 4
Height (cm) of 3-week-old CDC Leader kabuli chickpea inoculated with nine isolates of six *Fusarium* species under controlled conditions. Inoculum was incorporated into soil at planting and applied by soil drenching 10 days after planting.

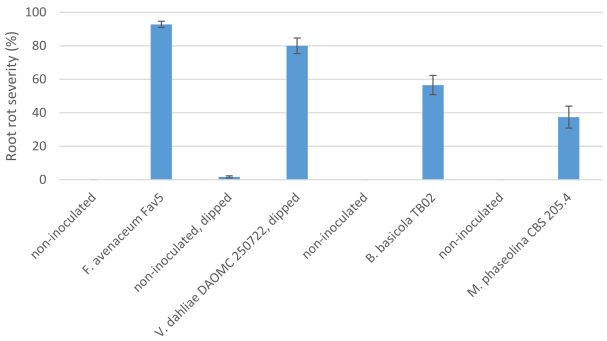

FIGURE 5
Root rot severity (%) caused by four pathogens on 3-week-old plants of CDC Leader kabuli chickpea under controlled conditions. Inoculum was incorporated into soil at planting or applied as a seedling dip, and applied by soil drenching 10 days after seeding or transplanting.

isolates of the four pathogens, with *F. avenaceum* causing the most damage to roots, followed by *V. dahliae*, *Berkeleyomyces* sp. and *M. phaseolina* under the test conditions (Figure 5). Infection by *F. avenaceum* resulted in totally collapsed brown hypocotyls and a small, brown tap root. Plants were severely stunted, dying or dead (Figure 6). Plants infected with *V. dahliae* developed brown lesions that encircled the hypocotyl. Disease development was more severe in experimental run 2, where *V. dahliae* infection affected the whole hypocotyl, epicotyl and tap root, and caused significant height reduction ($P = 0.009$). The impact on height observed in experimental run 2 was not statistically supported in pooled data. Symptoms caused by *Berkeleyomyces* sp. included black lesions on the hypocotyl that were generally not more than 1 cm in length and did not encircle the hypocotyl. Black lesions were also observed on hypocotyls of *M. phaseolina*-infected plants, but these were discrete lesions of limited size (Figure 6). Infection by *Berkeleyomyces* sp. and *M. phaseolina* did not impact plant height (data not shown).

Discussion

The increasing prominence of root rot diseases in pulse crops is an important issue facing agricultural systems on the Canadian prairies. Along with *Aphanomyces euteiches*, *Fusarium avenaceum* and *F. solani* are major pathogens of pea and lentil in this region (Chatterton et al., 2019). Chickpea cultivars grown in this region are susceptible to Fusarium root rot caused by *F. avenaceum* (S. Banniza, unpublished). During surveys of chickpea fields during 2020 and 2021, the typical pattern of patchy root rot development was observed under the prevailing hot, dry conditions. The 2021 survey focused upon regions where wilting, discoloration and/or stunting of chickpea were observed in 2020, which lead to a higher proportion of symptomatic plants and/or roots observed in 2021 as compared to 2020. No obvious geographical localization of individual root pathogens was detected in the chickpea production area surveyed. In both years, *F. redolens*, *F. avenaceum* and *F. solani* DNA detections

FIGURE 6
Root rot symptoms caused by four pathogens on 3-week-old plants CDC Leader kabuli chickpea under controlled conditions. Inoculum was incorporated into soil at planting or applied as a seedling dip, and applied by soil drenching 10 days after seeding or transplanting. From left to right: non-inoculated control, *Macrophomina phaseolina*, *Berkeleyomyces basicola*, *Verticillium dahliae*, *Fusarium avenaceum*.

were the most prevalent, with a prominent increase in *F. avenaceum* and *F. redolens* detection frequency in 2021 over that in 2020. The use of *M. phaseolina* species-specific primers gave misleading results due to non-specific amplification. Despite using a standard technique implemented successfully by other researchers (Mayék-Pérez et al., 2001; Cota-Barreras et al., 2022), this pathogen was never observed in PDA isolation plates, suggesting that *M. phaseolina* is not a current threat to chickpea production in Saskatchewan. Previously unreported pathogens *V. dahliae* and *Berkeleyomyces* sp. were detected in chickpea root tissue using molecular techniques, but whereas *Berkeleyomyces* sp. was isolated from chickpea roots, *V. dahliae* was never observed in isolation plates. While it is possible that isolation of *V. dahliae* would have benefitted from the use of semi-selective medium, other researchers have successfully used PDA for isolation of *V. dahliae* (Jabnoun-Khiareddine et al., 2010; Ashraf et al., 2012). Despite molecular detection of *V. dahliae* in 12 field samples, the pathogen could not be reliably isolated using these standard techniques. It is possible that the use of dry root tissue for isolation also did not favor *Verticillium* recovery. The impact of *V. dahliae* infection of chickpea under field conditions warrants further investigation, particularly given the wide host range of this pathogen and its potential for impact on canola, which is widely grown on the Canadian prairies (Hwang et al., 2017).

Pathogenicity studies involving the three most prevalent *Fusarium* species detected in surveys showed that three *F. redolens* isolates and three *F. solani* isolates caused only very mild symptoms on chickpea roots. This is supported by a previous study using two *F. redolens* isolates from durum which caused low to moderate disease on pea, desi chickpea and durum, with one of these isolates causing more disease on pea than on desi chickpea or durum (Esmaeili Taheri et al., 2011). Of the three *F. avenaceum* isolates in the current study, two caused severe disease on CDC Orkney kabuli chickpea, whereas only one of these, an isolate obtained from lentil, caused severe disease on CDC Leader kabuli chickpea. The lone chickpea isolate chosen for pathogenicity testing caused only minor symptoms. Some variation in the aggressiveness of 19 F. *avenaceum* isolates was previously observed on pea and chickpea (Safarieskandari et al., 2021). When compared to isolates of *F. solani*, *F. culmorum*, *F. redolens*, *F. oxysporum* and *F. acuminatum*, six of the 19 isolates of *F. avenaceum* were aggressive enough to kill pea plants, and one isolate caused only moderate symptoms on pea. A mixture of three of these *F. avenaceum* isolates with high aggressiveness on pea were inoculated onto two kabuli and two desi cultivars. Reduced emergence of one desi and one kabuli cultivar following inoculation using a seed soaking method was observed, and CDC Leader, a kabuli cultivar also used in the current study, did not emerge. Moderate root rot severity was reported for the chickpea cultivars that successfully emerged. The large variation in aggressiveness among *F. avenaceum* isolates reported by Safarieskandari et al. (2021) and observed in the current study suggests that further work is needed to investigate whether host origin relates to isolate aggressiveness and host preference. Given the potential for *F. avenaceum* to impact pulse and cereal crops, further research on this topic could be used to improve disease management strategies.

Three of the four *F. culmorum* isolates tested under controlled conditions caused moderate to severe root rot severity and significant height reduction in inoculated chickpea plants. Research comparing *Fusarium* sp. isolates from pea showed that isolates of *F. culmorum* caused root rot symptoms equivalent to that caused by the most aggressive *F. avenaceum* isolates on pea seedlings (Safarieskandari et al., 2021). During chickpea root rot surveys conducted during two dry, hot seasons, *F. culmorum* was not detected in root tissues collected in 2020, and only at low frequency in 2021. Isolation of *F. culmorum* from root tissue also occurred at low frequency in 2021. Given this pathogen's potential to cause severe root rot on chickpea and pea indoors where conditions are more moist and temperate, it is worthwhile continuing to learn about its role in the root rot complex of pulse and cereal crops.

Conducting disease survey work provided an opportunity to assess the potential threat of several previously unreported pathogens of chickpea in our region. Given that climate change threatens to modify growing conditions and may thereby shift the importance and composition of pathogen species and populations, creating an inventory of potential pathogens and assessing their relative pathogenicity is one small step toward system resiliency. No isolates of *F. oxysporum* f. sp. *ciceris* were recovered from diseased chickpea roots collected in disease surveys. An isolate of *F. oxysporum* f. sp. *ciceris* race 1 obtained from the US was included in growth chamber testing, where it failed to cause wilting or stunting of CDC Leader. As a pathogen with known impact on chickpea, these results may have been due to unsuitable test conditions, insufficient time for disease development, or resistance of CDC Leader to race 1 Fusarium wilt. Three additional root rot pathogens of chickpea with international significance, *Berkeleyomyces* sp., *V. dahliae* and *M. phaseolina*, were compared to a local, highly aggressive isolate of *F. avenaceum*. As these pathogens all have distinct biology and infection strategies, a direct, subjective comparison is somewhat difficult to attain. In addition, since these pathogens have not previously been reported in our region, we only had access to a single local isolate of *Berkeleyomyces* sp. and had to rely on single isolates of *V. dahliae* and *M. phaseolina* from culture collections. Despite these limitations, pathogenicity testing conducted using methods tailored to each pathogen provided some interesting insight. Although the inoculum density for the *F. avenaceum* isolate was the lowest of all four pathogens, this organism caused the most severe damage to chickpea seedlings under the test conditions. Within 20 days, chickpea inoculated with *F. avenaceum* Fav5 were dead or dying, and those inoculated with *V. dahliae* in one experimental run exhibited stunting. Chickpea seedlings inoculated with *Berkeleyomyces* sp. and *M. phaseolina* still appeared healthy above-ground but had hypocotyl lesions developing. Continued vigilance and assessment of the impact of emerging chickpea pathogens *V. dahliae* and *Berkeleyomyces* sp. under field conditions is recommended.

Data availability statement

The datasets presented in this study can be found in online repositories. The names of the repository/repositories and accession number(s) can be found below: https://www.ncbi.nlm.nih.gov/genbank/, OQ181356 OQ181357 OQ181358 OQ181359 OQ181360 OQ181361 OQ181362 OQ181363 OQ181364 OQ181365 OQ181366 OQ181367 OQ181368 OQ181369 OQ181370 OQ181371 OQ181372 OQ181373 OQ181374 OQ181375 OQ183436 OQ183437 OQ183438 OQ183439.

Author contributions

All authors listed have made a substantial, direct, and intellectual contribution to the work and approved it for publication. Cheryl Armstrong-Cho and Nimllash Thangam Sivachandra Kumar have contributed equally to this work and share first authorship.

Funding

Western Grains Research Foundation and the Agricultural Development Fund of the Saskatchewan Ministry of Agriculture, ADF project 20190243.

Acknowledgments

Technical support for pathogenicity testing was provided by Preetpal Kaur, Madison Muzyka and Dawson George. Our thanks to the many staff at the Saskatchewan Ministry of Agriculture, Saskatchewan Crop Insurance Corporation (SCIC), and Saskatchewan Association of Rural Municipalities (SARM) who coordinated survey activities, conducted field disease assessments, and collected chickpea roots. Isolates of *F. oxysporum* f. sp. *ciceris* were obtained from Dr. Weidong Chen at USDA-ARS at Washington State University. An isolate of *F. culmorum* (C1) was obtained from Dr. Syama Chatterton at AAFC Lethbridge. Identification of *F. inflexum* from lentil was conducted by Collins Bugingo in Mary Burrows' lab (Montana State University). The isolate of *Verticillium dahliae* was obtained from DAOMC, Ottawa and the *M. phaseolina* isolate was obtained from Westerdijk Fungal Biodiversity Institute, Utrecht, Netherlands. We are grateful for funding of this project from the Western Grains Research Foundation and the Agricultural Development Fund of the Saskatchewan Ministry of Agriculture.

We gratefully acknowledge that this work was conducted on Treaty 4 and Treaty 6 land and commit ourselves to the work of reconciliation in our community.

Conflict of interest

The authors declare that the research was conducted in the absence of any commercial or financial relationships that could be construed as a potential conflict of interest.

Publisher's note

Supplementary material

The Supplementary Material for this article can be found online at: https://www.frontiersin.org/articles/10.3389/fpls.2023.1117788/full#supplementary-material

References

Altschul, S. F., Gish, W., Miller, W., Myers, E. W., and Lipman, D. J. (1990). Basic local alignment search tool. *J. Mol. Biol.* 215, 403–410. doi: 10.1016/S0022-2836(05)80360-2

Ashraf, A., Rauf, A., Abbas, M. F., and Rehman, R. (2012). Isolation and identification of *Verticillium dahliae* causing wilt on potato in Pakistan. *Pak. J. Phytopathol.* 24, 112–116.

Babu, B. K., Saxena, A. K., Srivastava, A. K., and Arora, D. K. (2007). Identification and detection of *Macrophomina phaseolina* by using species-specific oligonucleotide primers and probe. *Mycologia* 99, 797–803.

Bowden, R. L., Wiese, M. V., Crock, J. E., and Auld, D. L. (1985). Root rot of chickpeas and lentils caused by *Thielaviopsis basicola*. *Plant Dis.* 69, 1089–1091.

Chatterton, S., Harding, M. W., Bowness, R., Mclaren, D. L., Banniza, S. , and Gossen, B. D. (2019). Importance and causal agents of root rot on field pea and lentil on the Canadian prairies 2014–2017. *Can. J. Plant Pathol.* 41, 98–114. doi: 10.1080/07060661.2018.1547792

Chen, W., Sharma, H. C., and Muehlbauer, F. J. (2011). *Compendium of chickpea and lentil diseases and pests* (St Paul, Minnesota, USA: The American Phytopathological Society).

Cota-Barreras, C. I., García-Estrada, R. S., Valdez-Torres, J. B., León-Félix, J., Valenzuela-Herrera, V., and Tovar-Pedraza, J. M. (2022). Molecular detection, virulence, and mycelial compatibility of *Macrophomina phaseolina* isolates associated with chickpea wilt in sinaloa and Sonora, Mexico. *Can. J. Plant Pathol* 44, 849-857. doi: 10.1080/07060661.2022.2084642

Coyne, C. J., Porter, L. D., Boutet, G., et al. (2019). Confirmation of fusarium root rot resistance QTL *Fsp-ps 2.1* of pea under controlled conditions. *BMC Plant Biol.* 19, 98.

Demeke, T., Clear, R. M., Patrick, S. K., and Gaba, D. (2005). Species-specific PCR-based assays for the detection of *Fusarium* species and a comparison with the whole seed agar plate method and trichothecene analysis. *Int. J. Food Micro.* 103, 271–284. doi: 10.1016/j.ijfoodmicro.2004.12.026

Erwin, D. C. (1958). Verticillium wilt of *Cicer arietinum* in southern California. *Plant Dis. Rep.* 42, 1111.

Esmaeili Taheri, A., Hamel, C., Gan, Y., and Vujanovic, V. (2011). First report of *Fusarium redolens* from Saskatchewan and its comparative pathogenicity. *Can. J. Plant Pathol.* 33, 559–564. doi: 10.1080/07060661.2011.620631

Esmaeili Taheri, A., Chatterton, S., Foroud, N. A., et al (2017). Identification and community dynamics of fungi associated with root, crown, and foot rot of field pea in western Canada. *Eur. J. Plant Pathol.* 147, 489–500.

Foroud, N. A., McCormick, S. P., MacMillan, T., Badea, A., Kendra, D. F., Ellis, B. E., et al. (2012). Greenhouse studies reveal increased aggressiveness of emergent Canadian *Fusarium graminearum* chemotypes in wheat. *Plant Dis.* 96, 1271–1279. doi: 10.1094/PDIS-10-11-0863-RE

Geiser, D. M., Jiménez-Gasco, M., Kang, S., Makalowska, I., Veeraraghavan, N., Ward, T. J., et al. (2004). FUSARIUM-ID v. 1.0: A DNA sequence database for identifying *Fusarium*. *Eur. J. Plant Pathol.* 110, 473–479. doi: 10.1023/B:EJPP.0000032386.75915.a0

Government of Saskatchewan (2021) *2021 specialty crop report*. Available at: https://www.saskatchewan.ca/business/agriculture-natural-resources-and-industry/agribusiness-farmers-and-ranchers/market-and-trade-statistics/crops-statistics/specialty-crop-report (Accessed Oct 1 2022).

Haware, M. P. (1998). "Diseases of chickpea," in *The pathology of food and pasture legumes*. Eds. D. J. Allen and J. M. Lenné (UK: CAB International Wallingford), 473–516.

Huang, J., and Kang, Z. (2010). Detection of *Thielaviopsis basicola* in soil with real-time quantitative PCR assays. *Microbiol. Res.* 165, 411–417. doi: 10.1016/j.micres.2009.09.001

Hwang, S. F., Strelkov, S. E., Ahmed, H. U., Zhou, Q., Fu, H., Fredua-Agyeman, R., et al. (2017). First report of *Verticillium dahliae* kleb. causing wilt symptoms in canola (*Brassica napus* l.) in north America. *Can. J. Plant Pathol.* 39, 514–526. doi: 10.1080/07060661.2017.1375996

Inderbitzin, P., Davis, R. M., Bostock, R. M., and Subbarao, K. V. (2013). Identification and differentiation of *Verticillium* species and v. longisporum lineages by simplex and multiplex PCR assays. *PloS One* 8, e65990. doi: 10.1371/journal.pone.0065990

Infantino, A., Kharrat, M., Riccioni, L., Coyne, C. J., McPhee, K. E., and Grünwald, N. J. (2006). Screening techniques and sources of resistance to root diseases in cool season food legumes. *Euphytica* 147, 201–221. doi: 10.1007/s10681-006-6963-z

Jabnoun-Khiareddine, H., Daami-Remadi, M., Barbara, D. J., and El Mahjoub, M. (2010). Morphological variability within and among *Verticillium* species collected in Tunisia. *Tunis. J. Plant Prot.* 5, 19–38.

Jha, U. C., Abhishek, B., Shailesh, P., and Kumar, P. S. (2020). Breeding, genetics, and genomics approaches for improving fusarium wilt resistance in major grain legumes. *Front. Genet.* 11, 1001. doi: 10.3389/fgene.2020.01001

Jiménez-Díaz, R. M., Castillo, P., Jiménez-Gasco, M. M., Landa, B. B., and Navas-Cortés, J. A. (2015). Fusarium wilt of chickpeas: Biology, ecology and management. *Crop Prot.* 73, 16–27. doi: 10.1016/j.cropro.2015.02.023

Jiménez-Fernández, D., Trapero-Casas, J. L., Landa, B. B., Navas-Cortés, J. A., Bubici, G., Cirulli, M., et al. (2016). Characterization of resistance against the olive-defoliating *Verticillium dahliae* pathotype in selected clones of wild olive. *Plant Pathol.* 65, 1279–1291. doi: 10.1111/ppa.12516

Jiménez-Gasco, M. M., and Jiménez-Díaz, R. M. (2003). Development of a specific polymerase chain reaction-based assay for the identification of *Fusarium oxysporum* f. sp. *ciceris* and its pathogenic races 0, 1A, 5, and 6. *Phytopathology* 93, 200–209. doi: 10.1094/PHYTO.2003.93.2.200

Kraft, J. M. (1969). Chickpea, a new host of *Fusarium solani* f. sp. *pisi*. *Plant Dis. Rep.* 53, 110–111.

Kulik, T. (2011). Development of TaqMan assays for 3ADON, 15ADON and NIV *Fusarium* genotypes based on Tri12 gene. *Cereal Res. Commun.* 39, 200–214. doi: 10.1556/CRC.39.2011.2.4

Mayék-Pérez, N., López-Castañeda, C., González-Chavira, M., Garcia-Espinosa, R., Acosta-Gallegos, J., de la Vega, O. M., et al. (2001). Variability of Mexican isolates of *Macrophomina phaseolina* based on pathogenesis and AFLP genotype. *Physiol. Mol. Plant Pathol.* 59, 257–264. doi: 10.1006/pmpp.2001.0361

Moussart, A., Even, M. N., and Tivoli, B. (2008). Reaction of genotypes from several species of grain and forage legumes to infection with a French pea isolate of the oomycete *Aphanomyces euteiches*. eur. *J. Plant Pathol.* 122, 321–333. doi: 10.1007/s10658-008-9297-y

Nel, W. J., Duong, T. A., Wingfield, B. D., Wingfield, M. J., and de Beer, Z. W. (2018). A new genus and species for the globally important, multihost root pathogen *Thielaviopsis basicola*. *Plant Pathol.* 67, 871–882. doi: 10.1111/ppa.12803

Nicholson, P., Simpson, D. R., Weston, G., Rezanoor, H. N., Lees, A. K., Parry, D. W., et al. (1998). Detection and quantification of *Fusarium culmorum* and *Fusarium graminearum* in cereals using PCR assays. *Physiol. Mol. Plant Pathol.* 53, 17–37. doi: 10.1006/pmpp.1998.0170

Safarieskandari, S., Chatterton, S., and Hall, L. M. (2021). Pathogenicity and host range of *Fusarium* species associated with pea root rot in Alberta, Canada. *Can. J. Plant Pathol.* 43, 162–171. doi: 10.1080/07060661.2020.1730442

Scibetta, S., Schena, L., Chimento, A., Cacciola, S. O., and Cooke, D. E. (2012). A molecular method to assess *Phytophthora* diversity in environmental samples. *J. Microbiol. Methods* 88, 356–368. doi: 10.1016/j.mimet.2011.12.012

Shah, D. A., and Madden, L. V. (2004). Nonparametric analysis of ordinal data in designed factorial experiments. *Phytopathology* 94, 33–43. doi: 10.1094/PHYTO.2004.94.1.33

Tabachnik, M., DeVay, J. E., Garber, R. H., and Wakeman, R. J. (1979). Influence of soil inoculum concentrations on host range and disease reactions caused by isolates of *Thielaviopsis basicola* and comparison of soil assay methods. *Phytopathology* 69, 974–977. doi: 10.1094/Phyto-69-974

Tekauz, A., McCallum, B., Ames, N., and Fetch, J. M. (2004). Fusarium head blight of oat - current status in western Canada. *Can. J. Plant Pathol.* 26, 473–479. doi: 10.1080/07060660409507167

Tekauz, A., McCallum, B., and Gilbert, J. (2000). Review: Fusarium head blight of barley in western Canada. *Can. J. Plant Pathol.* 22, 9–16. doi: 10.1080/07060660009501156

Untergasser, A., Ioana Cutcutache, I., Koressaar, T., Ye, J., Faircloth, B. C., Remm, M., et al. (2012). Primer3–new capabilities and interfaces. *Nucleic Acids Res.* 40, e115. doi: 10.1093/nar/gks596

Westerlund, F. V., Campbell, R. N., and Kimble, K. A. (1974). Fungal root rots and wilts of chickpea in California. *Phytopathology* 64, 432–436.

Willsey, T. L., Chatterton, S., Heynena, M., and Erickson, A. (2018). Detection of interactions between the pea root rot pathogens *Aphanomyces euteiches* and fusarium spp. using a multiplex qPCR assay. *Plant Pathol.* 67, 1912–1923. doi: 10.1111/ppa.12895

Xue, A. G., Armstrong, K. C., Voldeng, H. D., Fedak, G., and Babcock, C. (2004). Comparative aggressiveness of isolates of fusarium spp. causing head blight on wheat in Canada. *Can. J. Plant Pathol.* 26, 81–88. doi: 10.1080/07060660409507117

Zhou, Q., Yang, Y., Wang, Y., Jones, C., Feindel, D., Harding, M., et al. (2021). Phylogenetic, phenotypic and host range characterization of five *Fusarium* species isolated from chickpea in Alberta, Canada. *Can. J. Plant Pathol.* 43, 651–657. doi: 10.1080/07060661.2020.1869830

frontiers | Frontiers in Plant Science

TYPE Mini Review
PUBLISHED 09 February 2023
DOI 10.3389/fpls.2023.1132132

OPEN ACCESS

EDITED BY
Christophe Le May,
Institut Agro Rennes-Angers, France

REVIEWED BY
Catherine Rayon,
University of Picardie Jules Verne, France

*CORRESPONDENCE
Maïté Vicré
maite.vicre@univ-rouen.fr

SPECIALTY SECTION
This article was submitted to Plant Pathogen Interactions, a section of the journal Frontiers in Plant Science

RECEIVED 26 December 2022
ACCEPTED 16 January 2023
PUBLISHED 09 February 2023

CITATION
Fortier M, Lemaitre V, Gaudry A, Pawlak B, Driouich A, Follet-Gueye M-L and Vicré M (2023) A fine-tuned defense at the pea root caps: Involvement of border cells and arabinogalactan proteins against soilborne diseases.
Front. Plant Sci. 14:1132132.
doi: 10.3389/fpls.2023.1132132

A fine-tuned defense at the pea root caps: Involvement of border cells and arabinogalactan proteins against soilborne diseases

Mélanie Fortier, Vincent Lemaitre, Alexia Gaudry, Barbara Pawlak, Azeddine Driouich, Marie-Laure Follet-Gueye and Maïté Vicré*

Univ Rouen Normandie, GLYCOMEV UR 4358, SFR Normandie Végétal FED 4277, F-76000, Rouen, France

Plants have to cope with a myriad of soilborne pathogens that affect crop production and food security. The complex interactions between the root system and microorganisms are determinant for the whole plant health. However, the knowledge regarding root defense responses is limited as compared to the aerial parts of the plant. Immune responses in roots appear to be tissue-specific suggesting a compartmentalization of defense mechanisms in these organs. The root cap releases cells termed root "associated cap-derived cells" (AC-DCs) or "border cells" embedded in a thick mucilage layer forming the root extracellular trap (RET) dedicated to root protection against soilborne pathogens. Pea (*Pisum sativum*) is the plant model used to characterize the composition of the RET and to unravel its function in root defense. The objective of this paper is to review modes of action of the RET from pea against diverse pathogens with a special focus on root rot disease caused by *Aphanomyces euteiches*, one of the most widely occurring and large-scale pea crop diseases. The RET, at the interface between the soil and the root, is enriched in antimicrobial compounds including defense-related proteins, secondary metabolites, and glycan-containing molecules. More especially arabinogalactan proteins (AGPs), a family of plant extracellular proteoglycans belonging to the hydroxyproline-rich glycoproteins were found to be particularly present in pea border cells and mucilage. Herein, we discuss the role of RET and AGPs in the interaction between roots and microorganisms and future potential developments for pea crop protection.

KEYWORDS

associated cap-derived cells (AC-DCs), *Aphanomyces euteiches*, arabinogalactan-proteins (AGPs), root border cells, *Pisum sativum*, L., root defense, root extracellular trap (RET), root disease

1 Introduction

Legume seeds are an important source of dietary protein, carbohydrates, minerals, vitamins, and antioxidants presenting many advantages and great potential for human and animal nutrition. Garden pea (*Pisum sativum* L.) is one of the most widespread food legume crops cultivated in more than 90 countries all over the world (FAO, 2018) for its nutritional value and high-quality vegetable proteins. Its consumption is recognized to improve human diet and health by reducing cholesterol or preventing stomach cancer (Nazir et al., 2022). Several studies were dedicated to unravel pea proteins composition and properties making pea a widely used source of commercial proteins attracting attention in food industry (Karaca et al., 2011; Sun and Arntfield, 2012; Burger and Zhang, 2019). As compared to soybean (*Glycine max*) proteins, pea proteins present the advantage for food products to be deprived of allergen and being without genetic modification (Day, 2013; Krefting, 2017). Furthermore, pea is also a culture of interest as it does not require nitrogen fertilizer for its growth due to its capacity to fix atmospheric nitrogen *via* symbiosis with rhizobia thereby enriching the soil in nitrogen (Foyer et al., 2016). Therefore, pea is considered as an economical and environmental friendly crop, which improves crop productivity by reducing the demand for external nitrogen fertilizers in many farming systems. Despite its high nutritional value and remarkable advantages, the yield of the pea crop gets drastically reduced due to root diseases. More especially, *Aphanomyces euteiches* responsible of the root rot disease causes devastating damages to pea crops and significant economic losses (Gaulin et al., 2007). *A.euteiches* is particularly destructive on spring pea crops but also on other legumes such as green bean (*Phaseolus vulgaris*) or lentil (*Lens culinaris*). There is currently no effective way to control *A. euteiches* and root rot spreading, as neither the phyto-chemicals nor the resistant varieties are available. Avoidance of infested fields based on crop rotation remains the main used method to limit the spread of this disease. However, the long-term survival of *A. euteiches* oospores in the soil up to ten years is a serious limitation of this cropping management practice (Gibert, 2021). This results on an increasing need for new cropping systems and/or cultivar selection for pea producers in order to maintain sufficient yields. To this end, it is necessary to unravel the molecular dialogue at the root tip between pea and pathogens. This review summarizes current knowledge about the role of the root extracellular trap (RET) in pea root protection and presents the more promising strategies to control root disease with a special focus on root rot disease caused by *A. euteiches*.

2 Pea: the plant model to decipher the role of border cells in root defense

Plant defenses were mainly studied on the foliar parts whereas the belowground system remained ignored due to the difficulty of its access and the complexity of root-microbe interactions involving a diversity of beneficial and harmful soilborne microorganisms (Erb et al., 2011; Balmer et al., 2013). This is particularly true and crucial for legume roots which need to distinguish between mutualistic microbes and pathogens in order to allow symbiotic microorganisms such as rhizobia to colonize root tissues forming root nodules (Bozsoki et al., 2017). Immune signaling and responses in roots are not only different from leaves but are also compartmentalized within the different zones of this organ (Chuberre et al., 2018). Root elongation zone is recognized as the main entrance area for most of soilborne pathogens whereas root tip rarely develops lesions at early stages of infection (Gunawardena et al., 2005). This protection is due to atypical cells termed root "associated cap-derived cells" (AC-DCs) released from the root cap. "AD-DCs" are essential in root defense and comprise different cell populations according to their mode of detachment from the root: "root border cells" are AC-DCs released individually as in pea (Figure 1), whereas "border-like cells" are AC-DCs forming layers of cells that remain attached to the root cap as in *Arabidopsis thaliana* (Hawes, 1990; Vicré et al., 2005). The production of border cells was first described in pea (Hawes et al., 1998). Border cells, originally called "sloughed root cap" were defined as "living cells programmed to separate individually from the periphery of roots into the external environment" (Hawes and Pueppke, 1986). Border cells remain in close vicinity of the root cap as they are embedded in a thick mucilage acting as a "glue". Upon contact with water, the mucilage-that can hold 1,000 times its weight in water-swells leading to dispersion and release of border cells into the rhizosphere (Hawes et al., 1998). Experimentally, border cells can be easily visualized under binoculars by placing the root tip into water; the cells become dispersed in response to gentle agitation (Hawes and Lin, 1990). As they separate from pea root cap, border cells differentiation from root cap peripheral cells into border cells is accompanied by a switch in gene expression leading to the synthesis of a set of proteins and metabolites involved in root defense (Brigham et al., 1995; Wen et al., 2007; Wen et al., 2009). An array of 100 extracellular proteins was found to be released while border cell separation proceeds (Brigham et al., 1995). At the frontier between root and soil, root border cells are key elements controlling root interactions with microorganisms (Figure 2). Their functions are diverse according to both plant species and microorganisms. In pea, root border cells were clearly shown to be involved in root tip protection against *Nectria haematoccoca* infection (Gunawardena and Hawes, 2002; Gunawardena et al., 2005). Despite a formation of a mantle of hyphae covering the surface of the root tip, border cells detached from the root together with the pathogens leaving the root cap deprived of mycelium. This mostly happens at early stages of infection. Extracellular proteins secreted by border cells such as β-1-3,3 proteins as well as extracellular DNA were shown to contribute to pea root protection against *N. haematoccoca*. Border cells from pea were also shown to act as a "lure" against some species of fungi and nematodes by specifically attracting pathogens to the root tip for better neutralization (Hawes et al., 2000). When inoculating pea root with the pathogenic nematode *Meloidogyne incognita*, second-stage juveniles (J2) accumulated specifically at the root tip unsheathed by border cells. After a few minutes of contact with pea border cells, J2 lost their motility and entered into reversible quiescence (Zhao et al., 2000). Whereas J2 rapidly accumulated within clumps of *in vitro* detached border cells, no attraction was observed using pea root exudates. Reversible quiescence induced by pea root border cells was also reported with other nematodes but it should be noted the levels varied according to the green pea cultivars tested (Hiltpold et al.,

10.3389/fpls.2023.1132132

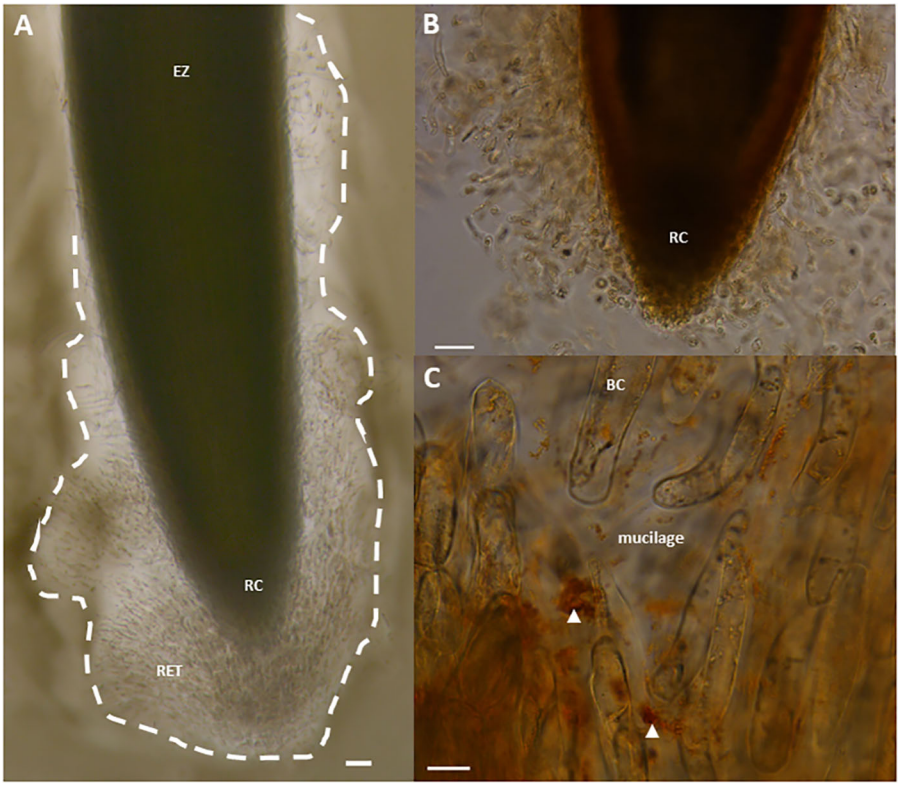

FIGURE 1
Light micrographs showing border cells and mucilage released by pea (*Pisum sativum* var. Astronaute) root tips, forming the RET, stained with India ink **(A)**, or with the β-glucosyl-Yariv reagent **(B, C)**. Note the observation of brown/red aggregates, indicated by white arrowheads, and signaling the presence of AGPs **(C)**. BC, border cell; EZ, elongation zone; RC, root cap; RET, Root Extracellular Trap. Scale bars, 100 µm **(A, B)** and 20 µm **(C)**.

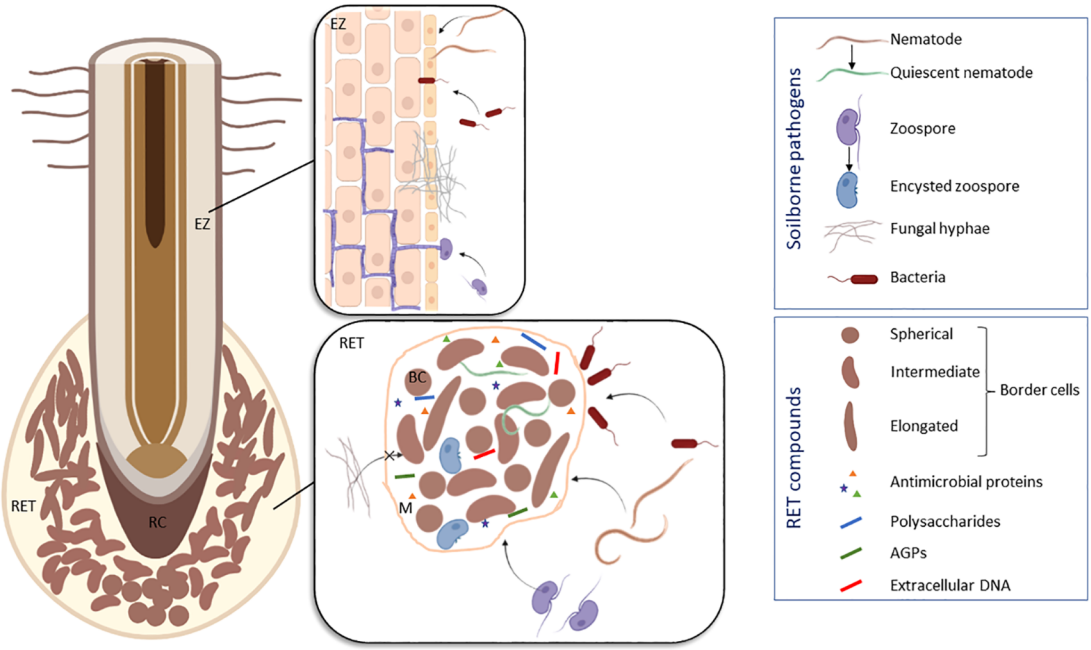

FIGURE 2
Schematic model illustrating the different modes of interaction between pea (*Pisum sativum*) roots and soilborne pathogens based on the results of Hawes et al., 2000; Gunawardena and Hawes, 2002; Gunawardena et al., 2005; Cannesan et al., 2011 and Zhao et al., 2000. To protect the root tip, the RET compounds are able to attract nematodes (e.g. *Meloidogyne incognita*) and to induce their quiescence, to trap oomycetes (e.g. *Aphanomyces euteiches*) and to induce their encystment, to prevent penetration of fungi (e.g. *Nectria haematoccoca*) and to exclude bacteria (e.g. *Pseudomonas aureofaciens*). Infection sites are usually located in the elongation zone of the root. BC, border cell; EZ, elongation zone; M, mucilage; RC, root cap; RET, Root Extracellular Trap. Figure created in BioRender.com.

2015). Such positive chemotaxis of nematodes by root border cells was species-dependent for the legumes studied: no attraction was found to occur in snap bean whereas repulsion was induced by alfalfa (Zhao et al., 2000). It is therefore of high interest to identify the nature of molecules produced and secreted by pea root border cells involved in chemotaxis and able induce a state of reversible quiescence of parasitic nematodes. Root border cells produce a quite abundant extra-cellular mucilage that forms a protective shield at the root tip. Such halo of mucilage was even more induced upon inoculation of wheat border cells with *Agrobacterium tumefasciens*. In this case, the mucilage allows exclusion of bacteria from the surface of border cells. However, such mechanisms have not been reported in pea border cells and *A. tumefasciens* were able to access to the border cells surface. Pea root infection by *A. euteiches* occurs mainly in the elongation and root hair areas with the exception of the root cap and border cells. In contrary to what was reported regarding infection with *N. haeamatococca*, border cells surface was not covered by the presence of mycelium and encysted zoospores (Cannesan et al., 2011). Such findings are in support of the hypothesis that root border cells in pea are involved in local defense of the root tip against *A. euteiches* preventing root cap colonization at early stages of infection. More specifically, we speculated that spherical border cells are the more active cells involved in root defense as compared to intermediate and elongated border cells. Defense mechanisms provided at the root tip by border cells appeared particularly complex as different border cells populations from pea might not be involved at the same level in root protection.

Border cells from pea present selective interactions with soilborne microorganisms by attracting, repelling or even inhibiting the growth of fungal, bacterial or oomycete pathogens (Figure 2) (Sherwood, 1987; Hawes and Brigham, 1992; Wen et al., 2007; Wen et al., 2009; Cannesan et al., 2011; Cannesan et al., 2012). Zhu et al. (1997) demonstrated that the ability of pea border cells to induce *in vitro* expression of bacterial gene required for the establishment of plant-microbe associations was selective. Little to no *vir* (*A. tumefasciens*) gene or *pkz* (pathogenic *Pseudomonas aureofaciens*) gene induction occurred in response to co-cultivation of these pathogenic bacteria with border cells of pea. However, the presence of pea border cells induced a significant increase in the expression of nod genes of *Rhizobium leguminosarum bv viciae*, a strain that nodulated pea (Zhu et al., 1997). It is thus remarkable that border cells from pea can influence expression of some genes from symbiotic bacteria but not others. It was then proposed that border cells are important actors in controlling the ecology of the rhizosphere by regulating growth and gene expression in microbial populations (Hawes, 1990; Hawes and Brigham, 1992). It also became obvious that root border cells do not act alone but in synergy with the surrounding mucilage layer to provide root protection against pathogens. Based on the Neutrophil Extracellular Trap (NET) described in mammals, the Root Extracellular Trap (or RET) model was proposed to explain the interconnection between AC-DCs and the mucilage (Driouich et al., 2013). The mucilage is a fibrillary structure forming a web that enhances the adhesion of microorganisms and facilitate pathogen neutralization by defense molecules produced and released by AC-DCs. We have postulated that fine-tuned communications are connecting AC-DCs throughout the RET in a similar way to the biofilms formed by bacteria (Driouich et al., 2019). The molecular events involved in the structuration and cell communication at the RET level remain to be in-depth established in order to unravel belowground defense mechanisms of the pea root tip.

3 Molecular dialogue at the pea root tip: a focus on glycomolecules

It has been estimated that approximately 20 to 25% of the total reduced carbon released by maize roots is in the form of high molecular weight root mucilage (Chaboud, 1983). Root mucilage exocytosis from border cells of different plant species such as maize or pea mainly consist mainly of polysaccharides including hemicellulosic compounds and pectins (Chaboud, 1983; Rougier and Chaboud, 1985; Vicré et al., 2005; Mravec et al., 2017). Homogalacturonans are essential components of pea root mucilage and are involved in cementing root border cells together. It has been reported that partial inhibition of the pectin methylesterase (*rcpme1*) in transgenic pea roots was correlated to the formation of a cohesive clump of border cells that could not separate from the root cap (Wen et al., 1999; Durand et al., 2009; Mravec et al., 2017). Correct expression of *rcpme1* in the pea root caps is thus necessary to provide border cells separation and release from the root cap showing the importance of the degree and pattern of methyl esterification of homogalacturonan in these events. The presence of xylogalacturonan (XGA) epitope recognized by the mAb LM8 was also associated with pea border cells detachment and was found to be released within extracellular bodies at the root surface in the mucilage (Mravec et al., 2017). Although the precise role of XGA remains to be clearly established, the presence of xylose residues prevents polysaccharides to be enzymatically degraded by pathogenic agents upon root infection (Jensen et al., 2008). Consequently, XGA could contribute to the mechanical barrier preventing microbial invasion at the root tip. Interestingly, Knee et al. (2001) reported that monosaccharide composition from pea root mucilage appeared to contain specifically high amount of arabinose (Ara) and galactose (Gal) possibly related to the presence of arabinogalactan proteins (AGPs). Cannesan et al. (2012) detected the presence of epitopes associated with AGPs at the border cell surface and within the mucilage. The monosaccharide composition and profiles of AGPs from the pea root cap, border cells and mucilage were distinct from the rest of the root system and were found to be species-specific. Furthermore, experimental data were consistent with the hypothesis that AGPs from pea root tips interfere with *in vitro* cell cycle of *A. euteiches*. *In vitro* assays showed that AGPs isolated from pea root cap and border cells were able to attract zoospores and inhibit subsequent cyst germination. AGPs are thought to be essential elements in root-microbe interactions in both pathogenic and beneficial microorganisms (Xie et al., 2012; Nguema-Ona et al., 2013). Xie et al. (2012) demonstrated the function of AGPs from

pea root in controlling *in vitro* surface attachment of *Rhizobium leguminosarum*. The authors suggest that AGPs could bind to one or both bacteria poles, thereby promoting their polar attachment to the root surface. A role of AGPs in *Agrobacterium* and *Rhizobium* adhesion to the root was previously reported in *Arabidopsis thaliana* supporting the importance of these proteoglycans in microorganisms attachment but the mechanisms of actions remains to be clarified (Gaspar et al., 2004; Vicré et al., 2005). However, it cannot be excluded that a complex including AGPs and different components could be involved in bacterial root adhesion. Interactions between AGPs and pectins such as homogalacturonans have been previously shown to occur although the exact linkage type are not determined (Oosterveld et al., 2002; Immerzeel et al., 2006; Cannesan et al., 2012). Classical AGPs bind reversibly to Ca^{2+} in a pH-dependent manner by glucuronic carboxyl groups. Ca^{2+}-driven cross-linking between the carboxyl groups of uronic acid in AGPs and pectins could lead to the formation of the adhesive properties of the mucilage (Huang et al., 2016). Such interactions might be essential in maintaining the structural properties of the RET but also in regulating adhesion and trapping of soilborne microorganisms. AGPs are promising candidates to be involved in early signaling and immune responses within the RET based several indications including: *i*) soluble AGPs could be released by cleavage of GPI-anchored moiety, *ii*) AGPs are involved in the Ca^{2+} signaling pathways, *iii*) enzymatic degradation by microorganisms releasing damage associated molecular pattern (DAMP) and *iv*) acting as of extracellular cargoe receptors initiating endocytosis (Wang et al., 2019). Therefore, to assess the precise contribution of AGPs in pea root protection the role of individual AGPs should be elucidated using transgenic lines affected in the protein backbone and/or in the glycan structure.

4 Future prospects for pea protection against root rot disease

To date, there is no registered chemical substances directed against *A. euteiches* and their use is not part of a sustainable agriculture. Furthermore, it should be taken into consideration that fungicides can also affect mycorrhizal fungal establishment leading to reductions in pea nitrogen fixation (Chang et al., 2013). Despites increasing progress in breeding for root rot disease resistance, no complete resistant pea cultivars are available (Pilet-Nayel et al., 2005; Lavaud et al., 2015; Lavaud et al., 2016). Avoidance of infested fields remains the more reliable method to manage root rot disease and assays were designed in order to evaluate the level of soil infectivity before subsequent pea sawing (Sauvage et al., 2007; Moussart et al., 2009; Gangneux et al., 2014). Oospores, the primary source of inoculum, can survive several years in soils before infesting host species such as pea (Papavizas and Ayers, 1974). Consequently, long-term rotations are necessary to avoid pea crop infestation. It is now recognized that several pathogens including *A. euteiches*, *Fusarium* spp., *Phytophthora* spp., *Pythium* spp., or *Rhizoctonia* spp. interact synergistically to infect the plant forming the pea root rot complex (PRRC) that aggravates pea root rot disease. The involvement of multi-species pathogens in the PRRC is a major limiting factor for plant breeding making complete pea resistance highly complex (Chatterton et al., 2019; Wille et al., 2021; Wu et al., 2022). However, plant beneficial microorganisms such as arbuscular mycorrhizal fungi (AMF) *Glomus intraradices* and *Glomus claroideum* were reported to slightly increase pea tolerance to root rot development (Thygesen et al., 2004). Field experiments suggest that AMF influence the reproductive stage of *A. euteiches* thus limiting the production of oospores within the infected plant tissues and their subsequent release into the soil (Bødker et al., 2002). Stimulating the immune defenses of pea was reported to be an interesting lever against root rot disease. Elicitation with oligogalacturonide fractions shown a protective effect in pea, with an induction of plant defense leading to a reduction in infection (Selim et al., 2017). The difficulties in controlling root rot disease have prompted a search for biological alternatives including the possibility of inter-cropping. French faba bean (*Vicia faba* L.) is a legume species recognized to be tolerant to root rot disease. Recently, root exudates from faba bean were shown to have a repellent effect on zoospores of *A. euteiches* (Laloum et al., 2021). Interestingly, experiments involving pea and faba bean co-cultivation resulted in reduced infection of root pea by *A. euteiches*. Similar data were also obtained when pea seedlings were inoculated with *A. euteiches* and cultivated in the presence of faba bean exudates. These findings highlight the *in vitro* protective effect of faba bean against pea root rot disease at early stages of infection. It is therefore of importance to investigate such protection under field conditions but also at a latest stage of infection to assess potential allopathic effects of faba bean. This study offers promising applications for the development of novel biocontrol agents and/or inter-cropping strategies for pea crop management. Extracts or root exudates from faba bean could be used in agriculture as bioactive natural compounds to improve pea protection against root rot disease caused by *A. euteiches* and the associated PRRC. It is also important, in order to contribute to sustainable agriculture, to investigate belowground interactions between pea roots and allopathic plant species with a special focus on the involvement of root AC-DCs and AGPs.

Author contributions

MF conceived and designed the figures. MV wrote the first draft. M-LF-G, AD, MF, VL, BP, AG and MV edited and improved the manuscript. All authors contributed to the article and approved the submitted version.

Funding

This work was supported by the University of Rouen Normandie. The Normandie Council and the European Union supported the work through the research project PROVEG

(Protéines Végétales, 2020-2022). MF received a PhD grant (2020-2023) from the Doctoral School EDnBISE (École Doctorale normande de Biologie Intégrative Santé Environnement). AG and VL received a PhD grant (respectively 2020-2023 and 2022-2025) from the Normandie Council. Financial support from Region Normandie and European Union (RIN Recherche Tremplin 2019 BEER) is also gratefully acknowledged.

Acknowledgments

This work was supported by the University of Rouen Normandie and the SFR Normandie Végétal FED 4277. We are grateful to Florian Barthes (RAGT2n) for providing pea seeds Astronaute.

Conflict of interest

The authors declare that the research was conducted in the absence of any commercial or financial relationships that could be construed as a potential conflict of interest.

Publisher's note

References

Bødker, L., Kjøller, R., Kristensen, K., and Rosendahl, S. (2002). Interactions between indigenous arbuscular mycorrhizal fungi and *Aphanomyces euteiches* in field-grown pea. *Mycorrhiza* 12, 7–12. doi: 10.1007/s00572-001-0139-4

Balmer, D., de Papajewski, D. V., Planchamp, C., Glauser, G., and Mauch-Mani, B. (2013). Induced resistance in maize is based on organ-specific defence responses. *Plant J.* 74, 213–225. doi: 10.1111/tpj.12114

Bozsoki, Z., Cheng, J., Feng, F., Gysel, K., Vinther, M., Andersen, K. R., et al. (2017). Receptor-mediated chitin perception in legume roots is functionally separable from nod factor perception. *Proc. Natl. Acad. Sci.* 114, E8118–E8127. doi: 10.1073/pnas.1706795114

Brigham, L. A., Woo, H.-H., Nicoll, M., and Hawes, M. C. (1995). Differential expression of proteins and mRNAs from border cells and root tips of pea. *Plant Physiol.* 109, 457–463. doi: 10.1104/pp.109.2.457

Burger, T. G., and Zhang, Y. (2019). Recent progress in the utilization of pea protein as an emulsifier for food applications. *Trends Food Sci. Technol.* 86, 25–33. doi: 10.1016/j.tifs.2019.02.007

Cannesan, M.-A., Durand, C., Burel, C., Gangneux, C., Lerouge, P., Ishii, T., et al. (2012). Effect of arabinogalactan proteins from the root caps of pea and *Brassica napus* on *Aphanomyces euteiches* zoospore chemotaxis and germination. *Plant Physiol.* 159, 1658–1670. doi: 10.1104/pp.112.198507

Cannesan, M.-A., Gangneux, C., Lanoue, A., Giron, D., Laval, K., Hawes, M. C., et al. (2011). Association between border cell responses and localized root infection by pathogenic *Aphanomyces euteiches*. *Ann. Bot.* 108, 459–469. doi: 10.1093/aob/mcr177

Chaboud, A. (1983). Isolation, purification and chemical composition of maize root cap slime. *Plant Soil* 73, 395–402. doi: 10.1007/BF02184316

Chang, K. F., Hwang, S. F., Ahmed, H. U., Gossen, B. D., Turnbull, G. D., and Strelkov, S. E. (2013). Management strategies to reduce losses caused by fusarium seedling blight of field pea. *Can. J. Plant Sci.* 93, 619–625. doi: 10.4141/cjps2012-293

Chatterton, S., Harding, M. W., Bowness, R., Mclaren, D. L., Banniza, S., and Gossen, B. D. (2019). Importance and causal agents of root rot on field pea and lentil on the Canadian prairies 2014–2017. *Can. J. Plant Pathol.* 41, 98–114. doi: 10.1080/07060661.2018.1547792

Chuberre, C., Plancot, B., Driouich, A., Moore, J. P., Bardor, M., Gugi, B., et al. (2018). Plant immunity is compartmentalized and specialized in roots. *Front. Plant Sci.* 9. doi: 10.3389/fpls.2018.01692

Day, L. (2013). Proteins from land plants – potential resources for human nutrition and food security. *Trends Food Sci. Technol.* 32, 25–42. doi: 10.1016/j.tifs.2013.05.005

Driouich, A., Follet-Gueye, M.-L., Vicré, M., and Hawes, M. C. (2013). Root border cells and secretions as critical elements in plant host defense. *Curr. Opin. Plant Biol.* 16, 489–495. doi: 10.1016/j.pbi.2013.06.010

Driouich, A., Smith, C., Ropitaux, M., Chambard, M., Boulogne, I., Bernard, S., et al. (2019). Root extracellular traps versus neutrophil extracellular traps in host defence, a case of functional convergence? *Biol. Rev* 94, 1685–1700. doi: 10.1111/brv.12522

Durand, C., Vicré-Gibouin, M., Follet-Gueye, M.-L., Duponchel, L., Moreau, M., Lerouge, P., et al. (2009). The organization pattern of root border-like cells of arabidopsis is dependent on cell wall homogalacturonan. *Plant Physiol.* 150, 1411–1421. doi: 10.1104/pp.109.136382

Erb, M., Balmer, D., De Lange, E. S., Von Merey, G., Planchamp, C., Robert, C., et al. (2011). Synergies and trade-offs between insect and pathogen resistance in maize leaves and roots. *Plant Cell Environ.* 34, 1088–1103. doi: 10.1111/j.1365-3040.2011.02307.x

FAO (2018) *FAOSTAT online database*. Available at: https://www.fao.org/faostat.

Foyer, C. H., Lam, H.-M., Nguyen, H. T., Siddique, K. H. M., Varshney, R. K., Colmer, T. D., et al. (2016). Neglecting legumes has compromised human health and sustainable food production. *Nat. Plants* 2, 1–10. doi: 10.1038/nplants.2016.112

Gangneux, C., Cannesan, M.-A., Bressan, M., Castel, L., Moussart, A., Vicré-Gibouin, M., et al. (2014). A sensitive assay for rapid detection and quantification of aphanomyces euteiches in soil. *Am. Phytopathological Soc.* 104, 1138–1147. doi: 10.1094/PHYTO-09-13-0265-R

Gaspar, Y. M., Nam, J., Schultz, C. J., Lee, L.-Y., Gilson, P. R., Gelvin, S. B., et al. (2004). Characterization of the arabidopsis lysine-rich arabinogalactan-protein AtAGP17 mutant (rat1) that results in a decreased efficiency of agrobacterium transformation. *Plant Physiol.* 135, 2162–2171. doi: 10.1104/pp.104.045542

Gaulin, E., Jacquet, C., Bottin, A., and Dumas, B. (2007). Root rot disease of legumes caused by *Aphanomyces euteiches*. *Mol. Plant Pathol.* 8, 539–548. doi: 10.1111/j.1364-3703.2007.00413.x

Gibert, S. (2021). Root rots in pea, characterisation and biocontrol of the parasitic complex of telluric origin including *Aphanomyces euteiches*. *Institut Natl. la Recherche Agronomique*.

Gunawardena, U., and Hawes, M. C. (2002). Tissue specific localization of root infection by fungal pathogens: Role of root border cells. *MPMI* 15, 1128–1136. doi: 10.1094/MPMI.2002.15.11.1128

Gunawardena, U., Rodriguez, M., Straney, D., Romeo, J. T., VanEtten, H. D., and Hawes, M. C. (2005). Tissue-specific localization of pea root infection by *Nectria haematococca*. mechanisms and consequences. *Plant Physiol.* 137, 1363–1374. doi: 10.1104/pp.104.056366

Hawes, M. C. (1990). Living plant cells released from the root cap: A regulator of microbial populations in the rhizosphere? *Plant Soil* 129, 19–27. doi: 10.1007/BF00011687

Hawes, M. C., and Brigham, L. A. (1992). Impact of root border cells on microbial populations in the rhizosphere. *Adv. Plant Pathol.* 8, 119–148.

Hawes, M. C., Brigham, L. A., Wen, F., Woo, H. H., and Zhu, Y. (1998). Function of root border cells in plant health: pioneers in the rhizosphere. *Annu. Rev. Phytopathol.* 36, 311–327. doi: 10.1146/annurev.phyto.36.1.311

Hawes, M. C., Gunawardena, U., Miyasaka, S., and Zhao, X. (2000). The role of root border cells in plant defense. *Trends Plant Sci.* 5, 128–133. doi: 10.1016/S1360-1385(00)01556-9

Hawes, M. C., and Lin, H.-J. (1990). Correlation of pectolytic enzyme activity with the programmed release of cells from root caps of pea (*Pisum sativum*) 1. *Plant Physiol.* 94, 1855–1859. doi: 10.1104/pp.94.4.1855

Hawes, M. C., and Pueppke, S. G. (1986). Sloughed peripheral root cap cells: Yield from different species and callus formation from single cells. *Am. J. Bot.* 73, 1466–1473. doi: 10.1002/j.1537-2197.1986.tb10892.x

Hiltpold, I., Jaffuel, G., and Turlings, T. C. J. (2015). The dual effects of root-cap exudates on nematodes: from quiescence in plant-parasitic nematodes to frenzy in entomopathogenic nematodes. *J. Exp. Bot.* 66, 603–611. doi: 10.1093/jxb/eru345

Huang, Y., Wang, Y., Tan, L., Sun, L., Petrosino, J., Cui, M.-Z., et al. (2016). Nanospherical arabinogalactan proteins are a key component of the high-strength adhesive secreted by English ivy. *Proc. Natl. Acad. Sci.* 113, E3193–E3202. doi: 10.1073/pnas.1600406113

Immerzeel, P., Eppink, M. M., De Vries, S. C., Schols, H. A., and Voragen, A. G. J. (2006). Carrot arabinogalactan proteins are interlinked with pectins. *Physiologia Plantarum* 128, 18–28. doi: 10.1111/j.1399-3054.2006.00712.x

Jensen, J. K., Sørensen, S. O., Harholt, J., Geshi, N., Sakuragi, Y., Møller, I., et al. (2008). Identification of a xylogalacturonan xylosyltransferase involved in pectin biosynthesis in arabidopsis. *Plant Cell* 20, 1289–1302. doi: 10.1105/tpc.107.050906

Karaca, A. C., Low, N., and Nickerson, M. (2011). Emulsifying properties of chickpea, faba bean, lentil and pea proteins produced by isoelectric precipitation and salt extraction. *Food Res. Int.* 44, 2742–2750. doi: 10.1016/j.foodres.2011.06.012

Knee, E. M., Gong, F. C., Gao, M., Teplitski, M., Jones, A. R., Foxworthy, A., et al (2001). Root mucilage from pea and its utilization by rhizosphere bacteria as a sole carbon source. *Mol. Plant Microbe Interact.* 14, 775–784. doi: 10.1094/MPMI.2001.14.6.775

Krefting, J. (2017). The appeal of pea protein. *J. Renal Nutr.* 27, e31–e33. doi: 10.1053/j.jrn.2017.06.009

Laloum, Y., Gangneux, C., Gügi, B., Lanoue, A., Munsch, T., Blum, A., et al. (2021). Faba bean root exudates alter pea root colonization by the oomycete *Aphanomyces euteiches* at early stages of infection. *Plant Sci.* 312, 111032. doi: 10.1016/j.plantsci.2021.111032

Lavaud, C., Baviere, M., Le Roy, G., Hervé, M. R., Moussart, A., Delourme, R., et al. (2016). Single and multiple resistance QTL delay symptom appearance and slow down root colonization by *Aphanomyces euteiches* in pea near isogenic lines. *BMC Plant Biol.* 16, 166. doi: 10.1186/s12870-016-0822-4

Lavaud, C., Lesné, A., Piriou, C., Le Roy, G., Boutet, G., Moussart, A., et al. (2015). Validation of QTL for resistance to *Aphanomyces euteiches* in different pea genetic backgrounds using near-isogenic lines. *Theor. Appl. Genet.* 128, 2273–2288. doi: 10.1007/s00122-015-2583-0

Moussart, A., Wicker, E., Le Delliou, B., Abelard, J.-M., Esnault, R., Lemarchand, E., et al. (2009). Spatial distribution of *Aphanomyces euteiches* inoculum in a naturally infested pea field. *Eur. J. Plant Pathol.* 123, 153–158. doi: 10.1007/s10658-008-9350-x

Mravec, J., Kračun, S. K., Rydahl, M. G., Westereng, B., Pontiggia, D., De Lorenzo, G., et al. (2017). An oligogalacturonide-derived molecular probe demonstrates the dynamics of calcium-mediated pectin complexation in cell walls of tip-growing structures. *Plant J.* 91, 534–546. doi: 10.1111/tpj.13574

Nazir, N., Badri, Z. A., Bhat, N. A., Bhat, F. A., Sultan, P., Bhat, T. A., et al. (2022). Effect of the combination of biological, chemical control and agronomic technique in integrated management pea root rot and its productivity. *Sci. Rep.* 12, 11348. doi: 10.1038/s41598-022-15580-1

Nguema-Ona, E., Vicré-Gibouin, M., Cannesan, M.-A., and Driouich, A. (2013). Arabinogalactan proteins in root–microbe interactions. *Trends Plant Sci.* 18, 440–449. doi: 10.1016/j.tplants.2013.03.006

Oosterveld, A., Voragen, A. G. J., and Schols, H. A. (2002). Characterization of hop pectins shows the presence of an arabinogalactan-protein. *Carbohydr. Polymers* 49, 407–413. doi: 10.1016/S0144-8617(01)00350-2

Papavizas, G. C., and Ayers, W. A. (1974). Aphanomyces species and their root diseases in pea and sugarbeet - a review, technical bulletin, agricultural research service. United States Department of Agriculture

Pilet-Nayel, M. L., Muehlbauer, F. J., McGee, R. J., Kraft, J. M., Baranger, A., and Coyne, C. J. (2005). Consistent quantitative trait loci in pea for partial resistance to *Aphanomyces euteiches* isolates from the united states and France. *Phytopathology®* 95, 1287–1293. doi: 10.1094/PHYTO-95-1287

Rougier, M., and Chaboud, A. (1985). Mucilages secreted by roots and their biological function. *Israel J. Bot.* 34, 129–146. doi: 10.1080/0021213X.1985.10677017

Sauvage, H., Moussart, A., Bois, F., Tivoli, B., Barray, S., and Laval, K. (2007). Development of a molecular method to detect and quantify aphanomyces euteiches in soil. *FEMS Microbiol. Lett.* 273, 64–69. doi: 10.1111/j.1574-6968.2007.00784.x

Selim, S., Sanssené, J., Rossard, S., and Courtois, J. (2017). Systemic induction of the defensin and phytoalexin pisatin pathways in pea (*Pisum sativum*) against *Aphanomyces euteiches* by acetylated and nonacetylated oligogalacturonides. *Molecules* 22, 1017. doi: 10.3390/molecules22061017

Sherwood, R. T. (1987). Papilla formation in corn root-cap cells and leaves inoculated with *Colletotricum graminicola*. *Phytopathology* 77, 930–934.

Sun, X. D., and Arntfield, S. D. (2012). Gelation properties of myofibrillar/pea protein mixtures induced by transglutaminase crosslinking. *Food Hydrocolloids* 27, 394–400. doi: 10.1016/j.foodhyd.2011.11.001

Thygesen, K., Larsen, J., and Bødker, L. (2004). Arbuscular mycorrhizal fungi reduce development of pea root-rot caused by *Aphanomyces euteiches* using oospores as pathogen inoculum. *Eur. J. Plant Pathol.* 110, 411–419. doi: 10.1023/B:EJPP.0000021070.61574.8b

Vicré, M., Santaella, C., Blanchet, S., Gateau, A., and Driouich, A. (2005). Root border-like cells of arabidopsis. microscopical characterization and role in the interaction with rhizobacteria. *Plant Physiol.* 138, 998–1008. doi: 10.1104/pp.104.051813

Wang, L., Cheng, M., Yang, Q., Li, J., Wang, X., Zhou, Q., et al. (2019). Arabinogalactan protein–rare earth element complexes activate plant endocytosis. *Proc. Natl. Acad. Sci.* 116, 14349–14357. doi: 10.1073/pnas.1902532116

Wen, F., VanEtten, H. D., Tsaprailis, G., and Hawes, M. C. (2007). Extracellular proteins in pea root tip and border cell exudates. *Plant Physiol.* 143, 773–783. doi: 10.1104/pp.106.091637

Wen, F., White, G. J., VanEtten, H. D., Xiong, Z., and Hawes, M. C. (2009). Extracellular DNA is required for root tip resistance to fungal infection. *Plant Physiol.* 151, 820–829. doi: 10.1104/pp.109.142067

Wen, F., Zhu, Y., and Hawes, M. C. (1999). Effect of pectin methylesterase gene expression on pea root development. *Plant Cell* 11, 1129–1140. doi: 10.1105/tpc.11.6.1129

Wille, L., Kurmann, M., Messmer, M. M., Studer, B., and Hohmann, P. (2021). Untangling the pea root rot complex reveals microbial markers for plant health. *Front. Plant Sci.* 12. doi: 10.3389/fpls.2021.737820

Wu, L., Fredua-Agyeman, R., Strelkov, S. E., Chang, K.-F., and Hwang, S.-F. (2022). Identification of novel genes associated with partial resistance to aphanomyces root rot in field pea by BSR-seq analysis. *Int. J. Mol. Sci.* 23, 9744. doi: 10.3390/ijms23179744

Xie, F., Williams, A., Edwards, A., and Downie, J. A. (2012). A plant arabinogalactan-like glycoprotein promotes a novel type of polar surface attachment by *Rhizobium leguminosarum*. *MPMI* 25, 250–258. doi: 10.1094/MPMI-08-11-0211

Zhao, X., Schmitt, M., and Hawes, M. C. (2000). Species-dependent effects of border cell and root tip exudates on nematode behavior. *Phytopathology®* 90, 1239–1245. doi: 10.1094/PHYTO.2000.90.11.1239

Zhu, Y., Pierson, L. S.III, and Hawes, M. C. (1997). Induction of microbial genes for pathogenesis and symbiosis by chemicals from root border cells. *Plant Physiol.* 115, 1691–1698. doi: 10.1104/pp.115.4.1691

frontiers | Frontiers in Plant Science

TYPE Original Research
PUBLISHED 20 February 2023
DOI 10.3389/fpls.2023.1115417

OPEN ACCESS

EDITED BY
Christophe Le May,
Institut Agro Rennes-Angers, France

REVIEWED BY
Magnus Karlsson,
Swedish University of Agricultural Sciences, Sweden
Mihir Kumar Mandal,
University of California, Davis, United States

*CORRESPONDENCE
Sean L. Bithell
sean.bithell@nsw.dpi.gov.au

SPECIALTY SECTION
This article was submitted to Plant Pathogen Interactions, a section of the journal Frontiers in Plant Science

RECEIVED 03 December 2022
ACCEPTED 31 January 2023
PUBLISHED 20 February 2023

CITATION
Bithell SL, Drenth A, Backhouse D, Harden S and Hobson K (2023) Inoculum production of *Phytophthora medicaginis* can be used to screen for partial resistance in chickpea genotypes.
Front. Plant Sci. 14:1115417.
doi: 10.3389/fpls.2023.1115417

Inoculum production of *Phytophthora medicaginis* can be used to screen for partial resistance in chickpea genotypes

Sean L. Bithell[1]*, Andre Drenth[2], David Backhouse[3], Steve Harden[1] and Kristy Hobson[1]

[1]Plant Systems, New South Wales Department of Primary Industries, Tamworth, NSW, Australia, [2]Centre for Horticultural Science, University of Queensland, Brisbane, QLD, Australia, [3]School of Environmental and Rural Science, University of New England, Armidale, NSW, Australia

Phytophthora root rot caused by *Phytophthora medicaginis* is an important disease of chickpeas (*Cicer arietinum*) in Australia with limited management options, increasing reliance on breeding for improved levels of genetic resistance. Resistance based on chickpea–*Cicer echinospermum* crosses is partial with a quantitative genetic basis provided by *C. echinospermum* and some disease tolerance traits originating from *C. arietinum* germplasm. Partial resistance is hypothesised to reduce pathogen proliferation, while tolerant germplasm may contribute some fitness traits, such as an ability to maintain yield despite pathogen proliferation. To test these hypotheses, we used *P. medicaginis* DNA concentrations in the soil as a parameter for pathogen proliferation and disease assessments on lines of two recombinant inbred populations of chickpea–*C. echinospermum* crosses to compare the reactions of selected recombinant inbred lines and parents. Our results showed reduced inoculum production in a *C. echinospermum* backcross parent relative to the *C. arietinum* variety Yorker. Recombinant inbred lines with consistently low levels of foliage symptoms had significantly lower levels of soil inoculum compared to lines with high levels of visible foliage symptoms. In a separate experiment, a set of superior recombinant inbred lines with consistently low levels of foliage symptoms was tested for soil inoculum reactions relative to control normalised yield loss. The in-crop *P. medicaginis* soil inoculum concentrations across genotypes were significantly and positively related to yield loss, indicating a partial resistance-tolerance spectrum. Disease incidence and the rankings for in-crop soil inoculum were correlated strongly to yield loss. These results indicate that soil inoculum reactions may be useful to identify genotypes with high levels of partial resistance.

KEYWORDS

root disease, phenotyping, tolerance, quantitative resistance, pathogen proliferation

Introduction

Phytophthora root rot (PRR) of chickpea (*Cicer arietinum*), caused by the Oomycete, *Phytophthora medicaginis*, is an important root disease of chickpea crops in the north-eastern Australian grain belt (Singh et al., 1994; Salam et al., 2011). For chickpea, similar to PRR of soybean, treatment of the seed with metalaxyl provides initial control during crop establishment, but protection across the whole growing season using cost-effective chemicals is not available (Dorrance and McClure, 2001). Absence of effective control methods has led to a focus on breeding for improved levels of resistance to provide a genetic solution to control PRR in chickpeas (Singh et al., 1994).

There are various types of resistance to plant pathogens that have different genetic basis. In this study, we examined partial resistance, which we define as resistance that confers reduced pathogen development, propagation, and spread of a disease in a plant population with a quantitative (non-major gene) genetic basis (Pariaud et al., 2009; St Clair, 2010) (Glossary Box). The term tolerance has also been used widely to refer to the performance of a genotype under disease pressure in the field, especially the ability to maintain yield in the presence of infection, although there have been considerable contradictions in its use and interpretation (Simms and Triplett, 1994; Erwin and Ribeiro, 1996; Pagan and Garcia-Arenal, 2020) (Glossary Box). From a general perspective of cause and effect between plant and pathogen, resistance is considered the effect of the plant on the pathogen, whereas tolerance is considered the effect of the pathogen on the plant. To discriminate among genotypes with partial resistance or tolerant phenotypes, it is necessary to compare the fitness or productivity of genotypes under the same levels of pathogen colonisation (Schafer, 1971; Pagan and Garcia-Arenal, 2020). Pagan and Garcia-Arenal (2020), when reviewing this area, observed that it is technically difficult to ensure the same level of pathogen colonisation even in non-field-based phenotyping systems but that quantifying the amount of disease or inoculum in the relevant infected tissue provided an effective method of comparing reactions and that fitness could be normalised against control treatments.

Glossary box

Partial resistance: the resistance that confers reduced pathogen development, propagation, and spread of a disease in a plant population with a quantitative (non-major gene) genetic basis.

Tolerance: the performance of a genotype under disease pressure in the field, especially the ability to maintain yield in the presence of infection.

The evaluation of material to provide improved resistance to *P. medicaginis* in chickpeas is ongoing. Early field and glasshouse screening studies of chickpea germplasm identified lines with improved survival times, but findings demonstrated inconsistent responses between field and glasshouse reactions (Dale and Irwin, 1991). *C. arietinum*-based chickpea varieties, such as var. Yorker, were released with a moderately resistant rating for PRR based on foliage symptom assessments (Knights et al., 2009). Although Yorker has a level of improved resistance, field evaluations showed that this resistance was not effective under conditions of high disease pressure and in seasons conducive to PRR development (Bithell et al., 2021). Furthermore, var. Yorker produced high *P. medicaginis* inoculum concentrations in soil at the end of the season even under moderately conducive conditions (Bithell et al., 2021). The inoculum and yield results for var. Yorker were indicative of a tolerance-type reaction or weak partial resistance. The absence of effective resistance sources in *C. arietinum* to *P. medicaginis* led to the evaluation of alternative resistance sources including wild relatives of chickpeas (Singh et al., 1994; Li et al., 2015). Among a range of wild relatives of chickpeas, *Cicer echinospermum* accessions provided the longest survival times in the presence of PRR infection; partial resistance was demonstrated by an absence of absolute resistance with the *C. echinospermum* accessions eventually dying from PRR (Knights et al., 2008). Resistance from *C. echinospermum* was successfully transferred to the progeny of crosses with chickpeas, and loci were identified for a complex quantitative genetic basis to the partial resistance (Knights et al., 2008; Amalraj et al., 2019).

Consistent selection or phenotyping across seasons, in systems with partial resistance, can be challenging, as the expression of resistance is highly dependent on the prevailing environmental conditions. Genotype-by-environment interactions involving partial resistance may be due to differing resistance thresholds among genotypes across a pathogen density gradient resulting in differing infection intensities among genotypes (Price et al., 2004). Recombinant inbred lines (RILs) of two chickpea–*C. echinospermum* populations provided a number of major quantitative trait loci (QTL) for resistance to *P. medicaginis* that showed negligible interactions for environments, while other resistance QTL showed strong environmental interactions (Amalraj et al., 2019). In some pathosystems, partial resistance may occur in combination with tolerance traits (Poland et al., 2009; Mikaberidze and McDonald, 2020). However, determination of the relative contribution of partial resistance and tolerance traits to disease reaction outcomes in variable field environments is difficult (Simms and Triplett, 1994; Masini et al., 2019; Pagan and Garcia-Arenal, 2020). The selection of material containing both partial resistance and disease tolerance traits was shown in one case to provide an inadvertent selection of tolerance over resistance traits (Mikaberidze and McDonald, 2020).

Current Australian chickpea breeding objectives involve finding the most beneficial combination of alleles to achieve high levels of disease resistance with high grain yield and quality. We sought to determine if selection for high-yielding lines under PRR disease pressure also selects material with high levels of partial resistance. It was also important to determine if changes in the amount of *P. medicaginis* inoculum and levels of disease severity are linked to other traits that may be more easily measured in a high-throughput breeding program to improve the selection process for high-yielding partially resistant material.

We specifically sought to determine if

1. inoculum production differs among RIL and RIL parents with differing levels of PRR resistance,
2. inoculum production differs relative to normalised yield loss among RIL lines selected for low levels of PRR development, and
3. there are disease or plant parameters that relate to *P. medicaginis* inoculum production values.

An in-depth understanding of disease assessment methods, inoculum responses, and trait composition is required to maximise sustainable yield and achieve genetic gain for resistance in chickpeas against *P. medicaginis* in breeding programs.

Materials and methods

To test our hypotheses, we used two RIL populations of a *C. echinospermum* backcross*susceptible population and a *C. echinospermum* backcross*tolerant population. The populations were phenotyped for their levels of PRR resistance in field experiments, including grain yield and *P. medicaginis* soil inoculum development at the harvest of selected RIL material.

RIL development and seed sources

A moderately PRR-resistant breeding line, 04067-81-2-1-1(B), which is a *C. arietinum* backcross *C. echinospermum* (Howzat/ILWC 245//99039-1013), was used to develop two F6-derived RIL populations by the National Chickpea Breeding Program based at the New South Wales Department of Primary Industries, Tamworth. The first population (D09008) was a cross of 04067-81-2-1-1(B) and an Australian PRR-susceptible chickpea variety, Rupali (pedigree: FLIP84-15C/ICCV88516//Amethyst); this is hereafter referred to as the BC*susceptible RIL population. The second population (D09024) was a cross of 04067-81-2-1-1(B) and an Australian desi chickpea variety, Yorker (pedigree: 8507-28H/946-31); this is hereafter referred to as the BC*tolerant RIL population. Yorker was released as a PRR moderately resistant chickpea variety, with resistance ratings based on foliage symptoms (Knights et al., 2009).

Isolates and inoculum production

P. medicaginis is a homothallic species. Ten isolates of *P. medicaginis* were used (as a mixture) in all experiments, storage, and isolate culturing as described in Bithell et al. (2022). Prior to inoculum production, each isolate was passaged through plants in a glasshouse using the very susceptible chickpea variety Sonali to ensure pathogenicity. With the use of low-strength V8 media (100 ml of V8 juice, 10 g of agar, 2.5 g of calcium carbonate, and 900 ml of Milli-Q water), an oospore suspension was prepared by macerating cultures with a hand-held Braun 600W blender and then added to flooded (Milli-Q water) cups of seedlings in potting mix, which were then drained after 48 h. After the observation of wilting, chlorosis, and canker development on the seedlings, stem tissue at the margin of the canker was used to re-isolate the pathogen on corn meal agar. Cultures were hyphal tipped and then grown on low-strength V8 media. Subcultures of these freshly passaged isolates were used to produce 90-mm-diameter Petri dish cultures of each isolate, which were grown in the dark at 21°C–23°C for at least 6 weeks prior to mixing with Milli-Q water (10% V/V) and macerating using a hand-held Braun 600W blender for approximately 3 min. Average oospore concentrations for each isolate were determined using counts under a 20 * 50-mm coverslip to prepare inoculum mixtures containing equal oospore concentrations.

RIL population disease status and phenotype selection

The two RIL populations were phenotyped for the severity of PRR development in inoculated field experiments in order to select RILs with high and low disease phenotypes.

Field experiments: The BC*susceptible RIL (n = 181) and the BC*tolerant RIL (n = 165) population were sown on 18 and 19 June 2014 in separate experiments at Hermitage Research Facility, Queensland (−28.204908 S, 152.102689 E) in 2014. The methods used for the RIL field experiments are described by Amalraj et al. (2019). Briefly, the plots were sown with a four-row seeder with separate in-furrow delivery of in-solution *Mesorhizobium ciceri* rhizobia inoculant and the 10 isolate mixture of *P. medicaginis* at sowing at a concentration of ~1,500 oospores/seed. Each plot had 20 seeds per single 1.2-m row plot. The experiments had a randomised block design with four replicates. Check varieties covering a resistance spectrum were supra-replicated on block and sub-block basis. The soil type at the Hermitage site was a deep, self-mulching, black vertosol (Thomson et al., 2007). No in-crop irrigation was applied, and 97 mm of in-crop rainfall was received during the field experiments.

Establishment and disease assessments: The number of seedlings in each plot was counted 48 days after sowing (DAS) to determine establishment. A minimum of three disease assessments were then made; the first assessment was performed when early disease symptoms were evident in susceptible check varieties (85 DAS, pre-flowering 12–14 nodes), the second assessment was made mid-season (118 DAS, immature pods present), and the final assessment (135 DAS) occurred at the beginning of pod maturity. At each disease assessment, separate counts of the number of chlorotic, dead, and total number of plants were made. Late-season assessments were carried out before widespread plant senescence had occurred. At the final assessment, dead plants were categorised into development categories as having produced no pods (died as seedlings prior to flowering) or as podded, and counts of each category were made. At this assessment, counts were also made of the number of chlorotic, senescent, and healthy non-senesced plants.

Selected RIL disease phenotype groups: To select RILs with high and low disease phenotypes, the proportion of plants that had died at the 135 DAS assessment timing was used as the criterion. From each RIL population, six lines were randomly selected as low disease lines using a random number function in Excel (Microsoft Office Standard, 2016) on the basis of having no plant death. Six high-disease RILs were randomly selected from each RIL population based on more than 30% plant death for the BC*susceptible RIL and greater than 10% plant death for the BC*tolerant RIL.

High and low disease RIL inoculum relationship

The soil beneath the 24 selected RIL and parents of the two RIL populations was sampled to evaluate *P. medicaginis* inoculum

concentrations across different disease phenotypes. Each plot of the selected RIL in the above experiments was soil sampled 145 days after sowing (DAS), by taking four separate 45-mm-diameter 100-mm-depth soil cores, each 250 mm apart; two were collected from either side of each row, approximately 20 mm from the closest stem base, placed in bags and dried at 40°C for 72 h. A 500-g sub-sample was then sent to the Root Disease Testing Service at the South Australian Research and Development Institute (Adelaide, Australia) to quantify the *P. medicaginis* soil DNA concentration as described by Bithell et al. (2021).

Superior RIL yield loss and inoculum production

We compared selected RIL to determine if inoculum production relative to normalised yield loss differed. We used a set of eight superior RIL, which had provided consistently low disease reactions (BC*susceptible (n = 3), the maximum proportion of dead plants from back-transformed logits for the three selected RIL, range 0.015 to 0.049; and BC*tolerant (n = 5), the maximum proportion of dead plants from back-transformed logits for the five selected RIL, 0 to 0.018) across three phenotyping experiments per population (Amalraj et al., 2019). A four-row plot (each 15 m^2) experiment was conducted at Hermitage, as a randomised complete block design with three replicates. The experiment was sown on 27 June 2017 with an in-furrow delivery of in-solution *M. ciceri* rhizobia. All seeds had a seed treatment of 360 g/L of thiram and 200 g/L of thiabendazole. There was an uninoculated control (−Pm) treatment, where the seed was also treated with metalaxyl (350 g/L of metalaxyl-M, 75 ml/100 kg seeds), and the plots received metalaxyl soil drenches [Ridomil Gold 480 SL (480 g/L of metalaxyl-M, 0.4 mL/L water/m of row)] at six weekly intervals after sowing. There was a *P. medicaginis* inoculated (+Pm) treatment, where an in-furrow application of a solution of *P. medicaginis* oospores and mycelium was applied at sowing as described for the earlier experiment. When the −Pm treatment received metalaxyl soil drenches, the +Pm treatment received water drenches equivalent to the metalaxyl application (1 L water/m of row).

Plots were sown at calculated seed densities to achieve a target population of 35 plants/m^2. Around each experimental plot, four-row buffer plots of metalaxyl-treated var. Yorker seeds were planted to prevent the movement of *P. medicaginis* between treatments. Supplementary irrigation of 31 mm was applied with dripper tape (T-tape, Rivulas Irrigation) over a 5-day period starting 35 DAS. There was 137 mm of in-crop rainfall during this field experiment. Disease assessments were carried out on the middle two rows of each plot. The number of chlorotic and/or dead plants was counted in each plot at approximately 6-week intervals. Plant heights were recorded by measuring two plants per plot at physiological maturity (141 DAS). The proportional area of early senescence was also assessed for each plot on this date. The middle two rows of each plot were machine harvested at 169 DAS to determine grain yield.

To determine inoculum production in-crop (140 DAS) and postharvest (170 DAS), five soil cores were collected from each of the middle two rows of each plot, using 45-mm-diameter 100-mm-depth soil cores collected approximately 20 mm from the closest stem base. The pooled cores from each plot were dried at 40°C for 72 h. All plots were sampled at 170 DAS, but only the BC*tolerant RIL and parents (n = 7) were sampled at 140 DAS. After being dried, a 500-g sub-sample was collected using the level surface sub-sampling method described by Schroth (2003) and sent for *P. medicaginis* DNA concentration analysis as previously described.

Design and analyses

All experiment layouts were designed using DiGGer ver. 1.0.2 (Coombes, 2016). The two RIL population experiments that included check varieties were supra-replicated on block and sub-block basis. Residuals were examined, and if necessary, data were appropriately transformed to meet requirements for residuals to be normally distributed. Residual degrees of freedom are presented for each analysis.

Hermitage RIL population experiments: For the two whole RIL population experiments, RIL with complete data across all replicates was selected for analysis. This provided 173 RIL for the BC*susceptible population and 164 RIL for the BC*tolerant population. Analysis of the proportion of dead seedlings (dead with no pods), dead podded plants, chlorotic or senescent podded plants, non-symptomatic podded plants, and all plants with pods from the final disease assessment was made with a generalized linear mixed model (GLMM) with a binominal distribution logit link and the Wald test. The back-transformed logit values for each RIL were then used for whole-population comparisons among disease and development parameters. For the RIL from the high and low disease classes, ANOVA with RIL nested within the disease class was used to compare *P. medicaginis* DNA concentrations and disease parameters.

Superior RIL yield loss and inoculum production: A GLMM binominal distribution logit link and the Wald test was used for the analysis of the proportion of dead and chlorotic plants. Grain yield and height reduction data were normalised relative to the metalaxyl-protected control treatment as outlined for the determination of point tolerance responses (Pagan and Garcia-Arenal, 2020). After the evaluation of a range of models, regression with an exponential function was used to assess the relationship between the proportion of infected plants and normalised yield, and linear regression was used to assess the relationship between other parameters.

All statistical analyses were carried out with GenStat 19th edition (Anon, 2018).

Results

RIL population disease status at maturity and phenotype selection

The distribution of PRR disease of RIL in both populations was used to select groups of RIL with high and low disease phenotypes. Seasonal conditions in 2014 were not conducive to high levels of PRR development, but the BC*susceptible RIL had close to a proportion of 0.5 of plants dying as either seedlings or podded plants (Figure 1A). Recombinant inbred lines with proportional total mortality (dead seedling plus dead podded plants) values ranging from 0.32 to 0.62

were selected as the high disease group. For the BC*tolerant RIL, few lines had a greater proportion than 0.20 mortality in any development category (Figure 1B). Lines selected from this population for the high disease group had total mortality proportional values ranging from 0.11 to 0.31. Comparison of the maturity status at the final assessment for the selected RIL between the two populations showed that the selected BC*tolerant RIL had three lines with a higher proportion of dead podded plants than dead seedlings. In contrast for the selected BC*susceptible RIL, the proportion of dead seedlings was as high as dead podded plants.

High and low disease RIL inoculum relationships

This analysis was completed to test for differences in *P. medicaginis* inoculum between the high and low disease phenotypes in each of the contrasting RIL populations.

For the BC*susceptible RIL population, there was a significant ($p < 0.05$, df = 33, least significant difference (LSD) = 1.77) difference in log-transformed soil *P. medicaginis* DNA values among the two disease groups, the high disease group had a value of 9.9, and the low disease group had a value of 7.9 (Figure 2A). However, log-transformed soil *P. medicaginis* DNA values did not differ significantly ($p > 0.05$) between the two parents, 04067-81-2-1-1(B) (6.0) and Rupali (5.9). 04067-81-2-1-1(B) and Rupali differed significantly (chi probability = 0.003) in the proportion of non-symptomatic plants that produced pods, with respective back-transformed logit proportions of 0.94 and 0.51. The *C. arietinum* parent of the BC*tolerant population, var. Yorker, was included as a check in this BC*susceptible RIL population experiment and provided a high (11.1) postharvest *P. medicaginis* DNA value.

For the BC*tolerant RIL population, there was also a significant ($p < 0.05$, df = 33, LSD = 1.54) difference in log-transformed soil *P. medicaginis* DNA values among the two disease groups, the high disease group had a value of 10.2 and the low disease group a value of 7.8 (Figure 2B). For the parents of this population, log-transformed soil *P. medicaginis* DNA values differed significantly ($p < 0.05$, residual df = 3, LSD = 1.81) between 04067-81-2-1-1(B) (7.4) and var. Yorker (10.0). 04067-81-2-1-1(B) and Yorker differed significantly (chi probability < 0.001) in the proportion of non-symptomatic plants that produced pods, with respective back-transformed logit proportions of 1.00 and 0.851.

Superior RIL yield loss and inoculum production

This experiment tested whether inoculum production relative to normalised yield loss differed among three RIL from the BC*susceptible RIL population and five RIL from the BC*tolerant population selected for superior performance and two parents. In addition, we sought to identify which disease or plant parameters may relate to genotype inoculum production values.

There was a significant range in the proportion of PRR symptomatic (dead plus chlorotic) plants, especially among the parents of the BC*tolerant RIL population where var. Yorker had a high symptomatic proportion (0.76), while the other parent 04067-

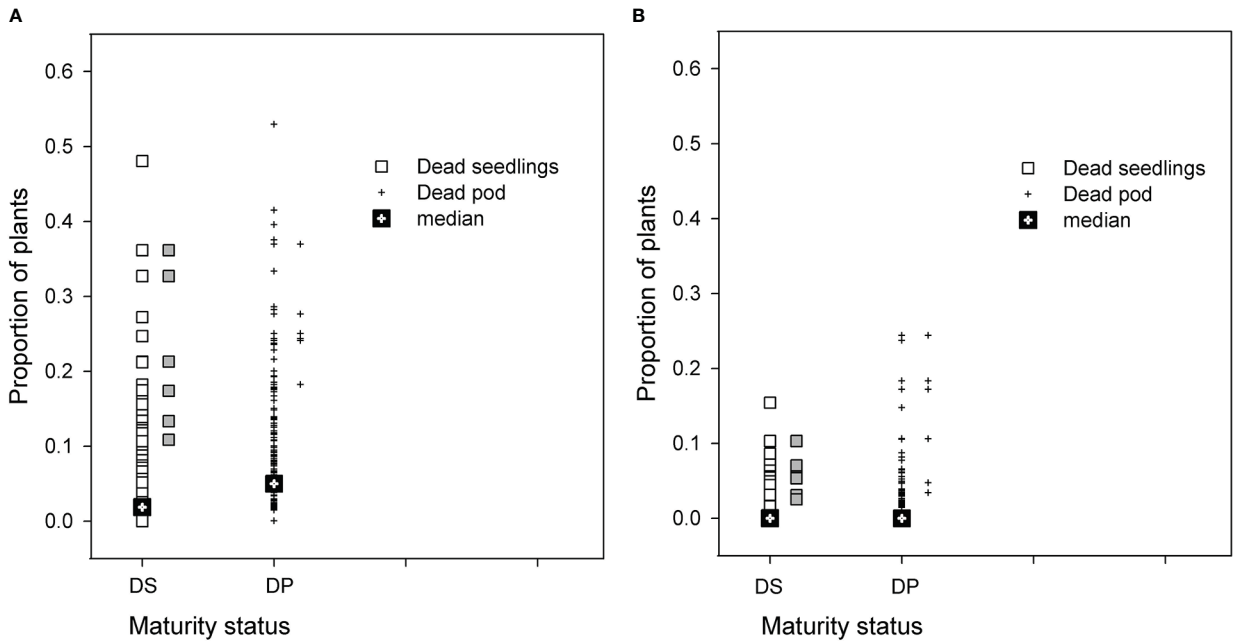

FIGURE 1
Results for two recombinant line (RIL) populations, **(A)** *Cicer echinospermum* backcross*susceptible (BC*susceptible) and **(B)** *C. echinospermum* backcross*tolerant (BC*tolerant), in two *Phytophthora medicaginis* inoculated single-row experiments, for proportions of plants dead at the final assessment with a development status categorised as dead seedlings (DS, □) or dead podded plants (DP, +). Median values for each category presented and symbols in grey to the right of each population plot are the six selected high disease RIL that were postharvest soil sampled.

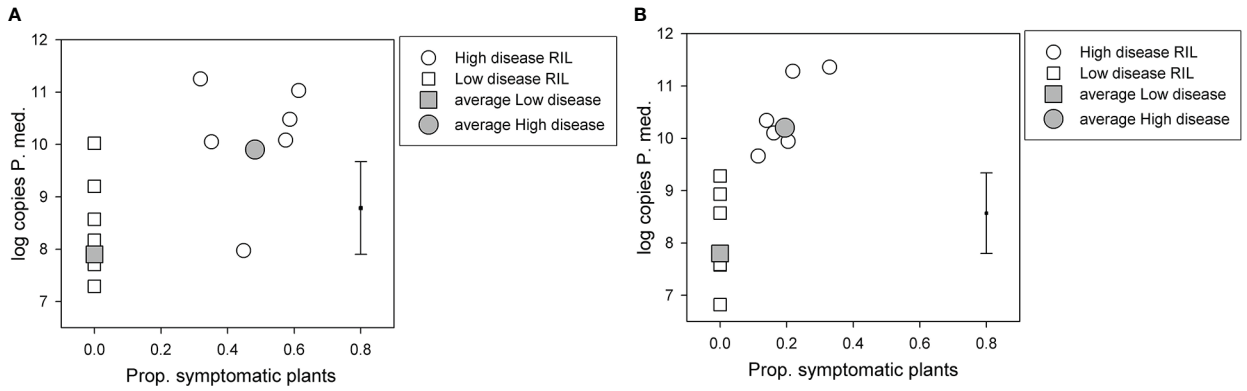

FIGURE 2
Results for selected recombinant inbred lines (RILs) in two *Phytophthora medicaginis* inoculated single-row experiments, with six low disease and six high disease lines from **(A)** *Cicer echinospermum* backcross*susceptible (BC*susceptible) and **(B)** *C. echinospermum* backcross*tolerant (BC*tolerant) populations, with the proportion of plants with foliage symptoms (chlorotic plus dead) plotted against the log-transformed postharvest soil *P. medicaginis* (P.med) DNA concentrations (number of sequence copies/g soil) for individual RIL and high and low disease group averages. Error bar shows LSD ($p < 0.05$) for disease group analysis. LSD, least significant difference.

81-2-1-1(B) and five other RIL had values below 0.03 (Table 1). The RIL with the highest symptomatic proportion of 0.13 was from the BC*susceptible population.

The area of early senescence differed among *Phytophthora* treatments ($p < 0.001$, −Pm 16.2%, +Pm 46.7%, LSD = 10.86) and among genotypes ($p < 0.001$), but there was no significant interaction. For grain production, there was a significant interaction ($p < 0.05$) where four RIL and the parent, 04067-81-2-1-1(B), did not have a significant reduction in yield in the +Pm treatment relative to −Pm. In addition, for the +Pm treatment, two RILs had higher yields than three other RILs, including two from the same BC*tolerant population. The four genotypes that had significant reductions in yield were also the only genotypes to have early senescence values of 35% or greater.

Comparison of genotype traits for relationships between disease, plant height, yield, in-crop, and postharvest inoculum production parameters was based on the use of normalised results. For genotype effects (df = 29), there were significant differences for normalised plant heights ($p < 0.001$), normalised yield losses ($p < 0.05$), and postharvest soil *P. medicaginis* inoculum concentrations ($p < 0.05$).

The proportions of symptomatic plants, normalised height reduction, and area of early senescence were significantly and positively related to normalised yield loss. The proportion of symptomatic plants accounted for 65% ($p < 0.05$, df = 7) of the variance in normalised yield loss across the RIL and parents (Figure 3A). Normalised height reduction ($p < 0.01$, $R^2 = 69.4$) and the area of early senescence in the +Pm treatment ($p < 0.001$, $R^2 = 73.8$) both accounted for a substantial proportion of the variance in

TABLE 1 Superior recombinant inbred line (RIL) disease (proportion of symptomatic plants), early senescence (Early Sen.) results for Phytophthora medicaginis (+Pm) inoculated RIL and yield results from control (-Pm) and inoculated RIL from the Cicer echinospermum backcross*susceptible (BC*sus.) and C. echinospermum backcross*tolerant (BCxtol.) populations and two RIL parents.

		Prop. Symp.	Early Sen.	Grain, kg/ha	
Population	Genotype	+Pm	% area	−Pm	+Pm
	04067-81-2-1-1(B)	0.02	13.3	2,885	2,148
BC*sus.	D09008B>F6RIL>046	0.01	47.5	3,354	2,117
BC*sus.	D09008C>F6RIL>007	0.06	32.1	3,771	2,796
BC*sus.	D09008D>F6RIL>016	0.13	50.8	3,075	1,990
BC*tol.	D09024B>F6RIL>020	0.08	35.0	3,403	1,639
BC*tol.	D09024B>F6RIL>030	0.02	10.0	2,456	1,948
BC*tol.	D09024B>F6RIL>040	0.01	13.3	3,044	3,093
BC*tol.	D09024C>F6RIL>010	0.04	25.4	2,886	2,346
BC*tol.	D09024D>F6RIL>028	0.01	20.0	3,483	3,093
	Yorker	0.76	77.5	3,135	527
Wald/LSD		122.1[W]	24.27	1,014.7	

Wald statistic presented for the proportion of symptomatic (Prop. Symp.) plants, Wald tests, [W]$p < 0.001$. Least significant difference (LSD) presented for area of early senescence (Early Sen.), and grain yields for the control (−Pm) and +Pm treatments in 2017 yield loss experiment.

normalised yield loss (Figures 3B,C), although RIL with the least height reduction did not have the lowest yield loss and vice versa. Normalised height reduction also accounted for approximately half of the variance in the area of early senescence in the +Pm treatment ($p < 0.05$, $R^2 = 50.7$) (Figure 3D).

In-crop soil *P. medicaginis* DNA concentrations were assessed for the BC*tolerant population RIL and parents. For comparisons with proportional yield loss, one RIL D09024C>F6RIL>010 had the highest in-crop *P. medicaginis* DNA value but less than 20% proportional yield loss. When that particular RIL was excluded as an outlier, the in-crop soil *P. medicaginis* DNA concentrations accounted for a large ($p < 0.05$, $R^2 = 79.7$) proportion of the variance in proportional yield loss. With no exclusions, there was no significant ($p > 0.05$) relationship (Figure 3E). Postharvest soil *P. medicaginis* DNA concentrations were assessed for all entries, but a different RIL (D09008B>F6RIL>046) provided high *P. medicaginis* DNA values but mid-range proportional yield loss values. When that particular RIL was excluded, the postharvest soil *P. medicaginis* DNA concentrations accounted for a moderate ($p < 0.05$, $R^2 = 38.8$) proportion of the variance in proportional yield loss (Figure 3F).

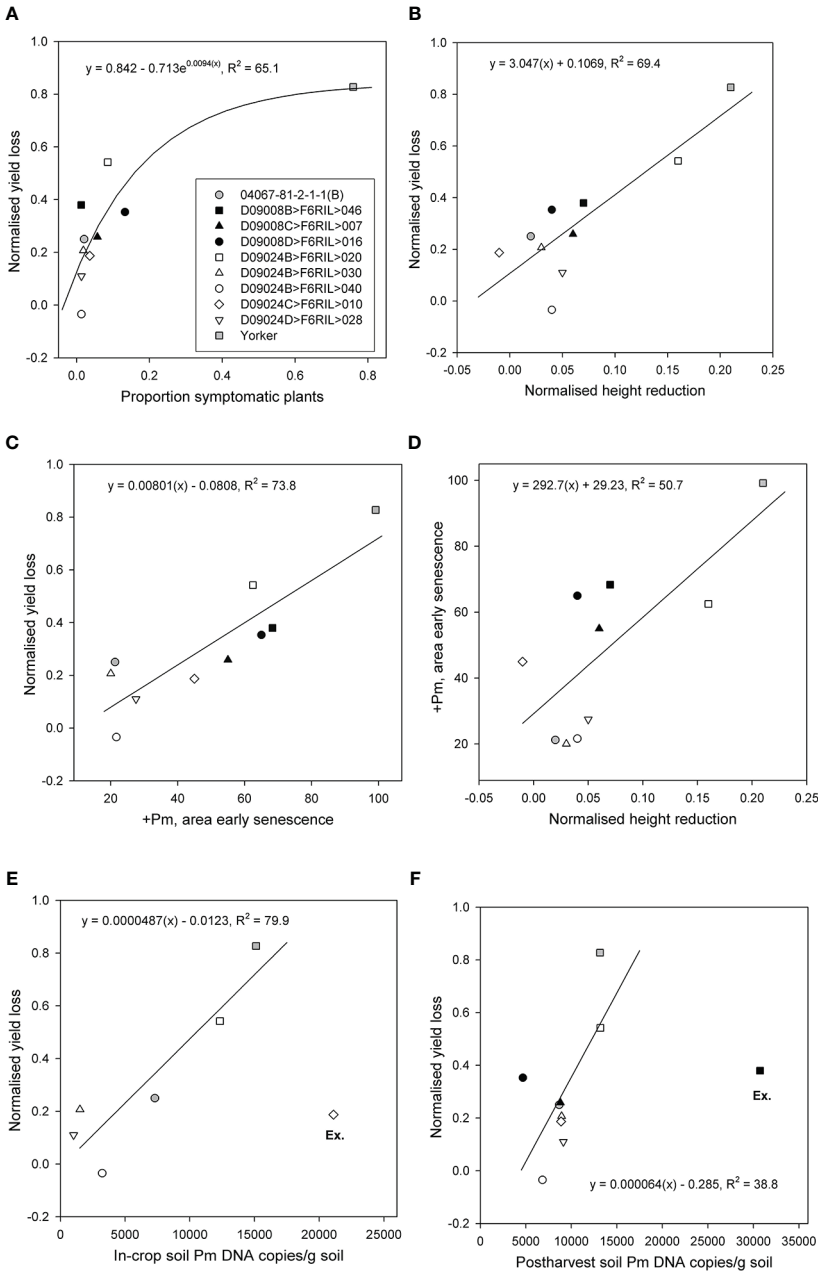

FIGURE 3
Relationships for eight superior recombinant inbred lines (RIL) from two populations (*Cicer echinospermum* backcross*susceptible (D09008) and *C. echinospermum* backcross*tolerant (D09024)) and two parents for plots of **(A)** back-transformed proportion of symptomatic plants *vs.* normalised yield loss, **(B)** normalised height reduction *vs.* normalised yield loss, **(C)** area of early senescence *vs.* normalised yield loss, **(D)** normalised height reduction *vs.* area of early senescence, **(E)** in-crop *Phytophthora medicaginis* (Pm) DNA concentrations *vs.* normalised yield loss, and **(F)** postharvest *P. medicaginis* DNA concentrations *vs.* normalised yield loss. Fitted regression lines and equations are presented. For **(E, F)**, one RIL was excluded (Ex.) from each regression.

Comparison of RIL performance across multiple parameters that identified three of the five RILs from the BC*tolerant population provided low-range normalised height reductions and early senescence values, in addition to consistently low in-crop and postharvest *P. medicaginis* DNA concentration results (Figure 3). For the six genotypes used in the in-crop inoculum regression, genotype in-crop inoculum values were significantly ($p < 0.05$) correlated with both normalised height reduction (0.883) and early senescence (0.892). However, the rankings of genotypes with low in-crop inoculum values against normalised yield loss more closely matched the rankings of genotypes with low early senescence against normalised yield loss than height reduction-based genotype rankings. The genotype rankings for normalised yield relationships with the proportion of symptomatic plants, area of early senescence, and in-crop inoculum showed that two RILs (D09024D>F6RIL>028, D09024B>F6RIL>040) were consistently at the lower end of these three normalised yield loss relationships.

Discussion

We evaluated *P. medicaginis* soil inoculum production of RIL from two chickpea–*C. echinospermum* populations. For groups of RIL with differing levels of foliage symptoms, *P. medicaginis* inoculum concentrations were higher for high disease phenotypes than low disease phenotypes in both RIL populations. Analysis of the soil inoculum reactions relative to control normalised yield loss for a set of RIL with superior PRR resistance required the exclusion of some RILs due to an apparent uneven distribution of inoculum in the field experiment. However, in-crop *P. medicaginis* soil inoculum concentrations were significantly related to normalised yield loss and indicated a putative partial resistance-tolerance spectrum.

Differences between the two disease phenotype categories in inoculum concentrations of RIL were related to the susceptibility and resistance of the RIL parents. The differences between high and low disease phenotypes for RIL from the BC*tolerant population could be related to differences in inoculum production values of their parents, where var. Yorker had significantly higher *P. medicaginis* soil inoculum concentrations than the backcross, 04067-81-2-1-1(B). Higher soil *P. medicaginis* inoculum production with var. Yorker was also confirmed in the BC*susceptible population experiment. The var. Yorker in-crop soil *P. medicaginis* inoculum concentrations were more than double those of 04067-81-2-1-1(B) in a separate study where genotypes were inoculated with the same equal oospore-based isolate mixture used in this study (Bithell et al., 2022). Furthermore, when soil *P. medicaginis* inoculum concentrations are expressed relative to root weight, var. Yorker had more than a 15-fold higher pathogen DNA concentration than 04067-81-2-1-1(B). Together, these results provide consistent evidence that the *C. echinospermum* backcross 04067-81-2-1-1(B) produced significantly less *P. medicaginis* inoculum than the moderately susceptible *C. arietinum* variety var. Yorker under field conditions. The lower inoculum production of 04067-81-2-1-1(B) could be attributed to the effects of partial resistance resulting in less extensive pathogen proliferation, as reported with other partially resistant material in similar pathosystems (Dorrance et al., 2001; Mideros et al., 2007). It follows that the *P. medicaginis* inoculum concentrations of the BC*tolerant RIL with high disease phenotypes were also similar to var. Yorker with elevated soil DNA values.

There was also evidence for particular RIL parents with differing PRR resistance to have similar *P. medicaginis* soil concentrations. We showed there was no difference in soil *P. medicaginis* concentrations in the soil among the parents of the BC*susceptible RIL population, viz., the very susceptible rated variety Rupali and 04067-81-2-1-1(B). In a prior study, *P. medicaginis* inoculum concentrations in the soil for another very susceptible PRR-rated variety, var. Sonali, showed a large decline in DNA concentrations from when peak disease and premature plant death occurred early in the growing season (Bithell et al., 2021). For this current study, of the three parents in the RIL population experiments, the very susceptible var. Rupali had the highest proportion of symptomatic plants (~49%) of all RIL parents. The high disease incidence included premature plant death for Rupali, which may be expected to have contributed to inoculum decline occurring prior to the inoculum sampling at the end of the growing season However, in contrast to results for the BC*tolerant RIL, five high disease BC*susceptible RILs had high inoculum concentrations, indicating that post-peak disease inoculum decline was not a trait of high disease BC*susceptible RIL.

Pathogen proliferation and normalised fitness assessments are key methods for the separation of genotypes with putative partial resistance or tolerance traits. It has been established in a number of soil-borne pathosystems, including those with oomycetes, that inoculum is often clustered in foci as opposed to a homogenous distribution (Campbell and Noe, 2003; Moussart et al., 2009). We demonstrated a large and significant range of normalised yield loss reactions to PRR infection among parents and eight chickpea–*C. echinospermum* RIL. However, we also identified issues probably related to the uneven distribution of *P. medicaginis* inoculum in the experiment. The uneven distribution of *P. medicaginis* inoculum may have contributed to variable inoculum results for some genotypes in the large plot yield loss experiment, as these also had a lower soil sampling intensity than the single-row plots in the first two experiments. It was necessary to exclude two genotypes from the analyses due to inconsistent soil inoculum values; however, analyses of the available data provided a number of useful findings. It will be important to identify *P. medicaginis*-free areas for experiments or to carry out plot-level sampling prior to sowing in order to reduce potential spatial variation in *P. medicaginis* populations across experimental sites. Issues of sample variability effects on cereal root pathogen detection can be addressed through the use of larger (250 g) sub-samples and the separation and grinding of soil organic matter prior to sub-sampling (Herdina and Roget, 2000). Prior to root decomposition, the highest concentrations of *P. medicaginis* inoculum are in root tissues. To reduce *P. medicaginis* detection variability, it may be appropriate to evaluate more samples and larger sample sizes (through a greater coring intensity per plot) and then separate and grind the organic matter in soil samples for re-inclusion with soil prior to DNA analyses.

Results for var. Yorker demonstrated a tolerance-type reaction due to substantial pathogen proliferation in association with the collapse of yield under high disease pressure. Both of these aspects were identified previously for var. Yorker but not in relation to control normalised yield loss (Bithell et al., 2021). Similar observations have been made in related pathosystems such as the PRR of soybean for genotypes with low levels of partial resistance, where under high inoculum and

favourable environmental conditions, substantial yield losses could not be prevented from occurring (Dorrance et al., 2003). Based on our findings for var. Yorker, we determined that var. Yorker was a tolerant genotype through the demonstration of reduced fitness or productivity relative to pathogen proliferation (Pagan and Garcia-Arenal, 2020). From the identification of var. Yorker as tolerant, we were then able to interpret the positions of the remaining genotypes in the inoculum–yield loss relationship as representing a partial resistance-tolerance spectrum. The in-crop inoculum–yield loss relationship identified the BC*tolerant RILs that had the lowest in-crop and postharvest *P. medicaginis* concentrations and low PRR yield loss values. These RILs were therefore interpreted to have the highest levels of partial resistance. A number of QTL associated with both Yorker and the *C. echinospermum* backcross 04067-81-2-1-1(B) from analysis of foliage symptoms caused by PRR were assumed to represent partial resistance traits (Amalraj et al., 2019). The research presented in this current study provides evidence that some QTL associated with var. Yorker may be linked to tolerance traits. These findings reinforce the need for an improved understanding of the genetic basis of partial resistance and tolerance traits in *C. echinospermum* derivatives. In addition, it may be possible to determine the effect of crossing on QTL pyramiding and trait composition in *C. echinospermum* derivatives. Of relevance to these goals is research on crown rot of wheat caused by *Fusarium pseudograminearum*, which has shown the capability to separately identify partial resistance from tolerance QTL for a number of traits (Rahman et al., 2021).

There was evidence for both pre-flowering and post-flowering PRR disease effects on normalised yield loss. In studies of PRR-affected soybean varieties with differing levels of partial resistance, the ratio of plants producing grain in yield component analysis was the most critical factor contributing to yield loss (Tooley and Grau, 1984). Chickpea yield is a highly heritable trait, with overall yields of desi chickpeas in semi-arid environments largely dependent on two yield components: pods per unit area and seed weight (Gan et al., 2003; Ali et al., 2009). Pre-flowering PRR disease reduces the potential number of chickpea pods, but in our yield loss experiment, there were minor to nil foliage symptoms or plant death across all RIL in pre-flowering assessments (data not presented). The importance of the final proportion of symptomatic plants on normalised yield loss may then be linked to post-flowering effects. In contrast, we found that root disease effects on genotype vegetative growth (normalised height reduction) accounted for a substantial proportion of the variation in normalised yield loss, but only one RIL genotype had more than a 10% PRR incidence based on foliage symptoms prior to physiological maturity when height measurements were taken. The reductions in height had been induced in the preceding months when most of the foliage was non-symptomatic. For soybean, reductions in plant height from PRR infection were correlated with final disease incidence and severity but were not a predictor of yield loss (Tooley and Grau, 1984). Pre-flowering destructive root disease assessments would be required to determine the relationship between chickpea height reduction and disease severity effects on grain yield.

It was notable that relationships among parameters varied in some respects. The positive but non-linear relationship between proportional infection and normalised yield loss indicated that the extent of proportional yield loss was lower at the high level of infection for var. Yorker. However, linear relationships that included var. Yorker were observed between the parameters normalised height reduction, area of early senescence, and in-crop inoculum production. The non-linear normalised yield to disease incidence relationship may be linked to increased seed production from surviving plants in plots due to higher levels of pathogen resistance, reduced interplant completion, or a combination of these factors as reported for *P. medicaginis*- and *Phytophthora sojae*-inoculated chickpea and soybeans plants, respectively, in field experiments (Wilcox and St Martin, 1998; Miranda, 2019).

Alternative methods of identifying material with low levels of pathogen proliferation may be useful. Comparison of genotype rankings among parameters related to normalised yield loss showed the proportion of symptomatic plants and area of early senescence as the parameters that provided genotype rankings that most closely matched those at the base of in-crop inoculum–normalised yield loss relationship. Notably, both of these parameters in this experiment were expressed post-flowering, and this may be a period when differential *P. medicaginis* inoculum production occurs among genotypes.

Both potential parameters indicative of inoculum production were PRR disease based. Findings for ranking similarities for the two genotypes at the base of the in-crop inoculum–yield loss and the proportion of symptomatic plants or early senescence-normalised yield loss relationships suggested simplistic relationships, whereby those genotypes with the least symptomatic plants or early senescence and yield loss will also provide lower inoculum development. If this is true, then yield loss experiments will need to be managed carefully to ensure that there is adequate disease pressure for foliage symptom development, as the two RIL disease phenotype experiments showed that differential inoculum production occurred under low disease RIL that did not develop foliage symptoms under dryland conditions and a low rainfall growing season. The differences in early senescence among chickpea genotypes may represent the effects of root disease damage contributing to premature foliage or crop maturity as shown in other pathosystems (Yang et al., 2016; Calamita et al., 2021). However, as shown for PRR of soybean where genotype maturity was evaluated for association with partial resistance (McBlain et al., 1991), chickpea genotype maturity may need to be considered as a contributing factor to the timing of senescence. If the priority is to identify RIL with low levels of *P. medicaginis* multiplication, then the evaluation of the proportion of symptomatic plants and area of early senescence as alternative parameters appears warranted.

In conclusion, we found some support for the hypothesis that *P. medicaginis* inoculum production differs among chickpea–*C. echinospermum* RIL and RIL parents with differing PRR resistance phenotypes. We found support for the hypothesis that inoculum production differs relative to normalised yield loss among RIL selected for low levels of PRR; however, comparisons were limited to a small set of genotypes due to variable inoculum measurements. We also found support for the evaluation of other parameters that were related to in-crop *P. medicaginis* inoculum production among chickpea genotypes.

Data availability statement

The original contributions presented in the study are included in the article. Further inquiries can be directed to the corresponding author.

Author contributions

SB, AD, DB, SH, and KH designed and conceived the study. SB and SH designed the experiments. SB and KH conducted the experiments. SB collected data and drafted the manuscript. All authors contributed to the article and approved the submitted version.

Conflict of interest

The authors declare that the research was conducted in the absence of any commercial or financial relationships that could be construed as a potential conflict of interest.

Acknowledgments

We acknowledge co-investment by New South Wales Department of Primary Industries (NSW DPI) and the Grains Research and Development Corporation (GRDC) under project DAN00172. The management of field experiments at the Hermitage Research Facility by William Martin at the Department of Agriculture and Fisheries Queensland is greatly appreciated.

Publisher's note

References

Ali, M. A., Nawab, N. N., Abbas, A., Zulkiffal, M., and Sajjad, M. (2009). Evaluation of selection criteria in *Cicer arietinum* l. using correlation coefficients and path analysis. *Aust. J. Crop Sci.* 3 (2), 65–70.

Amalraj, A., Taylor, J., Bithell, S., Li, Y., Moore, K., Hobson, K., et al. (2019). Mapping resistance to phytophthora root rot identifies independent loci from cultivated (*Cicer arietinum* l.) and wild (*Cicer echinospermum* P.H. Davis) chickpea. *Theor. Appl. Genet.* 132 (4), 1017–1033. doi: 10.1007/s00122-018-3256-6

Anon (2018). "GenStat committee," in *The guide to GenStat release 19.1* (Oxford: VSN International).

Bithell, S. L., Backhouse, D., Harden, S., Drenth, A., Moore, K., Flavel, R. J., et al. (2022). Aggressiveness of *Phytophthora medicaginis* on chickpea: Phenotyping method determines isolate ranking and host genotype-isolate interactions. *Plant Pathol.* 71, 1076–1091. doi: 10.1111/ppa.13547

Bithell, S. L., Moore, K., McKay, A., Harden, S., and Simpfendorfer, S. (2021). Phytophthora root rot of chickpea: Inoculum concentration and seasonally dependent success for qPCR based predictions of disease and yield loss. *Australas. Plant Pathol.* 50 (1), 91–103. doi: 10.1007/s13313-020-00752-2

Calamita, F., Imran, H. A., Vescovo, L., Mekhalfi, M., and La Porta, N. (2021). Early identification of root rot disease by using hyperspectral reflectance: The case of pathosystem Grapevine/Armillaria. *Remote Sens* 13 (13), 2436. doi: 10.3390/rs13132436

Campbell, C., and Noe, J. (2003). The spatial analysis of soilborne pathogens and root diseases. *Annu. Rev. Phytopathol.* 23, 129–148. doi: 10.1146/annurev.py.23.090185.001021

Coombes, N. (2016). *DiGGer: DiGGer design generator under correlation and blocking*. R package version 1.0.0.

Dale, M. L., and Irwin, J. A. G. (1991). Glasshouse and field screening of chickpea cultivars for resistance to *Phytophthora megasperma* f.sp. *medicaginis*. *Aust. J. Exp. Agric.* 31 (5), 663–667. doi: 10.1071/ea9910663

Dorrance, A. E., Inglis, D. A., Helgeson, J. P., and Brown, C. R. (2001). Partial resistance to *Phytophthora infestans* in four solanum crosses. *Am. J. Potato Res.* 78 (1), 9–17. doi: 10.1007/bf02874820

Dorrance, A. E., and McClure, S. A. (2001). Beneficial effects of fungicide seed treatments for soybean cultivars with partial resistance to *Phytophthora sojae*. *Plant Dis.* 85 (10), 1063–1068. doi: 10.1094/pdis.2001.85.10.1063

Dorrance, A. E., McClure, S. A., and St. Martin, S. K. (2003). Effect of partial resistance on phytophthora stem rot incidence and yield of soybean in Ohio. *Plant Dis.* 87 (3), 308–312. doi: 10.1094/PDIS.2003.87.3.308

Erwin, D. C., and Ribeiro, O. K. (1996). "Control by host resistance," in *Phytophthora diseases worldwide*. Eds. D. C. Erwin and O. K. Ribeiro (St. Paul: American Phytopathological Society), 186–210.

Gan, Y. T., Liu, P. H., Stevenson, F. C., and McDonald, C. L. (2003). Interrelationships among yield components of chickpea in semiarid environments. *Can. J. Plant Sci.* 83 (4), 759–767. doi: 10.4141/p02-145

Herdina,, and Roget, D. K. (2000). Prediction of take-all disease risk in field soils using a rapid and quantitative DNA soil assay. *Plant Soil* 227 (1/2), 87–98. doi: 10.1023/A:1026566711399

Knights, T., Moore, K., and Cummings, G. (2009). *Yorker Desi chickpea*. (Pulse Australia: Pulse Variety Management Package New South Wales). 03, 2.

Knights, E. J., Southwell, R. J., Schwinghamer, M. W., and Harden, S. (2008). Resistance to *Phytophthora medicaginis* Hansen and Maxwell in wild cicer species and its use in breeding root rot resistant chickpea (*Cicer arietinum* l.). *Aust. J. Agric. Res.* 59 (4), 383–387. doi: 10.1071/AR07175

Li, H., Rodda, M., Gnanasambandam, A., Aftab, M., Redden, R., Hobson, K., et al. (2015). Breeding for biotic stress resistance in chickpea: progress and prospects. *Euphytica* 204 (2), 257–288. doi: 10.1007/s10681-015-1462-8

Masini, L., Grenville-Briggs, L. J., Andreasson, E., Raberg, L., and Lankinen, A. (2019). Tolerance and overcompensation to infection by *Phytophthora infestans* in the wild perennial climber *Solanum dulcamara*. *Ecol. Evol.* 9 (8), 4557–4567. doi: 10.1002/ece3.5057

McBlain, B. A., Hacker, J. K., Zimmerly, M. M., and Schmitthenner, A. F. (1991). Tolerance to phytophthora rot in soybean 2. evaluation of 3 tolerance screening methods. *Crop Sci.* 31 (6), 1412–1417. doi: 10.2135/cropsci1991.0011183X003100060003x

Microsoft Office Standard (2016). *Microsoft® Excel® 2016 (16.0.5239.1001) MSO.*

Mideros, S., Nita, M., and Dorrance, A. E. (2007). Characterization of components of partial resistance, Rps2, and root resistance to *Phytophthora sojae* in soybean. *Phytopathology* 97 (5), 655–662. doi: 10.1094/PHYTO-97-5-0655

Mikaberidze, A., and McDonald, B. A. (2020). A tradeoff between tolerance and resistance to a major fungal pathogen in elite wheat cultivars. *New Phytol.* 226 (3), 879–890. doi: 10.1111/nph.16418

Miranda, J. H. (2019). Single plant selection for improving root rot disease (*Phytophthora medicaginis*) resistance in chickpeas (*Cicer arietinum* l.). *Euphytica* 215 (5), 18. doi: 10.1007/s10681-019-2389-2

Moussart, A., Wicker, E., Delliou, B., Abelard, J. M., Esnault, R., Lemarchand, E., et al. (2009). Spatial distribution of *Aphanomyces euteiches* inoculum in a naturally infested pea field. *Eur. J. Plant Pathol.* 123 (2), 153–158. doi: 10.1007/s10658-008-9350-x

Pagan, I., and Garcia-Arenal, F. (2020). Tolerance of plants to pathogens: A unifying view. *Annu Rev Phytopathol* 58, 77–96. 58Annual Review of Phytopathology. doi: 10.1146/annurev-phyto-010820-012749

Pariaud, B., Ravigné, V., Halkett, F., Goyeau, H., Carlier, J., and Lannou, C. (2009). Aggressiveness and its role in the adaptation of plant pathogens. *Plant Pathol.* 58 (3), 409–424. doi: 10.1111/j.1365-3059.2009.02039.x

Poland, J. A., Balint-Kurti, P. J., Wisser, R. J., Pratt, R. C., and Nelson, R. J. (2009). Shades of gray: the world of quantitative disease resistance. *Trends Plant Sci.* 14 (1), 21–29. doi: 10.1016/j.tplants.2008.10.006

Price, J. S., Bever, J. D., and Clay, K. (2004). Genotype, environment, and genotype by environment interactions determine quantitative resistance to leaf rust (*Coleosporium asterum*) in *Euthamia graminifolia* (Asteraceae). *New Phytol.* 162 (3), 729–743. doi: 10.1111/j.1469-8137.2004.01082.x

Rahman, M. M., Davies, P., Bansal, U., Pasam, R., Hayden, M., and Trethowan, R. (2021). Relationship between resistance and tolerance of crown rot in bread wheat. *Field Crops Res.* 265. doi: 10.1016/j.fcr.2021.108106

Salam, M., Davidson, J., Thomas, G., Ford, R., Jones, R. C., Lindbeck, K., et al. (2011). Advances in winter pulse pathology research in Australia. *Australas. Plant Pathol.* 40 (6), 549–567. doi: 10.1007/s13313-011-0085-3

Schafer, J. F. (1971). Tolerance to plant disease. *Annu. Rev. Phytopathol.* 9 (1), 235–252. doi: 10.1146/annurev.py.09.090171.001315

Schroth, G. (2003). *Root systems*. In: Eds. G. Schroth and F. L. Sinclair CABI, Wallingford: Trees, Crops and Soil Fertility Concepts and Research Method, 235–257.

Simms, E. L., and Triplett, J. (1994). Costs and benefits of plant responses to disease: Resistance and tolerance. *Evolution* 48 (6), 1973–1985. doi: 10.1111/j.1558-5646.1994.tb02227.x

Singh, K. B., Malhotra, R. S., Halila, M. H., Knights, E. J., and Verma, M. M. (1994). Current status and future strategy in breeding chickpea for resistance to biotic and abiotic stressees. *Euphytica* 73 (1-2), 137–149. doi: 10.1007/bf00027190

St Clair, D. A. (2010). Quantitative disease resistance and quantitative resistance loci in breeding. *Annu. Rev. Phytopathol.* 48, 247–268. doi: 10.1146/annurev-phyto-080508-081904

Thomson, S. J., Cameron, J. A. L., Dalal, R. C., and Hoult, E. (2007). Alternate wet-dry regime during fallow failed to improve nitrogen release from added legume residues in legume-wheat rotations on a vertisol. *Aust. J. Exp. Agric.* 47 (7), 855–861. doi: 10.1071/ea05290

Tooley, P. W., and Grau, C. R. (1984). The relationship between rate-reducing resistance to *Phytophthora megasperma* f.sp. *glycinea* and yield of soyabean. *Phytopathology* 74 (10), 1209–1216. doi: 10.1094/Phyto-74-1209

Wilcox, J. R., and St Martin, S. K. (1998). Soybean genotypes resistant to phytophthora sojae and compensation for yield losses of susceptible isolines. *Plant Dis.* 82 (3), 303–306. doi: 10.1094/pdis.1998.82.3.303

Yang, C., Odvody, G. N., Thomasson, J. A., Isakeit, T., and Nichols, R. L. (2016). Change detection of cotton root rot infection over 10-year intervals using airborne multispectral imagery. *Comput. Electron. Agric.* 123, 154–162. doi: 10.1016/j.compag.2016.02.026

frontiers | Frontiers in Plant Science

TYPE Original Research
PUBLISHED 14 March 2023
DOI 10.3389/fpls.2023.1114408

OPEN ACCESS

EDITED BY
Christophe Le May,
Institut Agro Rennes-Angers, France

REVIEWED BY
Bita Naseri,
Agricultural Research, Education and Extension Organization (AREEO), Iran
Kevin E. McPhee,
Montana State University, United States

*CORRESPONDENCE
Carol Kälin
carol.kalin@slu.se

SPECIALTY SECTION
This article was submitted to Plant Pathogen Interactions, a section of the journal Frontiers in Plant Science

RECEIVED 02 December 2022
ACCEPTED 27 February 2023
PUBLISHED 14 March 2023

CITATION
Kälin C, Kolodinska Brantestam A, Arvidsson A-K, Dubey M, Elfstrand M and Karlsson M (2023) Evaluation of pea genotype PI180693 partial resistance towards aphanomyces root rot in commercial pea breeding. *Front. Plant Sci.* 14:1114408. doi: 10.3389/fpls.2023.1114408

Evaluation of pea genotype PI180693 partial resistance towards aphanomyces root rot in commercial pea breeding

Carol Kälin[1]*, Agnese Kolodinska Brantestam[2], Anna-Kerstin Arvidsson[2], Mukesh Dubey[1], Malin Elfstrand[1] and Magnus Karlsson[1]

[1]Department of Forest Mycology and Plant Pathology, Swedish University of Agricultural Sciences, Uppsala, Sweden, [2]Nomad Foods Ltd., Findus Sverige AB, Bjuv, Sweden

The cultivation of vining pea (*Pisum sativum*) faces a major constraint with root rot diseases, caused by a complex of soil-borne pathogens including the oomycetes *Aphanomyces euteiches* and *Phytophtora pisi*. Disease resistant commercial varieties are lacking but the landrace PI180693 is used as a source of partial resistance in ongoing pea breeding programs. In this study, the level of resistance and their interaction with *A. euteiches* virulence levels of six new back-crossed pea breeding lines, deriving from the cross between the susceptible commercial cultivar Linnea and PI180693, were evaluated for their resistance towards aphanomyces root rot in growth chamber and green house tests. Resistance towards mixed infections by *A. euteiches* and *P. pisi* and commercial production traits were evaluated in field trials. In growth chamber trials, pathogen virulence levels had a significant effect on plant resistance, as resistance was more consistent against *A. euteiches* strains exhibiting high or intermediate virulence compared with lowly virulent strains. In fact, line Z1701-1 showed to be significantly more resistant than both parents when inoculated with a lowly virulent strain. In two separate field trials in 2020, all six breeding lines performed equally well as the resistant parent PI180693 at sites only containing *A. euteiches*, as there were no differences in disease index. In mixed infections, PI180693 exhibited significantly lower disease index scores than Linnea. However, breeding lines displayed higher disease index scores compared with PI180693, indicating higher susceptibility towards *P. pisi*. Data on seedling emergence from the same field trials suggested that PI180693 was particularly sensitive towards seed decay/damping off disease caused by *P. pisi*. Furthermore, the breeding lines performed equally well as Linnea in traits important for green pea production, again emphasizing the commercial potential. In summary, we show that the resistance from PI180693 interacts with virulence levels of the pathogen *A. euteiches* and is less effective towards root rot caused by *P. pisi*. Our results show the potential use of combining PI180693 partial resistance against aphanomyces root rot with commercially favorable breeding traits in commercial breeding programs.

KEYWORDS

***Aphanomyces euteiches*, pea root rot, *Phytophthora pisi*, resistance, breeding**

1 Introduction

The production of pea (*Pisum sativum* L.) is globally on the rise as the easy-to-grow crop poses an important source for food and feed (https://www.fao.org). Peas are widely cultivated as an environmentally sustainable alternative to soybean in many plant-based products, due to their high nutritional value and protein content (Xiong et al., 2018; Wei et al., 2020). *P. sativum* can be grown worldwide in temperate to cool climates with Sweden being one of the northernmost regions of pea cultivation. In Sweden, different pea cultivars have been grown since Neolithic times and the plant has remained one of the country's most important crop species alongside cereals (Osvald, 1959; Hjelmqvist, 1979; Leino et al., 2013).

Root rot, a soil-borne disease caused by a complex of fungal and oomycete pathogens, poses a major threat to commercial pea production. Oomycetes resemble fungi in morphology and growth but are able to reproduce both asexually *via* motile zoospores and with the production of sexual oospores. The oospores are resilient to desiccation and can remain in the soil as inoculum for several years (Mitchell and Yang, 1966; Cannesan et al., 2011). Among these root rot pathogens, *Aphanomyces euteiches* is the main causal agent for pea root rot. Its symptoms include discoloration of roots and epicotyl, root damage, wilting and eventual severe yield losses (Malvick et al., 2001; Wu et al., 2018). Another emerging oomycete infecting pea roots is *Phytophthora pisi*, which was first shown to cause root disease in pea in Sweden. Disease symptoms in pea are similar between the two oomycete pathogens, but symptoms of *P. pisi* are rarely observed on the epicotyl (Heyman et al., 2013). Furthermore, oospores of *P. pisi* can be morphologically differentiated from *A. euteiches* oospores under the microscope (Heyman et al., 2013). Differences in virulence among *A. euteiches* strains are observed in controlled infection experiments (Quillévéré-Hamard et al., 2018; Kälin et al., 2022) but prove difficult for the prediction of cultivar performance in the field where soil microbial compositions are complex (Wille et al., 2020).

Agro-ecological factors have been shown to influence soil microbial abundance and community composition in other legume crops (Naseri and Ansari Hamadani, 2017). The co-occurrence of several pathogens in the pea root rot complex (PRRC) has been reported but their interactions remain largely uncharacterized (Baćanović-Šišić et al., 2018; Chatterton et al., 2019). However, the increased susceptibility to single pathogens of the PRRC in presence of other pathogen species has been shown in controlled greenhouse experiments. Using co-inoculation experiments with *A. euteiches* and several *Fusarium* spp., Willsey et al. (2018) reported a disease reinforcement effect in presence of multiple pathogens. Peters and Grau (2002) showed that co-inoculations of pea with a non-pathogenic *F. solani* strain and *A. euteiches* resulted in significantly more severe disease symptoms compared to single infections with *A. euteiches*. Further, other important factors such as the significant effect of sowing date and depth on fusarium wilt development in chickpea cultivars have been shown by Younesi et al. (2020). Historically, breeding for resistance towards aphanomyces root rot has been most successful combining results from plant-pathogen interactions in both growth chambers and field experiments (Moussart et al., 2001; Wicker et al., 2003; Pilet-Nayel et al., 2005; Abdullah et al., 2017).

In Swedish pea production, current control measures against root rot pathogens focus on diagnosis of occurrence in the field and prevention of high pathogen inoculum levels in fields. Soil testing prior to sowing has been a reliable method for the avoidance of highly infested fields and long periods of crop rotation can prevent inoculum accumulation in the soil (Moussart et al., 2009; Moussart et al., 2013). The production of vining peas for quick-freezing are especially challenging since crop production has to be carried out in proximity of factory sites. Breeding for increased resistance against *A. euteiches* remains the most promising approach in disease control. However, sources of partial resistance in pea are scarce, polygenically inherited and largely affected by environmental effects (Hamon et al., 2013; Desgroux et al., 2016; Lavaud et al., 2016). Pea cultivars with complete resistance to aphanomyces root rot are lacking, but several cultivars with partial resistance have been used in breeding programs. Among them, the landrace PI180693 has been identified as a source of resistance towards *A. euteiches* by Lockwood (1960) and has been used in several studies for its potential to tolerate *A. euteiches* infection (Pilet-Nayel et al., 2002; Wicker et al., 2003). Further, PI180693 has shown to maintain high levels of resistance towards fusarium root rot in both controlled and greenhouse conditions (Grünwald et al., 2003; Infantino et al., 2006; Coyne et al., 2019). However, the landrace is associated with unfavorable breeding traits, such as extremely long internode length (long haulm), pale peas, normal leaves and round seeds with a starchy flavor. In modern crop production, semi-leafless and shorter varieties are preferred, as they will remain more erect at harvest, which reduces the risk of picking up small stones and soil particles that can contaminate the produce. Further, peas for quick freezing should have a 'sweet flavor' as well as a uniform, bright and attractive green color. Therefore, PI180693's growth phenotype is unsuitable for commercial cultivation and quick-freezing.

Our study aimed at evaluating the usefulness of the partial resistance against aphanomyces root rot originating from PI180693 in practical pea breeding, with emphasis on disease range and intraspecific pathogen variation, effectiveness and consistency. We used six back-crossed pea lines from a cross between PI180693 and the commercial variety Linnea to investigate (i) variation in disease resistance between breeding lines, (ii) interactive effects between disease resistance and virulence of *A. euteiches* strains, and (iii) the predictive power of climate chamber and greenhouse pot bioassays for estimating pea field performance. We show that the partial resistance towards aphanomyces root rot derived from PI180693 is useful for applied, commercial breeding and how monitoring the presence and virulence levels of pathogen populations is important for development and deployment of durable root rot resistant cultivars.

2 Materials and methods

2.1 *Aphanomyces euteiches* cultivation and growth

The *A. euteiches* strains used in this experiment originate from Sweden (SE51 and SE58) and the United Kingdom (UK16). All strains have been used in commercial breeding experiments, as they

are known to differ in virulence on pea. Strain SE58 was previously included in a phenotyping assay and shown to be of intermediate virulence. All three strains were described to belong to the same genetic cluster in previous population genetic analyses and were maintained as described in Kälin et al. (2022). Prior to be used as inoculum, strains were grown for two weeks on corn meal agar (CMA, BD Biosciences, San Jose, CA) at 20°C in the dark.

2.2 Pea breeding material

Two BC1F8 lines (Z1654-1 and Z1656-1) and four BC2F6 lines (Z1701-1, Z1701-2, Z1707-1 and Z1707-02) were included in this study. These six lines where selected based on screening results of various lines in greenhouse tests (data not shown). The selected lines showed better agronomic performance (yield component parameters and morphology) and tolerance against *A. euteiches* compared to their sibling lines in initial large-scale screenings. The BC1F8 lines were backcrossed once to Linnea, after an initial cross between Linnea and PI180693, whereas BC2F6 lines represents second backcrosses to Linnea in the sixth generation selfed (Table 1).

2.3 Growth chamber and greenhouse assays and phenotyping

Seed surface sterilization was performed following the protocol described in (Kälin et al., 2022) with minor changes. Square plastic pots (0,254 l) were filled with a first layer of vermiculite (Sibelco, Antwerpen, Belgium), on which an agar plate discs (8,5 cm diameter) with *A. euteiches* mycelium were placed in all pathogen treatments. For the infections, only plates fully covered with mycelia were used. The pots were then filled up with vermiculite in which five holes (3 cm depth, 1 cm diameter) were made to place the sterilized seeds. Tools used for the inoculation of *A. euteiches* were sterilized with 70% ethanol between inoculations, to prevent cross-contamination. Pots inoculated with one *A. euteiches* strain were kept together on a separate tray throughout the incubation in the growth chamber (CMP6050, Conviron) at 22°C, 55% humidity and 150 µmol light intensity in a 12 h light, 12 h dark cycle. Uninoculated pots of each cultivar were used as controls. For maintaining optimal pathogen growth conditions, the trays were filled with 2 cm of water and randomly moved within the chamber to account for uneven light or humidity conditions. The experiment was conducted with five pots with five plants each (biological and technical replicates, respectively). Disease scoring was done after three weeks of incubation and root disease symptoms were graded on a scale from 0 (completely healthy) to 100 (completely dead), by two different persons for every plant and then averaged on pot level. Assays in the greenhouse followed the same protocol but with 10 seeds per pot, five replicates, and 16h light, 8h dark cycle at 20°C and 19°C, respectively. For root dry weight measurements, all roots were harvested per biological replicate (pot) and dried over two days at 60°C before weighing on a Precisa 360 ES (growth chamber trials) or Mettler AT261 Delta Range scale (greenhouse trials).

2.4 Field trials and phenotyping

In 2020, two field trials were sown on the 2nd of April (Z20EA) and on the 5th of May (Z20EB) in randomized 1 m^2 plots (two blocks), whereas a single trial in 2022 was sown on the 23rd of March (R-22-10-91) in randomized 12 m^2 plots (4 blocks). All trials were conducted in southern Sweden (Skåne) and the choice of fields was made based on information from biotest indicating moderate infection rate by *A euteiches*. The soil biotest test prior season showed disease index 34 for Z20EA, disease index 76 for Z20EB and disease index 36 for R-22-10-91 trials. At the location for Z20EB both *A. euteiches* and *P. pisi* were detected, see Supplementary Table 1 for field coordinates and soil test scores. For phenotyping, ten plants from each plot were taken to rate the infection on roots and provide a disease index score based on root discoloration, between 0 (completely healthy) to 100 (completely dead). The field Z20EA was scored on the 1st of July 2020, Z20EB on the 7th of July 2020 and field R-22-10-91 on the 7th of June 2022, just before flowering to avoid root darkening due to natural maturation processes. Plant emergence was recorded as the percentage of emerged plants in relation to sowed plants in both field trials in 2020 and as the absolute number of emerged plants per square meter in the 2022 field trial. In field R-22-10-91, plant height, yield (at TR100, kg/ha) and the ratio of

TABLE 1 Information about pea cultivars used in the study.

ID	Type of material	Earliness class*	Leaf type	Flower color	Seed shape
Z1654-1	Breeding line (BC1F8)	+12	semi-leafless	white	wrinkled
Z1656-1	Breeding line (BC1F8)	+12	semi-leafless	white	wrinkled
Z1701-1	Breeding line (BC2F6)	+12	semi-leafless	white	wrinkled
Z1701-2	Breeding line (BC2F6)	+12	semi-leafless	white	wrinkled
Z1707-1	Breeding line (BC2F6)	+12	semi-leafless	white	wrinkled
Z1707-2	Breeding line (BC2F6)	+12	semi-leafless	white	wrinkled
Linnea	Commercial variety (used for BC)	+12	semi-leafless	white	wrinkled
PI180693	Landrace (source of resistance)	+12	leaved	pink	Non-wrinkled

*Earliness class indicated the number of days the cultivar is delayed in green pea harvest relative to reference variety 'Cabree' (earliness class 0). BC, backcross number; F, selfing cycle.

10.3389/fpls.2023.1114408

green peas compared to the total plant biomass as well as additional growth parameters were measured.

2.5 Statistical analyses

In the growth chamber experiment, all disease score values were treated as an average of the disease score values scored by the two scorers. Data were tested for normality and mock scores were excluded from further analyses to approach normal distribution. Two two-way analyses of variance (ANOVA) in R using the aov function (package stats ver. 4.1.0, R Core Team, 2021) were performed to assess the effects of the two factors cultivar and strain on disease index and root dry weight, including the factor's interactions. Data on root dry weight of uninfected plants was assessed separately using Fisher LSD test on one-way ANOVA residuals. For the analysis of greenhouse trials, we used one-way ANOVAs for disease index and root dry weight including cultivar as independent variable, with Fisher LSD *post-hoc* tests. The correlation coefficient for disease index and root dry weight in the growth chamber trials, and for disease index and germination in the field trials, was calculated using Pearson correlation for normal distributions in R (cor.test function). Field data was analyzed separately for each field. For 2020 fields, one-way ANOVAs on the interaction of disease index and emergence with cultivar were performed and Fisher LSD test was used for mean comparisons between groups. For the 2022 field trial, we performed a two-way ANOVA on disease index including cultivar and block effect and one-way ANOVAs were performed for the breeding traits. The correlations of yield with disease index and emergence for each cultivar were analyzed using linear regression modelling.

2.6 Climate data

For the duration of the 2020 field trials, data on temperature, rainfall and relative humidity were retrieved from the closest weather station (56°03'04" N, 12°76'28" E), publicly available on https://www.smhi.se/data/meteorologi/ladda-ner-meteorologiska-observationer. For the 2022 field trial, average air temperature, precipitation (rain) and relative humidity were measured using a mobile weather station installed next to the field (56°01'07.8"N 12° 58'16.1"E). In both cases, daily measurements were retrieved and the averages over two weeks were calculated and used in Supplementary Figure 3.

3 Results

3.1 Disease resistance in growth chamber trials

The growth chamber pot assay showed significant effects of strain ($p < 0.001$), cultivar ($p < 0.001$) and their interaction ($p < 0.01$), on disease index (Table 2). *A. euteiches* strains differed in virulence with UK16 being most virulent on all lines, SE51 was of

TABLE 2 Results from analyses of variance of growth chamber and field trials.

Factor	Growth chamber*			Field R-22-10-91*				Field Z20EA#		Field Z20EB#	
	DI ~cultivar	RDW ~cultivar	DI ~cultivar	Emergence ~cultivar	Yield ~cultivar	Pea biomass ~cultivar	Plant length ~cultivar	DI ~cultivar	Emergence ~cultivar	DI ~cultivar	Emergence ~cultivar
Strain	***	***									
Cultivar	***	***	*	**	*	*	***	*	***	*	**
Strain:cultivar	**	***									
Block			**	***	**	***	**				
Cultivar:block			.	x	.	x	x				

*Two-way ANOVA. #One-way ANOVA. DI, disease index; RDW, root dry weight; significance codes: '***' 0.001 '**' 0.01 '*' 0.05 '.' 0.1 'x' 1.

intermediate virulence while SE58 was least virulent on all lines (Figure 1A). With low pathogen virulence, i.e. infection with SE58, larger variation in disease symptoms between breeding lines was observed, compared with infection with more virulent strains. The disease index of PI180693 was more consistent upon infection with *A. euteiches* strains differing in virulence (Figure 1A). Using Fisher LSD test, breeding lines Z1654-1, Z1656-1, Z1701-1, Z1701-2 and Z1707-2 had significantly ($p < 0.05$) lower disease indices than Linnea upon infection with highly virulent strain UK16 (Supplementary Figure 1A; Supplementary Table 2). In response to intermediate virulence (strain SE51), the same breeding lines were also significantly more resistant than their susceptible parent (Supplementary Figure 1B). However, only line Z1701-1 showed significantly lower disease indices than in Linnea upon infection with the lowly virulent strain SE58 (Supplementary Figure 1C).

3.1.1 Root dry weight in growth chamber trials

We measured lowest root dry weight in cultivars infected with the most virulent *A. euteiches* strain UK16 and highest root dry weight in roots of cultivars infected with the SE58 low virulent *A. euteiches* strain (Figure 1B). In PI180693, however, the root dry weight was highest in plants infected with SE51 and the difference in root dry weight between roots infected with the three strains was lower compared to other cultivars. Both *A. euteiches* strains and pea cultivars, as well as their interaction, showed to have a highly significant ($p < 0.001$) effect on root dry weight in the growth chamber pot trials (Table 2). Fisher LSD tests on cultivar comparisons revealed that upon infection with highly virulent strain UK16, only line Z1707-2 had significantly higher root dry weight than Linnea (Supplementary Figure 2A; Supplementary Table 2). In response to intermediate virulence (strain SE51), breeding lines Z1654-1, Z1701-1, Z1701-2, Z1707-1 and Z1707-2 scored significantly higher root dry weight than the susceptible parent (Supplementary Figure 2B). The same breeding lines, with exception of Z1707-1, also scored higher root dry weight upon infection with the lowly virulent strain SE58, including line Z1656-1 (Supplementary Figure 2C)

Root dry weight measurements of the non-inoculated controls showed natural variation in root volume between cultivars. With an average root dry weight of 0.36 g per biological replicate, breeding line Z1654-1 showed to have non-significantly ($p > 0.05$) lower root dry weight scores than PI180693 (average 0.396g) whereas dried roots of line Z1707-1 did not differ from Linnea (0.237g and 0.19g, respectively). All other breeding lines had intermediate root dry weight scores compared to their parent cultivars (Table 3).

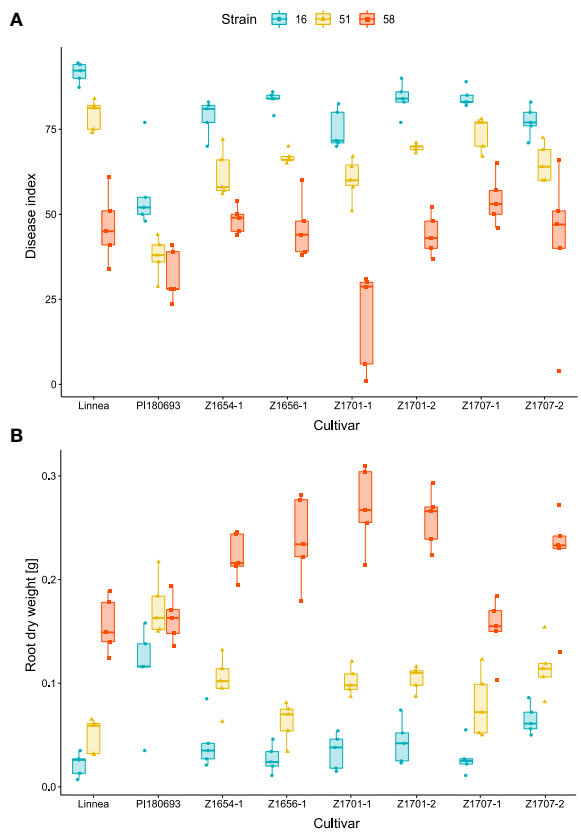

FIGURE 1
Virulence of *Aphanomyces euteiches* strains on pea cultivars. Disease indices **(A)** and root dry weight measurements **(B)** were assessed in growth chamber trials including six pea breeding lines and the two parental lines upon infection with *A. euteiches* strains UK16 (high virulence), SE51 (intermediate virulence) and SE58 (low virulence). Disease index scores (0 = completely healthy plant, 100 = completely diseased) and root dry weight measurements [g] are averages of five biological replicates.

3.2 Disease resistance and root dry weight in greenhouse trials

The effect of cultivar on measured disease indices showed to be highly significant ($p < 0.001$) in the greenhouse trials (Table 2). Fisher LSD tests on the ANOVA results showed that only breeding line Z1654-1 was significantly ($p < 0.05$) more resistant than Linnea upon infection with the intermediately virulent *A. euteiches* strain SE51 (Figure 2A). The effect on root dry weight was also highly significant ($p < 0.001$, Table 2). PI180693 displayed the highest root

TABLE 3 Root dry weight of uninfected pea cultivars in growth chamber experiments.

Cultivar	Root dry weight [g]*	Standard deviation	Fisher LSD#
Linnea	0.1894	0.04159086	e
PI180693	0.3962	0.07156256	a
Z1654-1	0.3598	0.03089822	ab
Z1656-1	0.3314	0.03415845	b
Z1701-1	0.3280	0.03205464	bc
Z1701-2	0.2698	0.04702871	cd
Z1707-1	0.2372	0.02060825	de
Z1707-2	0.2714	0.06148008	cd

*Roots were harvested after three weeks, and root dry weight values correspond to the average across five biological replicates (pots) with five plants each. #Fisher LSD test was applied on one-way ANOVA residuals. Letters a-e indicate significant ($p < 0.05$) different between group means.

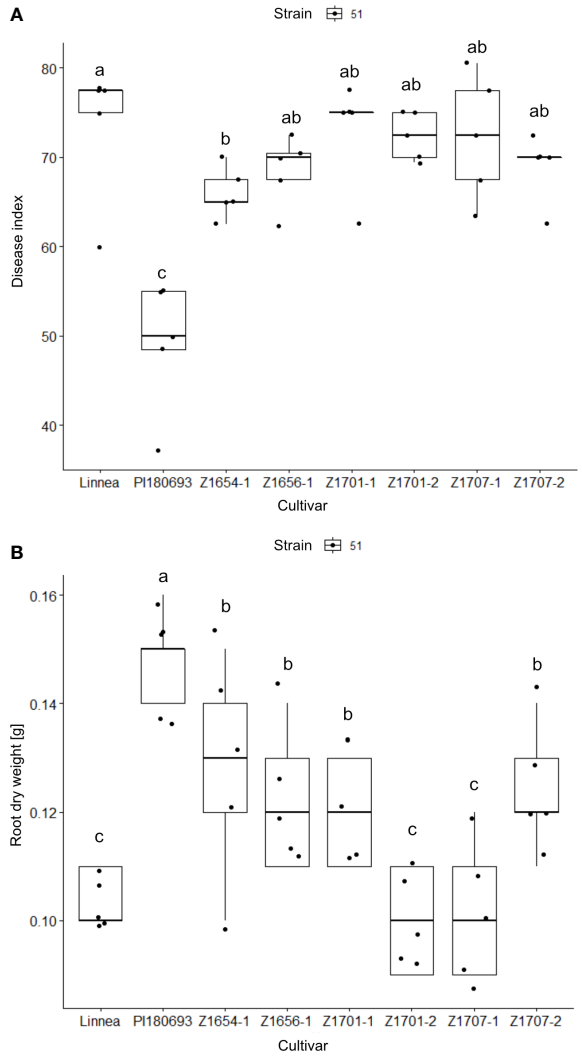

FIGURE 2
Disease index and root dry weight measurements in greenhouse trials. Disease index scores **(A)** and root dry weight measurements **(B)** in greenhouse trials, including six breeding lines and the two parental lines, upon infection with *A. euteiches* strain SE51 with intermediate virulence Disease index scores (0 = completely healthy plant, 100 = completely diseased) and root dry weight measurements [g] are averages of five biological replicates. Letters a-c indicate Fisher's significant ($p > 0.05$) differences between means of disease indexes and root dry weight between cultivars.

dry weight, whereas root dry weights of breeding lines Z1656-1, Z1701-1, Z1654-1 and Z1707-2 were significantly ($p < 0.05$) higher than Linnea and lower than PI180693 (Figure 2B).

3.3 Disease resistance and plant emergence in 2020 field trials

A. euteiches oospores were identified microscopically in fields Z20EA and Z20EB. In field Z20EB, *P. pisi* was also detected in soil tests and disease indices were higher on average. During the 2020 field seasons, air temperatures and relative humidity were lower than in year 2022 (Supplementary Figure 3).

In field Z20EA, Linnea was the most susceptible genotype with a significantly ($p < 0.05$) higher disease index compared with PI180693 and all breeding lines (Figure 3A). There were no differences in disease index between PI180693 and breeding lines. There was also a significant ($p < 0.001$) cultivar-effect on emergence in field Z20EA (Table 2), where Linnea showed a lower ($p < 0.05$) emergence compared with PI180693 and all breeding lines (Figure 3C). Disease index and emergence were significantly negatively correlated in field Z20EA (Pearson R = -0.637, $p < 0.01$).

In field Z20EB, where *P. pisi* co-occurred with *A. euteiches*, cultivar Linnea displayed the highest disease index, while PI180693 had the lowest ($p < 0.05$, Figure 3B). Only breeding line Z1656-1 had significantly ($p < 0.05$) lower disease index compared with Linnea (Figure 3B). Seedling emergence was significantly ($p < 0.05$) higher in breeding lines Z1707-2, Z1654-1 and Z1701-1 compared with Linnea (Figure 3D). Interestingly, no difference in seedling emergence was observed between PI180693 and Linnea (Figure 3D). Unlike in field Z20EA, there was no correlation between disease index and emergence in field Z20EB (Pearson R = 0.331, $p > 0.05$).

3.4 Disease resistance and plant emergence in 2022 field trial

As plots in field R-22-10-91 were larger than in fields Z20EA and Z20EB, we analyzed the effect of block size in our two-way ANOVA. Both cultivar and block had a significant effect on disease index ($p < 0.05$ and $p < 0.01$). The interaction effect of block and cultivar was not significant ($p > 0.1$, Table 2). Overall disease indices in field R-22-10-91 were lower compared with measured disease severity in the 2020 field trials but warmer average air temperature, less precipitation and higher relative humidity, especially during the sowing period, were measured in the 2022 field season (Supplementary Figure 3). Surprisingly, PI180693 scored the highest average disease index compared to all other cultivars ($p < 0.05$). Fisher comparisons between means of disease index per cultivar showed that no breeding line was significantly ($p < 0.05$) more resistant than the susceptible parent Linnea (Figure 4A).

Both cultivar and block had a significant effect on seedling emergence in field R-22-10-91 ($p < 0.01$ and $p < 0.001$, respectively, Table 2). Seedling emergence was significantly ($p < 0.5$) higher in PI180693 and breeding lines Z1707-2, Z1656-1, Z1701-1 and Z1654-1 than in Linnea (Figure 4B). In field R-22-10-91, the correlation between disease index and emergence was non-significantly negative (Pearson R = -0.308, $p > 0.05$).

3.4.1 Yield

In field R-22-10-91, block had a significant ($p < 0.01$) effect on yield, as well as cultivar ($p < 0.05$, Table 2). Breeding lines Z1701-2 and Z1707-2 had significantly ($p < 0.05$) lower yields than Linnea, but the yield of the other breeding lines did not differ from their commercially used parent. Interestingly, disease indices of lines Z1656-1 and Z1707-2 correlated positively with yield while all other cultivars showed a negative correlation (Figure 5A). The same two

10.3389/fpls.2023.1114408

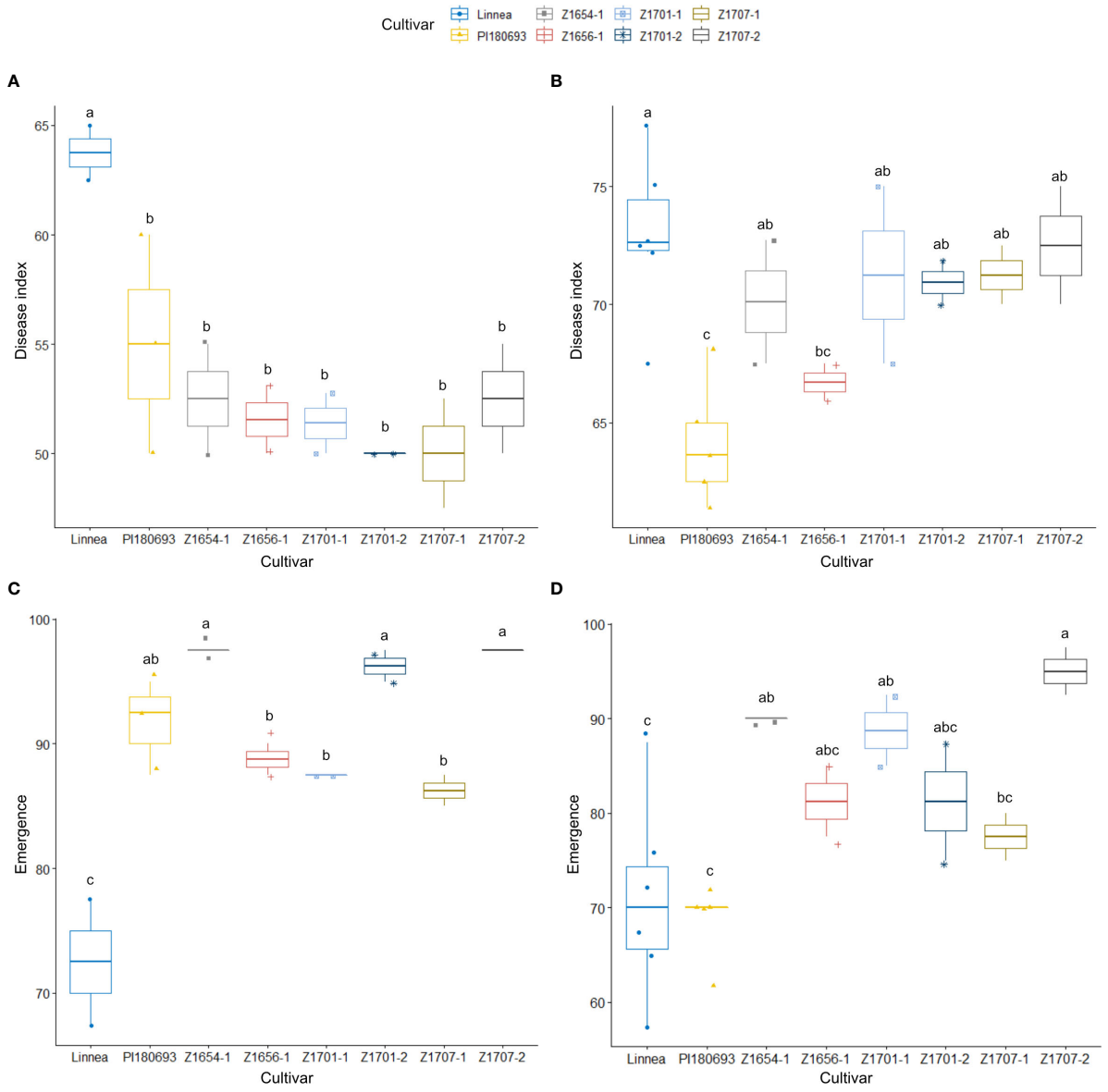

FIGURE 3
Disease index scores and emergence rates in 2020 field trials. Disease index scores **(A)** and emergence rates **(C)** for field Z20EA and field Z20EB with co-occuring *P. pisi*, **(B, D)**, respectively, are averages of two replicates for every breeding line and additional replicates for PI180693 and Linnea. Disease index is measured on a scale from 0 (completely healthy plant) to 100 (completely diseased) and emergence levels indicate the percentage of plants emerged compared to seeds sown. Letters a-c indicate Fisher's significant ($p > 0.05$) differences between means of disease indexes and emergence rates.

breeding lines also showed positive correlations between yield and emergence in linear regression analyses (Figure 5B).

3.4.2 Percentage of green peas compared to total plant biomass

Both cultivar and block had a significant ($p \leq 0.05$) effect on the amount of green peas per total plant biomass in field R-22-10-91 (Table 2). The percentage of peas versus total plant biomass in breeding lines Z1701-1 (17.7%) and Z1654-1 (17.3%) did not differ compared to 14.1% in Linnea (Supplementary Table 3). Interestingly, there was no correlation between disease index and the amount of peas versus the total plant biomass (Pearson correlation coefficient, R = 0.23, $p > 0.05$).

3.4.3 Plant height

In field R-22-10-91, both cultivar and block had a significant ($p < 0.001$ and $p < 0.01$, respectively) effect on the average plant height (Table 2). Cultivar PI180693 grew the tallest with an average plant length of 151 cm (Supplementary Table 3). The average length of other breeding lines was comparable to Linnea, except lines Z1654-1 and Z1656-1 that grew significantly ($p < 0.05$) taller than Linnea with average plant lengths of 77.6 cm and 81.8 cm.

3.4.4 Number of pods per plant and average length of second node pod

In the 2022 field trial, the number of pods per plant as well as the length of the second node pod were measured and compared to the

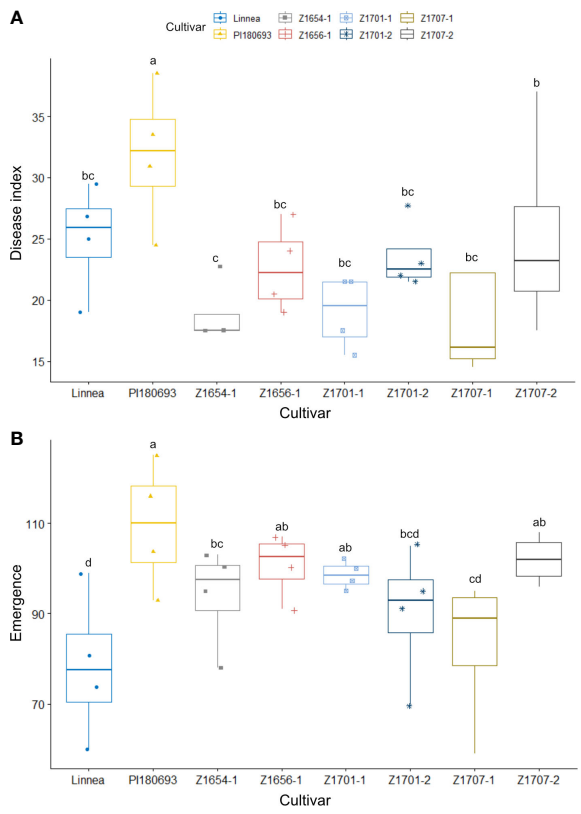

FIGURE 4
Disease index scores and emergence rates in the 2022 field trial. Disease index scores **(A)** and emergence rates **(B)** in field R-22-10-91. are averages of four replicates per cultivar. Disease index is measured on a scale from 0 (completely healthy plant) to 100 (completely diseased) and emergence levels indicate the percentage of plants emerged compared to seeds sown. Letters a-c indicate Fisher's significant ($p > 0.05$) differences between means of disease indexes and emergence rates.

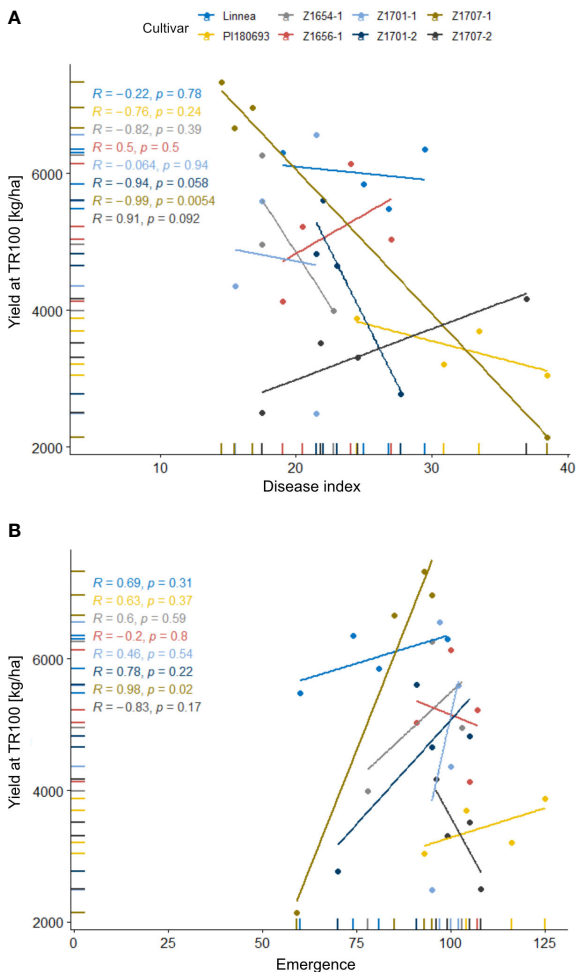

FIGURE 5
Correlations of yield with disease index scores and emergence rates in the 2022 field trial. Disease index scores **(A)** and yield and emergence rates **(B)** in field R-22-10-91are averages of four replicates per cultivar. Disease index is measured on a scale from 0 (completely healthy plant) to 100 (completely diseased) and emergence levels indicate the number of emerged plants per square meter. Lines represent linear regressions between the two factors, R values show Pearson correlation coefficients.

Linnea phenotype. Breeding line Z1707-2 had significantly less ($p < 0.05$, average 5.88) pods per plant than Linnea (average 7.5) while line Z1654-1 had more with an average of 9.12 (Supplementary Table 3). Comparing the average lengths of second node pods, breeding lines Z1656-1, Z1701-1 and Z1654-1 did not differ from the Linnea phenotype with an average length of 56.6 mm while the other breeding lines were comparable to the PI180693 phenotype with an average of 43.8 mm, (Supplementary Table 3).

4 Discussion

Taken together, our results show that the resistance from PI180693 can successfully be deployed in pea breeding line crosses. We found that some breeding lines are more resistant than their susceptible parent Linnea in field conditions and in growth chamber trials at low pathogen virulence levels. Line Z1654-1 scored lowest disease index on average (11.5% lower than Linnea) in both controlled experiments and scored on average 42% higher in root dry weight measurements compared to the susceptible parent. At lower pathogen pressure, line Z1701-1 showed to be significantly more resistant than both parents in the growth chamber trials with a 58.5% lower disease index than Linnea and 39.5% lower than PI180693. Interestingly, measured disease indices of PI180693 varied less in response to different virulence levels of *A. euteiches* compared with the breeding lines, indicating that the original source of resistance in PI180693 is more robust to varying pathogen virulence levels and partially lost during the breeding steps. This emphasizes the polygenic nature of the resistance and indicates that allele combinations for optimal disease resistance is yet to be achieved in the breeding lines. Along with this, we observed a negative correlation between pea root dry weight and disease index upon infections with *A. euteiches* across cultivars. Resistance QTLs in pea have previously been shown to be correlated with increased root volume and architecture (Desgroux et al., 2018). However, it remains to be investigated at which developmental stage the formation of roots is either fully inhibited or drastically reduced.

In our field experiments, the measured disease indices represented the overall plant health, including both root and shoot phenotype, and cannot be directly compared to disease indices in controlled conditions. Soil testing in fields Z20EA and Z20EB confirmed the presence of *A. euteiches* in the soil and in the latter the co-occurrence of *P. pisi*. We observed higher disease indices in field Z20EB compared to field Z20EA, indicating that presence of *P. pisi* enhanced disease levels. Comparing breeding line performance in field Z20EB, we did not find any indication that resistance in PI180693 is active against *P. pisi* infection. Whereas the genetic resistance in pea towards fusarium root rot caused by *Fusarium solani* f. sp. *phaseoli* is known to be inherited quantitatively (Mukankusi et al., 2011), little is yet known about the genes underlying the resistance to the emerging pathogen *P. pisi* (Heyman et al., 2013; Hosseini et al., 2014). In order to be able to make clearer predictions about the performance of the breeding lines upon infection with *P. pisi*, it will be essential to isolate virulent pathogen strains, and perform controlled single infections with the pathogen.

In field Z20EA where only *A. euteiches* was detected, all breeding lines had significantly higher emergence rates than Linnea, whereas in co-occurrence with *P. pisi* (field Z20EB), emergence rates were lower. We hypothesize that the additional presence of *P. pisi*, could have growth inhibiting effects in early plant growth stages and affect seed germination. When assessing emergence rates, natural variation in seed coat morphology must be taken into account, as for example PI180693 has shown to have a harder seed coat in seed germination tests (data not shown). In previous experiments we used pre-germinated pea seedlings that were able to germinate without pathogen pressure (Kälin et al., 2022). In these greenhouse and growth chamber trials we tried to spatially separate the inoculum from the seed, enabling the seeds to also germinate without pathogen pressure. In field conditions, however, seeds are subjected to *A. euteiches* and other root rot causing pathogens from the moment of sowing, which can lead to lower emergence rates. This emphasizes the importance of optimal timing of sowing within a growing season to reduce root rot disease in legume production (Nazer Kakhki et al., 2022).

In our 2022 field trial design, the size of blocks showed to have a significant effect on all analyzed parameters, which also corresponds to the typical patchy occurrence of *A. euteiches* in agricultural fields. Remarkably, PI180693 scored both highest disease indices and emergence rates in field R-10-22-91. None of the breeding lines showed disease index values that were significantly different from Linnea in this field trial, but four lines showed higher emergence rates than their susceptible parent. However, the 2022 season was very different compared with 2020, with moist soil conditions during sowing, followed by a very dry field season with high temperatures and low precipitation that were not conducive for root rot disease. It is known that levels of high soil moisture, due to heavy precipitation, poor drainage or high soil compaction, favor disease development in *A. euteiches* infections (Grath and Håkansson, 1992; Allmaras et al., 2003; Karppinen et al., 2020) and could therefore explain the observed patterns of lower average disease indices in field R-22-10-91, combined with a significant variation in emergence between cultivars.

With exception of two breeding lines, higher disease indices in field R-22-10-91 were associated with lower yield whereas four out of six breeding lines did not differ in yield compared to Linnea. Two of them (Z1701-1 and Z1654-1) were also comparable to Linnea in the ratio of green peas versus total plant biomass and average length of second node pod. Line Z1654-1 even scored more pods per plant than Linnea but inherited PI180693's tall growth phenotype. Our results confirm how breeding for robust resistance in pea is facing major challenges as resistance towards root rot is polygenically inherited and often associated with unfavorable breeding traits. Positive and negative associations between alleles controlling plant morphological traits, and resistance, suggesting pleiotropic genes involved in underlying resistance QTLs (Poland et al., 2009; Hamon et al., 2013). Desgroux et al. (2016) have reported a broken linkage between the traits of flower coloration and disease resistance against root rot in pea and recommend finer mapping techniques in future resistance breeding.

Our results further highlight the difficulty of predicting breeding line performance in the field based on results from experiments in controlled environments. In growth chamber experiments pressure from other pathogens is removed and only single or controlled co-infections at known virulence levels are assessed. In field conditions, however, the plants are exposed to a variety of PRRC pathogens with potential synergistic or antagonistic effects, as well as to a variety of other microbes (Wille et al., 2020). In summary, we showed the potential use of combining PI180693 partial resistance against aphanomyces root rot with commercially favorable breeding traits in commercial breeding programs.

Data availability statement

The raw data supporting the conclusions of this article will be made available by the authors, without undue reservation.

Author contributions

CK, MK, MD, AKB and ME planned and designed, and CK and MD carried out the growth chamber experiments. Field experiments were planned and performed by AKB and A-KA. Data analysis was done by CK and MK. All authors contributed to the article and approved the submitted version.

Funding

This work was funded by SLU Grogrund.

Acknowledgments

We acknowledge Claudia von Brömssen for her help with statistical analyses and Salim Bourras for his assistance throughout the study.

Conflict of interest

Authors AKB and A-KA are employed by Nomad Foods Ltd., Findus Sverige AB.

The remaining authors declare that the research was conducted in the absence of any commercial or financial relationships that could be construed as a potential conflict of interest.

Publisher's note

All claims expressed in this article are solely those of the authors and do not necessarily represent those of their affiliated organizations, or those of the publisher, the editors and the reviewers. Any product that may be evaluated in this article, or claim that may be made by its manufacturer, is not guaranteed or endorsed by the publisher.

Supplementary material

The Supplementary Material for this article can be found online at: https://www.frontiersin.org/articles/10.3389/fpls.2023.1114408/full#supplementary-material

SUPPLEMENTARY TABLE 2
Combined Fisher LSD test results for growth chamber, greenhouse and field trials.

References

Abdullah, A. S., Moffat, C. S., Lopez-Ruiz, F. J., Gibberd, M. R., Hamblin, J., and Zerihun, A. (2017). Host–Multi-Pathogen warfare: Pathogen interactions in Co-infected plants. *Front. Plant Sci.* 8, 1806. doi: 10.3389/fpls.2017.01806

Allmaras, R. R., Fritz, V. A., Pfleger, F. L., and Copeland, S. M. (2003). Impaired internal drainage and aphanomyces euteiches root rot of pea caused by soil compaction in a fine-textured soil. *Soil Tillage. Res.* 70, 41–52. doi: 10.1016/S0167-1987(02)00117-4

Baćanović-Šišić, J., Šišić, A., Schmidt, J. H., and Finckh, M. R. (2018). Identification and characterization of pathogens associated with root rot of winter peas grown under organic management in Germany. *Eur. J. Plant Pathol.* 151, 745–755. doi: 10.1007/s10658-017-1409-0

Cannesan, M. A., Gangneux, C., Lanoue, A., Giron, D., Laval, K., Hawes, M., et al. (2011). Association between border cell responses and localized root infection by pathogenic aphanomyces euteiches. *Ann. Bot.* 108, 459–469. doi: 10.1093/aob/mcr177

Chatterton, S., Harding, M. W., Bowness, R., Mclaren, D. L., Banniza, S., and Gossen, B. D. (2019). Importance and causal agents of root rot on field pea and lentil on the Canadian prairies 2014–2017. *Can. J. Plant Pathol.* 41, 98–114. doi: 10.1080/07060661.2018.1547792

Coyne, C. J., Porter, L. D., Boutet, G., Ma, Y., Mcgee, R. J., Lesné, A., et al. (2019). Confirmation of fusarium root rot resistance QTL fsp-ps 2.1 of pea under controlled conditions. *BMC Plant Biol.* 19, 98. doi: 10.1186/s12870-019-1699-9

Desgroux, A., Baudais, V. N., Aubert, V., Le Roy, G., De Larambergue, H., Miteul, H., et al. (2018). Comparative genome-wide-association mapping identifies common loci controlling root system architecture and resistance to aphanomyces euteiches in pea. *Front. Plant Sci.* 8, 2195. doi: 10.3389/fpls.2017.02195

Desgroux, A., L'anthoëne, V., Roux-Duparque, M., Rivière, J. P., Aubert, G., Tayeh, N., et al. (2016). Genome-wide association mapping of partial resistance to aphanomyces euteiches in pea. *BMC Genomics* 17, 124. doi: 10.1186/s12864-016-2429-4

Grath, T., and Håkansson, I. (1992). Effects of soil compaction on development and nutrient uptake of peas. *Swedish. J. Agric. Res.* 22, 13–17.

Grünwald, N. J., Coffman, V. A., and Kraft, J. M. (2003). Sources of partial resistance to fusarium root rot in the pisum core collection. *Plant Dis.* 87, 1197–1200. doi: 10.1094/PDIS.2003.87.10.1197

Hamon, C., Coyne, C. J., Mcgee, R. J., Lesné, A., Esnault, R., Mangin, P., et al. (2013). QTL meta-analysis provides a comprehensive view of loci controlling partial resistance to aphanomyces euteichesin four sources of resistance in pea. *BMC Plant Biol.* 13, 45. doi: 10.1186/1471-2229-13-45

Heyman, F., Blair, J. E., Persson, L., and Wikström, M. (2013). Root rot of pea and faba bean in southern Sweden caused by phytophthora pisi sp. nov. *Plant Dis.* 97, 461–471. doi: 10.1094/PDIS-09-12-0823-RE

Hjelmqvist, H. (1979). Beiträge zur kenntnis der prähistorischen nutzpflanzen in schweden. *Opera. Botanica* 47.

Hosseini, S., Heyman, F., Olsson, U., Broberg, A., Funck Jensen, D., and Karlsson, M. (2014). Zoospore chemotaxis of closely related legume-root infecting phytophthora species towards host isoflavones. *Plant Pathol.* 63, 708–714. doi: 10.1111/ppa.12137

Infantino, A., Kharrat, M., Riccioni, L., Coyne, C. J., Mcphee, K. E., and Grünwald, N. J. (2006). Screening techniques and sources of resistance to root diseases in cool season food legumes. *Euphytica* 147, 201–221. doi: 10.1007/s10681-006-6963-z

Kälin, C., Berlin, A., Kolodinska Brantestam, A., Dubey, M., Arvidsson, A.-K., Riesinger, P., et al. (2022). Genetic diversity of the pea root pathogen aphanomyces euteiches in Europe. *Plant Pathol.* 71, 1570–1578. doi: 10.1111/ppa.13598

Karppinen, E. M., Payment, J., Chatterton, S., Bainard, J. D., Hubbard, M., Gan, Y., et al. (2020). Distribution and abundance of aphanomyces euteiches in agricultural soils: effect of land use type, soil properties, and crop management practices. *Appl. Soil Ecol.* 150, 103470. doi: 10.1016/j.apsoil.2019.103470

Lavaud, C., Baviere, M., LE Roy, G., Hervé, M. R., Moussart, A., Delourme, R., et al. (2016). Single and multiple resistance QTL delay symptom appearance and slow down root colonization by aphanomyces euteiches in pea near isogenic lines. *BMC Plant Biol.* 16, 166. doi: 10.1186/s12870-016-0822-4

Leino, M. W., Boström, E., and Hagenblad, J. (2013). Twentieth-century changes in the genetic composition of Swedish field pea metapopulations. *Heredity* 110, 338–346. doi: 10.1038/hdy.2012.93

Lockwood, J. L. (1960). Pea introductions with partial resistance to aphanomyces root rot. *Phytopathology* 50, 621–624.

Malvick, D., Pfleger, F., and Grau, C. (2001). Aphanomyces root rot. *Compendium of Pea Diseases and Pests, 2nd edition*. St. Paul: APS Press, p. 9–13.

Mitchell, J., and Yang, C. (1966). Factors affecting growth and development of aphanomyces euteiches. *Phytopathology* 56, 917–922.

Moussart, A., Even, M. N., Lesné, A., and Tivoli, B. (2013). Successive legumes tested in a greenhouse crop rotation experiment modify the inoculum potential of soils naturally infested by aphanomyces euteiches. *Plant Pathol.* 62, 545–551. doi: 10.1111/j.1365-3059.2012.02679.x

Moussart, A., Wicker, E., Duparque, M., and Rouxel, F. (2001). "Development of an efficient screening test for pea resistance to aphanomyces euteiches," in *Proceedings of the 2nd International Aphanomyces Workshop, Section II: Epidemiology, Population Genetics & Host-Parasite Interactions. Proc. 4th Eur. Conf.* Grain Legumes, Cracow, Poland, Paris, France, 272–273.

Moussart, A., Wicker, E., Le Delliou, B., Abelard, J.-M., Esnault, R., Lemarchand, E., et al. (2009). Spatial distribution of aphanomyces euteiches inoculum in a naturally infested pea field. *Eur. J. Plant Pathol.* 123, 153–158. doi: 10.1007/s10658-008-9350-x

Mukankusi, C., Derera, J., Melis, R., et al. (2011). Genetic analysis of resistance to Fusarium root rot in common bean. *Euphytica* 182, 11–23. doi: 10.1007/s10681-011-0413-2

Naseri, B., and Ansari Hamadani, S. (2017). Characteristic agro-ecological features of soil populations of bean root rot pathogens. *Rhizosphere* 3, 203–208. doi: 10.1016/j.rhisph.2017.05.005

Nazer Kakhki, S. H., Taghaddosi, M. V., Moini, M. R., and Naseri, B. (2022). Predict bean production according to bean growth, root rots, fly and weed development under different planting dates and weed control treatments. *Heliyon* 8, e11322. doi: 10.1016/j.heliyon.2022.e11322

Osvald, H. (1959). *Åkerns nyttoväxter* (Stockholm: Sv. litteratur), p596.

Peters, R. D., and Grau, C. R. (2002). Inoculation with nonpathogenic fusarium solani increases severity of pea root rot caused by aphanomyces euteiches. *Plant Dis.* 86, 411–414. doi: 10.1094/PDIS.2002.86.4.411

Pilet-Nayel, L., Muehlbauer, F. J., Mcgee, R. J., Kraft, J. M., Baranger, A., and Coyne, C. J. (2002). Quantitative trait loci for partial resistance to aphanomyces root rot in pea. *Theor. Appl. Genet.* 106, 28–39. doi: 10.1007/s00122-002-0985-2

Pilet-Nayel, M. L., Muehlbauer, F. J., Mcgee, R. J., Kraft, J. M., Baranger, A., and Coyne, C. J. (2005). Consistent quantitative trait loci in pea for partial resistance to aphanomyces euteiches isolates from the united states and France. *Phytopathology* 95, 1287–1293. doi: 10.1094/PHYTO-95-1287

Poland, J. A., Balint-Kurti, P. J., Wisser, R. J., Pratt, R. C., and Nelson, R. J. (2009). Shades of gray: the world of quantitative disease resistance. *Trends Plant Sci.* 14, 21–29. doi: 10.1016/j.tplants.2008.10.006

Quillévéré-Hamard, A., Roy, L. G., Moussart, A., Baranger, A., Andrivon, D., Pilet-Nayel, M. L., et al. (2018). Genetic and pathogenicity diversity of aphanomyces euteiches populations from pea-growing regions in France. *Front. Plant Sci.* 9, 1673. doi: 10.3389/fpls.2018.01673

R Core Team. (2021). R: A language and environment for statistical computing. Vienna, Austria: R Foundation for Statistical Computing.

Wei, Y., Cai, Z., Wu, M., Guo, Y., Tao, R., Li, R., et al. (2020). Comparative studies on the stabilization of pea protein dispersions by using various polysaccharides. *Food Hydrocoll.* 98, 105233. doi: 10.1016/j.foodhyd.2019.105233

Wicker, E., Moussart, A., Duparque, M., and Rouxel, F. (2003). Further contributions to the development of a differential set of pea cultivars (Pisum sativum) to investigate the virulence of isolates of aphanomyces euteiches. *Eur. J. Plant Pathol.* 109, 47–60. doi: 10.1023/A:1022020312157

Wille, L., Messmer, M. M., Bodenhausen, N., Studer, B., and Hohmann, P. (2020). Heritable variation in pea for resistance against a root rot complex and its characterization by amplicon sequencing. *Front. Plant Sci.* 11, 542153. doi: 10.3389/fpls.2020.542153

Willsey, T. L., Chatterton, S., Heynen, M., and Erickson, A. (2018). Detection of interactions between the pea root rot pathogens aphanomyces euteiches and fusarium spp. using a multiplex qPCR assay. *Plant Pathol.* 67, 1912–1923. doi: 10.1111/ppa.12895

Wu, L., Chang, K.-F., Conner, R. L., Strelkov, S., Fredua-Agyeman, R., Hwang, S.-F., et al. (2018). Aphanomyces euteiches: A threat to Canadian field pea production. *Engineering* 4, 542–551. doi: 10.1016/j.eng.2018.07.006

Xiong, T., Xiong, W., Ge, M., Xia, J., Li, B., and Chen, Y. (2018). Effect of high intensity ultrasound on structure and foaming properties of pea protein isolate. *Food Res. Int.* 109, 260–267. doi: 10.1016/j.foodres.2018.04.044

Younesi, H., Chehri, K., Sheikholeslami, M., Safaee, D., and Naseri, B. (2020). Effects of sowing date and depth on fusarium wilt development in chick pea cultivars. *J. Plant Pathol.* 102, 343–350. doi: 10.1007/s42161-019-00423-2

frontiers | Frontiers in Plant Science

TYPE Original Research
PUBLISHED 27 March 2023
DOI 10.3389/fpls.2023.1140101

OPEN ACCESS

EDITED BY
Christophe Le May,
Institut Agro Rennes-Angers, France

REVIEWED BY
Magnus Karlsson,
Swedish University of Agricultural Sciences, Sweden
Hugo Germain,
Université du Québec à Trois-Rivières, Canada

*CORRESPONDENCE
Elodie Gaulin
elodie.gaulin@univ-tlse3.fr

SPECIALTY SECTION
This article was submitted to Plant Pathogen Interactions, a section of the journal Frontiers in Plant Science

RECEIVED 08 January 2023
ACCEPTED 24 February 2023
PUBLISHED 27 March 2023

CITATION
Kiselev A, Camborde L, Carballo LO, Kaschani F, Kaiser M, van der Hoorn RAL and Gaulin E (2023) The root pathogen *Aphanomyces euteiches* secretes modular proteases in pea apoplast during host infection.
Front. Plant Sci. 14:1140101.
doi: 10.3389/fpls.2023.1140101

The root pathogen *Aphanomyces euteiches* secretes modular proteases in pea apoplast during host infection

Andrei Kiselev[1], Laurent Camborde[1], Laura Ossorio Carballo[2], Farnusch Kaschani[3], Markus Kaiser[3], Renier A. L. van der Hoorn[2] and Elodie Gaulin[1]*

[1]Laboratoire de Recherche en Sciences Végétales (LRSV), Université de Toulouse, CNRS, UPS, Toulouse INP, Auzeville-Tolosane, France, [2]The Plant Chemetics Laboratory, Department of Plant Sciences, University of Oxford, Oxford, United Kingdom, [3]ZMB Chemical Biology, Faculty of Biology, University of Duisburg-Essen, Essen, Germany

To successfully colonize the host, phytopathogens have developed a large repertoire of components to both combat the host plant defense mechanisms and to survive in adverse environmental conditions. Microbial proteases are predicted to be crucial components of these systems. In the present work, we aimed to identify active secreted proteases from the oomycete *Aphanomyces euteiches*, which causes root rot diseases on legumes. Genome mining and expression analysis highlighted an overrepresentation of microbial tandemly repeated proteases, which are upregulated during host infection. Activity Based Protein Profiling and mass spectrometry (ABPP-MS) on apoplastic fluids isolated from pea roots infected by the pathogen led to the identification of 35 active extracellular microbial proteases, which represents around 30% of the genes expressed encoding serine and cysteine proteases during infection. Notably, eight of the detected active secreted proteases carry an additional C-terminal domain. This study reveals novel active modular extracellular eukaryotic proteases as potential pathogenicity factors in *Aphanomyces* genus.

KEYWORDS

***Aphanomyces*, root rot, plant pathogen, proteases, apoplast, extracellular, activity-based proteomics**

Introduction

Root rot diseases are a major global threat to the productivity of agricultural crops. The term 'root rot' has been widely used to describe a group of diseases characterized by softening and necrosis of the roots, producing a broad spectrum of lesions of various colors and sizes (Sharma et al., 2022). The widely spread oomycetes and fungi are the most prevalent soil-borne root rot pathogens (Dean et al., 2012; Becking et al., 2021). *Aphanomyces euteiches* root rot (ARR) disease is one of the major limiting factors in the

cultivation of North American (Papavizas and Ayers, 1974; Wu et al., 2018) and European pea (Quillévéré-Hamard et al., 2018; Quillévéré-Hamard et al., 2020), with some occurrence of this disease in Australian faba bean cultures (Watson et al., 2013).

Filamentous plant pathogenic oomycetes secrete several types of pathogenicity factors to facilitate infection, such as small secreted proteins (SSP), cellulose-binding proteins (CBELs) or plant DNA-damaging proteins (Gaulin et al., 2006; Ramirez-Garcés et al., 2016; Camborde et al., 2022). Before entering the root cells, these pathogens, including *A. euteiches*, may pass the apoplast. Due to its extracellular nature, the apoplast is involved in the perception and transduction of environmental signals (for a review, see Farvardin et al., 2020). On plant microbe detection, the plant cell wall is modified and the fluidic apoplast becomes a harsh environment equipped with antimicrobial compounds and various types of enzymes to restrict pathogen infection (Jashni et al., 2015; Dora et al., 2022). Basically, to survive in plant apoplast, phytopathogens depend on their ability to harvest nutrients, to hide from the host surveillance system and to attenuate host defense responses. Therefore, these pathogens produce cell-wall degrading enzymes (CWDE) and evolved molecular mechanisms to permit hiding, inhibition of defense-induced components, and detoxification/degradation of host components (Rocafort et al., 2020). Secreted proteases perform the two-last categories of actions and are present in the extracellular space of infected plant tissues. These proteases are found to originate from both the host and the pathogen (Jashni et al., 2015; Paulus et al., 2020).

Plant-secreted proteases are suspected to play major role during oomycete infection and numerous plant proteases are highly upregulated during infection, exemplified by aspartic protease StAsp from potato (Guevara et al., 2005) or the P69B serine protease from tomato (Tian et al., 2004; Paulus et al., 2020). Recent evidence has shown that proteases from oomycetes might also have a role to play during plant invasion. Expression profile of *in-silico* identified metalloprotease from *Phytophthora infestans* pinpointed a dozen of enzymes that potentially affect virulence of the pathogen (Schoina et al., 2021). Knockout-mutants of two secreted cysteine proteases from *Phytophthora parasitica* (PpCys44, 45) present a reduced virulence during *Nicotiana benthamiana* infection, while overexpression of both proteases in the plant apoplast triggers cell death (Zhang et al., 2020). In addition, a general counter-defense strategy used by invading oomycetes relies on the inhibition of host proteases. *P. infestans* secretes a large group of cystatin-like inhibitors (EPICs) known to target tomato Pip1, Rcr3 and C14 (Tian et al., 2007; Song et al., 2009; Kaschani et al., 2010; Van der Hoorn, 2011). Likewise, the Kazal-like serine protease inhibitors EP1 and EPI10 from *P. infestans* target tomato P69B subtilase (Tian et al., 2004, 2005). Interestingly, the *A. euteiches* genome, in addition to having numerous CWDE, is characterized by a large representation of putative extracellular proteases (Gaulin et al., 2018; Kiselev et al., 2022), suggesting a key role in infection.

To characterize the oomycete enzymes contributing to virulence, Meijer et al. (2014) performed a proteome profiling of the secretome from *P. infestans* grown on a plant-based medium and identified one aspartic protease, four cysteine proteases and two metalloproteases (Meijer et al., 2014). Similar studies on other *Phytophthora* species did not identify any proteases in the secretome (Severino et al., 2014; McGowan et al., 2020). These apparently contradicting results suggest that untargeted *in vitro* methods may be not ideally suited for protease identification. Activity-based protein profiling and mass spectrometry (ABPP-MS) uses highly selective active-site targeted chemical probes to label and characterize *in vivo*, active proteins including proteases (van der Hoorn et al., 2004; Kaschani et al., 2009). A set of probes were developed to target the different families of proteases, including papain-like cysteine proteases (PLCP), serine proteases, proteasomes, and metalloproteases (van der Hoorn, 2011; Morimoto and van der Hoorn, 2016). ABPP-MS has been used to identify a proteolytic cascade that activates immune proteases in tomato (Paulus et al., 2020), and to characterize secreted inhibitors from various pathogens (Shabab et al., 2008; Kaschani et al., 2010; Shindo et al., 2016).

Here we assessed whether the large repertoire of predicted *A. euteiches* proteases are active during host infection using ABPP-MS on infected-pea roots. We firstly defined the repertoire and genome organization of *A. euteiches* secreted proteases and evaluated their expression upon host infection. Then we identified 35 microbial proteases, among these, eight were original composite secreted proteases with a proteolytic domain associated to a non-catalytic domain that shows binding properties either for lipids or for carbohydrates. This work demonstrates ABPP-MS as an efficient *in vivo* tool to quickly substantiate genomics prediction of microbial pathogenicity factors. It allows the identification of original oomycete modular extracellular proteases, secreted by *A. euteiches* in the apoplastic host space in order to initiate the disease process.

Materials and methods

A. euteiches genome mining

Genome assembly (SRA accession SPR355760), predicted proteome sequence, and expression data (RNASeq) of *A. euteiches* ATCC201684 were accessed through the AphanoDB database (https://www.polebio.lrsv.ups-tlse.fr/aphanoDB/). The peptidases of *A. euteiches* were extracted as proteins harboring GO:0008233 and its child terms. To classify the genes into multigene families, the Markov Clustering Algorithm was applied (inflation rate 1,5) to cluster pairwise blast results (e-value < $1e^{-30}$). Tandemly repeated genes were identified as adjacent genes (blast e-value <$1e^{-80}$, coverage > 80%). Microsynteny search was performed using OGOB browser (McGowan et al., 2019) and FungiDB (Basenko et al., 2018) resource using the best blast hit of the corresponding organism. Secreted proteases were identified as those with a predicted signal peptide using SignalP v.5 (Almagro Armenteros et al., 2019) and those without transmembrane helices were predicted using TMHMM v.2.0 (Krogh et al., 2001).

For C1A cysteine-proteases phylogeny tree reconstruction, *Phytophthora infestans* T30-4 and *Saprolegnia parasitica* CBS223-65 sequences were downloaded from the FungiDB repository (Basenko et al., 2018). The proteins of the different genomes were

assigned with PFAM domain (PF00112) using InterProScan search (Sperschneider et al., 2015). The PF00112 domains were extracted and the phylogenetic tree was constructed and visualized in CLC Main Workbench v7.8.1(Qiagen), using ClustalW alignment and Neighbor-Joining (NJ) method with default parameters and bootstrap value of 1000.

Whole expression analysis (RNASeq)

Previously generated RNASeq reads of *M. truncatula* A17-Jemalong infected with *A. euteiches* ATCC201684 at 1, 3, 9 days post infection and *A. euteiches* mycelium (Gaulin et al., 2018) are accessible at NCBI SRA under reference SPR355760. The raw data were trimmed with TrimGalore (v.0.6.5) (https://github.com/FelixKrueger/TrimGalore) with cutadapt and FastQC options, and mapped to *M. truncatula* cv Jemalong A17 reference genome v.5.0 using Hisat2 (v.2.1.0) (Kim et al., 2019). Samtools (v.1.9) algorithms 'fixmate' and 'markdup' (Li et al., 2009) were used to clean alignments from duplicated sequences. Reads were counted with HTseq (v.0.9.1) (Anders et al., 2015) using the reference GFF file (Kiselev et al., 2022). The count files were normalized and differentially expressed genes (DEGs) were identified using the DESeq2 algorithm (Love et al., 2014).

Plant material, microbial strains and growth conditions

All experiments were carried out on the Précovil variety of *Pisum sativum* produced by the company Vilmorin (St Quentin Fallavier, France). Before germination, seeds were sterilised for 30 s in 96% EtOH, and 5 min in 5% bleach solution. After germination, the seeds were planted in 300 ml sterile pots filled with zeolite (1–5 mm fraction) and Fåhraeus media (Fåhraeus, 1957), supplemented with 5 mM NH_4NO_3 as nitrogen supplement. Zoospores of *A. euteiches* ATCC201684 were prepared as described elsewhere (Ramirez-Garcés et al., 2016). The plantelets were infected with 10^5 zoospores per plant one day after transfer to zeolite pots. Roots were harvested 15 days after infection. Pea apoplastic fluid was extracted using 3-times vacuum infiltration with ice-cold water. Two bars of pressure were applied 3 times during 10 min. Infiltrated roots were dried by rolling in a paper towel, placed in a 20 ml syringe and then introduced into a 50 ml falcon tube followed by centrifugation at 4°C, 2000 rpm with a slow acceleration/deceleration program.

Microscopy

Primary and upper secondary roots of pea infected or not by *A. euteiches*, were collected at 15 dpi for microscopic analysis. The primary root was placed directly on a holder and the secondary roots were embedded in 2,5% agarose and sliced using a vibrating-blade microtome (Leica VT1000 S) to 100 µm thickness. To specifically stain *A. euteiches* hyphae, wheat germ agglutinin coupled to Alexa Fluor 488 conjugate (WGA-488, Invitrogen) was used. Briefly, the specimens were stained in a 10 µg/ml staining solution for 5 min at room temperature and directly placed in a water drop on a microscope slide and observed using a confocal microscope. A confocal laser scanning microscope (Leica TCS SP8 operated on the LAS X software platform) was used to image the samples. Alexa Fluor 488 was detected between 500-565 nm using an OPSL 488 nm laser. Specimens were observed using a 10X dry objective (HC PL FLUOTAR 10x/0.30). All images were processed using ImageJ software version 1.53.

Labelling active apoplastic hydrolases and affinity purification

Three ml aliquots of pea apoplastic fluid (AF) per treatment were labelled with 4 µM of FP-biotin (Sigma) and 4 µM DCG04 (MedKoo Biosciences) during 4 h at room temperature under slow rotation (10 rpm). The reaction was buffered using 50 mM NaAc (pH 5) and 5 mM of dithiothreitol (DTT). No-probe control (NCP) samples were identical to labelled samples but instead of probes, an equal volume of DMSO was added to 3 ml of AF. Labelling reactions were stopped by chloroform/methanol precipitation. Cold chloroform+water+methanol mixture in the volume ratio 1:3:4 was added to the samples and mixed thoroughly. The precipitated samples were stored in the freezer at -20°C. Next, the samples were centrifuged at 3000 g for 30 min at 4°C. The aqueous top phase was removed without disturbing the interphase in which the proteins were present. Four volumes of cold methanol were then added, and the samples were centrifuged again for 45 min at 3000 g at 4°C. The supernatant was removed without disturbing the pellet and the precipitated proteins were left to dry at room temperature. The precipitated proteins were resuspended with 2 ml of 1.2% sodium dodecyl sulphate (SDS) phosphate saline buffer (PBS) (Life Technologies, 18912-014) for at least 40 min. The samples were then sonicated in a sonication bath at maximum power for 10 min. A further 5 ml of PBS was added to the samples and the proteins were denatured in a water bath at 90°C for 5 min. A further 3 ml of PBS was added to the samples to lower the SDS concentration to below 0.2%. To enrich the labelled proteins, 130 µl of PBS-washed avidin beads (Sigma, A9207) were added to each sample, including the NPC. The beads were incubated with resuspended proteins for 1 h at room temperature under rotation. The beads were then centrifuged for 1 min at 400 g and the supernatant was discarded. The Avidin beads were then washed 5 times with 10 ml of 1% SDS PBS buffer to remove nonspecific protein-beads interactions, and 3 times with 10 ml of ultra-pure HPLC-MS grade water. Finally, the beads were transferred into 2 ml LoBind protein tubes (Eppendorf, Z666505-100EA).

On-bead digestion and peptide purification

250 µl of 8 M Urea in 50 mM TrisHCl (pH 8) was added to the beads. The proteins were reduced by adding 500 mM of TCEP and incubating samples at 56°C for 30 min while shaking. The samples

were then cooled to room temperature before the alkylation step. 30 µl of 500 mM chloroacetamide was added and alkylation was performed at 36°C for 30 min in the dark. The samples were centrifuged at 2000 rpm for 3 min and the supernatant was removed. A vial of 20 µg of LysC endopeptidase enzyme (Wako, 125-02543) was resuspended into 1220 µl of 1 M urea in 50 mM Tris-HCl pH 8. 80 µl of this resuspended LysC was added to each sample. The tubes were sealed with a parafilm and LysC digestion was performed overnight at 37°C while shaking. The following day, trypsin endopeptidase (Trypsin gold MS grade Promega V5280) was reconstituted following manufacturer's instructions in 50 mM NaAc pH 5. 20 µg of the reconstituted trypsin was added to 1200 µl of 50 mM Tris-HCl pH 8. 80 µl of the diluted trypsin was added to each sample (2 µg per sample) and incubated for at least 8 h at 36°C. After trypsin digestion, tryptic peptides present in the supernatant were recovered in a new Lobind protein tube. Prior to mass spectrometry analysis of the peptidic composition, the tryptic peptides were purified using 100 µl Agilent Bond Elut OMIX pipette tips for micro extractions (Agilent, A57003100) using a 1 ml syringe coupled with a 1000 µl cut filter tip to push buffers and samples through the C18 column.

LC-MS/MS

Experiments were performed on an Orbitrap Fusion Lumos instrument (Thermo) coupled to an EASY-nLC 1200 liquid chromatography (LC) system (Thermo). LC was operated in the one-column mode. The analytical column was a fused silica capillary (75 µm × 46 cm) with an integrated PicoFrit emitter (New Objective) packed in-house with Reprosil-Pur 120 C18-AQ 1.9 µm resin (Dr. Maisch). The analytical column was encased by a column oven (Sonation) and attached to a nanospray flex ion source (Thermo). The column oven temperature was adjusted to 50 °C during data acquisition. The LC was equipped with two mobile phases: solvent A (0.1% formic acid, FA, in water) and solvent B (0.1% FA, 20% water and 80% acetonitrile, ACN). All solvents were of UPLC grade (Honeywell). Peptides were directly loaded onto the analytical column with a maximum flow rate that would not exceed the set pressure limit of 980 bar, usually around 0.6–0.8 µL/min. Peptides were subsequently separated on the analytical column by running a 140 min gradient of solvent A and solvent B (start with 8% B; gradient 8% to 35% B for 95 min; gradient 35% to 44% B for 20 min; gradient 44% to 100% B for 10 min and 100% B for 15 min) at a flow rate of 250 nl/min. The mass spectrometer was operated using Orbitrap Fusion Lumos Tune Application (version v3.3.2782.28) and Xcalibur (v4.3.73.11). The mass spectrometer was set in the positive ion mode. Precursor ion scanning was performed in the Orbitrap analyzer (FTMS; Fourier Transform Mass Spectrometry) in the scan range of m/z 375–1750 and at a resolution of 120000 with the internal lock mass option turned on (lock mass was 445.120025 m/z, polysiloxane) (Olsen et al., 2005). Product ion spectra were recorded in a data dependent fashion in the ion trap (ITMS) in variable scan range and at a rapid scan rate. The ionization potential (spray voltage) was set to 2.3 kV and the ion transfer tube temperature was 275°C. Peptides were analyzed using a repeating cycle (cycle time = 3 s) consisting of a full precursor ion scan (4.0×10^5 ions or 50 ms) and a variable number of product ion scans (1.0×10^4 ions, injection time set to 'auto'); peptides were isolated based on their intensity in the full survey scan (threshold of 5000 counts) for tandem mass spectrum (MS2) generation that permits peptide sequencing and identification. Stepped Higher-energy collisional dissociation (HCD) energy was set to 20, 35 and 40% for the generation of MS2 spectra. During MS2 data acquisition, the dynamic ion exclusion was set to 25 s (mass tolerance ±10 ppm) and a repeat count of 1. Ion injection time prediction, preview mode for the FTMS, monoisotopic precursor selection and charge state screening (charge states: 2 –6) were enabled.

Peptide and protein identification using MaxQuant

RAW spectra were submitted to Andromeda (Cox et al., 2011) search in MaxQuant (2.0.2.0) using default settings (Cox and Mann, 2008). Label-free quantification and match-between-runs was activated (Cox et al., 2014). The MS/MS spectral data were searched against the *A. euteiches* database (Kiselev et al., 2022) and the *P. sativum* database (Kreplak et al., 2019). All searches included a contaminants database search (as implemented in MaxQuant, 245 entries). The contaminants database containing known MS contaminants was included to estimate the level of contamination. Andromeda searches allowed oxidation of methionine residues (16 Da) and acetylation of the protein N-terminus (42 Da) as dynamic modifications and the static modification of cysteine (57 Da, alkylation with iodoacetamide). Enzyme specificity was set to 'Trypsin/P' with two missed cleavages allowed. The instrument type in Andromeda searches was set to Orbitrap and the precursor mass tolerance was set to ±20 ppm (first search) and ±4.5 ppm (main search). The MS/MS match tolerance was set to ±0.5 Da. The peptide spectrum match FDR and the protein FDR were set to 0.01 (based on target-decoy approach). The minimum peptide length was 7 amino acids. For protein quantification, unique and razor peptides were allowed. Modified peptides were allowed for quantification. The minimum score for modified peptides was 40. Label-free protein quantification was switched on, and unique and razor peptides were considered for quantification with a minimum ratio count of 2. Retention times were recalibrated based on the built-in nonlinear time-rescaling algorithm. Within parameter groups, MS/MS identifications were transferred between LC-MS/MS runs with the 'match between runs' (MBR) option in which the maximal match time window was set to 0.7 min and the alignment time window set to 20 min. The quantification was based on the 'value at maximum' of the extracted ion current. At least two quantitation events were required for a quantifiable protein. Further analysis and filtering of the results was done in Perseus v1.6.10.0. (Tyanova et al., 2016). For quantification, we combined related biological replicates to categorical groups and investigated only those proteins that were found in at least one categorical group in a minimum of 3 out of 4 biological replicates. Comparison of protein group quantities (relative quantification) between different MS runs is based solely on the LFQ's as calculated by MaxQuant, MaxLFQ algorithm (Cox et al., 2014).

Results

A. euteiches encodes numerous secreted proteases, tandemly duplicated in the genome

The AphanoDB, a database dedicated to the genus *Aphanomyces* (https://www.polebio.lrsv.ups-tlse.fr/aphanoDB/), contains 518 proteins with a PFAM-based GO Peptidase activity (GO:0008233), with trypsin S1 being the largest family (74 genes) in *A. euteiches* ATCC201684 strain (Supplementary Table S1). In a previous global analysis of the secretome we reported a large number of secreted proteases compared to the phytopathogen oomycete *P. infestans* (Gaulin et al., 2018; Kiselev et al., 2022). Accordingly, in this work we identified 151 proteins with a predicted signal peptide (+SP) and no transmembrane domain (-TM). Secreted proteases account for 28,5% of the total set of proteases indicating their significant enrichment in the secretome (Fischer exact's test $p < 0,05$), and represent 10% of a total *A. euteiches* secretome. As illustrated in Figure 1A, more than 80% of secreted proteases correspond to five families based on PFAM domains: serine proteases from S1, S8/S53, S28 (trypsin, subtilase and carboxypeptidase), papain-like cysteine proteases C1A (PLCPs) and metalloproteases M14. In all these five families, the number of secreted proteases is greater than non-secreted, as in metalloproteases M8 and M12A families. The *A. euteiches*

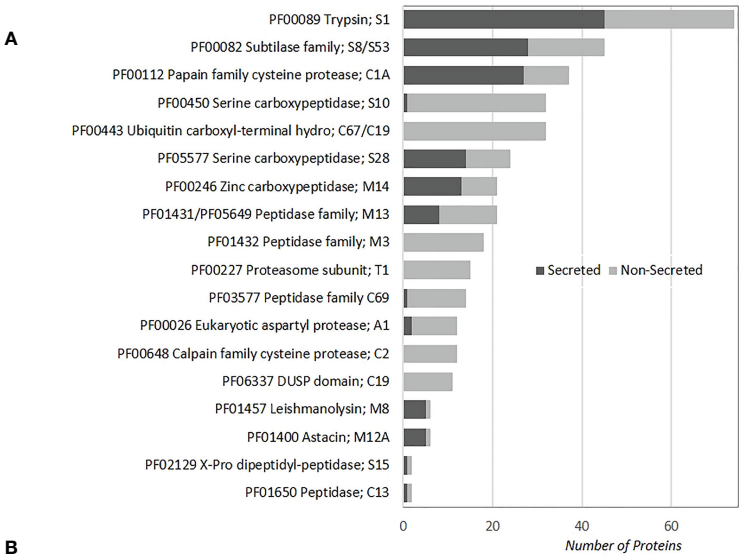

B

ID	Pfam-identified proteolytic domain	No of members per family	No of TR*/ No of genes/ No of genes per repeat	% of TR genes
1	Trypsin; S1	37	8/19/2,4	50
2	Papain; C1A	26	5/12/2,4	44
3	Subtilase; S8/S53	24	6/14/2,3	50
4	Serine carboxypeptidase; S28	14	2/5/2,5	35
5	Zinc carboxypeptidase; M14	12	1/5/5	41
6	Peptidase M13	8	0	0
7	Trypsin; S1	7	1/2/2	28
8	Leishmanolysin; M8	5	1/4/4	66
9	Astacin; M12	4	1/3/3	75
10	Subtilase S8/S53 + pro-kumanolisin	2	0	0

*TR – tandem repeats

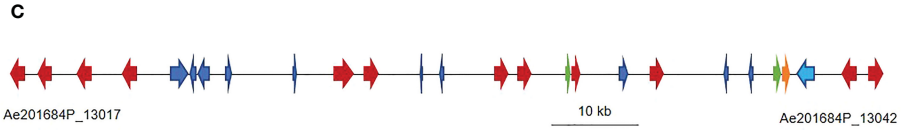

FIGURE 1
Mining of protease sequences from *A. euteiches* genome. **(A)** Repartition of proteolytic enzymes between secreted and non-secreted proteins in *A. euteiches* ATCC201684 genome. Proteolytic domains determined by InterProScan software against Pfam database. Secreted proteins (dark-grey) correspond to proteins with a predicted signal peptide (+SP) and without a predicted transmembrane domain (-TM). Data extracted from AphanoDB database (Madoui et al., 2007; Gaulin et al., 2018). **(B)** Distribution of secreted proteolytic enzymes in multigene families and tandem repeats in *A. euteiches*. Multigene families determined using Markov Cluster Algorithm (MCL) with a blast e-value < $1e^{-30}$, MCL inflation rate 1.5. Proteins considered in Tandem Repeats (TR), when having adjacent copy (blast e-value < $1e^{-80}$, coverage > 80%). **(C)** A 97 kb genome region (between Ae201684P_13017 and Ae201684P_13042 genes) in 2,7 Mb contig of *A. euteiches* enriched in tandemly repeated secreted subtilases (multigene family 3). The cluster contains 26 genes, corresponding to 11 secreted subtilases (red arrows), 1 non-secreted subtilase (orange arrow), 2 small secreted proteins (SSP, green arrows) and 13 non-secreted proteins with various functions (blue arrows). See Supplementary Table S4 for the detailed description of proteins present in the cluster.

secretome has very few carboxypeptidase (S10) X-Pro dipeptidyl-peptidase (S15), cysteine peptidases (C69 and C13) and aspartyl proteases (A1) and no M3 peptidases (Supplementary Table S2). Thus, the secretory repertoire of proteases in *A. euteiches* spans thirteen families among the 281 described in MEROPS.

Since tandem duplication of genes is a driving force for the expansion of oomycete sequences related to pathogenicity (McGowan et al., 2019), we looked for the genomic organization of the secreted proteases within the *A. euteiches* genome. Markov cluster algorithm (MCL) grouped the 138 secreted proteases (92%) from the genome sequence of *A. euteiches* into 10 multigene families (blast e-value < $1e^{-30}$, MCL inflation rate of 1,5), with sizes ranging from 2 members to 37 per family (average of 14) (Figure 1B). Only twelve secreted proteases did not present any paralog and were considered as singletons (Supplementary Table S3). We identified tandemly repeated proteases within each family by looking for proteins with an adjacent copy (blast e-value < $1e^{-80}$, coverage > 80%). For eight out of ten families, a large proportion (over 28%) of the genes were found to be tandemly replicated, while the two small multigene families containing metallopeptidases M13 and subtilases, and pro-kumanolisin prodomain, did not contain any tandem duplications. The tandem duplication rate of secreted proteases is in the range 33–60% in *A. euteiches*, while an average rate of 4–14% is reported for the whole genome in oomycetes (McGowan et al., 2019).

The identification of multigene families with a high proportion of tandemly repeated genes prompted us to localize the family members in the genome of *A. euteiches*. For each multigene family, a genome region consists mainly of the family members. As illustrated in Figure 1C, within a 97 kb genome region consisting of 26 genes, twelve correspond to secreted subtilases from the same multigene family (Figure 1C). Other genes from the cluster represent CYP450, endonuclease, Na/H exchanger, phosphatase, two Small Secreted Proteins (SSP), and proteins with unknown function (Supplementary Table S4). This genomic organization of subtilases was not detected in other oomycetes genomes when using FungiDB or OGOB synteny searches (Basenko et al., 2018; McGowan et al., 2019), despite the presence of orthologous genes both in Saprolegniales and Peronosporales orders. The absence of similar gene clusters in the animal pathogenic species from the *Aphanomyces* genus supports the hypothesis that the duplication of secreted proteases happened during adaptation to the host plant. Taken together, these data suggest that within *A. euteiches*, the secreted proteases are pathogenicity factors that evolved through tandem duplication events. This evolution could offer greater flexibility for a broad-range pathogen such as *A. euteiches*.

A. euteiches secreted proteases are induced during the infection process

To identify whether there is a transcriptional regulation of secreted proteases during infection of the host plant, dual RNA-Seq of the infection process of *A. euteiches* on susceptible *Medicago truncatula* line was analyzed (Gaulin et al., 2018). Overall, 118 secreted proteases were expressed, among which 79 were differentially expressed (DE, adjusted p-value <0,05) at 1-, 3- or 9-days post infection (dpi) as compared to a mycelium grown on synthetic media (Figure 2 and Supplementary Table S5). Several expression pattern can be distinguished. One includes almost all the trypsin S1 and zinc carboxypeptidase M14 genes, which are induced from 1 to 9 dpi. A second pattern identified around half of subtilase S8/S53, metallopeptidase M13 and of papain-like cysteine protease (PLCPs) belonging to protease family C1A, which are differentially upregulated overtime, while few genes are downregulated. Finally, some genes as subtilase S8 or trypsin S1 are respectively only express at the early stage of the infection or at a later stage. The tandemly repeated proteases do not show a common expression pattern since most of the astacin, M12 are slightly express from 3 to 9 dpi as the

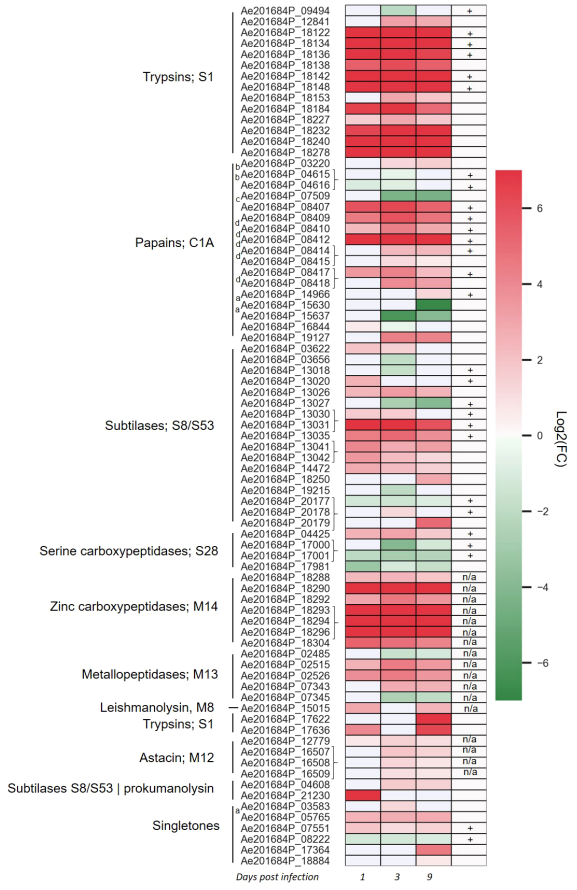

FIGURE 2
Aphanomyces euteiches differentially expressed genes coding for secreted proteases during *Medicago truncatula* infection. Three first columns of the heatmap represents log2(Fold Change) value of the significantly differentially expressed genes (DEG, p-value <0.05) during the time course of infection of *M. truncatula* roots (1, 3, 9 days post infection) as compared to the free-living mycelium. Braces on the right side of the gene name indicate adjacent tandemly repeated genes. The fourth column represents the identification of secreted proteases in activity-based proteome profiling proteomics (ABPP-MS) experiment using probes against active serine and cysteine hydrolases (+: identified by proteomics, blank: not identified by proteomics, n/a: probe not adapted for proteomics detection). Letter on the left side of the gene name indicate the presence of a binding domain within the secreted proteases [a: PAN/Apple domain (PF14295), b: ML domain (PF02221), c: fungal cellulose binding domain (PF00734), d: cysteine rich secretory domain CAP (PF00188)].

tandemly repeated C1A PLCPs, when the repeated subtilase S8 or zinc carboxypeptidase M14 genes are highly express at all stages. The transcriptomics evidence of massively upregulated secreted proteases during infection of *M. truncatula* roots underpins the role of these genes as pathogenicity factors in *A. euteiches*. In addition, the various expression pattern observed within similar proteins of the same multigene family suggests an independent transcriptional regulation and function of the tandemly repeated secreted proteases.

A. euteiches secretes active serine hydrolase and cysteine proteases into plant apoplast during pea infection

To evaluate the contribution of *A. euteiches* extracellular proteases during legume infection, we hypothesized that secreted proteases should be present within the apoplast of infected roots. A semi-sterile pathosystem using *Pisum sativum* was established to collect sufficient volume of apoplastic fluid (AF), after roots infection by *A. euteiches* (Supplemental Figure 1). To perform the ABPP-MS assay, isolated apoplastic fluids (AF) were incubated with a cocktail of commercially available FP-biotin and DCG-04 to label Ser hydrolases and PLCPs, respectively. To further identify natively biotinylated proteins, samples without probes were generated (NPC = No-Probe-Control) and all were subjected for mass spectrometry. Protein identification was performed with MaxQuant software using the latest genome assembly of *A. euteiches* (Kiselev et al., 2022) and *P. sativum* (Kreplak et al., 2019). The analysis revealed a total of 3641 proteins groups (PG) (Figure 3A). PGs can represent several similar proteins, which are not distinguishable from detected peptides and tandemly repeated *A. euteiches* proteins. The PGs containing *P. sativum* proteins were filtered out (525 PG), and 20 PGs having similarity with *A. euteiches* within non-infected samples (mock) were removed. For further analysis, 274 PGs were kept, which were detected in at least three out of four replicates of the infected samples. From the resulting list, 59 PGs were carrying a serine or cysteine hydrolase domain (Supplementary Table S6), and 52 of these were enriched in the probe samples when compared to the no-probe-control (p-value <0.05). Among the 52 PGs, 26 were predicted as secreted leading to a final set of 35 proteins (Supplementary Table S7). A large majority of the corresponding genes are differentially expressed (28) at least at one time point during the infection of *M. truncatula* roots (Figure 2). Overall, from the 115 annotated Cys and Ser hydrolases that could be labelled with the probes, 99 (~85%) have a transcript in at least one of the time points of the infection. Therefore, the ABPP-MS approach allows identification of 30% of the *A. euteiches* expressed sequence during legume root colonization.

The set of the MS-identified secreted proteins consists of 4 PGs with subtilases that include seven proteins; four PGs with trypsins (eight proteins), one PG with Ser carboxypeptidase S10 (one protein); four PGs with Ser carboxypeptidase S28 (four proteins); five PGs with PLCPs (five proteins) (Figure 3B). In addition, six PGs include eight secreted modular proteins, in which an additional PFAM domain is associated with the proteolytic domain at the C-terminus. These correspond to: one PG with a subtilase connected to a PAN domain (PF14295, two proteins); two PGs with a PLCP connected to a Cys-rich secretory protein-CAP (PF00188, two proteins); two PGs with a PLCP connected to a ML domain (PF02221, two proteins) and one PG of a PLCP connected to a fungal cellulose binding domain (PF00734, one protein) or to a ML domain (PF02221, one protein). All the MS-identified serine subtilases are present in one gene cluster located in contig 762

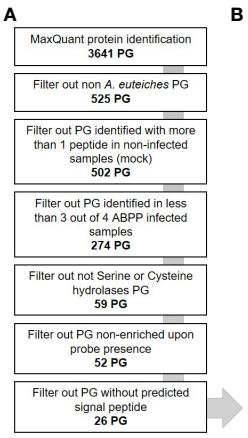

B

PFAM annotation	No of Protein Groups (PG)/Proteins	Genes *	
PF00082 Subtilase family	4/7	Ae201684P_13042 Ae201684P_13035 Ae201684P_13031/18 Ae201684P_13030/27/20	Serine proteases
PF00089 Trypsin	4/8	Ae201684_18136 Ae201684_18143/21/22/42/48 Ae201684_18134 Ae201684_9494	
PF00450 Serine carboxypeptidase S10	1/1	Ae201684P_8222	
PF05577 Serine carboxypeptidase S28	4/4	Ae201684P_17000 Ae201684P_17001 Ae201684P_18544 Ae201684P_4425	
PF00082 Subtilase family/ PF14295 PAN domain	1/2	Ae201684P_20178/77	
PF00112 Papain family cysteine protease	5/5	Ae201684P_3220 Ae201684P_7551 Ae201684P_7509 Ae201684P_8409 Ae201684P_8417	Cysteine proteases
PF00112 Papain family cysteine protease/ PF08246 Cathepsin propeptide inhibitor domain	2/2	Ae201684P_16844 Ae201684P_14966	
PF00112 Papain family cysteine protease/ PF00188 Cysteine-rich secretory protein family	2/2	Ae201684P_8414 Ae201684P_8415	
PF00112 Papain family cysteine protease/ PF02221 ML domain / PF08246 Cathepsin propeptide inhibitor domain	2/2	Ae201684P_4616 Ae201684P_4615	
PF00112 Papain family cysteine protease/ PF00734 Fungal cellulose binding domain or PF00188 Cysteine-rich secretory protein family	1/2	Ae201684P_8407/12	

*Genes listed in one line identified in the same PG

FIGURE 3
Data analysis workflow of secreted proteases from *A. euteiches*. **(A)** Downstream analysis of the MaxQuant assigned Protein Groups (PG). The number of PGs on each step is indicated in bold. **(B)** List of the mass spectrometry identified extracellular serine and cysteine proteases from *A. euteiches* present in apoplastic fluid of pea, 15 days post infection. Gene IDs according to AphanoDB nomenclature. Note that the sequences given in each line of the table belong to the same PG. See Supplementary Tables S6–S8 for complete data.

presented in Figure 1C. The trypsin proteases originated also from one gene cluster in contig 60. A third cluster present on contig 595, corresponds to the PLCPs with or without an additional PFAM domain. Furthermore, two couples of tandemly repeated proteins were identified: carboxypeptidases (Ae201684P_17000 and _17001) and PLCPs-CAP proteins (Ae201684P_8414 and _8415). Both proteins of each of repeats are identified as a separate PG indicating their presence in the sample. Taken together, the ABPP-MS approach supports the prediction of proteases gene clusters and tandemly repeated sequences in *A. euteiches* genome.

A. euteiches produces modular extracellular serine and cysteine proteases during legume infection

Most families of fungal, oomycetes serine or cysteine proteases correspond to a single-domain protein (Muszewska et al., 2017). The identification by MS of multidomain extracellular proteases may suggest a specific function for these enzymes for *A. euteiches* invasion. The identified multidomain proteases harbor an additional binding region consisting of a PAN/Apple domain (PF14295) for subtilases and a ML lipid binding domain (PF02221), a Cys-rich secretory CAP domain (PF00188) or a CBM1 fungal cellulose binding domain (PF00734) for PLCPs. PAN/Apple and CBM1 have been suggested to mediate protein/carbohydrate or protein/protein interactions (Tordai et al., 1999), while CAP and ML domains are related to sterol and lipid binding capacities, respectively (Inohara and Nuñez, 2002; Schneiter and Di Pietro, 2013). InterProScan domain architecture searches revealed the large distribution within eukaryotes of modular PAN-trypsin proteases with a large representation in animals, but the association of a PAN/Apple domain with a subtilase is unique to the *Aphanomyces* genus. The combination of a cysteine C1A domain (PF00112) with a lipid-binding ML domain (C1A:ML) is present in several Stramenopila, including oomycetes, the yellow-green algae (Xanthophyceae, *Tribonema minus*), and brown algae (Phaeophyceae, *Ectocarpus siliculosus*), but the C1A:CBM1 and C1A:CAP associations are restricted to the *Aphanomyces* genus. Only heterotrophic Amoebozoan slime molds protists (*Planoprotselium fungivorum, Dictyostelium purpureum, Polysphondylium pallidum*) harbor predicted extracellular proteins with domains organized in the reverse order (e.g. CAP:C1A). The gene cluster encoding PLCPs identified by MS displays the unique structure of modular cysteine proteases. Within 50 kb on contig 595, this gene cluster contains 12 extracellular PLCP-encoding genes, which have a conserved C1A domain at the N-terminal region associated with a variable C-terminal region consisting either of CBM1, CAP or no domains. The domains are commonly separated by a disordered linker often represented as a PT-repeat (Figure 4A). Phylogenetic analysis of C1A-domain from PCLPs sequences from *P. infestans*, *S. parasitica* with *A. euteiches*, identified 12 multidomain members of the clustered-PLCP of the root pathogen in one group derived from a unique C1A-containing protein (Figure 4B). Within this group, CAP and CBM1 additional domains form two subgroups, suggesting a first duplication of the catalytic domain followed by acquisition of an additional 'binding' module for modifying the initial function of the C1A domain. (Figure 4B). The others C1A-containing proteins of *A. euteiches* are mainly detected in two groups, related to the fish pathogen *S. parasitica* with the exception of C1A-ML multidomain PLCPs more related to *P. infestans*. To predict whether the additional domain within the original PLCPs may modulate the activity of the corresponding enzyme, the structure of the catalytic and binding domains of each protease was predicted with Alpha-Fold2 (Jumper et al., 2021). Superpositions of the predicted 3D modelling with a reference structure for each domain are shown in Figures 4C–E. All the modular proteins keep a structural homology (RMSDE score <= 1) with the reference structure. Despite a slightly higher RMSDE score of ~4, the structural alignment of the ML-domain also revealed a structural topology to immunoglobulin (PDB 1AHM). According to the modelling results, the additional binding domain detected in the extracellular PCLP of *A. euteiches* may serve for the adhesion of a protease to a specific substrate to enhance its activity during infection.

Discussion

The genome of the detrimental-roots colonizing filamentous oomycete *A. euteiches* is predicted to have a large set of proteolytic enzymes (Kiselev et al., 2022). Here we explored the genomic organization of protease sequences, their expression during host infection, and characterized whether they are present and active during root colonization using an ABPP-MS approach. We identified original modular secreted serine subtilisin and PCLPs in the apoplast of infected roots that may contribute to *A. euteiches* pathogenicity.

The curated annotation of the predicted proteases from the long-read sequenced ATCC201684 strain of *A. euteiches* showed that the proteases consist mainly of trypsin (serine protease, S1 class) and papain (cysteine protease, C1 class) families. Up to 60% of secreted protease genes were found tandemly repeated and frequently organized in large clusters enriched in proteases (e.g. over 50% of genes within a cluster encode proteases). McGowan et al. (2019) identified that 40% of the 20 oomycete species analyzed, displayed GO terms enrichment in terms linked to pathogenicity such as 'catalytic activity, acting on protein' (GO:140096) and 'peptidase activity' (GO:0008233), in tandem duplicate genes. Tandem gene duplication in combination with homologous recombination are postulated to accelerate pathogenicity factors evolution within oomycete genomes (Haas et al., 2009; Fitzpatrick et al., 2010; Liang et al., 2020). In *A. euteiches*, we suspected that neo-functionalization occurs after tandem duplication of the secreted cysteine protease family, due to the presence at the C-terminal part of the enzymes of various additional domain associated either to carbohydrate-binding capacity (CBM1, PAN/Apple) or to sterol/lipid affinity (ML, CAP).

The whole pathogen's transcriptome analysis of *M. truncatula* roots infected by *A. euteiches*, revealed induction of serine (trypsin, subtilisin), PLCP and zinc carboxypeptidases (M14) during infection. Most of the serine proteases and PLCP showed induced expression from the first day of infection, with an increase in the number of induced genes in 3 and 9 dpi, suggesting their key role in plant invasion. The differential pattern of expression is likely related to the hemibiotrophic life style of the pathogen. From one day to six

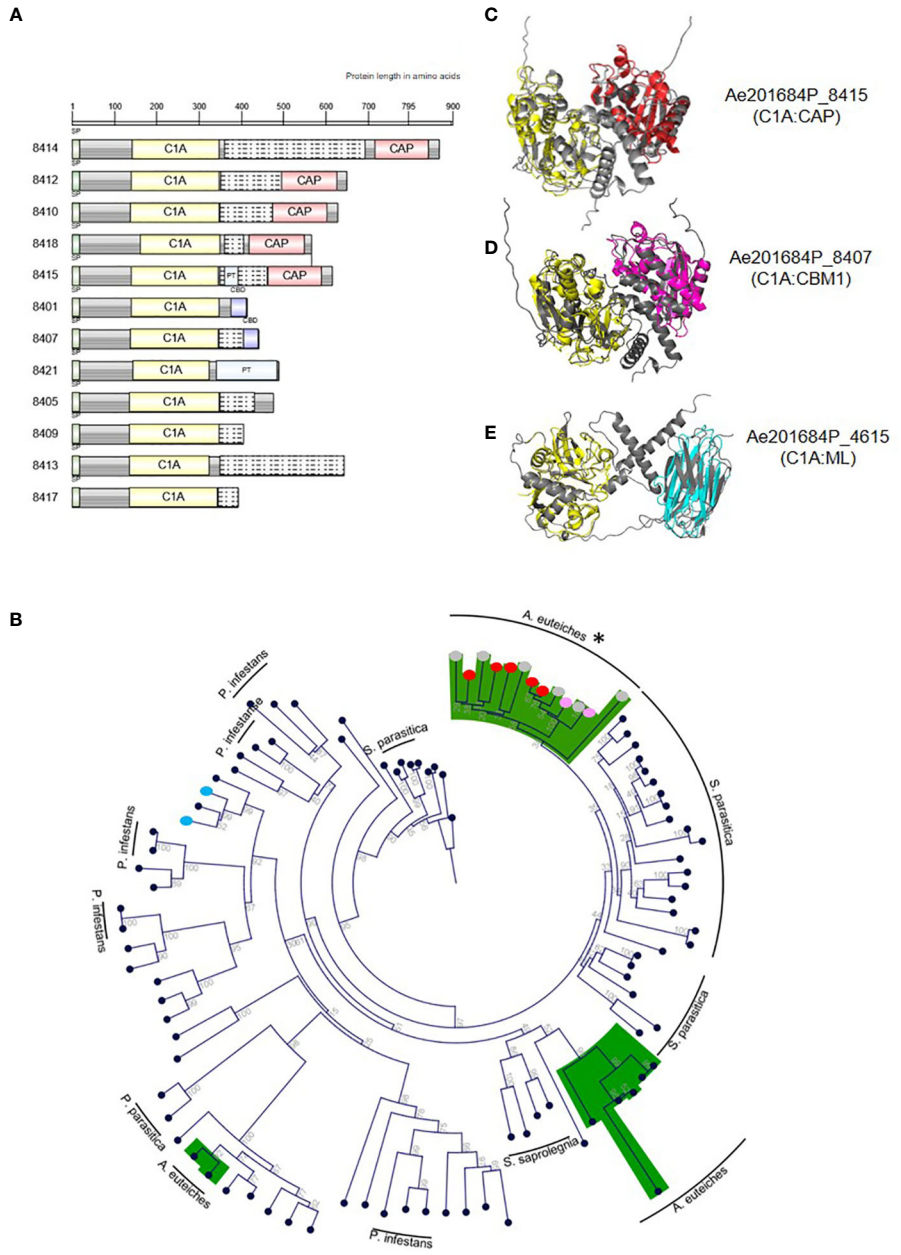

FIGURE 4
Modular papain-like cysteine proteases (PLCP) from *A. euteiches* identified in pea apoplastic fluids. **(A)** Protein domain architecture of the clustered PCLPs from *A. euteiches*. C1A: cysteine protease domain type C1A (PF00112); CBD: carbohydrate-binding module CBM1 (PF00734), CAP: Cysteine-rich secretory protein (PF00188), PT: PT-repeat (PF04886). Grey boxes: no domain predicted, Grey boxes with dashed lines: disorder region predicted by InterProScan. Scale = amino acids. **(B)** Phylogenetic tree constructed using the predicted C1A domain (PF00112) present in PLCPs from the plant pathogen *Phytophthora infestans*, the animal pathogen *Saprolegnia parasitica* and *A. euteiches*. Green color indicates the main group for *A. euteiches*. Asterik identified the clustered extracellular PCLPs of the pathogen. Colored dots indicated the associated domain of multidomain PLCPs of *A. euteiches* (red: CAP; pink: CBD; blue: ML-domain; grey: no domain). Neighbor-Joining method was used and boostrap are indicated **(C-E)**. PyMol representation of selected *A. euteiches* modular C1A cysteine proteases (grey). 3D structures superposition with a reference domain (colored) was performed, **(C)** Ae201684P_8415, cysteine protease C1A (PDB 1BP4, yellow), CAP domain (PDB 1SMB, red). RMSD scores: C1A domains = 0.877, CAP-domains = 1.077; **(D)** Ae201684P_8407, cysteine protease C1A (PDB 1BP4, yellow), CBM1 domain (PDB 5X34, magenta). RMSD scores: C1A domains 0.787, CBM1-domains = 0.937; **(E)** Ae201684P_4615, cysteine protease C1A (PDB 1BP4, yellow), ML-domain (PDB 1AHM, cyan). RMSD scores: C1A domains 0.674, ML-domains = 4.475. Structural predictions were performed using AlphaFold2.

day after infection the pathogen colonized almost all the cortex root tissues of *M. truncatula*, before invading the stele and vascular tissues in fifteen days, causing root rot symptoms (Djébali et al., 2009). Thus, before turning necrotrophic, extracellular peptidases of *A. euteiches* can contribute to the degradation of host proteins located into the apoplast or structural proteins from the plant cell wall. At later stage of the infection, secreted proteases may counteract apoplastic immunity through degrading host-derived defense proteins, be directly toxic for the root tissues or have a role for nutrient acquisition by digesting host tissues.

Several studies on plant-microbe interactions (van der Hoorn et al., 2004; Meijer et al., 2014) have reported the presence of plant proteases within infected tissues, and only few microbial proteases have been functionally characterized. The developed ABPP-MS assay on apoplastic fluid from pea roots infected by *A. euteiches* using probes that target serine (FP) and cysteine (DCG04) proteases, allows the identification of 35 *A. euteiches* extracellular active proteases. This set of active enzymes covers ~30% of total number of expressed genes during *M. truncatula* infection, demonstrating the efficiency of ABBP-MS assay to identify putative pathogenicity factors. The remarkable signature of the identified proteases in the apoplastic fluid of infected-pea roots, correspond to multidomain proteases with an additional 'binding domain' having affinity for carbohydrates or lipids/sterols. Eukaryotic proteases are rarely associated with a non-catalytic domain, but *A. euteiches* produces several different combinations of extracellular multidomain proteases: serine proteases with PAN/Apple domain and cysteine proteases with CBM1, ML, CAP domains. Some domain combinations, like C1A:CBM1 and C1A:CAP, are only detected in the genus *Aphanomyces*. In addition, twelve of C1A-multidomain proteases identified by MS are organized in one cluster within the genome of *A. euteiches*. The members of the cluster are found in one phylogenetic group divided in two classes with single or multidomain PCLPs, suggesting independent acquisition of the additional 'binding' domain. The other PLCPs of *A. euteiches* are identified in two main groups related to the fish pathogenic oomycete *S. parasitica*, except the C1A:ML multidomain proteases which are more closely related to single domain proteases of the plant pathogen *P. infestans*. Structural prediction of the modular C1A proteases of *A. euteiches* indicates that the additional domain does not form a lid structure or an occluding loop that can cover the active site, suggesting the evolution of specialized functions for these PLCPs. Inappropriate activity of proteases can be deleterious to the cell or the organism that produces them, thus, proteases activity is regulated to allow proteolysis event only in an adapted environment or cellular compartment (for review see Kopitar-Jerala, 2012). Here we suggest that the non-catalytic protease-associated domain found in *A. euteiches* corresponds to regions responsible for regulation or targeting of the enzymes.

To conclude, the ABPP-MS approach allows the characterization of original active extracellular multidomain apoplastic proteases from a soil-borne oomycete that could play a key role in root infection. This system can be easily translated to other pathosystems and will facilitate addressing the global challenge in the selection of microbial candidate genes for functional analysis.

Data availability statement

The datasets presented in this study can be found in online repositories. The names of the repository/repositories and accession number(s) can be found in the article/Supplementary Material.

Author contributions

AK, EG, RH planned and designed the experiments. AK, LC, LOC performed the experiments. FK, MK performed proteomics analysis. AK, EG analysed the data. AK, EG wrote the manuscript with help of all authors. All authors contributed to the article and approved the submitted version.

Funding

This research was funded by the European Union's Horizon 2020 research program under grant no. 766048 (MSCA-ITN-2017 PROTECTA).

Conflict of interest

The authors declare that the research was conducted in the absence of any commercial or financial relationships that could be construed as a potential conflict of interest.

Publisher's note

Supplementary material

The Supplementary Material for this article can be found online at: https://www.frontiersin.org/articles/10.3389/fpls.2023.1140101/full#supplementary-material

SUPPLEMENTARY FIGURE 1
Semi-sterile *in vitro* system for ABPP-MS assay between *Pisum sativum cv Précovil* and *A. euteiches*. Roots of infected (left) and non-infected pea (right) at 15 days post infection with 10^5 zoospores of *A. euteiches*. Plants were maintained at 21°C in a semi-sterile condition in pots filled with zeolite as a solid substrate and Fåhraeus media as the nutritive solution under 18h/6h-light/dark alternance. The black arrow points to root rot symptoms; scale bar = 1 cm. The cross sections of primary roots were stained with Wheat Germ Agglutinin-Alex Fluor 555 conjugate to detect *A. euteiches* hyphae (green). UV fluorescence reveals phenolic compounds (blue) and pericycle cells reinforcement (red arrow) in infected roots. Note that the pathogen is restricted to the root cortex as previously reported upon infection of a tolerant line of the model legume *Medicago truncatula* (i.e., Jemalong A17) by the same strain of *A. euteiches* (Djébali et al., 2009). Scale bar = 100 µm.

References

Almagro Armenteros, J. J., Tsirigos, K. D., Sønderby, C. K., Petersen, T. N., Winther, O., Brunak, S., et al. (2019). SignalP 5.0 improves signal peptide predictions using deep neural networks. *Nat. Biotechnol.* 37, 420–423. doi: 10.1038/s41587-019-0036-z

Anders, S., Pyl, P. T., and Huber, W. (2015). HTSeq–a Python framework to work with high-throughput sequencing data. *Bioinformatics* 31, 166–169. doi: 10.1093/bioinformatics/btu638

Basenko, E., Pulman, J., Shanmugasundram, A., Harb, O., Crouch, K., Starns, D., et al. (2018). FungiDB: An integrated bioinformatic resource for fungi and oomycetes. *JoF* 4, 39. doi: 10.3390/jof4010039

Becking, T., Kiselev, A., Rossi, V., Street-Jones, D., Grandjean, F., and Gaulin, E. (2021). Pathogenicity of animal and plant parasitic *Aphanomyces* spp and their economic impact on aquaculture and agriculture. *Fungal Biol. Rev* 40, 1–18. doi: 10.1016/j.fbr.2021.08.001

Camborde, L., Kiselev, A., Pel, J. M. C., Le Ru, A., Jauneau, A., Pouzet, C., et al. (2022). An oomycete effector targets a plant RNA helicase involved in root development. *New Phytol.* 233, 2232–2248. doi: 10.1111/nph.17918

Cox, J., Hein, M. Y., Luber, C. A., Paron, I., Nagaraj, N., and Mann, M. (2014). Accurate proteome-wide label-free quantification by delayed normalization and maximal peptide ratio extraction, termed MaxLFQ. *Mol. Cell. Proteomics* 13, 2513–2526. doi: 10.1074/mcp.M113.031591

Cox, J., and Mann, M. (2008). MaxQuant enables high peptide identification rates, individualized p.p.b.-range mass accuracies and proteome-wide protein quantification. *Nat. Biotechnol.* 26, 1367–1372. doi: 10.1038/nbt.1511

Cox, J., Neuhauser, N., Michalski, A., Scheltema, R. A., Olsen, J. V., and Mann, M. (2011). Andromeda: A peptide search engine integrated into the MaxQuant environment. *J. Proteome Res.* 10, 1794–1805. doi: 10.1021/pr101065j

Dean, R., Van Kan, J. A. L., Pretorius, Z. A., Hammond-Kosack, K. E., Di Pietro, A., Spanu, P. D., et al. (2012). The top 10 fungal pathogens in molecular plant pathology: Top 10 fungal pathogens. *Mol. Plant Pathol.* 13, 414–430. doi: 10.1111/j.1364-3703.2011.00783.x

Djébali, N., Jauneau, A., Torregrosa, C., Chardon, F., Jaulneau, V., Mathé, C., et al. (2009). Partial resistance of *Medicago truncatula* to *Aphanomyces euteiches* is associated with protection of the root stele and is controlled by a major QTL rich in proteasome-related genes. *Mol. Plant-Microbe Interact.* 22, 1043–1055. doi: 10.1094/MPMI-22-9-1043

Dora, S., Terrett, O. M., and Sánchez-Rodríguez, C. (2022). Plant–microbe interactions in the apoplast: Communication at the plant cell wall. *Plant Cell* 34, 1532–1550. doi: 10.1093/plcell/koac040

Fåhraeus, G. (1957). The infection of clover root hairs by nodule bacteria studied by a simple glass slide technique. *Microbiology* 16, 374–381. doi: 10.1099/00221287-16-2-374

Farvardin, A., González-Hernández, A. I., Llorens, E., García-Agustín, P., Scalschi, L., and Vicedo, B. (2020). The apoplast: A key player in plant survival. *Antioxidants* 9, 604. doi: 10.3390/antiox9070604

Fitzpatrick, D. A., O'Gaora, P., Byrne, K. P., and Butler, G. (2010). Analysis of gene evolution and metabolic pathways using the *Candida* gene order browser. *BMC Genomics* 11, 290. doi: 10.1186/1471-2164-11-290

Gaulin, E., Dramé, N., Lafitte, C., Torto-Alalibo, T., Martinez, Y., Ameline-Torregrosa, C., et al. (2006). Cellulose binding domains of a *Phytophthora* cell wall protein are novel pathogen-associated molecular patterns. *Plant Cell* 18, 1766–1777. doi: 10.1105/tpc.105.038687

Gaulin, E., Pel, M. J. C., Camborde, L., San-Clemente, H., Courbier, S., Dupouy, M.-A., et al. (2018). Genomics analysis of aphanomyces spp. identifies a new class of oomycete effector associated with host adaptation. *BMC Biol.* 16, 43. doi: 10.1186/s12915-018-0508-5

Guevara, M. G., Almeida, C., Mendieta, J. R., Faro, C. J., Veríssimo, P., Pires, E. V., et al. (2005). Molecular cloning of a potato leaf cDNA encoding an aspartic protease (StAsp) and its expression after *P. infestans* infection. *Plant Physiol. Biochem.* 43, 882–889. doi: 10.1016/j.plaphy.2005.07.004

Haas, B. J., Kamoun, S., Zody, M. C., Jiang, R. H., Handsaker, R. E., Cano, L. M., et al. (2009). Genome sequence and analysis of the Irish potato famine pathogen *Phytophthora infestans*. *Nature* 461, 393–398. doi: 10.1038/nature08358

Inohara, N., and Nuñez, G. (2002). ML — a conserved domain involved in innate immunity and lipid metabolism. *Trends Biochem. Sci.* 27, 219–221. doi: 10.1016/S0968-0004(02)02084-4

Jashni, M. K., Dols, I. H. M., Iida, Y., Boeren, S., Beenen, H. G., Mehrabi, R., et al. (2015). Synergistic action of a metalloprotease and a serine protease from *Fusarium oxysporum* f. sp. *lycopersici* cleaves chitin-binding tomato chitinases, reduces their antifungal activity, and enhances fungal virulence. *MPMI* 28, 996–1008. doi: 10.1094/MPMI-04-15-0074-R

Jumper, J., Evans, R., Pritzel, A., Green, T., Figurnov, M., Ronneberger, O., et al. (2021). Highly accurate protein structure prediction with AlphaFold. *Nature* 596, 583–589. doi: 10.1038/s41586-021-03819-2

Kaschani, F., Gu, C., Niessen, S., Hoover, H., Cravatt, B. F., and van der Hoorn, R. A. L. (2009). Diversity of serine hydrolase activities of unchallenged and *Botrytis*-infected *Arabidopsis thaliana*. *Mol. Cell. Proteomics* 8, 1082–1093. doi: 10.1074/mcp.M800494-MCP200

Kaschani, F., Shabab, M., Bozkurt, T., Shindo, T., Schornack, S., Gu, C., et al. (2010). An effector-targeted protease contributes to defense against *Phytophthora infestans* and is under diversifying selection in natural hosts. *Plant Physiol.* 154, 1794–1804. doi: 10.1104/pp.110.158030

Kim, D., Paggi, J. M., Park, C., Bennett, C., and Salzberg, S. L. (2019). Graph-based genome alignment and genotyping with HISAT2 and HISAT-genotype. *Nat. Biotechnol.* 37, 907–915. doi: 10.1038/s41587-019-0201-4

Kiselev, A., San Clemente, H., Camborde, L., Dumas, B., and Gaulin, E. (2022). A comprehensive assessment of the secretome responsible for host adaptation of the legume root pathogen *Aphanomyces euteiches*. *JoF* 8, 88. doi: 10.3390/jof8010088

Kopitar-Jerala, N. (2012). The role of cysteine proteinases and their inhibitors in the host-pathogen cross talk. *CPPS* 13, 767–775. doi: 10.2174/138920312804871102

Kreplak, J., Madoui, M.-A., Cápal, P., Novák, P., Labadie, K., Aubert, G., et al. (2019). A reference genome for pea provides insight into legume genome evolution. *Nat. Genet.* 51, 1411–1422. doi: 10.1038/s41588-019-0480-1

Krogh, A., Larsson, B., von Heijne, G., and Sonnhammer, E. L. L. (2001). Predicting transmembrane protein topology with a hidden markov model: application to complete genomes. edited by f. Cohen. *J. Mol. Biol.* 305, 567–580. doi: 10.1006/jmbi.2000.4315

Li, H., Handsaker, B., Wysoker, A., Fennell, T., Ruan, J., Homer, N., et al. (2009). The sequence alignment/map format and SAMtools. *Bioinformatics* 25, 2078–2079. doi: 10.1093/bioinformatics/btp352

Liang, D., Andersen, C. B., Vetukuri, R. R., Dou, D., and Grenville-Briggs, L. J. (2020). Horizontal gene transfer and tandem duplication shape the unique CAZyme complement of the mycoparasitic oomycetes *Pythium oligandrum* and *Pythium periplocum*. *Front. Microbiol.* 11. doi: 10.3389/fmicb.2020.581698

Love, M. I., Huber, W., and Anders, S. (2014). Moderated estimation of fold change and dispersion for RNA-seq data with DESeq2. *Genome Biol.* 15, 550. doi: 10.1186/s13059-014-0550-8

Madoui, M.-A., Gaulin, E., Mathé, C., San Clemente, H., Couloux, A., Wincker, P., et al. (2007). AphanoDB: A genomic resource for *Aphanomyces* pathogens. *BMC Genomics* 8, 471. doi: 10.1186/1471-2164-8-471

McGowan, J., Byrne, K. P., and Fitzpatrick, D. A. (2019). Comparative analysis of oomycete genome evolution using the oomycete gene order browser (OGOB). *Genome Biol. Evol.* 11, 189–206. doi: 10.1093/gbe/evy267

McGowan, J., O'Hanlon, R., Owens, R. A., and Fitzpatrick, D. A. (2020). Comparative genomic and proteomic analyses of three widespread *Phytophthora* species: *Phytophthora chlamydospora, phytophthora gonapodyides* and *Phytophthora pseudosyringae*. *Microorganisms* 8, 653. doi: 10.3390/microorganisms8050653

Meijer, H. J. G., Mancuso, F. M., Espadas, G., Seidl, M. F., Chiva, C., Govers, F., et al. (2014). Profiling the secretome and extracellular proteome of the potato late blight pathogen *Phytophthora infestans*. *Mol. Cell. Proteomics* 13, 2101–2113. doi: 10.1074/mcp.M113.035873

Morimoto, K., and van der Hoorn, R. A. L. (2016). The increasing impact of activity-based protein profiling in plant science. *Plant Cell Physiol.* 57, 446–461. doi: 10.1093/pcp/pcw003

Muszewska, A., Stepniewska-Dziubinska, M. M., Steczkiewicz, K., Pawlowska, J., Dziedzic, A., and Ginalski, K. (2017). Fungal lifestyle reflected in serine protease repertoire. *Sci. Rep.* 7, 9147. doi: 10.1038/s41598-017-09644-w

Olsen, J. V., de Godoy, L. M. F., Li, G., Macek, B., Mortensen, P., Pesch, R., et al. (2005). Parts per million mass accuracy on an orbitrap mass spectrometer *via* lock mass injection into a c-trap. *Mol. Cell. Proteomics* 4, 2010–2021. doi: 10.1074/mcp.T500030-MCP200

Papavizas, G. C., and Ayers, W. A. (1974). *Aphanomyces species and their root diseases in pea and sugarbeet: A review* (Technical Bulletins 158606, United States Department of Agriculture, Economic Research Service).

Paulus, J. K., Kourelis, J., Ramasubramanian, S., Homma, F., Godson, A., Hörger, A. C., et al. (2020). Extracellular proteolytic cascade in tomato activates immune protease Rcr3. *Proc. Natl. Acad. Sci. U. S. A.* 117, 17409–17417. doi: 10.1073/pnas.1921101117

Quillévéré-Hamard, A., Le Roy, G., Lesné, A., Le May, C., and Pilet-Nayel, M.-L. (2020). Aggressiveness of diverse French *Aphanomyces euteiches* isolates on pea near-Isogenic-Lines differing in resistance QTL. *Phytopathology* 111, 695–702. doi: 10.1094/PHYTO-04-20-0147-R

Quillévéré-Hamard, A., Le Roy, G., Moussart, A., Baranger, A., Andrivon, D., Pilet-Nayel, M.-L., et al. (2018). Genetic and pathogenicity diversity of *Aphanomyces euteiches* populations from pea-growing regions in France. *Front. Plant Sci.* 9. doi: 10.3389/fpls.2018.01673

Ramirez-Garcés, D., Camborde, L., Pel, M. J. C., Jauneau, A., Martinez, Y., Néant, I., et al. (2016). CRN13 candidate effectors from plant and animal eukaryotic pathogens are DNA-binding proteins which trigger host DNA damage response. *New Phytol.* 210, 602–617. doi: 10.1111/nph.13774

Rocafort, M., Fudal, I., and Mesarich, C. H. (2020). Apoplastic effector proteins of plant-associated fungi and oomycetes. *Curr. Opin. Plant Biol.* 56, 9–19. doi: 10.1016/j.pbi.2020.02.004

Schneiter, R., and Di Pietro, A. (2013). The CAP protein superfamily: Function in sterol export and fungal virulence. *BioMol. Concepts* 4, 519–525. doi: 10.1515/bmc-2013-0021

Schoina, C., Rodenburg, S. Y. A., Meijer, H. J. G., Seidl, M. F., Lacambra, L. T., Bouwmeester, K., et al. (2021). Mining oomycete proteomes for metalloproteases leads to identification of candidate virulence factors in *Phytophthora infestans*. *Mol. Plant Pathol.* 22, 551–563. doi: 10.1111/mpp.13043

Severino, V., Farina, A., Fleischmann, F., Dalio, R. J. D., Di Maro, A., Scognamiglio, M., et al. (2014). Molecular profiling of the *Phytophthora plurivora* secretome: a step towards understanding the cross-talk between plant pathogenic oomycetes and their hosts. *PloS One* 9, e112317. doi: 10.1371/journal.pone.0112317

Shabab, M., Shindo, T., Gu, C., Kaschani, F., Pansuriya, T., Chintha, R., et al. (2008). Fungal effector protein AVR2 targets diversifying defense-related cys proteases of tomato. *Plant Cell* 20, 1169–1183. doi: 10.1105/tpc.107.056325

Sharma, A., Rani, M., Lata, H., Thakur, A., Sharma, P., Kumar, P., et al. (2022). Global dimension of root rot complex in garden pea: Current status and breeding prospective. *Crop Prot.* 158, 106004. doi: 10.1016/j.cropro.2022.106004

Shindo, T., Kaschani, F., Yang, F., Kovács, J., Tian, F., Kourelis, J., et al. (2016). Screen of non-annotated small secreted proteins of *Pseudomonas syringae* reveals a virulence factor that inhibits tomato immune proteases. *PloS Pathog.* 7, e1005874. doi: 10.1371/journal.ppat.1005874

Song, J., Win, J., Tian, M., Schornack, S., Kaschani, F., Ilyas, M., et al. (2009). Apoplastic effectors secreted by two unrelated eukaryotic plant pathogens target the tomato defense protease Rcr3. *Proc. Natl. Acad. Sci. U. S. A.* 106, 1654–1659. doi: 10.1073/pnas.0809201106

Sperschneider, J., Dodds, P. N., Gardiner, D. M., Manners, J. M., Singh, K. B., and Taylor, J. M. (2015). Advances and challenges in computational prediction of effectors from plant pathogenic fungi. *PLoS Pathog.* 11:e1004806. doi: 10.1371/journal.ppat.1004806

Tian, M., Benedetti, B., and Kamoun, S. (2005). A second kazal-like protease inhibitor from *Phytophthora infestans* inhibits and interacts with the apoplastic pathogenesis-related protease P69B of tomato. *Plant Physiol.* 138, 1785–1793. doi: 10.1104/pp.105.061226

Tian, M., Huitema, E., da Cunha, L., Torto-Alalibo, T., and Kamoun, S. (2004). A kazal-like extracellular serine protease inhibitor from *Phytophthora infestans* targets the tomato pathogenesis-related protease P69B. *J. Biol. Chem.* 279, 26370–26377. doi: 10.1074/jbc.M400941200

Tian, M., Win, J., Song, J., van der Hoorn, R. A. L., van der Knaap, E., and Kamoun, S. (2007). A *Phytophthora infestans* cystatin-like protein targets a novel tomato papain-like apoplastic protease. *Plant Physiol.* 143, 364–377. doi: 10.1104/pp.106.090050

Tordai, H., Bányai, L., and Patthy, L. (1999). The PAN module: the n-terminal domains of plasminogen and hepatocyte growth factor are homologous with the apple domains of the prekallikrein family and with a novel domain found in numerous nematode proteins. *FEBS Lett.* 461, 63–67. doi: 10.1016/S0014-5793(99)01416-7

Tyanova, S., Temu, T., Sinitcyn, P., Carlson, A., Hein, M. Y., Geiger, T., et al. (2016). The Perseus computational platform for comprehensive analysis of (prote)omics data. *Nat. Methods* 13, 731–740. doi: 10.1038/nmeth.3901

van der Hoorn, R. A. L. (2011). Mining the active proteome of. *Arabidopsis thaliana Front. Plant Sci.* 2. doi: 10.3389/fpls.2011.00089

van der Hoorn, R. A. L., Leeuwenburgh, M. A., Bogyo, M., Joosten, M. H. A. J., and Peck, S. C. (2004). Activity profiling of papain-like cysteine proteases in plants. *Plant Physiol.* 135, 1170–1178. doi: 10.1104/pp.104.041467

Vizcaíno, J. A., Csordas, A., del-Toro, N., Dianes, J. A., Griss, J., Lavidas, I., et al. (2016). 2016 update of the PRIDE database and its related tools. *Nucleic Acids Res.* 44, D447–D456. doi: 10.1093/nar/gkv1145

Watson, A., Browne, S. L., Snudden, M. G., and Mudford, E. M. (2013). *Aphanomyces* root rot of beans and control options. *Australas. Plant Pathol.* 42, 321–327. doi: 10.1007/s13313-012-0180-0

Wu, L., Chang, K.-F., Conner, R. L., Strelkov, S., Fredua-Agyeman, R., Hwang, S.-F., et al. (2018). *Aphanomyces euteiches*: A threat to Canadian field pea production. *Engineering* 4, 542–551. doi: 10.1016/j.eng.2018.07.006

Zhang, Q., Li, W., Yang, J., Xu, J., Meng, Y., and Shan, W. (2020). Two *Phytophthora parasitica* cysteine protease genes, *PpCys44* and *PpCys45*, trigger cell death in various *Nicotiana* spp. and act as virulence factors. *Mol. Plant Pathol.* 21, 541–554. doi: 10.1111/mpp.12915

frontiers | Frontiers in Plant Science

TYPE Original Research
PUBLISHED 14 April 2023
DOI 10.3389/fpls.2023.1125551

OPEN ACCESS

EDITED BY
Marie-Laure Pilet-Nayel,
INRAE Bretagne Normandie, France

REVIEWED BY
Pascal Ratet,
UMR9213 Institut des Sciences des Plantes de Paris Saclay (IPS2), France
Béatrice Teulat,
Institut Agro Rennes-Angers, France

*CORRESPONDENCE
Martina Rickauer
martina.rickauer@toulouse-inp.fr

SPECIALTY SECTION
This article was submitted to Plant Pathogen Interactions, a section of the journal Frontiers in Plant Science

RECEIVED 16 December 2022
ACCEPTED 20 March 2023
PUBLISHED 14 April 2023

CITATION
Fartash AH, Ben C, Mazurier M, Ebrahimi A, Ghalandar M, Gentzbittel L and Rickauer M (2023) *Medicago truncatula* quantitative resistance to a new strain of *Verticillium alfalfae* from Iran revealed by a genome-wide association study.
Front. Plant Sci. 14:1125551.
doi: 10.3389/fpls.2023.1125551

Medicago truncatula quantitative resistance to a new strain of *Verticillium alfalfae* from Iran revealed by a genome-wide association study

Amir Hossein Fartash[1], Cécile Ben[1,2], Mélanie Mazurier[1], Asa Ebrahimi[3], Mojtaba Ghalandar[4], Laurent Gentzbittel[1,2] and Martina Rickauer[1]*

[1]Laboratoire écologie fonctionnelle et environnement, Université de Toulouse, Centre National de Recherche Scientifique, Toulouse Institut National Polytechnique, Université Toulouse 3 – Paul Sabatier (UPS), Toulouse, France, [2]Project Center for Agro Technologies, Skolkovo Institute of Science and Technology, Moscow, Russia, [3]Department of Plant Breeding and Biotechnology, Science and Research Branch, Islamic Azad University, Tehran, Iran, [4]Plant Protection Department, Markazi Agricultural and Natural Resources Research and Education Center, Arak, Iran

Verticillium wilt is a major threat to many crops, among them alfalfa (*Medicago sativa*). The model plant *Medicago truncatula*, a close relative of alfalfa was used to study the genetic control of resistance towards a new *Verticillium alfalfae* isolate. The accidental introduction of pathogen strains through global trade is a threat to crop production and such new strains might also be better adapted to global warming. Isolates of *V. alfalfae* were obtained from alfalfa fields in Iran and characterized. The Iranian isolate AF1 was used in a genome-wide association study (GWAS) involving 242 accessions from the Mediterranean region. Root inoculations were performed with conidia at 25°C and symptoms were scored regularly. Maximum Symptom Score and Area under Disease Progess Curve were computed as phenotypic traits to be used in GWAS and for comparison to a previous study with French isolate V31.2 at 20°C. This comparison showed high correlation with a shift to higher susceptibility, and similar geographical distribution of resistant and susceptible accessions to AF1 at 25°C, with resistant accessions mainly in the western part. GWAS revealed 30 significant SNPs linked to resistance towards isolate AF1. None of them were common to the previous study with isolate V31.2 at 20°C. To confirm these *loci*, the expression of nine underlying genes was studied. All genes were induced in roots following inoculation, in susceptible and resistant plants. However, in resistant plants induction was higher and lasted longer. Taken together, the use of a new pathogen strain and a shift in temperature revealed a completely different genetic control compared to a previous study that demonstrated the existence of two major QTLs. These results can be useful for *Medicago* breeding programs to obtain varieties better adapted to future conditions.

KEYWORDS

alfalfa, biotic stress, fungal pathogen, gene expression, global warming, legume, vascular wilt, quantitative disease resistance

1 Introduction

Plants are continuously in contact with a myriad of microorganisms of which some are pathogenic. However, thanks to their innate immunity system, disease is rather the exception than the rule, at least in undisturbed environments. Disease resistance in plants has been described as qualitative (complete, gene-for-gene) disease resistance (Flor, 1971) and quantitative (partial) disease resistance (QDR) (Poland et al., 2009). Qualitative resistance which is governed by a single gene can be neutralized easily by the evolution of new pathogen strains (Flor, 1971; Poland et al., 2009). QDR which is controlled by the contribution of multiple genes of (usually) small effect and their cumulative actions is characterized by a continuous phenotypic variation among populations, from total resistance to high susceptibility (Poland et al., 2009) and varies with environmental conditions (Bartoli and Roux, 2017). Due to the polygenic heredity QDR is more durable (Roumen, 1994).

Plants' defense mechanisms and pathogens' pathogenicity have undergone a series of adaptive changes during co-evolution. When a pathogen overcomes preformed defense structures, the plant's innate immune system is activated by recognition of conserved pathogen-associated molecular patterns (PAMPs) also named microbe-associated molecular patterns (MAMPs) (Ausubel, 2005) or damage-associated molecular patterns (DAMPs) through pattern recognition receptors (PRRs) (Bigeard et al., 2015; Miller et al., 2017). The detection of MAMPs/PAMPs and DAMPs triggers an array of defense responses known as pathogen-triggered immunity, PAMP-triggered immunity (PTI), or MAMP-triggered immunity (MTI) (Bigeard, Colcombet and Hirt, 2015). PTI/MTI involves the production of antimicrobial compounds and pathogenesis-related (PR) proteins in the plant (Bigeard et al., 2015; Miller et al., 2017; Kamle et al., 2020).

As adaptive response pathogens evolved to produce and release effectors into the host plant cells which suppress PTI/MTI. The plants' response was to adapt their immune system by recruiting a second layer of defense that directly or indirectly detects pathogen effectors through plant resistance (R) proteins leading to Effector-Triggered Immunity (ETI) (Zipfel, 2014; Miller et al., 2017; Kamle et al., 2020).

Recognition of the pathogen through perception of PAMPs/MAMPs, in the case of PTI/MTI or effectors, in the case of ETI, is followed by cascades of signaling pathways such as ion fluxes and phosphorylation of proteins (Shen et al., 2017) leading finally to defense mechanisms such as strengthening of cell walls (Vogel and Somerville, 2000; Zhang et al., 2022), production of reactive oxygen species (ROS), pathogenesis related proteins (PRs) and phytoalexins (Wojtaszek, 1997; Okada et al., 2015; Rout et al., 2016), either locally or systemically.

This fragile balance between plants resistance and pathogens' virulence is more and more threatened by anthropogenic factors such as global trade. The exchange of seeds and plants worldwide has led to the spread of pathogens in areas where they were absent before and to which local plants may not have evolved resistance mechanisms.

Verticillium wilt is a vascular disease caused by the soil-borne fungus *Verticillium* spp. This disease is one of the most destructive fungal diseases in the world and affects more than 200 different hosts, among them many economically important crops (Klosterman et al., 2011). It is found mainly in temperate regions, but can also occur in hotter climates (Erwin and Howell, 1998; Klosterman et al., 2011). The fungus enters the roots of its host plants through natural cracks or wounds and colonizes the xylem vessels which leads to their plugging through the production of gels in susceptible hosts (Cooper and Wood, 1980; Fradin and Thomma, 2006; Inderbitzin et al., 2014). Visible symptoms are yellowing, wilting and finally death of the plant. *Verticillium* species are able to survive in the soil for many years (Pegg and Brady, 2002; Agrios, 2005) through the production of thick-walled pigmented resting structures. This feature greatly reduces the possibilities of disease management (Inderbitzin et al., 2011). The best strategy so far is breeding of resistant crop varieties.

Verticillium dahliae is the most important and best studied *Verticillium* species due to the high number of its host plants and the economic impact of the disease (Klosterman et al., 2011; Inderbitzin and Subbarao, 2014). *V. alfalfae* which has a narrower host range and is most aggressive on alfalfa is a major threat to this important forage crop worldwide (Acharya and Huang, 2003; Graham and Vance, 2003). The tetraploid and outcrossing nature of alfalfa makes genetic studies of disease resistance difficult, but synteny and sequence homologies with model plants such as *Medicago truncatula* can be of great help.

Medicago truncatula, a diploid autogamous wild plant and close relative of alfalfa, has been established as a model plant for legume crops (Cook, 1999). It is native to the Mediterranean region, presents high biodiversity, and many genomic and genetic resources are available (Ellwood et al., 2006; Gentzbittel et al., 2015). It is a host to *V. alfalfae* and quantitative resistance to this fungus relying on several QTLs has been reported (Ben et al., 2013). Resistant plants were shown to stop fungal colonization of their roots at early stages, and exhibited transcriptional responses related to innate immunity (Toueni et al., 2016). Based on the interaction between *M. truncatula* and *V. alfalfae* our group has studied the link between genome admixture and resistance to this pathogen, using geographical origin of plant accessions as covariates (Gentzbittel et al., 2019).

This study revealed that resistant accessions were mostly found in populations from the western part of the Mediterranean basin, with a gradient of susceptibility to resistance from east to west. This led to the hypothesis that host plant and pathogen strain may have co-evolved, and that an isolate from the east might reveal a different pattern of the plant's genetic control of resistance.

To test this hypothesis a new *Verticillium alfalfae* isolate was obtained from Iran, the far eastern part of the plant's natural habitat. Inoculations were performed at 25°C, in agreement with the pathogen's optimum temperature for sporulation and growth, and the geographical distribution of resistance and susceptibility was plotted.

Loci involved in the plant's response were identified by a genome-wide association study (GWAS) taking advantage of the

international MtHapMap project (Tang et al., 2014) which provides genomics data on a large number of accessions.

Results were compared to those obtained in a previous GWAS study, with a French *V. alfalfae* isolate and at 20°C. A high correlation between the two studies was observed concerning the geographical distribution of resistant and susceptible accessions. However no common *loci* associated to resistance were detected by SNPs. The expression study of some genes underlying the *loci* showed that they were all expressed in roots and induced by inoculation with *V. alfalfae*.

2 Material and methods

2.1 Fungal isolates

2.1.1 Isolation of fungal strains and selection of *Verticillium alfalfae*

Symptomatic alfalfa plants were collected from six different regions in Iran (Figure 1) and dried between paper for conservation. Their stems were cut into 2 cm long fragments above the first node and after surface sterilization (15 sec in 70% ethanol and 6 minutes in 0.96% commercial bleach), the fragments were incubated on PDA containing 50 µg/ml streptomycin and incubated at 25°C (Mazurier, 2018). After 3 days, outgrowing mycelium was subcultured on fresh PDA, and purified by further subculturing. Monospore cultures were prepared when isolates were pure by visual assessment. The isolates were cultured on water agar at 25°C for observation of conidiophores under the microscope. Samples exhibiting the characteristic verticillate form of conidiophores were considered as *Verticillium* sp. and were retained for further identification steps.

FIGURE 1
Map of Iran showing provinces where alfalfa plants with wilting symptoms were collected for fungus isolation. The green stars show the provinces where fungal isolates were confirmed by PCR to be *V. alfalfae*, the red stars show provinces where the fungal isolates were not confirmed as *V. alfalfae*. Map adapted from Pešić et al. (2014).

2.1.2 Molecular identification of fungal isolates

The fungal isolates were grown in Potato Dextrose Broth (PDB) for 2 weeks and the mycelium was harvested by filtration and stored at −20°C.

DNA was extracted from frozen mycelium using the CTAB protocol (Carter-House et al., 2020). The quantity and quality of DNA was assessed with a nanodrop (NanoDrop nd-1000 Spectrophotometer).

Molecular identification was performed by PCR using the species-specific primers AlfF/AlfD1r (for *V. alfalfae*) and NoF/NoNuR (for *V. nonalfalfae*) (Inderbitzin et al., 2013). The ITS universal fungal primers (White et al., 1990) were used as a quality control (Supplementary Table 1). The PCR reaction mix contained: 1X PCR buffer, 2 mM MgCl2, 25 µM dNTPs, 1 µM each primer, 1.4 U Taq polymerase. Amplification was performed in 30 reaction cycles (1 min at 94°C, 1 min at 50°C for ITS primers, 62°C for AlfF/AlfD1r and 65°C for NoF/NoNuR primers, and 2 min at 72°C) after denaturation for 10 min at 94°C, and was followed by extension for 10 min at 72°C. Amplicons were electrophoresed on a 1% and 1.5% agarose gel containing Ethidium bromide, for amplification with ITS1-ITS4 and species-specific primers respectively. DNA bands were visualized through the Quantum st5 gel documentation system.

2.1.3 Analysis of *Verticillium alfalfae* growth and sporulation

Small disks (0.8 cm) of mycelium were punched from the border of 2-week-old cultures and inoculated in the center of Petri dishes containing 15 ml PDA. The diameter of the colony was measured at regular intervals for 2 weeks at 20°C, 25°C, and 28°C in the dark.

After 14 days, 20 mL of sterile water was added to every culture and the surface of the mycelium was rubbed gently with a bent Pasteur pipette to release the conidia. The conidia were collected and their concentration was determined under the microscope with a Malassez counting chamber.

The study was performed in three independent experiments including two independent blocks through augmented split-plot design where the whole-plot factor was assigned to temperature (three separate incubators) and split-plot factor was assigned to the fungal strains. In each experiment three Petri dishes were used per strain per condition.

The linear mixed model was used to analyze the effect of temperature on hyphal growth and sporulation as follows:

$$\mathbf{Y} = \mathbf{Xb} + \mathbf{Zu} + \mathbf{e} \qquad \text{(Equ. 1)}$$

where Y is the response vector (observed values of hyphal growth or spore production) X is the N x p design matrix for the p fixed factor including the grand mean of the trait (hyphal growth or spore production), temperatures and the different strains, and Z represents N x q_j design matrix for the q random effects of experiments (defined as the combination of blocks within repeats, repeats and temperature).

An analysis of variance (ANOVA) was performed using the lmer function of the lmerTest package (Kuznetsova et al., 2017) of the R 4.1.0 statistical software (R Core Team, 2020) to determine

variability for growth and sporulation among the *V. alfalfae* isolates. The least square means (LSmeans) (Lenth, 2013) for each strain were computed and the mean comparison grouping was performed by the Tukey method.

2.2 Plant material and genome-wide association mapping

2.2.1 Plant growth, inoculation and phenotyping

The MtHapMap collection was multiplied in our greenhouse in 2014 for a GWAS study at 20°C (Mazurier, 2018). A set of 242 *Medicago truncatula* accessions was selected based on the number of available seeds (Supplementary Table 2) for the present study.

They were scarified manually with sandpaper and incubated at 5°C in Petri dishes between layers of moist filter paper for 2–3 days, then were transferred to room temperature for 24h. Germinated seeds were transplanted into Jiffy substrate (jiffy®-7 diameter 33cm) and seedlings were grown in a phytotron with 25°C day/23°C night and a photoperiod of 16h.

Ten-day-old seedlings were subjected to root inoculation with conidia of isolate AF1 at a concentration of 10^6 spores/ml and symptom development was scored regularly on a scale from 0 to 4, as described by Ben et al. (2013) during 4 weeks under the same conditions as for growing.

Disease intensity and progress were evaluated through Maximum Symptom Scores (MSS, the score on the last day of symptom scoring) and Area Under the Disease Progress Curves (AUDPC) respectively.

In total, 8,442 inoculated plants were assessed through an augmented block design with three independent experiments for all 242 accessions; 4 accessions (F83005.5, DZA315.16, DZA45.5, and A17) were included in each block as check lines to evaluate the block effects. Each experiment contained 6–12 plants per accession, while the check accessions were consistently six plants per block.

2.2.2 Data analysis

For data analysis the Mixed Linear Model (MLM) approach was applied. Estimated breeding values corresponding to the traits (AUDPC and MSS) were calculated as BLUEs (Best Linear Unbiased Estimation) through the following mixed linear model:

$$\mathbf{Y} = \mathbf{Xb} + \mathbf{Zu} + \mathbf{e} \qquad \text{(Equ. 2)}$$

The BLUEs were extracted from the model to be used for genome-wide association mapping.

Data transformation was deployed whenever it was needed to homogenize variances and normalize residuals of the ANOVAs.

Multiple mean comparisons were performed using Tukey (pairwise comparisons) tests at p-value ≤ 0.05 using the cld function of the multcomp R package to group the accessions with regard to their response to inoculation with the selected Iranian *V. alfalfae* isolate.

The broad sense heritability (H^2) was calculated through the variance components method on raw phenotypic data while the blocks and repeats were regarded as fixed effects and the accession regarded as random effect.

For comparison of the results of the current study with a previous one performed with the French *V. alfalfae* strain V31.2 at 20°C, the extracted BLUE values from the adjusted mean values of MSS were used, and the correlation among them was calculated.

2.2.3 Genome-wide association mapping

To fine map the genomic regions of *M. truncatula* with additive effects associated with AUDPC and MSS, TASSEL 5.2.50 was used (Bradbury et al., 2007). Single Nucleotide Polymorphism (SNP) data were obtained from the *Medicago truncatula* HapMap project (http://www.medicagohapmap.org/) and were filtered with a minimum allele frequency (MAF) of 5% and minimum count to 200, which resulted in 5,671,743 SNPs retained.

A total of five GWAS statistical models were tested including General Linear Model (GLM) without any correction for population structure (naive model), GLM Q-Model with Q-matrix as correction for population structure and three Mixed Linear Models (K model, Q model and K + Q model) with K-matrix and/or Q-matrix respectively as correction for kinship relationships and population structure. The population structure (Q matrix) is based on population admixture proportions of *M. truncatula* individuals. The kinship matrix (K matrix) was computed from a 840K LD-pruned SNP dataset. Both matrices have been described earlier by Gentzbittel et al. (2019). To reduce computing time, the Population Parameter Previously Determined (P3D) algorithm (Zhang et al., 2010) was used to fit mixed linear models.

For all models, the Q-Q plot was plotted to evaluate which was the best fitted model for this study. Manhattan plots were computed to illustrate the association of SNPs with AUDPC and MSS.

For plotting the Manhattan graph the association score of SNPs was calculated through p-values of all SNPs as follows - log10 (p-values).

To correct for multiple testing, Bonferroni and False Discovery Rate (FDR) corrections were used. Multiple testing adjustment was conducted at $\alpha = 0.05$.

2.3 Gene expression studies

2.3.1 Selection of candidate genes and primer design

The suggestive line which was proposed by the qqman R package (D. Turner, 2018) was very close to the FDR, thus it was chosen as the main threshold for selecting the significant candidate SNPs. Hence, SNPs with association score values equal or greater than 5 were selected. Based on data on linkage disequilibrium and recombination rates described for *M. truncatula* in a previous study (Branca et al., 2011), the regions 10 kb upstream and downstream of these SNPs were explored on the JBrowser site (Buels et al., 2016). Genes with functional annotation associated to defense pathways which were located within these areas were favoured as possible candidate genes. In addition, two genes encoding hypothetical

proteins were included for further steps because of their high association score.

The full sequence of selected candidate genes was obtained from the MtHapMap site (http://www.medicagohapmap.org/fgb2/gbrowse/mt40/). Primers for quantitative real-time PCR (qRT-PCR) were designed using the primer3plus web interface for primer3 (Primer3Plus Version: 2.4.2, https://primer3plus.com/cgi-bin/dev/primer3plus.cgi). For each candidate gene, primer pairs were designed based on exon-exon junction and were examined for primer stability (https://www.ncbi.nlm.nih.gov/tools/primer-blast/) and specific amplification through blast on the *M. truncatula* A17 genome (http://www.medicagohapmap.org/tools/blastform; https://blast.ncbi.nlm.nih.gov/Blast.cgi?PROGRAM=blastn&PAGE_TYPE=BlastSearch&LINK_LOC=blasthome). The primer pairs for qRT-PCR were selected based on the results of primer efficiency tests with a mix of cDNA from all conditions and time points (Supplementary Table 3).

2.3.2 Inoculation of plants and quantitative real-time PCR

Gene expression studies were performed in three independent experiments. Twelve of the most susceptible and resistant accessions based on the Tukey's multiple comparison of BLUEs values of AUDPC were selected (Supplementary Table 4). Germinated seedlings were transferred to plug trays containing a mixture of sand-perlite (2/3 sand, 1/3 perlite), and grown for 10 days in a phytotron under the same conditions as described above.

Root inoculation and maintenance of the inoculated seedlings was performed under the same conditions as described for phenotyping before.

Roots and aerial parts of plants were harvested separately at 0, 4, 24 and 96 hours post inoculation (hpi) and pooled into a resistant and a susceptible group for each harvesting time. Total RNA was extracted using 200 mg of frozen root tissue samples following the TRIzol method (Invitrogen). After DNase I treatment (Promega) RNA quality was analyzed by NanoDrop nd-1000 Spectrophotometer and subsequently purified by the LiCl precipitation method (Cathala et al., 1983).

cDNA was synthesized from one microgram of pure RNA with the ImProm-II ™ Reverse Transcription System kit (Promega, A3800) using Oligo $(dT)_{15}$ primer following the manufacturer's instructions.

qRT-PCR was performed with the EurobioGreen® mix qPCR 2X Lo-Rox Kit (Eurobio Scientific, Reference GAEMMX02L-8T) in the QuantStudio™ 6 Flex Real-Time PCR System (Applied Biosystems). At least two technical replicates were run for all samples.

The reaction consisted of one step of 95°C for 3 min for cDNA denaturation, followed by 40 cycles of denaturation and annealing/polymerization (95°C/15sec, 60°C/30 sec). To assess the quality of qRT-PCR reactions the melting curve was implemented at the end of the reaction (95°C/15 sec, 60°C/15 sec, 95°C/15 sec). In order select the primers for gene expression studies we checked primer efficiency with a dilution series of an equimolar mix of cDNA from mock-inoculated and inoculated roots of the susceptible and resistant plants.

The C_T values were extracted through Design & Analysis software (V.2.4.3). Relative gene expression levels were analyzed by the comparative C_T method (Schmittgen and Livak, 2008). The Medtr2g008050 (Actin) and Medtr4g097170 (H3L) housekeeping genes were used for normalization. ΔC_T values were normalized against the harmonic mean of the two housekeeping genes.

3 Results

3.1 *Verticillium alfalfae* isolates from Iran differ from the French strain V31.2

In order to obtain *V. alfalfae* strains from a region east of the Mediterranean basin with higher temperatures than France, samples from alfalfa fields exhibiting typical wilting symptoms were collected during two field trips in Iran (Figure 1).

Putative *V. alfalfae* isolates were obtained from diseased alfalfa plants and after visual assessment sixteen were further analyzed by PCR with *V. alfalfae*-specific (AlfF/AlfD1r) and *V. nonalfalfae*-specific (NoF/NoNuR) primers. Amplification with AlfF/AlfD1r resulted in a band of the expected size of 1060 bp (Inderbitzin et al., 2013) for ten Iranian isolates and the French strain V31.2. No band was obtained with the negative controls *V. dahliae* strain JR2 and *V. non-alfalfae* strain LPP0323 (data not shown). Inversely, PCR with the *V. non-alfalfae* specific primers amplified only DNA from strain LPP0323 but not from Iranian isolates and the French strain V31.2 (data not shown).

In contrast to the French isolate, discoloration and formation of dark sections (black resting structures) were observed for the Iranian isolates and they occurred more frequently at 25°C than at 20°C.

To investigate vegetative and reproductive features of the Iranian isolates, hyphal growth and the amount of produced conidia were examined at three different temperatures (Figure 2).

Radial growth of seven Iranian *V. alfalfae* isolates and the French strain V31.2 on PDA medium showed similar behavior for all isolates with linear growth for up to two weeks. Growth was best at 25°C and very poor at 28°C (Supplementary Figure 1). Compared to the French strain, the Iranian isolates grew less at all three temperatures.

Statistical analysis by ANOVA confirms a significant effect of both strain and temperature on growth rate (Table 1). The Iranian strains belong to one group and the French strain belongs to a distinct group for vegetative growth (Figure 2A), as revealed by Tukey multiple means comparison test. Twenty-five °C was the best temperature for all isolates, followed by 20°C (Figure 2B).

Assessment of *in-vitro* sporulation also showed a significant effect of strain and temperature as well as a significant interaction strain x temperature as confirmed by ANOVA (Table 1). Again, LS means grouping showed that except at 28°C where no distinct difference between strains can be observed, the Iranian isolates are all in a group distinct from the French strain, with 25°C as the best temperature for all (Figure 2C). However, in contrast to hyphal growth where the French isolate had higher growth rates than the Iranian ones, sporulation of the Iranian isolates was superior to that of the French strain.

10.3389/fpls.2023.1125551

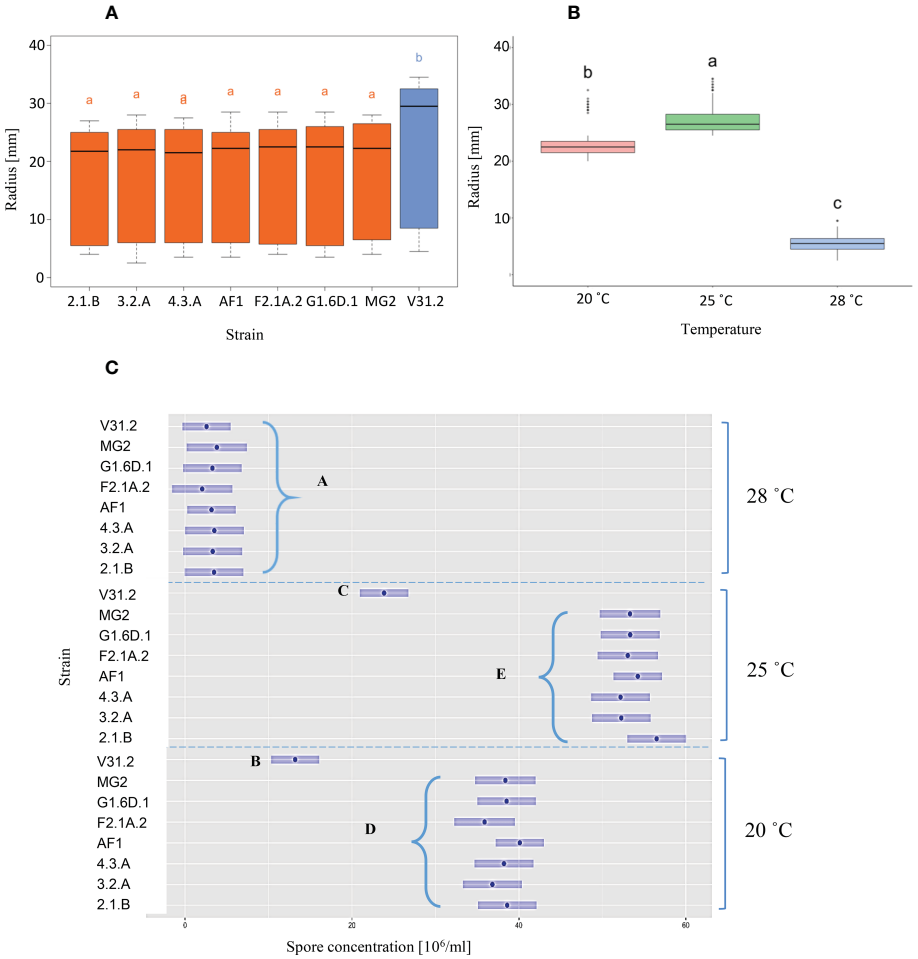

FIGURE 2
Radial growth and sporulation of *V. alfalfae* strains at 20 °C, 25 °C and 28 °C. Fungal isolates were cultured on PDA in darkness and hyphal growth was measured as radius during 14 days at regular intervals. Spores were harvested after 14 days. **(A)** Boxplot of strains' effect on radius after 14 days of growth, **(B)** Boxplot of temperatures' effect on radius after 14 days of growth. **(C)** Spore production as function of strain and temperature. The letters represent distinct groups by LSmeans based on the Tukey's test. The experiment was performed in 3 independent repetitions, each with 3 Petri dishes per condition and strain.

3.1.1 Phenotypic evaluation of *Medicago truncatula* response to an Iranian isolate points to quantitative resistance and reveals similar geographical correlation as with a French isolate

Given the homogenous growth and sporulation rates among the Iranian isolates, isolate AF1 was retained for the following study.

Ten-day-old *M. truncatula* plants were root-inoculated with spores of *V. alfalfae* isolate AF1 and symptoms were scored regularly for four weeks. Appearance of symptoms was observed 7–10 days after inoculation in susceptible *M. truncatula* lines, highly susceptible lines reaching the ultimate score of 4 (dead plant) after 3 weeks. A wide range of variation in the response, typical for quantitative traits, was observed among the 242 *M. truncatula* accessions, as shown by Area Under Disease Progress Curve (AUDPC) and Maximum Symptom Score (MSS) values (Supplementary Figure 2, Supplementary Tables 5, 6).

TABLE 1 Analysis of Variance of the effect of temperature and fungal strain on vegetative growth and sporulation.

Type III Analysis of Variance Table with Satterthwaite's method							
		Radial Growth			Sporulation		
Source of variation	NumDF	Mean Sq	F value	Pr(>F)	Mean Sq	F value	Pr(>F)
Strain	7	292.4	8.33	1.25e-08 ***	708	106.1	2e-16 ***
Temperature	2	19344.0	551.56	2.2e-16 ***	8531	1278.3	8.3e-16 ***
Strain: Temperature	14	49.0	1.39	0.1465	171	25.6	2e-16 ***

Data were obtained from 3 independent experiments, each with 3 Petri dishes, (***) represent p-value less than 0.001.

Broad sense heritability (H2) values for AUDPC and MSS were 0.719 and 0.724 respectively; the correlation between AUDPC and MSS was 0.96.

These results show that the population and the phenotype scoring method are suitable to implement a genome-wide association study in order to investigate the genetic architecture of *M. truncatula* response towards Iranian *V. alfalfae*.

When the results of our study were compared to those of a previous one with French isolate V31.2 at 20°C, the Pearson coefficient shows a high correlation between the two studies (R = 0,81, p < 2,2e-16) (Figure 3A). It also appeared that the plants' response in the current study had a tendency towards higher values of disease parameters, *i.e.* plants were more susceptible (Figure 3B). Some accessions presented a different response between the two studies. Only 5 accessions were strictly resistant to AF1 at 25°C with MSS values lower than 1.5, as compared to 63 accessions in the study with V31.2 at 20°C. Among these 63 accessions 16 became truly susceptible when inoculated with AF1 at 25°C, with MSS values ≥ 2.5.

When geographical origin and response to AF1 were plotted, a gradient from east to west of susceptible and resistant accessions was evidenced, similar to the previous study with the French isolate V31.2 at 20°C (Figure 4).

3.1.2 Genome-wide association study reveals the presence of numerous *loci* linked to resistance towards *Verticillium alfalfae* isolate AF1 in *Medicago truncatula*

In order to detect *loci* related to *M. truncatula* resistance against the Iranian isolate AF1, a genome-wide association study was undertaken using 5,671,743 high density SNP markers from the *Medicago truncatula* HapMap project.Statistical models for the association of genotype and phenotype were tested with the disease parameters MSS and AUDPC using the Tassel 5 software as in a previous study (Mazurier, 2018), and compared by Q-Q plot. As judged by this analysis, the most suitable model was a MLM Q-model which accounts for population structure for both traits, and uses the identity matrix to model kinship among random effects (Figure 5, Supplementary Figure 3). The K and Q + K models of MLMs showed deflation of p-values suggesting overfitting (Supplementary Figure 3G–J).

Analysis of the association between SNPs and AUDPC (Figure 6A) and SNPs and MSS (Figure 6B) revealed a high number of strongly associated *loci*. After conservative correction for multiple testing based on SNPs association score >= 5 as determined by the suggestive line, 24 and 14 significant SNPs were identified respectively for the AUDPC and MSS parameters on seven and six chromosomes respectively (Table 2). Among these significant SNPs, eight SNPs were common to AUDPC and MSS, with chromosome 8 containing five significant common SNPs. Chromosomes 1, 4 and 7 contain only one common SNP each.

3.2 Expression of selected candidate genes is induced by inoculation and differs in resistant and susceptible plants

To identify genes underlying the resistance-related *loci* revealed by GWAS, annotated genes in a span of 10 Kb upstream and downstream of each significant SNP were analyzed.

In a first step, 79 and 43 putative candidate genes were identified with the parameters AUDPC and MSS respectively. To reduce these numbers for expression studies, genes whose functional annotation suggested involvement in resistance, either by defense mechanisms

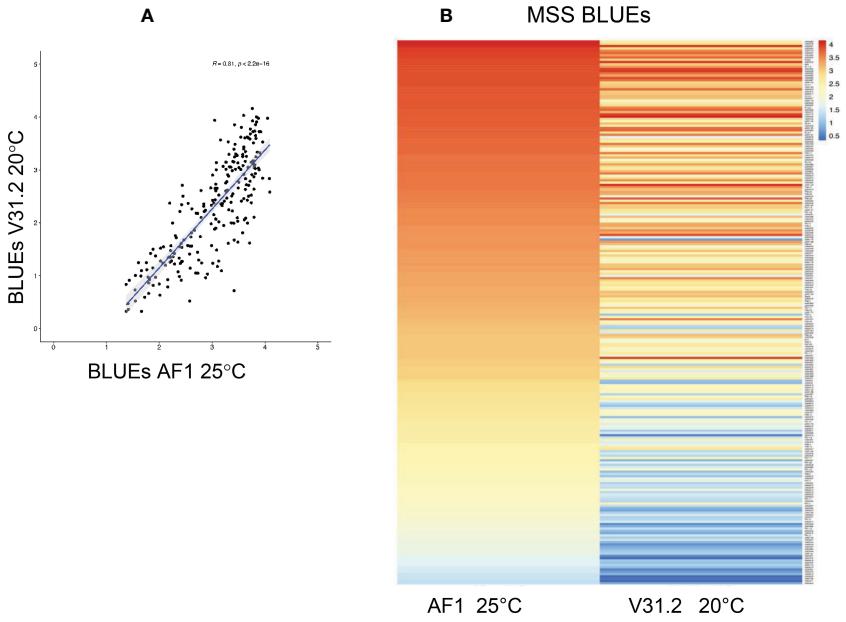

FIGURE 3
Comparison of the Maximum Symptom Score (MSS) response of a panel of 242 *M. truncatula* accessions inoculated with *Verticillium alfalfae* strain AF-1 at 25 °C and strain V31.2 at 20 °C. **(A)** Pearson correlation coefficient. **(B)** Heatmap of MSS response.

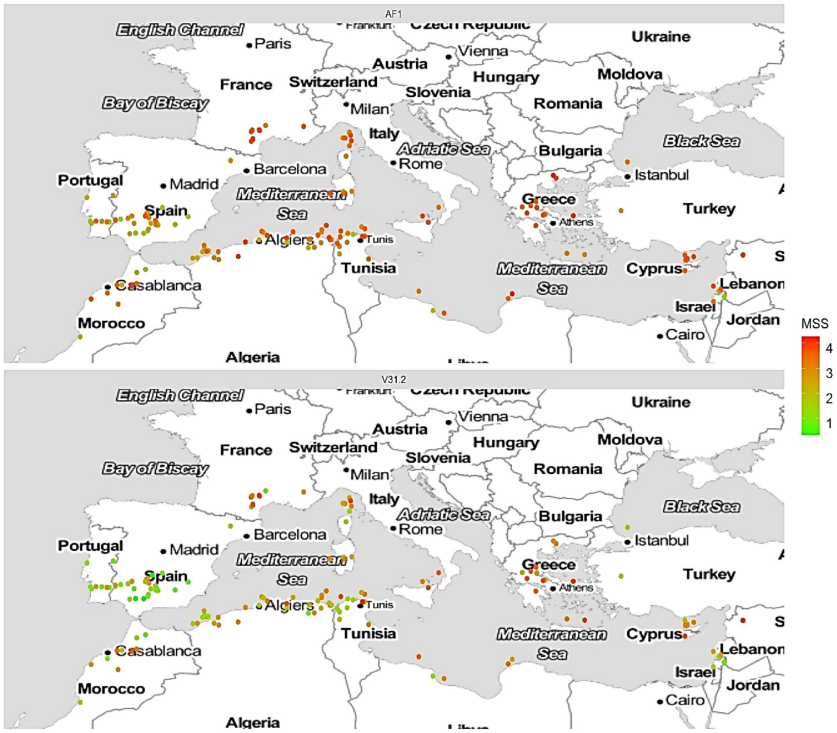

FIGURE 4
Comparison of the Maximum Symptom Score (MSS) response of a panel of 242 *M. truncatula* accessions inoculated with *Verticillium alfalfae* strain AF1 at 25°C and strain V31.2 at 20°C, across their natural geographical origins. Geographical documented origin of the 242 accessions of *M. truncatula* for which the response to the two strains of *V. alfalfae* has been evaluated is plotted on the map. Each accession is represented by a dot whose color varies according to the corrected MSS after inoculation by AF1 (upper panel) and V31.2 (lower panel). The color scale is shown on the right side, red is for susceptible, green for resistant response.

or signaling pathways alongside with genes with high association score and encoding hypothetical proteins, were retained. This resulted in 52 and 27 candidate genes for AUDPC and MSS respectively. In the next step only genes that were common for AUDPC and MSS were considered which led to 21 candidate genes. Among them nine genes were chosen for expression studies (Supplementary Table 3), based on the availability of efficient primers in qRT-PCR.

They encode proteins such as Rho-like GTP-binding protein (Medtr8g075240), casein kinase I-like protein (Medtr1g042280), MATH domain protein (Medtr1g042160), proteasome subunit alpha type-7-A protein (Medtr8g075320), osmosensor histidine kinase (Medtr8g075340), 3-hydroxyisobutyrate dehydrogenase-like 1/6-phosphogluconate dehydrogenase NAD-binding domain protein (Medtr8g102470), glycoside hydrolase family 1 protein (Medtr4g023000), pathogenesis-related thaumatin family protein (Medtr8g075550), and finally a hypothetical protein without known function (Medtr1g087500).

Their expression was studied in roots inoculated with spores of *V. alfalfae* AF1 versus control condition, at early (0, 4, and 24 hpi)

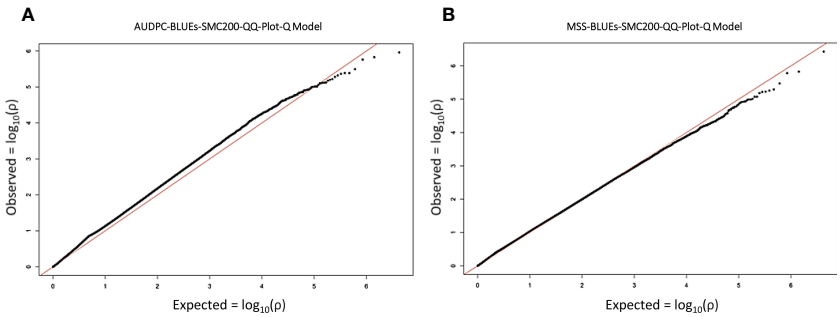

FIGURE 5
QQ plots of the MLM Q-model extracted from GWAS results. **(A)** AUDPC, **(B)** MSS. Each point represents the observed value of the P-value as a function of its theoretical value for an SNP, the more the points follow the bisector (red line), the more efficient the model. MLM, Mixed Linear Model. BLUE, the Best Linear Unbiased estimator. SMC200 refers to the site minimum count in the tassel program that was set to the 200.

and intermediate (96 hpi) time points. In order to erase individual differences due to the genetic background, pools of the most resistant and the most susceptible accessions were used for RNA extraction (Supplementary Table 4).

Expression analysis by qRT-PCR showed that all selected genes were expressed in roots of the susceptible and resistant plants (Figure 7). Moreover, their expression was induced transiently by inoculation and induction was generally stronger in plants of the resistant pool with induction factors up to 89 fold for gene Medtr8g075550 (Figure 7D).

Based on the time course of their expression the genes were classified into four groups (Figure 7). The first group contains the genes Medtr4g023000 (glycoside hydrolase family 1 protein), Medtr8g075340 (osmosensor histidine kinase) and Medtr8g102470 (3-hydroxyisobutyrate dehydrogenase-like 1/6-phosphogluconate dehydrogenase NAD-binding domain protein). They showed a very early induction at 4 hpi in both susceptible and resistant plants which decreased thereafter. Expression returned to basic levels in susceptible plants but stayed at induced levels for at least 24h in the resistant plants (Figure 7A).

The second group contains the genes Medtr1g042280 (casein kinase I-like protein), Medtr1g042160 (MATH domain protein) and Medtr1g087500 (hypothetical protein). They also exhibited very early induction at 4 hpi in both susceptible and resistant plants which was higher in resistant plants, but compared to genes of the first group their maximum expression was at 24 hpi and their induction lasted until 96 hpi (Figure 7B).

The third group contains only one gene, Medtr8g075240 (Rho-like GTP-binding protein), and exhibited induction at 4 hpi in resistant plants which increased until 96 hpi whereas in susceptible plants only a weak induction at 24h was observed (Figure 7C).

The fourth group containing the genes Medtr8g075320 (proteasome subunit alpha type-7-A protein) and Medtr8g075550 (pathogenesis-related thaumatin family protein) exhibited strong

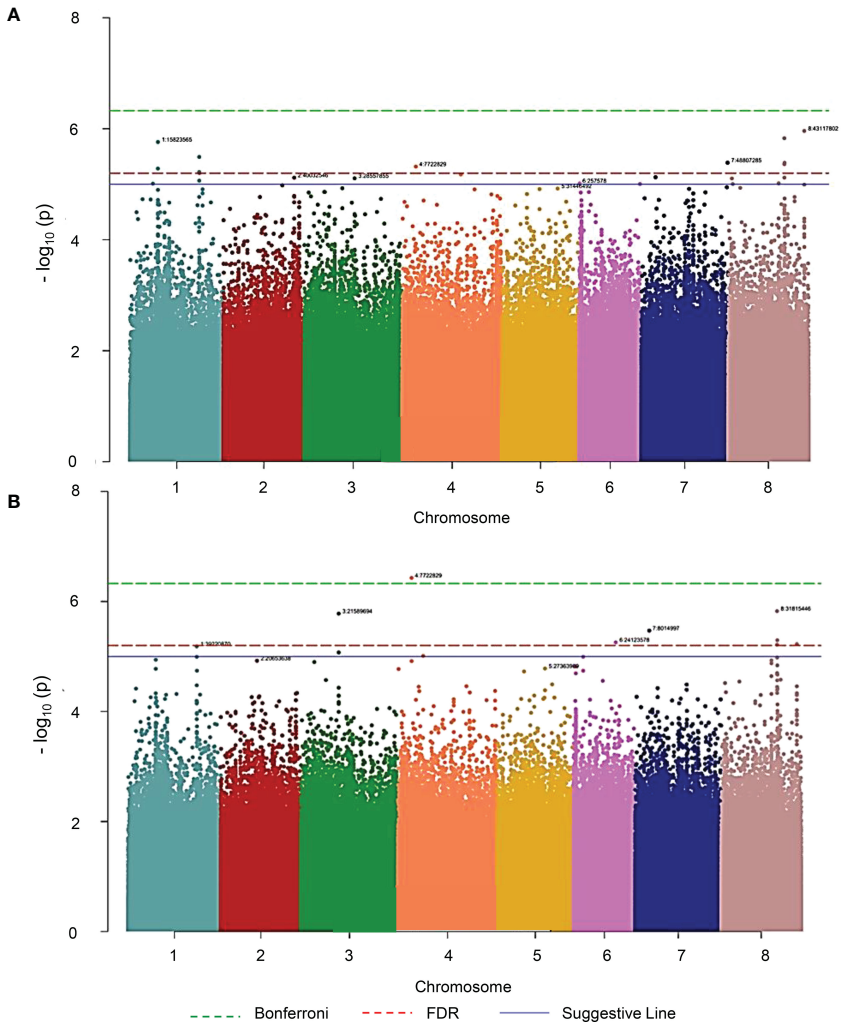

FIGURE 6
Manhattan plot illustration of the response of *M. truncatula* to *V. alfalfae* strain AF1 revealed by GWAS analysis. **(A)** AUDPC, **(B)** MSS. The green dashed line represents the Bonferroni threshold, the red dashed line the FDR threshold and the blue solid line the suggestive line of the qqman R package. AUDPC and MSS phenotypes were evaluated in 242 root-inoculated accessions of the MtHapMap collection. Association genetic analysis was performed using a Mixed linear model - Q Model. Each point represents a SNP. The X-axis shows the 8 chromosomes ordered by number, the Y-axis represents the association score, i.e. the probability that the SNP is related to the studied phenotype, is calculated as -log10[p-value].

TABLE 2 Most significant Single Nucleotide Polymorphism (SNP) markers associated to the response of *Medicago truncatula* to *Verticillium alfalfae* strain AF1.

Trait	SNP marker	Chr	Position	df	p	MarkerR2	score	Allele	Effect
AUDPC	1:12964012	1	12964012	2	9,742E-06	0,092	5,011	A/G	0,007/0,004
AUDPC	1:15800708	1	15800708	2	5,228E-06	0,105	5,282	A/G	-0,009/-0,005
AUDPC	1:15823565	1	15823565	2	1,732E-06	0,112	5,761	C/T	-0,005/0,001
AUDPC	**1:39220870**	**1**	**39220870**	**2**	**3,220E-06**	**0,097**	**5,492**	**A/G**	**-0,008/-0,004**
AUDPC	1:39222678	1	39222678	2	6,012E-06	0,097	5,221	A/T	0,002/-0,002
AUDPC	1:39226123	1	39226123	2	8,624E-06	0,089	5,064	A/G	-0,008/-0,004
AUDPC	1:39333665	1	39333665	2	6,292E-06	0,090	5,201	A/T	0,004/-0,0001
AUDPC	2:33302078	2	33302078	2	4,598E-06	0,098	5,337	A/T	0,001/0,007
AUDPC	2:40032546	2	40032546	2	7,623E-06	0,087	5,118	C/T	0,003/-0,001
AUDPC	3:28557855	3	28557855	2	7,810E-06	0,092	5,107	C/T	-0,006/-0,003
AUDPC	**4:7722829**	**4**	**7722829**	**2**	**4,808E-06**	**0,099**	**5,318**	**G/T**	**-0,005/0,0004**
AUDPC	4:33221889	4	33221889	2	6,654E-06	0,090	5,177	A/G	0,001/0,009
AUDPC	6:257578	6	257578	2	9,656E-06	0,101	5,015	A/T	0,002/-0,005
AUDPC	6:34475434	6	34475434	2	9,889E-06	0,092	5,005	A/G	0,011/0,002
AUDPC	**7:8014997**	**7**	**8014997**	**2**	**7,468E-06**	**0,093**	**5,127**	**A/T**	**-0,01/-0,006**
AUDPC	7:48807285	7	48807285	2	4,102E-06	0,111	5,387	A/C	-0,005/0,001
AUDPC	8:2106964	8	2106964	2	7,865E-06	0,090	5,104	G/T	-0,008/-0,004
AUDPC	8:2597013	8	2597013	2	9,890E-06	0,098	5,005	C/T	-0,008/-0,003
AUDPC	**8:28608045**	**8**	**28608045**	**2**	**9,622E-06**	**0,095**	**5,017**	**C/G**	**-0,01/-0,006**
AUDPC	**8:31815446**	**8**	**31815446**	**2**	**1,482E-06**	**0,105**	**5,829**	**A/G**	**-0,0003/-0,007**
AUDPC	8:31823520	8	31823520	2	4,349E-06	0,094	5,362	A/G	0,004/-0,001
AUDPC	**8:31847916**	**8**	**31847916**	**2**	**7,590E-06**	**0,117**	**5,120**	**C/T**	**-0,0002/-0,007**
AUDPC	**8:31944993**	**8**	**31944993**	**2**	**4,112E-06**	**0,095**	**5,386**	**A/G**	**-0,0003/-0,005**
AUDPC	**8:43117802**	**8**	**43117802**	**2**	**1,094E-06**	**0,104**	**5,961**	**C/T**	**0,006/-0,003**
MSS	**1:39220870**	**1**	**39220870**	**2**	**6,572E-06**	**0,089**	**5,182**	**A/G**	**-6,218/-2,906**
MSS	3:21589694	3	21589694	2	1,660E-06	0,110	5,780	G/T	1,83/5,333
MSS	3:21589926	3	21589926	2	8,462E-06	0,085	5,073	C/T	-4,586/-1,384
MSS	3:21589932	3	21589932	2	8,462E-06	0,085	5,073	C/T	-1,384/-4,586
MSS	**4:7722829**	**4**	**7722829**	**2**	**3,732E-07**	**0,118**	**6,428**	**G/T**	**-4,438/0,674**
MSS	4:14324686	4	14324686	2	9,742E-06	0,095	5,011	G/T	4,156/-1,281
MSS	6:24123578	6	24123578	2	5,540E-06	0,088	5,257	A/G	-1,457/1,346
MSS	**7:8014997**	**7**	**8014997**	**2**	**3,388E-06**	**0,098**	**5,470**	**A/T**	**-8,927/-5,172**
MSS	**8:28608045**	**8**	**28608045**	**2**	**9,870E-06**	**0,092**	**5,006**	**C/G**	**-7,034/-3,649**
MSS	8:28608060	8	28608060	2	8,712E-06	0,094	5,060	A/T	1,653/-1,706
MSS	**8:31815446**	**8**	**31815446**	**2**	**1,496E-06**	**0,102**	**5,825**	**A/G**	**-0,384/-6,424**
MSS	**8:31847916**	**8**	**31847916**	**2**	**6,065E-06**	**0,114**	**5,217**	**C/T**	**-0,319/-6,458**
MSS	**8:31944993**	**8**	**31944993**	**2**	**5,069E-06**	**0,091**	**5,295**	**A/G**	**-0,403/-4,639**
MSS	**8:43117802**	**8**	**43117802**	**2**	**5,934E-06**	**0,088**	**5,227**	**C/T**	**4,966/-2,522**

Significant SNPs in common between AUDPC and MSS are highlighted in bold.
SNPs were filtered by p-value using the MLM Q-Model for AUDPC and MSS traits in response to inoculation with AF1.

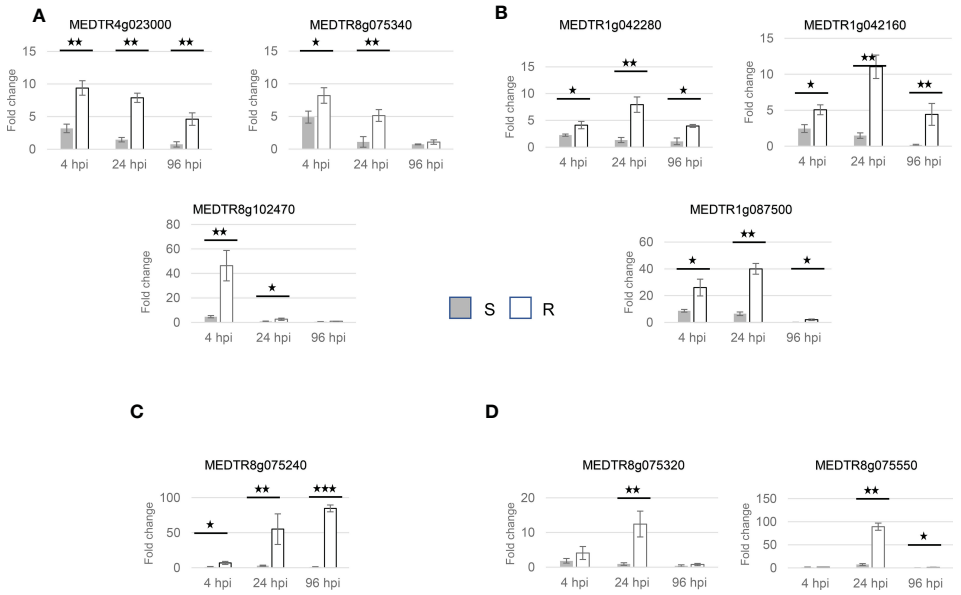

FIGURE 7
Gene expression in roots inoculated with *V. alfalfae* strain AFI, grouped by expression patterns. **(A)** Glycoside hydrolase family 1 protein (MEDTR4g023000), Osmosensor histidine kinase (MEDTR8g075340), 6-phosphogluconate dehydrogenase NAD-binding domain protein/3-hydroxyisobutyrate dehydrogenase-like 1 (MEDTR8g102470). **(B)** Casein kinase I-like protein (MEDTR1g042280), MATH domain protein (MEDTR1g042160), hypothetical protein MTR_1g087500 (MEDTR1g087500). **(C)** Rho-like GTP-binding protein (MEDTR8g075240). **(D)** Proteasome subunit alpha type-7-A protein (MEDTR8g075320), Pathogenesis-related thaumatin family protein (MEDTR8g075550). The fold change (expression in inoculated roots over expression in mock-inoculated roots) is calculated through ΔΔ CT by $2^{-(\Delta\Delta CT)}$. The error bars represent the standard deviation of the fold-change. The fold change is calculated through ΔΔ CT by $2^{-(\Delta\Delta CT)}$. The stars present significance levels derived from the T-test of mean comparison between treated susceptible and resistant pools at each time point. (*) represent p-value less than 0.05, (**) less than 0.01, (***) less than 0.001.

induction at 24 hpi which decreased thereafter in resistant plants. In susceptible plants the expression was induced weakly only for Medtr8g075550, at 24h and even slightly suppressed for both genes at 96hpi (Figure 7D).

Taken together, the expression patterns of all candidate genes detected under *loci* identified by GWAS support the involvement of these *loci* in the resistance response to *V. alfalfae*. Although all selected candidate genes were induced to some level in both susceptible and resistant plants, the difference between the resistant and susceptible plants was statistically significant at most time points, with induction factors consistently higher in the resistant plants (Pešić et al., 2014).

4 Discussion

The first report of Verticillium wilt disease due *V. alfalfae* in Iran was published in 2004 (Ghalandar et al., 2004) describing the pathogen in alfalfa fields of the Markazi Province. Fourteen years after this publication, the samples we collected from different parts of Iran reveal that this disease has spread since then to various areas of the Markazi and neighboring Hamedan provinces and up to the Teheran region. Since alfalfa culture in Iran depends on irrigation, it can be supposed that the pathogen spread has been favoured by irrigation systems, as has been reported for *V. dahliae* on olive tree (Jiménez-Díaz et al., 2011; López-Escudero and Mercado-Blanco, 2011). Seed companies in Iran and neighboring countries should thus include partial resistance to Verticillium wilt in future alfalfa breeding programs and survey alfalfa producing regions for occurrence of this disease in production fields.

By hyphal growth and sporulation all Iranian isolates are in one statistical group as opposed to the French isolate. A negative correlation between hyphal growth and sporulation as observed in our study has been reported earlier for other fungal species such as *Aspergillus Niger* (Muller, 1956), *V. agaricinum* and *Schizosaccharomyces pombe* (McKoy and Trinci, 1987) and *Ascochyta rabiei* (Mahiout et al., 2015).

Together with the observation that mycelia of Iranian strains develop black pigmentation after prolonged growth on PDA whereas the French strain does not, this indicates strongly that *V. alfalfae* in Iran belongs to a different genotype. An Iranian strain could thus be used to study the disease response of *M. truncatula* in a perspective of putative invasion of new pathogen strains through global trade. Also, in order to take into account a predicted increase in future temperatures, root-inoculated plants were maintained at 25°C instead of the standard temperature of 20°C which is the standard temperature for the assessment of commercial alfalfa varieties and was used in previous works (Ben et al., 2013; Toueni et al., 2016). The here described work should thus lead to detecting putatively new *loci* involved in the genetic control of resistance compared to previous studies (Ben et al., 2013; Toueni et al., 2016; Mazurier, 2018), in a scenario of globalization and global warming.

Despite the fact that two parameters have been changed (temperature and strain), there was still a high correlation

between the current study at 25°C and the previous one at 20°C (Mazurier, 2018), but with a tendency towards higher susceptibility of plants towards AF1 at 25°C. This tendency could be due to the higher aggressiveness of AF1, or to the higher temperature or to a combination of both. Previous work has indeed shown that *V. alfalfae* V31.2 was more aggressive at 25°C compared to 20°C (Sbeiti et al., 2023). Studies on Fusarium wilt on two different host plants have also reported higher disease severity at higher temperature (Ferrocino et al., 2013; Chitarra et al., 2015). However, the observation that a small number of accessions changed from resistant to susceptible under the new conditions might also indicate the combined effects of strain, temperature and genotype.

The geographical distribution of susceptible and resistant accessions was similar to that revealed by the WhoGEM approach, *i.e.* resistant accessions are located in western regions of the Mediterranean basin while the susceptible ones are located in the eastern parts (Gentzbittel et al., 2019). The present results confirmed that resistance to *V. alfalfae* among *M. truncatula* accessions is structured by genome admixture and geographical origin, in a similar way independent of the pathogen's geographical origin (Figure 4). However, our knowledge about Verticillium wilt in Iran is limited. Although our observations and results suggest that the Iranian *V. alfalfae* isolates belong to a different genotype than the French strain, we do not know if the pathogen is indigenous to Iran or not. It would be interesting to enlarge the study to isolates from other countries of the Mediterranean basin, east and west.

The continuous distribution of AUDPC and MSS scores through the panel of *M. truncatula* accessions indicates that resistance to the Iranian strain of *V. alfalfae* is controlled in a polygenic manner. The broad sense heritability (H^2) calculated values for both traits (AUDPC=0.719, MSS=0.724) suggests that their variability is linked to a combination of genetic and environmental factors with a higher contribution of genetic variance.

Taken together, the range of phenotypic variation of the plants' response to the pathogen and high heritability indicated that population and traits are suitable for studying the genetic architecture of *M. truncatula* resistance towards the Iranian *V. alfalfae* isolate through genome-wide association mapping.

GWAS evaluates the statistical significance of the association between quantitative differences of a particular phenotype and specific genetic polymorphisms in a set of genetically distinct individuals (Ogura and Busch, 2015). A first step of GWAS was to select an appropriate statistical model which reduces false positives and copes with spurious associations due to population structure (Balding, 2006; Yu and Buckler, 2006; Wang et al., 2012) and population admixture (Chen et al., 2014; Gay et al., 2020) as much as possible. Based on these criteria we selected a MLM-Q Model.

A previous study (Ben et al., 2013) has reported a major QTL controlling resistance to *V. alfalfae* strain V31.2 on chromosome 7 as well as QTLs on chromosomes 2 and 6. The major QTL on chromosome 7 was later confirmed by GWAS through co-localisation of 11 and 4 different SNPs respectively related to AUDPC and MSS (Mazurier, 2018). Our present study with an Iranian strain and conducted at higher temperature (25°C *versus* 20°C) revealed a higher number of *loci* and did not show overlap with the Mazurier study (2018) except for the *locus* on chromosome 1 with a common candidate gene *Medtr1g042160* encoding a MATH domain protein. A comparison between the two studies also showed that five resistant accessions in the previous study (Mazurier, 2018), [L000411, L000513 and L000443 originating from Spain, L000620 originating from France and A17 which is predicted to originate from Spain (Gentzbittel et al., 2019)] are still categorized as resistant in our work. However, we do not know the genetic basis of the resistance in these particular accessions. It might be based on the same *loci* or might be the result of different QTLs/genes/proteins that finally led to the same phenotypic outcome.

Taken together, our results show that a simple shift in temperature combined with a new pathogen strain drastically changes the architecture of genetic control of resistance to the pathogen and notably does not involve the strong QTL on chromosome 7 which is effective against strain V31.2 at 20°C (Ben et al., 2013; Mazurier, 2018).

The high synteny between *M. truncatula* and alfalfa makes it possible to use markers from one species in the other one, as has been shown for several genes involved in the symbiosis with Rhizobium (Zhu et al., 2005). A study on resistance to Verticillium wilt in alfalfa reported significant SNP markers on five chromosomes (Zhang et al., 2014) and suggested that those on chromosome 2 and 7 might have similar locations as QTLs identified in *M. truncatula* by Ben et al. (2013). Comparing the SNPs identified in our work and those of Zhang and co-workers (2014), the positions of markers 4:14324686 and 8:28608045 indicate additional similar locations on the alfalfa chromosomes, supporting the idea that results obtained in *M. truncatula* can be used to improve cultivated crops. A GWAS by Yu et al. (2017) described ten SNPs associated to resistance to *V. alfalfae*, some of them on the same chromosomes as in our study. However they were not near the SNPs we detected. All nine genes for which we studied expression in *M. truncatula* roots, have homologs in alfalfa (https://medicago.legumeinfo.org/tools/sequenceserver/), with more than 90% identity, though the coverage was low for three among them.

In order to validate the *loci* detected by GWAS, we selected genes in the areas 10 kb upstream and downstream of all significant SNPs. This distance is based on data on linkage disequilibrium and recombination rates described for *M. truncatula* in a previous study (Branca et al., 2011).

Chromosome 8 shows the highest number of genes putatively involved in resistance towards AF1 with 31 and 17 genes for AUDPC and MSS respectively.

One gene (Medtr1g042160) on chromosome 1 which was detected through AUDPC was common to the previous study with the French strain at 20°C (Mazurier, 2018). This gene encodes a MATH domain and coiled-coil domain-containing protein homologous to At3g58250. Meprin and TRAF-C Homology (MATH) domain is a protein-protein interaction domain composed of seven anti-parallel p-helices (Zapata et al., 2007) which is reported to play a role in plant–fungal interactions (Oelmuller et al., 2005) and also in plant responses to abiotic stress in Arabidopsis and rice as well as to pathogen attack in rice

(Kushwaha et al., 2016). In our study its expression was induced by inoculation in roots at 4 hpi, to a higher level in resistant plants compared to susceptible ones. This candidate gene that was detected by two independent GWAS in response to two different strains of *V. alfalfae* and temperatures is a very promising breeding target to improve *Verticillium* resistance in Medics. Further analyses will be implemented to validate its role in the interaction between *Medicago* sp. and *Verticillium* and maybe develop molecular markers for marker-assisted selection.

In addition to the MATH gene, expression of eight other genes from *loci* on chromosomes 1, 4, 7 and 8 was studied in roots of susceptible and resistant plants after root inoculation.

These genes encode proteins mainly related to signaling and defense in stress resistance.

Genes encoding a casein kinase 1 like protein, an osmosensor histidine kinase, and a Rho-like GTP binding protein were induced at 4 hpi in *M. truncatula* roots inoculated with AF1, to a higher level in resistant plants compared to susceptible ones. Kinases through phosphorylation of their targets participate in many signaling pathways, as do GTP-binding proteins, and have putative roles in phytohormone signaling and defense against biotic stress (Pham et al., 2012; Yin et al., 2015; Klessig et al., 2018; Li et al., 2019; Zhao et al., 2020).

The gene encoding a proteasome subunit alpha type-7-A protein was induced at 4 hpi, to a higher level in resistant plants compared to susceptible ones. Ubiquitination is also an important part of signaling pathways in response to pathogens (Marino et al., 2012).

Other proteins participate more directly to defense such as the pathogenesis-related proteins to which belong thaumatin and glycoside hydrolases (Ali et al., 2018). The induction of the gene encoding the thaumatin family protein was later than that of the eight other genes, which is consistent with a role as defense protein, whereas the gene encoding glycoside hydrolase family 1 protein had its highest induction at 4hpi which indicates a possible signaling involvement of this protein.

Finally, the genes encoding a 6-phosphogluconate dehydrogenase NAD-binding domain protein/probable 3-hydroxyisobutyrate dehydrogenase-like 1 protein and a hypothetical protein, are representatives of primary metabolism and unknown functions. They were also induced in roots by AF1 inoculation, early and stronger in resistant plants, indicating their putative involvement in the plants' resistance response.

Taken together, the expression patterns of these genes, *i.e.* strong induction in resistant plants vs. weak induction in susceptible plants, are in agreement with the claim that the *loci* identified by GWAS have significant contributions to resistance. The evaluation of the response of the association panel to the French *Verticillium* isolate V31.2 at 20°C in a previous study led to the identification of 34 candidate genes (Mazurier, 2018). Our present study with the Iranian *Verticillium* isolate AF1 at 25°C identified 93 candidate genes, with only one gene (Medtr1g042160) in common, which corresponds to about 1% overlap between the two studies. Due to the high number of candidate genes and the small contribution of each *locus* to resistance, it did not seem reasonable to go further for functional studies.

In addition, since two variables (temperature and pathogen strain) have been changed, it is not possible to separate their effects on the outcome of the interaction between *M. truncatula* and *V. alfalfae.* However, the results show that such combined effects can completely change the genetic architecture of plant disease resistance and should be a warning to breeders and institutions that control exchange of plant material.

Data availability statement

The raw data supporting the conclusions of this article will be made available by the authors, without undue reservation.

Author contributions

AF performed all experiments, analyzed the data and wrote a first draft of the manuscript. CB contributed substantially to the data analysis and interpretation and critically revised the manuscript. AE contributed to collecting the samples and acquisition of funding, and revised the manuscript. MM provided phenotypic data and interpretation of data. MG contributed to collecting and identifying the samples. LG contributed substantially to the conception and design of the work and supervised statistical analysis and interpretation of data. MR conceived and supervised the project, contributed to acquire funding, and revised the manuscript. All authors contributed to the article and approved the submitted version.

Funding

This work has been supported with project PHC Gundishapur N° 38423VK through funding field trips to Iran. AF was supported by the Iranian NanoBioTechnologist laboratory (INBTCo.), Tehran, Iran with a PhD grant.

Acknowledgments

This work has been supported by the Center for International Scientific Studies & Collaboration (CISSC) and the French Embassy in Iran. The authors also thank the staff at GeT-PlaGe for assistance and use of the QuantStudio™ 6 Flex Real-Time PCR System, and Genotoul Bioinformatics platform Toulouse Occitanie (Bioinfo Genotoul, doi: 10.15454/1.5572369328961167E12) for providing hardware infrastructure, help, computing and storage resources.

Conflict of interest

The authors declare that the research was conducted in the absence of any commercial or financial relationships that could be construed as a potential conflict of interest.

Publisher's note

All claims expressed in this article are solely those of the authors and do not necessarily represent those of their affiliated

organizations, or those of the publisher, the editors and the reviewers. Any product that may be evaluated in this article, or claim that may be made by its manufacturer, is not guaranteed or endorsed by the publisher.

Supplementary material

The Supplementary Material for this article can be found online at: https://www.frontiersin.org/articles/10.3389/fpls.2023.1125551/full#supplementary-material

References

Acharya, S. N., and Huang, H. C. (2003). Breeding alfalfa for resistance to verticillium wilt: A sound strategy, In *Advances in Plant Disease management*. eds. H. C. Huang and S. N. Acharya, (Research Signpost Trivandrum), 345–371.

Agrios, G. (2005). *Plant pathology. 5th Edition* (Burlington: Elsevier Academic Press).

Ali, S., Ganai, B. A., Kamili, A. N., Bhat, A. A., Mir Zahoor, A., Bhat, J. A., et al. (2018). 'Pathogenesis-related proteins and peptides as promising tools for engineering plants with multiple stress tolerance'. *Microbiological Res.* 212–213 (March), 29–37. doi: 10.1016/j.micres.2018.04.008

Ausubel, F. M. (2005). Are innate immune signaling pathways in plants and animals conserved? *Nat. Immunol.* 6 (10), 973–979. doi: 10.1038/ni1253

Balding, D. J. (2006). A tutorial on statistical methods for population association studies. *Nat. Rev. Genet.* 7 (10), 781–791. doi: 10.1038/nrg1916

Bartoli, C., and Roux, F. (2017). Genome-wide association studies in plant pathosystems: Toward an ecological genomics approach. *Front. Plant Sci.* 8 (May). doi: 10.3389/fpls.2017.00763

Ben, C., Maoulida, T., Montanari, S., Tardin, M.-C., Fervel, M., Negahi, A., et al. (2013). Natural diversity in the model legume medicago truncatula allows identifying distinct genetic mechanisms conferring partial resistance to verticillium wilt. *J. Exp. Bot.* 64 (1), 317–332. doi: 10.1093/jxb/ers337

Bigeard, J., Colcombet, J., and Hirt, H. (2015). Signaling mechanisms in pattern-triggered immunity (PTI). *Mol. Plant Elsevier Ltd* 8 (4), 521–539. doi: 10.1016/j.molp.2014.12.022

Bradbury, P. J., Zhang, Z., Kroon, D. E., Casstevens, T. M., Ramdoss, Y., and Buckler, E. S. (2007). TASSEL: software for association mapping of complex traits in diverse samples. *Bioinformatics* 23 (19), 2633–2635. doi: 10.1093/bioinformatics/btm308

Branca, A., Paape, T. D., Zhou, P., Briskine, R., Farmerd, A. D., Mudge, J., et al. (2011). Whole-genome nucleotide diversity, recombination, and linkage disequilibrium in the model legume medicago truncatula. *Proc. Natl. Acad. Sci. United States America* 108 (42), E864–E870. doi: 10.1073/pnas.1104032108

Buels, R., Yao, E., Diesh, C. M., Hayes, R. D., Munoz-Torres, M., Helt, G., et al. (2016). 'JBrowse: a dynamic web platform for genome visualization and analysis'. *Genome Biol. Genome Biol.* 17 (1), 66. doi: 10.1186/s13059-016-0924-1

Carter-House, D., Stajich, J. E., Unruh, S., and Kurbessoian, T. (2020). Fungal CTAB DNA extraction. In protocols.io, doi: 10.17504/protocols.io.bhx8j7rw. protocols.io.

Cathala, G., Savouret, J. F., Mendez, B., West, B. L., Karin, M., Martial, J. A., et al. (1983). A method for isolation of intact, translationally active ribonucleic acid. *DNA* 2 (4), 329–335. doi: 10.1089/dna.1983.2.329

Chen, M., Yang, C., Li, C., Hou, L., Chen, X., and Zhao, H. (2014). Admixture mapping analysis in the context of GWAS with GAW18 data. *BMC Proc.* 8 (suppl1), 1–5. doi: 10.1186/1753-6561-8-S1-S3

Chitarra, W., Siciliano, I., Ferrocino, I., Gullino, M. L., and Garibaldi, A. (2015). Effect of elevated atmospheric CO2 and temperature on the disease severity of rocket plants caused by fusarium wilt under phytotron conditions. *PloS One* 10 (10), e0140769. doi: 10.1371/journal.pone.0140769

Cook, D. R. (1999). Medicago truncatula — a model in the making! *Curr. Opin. Plant Biol. Curr. Biol. Ltd* 2 (4), 301–304. doi: 10.1016/S1369-5266(99)80053-3

Cooper, R. M., and Wood, R. K. S. (1980). Cell wall degrading enzymes of vascular wilt fungi. III. possible involvement of endo-pectin lyase in verticillium wilt of tomato. *Physiol. Plant Pathol.* 16 (2), 285–300. doi: 10.1016/0048-4059(80)90043-0

Ellwood, S. R., D'Souza, N. K., Kamphuis, L. G., Burgess, T. I., Nair, R. M., and Oliver, R. P. (2006). SSR analysis of the medicago truncatula SARDI core collection reveals substantial diversity and unusual genotype dispersal throughout the Mediterranean basin. *Theor. Appl. Genet.* 112 (5), 977–983. doi: 10.1007/s00122-005-0202-1

Erwin, D. C., and Howell, A. B. (1998). Verticillium survives heat in Mojave desert alfalfa. *California Agric.* 52 (4), 24–26. doi: 10.3733/ca.v052n04p24

Ferrocino, I., Chitarra, W., Pugliese, M., Gilardi, G., Gullino, M. L., and Garibaldi, A. (2013). Effect of elevated atmospheric CO2 and temperature on disease severity of fusarium oxysporum f.sp. lactucae on lettuce plants. *Appl. Soil Ecol.* 72, 1–6. doi: 10.1016/j.apsoil.2013.05.015

Flor, H. H. (1971). 'Current status of the gene-fob-gene concept'. *Annu. Rev. Phytopathol.* 9, 275–296. doi: 10.1146/annurev.py.09.090171.001423

Fradin, E. F., and Thomma, B. P. H. J. (2006). Physiology and molecular aspects of verticillium wilt diseases caused by v. dahliae and v. albo-atrum. *Mol. Plant Pathol.* 7 (2), 71–86. doi: 10.1111/j.1364-3703.2006.00323.x

Gay, N. R., Gloudemans, M., Antonio, M. L., Abell, N. S., Balliu, B., Park, Y., et al. (2020). 'Impact of admixture and ancestry on eQTL analysis and GWAS colocalization in GTEx'. *Genome Biol.* 21 (1), 233. doi: 10.1186/s13059-020-02113-0

Gentzbittel, L., Andersen, S. U., Ben, C., Rickauer, M., Stougaard, J., and Young, N. D. (2015). 'Naturally occurring diversity helps to reveal genes of adaptive importance in legumes'. *Front. Plant Sci.* 6. doi: 10.3389/fpls.2015.00269

Gentzbittel, L., Ben, C., Mazurier, M., Shin, M. G., Lorenz, T., Rickauer, M., et al. (2019). 'WhoGEM: an admixture-based prediction machine accurately predicts quantitative functional traits in plants'. *Genome Biol. Genome Biol.* 20 (1), 106. doi: 10.1186/s13059-019-1697-0

Ghalandar, M., Clewes, E., Barbara, D. J., Zare, R., and Heydari, A. (2004). Verticillium wilt (Verticillium albo-atrum) on medicago sativa (alfalfa) in Iran. *Plant Pathol.* 53 (6), 812–812. doi: 10.1111/j.1365-3059.2004.01081.x

Graham, P. H., and Vance, C. P. (2003). 'Update on legume utilization Legumes: Importance and constraints to greater use'. *Plant Physiol.* 131 (March), 872–877. doi: 10.1104/pp.017004.872

Inderbitzin, P., Bostock, R. M., Davis, R. M., Usami, T., Platt, H. W., and Subbarao, K. V. (2011). Phylogenetics and taxonomy of the fungal vascular wilt pathogen verticillium, with the descriptions of five new species. *PloS One* 6 (12), e28341. doi: 10.1371/journal.pone.0028341

Inderbitzin, P., Davis, R. M., Bostock, R. M., and Subbarao, K. V. (2013). Identification and differentiation of verticillium species and v. longisporum lineages by simplex and multiplex PCR assays. *PloS One* 8 (6), 1–12. doi: 10.1371/journal.pone.0065990

Inderbitzin, P., Thomma, B. P. H. J., Klosterman, S. J., and Subbarao, K. V. (2014). 'Verticillium alfalfae and V . dahliae, agents of verticillium wilt diseases,' in *Genomics of plant-associated fungi and oomycetes: Dicot pathogens* R. Dean, A. Lichens-Park and C. Kole (eds) (Berlin Heidelberg: Springer), 65–97. doi: 10.1007/978-3-662-44056-8_4

Inderbitzin, P., and Subbarao, K. V. (2014). *Verticillium* systematics and evolution: How confusion impedes verticillium wilt management and how to resolve it. *Phytopathology* 104 (6), 564–574. doi: 10.1094/PHYTO-11-13-0315-IA

Jiménez-Díaz, R. M., Olivares-García, C., Landa, B. B., Del Mar Jiménez-Gasco, M., and Navas-Cortés, J. A. (2011). Region-wide analysis of genetic diversity in verticillium dahliae populations infecting olive in southern Spain and agricultural factors influencing the distribution and prevalence of vegetative compatibility groups and pathotypes. *Phytopathology* 101 (3), 304–315. doi: 10.1094/PHYTO-07-10-0176

Kamle, M., Borah, R., Bora, H., Jaiswal, A. K., Singh, R. K., and Kumar, P. (2020). Systemic acquired resistance (SAR) and induced systemic resistance (ISR): Role and mechanism of action against phytopathogens. In: *Fungal Biotechnology and Bioengineering*., A. L. Hesham, R. Upadhyay, G. Sharma, C. Manoharachary and V. Gupta (eds), Springer, Cham. 457–470. doi: 10.1007/978-3-030-41870-0_20

Klessig, D. F., Choi, H. W., and Dempsey, D. A. (2018). Systemic acquired resistance and salicylic acid: Past, present, and future. *Mol. Plant-Microbe Interact.* 31 (9), 871–888. doi: 10.1094/MPMI-03-18-0067-CR

Klosterman, S. J., Subbarao, K. V., Kang, S., Veronese, P., Gold, S. E., Thomma, B. P. H. J., et al. (2011). Comparative genomics yields insights into niche adaptation of plant vascular wilt pathogens. *PloS Pathog.* 7 (7), 1–19. doi: 10.1371/journal.ppat.1002137

Kushwaha, H. R., Joshi, R., Pareek, A., and Singla-Pareek, S. L. (2016). 'MATH-domain family shows response toward abiotic stress in arabidopsis and rice'. *Front. Plant Science.* 7. doi: 10.3389/fpls.2016.00923

Kuznetsova, A., Brockhoff, P. B., and Christensen, R. H. B. (2017). lmerTest package: Tests in linear mixed effects models. *J. Stat. Software* 82 (13), 1–26. doi: 10.18637/jss.v082.i13

Lenth, R. V. (2013). 'Using the lsmeans package'. *CRAN R Project* 50 (60), 70.

Li, N., Han, X., Feng, D., Yuan, D., and Huang, L. J. (2019). Signaling crosstalk between salicylic acid and ethylene/Jasmonate in plant defense: Do we understand what they are whispering? *Int. J. Mol. Sci.* 20 (3), 1–15. doi: 10.3390/ijms20030671

López-Escudero, F. J., and Mercado-Blanco, J. (2011). Verticillium wilt of olive: a case study to implement an integrated strategy to control a soil-borne pathogen. *Plant Soil* 344 (1–2), 1–50. doi: 10.1007/s11104-010-0629-2

Mahiout, D., Bendahmane, B. S., Youcef Benkada, M., and Rickauer, M. (2015). Physiological characterisation of ascochyta rabiei (Pass.) lab. isolated from diseased chickpea fields in six regions of northwestern Algeria. *American-Eurasian J. Agric. Environ. Sci.* 15 (6), 1136–1146. doi: 10.5829/idosi.aejaes.2015.15.6.94125

Marino, D., Peeters, N., and Rivas, S. (2012). Ubiquitination during plant immune signaling. *Plant Physiol.* 160 (1), 15–27. doi: 10.1104/pp.112.199281

Mazurier, M. (2018). Biodiversity and adaptation to root pathogen verticillium alfalfae at medicago truncatula. importance of micro-evolution [Ph.D. dissertation]. [Toulouse (France)] (Université Toulouse 3 Paul Sabatier). Available at: https://tel.archives-ouvertes.fr/OMP-ECOLAB-TEL/tel-01927066v1.

McKoy, J. F., and Trinci, A. P. J. (1987). Sporulation of verticillium agaricinum and schizosaccharomyces pombe in batch and chemostat culture. *Trans. Br. Mycological Society. Br. Mycological Soc.* 88 (3), 299–307. doi: 10.1016/s0007-1536(87)80002-5

Miller, R. N. G., Alves, G. S. C., and Van Sluys, M. A. (2017). Plant immunity: Unravelling the complexity of plant responses to biotic stresses. *Ann. Bot.* 119 (5), 681–687. doi: 10.1093/aob/mcw284

Muller, W. H. (1956). Influence of temperature on growth and sporulation of certain fungi. *Botanical Gazette.* 117 (4), 336–343. doi: 10.1086/335920

Oelmüller, R., Peškan-Berghöfera, T., Shahollaria, B., Trebickab, A., Sherametia, I., and Varma, A. (2005). MATH domain proteins represent a novel protein family in arabidopsis thaliana, and at least one member is modified in roots during the course of a plant-microbe interaction. *Physiologia Plantarum* 124 (2), 152–166. doi: 10.1111/j.1399-3054.2005.00505.x

Ogura, T., and Busch, W. (2015). From phenotypes to causal sequences: Using genome wide association studies to dissect the sequence basis for variation of plant development. *Curr. Opin. Plant Biol.* 23, 98–108. doi: 10.1016/j.pbi.2014.11.008

Okada, K., Abe, H., and Arimura, G. I. (2015). Jasmonates induce both defense responses and communication in monocotyledonous and dicotyledonous plants. *Plant Cell Physiol.* 56 (1), 16–27. doi: 10.1093/pcp/pcu158

Pegg, G. F., and Brady, B. L. (2002). *Verticillium wilts. illustrate* Vol. 552. Ed. B. L. Brady. (Wallingford, Oxon OX10 8DE, UK: CABI Pub., CAB International). Available at: https://books.google.fr/books/about/Verticillium_Wilts.html?id=Ks4tbrkiR8cC&redir_esc=y.

Pešić, V., Smit, H., and Saboori, A. (2014). Checklist of the water mites (Acari, hydrachnidia) of Iran: Second supplement and description of one new species. *Ecologica Montenegrina* 1 (1), 30–48. doi: 10.37828/em.2014.1.6

Pham, J., Liu, J., Bennett, M. H., Mansfield, J. W., and Desikan, R. (2012). Arabidopsis histidine kinase 5 regulates salt sensitivity and resistance against bacterial and fungal infection. *New Phytol.* 194 (1), 168–180. doi: 10.1111/j.1469-8137.2011.04033.x

Poland, J. A., Balint-Kurti, P. J., Wisser, R. J., Pratt, R. C., and Nelson, R. J. (2009). Shades of gray: the world of quantitative disease resistance. *Trends Plant Sci.* 14 (1), 21–29. doi: 10.1016/j.tplants.2008.10.006

R Core Team (2020). *'R: A language and environment for statistical computing. r foundation for statistical computing'* (Vienna; Austria: R Foundation for Statistical Computing). Available at: http://www.r-project.org/.

Roumen, E. C. (1994). The inheritance of host plant resistance and its effect on the relative infection efficiency of magnaporthe grisea in rice cultivars. *Theor. Appl. Genet.* 89 (4), 498–503. doi: 10.1007/BF00225386

Rout, E., Nanda, S., and Joshi, R. K. (2016). Molecular characterization and heterologous expression of a pathogen induced PR5 gene from garlic (Allium sativum l.) conferring enhanced resistance to necrotrophic fungi. *Eur. J. Plant Pathol.* 144 (2), 345–360. doi: 10.1007/s10658-015-0772-y

Sbeiti, A. A., Mazurier, M., Ben, C., Rickauer, M., and Gentzbittel, L. (2023). 'Temperature increase modifies susceptibility to verticillium wilt in medicago spp and may contribute to the emergence of more aggressive pathogenic strains'. *Front. Plant Science.* 14. doi: 10.3389/fpls.2023.1109154

Schmittgen, T. D., and Livak, K. J. (2008). Analyzing real-time PCR data by the comparative CT method. *Nat. Protoc.* 3 (6), 1101–1108. doi: 10.1038/nprot.2008.73

Shen, Y., Liu, N., Li, C., Wang, X., Xu, X., Chen, W., et al. (2017). 'The early response during the interaction of fungal phytopathogen and host plant'. *Open Biol.* 7 (5), 170057. doi: 10.1098/rsob.170057

Tang, H., Krishnakumar, V., Bidwell, S., Rosen, B., Chan, A., Shiguo Zhou, S., et al. (2014). An improved genome release (version Mt4.0) for the model legume medicago truncatula. *BMC Genomics* 15 (1), 1–14. doi: 10.1186/1471-2164-15-312

Toueni, M., Ben, C., Le Ru, A., Gentzbittel, L., and Rickauer, M. (2016). 'Quantitative resistance to verticillium wilt in medicago truncatula involves eradication of the fungus from roots and is associated with transcriptional responses related to innate immunity'. *Front. Plant Sci.* 7 (September). doi: 10.3389/fpls.2016.01431

Turner, S. D. (2018). 'qqman: an r package for visualizing GWAS results using q-q and manhattan plots'. *J. Open Source Software* 3 (25), 731. doi: 10.21105/joss.00731

Vogel, J., and Somerville, S. (2000). Isolation and characterization of powdery mildew-resistant arabidopsis mutants. *Proc. Natl. Acad. Sci. United States America* 97 (4), 1897–1902. doi: 10.1073/pnas.030531997

Wang, M., Jiang, N., Jia, T., Leach, L., Cockram, J., Waugh, R., et al. (2012). Genome-wide association mapping of agronomic and morphologic traits in highly structured populations of barley cultivars. *Theor. Appl. Genet.* 124 (2), 233–246. doi: 10.1007/s00122-011-1697-2

White, T.J., Bruns, T., Lee, S., and Taylor, J. (1990). 'Amplification and direct sequencing of fungal ribosomal rand genes for phylogenetics'. in: *PCR protocols a guide to methods and applications*., eds: M. A. Innis, D. H. Gelfand, J. J. Sninsky and T. J. White (San Diego: Academic Press), 315–322. doi: 10.1016/B978-0-12-372180-8.50042-1

Wojtaszek, P. (1997). Oxidative burst: An early plant response to pathogen infection. *Biochem. J.* 322 (3), 681–692. doi: 10.1042/bj3220681

Yin, C.-C., Ma, B., Collinge, D. P., Pogson, B. J., He, S. J., Xiong, Q., et al. (2015). Ethylene responses in rice roots and coleoptiles are differentially regulated by a carotenoid isomerase-mediated abscisic acid pathway. *Plant Cell* 27 (4), 1061–1081. doi: 10.1105/tpc.15.00080

Yu, J., and Buckler, E. S. (2006). Genetic association mapping and genome organization of maize. *Curr. Opin. Biotechnol.* 17 (2), 155–160. doi: 10.1016/j.copbio.2006.02.003

Yu, L.-X., Zheng, P., Zhang, T., Rodringuez, J., and Main, D. (2017). Genotyping-by-sequencing-based genome-wide association studies on verticillium wilt resistance in autotetraploid alfalfa (Medicago sativa l.). *Mol. Plant Pathol.* 18 (2), 187–194. doi: 10.1111/mpp.12389

Zapata, J. M., Martínez-García, V., and Lefebvre, S. (2007). 'Phylogeny of the TRAF/MATH domain', in *TNF receptor associated factors (TRAFs)* (New York, NY: Springer New York), 1–24. doi: 10.1007/978-0-387-70630-6_1

Zhang, Z., Ersoz, E., Lai, C.-Q., Todhunter, R. J., Tiwari, H. K., Gore, M. A., et al. (2010). Mixed linear model approach adapted for genome-wide association studies. *Nat. Genet.* 42 (4), 355–360. doi: 10.1038/ng.546

Zhang, T., Yu, L.-X., McCord, P., Miller, D., Bhamidimarri, S., Johnson, D., et al. (2014). 'Identification of molecular markers associated with verticillium wilt resistance in alfalfa (Medicago sativa l.) using high-resolution melting'. *PloS One* 9 (12), e115953. doi: 10.1371/journal.pone.0115953

Zhang, L., Liu, J., Cheng, J., Sun, Q., Zhang, Y., Liu, J., et al. (2022). 'lncRNA7 and lncRNA2 modulate cell wall defense genes to regulate cotton resistance to verticillium wilt'. *Plant Physiol.* 189 (1), 1–21. doi: 10.1093/plphys/kiac041

Zhao, H., Duan, K.-X., Ma, B., Yin, C. C., Hu, Y., Tao, J. J., et al. (2020). 'Histidine kinase MHZ1/OsHK1 interacts with ethylene receptors to regulate root growth in rice'. *Nat. Commun.* 11 (1), 518. doi: 10.1038/s41467-020-14313-0

Zhu, H., Choi, H. K., Cook, D. R., and Shoemaker, R. C. (2005). Bridging model and crop legumes through comparative genomics. *Plant Physiol.* 137 (4), 1189–1196. doi: 10.1104/pp.104.058891

Zipfel, C. (2014). Plant pattern-recognition receptors. *Trends Immunol. Elsevier Ltd* 35 (7), 345–351. doi: 10.1016/j.it.2014.05.004

frontiers | Frontiers in Plant Science

TYPE Original Research
PUBLISHED 09 May 2023
DOI 10.3389/fpls.2023.1115420

OPEN ACCESS

EDITED BY
Tika Adhikari,
North Carolina State University,
United States

REVIEWED BY
Adnan Šišić,
University of Kassel, Germany
Kurt Heungens,
Fisheries and Food Research (ILVO),
Belgium

*CORRESPONDENCE
Syama Chatterton
syama.chatterton@agr.gc.ca

SPECIALTY SECTION
This article was submitted to
Plant Pathogen Interactions,
a section of the journal
Frontiers in Plant Science

RECEIVED 04 December 2022
ACCEPTED 03 April 2023
PUBLISHED 09 May 2023

CITATION
Chatterton S, Schwinghamer TD, Pagé A, Davidson RB, Harding MW and Banniza S (2023) Inoculum dose–disease response relationships for the pea root rot pathogen, *Aphanomyces euteiches*, are dependent on soil type and other pathogens.
Front. Plant Sci. 14:1115420.
doi: 10.3389/fpls.2023.1115420

Inoculum dose–disease response relationships for the pea root rot pathogen, *Aphanomyces euteiches*, are dependent on soil type and other pathogens

Syama Chatterton[1]*, Timothy D. Schwinghamer[1], Antoine Pagé[2], Robyne Bowness Davidson[3], Michael W. Harding[4] and Sabine Banniza[5]

[1]Lethbridge Research and Development Centre, Agriculture and Agri-Food Canada, Lethbridge, AB, Canada, [2]Aquatic and Crop Resource Development, National Research Council Canada, Montreal, QC, Canada, [3]Applied Research, Lakeland College, Lacombe, AB, Canada, [4]Plant and Bee Health Surveillance, Alberta Ministry of Agriculture and Irrigation, Brooks, AB, Canada, [5]Crop Development Centre, University of Saskatchewan, Saskatoon, SK, Canada

The oomycete pathogen, *Aphanomyces euteiches*, was implicated for the first time in pea and lentil root rot in Saskatchewan and Alberta in 2012 and 2013. Subsequent surveys from 2014 to 2017 revealed that *Aphanomyces* root rot (ARR) was widespread across the Canadian prairies. The absence of effective chemical, biological, and cultural controls and lack of genetic resistance leave only one management option: avoidance. The objectives of this study were to relate oospore levels in autoclaved and non-autoclaved soils to ARR severity across soil types from the vast prairie landscape and to determine the relationship of measured DNA quantity of *A. euteiches* using droplet digital PCR or quantitative PCR to the initial oospore inoculum dose in soils. These objectives support a future end goal of creating a rapid assessment method capable of categorizing root rot risk in field soil samples to aid producers with pulse crop field selection decisions. The ARR severity to oospore dose relationship was statistically significantly affected by the soil type and location from which soils were collected and did not show a linear relationship. For most soil types, ARR did not develop at oospore levels below 100/g soil, but severity rose above this level, confirming a threshold level of 100 oospores/g soil for disease development. For most soil types, ARR severity was significantly higher in non-autoclaved compared to autoclaved treatments, demonstrating the role that other pathogens play in increasing disease severity. There was a significant linear relationship between DNA concentrations measured in soil and oospore inoculum concentration, although the strength of the relationship was better for some soil types, and in some soil types, DNA measurement results underestimated the number of oospores. This research is important for developing a root rot risk assessment system for the Canadian prairies based on soil inoculum quantification, following field validation of soil quantification and relationship to root rot disease severity.

KEYWORDS

***Aphanomyces* root rot, oospore, inoculum dose, PEA, droplet digital PCR, soil texture**

Introduction

Aphanomyces euteiches is the most destructive root rot pathogen of pea in areas with a humid climate (Levenfors et al., 2003). This pathogen is widespread in North America, Europe, Japan, Australia, and New Zealand (Gangneux et al., 2014), but, until 2012, it was not considered a pathogen of concern to pea fields in Alberta and Saskatchewan (Banniza et al., 2013; Chatterton et al., 2015). Intego Solo (a.i., ethaboxam) is the only product registered for early-season suppression of *Aphanomyces* root rot, but it does not reduce disease severity ratings of root rots occurring past the seedling stage (Willsey et al., 2021). Dinitroaniline (e.g., Edge and Treflan) herbicides were effective in Japan and the United States in field trials (Jacobsen and Hopen, 1981), but they are currently not used extensively for disease management. Biological control products were efficacious in field trials conducted in Canada (Xue, 2003), but the suppressive effects can be variable, and there are no commercially available biological control products registered for root rot suppression or management. Incorporation of green manures from Brassicaceae or other soil amendments (e.g., spent lime) suppressed *Aphanomyces* root rot, but the implementation in large-scale field operations is limited (Williams-Woodward et al., 1997; Heyman et al., 2007; Hossain et al., 2012). Therefore, there are currently no efficacious in-crop or preventative treatments available to reduce the impact of *Aphanomyces* root rot. Crop rotation is ineffective in the short term due to the long-term viability of oospores in the soil (Pfender and Hagedorn, 1983), although resistant pulse crops (e.g., faba bean or chickpeas) can be planted instead of susceptible host crops (peas, lentil, alfalfa, and dry bean) (Hughes and Grau, 2007). *Aphanomyces* root rot-resistant pulse crops are not a viable option in all of the growing regions of Saskatchewan and Alberta and may not be attractive alternatives due to market constraints. There are currently no resistant field pea varieties available in North America, although partially resistant germplasm was identified, and new quantitative trait loci were described by Hamon et al. (2013) and McGee et al. (2012). The absence of effective chemical, biological, and cultural control and lack of genetic resistance leave only one management option: growing pulse crops in low-risk fields.

In areas with endemic *A. euteiches* problems, the most recommended practice is disease avoidance based on determining inoculum potential of field soil indexing through greenhouse grow-out tests in field soils (Levenfors et al., 2003; Hughes and Grau, 2007; Sauvage et al., 2007; Gangneux et al., 2014; Harveson et al., 2014). Inoculum potential is an index of potential disease activity of the soil dependent on pathogen infectivity and density and soil factors that can either inhibit or promote infection (Malvick et al., 1994; Moussart et al., 2009). Historically, inoculum potential was determined in a greenhouse bioassay by growing a susceptible pea cultivar in collected field soils under conditions that are conducive to disease development (e.g., seeds treated with metalaxyl and water-saturated conditions; Malvick et al., 1994). A strong positive correlation between disease severities obtained in the greenhouse compared to those observed in the field allows this bioassay to be used as a predictive test. Predictive tests were, however, labor and time intensive, and they often failed to motivate stakeholders, owing to the expense and lack of real-time information. Quantitative molecular techniques like droplet digital PCR or quantitative PCR can be a more efficient method to determine the presence and quantity of *A. euteiches* in soil (Gangneux et al., 2014; Gibert et al., 2021).

Although *A. euteiches* is the most destructive pathogen to pea roots, it often is detected as a complex with other soilborne pathogens (Chatterton et al., 2019). A number of *Fusarium* species were commonly isolated from pea roots in southern Alberta, Canada (Esmaeili Taheri et al., 2017), and *F. avenaceum* and *F. solani* were the most aggressive among tested species (Safarieskandari et al., 2021). Co-inoculation of *A. euteiches* with these two species, and the weakly aggressive *F. redolens*, resulted in statistically significantly higher disease severity ratings compared to single-species inoculation (Willsey et al., 2018). Therefore, the synergistic interactions of *A. euteiches* with other soil pathogens may affect disease severity. In this context, the bioassay may be more predictive, in some cases, than DNA-based analyses of *A. euteiches* alone.

Currently, pulse producers in the Canadian prairies can submit root and soil samples to several commercial laboratories to obtain confirmation on the presence or absence of *A. euteiches*, but no meaningful information on the risk of growing a susceptible crop is provided. A new TaqMan-based multiplex quantitative PCR (qPCR) assay for *A. euteiches*, *Fusarium avenaceum*, and *F. solani* for the purpose of quantifying these pathogens in root tissue (Willsey et al., 2018), a SYBR-green-based qPCR assay (Gangneux et al., 2014), and a ddPCR assay (Gibert et al., 2021) for *A. euteiches* oospores in soil were recently published. There are, however, challenges with detection and quantification of pathogen DNA in soil. First, obtaining representative samples from entire fields is extremely challenging due to field sizes on the Prairies and the irregular distribution of soilborne pathogens. Second, the presence of PCR inhibitors in soil can suppress amplification. Both challenges can lead to false negative results. Adequate sample collection, proper soil preparation, and homogenization can reduce the confounding impact of patchy pathogen distribution in soils. Droplet digital PCR is presumably less sensitive to PCR inhibitors because the inhibitor substances may become sequestered in the individual nano-droplets from DNA molecules (Gibert et al., 2021). As a result, improvements in sample collection, preparation/homogenization, and PCR methodologies can help to ameliorate these challenges.

Field pea is cultivated in a large geographical area across the Canadian prairies, as production spans three major soil zones (black, dark brown, and brown chernozemic soils) owing in part to differences in precipitation, temperature, and native vegetation (Fuller, 2010). Black soils are characterized by high organic matter (5–8.5%) and a low mean annual water deficit of 6.5–13 cm; dark brown by high clay content, moderate organic matter (3.5%–5%), and water deficit (13–19 cm); and the semi-arid brown soil zone with the lowest organic matter (2.5%–3.4%) and highest water deficit (19–38 cm) (Fuller, 2010). Moderate to severe levels of *Aphanomyces* root rot occurs in all of these soil zones (Chatterton et al., 2019). Inoculum potential can be affected by soil type and characteristics (Persson and Olsson, 2000).

With the long-term goal of developing a molecular-based quantification system for measuring *A. euteiches* inoculum potential of prairie soils, the objectives of this study were to 1) relate spiked oospore levels in soils to disease severity for the three common soil zones and types of the Prairies (treatment = three soil zones comprising four soil types); 2) determine whether global soil microbiomes affect the above relationships (treatment = autoclaved or raw (non-autoclaved) soils); and 3) adapt a droplet digital protocol for quantification of *A. euteiches*, *F. avenaceum*, and *F. solani* in soils and use the assay to determine the relationship of measured DNA quantity of *A. euteiches* using ddPCR and qPCR to the starting oospore inoculum dose in soils and determine whether background levels of the two *Fusarium* species affected the disease severity. These objectives support a future end goal of creating a rapid assessment method capable of categorizing root rot risk in field soil samples, aiding producers in pulse crop field selection decisions on the Canadian Prairies.

Materials and methods

Soil samples

Soil samples were collected from three soil zones (black, dark brown, and brown) from different fields in Alberta and Saskatchewan in fall of 2015 and 2016. Fields without a history of pulse production were chosen for sampling with the assumption that they would not contain natural inoculum of *A. euteiches*, as the frequency of legumes cropped in a soil is a major indicator of disease risk (Oyarzun et al., 1993). Bulk soil from the top 0–20 cm was collected in large plastic tubs and stored at 4°C. Five days prior to the start of a trial, half of the soil from each location was autoclaved three times at 121°C for 60 min, mixed by shaking the autoclave bag, followed by a 24-h rest period between runs. Soil was autoclaved with the intention of removing any soilborne pathogens and determining the effect of the absence of a global microbiome on disease severity responses. The other half was not autoclaved and served as the raw or non-autoclaved treatment. Soil was then air-dried for 2 days in a drying room so that moisture was roughly equivalent between all soil batches, but the starting soil moisture level was not measured. The soil texture (% sand, silt, and clay) and total percent nitrogen and organic carbon were determined by a commercial soil testing lab (Down to Earth Labs; Lethbridge, AB).

Preparation of oospores and soil inoculations

Four isolates (Ae1, Ae4, Ae6, and Ae7) of *A. euteiches*, obtained previously from diseased pea roots in Alberta and Saskatchewan (Sivachandra Kumar et al., 2021), were maintained on cornmeal agar (CMA, Sigma-Aldrich, Oakville ON) at room temperature. A mycelia plug of each isolate was transferred to CMA and grown for 3 days, before transfer to homogenized and filtered oatmeal broth in Erlenmeyer flasks (5 plugs/30 ml broth) (Windels, 2000). Each isolate was grown separately with five flasks per isolate. The flasks were then incubated in the dark for 30–45 days. After incubation, the mycelial mats with oospores were homogenized in a Waring blender for 5 min and filtered through four layers of cheesecloth to separate the oospores (Gangneux et al., 2014). The resulting suspension was then centrifuge filtered through 100-µm cell strainers (VWR, Edmonton AB) at 4,000 rpm. The concentration of oospores in the suspension of each isolate was counted using a hemocytometer. The volume of initial oospore suspension of each isolate needed to result in total oospore concentrations of 1,000, 500, 100, 10, and 1 oospores/g soil was calculated, and appropriate amounts to give an equal concentration of each isolate in the mixture were then added to 250 ml of sterile distilled water (SDW). This was then added to 1,250 g of each autoclaved and non-autoclaved soil batch for each target concentration and mixed thoroughly by hand. For the control (0 oospore/g soil), 250 ml of SDW was added to the soils. Square pots (5 cm) were filled with 250 g of soil, with four replicates per treatment, and each pot was placed into a 1-lb plastic bag to catch water run-off and reduce cross-contamination between pots. The experimental layout was as follows: (1) three soil zones (brown, dark brown, and black) collected from one different field per year (2015 and 2016) and per province (Saskatchewan and Alberta) for a total of 12 sources; (2) oospore concentrations, 0, 1, 10, 100, 500, and 1,000 oospores/g soil with an equal amount of each isolate; and (3) autoclaved or non-autoclaved soil. The trial was performed as a randomized complete block design, with all treatment combinations for each year (72 in total per trial) randomized within four trays (24 pots per tray), which were considered to represent one block. Trials were conducted within 2–3 months of collecting the soil and performed twice for each soil source.

Plant growth and disease rating

Five pea seeds (cv. CDC Meadow) were planted into each pot containing soil prepared as described above. Seeds were surface disinfested for 5 min in 0.5% NaOCl (10% bleach) with a drop of Tween 20 and then washed three times with sterile distilled water (SDW) prior to planting. A preliminary trial was performed to determine whether the different soil types required different watering regimes based on water holding capacity. While some soil types drained faster than others, there did not appear to be any advantage in watering the different soil types with varying volumes of water. As the extra labor and time required did not outweigh small but non-significant differences in disease observed, all experimental pots were watered until run-off every other day. This watering regime kept all soil types sufficiently saturated for disease development. Plants were grown for 5 weeks under standard greenhouse conditions (16:8 h photoperiod, 22°C and 18°C day/night). Roots were washed, and each plant rated for disease on a 0 (no disease)–5 (dead) *Aphanomyces* root rot scale, based on percentage discoloration of the roots, 1 = 1%–25% root discoloration; 2 = 26%–50% root discoloration; 3 = 51%–75% root discoloration; 4 = 76%–100% discoloration; and 5 = dead plant (Papavizas and Ayers, 1974). The disease severity ratings for each pot were converted to a disease severity index (DSI) from 0 to 1

by summing the product of the number of plants in each category by each disease rating category and dividing by the total number of plants rated multiplied by the maximum disease scale. Tests for unequal variance (Levene's and Bartlett's) between trials were not significant (JMP 16.0, SAS Institute Inc., Cary, NC), allowing the DSI values from repeated trials for each soil to be pooled for analysis. Although isolations were not performed from all of the roots rated in the experiments due to the overwhelming number of roots generated, random roots from some of the zero oospores soils that showed disease symptoms were plated out after surface disinfestation onto PDA amended with 0.15 g L^{-1} penicillin (Gold Biotechnology, St. Louis, MO, USA) and 0.15 g L^{-1} streptomycin sulfate (Sigma-Aldrich, St. Louis, MO, USA) as described in Esmaeili Taheri et al. (2017). Cultures growing from roots were noted and a presumptive identification made based on colony morphology, but the precise numbers of each colony type were not counted nor were cultures further identified to species.

DNA extraction and pathogen quantification

Immediately after adding oospores to the soil at the various doses from the samples tested in 2016 only, an aliquot (~50 g) was removed from each treatment batch. This soil was stored at −20°C until processing for extraction. DNA was extracted in duplicate from 250 mg soil samples from each repeated trial (= 4 biological replicates per oospore treatment level), collected from the 50 g retained soil aliquot, using the PowerSoil DNA extraction kit according to manufacturer's instructions (Qiagen, Toronto, ON). A tetraplex BioRad digital droplet PCR (ddPCR) assay was optimized to quantify three pea root rot pathogens in each DNA extract, using the following targets: the Internal Transcribed Spacer region (ITS) of *Aphanomyces euteiches* (Ae), partial translation elongation factor (TEF) gene of *Fusarium solani* (Fs) and *Fusarium avenaceum* (Fa), and the lipid transfer protein 3 gene from *Triticum aestivum* (TaLTP3) as an internal standard to ensure that amplification had occurred in the event that all of the pathogen targets within a sample were zero (Table 1). A total of 10 µl of 10^5 copies/µl of TaLTP3 gBlock synthetic DNA [Integrated DNA Technologies (IDT), Coralville, IA] was added to each 250 mg soil sample prior to extraction. The optimized parameters included the primer/probe concentration, the template volume (2–8 µl), and the addition of bovine serum albumin (BSA) at high template volumes to eliminate a previously observed "rain" effect (Hughesman et al., 2016). Primer/probes were tested sequentially using different concentrations ranging from 0.25 to 0.75 µM, except for *F. solani*, which was tested up to 1.0 µM, so that two targets could be separated based on amplitude while using the same fluorophore (Supplementary Table S1, Biorad, 2016). Higher primer concentrations were assigned to the target that displayed higher fluorescence values during droplet analysis, which helped separate the target droplets with sufficient margin for a clear cut-off value. For Ae and TaLTP3, differing template volumes of 2–8 µl (Supplementary Table S1) were added to the reactions to determine if increasing template volume allowed for better detection of the target if present at a low concentration (e.g., low infested field soil). Although detection frequency of low-target copies improved with increased DNA template volume, the "rain" effect increased, which made it difficult to separate out targets (data not shown). BSA was added at low concentrations (Supplementary Table S1) to mitigate the "rain" effect from high concentration samples (Biorad technical support personal communication, 2016), lowering the chance of a false positive, but this did not improve detection. Therefore, 2 µl (50 ng total) of template DNA was used for the soil DNA assays. The final optimized 25 µl ddPCR reaction consisted of 12.5 µl ddPCR™ Supermix for Probes no UTP (BioRad, Mississauga, ON), 5.71 µl of primer/probe pool as shown in Table 1, 2 µl of sample, and 4.79 µl ddH_2O. A no template control (NTC) and DNA extracted from oospores of each *A. euteiches* isolate at 10, 100, and 2,500 oospores/ml were included as a positive control. Preliminary testing had indicated that 2,500 oospores/ml was the upper limit of detection, and targets became oversaturated above this level. DNA extracted from 1,000 spores/ml of the two *Fusarium* species was also included as a positive control. The ddPCR reactions were then loaded onto a ddPCR™ 96-well plate, heat sealed using the PX1 plate sealer (BioRad, Mississauga, ON) with pierceable foil heat seal, then loaded onto the QX200 Automated Droplet Generator (AutoDG, BioRad, Mississauga, ON). The AutoDG was loaded as per the specifications of the manufacturer. Briefly, DG32 automated droplet generator cartridges, 2–120 µl pipets for AutoDG system, the sealed ddPCR plate, a cold block with a sample-receiving plate, and automated droplet generation oil for probes were loaded into their respective positions and run. After droplet generation, the sample plate was sealed with foil, then loaded onto the BioRad C1000 touch thermal cycler (BioRad). The ddPCR program was as follows: 98°C for 10 min followed by 40 cycles of 94°C for 30 s and 60°C for 1 min and finally 98 °C for 10 min. The ddPCR plate was then transferred to the QX200 droplet reader (BioRad) for droplet analysis. DNA quantification results were returned as the number of target gene copies per microliter of reaction calculated by the QuantaSoft software (BioRad). The copies per microliter value of the no template control was subtracted from all values of the sample wells before proceeding with analysis.

To compare the generated ddPCR data for *A. euteiches* to previously published quantitative PCR (qPCR) data (Willsey et al., 2018), analyses were subsequently conducted using a QuantStudio™ Analysis Pro instrument (Applied Biosystems, Mississauga, ON) with the same DNA extracts using the protocol described in Willsey et al., 2018. The Ct values were used to calculate copies per microliter of reaction based on a standard curve using gBlock synthetic DNA [Integrated DNA Technologies (IDT), Coralville, IA] of the target gene sequences from 10 to 10^6 copies/µl that was included with each qPCR assay run. The generated Ct values were automatically converted to gene copies/microliter by the QuantStudio real-time PCR program (Applied Biosystems) based on the standard curve. For both ddPCR and qPCR, gene copies per microliter were then used to calculate the number of cells per gram of soil based on the assumption that there are 190 ITS copies per *A. euteiches* diploid oospore (Gangneux et al., 2014), which were then transformed using $\log_{10} + 1$ to account for zeroes in the spiked and measured oospore concentration. For

TABLE 1 Primer and probe sequences and their concentrations used in the tetraplex multiplex assay.

Oligonucleotide Name	Sequence (5`-3`)	Concentration in ddPCR (μM)	Reference
Ae1.2-ITS_Fwd	CCT GCG GAA GGA TCA TTA CC	0.38	Willsey et al. (2018)
Ae1.2-ITS_Rev	AAA ATT ACA TCG GTT CCT TGC G	0.38	
Ae1.2-ITS Probe	56-FAM/TTC TTT ATG/ZEN/AGG CTT GTG CTC TT/ 3IABkFQ	0.20	
F_Sol_Fwd	GCG CCT TAC TAT CCC ACA TC	1.00	Zitnick-Anderson et al. (2018)
F_Sol_Rev	TTT TGT GAC TCG GGA GAA GC	1.00	
F_Sol_Probe	56-FAM/CCT CCG/ZEN/CGA CAC GCT CT/3IABkFQ	0.50	
FaveSS-Fwd	AAG GCA TGG TGT GA	0.75	designed in house
FaveSS-Rev	TCG CTC TCT GGA AGT TCG	0.75	
Fave-SS-Probe	5-HEX/ACT CCT CGC/ZEN/TAC TAT GTC ACC GTC A/ 3IABkFQ	0.38	
TaLTP3-178F	GCAGGTGGACTCCAAGCTC	0.38	Foroud (2011)
TaLTP3-320R	GGCACCTGCACGCTATCT	0.38	
TaLTP3 Probe	5-HEX/CTC GAT CAG/ZEN/CAA GGA GTG CT/3IABkFQ	0.20	

Ae, *Aphanomyces euteiches*; F. sol, *Fusarium solani*; F. ave, *Fusarium avenaceum*; TaLTP3, lipid transfer protein 3 gene from *Triticum aestivum*.

estimated concentration of the two *Fusarium* species in soil, the number of TEF1 gene copies per gram soil was $\log_{10}$ + 1 transformed prior to statistical analysis.

Statistical modeling of disease severity index data

Statistical modeling of the DSI data was performed in two steps, both conducted with software suite SAS 9.4 (SAS Institute Inc., Cary, NC). This process was selected to sequentially a) assess the impact that differences in the predictor variables (oospore level, soil zone, soil type, treatment, and year) have on the response variable DSI and b) precisely describe the soil *A. euteiches* oospore level to pea disease severity (DSI) relationships.

The effects of the predictor variables on the response variable DSI were estimated by generalized linear mixed modeling with the GLIMMIX procedure. As the distribution of percentage data is beta-distributed, the beta distribution was specified (DIST = BETA) for the modeling of DSI with the SAS PROC GLIMMIX default logit (log-odds) link function for a beta model. The assumption of variance homogeneity was tested based on the Bayesian information criterion (BIC) goodness of fit estimator. The Gaussian normal distribution of the residuals was not assumed, the models were therefore "generalized." The fixed effects of oospore level, soil zone, soil type, treatment, year, and the interaction effects on the response variable DSI were evaluated using a series of effect slices. Year was included in the model to account for soils that were collected from the same general location (or closest town) so had the same texture and soil zone profile, but were from a different field that may have had different cropping histories and global microbiome. However, this term also includes the effect of experiment variation, as experiments were performed in the different years in which the soils were collected. The effect of trial was included as an initial term in the analysis, but this term is a covariate of the "texture × type × year" interaction, since different "texture × type × year" combinations were tested in different trials. Effect slices of trial by oospore concentration, treatment, and each texture × type × year combination showed that the measured DSI was different in repeated trials for 10 out of the total of 144 combinations (data not shown). Thus, measurement of DSI was fairly consistent over repeated trials, and subsequently trial was not included in the final model. To visualize the relationship between oospore level and DSI, graphs were produced in SigmaPlot 14.5 using the PROC GLIMMIX estimates of inverse-linked least squares-means and standard errors.

Comparison of methods for the quantification of *A. euteiches* oospore levels in soil

The *A. euteiches* qPCR (Ct value standard curve to gene copy number) and ddPCR (gene copy number) results were converted to $\log_{10}$ (oospores + 1)/g soil so that they could be directly compared to each other and to the starting concentrations of $\log_{10}$ (oospores + 1)/g soil applied to the soils. The relationships between oospore levels measured using PCR quantification methods and starting oospore inoculum levels was analyzed using linear regressions, and slopes and intercepts were significant for each regression. The least square means and standard errors for each treatment level was determined using JMP 16.0 using the fit model function, and figures were then produced using Microsoft Excel M365 to visualize the relationship. The effects of PCR type (qPCR or ddPCR), treatment (soil autoclaved or non-autoclaved), and field location, and their interaction on regression parameters [intercept (shifted-*t*

distribution) and slope (gamma distribution)] were determined using the GLIMMIX procedure of the statistical software suite SAS 9.4 with output generated from PROC REG estimates of the linear regression intercepts and slopes.

Quantification of *Fusarium* spp. cell levels in soil

The least square means and standard errors of *F. avenaceum* and *F. solani* $\log_{10}$ (TEF1 gene copies + 1)/g soil for each location and treatment level in 2016 were compared using the fit model function in JMP 16.0 and means separated by Tukey's honestly significant difference (HSD).

Results

Soil properties

Although soil was collected from fields according to soil zone, the soil texture analysis revealed that soil zone and soil texture did not always match (Table 2). For example, silt loam soils were collected from locations in the black, brown, and dark brown soil zones in Saskatchewan in 2016. Although there was some variation in the percentage of sand and clay between soils from these three locations, they were all comprised of approximately 50% silt. Therefore, for the analysis of the oospore dose–disease response curves, soil type (texture), soil zone, and year were all used as predictor variables to represent each unique location.

Statistical modeling of disease severity index data

The *F*-tests performed to assess the impact of predictor variables on the response variable DSI demonstrated that differences in the value of predictor variables oospore level, soil zone, soil texture, treatment, and year all had significant contributions to the observed variations in DSI (Table 3). Several variable interactions were also noted, including the four-way interaction soil zone × soil texture × treatment × year (nested in oospore level). Since this interaction was significant, the GLIMMIX analysis was performed again using location as fixed factor. There was a significant difference between locations, oospore level, and all interaction terms, including location × oospore level × treatment (Supplementary Table S2). This test confirmed results of the analysis with the individual terms, but inclusion of the individual terms allowed direct comparisons between factors. Subsequent tests of effect slices indicated that the soil zone, soil texture, and year means of DSI were not equal for various combinations of treatment effects. The tests of effect slices sliced by "soil zone × texture × oospore × treatment" indicated that there were significant differences in DSI between years (2015 and 2016) for the black loam (Figure 1), brown clay loam (Figure 2), and dark brown silty loam and clay loam soils (Figure 3) at several oospore levels in both autoclaved and non-autoclaved soils (Supplementary Table S3).

For the test of effects sliced by "texture × oospore level × treatment × year," there were significant differences between soil zones within each soil texture. Clay loam soils in 2015 were sampled from brown and dark brown soil zones (Figures 2, 3), and there were significant differences between the DSI responses for non-autoclaved soils only (Supplementary Table S4). Silty loam soils were sampled in 2016 from dark brown, brown, and black soil zones (Figures 1–3), and the effect slices indicated that there were significant differences between these soil zones for DSI response at several oospore levels in both autoclaved and non-autoclaved treatments (Supplementary Table S4).

To determine the effect of soil texture on the DSI response, effects were sliced by "zone × oospore level × treatment × year." Loam, sandy loam, and silty loam soils were collected from the black soil zone in 2015 (Figure 1), and DSI differed significantly between these three soil textures in non-autoclaved soils at 10, 100,

TABLE 2 Soil zone, soil type, year, province, closest town, and soil properties for soils used in oospore addition experiments.

Soil Zone	Soil Type	Year	Province	Location	Sand (%)	Silt (%)	Clay (%)	Nitrogen (%)	Organic C (%)
Black	Sandy loam	2015	AB	Lacombe	56.6	27.4	16	0.328	4.035
Black	Silty loam	2016	SK	Melfort	16.5	55.4	28	0.627	6.862
Black	Loam	2015	SK	Rosthern	30.6	47.4	22	0.299	3.525
Black	Loam	2016	AB	Lacombe2	40.5	41.5	18	0.388	4.821
Brown	Loam	2015	SK	Swift Current	38.6	41.4	20	0.142	1.477
Brown	Silty loam	2016	SK	Swift Current2	28.4	51.6	20	0.15	1.459
Brown	Clay loam	2015	AB	Lethbridge	30.6	39.4	30	0.243	2.612
Brown	Clay loam	2016	AB	Rosemary	20.4	43.6	36	0.286	2.775
Dark Brown	Clay loam	2015	AB	Drumheller	32.5	35.5	32	0.468	5.581
Dark Brown	Clay loam	2016	AB	Lethbridge2	28.6	37.4	34	0.304	3.217
Dark Brown	Silty loam	2015	SK	Saskatoon	24.5	55.5	20	0.283	2.915
Dark Brown	Silty loam	2016	SK	Biggar	30.6	51.4	18	0.272	3.531

TABLE 3 Type III tests of fixed effects and their interactions included in the nested GLIMMIX analysis of variables that affected the disease severity index of pea grown in soils collected from three soil zones and four soil textures, autoclaved or non-autoclaved (Treatment), and then inoculated with 0,1, 10, 100, 500, or 1,000 oospores/g soil.

Effect	Num DF*	*F* Value	*p*
Year	1	61.08	<.0001
Zone	2	15.90	<.0001
Texture	3	60.60	<.0001
Treatment	1	5.79	0.0164
OosporeLevel	5	257.07	<.0001
Treatment×Year	1	3.14	0.0770
OosporeLevel×Year	5	2.85	0.0148
Zone×Treatment	2	7.57	0.0006
Zone×OosporeLevel	10	1.09	0.3689
Texture×Treatment	3	5.85	0.0006
Texture×OosporeLevel	15	4.33	<.0001
OosporeLev×Treatment	5	0.56	0.7315
Zone×Texture×Treat(Oos)	49	1.97	0.0001
Zone×Texture×Treat×Year(Oos)	17	3.06	<.0001

*Num DF, numerator degrees of freedom. Denominator degrees of freedom was 794.

and 500 oospores/g soil only (Supplementary Table S5). Loam and clay loam soils were collected in the brown soil zone in 2015 (Figure 2), and the DSI differed between these soil textures at all oospore levels from 0 to 100 in both autoclaved and non-autoclaved treatments, except the autoclaved 0 treatment. Clay loam and silty loam soils were sampled from the brown soil zone in 2016 (Figure 2), and DSI differed between these two soil types at all oospore and treatment levels, except the autoclaved 0 level. Clay loam and silty loam soils were sampled from the dark brown soil zone in 2015 (Figure 3), and there were significant differences between these soil types at several oospore levels in the autoclaved and non-autoclaved treatments.

For the effect of treatment, there were significant differences between autoclaved and non-autoclaved soils for the following combinations: black loam soil in 2015 at 100 and 500 oospores/g soil; black silty loam in 2016 at 100, 500, and 1000 oospores/g soil; brown clay loam in 2015 at 0, 1, and 500 oospores/g soil; and brown clay loam in 2016 at 1,000 oospores/g soil; brown loam in 2015 at 100 and 500 oospores/g soil; brown silty loam in 2016 at 0 and 1 oospores/g soil; dark brown silty loam in 2015 at 1 oospore/g soil; and dark brown silty loam in 2016 at 500 oospores/g soil (Supplementary Table S6). The test of effects sliced by "zone × texture × treatment × year" indicated that there were significant differences between oospore levels for all combinations, and the differences were explored further using simple effect comparison of the means using Scheffe's multiple grouping method.

Low to moderate levels (0.2–0.4 DSI) of disease were observed in the control autoclaved and non-autoclaved soils for all of the "soil zones × texture" combinations (Figures 1–4). For all "soil zone × textures," there was no statistical difference between 0, 1, and 10 oospore levels, except at 10 oospores/g soil in the dark brown silty loam 2015 soil (Figure 3). The DSI at 100 oospores/g soil was significantly higher than the DSI at 0, 1, or 10 oospores/g soil at the following locations and treatments: black silty loam 2016, black loam 2015, dark brown silty loam 2016, and brown loam 2015. For all other locations, except black loam 2016 and dark brown clay loam 2016, the DSI at 100 oospores/g soil was between that at 10 and 500 oospores/g soil and was above 0.5 DSI. In the dark brown clay loam 2016 (Lethbridge2) soil, there was no difference between DSI at any of the oospore levels in the non-autoclaved treatment (Figure 3). For black loam 2016 (Lacombe2), only the DSI at 1,000 oospores/g in the non-autoclaved soil was significantly higher from all of the other oospore levels (Figure 1). For almost all "soil zone × texture" datasets, the maximum DSI ranged from 0.8 to 0.97 at the highest oospore level of 1,000 oospores/g soil (Figures 1–3). The exceptions were dark brown clay loam 2016 (Lethbridge2) and black loam 2016 (Lacombe2), where maximum disease severity was 0.26 and 0.44, respectively, in the non-autoclaved soil, and 0.58 and 0.66, respectively, in the autoclaved soil, at 1,000 oospores/g soil.

DNA quantification of *A. euteiches* levels in soil

The type III tests of fixed effects [field location, PCR type (ddPCR and qPCR), and treatment (autoclaved or non-autoclaved soils)] of the slopes determined from linear regressions between measured oospores and added oospores (Figure 5) showed that all factors, including location (soil zone × texture), and their interactions were significant (Table 4). There was significant difference in the slopes of the regression lines calculated for qPCR and ddPCR for dark brown silty loam, dark brown clay loam, and brown clay loam, with the slope of the qPCR line higher than those of the ddPCR lines (Figure 5, Supplementary Figure S1A, Supplementary Table S8). The slopes for the dark brown clay loam (Lethbridge2) autoclaved ddPCR and qPCR lines were the lowest at 0.61 and 0.66, respectively, indicating significant underestimation of oospore levels in the soil compared to the actual amounts added (Supplementary Figure S1A, Supplementary Table S8). The slopes for the black silty loam (Melfort) autoclaved qPCR and ddPCR lines were the highest at 1.19 and 1.17, respectively, and R^2 values were 0.94 and 0.98 (Supplementary Figure S1A, Supplementary Table S8). For treatment × field location interactions, there were significant differences in the slopes of the lines for autoclaved and non-autoclaved soils from dark brown silty loam, dark brown clay loam, black silty loam, and brown silty loam locations (Figure 5, Supplementary Figure S1A). For dark brown silty loam, dark brown clay loam, and brown silty loam, the slopes for the autoclaved soil lines were lower than the non-autoclaved lines, but the reverse was true for black silty loam.

The type III tests of fixed effects [field location, PCR type (ddPCR and qPCR), and treatment (autoclaved or non-autoclaved soils)] of the intercepts calculated from linear

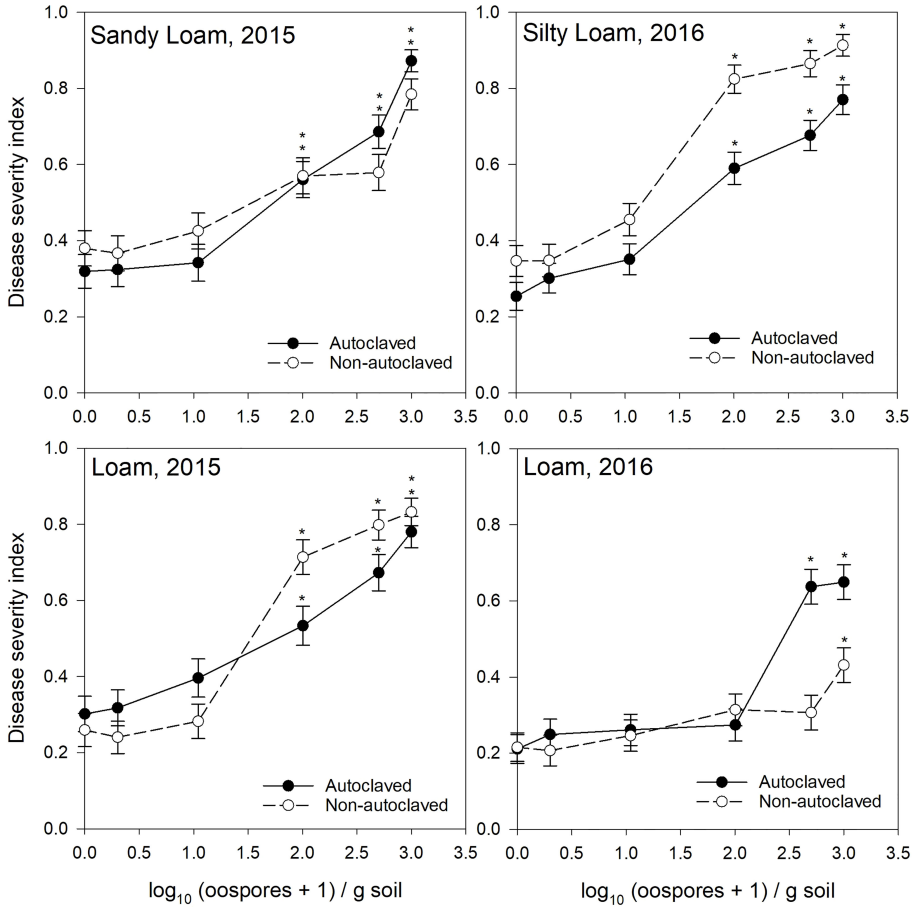

FIGURE 1
Relationship between spiked oospore concentration (log10 + 1 oospores/g dry soil) and disease severity index of *Aphanomyces* root rot on pea grown in autoclaved or non-autoclaved soils collected from black soil zones. Error bars represent the mean population standard error of the experiment. Asterisks (*) indicate treatment combinations that were significantly different from their respective (autoclaved or non-autoclaved) zero spiked oospore control. ** indicates both autoclaved and non-autoclaved treatments were significantly different from the controls.

regressions between measured oospores and added oospores (Figure 5) revealed that only location and the interaction between location and PCR type were significant (Table 4). The intercepts for black loam, brown clay loam, and brown silty loam were significantly different between qPCR and ddPCR (Supplementary Figure S1B). Although there was a large numerical difference between the intercepts for the autoclaved and non-autoclaved black silty loam soil, this difference was not significant due to the large upper and lower confidence limits (Supplementary Figure S1B). The intercepts ranged from as low as −0.41 (ddPCR autoclaved, black silty loam) to as high as 0.76 (qPCR non-autoclaved, black silty loam) (Supplementary Figure S1B, Supplementary Table S8).

Fusarium levels in soil

Levels of *F. avenaceum* and *F. solani* were quantified in soils collected in 2016 using ddPCR. *F. avenaceum* was present in soils from all locations, but levels were very low in brown silty loam (Figure 6). *Fusarium solani* was also present in all soils, but levels were lower in brown silty loam and dark brown silty loam than the other soils (Figure 6). Autoclaving soils significantly reduced the levels of *F. avenaceum* and *F. solani* compared to the non-autoclaved soils but did not completely eliminate their DNA from soils. Although we did not perform isolations from all roots in all of the trials, periodic plating of random root samples from the zero oospore treatments yielded various *Fusarium* species, primarily presumptive *F. avenaceum*, *F. solani*, and *F. redolens* based on colony morphology and common saprophytes like *Rhizopus* and *Penicillium* spp. (data not shown).

Discussion

The primary objective of this study was to relate oospore levels of *A. euteiches* in soil to disease severity for the common soil zones of the Prairies. Care was taken to select a balanced number of fields in each soil zone (black, dark brown, and brown) in each province and year for subsequent testing of the inoculum dose–disease response relationship. However, because there were different soil textures across soil zones, this resulted in an unbalanced design

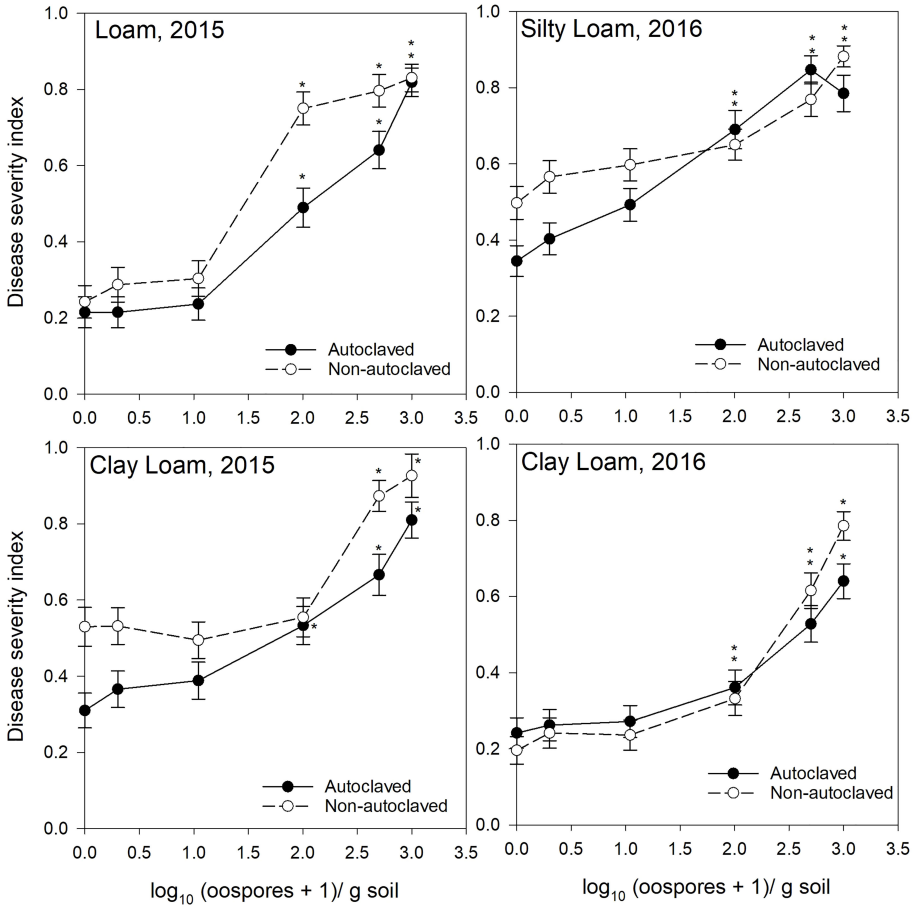

FIGURE 2
Relationship between spiked oospore concentration (log10 + 1 oospores/g dry soil) and disease severity index of *Aphanomyces* root rot on pea grown in autoclaved or non-autoclaved soils collected from brown soil zones. Error bars represent the mean population standard error of the experiment. Asterisks (*) indicate treatment combinations that were significantly different from their respective (autoclaved or non-autoclaved) zero spiked oospore control. ** indicates both autoclaved and non-autoclaved treatments were significantly different from the controls.

when accounting for soil texture × zone interactions. Thus, for statistical analysis, generalized linear mixed modeling with nested factors was used to account for the unbalanced design. This analysis, along with the graphical representation of disease severity levels, clearly showed that there was a differential disease severity outcome to oospore concentrations for each of the different soil textures and zone combinations. Therefore, although the intention of this research was to develop a generalized disease severity–oospore dose model, the nature of the interaction of disease development with the large array of soil zones and textures within the Canadian prairies renders this relationship more complex.

Soil zones are defined by their biogeographic properties that include differences in annual precipitation, temperature, organic matter, and native vegetation (Fuller, 2010), all of which will affect the soil microbiome and ecology. Soil texture, on the other hand, refers to the percent composition of silt, clay, and sand. The percentage of these components affect water holding capacity and drainage, and the physical nature of oospore interactions with soil particles. The combination of both soil zone and texture defines the soil's physicochemical properties, which are known to affect *Aphanomyces* root rot development (Persson and Olsson, 2000). Thus, it was not surprising that both soil zone, texture, and their interaction resulted in differential DSI responses to oospore concentrations in soil. For example, some glacial clay soils (35%–40% clay content) were more conducive to *Aphanomyces* root rot of pea than till clay soils due to their different source material and thus different physicochemical properties (Persson and Olsson, 2000). Generally, high clay soils are more compact with low water permeability, which favors root infection by zoospore-producing pathogens (Persson and Olsson, 2000).

Year was also included in the model, as soils were collected in two different years, and the experiments with each soil set were also performed in two different years. This term was thus included in the model because soil collection year could have affected biological properties (e.g., the global microbiome) of the soil. The year 2015 was warmer and drier than average in Alberta and Saskatchewan, while 2016 was wetter and cooler than average resulting in higher root rot prevalence and incidence in 2016 (Chatterton et al., 2019). Although soils were dried prior to spiking with oospores, differences in weather and local edaphic condition soils experienced prior to collection could have affected microbial community composition

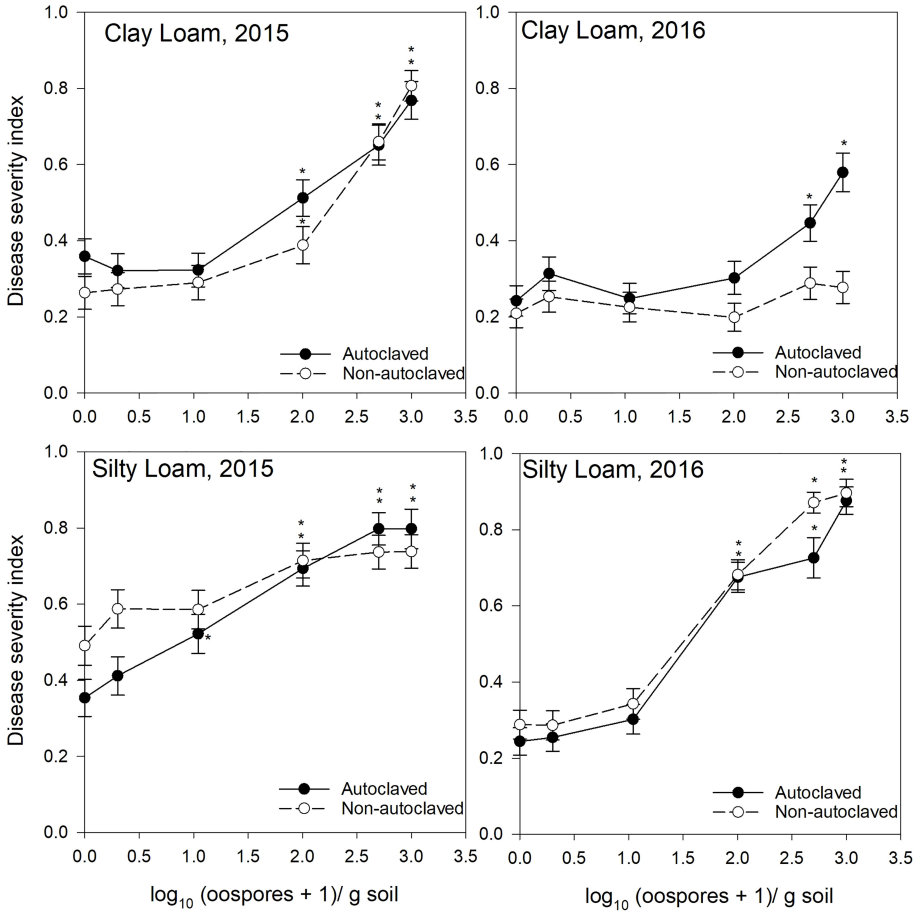

FIGURE 3
Relationship between spiked oospore concentration (log10 + 1 oospores/g dry soil) and disease severity index of *Aphanomyces* root rot on pea grown in autoclaved or non-autoclaved soils collected from dark brown soil zones. Error bars represent the mean population standard error of the experiment. Asterisks (*) indicate treatment combinations that were significantly different from their respective (autoclaved or non-autoclaved) zero spiked oospore control. ** indicates both autoclaved and non-autoclaved treatments were significantly different from the controls.

(Bainard et al., 2016); for example, frequency of pea root rot pathogens was affected by year (Esmaeili Taheri et al. 2017). In addition to the influence of weather on soil microbial communities, the effect of year on experimental variance cannot be fully discounted. Soils collected in 2015 were performed as one experimental batch with two repeated trials, and those collected in 2016 were performed as a separate experimental batch. Therefore, the significance of year in the model could also be due to the variation between experiments. The precise differences in specific soil properties as a combination of soil texture, soil zone, and year (weather and edaphic factors) that account for the differential disease–response relationship observed in this study should be explored further but were beyond the scope of this project.

Even within similar soil zone × texture groups, there were dissimilar responses for the Lethbridge2 (dark brown and clay loam) and Lacombe2 (black and loam) soils from the other locations within their respective soil groupings. Disease severity in these two soils remained low at almost all oospore levels, including 1,000 oospores/g soil, suggesting a suppressive soil effect. Oospore inoculations of the autoclaved soils resulted in some, but not complete, restoration of higher disease levels, suggesting that the suppressive effect is both biotic and abiotic. Both of these fields had a history of compost application. Although compost has been linked to building suppressive soils (Hadar and Papadopoulou, 2012), further investigations of these soils is required to confirm the suppressive effect and elucidate mechanisms.

The other major factor affecting the disease severity–dose response relationship was whether the soil had been autoclaved prior to inoculations. Although autoclaving can alter soil properties (Berns et al., 2008), the primary purpose of autoclaving the soil was to eliminate any other native pathogens in the soil and to also determine the effect of the global soil microbiome by comparing the response between autoclaved and non-autoclaved soils. The response to autoclaving also varied by soil texture and zone. For some soil zones × texture (clay loam–dark brown and brown, and silty loam–dark brown), there was no difference in disease severity at the various oospore levels between autoclaved and non-autoclaved soils, whereas for other locations, disease severity at each oospore concentration was generally higher in non-autoclaved treatments than autoclaved treatments. This could indicate that other organisms within the soil contribute to enhancing disease,

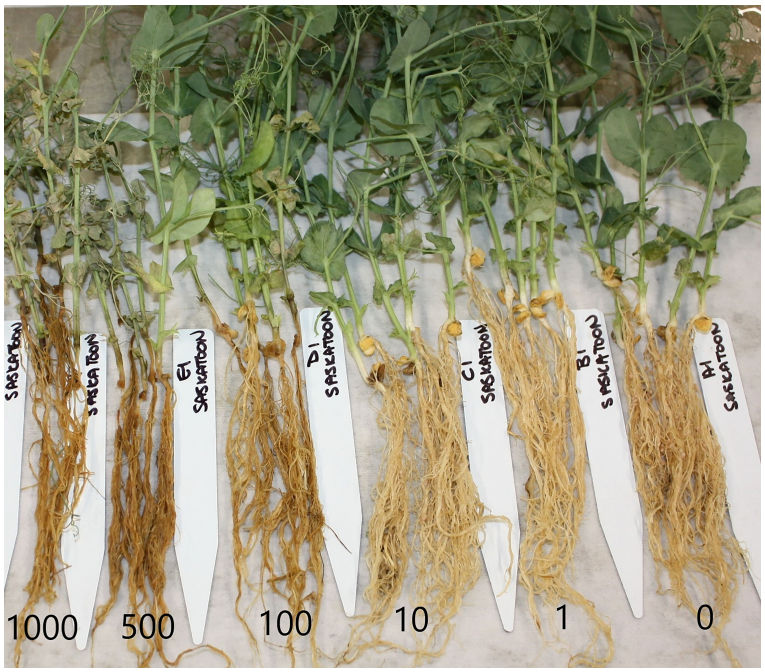

FIGURE 4
Disease symptoms on pea plants grown in non-autoclaved soil from Saskatoon (dark brown silt loam) in 2015 inoculated with 0 (right) – 1,000 (left) oospores/g soil.

although the confounding effects of autoclaving on changing the soil parameters cannot be fully discounted. However, assessment of two *Fusarium* species that are commonly associated with the pea root rot complex (Esmaeili Taheri et al. 2017, Chatterton et al., 2019) showed that *F. avenaceum* and *F. solani* were present at higher levels in all of the non-autoclaved soils, although concentration varied between soils. Although we did not perform isolations from all roots from all of the locations, presumptive *F. avenaceum*, *F. solani*, and *F. redolens* isolates, based on colony morphology, were observed on root pieces in culture, as were common saprophytes like *Rhizopus* and *Penicillium* spp. (data not shown). In greenhouse trials, co-inoculation of *A. euteiches* with *F. avenaceum* and/or *F. solani* resulted in significantly higher disease severity levels than any of the pathogens occurring singly (Willsey et al., 2018).

One of the challenges with interpreting the results from this study is that root browning was often observed in the non-inoculated (zero oospores/g soil) treatments for all soils. These roots were often scored with a disease rating of 1 (<25% of roots browned), but it was difficult to determine if it was due to pathogen infection or root staining from the soils. This was observed even in autoclaved soils, and for the most part, disease severity did not differ between the autoclaved and non-autoclaved soils without oospore treatments. The exception was in silty loam soils where the non-autoclaved soils had a higher disease severity than the autoclaved soils without any addition of oospores. The silty loam soils were all collected in 2016, and all of these soils had *F. avenaceum* and/or *F. solani* at various levels. Soils were collected from fields that did not have any prior history of *A. euteiches*, with the assumption that they would be free from *A. euteiches*, as soils with a cropping history of pulses are at higher risk of *A. euteiches* infestation (Pfender and Hagedorn, 1983). It is possible that some soils may have had low levels of *A. euteiches*, since research in Saskatchewan showed that soils from native pastures can contain low levels of *A. euteiches* (Karppinen et al., 2020). This seems particularly likely for the black silty loam soil that showed *A. euteiches* in the non-autoclaved, non-inoculated treatment in both the qPCR and ddPCR results. Other pathogens such as *Pythium* spp., *Rhizoctonia solani*, or other *Fusarium* spp. may also have been present in the soil or on the seed and confounded disease severity ratings.

Visual representation of the relationship between oospore dose and disease severity clearly showed that the relationship was not log-linear. Linear regression using the whole data set was attempted but resulted in a low R^2 value (data not shown), likely due to the differential responses for DSI between soil zones × textures. Previous research with soils from France and Sweden showed a log-linear relationship between oospore dose and disease severity (Persson et al., 1999; Sauvage et al., 2007; Gangneux et al., 2014). In our study, either disease did not develop, or severity was not significantly different from zero oospores, when oospore levels were below 100 oospores/g soil for all soil zone by textures. Similar to these previous studies, we did observe that disease reached a maximum level (i.e., DSI = 1) at 1,000 oospores/g soil for several soil types. Previous studies used a larger range of oospore concentrations, but fewer soil sources, and soils were only inoculated with one *A. euteiches* isolates (Sauvage et al., 2007; Gangneux et al., 2014). In our study, we inoculated soils with a mixture of four *A. euteiches* isolates and used a smaller range of oospore concentrations because of the large number of soils that were being evaluated. In the range of 10 of 1,000 oospores, which is

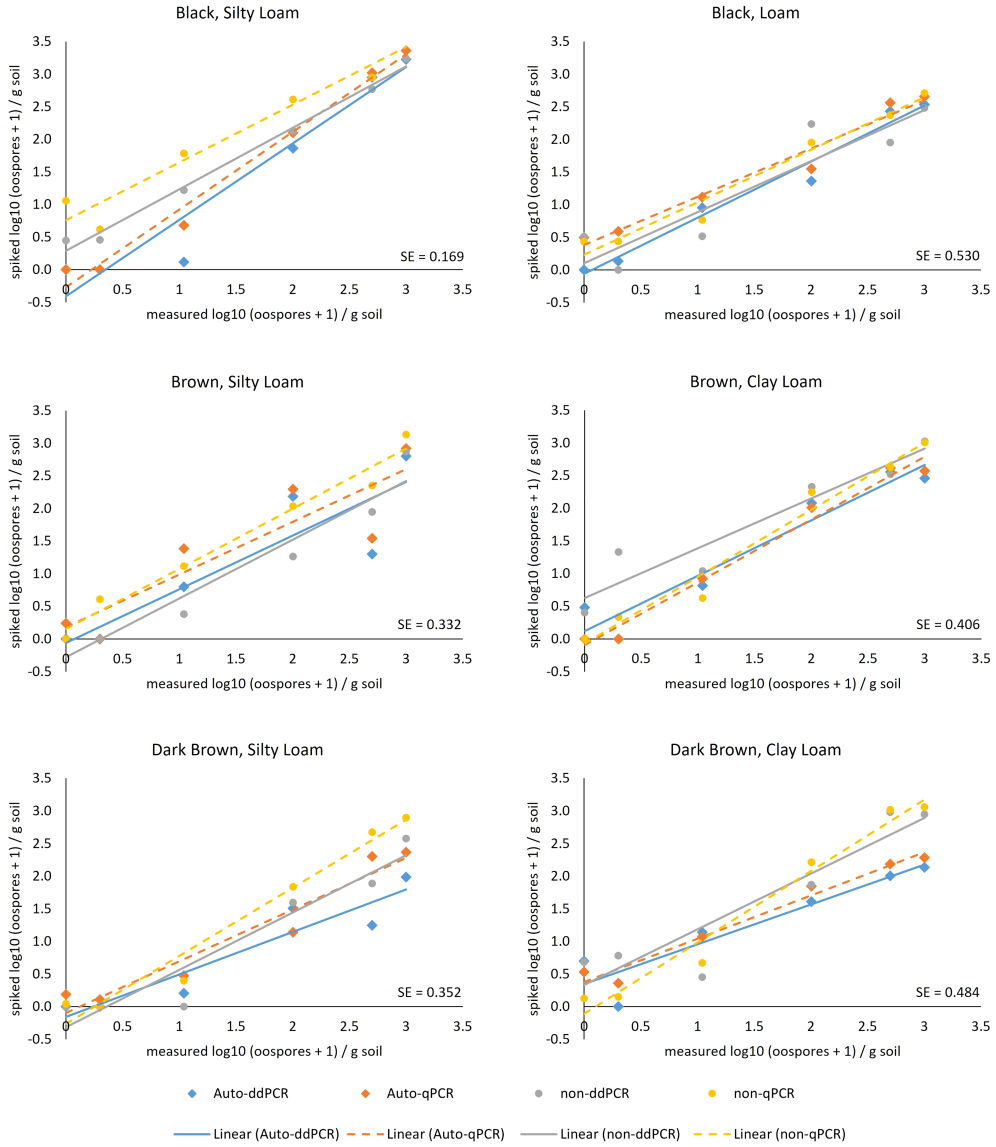

FIGURE 5
Relationship between number of oospores/g soil calculated from ddPCR (solid line) and qPCR (dashed line) analysis of DNA extracted from soils that were autoclaved (diamonds) or non-autoclaved (circles) from six locations (= unique soil zone and texture) with 0, 1, 10, 100, 500, and 1,000 oospores added. Oospore levels were calculated from ITS copies/microliter for ddPCR and ITS copies standard curve (*via* Ct values) for qPCR, based on the assumption of 190 ITS copies per oospore and a DNA extraction from 250 mg soil. Standard error bars are not shown, but the mean population standard error (SE) for each location is given in the lower right-hand corner of the graph.

comparable to these other studies, a linear relationship was apparent for some soils. There can be a significant variation in aggressiveness among *A. euteiches* isolates (Sivachandra Kumar et al., 2021), so it is possible that using a mixture of isolates contributed to the non-linear relationships observed. Of the four isolates that were used in this study, three (Ae4, Ae6, and Ae7) were highly aggressive towards CDC Meadow, and one (Ae1) was moderately aggressive, while two isolates (Ae6 and Ae7) also caused moderate disease severity on the partial resistant line PI660736 (Sivachandra Kumar et al., 2021). Furthermore, while care was taken to ensure that there was an equal concentration of oospores from each isolate in the inoculation mix, our personal observations repeatedly working with these isolates is that some consistently produce more oospores and zoospores than others (e.g., Ae1 produces more zoospores but fewer oospores than Ae6). These intrinsic properties of the different isolates could also affect resulting disease severity.

Finally, we also compared the use of qPCR and ddPCR to quantify *A. euteiches* DNA in the initial soil dilution series to determine whether these tools can be used to accurately measure oospore concentrations in different soils. In order to compare qPCR and ddPCR, the returned Ct values (qPCR) and ITS copy number per microliter (ddPCR) were converted to an estimate of oospore numbers per gram of soil. Although the ITS copy number is variable among isolates (Gangneux et al., 2014), we used an average of 190 ITS copies per diploid cell for ease of calculations and because it is

TABLE 4 Type III tests of the fixed effects of field location (= unique soil zone × texture), PCR type (qPCR or ddPCR), and treatment (autoclaved or non-autoclaved) on the regression parameters for the regression analysis of log10 (oospores +1)/g soil added to the soils versus the calculated concentration of log10 (oospores +1)/g soil measured in soil using qPCR or ddPCR.

Effect	Numerator DF*	*F* Ratio	*p*
Slope (b_1)			
Location	5	66.40	0.0001
PCR type	1	58.48	0.0006
Treatment	1	73.38	0.0004
Location×PCR type	5	22.30	0.0020
Location×Treatment	5	89.36	<.0001
Treatment×PCR type	1	13.43	0.0145
Intercept (b_0)			
Location	5	14.59	0.0053
PCR type	1	0.69	0.4428
Treatment	1	2.36	0.1854
Location×PCR type	5	7.58	0.0221
Location×Treatment	5	4.31	0.0673
Treatment×PCR type	1	3.10	0.1385

*Denominator degree of freedom = 5.

close to the mean of 95 ± 22 copies per cell calculated for 40 *A. euteiches* isolates (Gangneux et al., 2014). More precise measurement of actual copy number per cell was described by Gibert et al. (2021) by also using a single-copy *A. euteiches* gene target (Sauvage et al., 2007), but this method does not work well for soil due to the low sensitivity of quantifying a single-gene target sequence. For the purposes of estimating *A. euteiches* inoculum levels in soil and developing a test that can easily be implemented by commercial labs, our results show that using an average of 190 ITS copies per cell for calculating oospores per gram soil works well, since for most soils, there was a significant correlation between initial oospore concentration and calculated oospore concentration, with slopes close to 1. As expected, quantification below 10 oospores/g soil was not accurate, as this quantity is reaching the theoretical limit of detection from 250 mg of soil (Willsey et al., 2018) and resulted in the intercepts for several soils falling below or above zero. Digital droplet PCR has the potential to be more sensitive for quantifying DNA of a relatively rare target in soil than qPCR (Gibert et al., 2021). However, in the side-by-side comparison of qPCR and ddPCR amplification of inoculated oospores, for several soil types, the slope of the line for the ddPCR assays was significantly lower than for the qPCR assays. In most cases, this resulted in an underestimation of oospores per gram of soil compared to the actual amount for the ddPCR assays. Gibert et al. (2021) used 200 ng of soil matrix DNA per PCR mixture in order to obtain increased sensitivity. In our study, increasing the amount of soil DNA resulted in a greater rain effect, which inhibited differentiation of the four targets in the multiplex assay, and thus, only 50 ng of total soil DNA was used per reaction. On the other hand, the qPCR assay was performed as a singleplex for *A. euteiches* only, and thus, it is possible that some sensitivity was lost in the multiplex ddPCR assay. However, a multiplex assay that can target multiple species within the root rot complex would be beneficial for reducing per sample assay costs and for more precise risk prediction, given that multiple species interact together to increase disease severity. Therefore, further research into enhancing the sensitivity of a multiplex ddPCR assay would be beneficial.

Both qPCR and ddPCR assays were affected by soil texture × soil zone and autoclave treatment. For ddPCR, the black silt loam soil had the highest R^2 and slope closest to 1, while the dark brown clay loam soil had the lowest R^2 and slope. For qPCR, dark brown silt loam, black silt loam, and brown clay loam soils had the highest R^2 values and slopes closest to 1, while the black loam soil had the lowest R^2 and slope. Although organic matter, humic acid, and clay content can all affect DNA quantification results from soils (Frostegård et al., 1999; Almquist et al., 2016; Gibert et al., 2021),

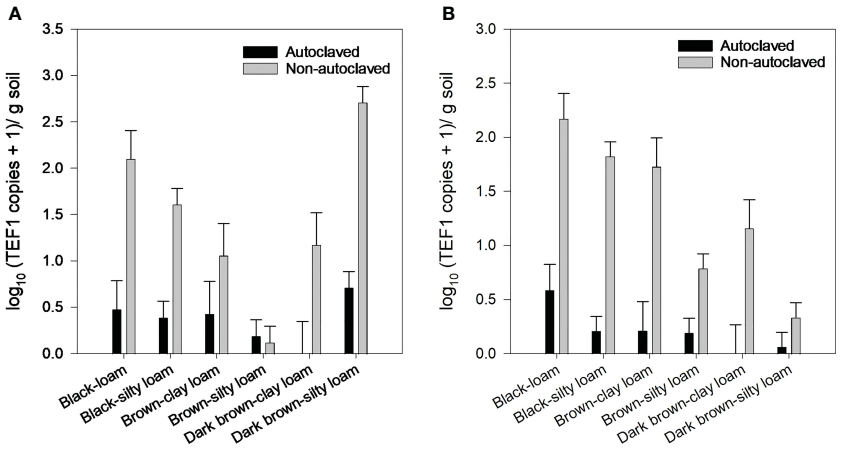

FIGURE 6
Fusarium avenaceum **(A)** and *Fusarium solani* **(B)** concentration [$\log_{10}$ (TEF1 gene copies + 1)/g soil] in soils from six locations (=unique soil zone and texture) that were autoclaved or non-autoclaved from 2016 soil collections. Error bars represent the mean population standard error of the experiment.

there did not appear to be any clear trends on the effects of these factors with the soils we tested. The two black soils had the highest organic matter, but the black silt loam soil performed the best for ddPCR and qPCR, while the black loam soil performed the worst. Similarly, the two clay loam soils had contrasting performance for both qPCR and ddPCR assays. The finding that soil type influences oospore quantification has been described for related species, *Aphanomyces cochlioides* where oospore detection limits were higher in high clay soils (Almquist et al., 2016) and *Phytophthora medicaginis* where quantification was lower in sand than in soil (Bithell et al., 2021). In terms of the effect of autoclaving, dark brown silt loam, black silt loam, and dark brown clay loam soils had significantly different slopes between autoclaved and non-autoclaved treatments, even though oospores were added after autoclaving. Autoclaving can affect soil properties, causing, for example, a decrease in aggregation, a corresponding increase in the clay fraction, and more dissolved organic matter (Berns et al., 2008). Changes in these properties could have affected performance of the ddPCR and qPCR reactions, although it is not clear why only some soils were affected. Autoclaved soils could also have a different microbiome if the native soil microbiome was rapidly replaced by fast colonizers. As discussed above, the disease severity and oospore dose relationship may also have been affected by changes in soil properties due to autoclaving, but other soil sterilization procedures may also result in changes to soil properties (Berns et al., 2008), and other sterilization equipment are not as readily available as an autoclave. It is possible that this differential effect was due to the different spiking events and random variation in oospore distribution when collecting 2 × 250 mg samples from each spiking event. Taken together, the results for the effects of soil texture and zone and autoclaving suggest that soil properties may affect the performance of both qPCR and ddPCR, although the exact nature requires further research. This is being tested with more replicates on a larger number of soil samples to determine if random variation in sampling is the biggest factor.

This research demonstrated that developing a model for predicting severity of *Aphanomyces* root rot based on DNA quantification of soils will not be an easy task for the large geographical area under which pea is cultivated in the Canadian prairies. The vast area encompasses several biogeographical zones and soil types. Our research clearly showed that the relationship between disease severity and oospore concentration was different based on soil zone and texture. In addition, the presence of other pathogens and potentially, beneficial organisms, in the soil further complicates this relationship. Furthermore, using DNA quantification tools to estimate initial oospore concentration in the soil was also affected by soil properties. Nonetheless, this research is the first step towards understanding inoculum thresholds that are required for disease progression in Canadian prairies soils and defining the relationship between pathogen inoculum and disease severity. Further research to better understand the factors that affect DNA quantification accuracy and sensitivity is currently underway by testing a much larger set of soils from across the Canadian prairies.

Data availability statement

The raw data supporting the conclusions of this article will be made available by the authors, without undue reservation.

Author contributions

SC performed the research and wrote the manuscript, TS analyzed the data, AP assisted with manuscript writing, RD, MH and SB provided soil samples and manuscript review and editing. All authors contributed to the article and approved the submitted version.

Funding

Funding was provided by the Alberta Pulse Growers and the Saskatchewan Pulse Growers Associations.

Acknowledgments

We gratefully acknowledge the technical assistance of Anthony Erickson, Christine Vucurevich, and Scott Erickson. Funding was provided by the Alberta Pulse Growers and the Saskatchewan Pulse Growers Associations.

Conflict of interest

The authors declare that the research was conducted in the absence of any commercial or financial relationships that could be construed as a potential conflict of interest.

Publisher's note

Supplementary material

The Supplementary Material for this article can be found online at: https://www.frontiersin.org/articles/10.3389/fpls.2023.1115420/full#supplementary-material

References

Almquist, C., Persson, L., Olsson, Å., Sundström, J., and Jonsson, A. (2016). Disease risk assessment of sugar beet root rot using quantitative real-time PCR analysis of *Aphanomyces cochlioides* in naturally infested soil samples. *Eur. J. Plant Pathol.* 145, 731–742. doi: 10.1007/s10658-016-0862-5

Bainard, L. D., Hamel, C., and Gan, Y. (2016). Edaphic properties override the influence of crops on the composition of the soil bacterial community in a semiarid agroecosystem. *Appl. Soil Ecol.* 105, 160–168. doi: 10.1016/j.apsoil.2016.03.013

Banniza, S., Bhadauria, V., Peluola, C. O., Armstrong-Cho, C., and Morrall, R. A. A. (2013). First report of *Aphanomyces euteiches* in Saskatchewan. *Can. Plant Dis. Surv.* 93, 163–164.

Berns, A. E., Philipp, H., Narres, H.-D., Burauel, P., Vereecken, H., and Tappe, W. (2008). Effect of gamma-sterilization and autoclaving on soil organic matter structure as studied by solid state NMR, UV and fluorescence spectroscopy. *Eur. J. Soil Sci.* 59, 540–550. doi: 10.1111/j.1365-2389.2008.01016.x

Biorad (2016) *Bulletin 6407 - droplet DigitalTM PCR applications guide*. Available at: https://www.bio-rad.com/fr-ca/life-science/digital-cr?ID=M9HE2R15&source_wt=ddPCRAppGuide_surl.

Bithell, S., Moore, K., Herdina, McKay, A., Harden, S., and Simpfendorfer, S. (2021). Phytophthora root rot of chickpea: inoculum concentration and seasonally dependent success for qPCR based predictions of disease and yield loss. *Australas. Plant Pathol.* 50, 91–103. doi: 10.1007/s13313-020-00752-2

Chatterton, S., Bowness, R. T., and Harding, M. W. (2015). First report of root rot of field pea caused by *Aphanomyces euteiches* in Alberta, Canada. *Plant Dis.* 99, 288. doi: 10.1094/PDIS-09-14-0905-PDN

Chatterton, S., Harding, M. W., Bowness, R., McLaren, D. L., Banniza, S., and Gossen, B. D. (2019). Importance and causal agents of root rot on field pea and lentil on the Canadian prairies 2014–2017. *Can. J. Plant Pathol.* 41, 98–114. doi: 10.1080/07060661.2018.1547792

Esmaeili Taheri, A., Chatterton, S., Foroud, N. A., Gossen, B. D., and McLaren, D. L. (2017). Identification and community dynamics of fungi associated with root, crown, and foot rot of field pea in western Canada. *Eur. J. Plant Pathol.* 147, 489–500. doi: 10.1007/s10658-016-1017-4

Foroud, N. A. (2011). *Investigating the molecular mechanisms of fusarium head blight resistance in wheat* (Vancouver, BC, Canada: University of British Columbia). PhD Thesis.

Frostegård, Å., Courtois, S., Ramisse, V., Clerc, S., Bernillon, D., Gall, F. L., et al. (1999). Quantification of bias related to the extraction of DNA directly from soils. *App. Env. Microbiol.* 65, 5409–5420. doi: 10.1128/AEM.65.12.5409-5420.1999

Fuller, L. (2010). Chernozemic soils of the prairie region of Western Canada. *Prairie Soils Crops* 3, 37–45.

Gangneux, C., Cannesan, M. A., Bressan, M., Castel, L., Moussart, A., Vicré-Gibouin, M., et al. (2014). A sensitive assay for rapid detection and quantification of *Aphanomyces euteiches* in soil. *Phytopathology* 104, 1138–1147. doi: 10.1094/PHYTO-09-13-0265-R

Gibert, S., Edel-Hermann, V., Moussa Mcolo, R., Gautheron, E., Michel, J., Bernaud, E., et al. (2021). Risk assessment of aphanomyces euteiches root rot disease: quantification of low inoculum densities in field soils using droplet digital PCR. *Eur. J. Plant Pathol.* 161, 503–528. doi: 10.1007/s10658-021-02325-5

Hadar, Y., and Papadopoulou, K. K. (2012). Suppressive composts: microbial ecology links between abiotic environments and healthy plants. *Annu. Rev. Phytopathol.* 50, 133–153. doi: 10.1146/annurev-phyto-081211-172914

Hamon, C., Coyne, C. J., McGee, R. J., Lesne, A., Esnault, R., Mangin, P., et al. (2013). QTL meta-analysis provides a comprehensive view of loci controlling partial resistance to *Aphanomyces euteiches* in four sources of resistance in pea. *BMC Plant Biol.* 13, 45. doi: 10.1186/1471-2229-13-45

Harveson, R. M., Nielsen, K. A., and Eskridge, K. M. (2014). Utilizing a preplant soil test for predicting and estimating root rot severity in sugar beet in the central high plains of the united states. *Plant Dis.* 98, 1248–1252. doi: 10.1094/PDIS-11-13-1186-RE

Heyman, F., Lindahl, B., Persson, L., Wikström, M., and Stenlid, J. (2007). Calcium concentrations of soil affect suppressiveness against aphanomyces root rot of pea. *Soil Biol. Biochem.* 39, 2222–2229. doi: 10.1016/j.soilbio.2007.03.022

Hossain, S., Bergkvist, G., Berglund, K., Mårtensson, A., and Persson, P. (2012). Aphanomyces pea root rot disease and control with special reference to impact of brassicaceae cover crops. *Acta Agriculturae Scandinavica Section B — Soil Plant Sci.* 62, 477–487. doi: 10.1080/09064710.2012.668218

Hughes, T. J., and Grau, C. R. (2007). Aphanomyces root rot or common root rot of legumes. *Plant Health Instructor*. doi: 10.1094/PHI-I-2007-0418-01

Hughesman, C. B., Lu, X. J. D., Liu, K. Y. P., Zhu, Y., Poh, C. F., and Haynes, C. (2016). A robust protocol for using multiplexed droplet digital PCR to quantify somatic copy number alterations in clinical tissue specimens. *PloS One* 11 (8), e0161274. doi: 10.1371/journal.pone.0161274

Jacobsen, B. J., and Hopen, H. J. (1981). Influence of herbicides on aphanomyces root rot of peas. *Plant Dis.* 65, 11–16. doi: 10.1094/PD-65-11

Karppinen, E. M., Payment, J., Chatterton, S., Bainard, J. D., Hubbard, M., Gan, Y., et al. (2020). Distribution and abundance of *Aphanomyces euteiches* in agricultural soils: effect of land use type, soil properties, and crop management practices. *Appl. Soil Ecol.* 150, 103470. doi: 10.1016/j.apsoil.2019.103470

Levenfors, J. P., Wikström, M., Persson, L., and Gerhardson, B. (2003). Pathogenicity of aphanomyces spp. from different leguminous crops in Sweden. *Eur. J. Plant Pathol.* 109, 535–543. doi: 10.1023/A:1024711428760

Malvick, D., Percich, J., Pfleger, F., Givens, J., and Williams, J. (1994). Evaluation of methods for estimating inoculum potential of *Aphanomyces euteiches* in soil. *Plant Dis.* 78, 361–365. doi: 10.1094/PD-78-0361

McGee, R. J., Coyne, C. J., Pilet-Nayel, M. L., Moussart, A., Tivoli, B., Baranger, A., et al. (2012). Registration of pea germplasm lines partially resistant to aphanomyces root rot for breeding fresh or freezer pea and dry pea types. *J. Plant Regis.* 6, 203–207. doi: 10.3198/jpr2011.03.0139crg

Moussart, A., Wicker, E., Le Delliou, B., Abelard, J. M., Esnault, R., Lemarchand, E., et al. (2009). Spatial distribution of aphanomyces euteiches inoculum in a naturally infested pea field. *Eur. J. Plant Pathol.* 123, 153–158. doi: 10.1007/s10658-008-9350-x

Oyarzun, P., Gerlagh, M., and Hoogland, A. E. (1993). Relation between cropping frequency of peas and other legumes and foot and root rot in peas. *Neth. J. Plant Pathol.* 99, 35–44. doi: 10.1007/BF01974783

Papavizas, G. C., and Ayers, W. A. (1974). Aphanomyces species and their root diseass on pea and sugarbeet. *Tech. Bull. Agric. Res. Serv. US Dept. Agric.* 1485, 1–158.

Persson, L., Larsson-Wikström, M., and Gerhardson, B. (1999). Assessment of soil suppressiveness to aphanomyces root rot of pea. *Plant Dis.* 83, 1108–1112. doi: 10.1094/PDIS.1999.83.12.1108

Persson, L., and Olsson, S. (2000). Abiotic characteristics of soils suppressive to aphanomyces root rot. *Soil Biol. Biochem.* 32, 1141–1150. doi: 10.1016/S0038-0717(00)00030-4

Pfender, W. F., and Hagedorn, D. J. (1983). Disease progress and yield loss in aphanomyces root rot of peas. *Phytopathology* 73, 1109–1113. doi: 10.1094/Phyto-73-1109

Safarieskandari, S., Chatterton, S., and Hall, L. M. (2021). Pathogenicity and host range of fusarium species associated with pea root rot in Alberta, Canada. *Can. J. Plant Pathol.* 43, 162–171. doi: 10.1080/07060661.2020.1730442

Sauvage, H., Moussart, A., Bois, F., Tivoli, B., Barray, S., and Laal, K. (2007). Development of a molecular method to detect and quantify *Aphanomyces euteiches* in soil. *FEMS Microbiol. Lett.* 273, 64–69. doi: 10.1111/j.1574-6968.2007.00784.x

Sivachandra Kumar, N. T., Caudillo-Ruiz, K. B., Chatterton, S., and Banniza, S. (2021). Characterization of *Aphanomyces euteiches* pathotypes infecting peas in Western Canada. *Plant Dis.* 105, 4025–4030. doi: 10.1094/PDIS-04-21-0874-RE

Williams-Woodward, J. L., Pfleger, F. L., Fritz, V. A., and Allmaras, R. R. (1997). Green manures of oat, rape and sweet corn for reducing common root rot in pea *(Pisum sativum)* caused by *Aphanomyces euteiches*. *Plant Soil* 188, 43–48. doi: 10.1023/A:1004260214107

Willsey, T. L., Chatterton, S., Heynen, M., and Erickson, A. (2018). Detection of interactions between the pea root rot pathogens *Aphanomyces euteiches* and fusarium spp. using a multiplex qPCR assay. *Plant Pathol.* 67, 1912–1923. doi: 10.1111/ppa.12895

Willsey, T., Patey, J., Vucurevich, C., Chatterton, S., and Carcamo, H. (2021). Evaluation of foliar and seed treatments for integrated management of root rot and pea leaf weevil in field pea and faba bean. *Crop Protect* 143, 105538. doi: 10.1016/j.cropro.2021.105538

Windels, C. E. (2000). Aphanomyces root rot on sugar beet. *Plant Health Prog.* 1:1. doi: 10.1094/PHP-2000-0720-01-DG

Xue, A. G. (2003). Efficacy of *Clonostachys rosea* strain ACM941 and fungicide seed treatments for controlling the root rot complex of field pea. *Can. J. Plant Sci.* 83, 519–524. doi: 10.4141/P02-078

Zitnick-Anderson, K., Simons, K., and Pasche, J. S. (2018). Detection and qPCR quantification of seven *Fusarium* species associated with the root rot complex in field pea. *Can. J. Plant Pathol.* 40, 261–271. doi: 10.1080/07060661.2018.1429494

frontiers | Frontiers in Plant Science

TYPE Review
PUBLISHED 02 June 2023
DOI 10.3389/fpls.2023.1165658

OPEN ACCESS

EDITED BY
Marie-Laure Pilet-Nayel,
INRAE Bretagne Normandie, France

REVIEWED BY
Jiban Shrestha,
Nepal Agricultural Research Council, Nepal
Robyne Davidson,
Lakeland College, Canada

*CORRESPONDENCE
Haitian Yu
haitian7@ualberta.ca/haitianlegume@outlook.com
Yuhua He
hyhyaas@163.com
Meiyuan Lv
lvmeiyang01@163.com

RECEIVED 14 February 2023
ACCEPTED 03 May 2023
PUBLISHED 02 June 2023

CITATION
Yu H, Yang F, Hu C, Yang X, Zheng A, Wang Y, Tang Y, He Y and Lv M (2023) Production status and research advancement on root rot disease of faba bean (*Vicia faba* L.) in China. *Front. Plant Sci.* 14:1165658. doi: 10.3389/fpls.2023.1165658

Production status and research advancement on root rot disease of faba bean (*Vicia faba* L.) in China

Haitian Yu[1,2*], Feng Yang[1], Chaoqin Hu[1], Xin Yang[1], Aiqing Zheng[1], Yubao Wang[1], Yongsheng Tang[3], Yuhua He[1*] and Meiyuan Lv[1*]

[1]Institute of Food Crops, Yunnan Academy of Agricultural Science, Kunming, Yunnan, China, [2]Department of Agricultural, Food and Nutritional Science, University of Alberta, Edmonton, AB, Canada, [3]Qujing Academy of Agricultural Sciences, Qujing, Yunnan, China

China is the largest producer of faba bean with a total harvested area of 8.11×10^5 ha and a total production of 1.69×10^6 tons (dry beans) in 2020, accounting for 30% of the world production. Faba bean is grown in China for both fresh pods and dry seed. East China cultivates large seed cultivars for food processing and fresh vegetables, while northwestern and southwestern China grow cultivars for dry seeds, with an increased production of fresh green pods. Most of the faba bean is consumed domestically, with limited exports. The absence of unified quality control measures and simple traditional cultivation practices contributes to the lower competitiveness of the faba bean industry in international markets. Recently, new cultivation methods have emerged with improved weed control, as well as better water and drainage management, resulting in higher quality and income for producers. Root rot disease in faba bean is caused by multiple pathogens, including *Fusarium* spp., *Rhizoctonia* spp., and *Pythium* spp. *Fusarium* spp. is the most prevalent species causing root rot in faba bean crops and is responsible for severe yield loss, with different species causing the disease in different regions in China. The yield loss ranges from 5% to 30%, up to 100% in severely infected fields. The management of faba bean root rot disease in China involves a combination of physical, chemical, and bio-control methods, including intercropping with non-host crops, applying rational nitrogen, and treating seeds with chemical or bio-seed treatments. However, the effectiveness of these methods is limited due to the high cost, the broad host range of the pathogens, and potential negative impacts on the environment and non-targeted soil organisms. Intercropping is the most widely utilized and economically friendly control method to date. This review provides an overview of the current status of faba bean production in China, the challenges faced by the industry due to root rot disease, and the progress in identifying and managing this disease. This information is critical for developing integrated management strategies to effectively control root rot in faba bean cultivation and facilitating the high-quality development of the faba bean industry.

KEYWORDS

Vicia faba, production, root rot, identification, management

1 Introduction

Faba bean (*Vicia faba* L.), native to the Mediterranean and Central Asia, is an important legume crop that can be used as food for human consumption and as livestock feed (Crépon et al., 2010). The characteristics of high protein content in seed and straw, the high efficacy of root-rhizobia in nitrogen fixation, the good potential in soil quality improvement (Duchene et al., 2017), and the good adaptation in different habitats (Singh et al., 2013) make it well recognized and widely cultivated in the world.

While the production of primary crops such as wheat, rice, maize, and sugarcane has increased 52% from 2000 to 2021 (9.3 billion tons) (FAOSTAT, 2022), the challenges posed by climate change and loss of quality and area of arable land are limiting crop production (Döös, 2002; Shi et al., 2016; Snowdon et al., 2021). Additionally, global water stress and rising hunger (Alcamo et al., 2007; Oxford Analytica, 2019), with most of the undernourished population living in Asia and Africa, are increasing stress on agricultural production. To meet the food needs of the rapidly growing world population, a 70% increase in food production by 2050 is suggested by the FAO (Food and Agriculture Organization of the United Nations) (Kuttibai et al., 2022). The overuse of chemical fertilizers and pesticides to achieve high yield, although to a lesser extent, also impairs agricultural sustainability and human health (Liu and Wu, 2022). As reported by the FAO, over 200 million tons of fertilizers, with 56% nitrogen, were applied in 2020 and pesticide use has increased by 30% since 2000. These factors emphasize the importance of increasing the cultivation and utilization of legume crops in agriculture, which will diversify the agroecosystem, reduce pest stress, lower nitrogen fertilizer inputs, improve soil quality, and increase the availability of legume protein for nourishing the needy population (Costanzo and Bàrberi, 2014; Duchene et al., 2017; Blesh, 2019; Zhang et al., 2019).

The production of legume crops, including faba bean, is crucial to alleviate the increasing challenges in crop production such as global food stress, land degradation, and overuse of chemicals. However, various abiotic and biotic factors can hamper legume productivity (Varshney et al., 2009). Root rot disease associated with Fusarium wilt is considered as one of the major constraints on legume production (Liebenberg, 2002; Infantino et al., 2006; Singh and Schwartz, 2010) and has been reported to cause severe disease in faba bean (Sillero et al., 2010; Hou et al., 2011; Paul and Gupta, 2021). In faba bean production in China, root rot and wilt disease caused by various fungi including *Fusarium* spp., *Rhizoctonia solani*, and *Pythium debaryanum* are a major challenge, leading to yield losses of 5%–30% and even up to 100% under favorable environmental conditions (Dong et al., 2014a; Zhang et al., 2018). Charcoal rot caused by *Macrophomina phaseolina* has also been recently reported in Yunnan province (Sun et al., 2019; Yu et al., 2021). This review summarizes the status of faba bean production in China and the research advancement on root rot and wilt diseases, providing crucial information for future strategies in the development of the faba bean industry and integrated disease management.

2 Status of faba bean production of China

According to data from the FAO from 2001 to 2020, China led the world in faba bean production, with total harvested area and production of dry bean both accounting for more than 30% of the total global amount. In 2020, China and the world produced 1.69×10^6 and 5.68×10^7 metric tons of faba beans, respectively, with total harvested areas of 8.11×10^5 and 2.66×10^6 ha, respectively (dry beans), followed by Ethiopia, Australia, and the UK (FAOSTAT, 2022). In the past 20 years in China (Figures 1, 2), the lowest area harvested and the resulting production of faba bean was seen in 2014, which then reached a relatively stable level between 2016 and 2020. Compared to 2001, the harvested area and production of faba bean have decreased by 37.62% and 11.61%, respectively, by 2020. The shift in land use in Yunnan province from faba bean cultivation to vegetable cultivation, due to the desire for higher income crops, contributed to the decrease (Yu et al., 2019a). Despite the reduction in the harvested area and production, the increase in average yield of faba bean, from 1.47 tons·ha^{-1} to 2.12 tons·ha^{-1} (FAOSTAT, 2022), has helped compensate for the losses. Furthermore, there is still a huge potential for improvement, as the yield of faba bean in the regional trials in Yunnan was more than 3.0 tons·ha^{-1}. In China, most of the fresh beans and over 90% of the dry products were consumed domestically. However, importation of fresh beans has not been reported since 1961 and imports of dry beans, from 2014 to 2020, was limited to a few hundred kilograms, with most of the faba bean imported from ICARDA and used as germplasm for research purposes. Furthermore, the quantity of dry seeds exported out of China accounted for only 0.5%–2.5% of the total production in China and 0.66%–8.24% of the total production in the world (Figures 3, 4). The trend of decreased exports has lasted for more than 10 years (FAOSTAT, 2022). The low level of importation suggests a high degree of self-sufficiency, and a low level of export is attributed to the low consistency and quality of the faba bean product. Conversely, Australia, the third leading producer of faba bean, is the leading exporter (Johnson et al., 2021; Dhull et al., 2022) and is highly competitive in international markets

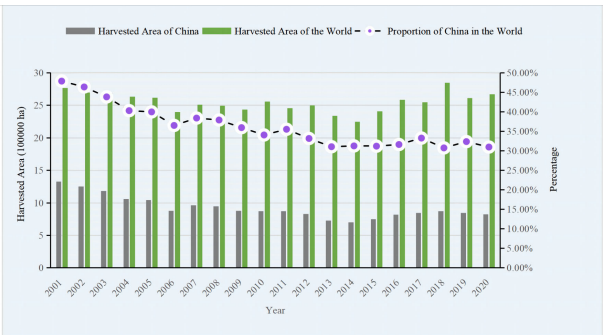

FIGURE 1
Harvested area of faba bean of china and the World from 2001 to 2020.

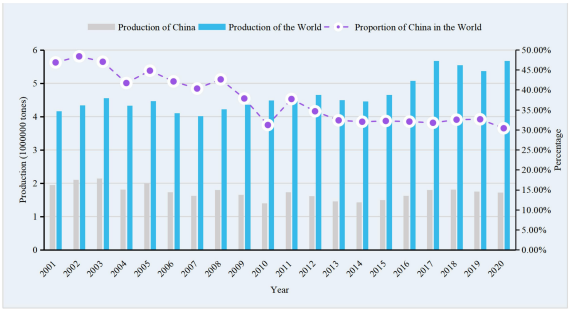

FIGURE 2
Production of faba bean of China and the World from 2001 to 2020.

because of consistent, high-quality commodity production (AEGIC, 2019).

Faba bean is traditionally cultivated in most parts of China, except for the northeast provinces of Heilongjiang, Jilin, and Changchun (Ye et al., 2003). The cultivation region of faba bean crosses large latitudinal and longitudinal ranges. The ecotype of faba bean was classified into the winter ecotype (between 21°N and 35°N latitude), basically sown between August and December and harvested from March to May of the next year, and the spring ecotype (between 31°N and 53°N latitude), sown between February and May and maturing in the fall season (Ye et al., 2003; Wang et al., 2012; Yu et al., 2019a). Typically, the northern and northwestern provinces are the regions for the spring ecotype, whereas the central, east, and southwest areas of China normally cultivate the winter faba bean (Lang et al., 1993; Wang et al., 2012). All parts of the faba bean plant, fresh or dry, were well utilized in China, usually eaten as a vegetable (fresh seed, pods, and plant shoots), used as food (dry seed), used in livestock (all parts), and used as a natural nitrogen resource for the agricultural system (all parts) (Ye et al., 2003; Yu et al., 2020), with dry beans being the major product. Cultivation of faba bean in China (Table 1) and the intended market is determined by seed size (Ye et al., 2003). Different cultivars have been developed for various purposes, with big seed cultivars [(hundred seed weight (HSW) > 120 g] used for both food processing and fresh vegetable use, while medium (70 g ≤ HSW ≤ 120 g) and small (HSW < 70 g) seed cultivars are mainly used for food processing and as fodder. The traditional landraces have been replaced by newly bred cultivars, which were developed by different agricultural science academies (Bao et al., 2008; Wang et al., 2020a; Xiang et al., 2022; Yu et al., 2019a). Besides the use of traditional cultivars, breeding and testing new germplasm, and breeding cultivars for special use are emerging purposes (Du, 2021; Yu et al., 2019b). For example, in Chongqing, there is a registered cultivar of faba bean that is used both as an ornamental plant, due to its pink color and defined inflorescence, and as a source of dry seed. This makes it unique when compared to other faba bean cultivars that are primarily grown for their pods or seed (Du, 2021).

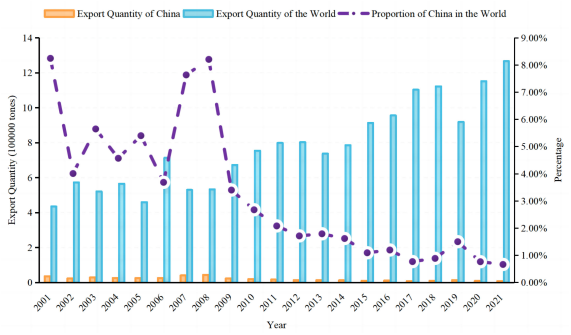

FIGURE 3
Exporting quantity of faba bean of China and the world from 2001 to 2020.

In East China, production of fresh green pods of faba bean has been commercially well-developed (Zhou et al., 2022). The cultivars of Tongcanxian series and Qidou series, the landraces Cixidabaican and Haimendaqingpi, and the introduced cultivar Lingxiyicun are commonly grown in East China, with a harvested area of approximately 7–8×10^4 ha. In the northwestern part of China, particularly the provinces of Qinghai, Gansu, Ningxia, and Xinjiang, faba bean is typically harvested for dry seed upon reaching maturity. The Qingdou and Lincan series cultivars are commonly grown in this region, with a harvested area of 2.4–3.0 ×10^4 ha and 7 × 10^4 ha, respectively. The cultivation area of faba bean in Gansu alone accounts for over 60% of the total spring faba bean cultivation area in China (Li and Nan, 2000; Hou et al., 2011). In the top-producing region of faba bean, located in southwest China, the crop is predominantly grown for dry seed with an increasing area for fresh green pods production (Yu et al., 2019a; Zhou et al., 2022). Yunnan and Sichuan are the first and second largest producers of faba bean in China, respectively, with more than 30% of faba bean cultivated in Yunnan (Yu et al., 2020). In Sichuan, approximately 1.4× 10^5 ha of faba bean were harvested in 2022 for both fresh and dry pods, with most of the dry faba bean processed into paste (Xiang et al., 2022).

The cultivation of faba bean in these regions usually involves crop rotation with paddy rice, wheat, oil crops, and other spring crops. In some southwest provinces, such as the mountainous region of Yunnan, early autumn and summer season cultivation is becoming more recognized as a special production of fresh faba bean at an altitude of 2,000 m above the sea level (Yu et al., 2019a). Additionally, Yunnan has a distinct advantage over other production regions, as it has a very diverse agricultural ecosystem at altitudes between 1,500 and 3,000 m above sea level that allows for the production of faba bean in multiple seasons, extending the marketing time (Bao, 2016; Yu et al., 2019a). Traditionally, farmers in Yunnan used broadcast sowing with surface soil tillage and crop rotation with dry land crops as well as direct seeding after rice (*Oryza sativa*) harvest. These methods were widely used due to their cost-effectiveness and high efficiency in nitrogen utilization for the succeeding crop. Recently, new cultivation patterns have been developed in Yunnan, including intercropping with perennial fruit trees such as grape, kiwi, date, and berry, as well as mulching-film side seeding, early autumn seeding, and off-season planting methods. These new methods have been recognized for their advantages, such as improved weed control, better capacity in

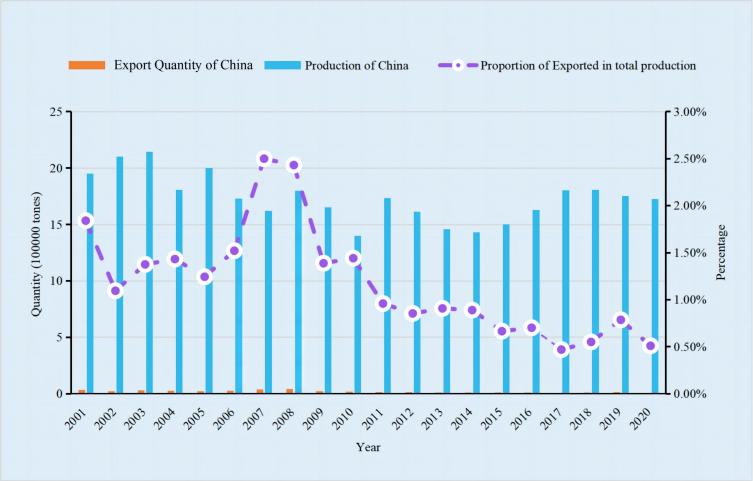

FIGURE 4
Proportion of Exporting quantity of faba bean in total production of China from 2001 to 2020.

providing or maintaining water and improving drainage, combined with higher quality and income for producers. Compared to traditional methods, these new patterns are more intensive and suitable for commercial and large-scale production of green beans, and have expanded the plantation region to cooler and higher elevation areas (Bao, 2016; Yu et al., 2018; Yu et al., 2019a).

In China, diverse habitats for cultivation provide a strong foundation for the high-quality and high-yield development of the faba bean industry. Over the past two centuries, based on the national developed research system, significant efforts have been made in cultivar breeding and improving cultural practices. However, the cultivation of faba bean in China is still challenged by the varying environmental conditions in different regions. Further research is necessary to enhance cultural practices that are tailored to the specific needs of each region and production purpose. This will contribute to the goal of achieving high-quality and high-yield production of faba bean. In addition, implementing a standardized quality testing system is critical to the growth and development of the faba bean industry in China.

TABLE 1 Harvested area of faba bean in the main producing province or autonomous region in China.

Province or autonomous region	Harvested area (ha)	Reference
Gansu	6.8×104	Li et al., 2018
Yunnan	>30×104	Yuan et al., 2020
Sichuan	14×104	Xiang et al., 2022
Chongqing	>6.6×104	He, 2019
Jiangsu	13×104	Minor Grain Crops, 2018
Zhejiang	5×104	Minor Grain Crops, 2018
Qinghai	2.6–2.7×104	Zhang et al., 2022

3 Identification of root rot disease in China

The root rot disease of faba bean can be caused by a number of different pathogens, including *Fusarium* spp., *Rhizoctonia* spp., *Pythium* spp., *Phoma* spp., and *Aphanomyces* spp. (Rubiales and Khazaei, 2022). The group of pathogens is often referred to as the root rot complex, with *Fusarium* spp. being the most commonly identified species causing foot and root rot, as well as wilt diseases, in faba bean in China (Table 2).

In Qinghai province, *Fusarium* spp. was responsible for severe yield loss, which caused wilt disease in the field with disease incidence ranging from 44% to 68% (Chen, 1999). Fusarium wilt, caused by *Fusarium oxysporum*, has been reported, but root rot caused by *Fusarium solani* is considered the major constraint on faba bean production in Qinghai (Wang et al., 2006). In the cold and humid regions of Gansu province, root rot disease caused by *Fusarium* spp. is a major constraint on faba bean production. The disease can result in yield losses of up to 90% under favorable conditions. *Fusarium solani* is the dominant species, followed by *Fusarium semitectum* and *Fusarium dimerum* (Hou et al., 2011). In addition, *Fusarium avenaceum* was also a commonly identified species causing root rot in faba bean crops. Other pathogens, including *Gliocladium roseum*, *F. oxysporum*, *Phoma* spp., *Pythium* spp., *Alternaria* spp., and *R. solani*, were also identified (Li and Nan, 1996). In Zhejiang province, located in the eastern part of China, the most significant pathogens causing root rot in faba bean were identified as *Fusarium acuminatum*, *F. oxysporum*, *Fusarium moniliforme*, *F. moniliforme* var. *subglutinans*, and *F. solani*. These species were determined based on their frequency of occurrence and pathogenicity index. Additionally, *F. semitectum* and *Fusarium tricinctum* were also confirmed (Bao et al., 1992). In Fujian province, the frequency of stem wilt disease caused by *F. oxysporum* increased since 2010, resulting in yield losses of 5% to 12% in 2013, and over 85% of the faba bean fields were infected (Wang, 2013). In Jiangsu province, a large amount of root and stem

TABLE 2 Disease incidence and yield losses caused by *Fusarium* spp. in a major producing province or autonomous region in China.

Province or autonomous region	Disease incidence (%)	Yield loss or plant death rate (%)	Main causal agents	Reference
Gansu	5–15	Up to 50	*Fusarium solani*; *Fusarium avenaceum*; *Fusarium oxysporum*	Hou et al., 2011; Zhang et al., 2018; Zhang et al., 2020; Liu and Wu, 2022
Xinjiang	4–15.5		*Fusarium solani*, *Fusarium incarnatum*, *Fusarium chlamydosporum* var. *fuscum*	Chu et al., 2019; Duan, 2021
Yunnan	20–30		*Fusarium* oxysporum, *Fusarium* avenaceum, *Fusarium* solani	Wang et al., 2002a; Wang et al., 2018
Jiangsu		10–30	*Fusarium oxysporum*, *Fusarium avenaceum*; *Fusarium moniliforme*	Ren et al., 2003
Zhejiang			*Fusarium acuminatum*, *Fusarium oxysporum*, *Fusarium moniliforme*, *Fusarium moniliforme* var. *subglutinans*, and *Fusarium solani*	Bao et al., 1992
Fujian		5–12	*Fusarium* oxysporum, *Fusarium* avenaceum, *Fusarium* moniliforme, and Fusarium equiseti	Wang, 2013
Qinghai	44–68		*Fusarium solani*	Chen, 1999; Wang et al., 2006

rot diseases were observed in the field, with 10% to 30% of plants dying and up to 40% in fields with severe infection. *Fusarium* spp. was identified as the major causal agent, the top four isolated species being *F. oxysporum*, *F. avenaceum*, *F. moniliforme*, and *Fusarium equiseti*. All the four species showed high virulence on faba bean (Ren et al., 2003).

In Yunnan province, wilt disease, stem rot, and root rot usually occurred in faba bean simultaneously (Figure 5), with major pathogens including *F. oxysporum*, *F. avenaceum*, *F. solani*, *R. solani*, and *P. debaryanum* Hesee (Wang et al., 2002a). Furthermore, after treatment with the secondary metabolite of *F. oxysporum*, the wilting symptom was also clearly observed on pea (*Pisum sativum*), common bean (*Phaseolus vulgaris*), cowpea (*Vigna unguiculata*), and maize (Wang et al., 2002b), which suggested the non-specific toxicity of the pathogen. *Fusarium oxysporum* is dominant at the seedling stage, causing stem rot, while *F. avenaceum* is more commonly associated with stem rot and wilt in mature plants (Wang et al., 1988). Based on a provincial survey on faba bean, *Fusarium* spp. is the main genus causing seedling root rot, with *F. oxysporum* and *F. avenaceum* being the most frequently isolated species. *Rhizoctonia solani* was identified as having the highest virulence among all the isolates, followed by *F. oxysporum* and *Fusarium sporotrichioides* (Ruan et al., 1986). Host range studies showed that *F. avenaceum*, isolated from the stem of faba bean, caused severe stem and root rot on faba bean and pea, and induced wilt and necrosis symptoms on the leaf of vetch (*Vicia cracce*). However, no infection was found on wheat, maize, common bean, or 35 other crops from 11 different genera (Ruan et al., 1982). Charcoal rot caused by *M. phaseolina* (Tassi) Goid has recently been reported as a problem for faba bean in Yunnan, causing serious yield losses due to root rot, leaf chlorosis, and wilting; eventually, plant death occurred with the necrosis leaf attached (Sun et al., 2019; Yu et al., 2021).

In Xinjiang province, root rot disease on faba bean has been a significant problem since 2009, leading to yield losses of nearly 100% in severely infected fields. The top three prevalent pathogens were identified as *Fusarium* spp., *Rhizoctonia* spp., and *Alternaria* spp. through molecular and morphological characterization (Duan, 2021). Additionally, *Fusarium chlamydosporum* var. *fuscum* was reported to cause severe root and basal stem rot diseases (Chu et al., 2019). In Hubei province, *Fusarium proliferatum* was reported as a causal agent of faba bean root rot (Zhao et al., 2011).

Generally, root rot and wilt diseases are prevalent in faba bean cultivation regions across China, which can cause 100% yield loss under severe conditions. The predominant causative agent of these diseases is the genus *Fusarium*, with different species dominating in

FIGURE 5
Root rot and wilt symptoms in faba bean in the field of Yunnan.

different regions. Similarly, *Fusarium* spp. has been reported as the most common pathogen causing foot and root rot in faba bean globally (Sillero et al., 2010; Šišić et al., 2020). However, the characterization of *Fusarium* spp. at diverse taxonomic levels and the impact of the pathogens on the disease development have been investigated to a lesser extent in China and worldwide, although it is crucial for the development of resistant varieties and integrated management strategies. Additionally, most of the studies conducted in China were carried out many years ago, highlighting the need for more recent studies to obtain more accurate information on the causal agents.

4 Management of root rot disease in China

Management strategies for root rot have included fungicide treatments, crop rotation, and variety selection, with the most cost-effective strategy being the use of resistant varieties (Marburger et al., 2014; Dolatabadian et al., 2022). However, the availability of resistance to root rot is limited (Rubiales and Khazaei, 2022). Crop rotation can also be an effective strategy but is limited by the broad host range of the pathogens (Bullock, 1992; Cook, 2006; Hwang et al., 2009; Marburger et al., 2014). Fungicide seed treatments are widely used but their efficacy varies depending on the specific species of *Fusarium* and may also have negative impacts on soil organisms and the environment (Munkvold and O'Mara, 2002; Broders et al., 2007; Ellis et al., 2011; Esker and Conley, 2012; Chang et al., 2014).

The management of faba bean root rot disease in China involves various methods, including physical, chemical, and bio-control approaches. One widely used strategy is intercropping with non-host crops, such as wheat, which has been shown to increase the diversity of rhizosphere fungi, reduce the incidence of faba bean root rot disease, and decrease the presence of *Fusarium* spp. in the soil (Luo et al., 2012). Intercropping with wheat has also been reported to decrease the content of citric and malic acid in the rhizosphere, resulting in reduced incidence and severity of Fusarium wilt disease caused by *F. oxysporum* (Xiao, 2013). Moreover, intercropping with wheat has been shown to increase the diversity of the rhizosphere microorganism, promote plant tissue integrity and growth, suppress the cinnamic acid-induced stress, alleviate the autotoxicity of faba bean, and increase the gene copy number of *Bacillus brevis*, which can alleviate the effects of Fusarium wilt on the faba bean crop (Dong et al., 2013a; Dong et al., 2017; Lv et al., 2020; Wang et al., 2020b; Guo et al., 2021; Zhang et al., 2023). Furthermore, intercropping faba bean with different wheat cultivars, such as Yunmai 42 and Yunmai 47, has been shown to significantly reduce the disease index of Fusarium wilt and improve rhizosphere microbial activity and diversity. The significant increase in the total content of organic acids and reduction in the levels of soluble sugar and free amino acids in the root exudates of Yunmai 42 and Yunmai 47 were identified as the main reason for the reduction in Fusarium wilt disease (Yang et al., 2014). In field conditions in Gansu, intercropping faba bean with potato in a 2:2 row ratio reduced Fusarium wilt incidence by 5.66% and disease index by 1.6 (Zhang et al., 2020). Faba bean density was also tested, with results showing that 12×10^5 plants per hectare had the lowest disease incidence and index, and the highest hundred seed weight and yield (Zhang et al., 2018). Under controlled environmental conditions, faba bean grown in soil collected from diseased fields had the lowest plant death rate at 50% water holding capacity (WHC), while growth parameters were significantly better at 50% WHC than at 30% or 70% WHC (Li and Nan, 2000).

The application of nitrogen has been found to be an effective method to control Fusarium wilt in faba bean by altering the composition and metabolic function of the rhizospheric microbial community and reducing the density of *F. oxysporum* (Dong et al., 2013b). In Zhejiang, a field study was conducted to investigate the effect of a 3% plant activator protein extracted from *Alternaria* spp. on root rot caused by *F. solani*. The results showed that leaf application of a 1,000-times diluted plant activator protein at the seedling stage reduced the disease index by 85.5% compared to the non-treated control (Wu et al., 2006). Similarly, the use of root exudates from different faba bean cultivars can increase resistance to Fusarium wilt by reducing the total content of free amino acids and soluble sugar and increasing organic acids (Dong et al., 2014b).

Inoculation of faba bean with arbuscular mycorrhizal fungi (AMF) species has also been found to enhance the plant's ability to resist Fusarium wilt and improve microbial carbon metabolic activity in the rhizosphere soil (Dong et al., 2019). Additionally, some rhizobacteria and *Bacillus subtilis* strains have been shown to inhibit the growth of *F. oxysporum* and *F. chlamydosporum* var. *fuscum*, respectively, which are known to cause root rot in faba bean (Wang et al., 2018; Chu et al., 2019). In Xinjiang, the use of bio-control agents, either as seed treatment, root irrigation, or applied at the time of seeding, showed a significant reduction in disease incidence and an increase in yield (Duan, 2014). The results of a study conducted in Qinghai indicated that the use of two biological pesticides, *Paenibacillus polymyxa* and *Trichoderma harzianum*, was effective in reducing the disease index of Fusarium wilt in faba bean. Application of 1 billion cfu·g^{-1} of *P. polymyxa* reduced the disease index by 74.23%, while application of ≥200 million live spores·g^{-1} of *T. harzianum* reduced it by 71.01% (Zhang et al., 2022).

A 2-year field study on faba bean root rot control found that applying triadimefon (0.01 g·kg−1 seed) showed the best efficacy, reducing disease index by 51.5% and death rate of mature plants by 31.9%–36%, while increasing seed yield by 19.6%–97.6% (Nan et al., 2002). *In vitro* tests demonstrated that tebuconazole and prochloraz were the most effective fungicides in inhibiting the growth of *Fusarium* spp. and the germination of conidia spores. In field trials, the best seed or root treatment was found to be a combination of prochloraz and *B. subtilis* at a ratio of 1:1 (v:v), with concentrations of 10^4 μg·ml^{-1} and 2×10^{10} cfu·ml^{-1}, respectively. This treatment reduced the disease index by 44.67%–52.21% across several field sites (Ren, 2002).

In China, a few cultivars with moderate to high resistance to *F. oxysporum* have been mentioned (Dong et al., 2014b), but the genetic basis of resistance has yet to be explored. Similarly, in Egypt, sources of resistance to *F. oxysporum* and *F. solani* were reported in

faba bean, mostly moderate resistance, but no further studies were conducted to explore the genetic mechanisms (Ali et al., 2019; Mahmoud and Abd El-Fatah, 2020).

In summary, various methods have been found to be effective in reducing the incidence of root rot and wilt disease in faba bean in China. Most of the research has focused on the pathogen *F. oxysporum*, and control of other *Fusarium* species and other pathogens has been less investigated. In Egypt, intercropping faba bean with garlic, as well as with onion and caraway, along with AMF inoculation can reduce root rot disease and enhance profitability and sustainable production (Abdel-Monaim and Abo-Elyousr, 2012; Mousa and El-Sayed, 2016; El-Mehy et al., 2022). Bio-control agents, such as *Paenibacillus* spp., *Bacillus* spp., and *Trichoderma* spp., all exhibited good potential in suppressing root-related disease in faba bean (Alfauomy and Atwa, 2020). Although biological control has shown promising results on the control of root rot disease, it has not been widely applied in faba bean production because of its cost. Chemical control is widely used, but the timing of application is crucial, as it can be difficult to control the disease once it has already started in the field. While resistance to stem, foot, and root rots has been reported in some germplasms of faba bean, no genetic information was reported. Understanding the genetic mechanism of resistance to *Fusarium* species and pathogens from other genera is essential for the development of effective disease control strategies, including resistance breeding. Developing an integrated management strategy that takes into account multiple factors and adopts a holistic approach is crucial to effectively controlling root rot disease in faba bean in China.

5 Conclusion

As a leading country, China plays an irreplaceable role in faba bean production worldwide. The long history of cultivation and diverse habitats across the country allow year-round and multipurpose production to meet domestic needs. However, the lack of standard criteria for quality control, as well as traditional extensive cultural practices, lowers the competitiveness of faba bean products in international markets. Root rot and wilt disease pose another threat to the development of the faba bean industry. Studies on the identification and control of these diseases are still in the primary stage, with little systemic understanding of exploiting the diversity of the causal agents to integrated disease management strategies. To facilitate the faba bean industry development domestically or internationally, it is extremely important to set unified standards for agricultural products, change cultural practices to more intensive methods, and conduct systemic projects to explore knowledge regarding the characteristics of the pathogens involved in root-related diseases and the integrated disease control methods for a specific single pathogen or for a pathogen complex.

Author contributions

HY: drafting the manuscript. FY, CH, and XY: analysis and/or interpretation of data. AZ, YT, and YW: acquisition of data. AS: revising the manuscript. HY, YH, and ML: revising the manuscript critically for important intellectual content and approval of the version of the manuscript to be published. All authors contributed to the article and approved the submitted version.

Funding

This work was supported by the Natural Science Foundation of Yunnan Province (202001AT070011), the International Plan of Talented Young Scientist Program (Egypt-19-046), and the Yunnan Key R&D Program (202202AE090003).

Acknowledgments

We thank members of the Innovation Team of Food Legume from the Food Crop Institute, Yunnan Academy of Agricultural Science for helpful discussion.

Conflict of interest

The authors declare that the research was conducted in the absence of any commercial or financial relationships that could be construed as a potential conflict of interest.

Publisher's note

References

Abdel-Monaim, M. F., and Abo-Elyousr, K. A. (2012). Effect of preceding and intercropping crops on suppression of lentil damping-off and root rot disease in new valley-Egypt. *Crop Protection.* 32, 41–46. doi: 10.1016/j.cropro.2011.10.011

AEGIC (2019) *Australian Pulses: quality, versatility, nutrition*. Available at: https://www.aegic.org.au (Accessed 6 February 2019).

Alcamo, J., Flörke, M., and Märker, M. (2007). Future long-term changes in global water resources driven by socio-economic and climatic changes. *Hydrological Sci. J.* 52 (2), 247–275. doi: 10.1623/hysj.52.2.247

Alfauomy, G. A., and Atwa, M. A. (2020). Influences of biological control on damping off diseases of faba beans as well as physico-chemical and

technological properties. *Middle East J. Agric. Res.* 9 (4), 812–827. doi: 10.36632/mejar/2020.9.4.64

Ali, M. B., Haridy, A. G., and Mahmoud, A. F. (2019). Evaluation of faba bean genotypes for yield and resistance to fusarium root rot under greenhouse and field conditions. *Int. J. Biosciences.* 14 (2), 374–385. doi: 10.12692/ijb/14.2.374-385

Bao, S. (2016). *Technology in production of faba bean* (Beijing: Beijing Education Press).

Bao, S., He, Y., Zong, X., Wang, L., Li, L., Enneking, D., et al. (2008). Collection of pea (*Pisum sativum*) and faba bean (*Vicia faba*) germplasm in yunnan. *Plant Genet. Resour. Newsletter.* 156, 11–22.

Bao, J. R., Wang, G. C., and Ye, C. M. (1992). Analysis on *Fusarium* pathogens on faba bean in zhejiang province. *Acta Agriculturae Universitatis Zhejiangensis.* 18 (3), 61–64.

Blesh, J. (2019). Feedbacks between nitrogen fixation and soil organic matter increase ecosystem functions in diversified agroecosystems. *Ecol. Applications: a Publ. Ecol. Soc. America.* 29 (8), e01986. doi: 10.1002/eap.1986

Broders, K. D., Lipps, P. E., Paul, P. A., and Dorrance, A. E. (2007). Evaluation of *Fusarium graminearum* associated with corn and soybean seed and seedling disease in Ohio. *Plant Disease.* 91, 1155–1160. doi: 10.1094/PDIS-91-9-1155

Bullock, D. G. (1992). Crop rotation. *Crit. Rev. Plant Sci.* 11 (4), 309–326. doi: 10.1080/07352689209382349

Chang, K. F., Conner, R. L., Hwang, S. F., Ahmed, H. U., McLaren, D. L., Gossen, B. D., et al. (2014). Effects of seed treatments and inoculum density of *Fusarium avenaceum* and *Rhizoctonia solani* on seedling blight and root rot of faba bean. *Can. J. Plant Sci.* 94 (4), 693–700. doi: 10.4141/cjps2013-339

Chen, Z. Q. (1999). Investigation and research on the incidence and harm of broad bean wilt disease in the main production areas of qinghai province. *Qinghai Agric. Forestry Sci. Technology.* 03, 14–17.

Chu, M., Gu, M. Y., Tang, Q. Y., Zhu, J., Hao, X. Y., and Zhang, Z. D. (2019). Identification of pathogenic fungi causing the root rot disease of dabancheng faba bean and analysis of antagonistic effect by the biocontrol bacteria. *Xinjiang Agric. Sci.* 56 (10), 1904–1911. doi: 10.6048/j.issn.001-4330.2019.010.016

Cook, R. J. (2006). Toward cropping systems that enhance productivity and sustainability. *Proc. Natl. Acad. Sci.* 103 (49), 18389–18394. doi: 10.1073/pnas.0605946103

Costanzo, A., and Bàrberi, P. (2014). Functional agrobiodiversity and agroecosystem services in sustainable wheat production. a review. *Agron. Sustain. Dev.* 34 (2), 327–348. doi: 10.1007/s13593-013-0178-1

Crépon, K., Marget, P., Peyronnet, C., Carrouee, B., Arese, P., and Duc, G. (2010). Nutritional value of faba bean (*Vicia faba* l.) seeds for feed and food. *Field Crops Res.* 115 (3), 329–339. doi: 10.1016/j.fcr.2009.09.016

Dhull, S. B., Kidwai, M. K., Noor, R., Chawla, P., and Rose, P. K. (2022). A review of nutritional profile and processing of faba bean (*Vicia faba* l.). *Legume Science.* 4 (3), e129. doi: 10.1002/leg3.129

Dolatabadian, A. R., Cornelsen, J., Huang, S. H., Zou, Z., and Fernando, W. D. (2022). Sustainability on the farm: breeding for resistance and management of major canola diseases in Canada contributing towards an IPM approach. *Can. J. Plant Pathology.* 44 (2), 157–190. doi: 10.1080/07060661.2021.1991480

Dong, Y., Dong, K., Tang, L., Zheng, Y., Yang, Z. X., Xiao, J. X., et al. (2013a). Relationship between rhizosphere microbial community functional diversity and faba bean fusarium wilt occurrence in wheat and faba bean intercropping system. *Acta Ecologica Sinica.* 33 (23), 7445–7454. doi: 10.5846/stxb201208281214

Dong, Y., Dong, K., Yang, Z. X., Zhu, J. H., Tang, L., and Zheng, Y. (2017). Effect of cinnamic acid on incidence of faba bean fusarium wilt and incidence-mitigating mechanisms of wheat and faba bean intercropping. *Acta Pedologica Sinica.* 54 (02), 503–515. doi: 10.11766/trxb201605030043

Dong, Y., Dong, K., Zheng, Y., Tang, L., and Yang, Z. X. (2014a). Faba bean fusarium wilt (*Fusarium oxysporum*) control and its mechanismin different wheat varieties and faba bean intercropping system. *Chin. J. Appl. Ecology.* 25 (7), 1979–1987. doi: 10.13287/j.1001-9332.20140505.001

Dong, Y., Dong, K., Zheng, Y., Yang, Z. X., Tang, L., and Xiao, J. X. (2014b). Allelopathic effects and components analysis of root exudates of faba bean cultivars with different degrees of resistance to *Fusarium oxysporum.* Chinese journal of eco-agriculture 22, 3, 292–299. doi: 10.3724/SP.J.1011.2014.31020

Dong, Y., Yang, Z. X., Dong, K., Tang, L., Zheng, Y., and Hu, G. B. (2013b). Effects of nitrogen application rate on faba bean fusarium wilt and rhizospheric microbial metabolic functional diversity. *Chin. J. Appl. Ecology.* 24 (4), 1101–1108. doi: 10.13287/j.1001-9332.2013.0265

Dong, Y., Zhao, S., Lv, J. X., and Dong, K. (2019). Synergistic effects of intercropping with wheat and inoculation with arbuscular mycorrhizal fungi on improvement of anti-fusarium wilt and rhizosphere microbial carbon metabolic activity of faba bean. *J. Plant Nutr. Fertilizers.* 25 (10), 1646–1656. doi: 10.11674/zwyf.18400

Döös, B. R. (2002). Population growth and loss of arable land. *Global Environ. Change.* 12 (4), 303–311. doi: 10.1016/S0959-3780(02)00043-2

Du, C. Z. (2021) *A breakthrough in the breeding of new varieties of broad beans* Available at: http://www.moa.gov.cn/xw/qg/202104/t20210429_6366977.htm

Duan, X. D. (2014). Evaluation of three biocontrol agents for managing root rot in faba bean. *Rural Sci. Technology.* 10, 26–27. doi: 10.3969/j.issn.1002-6193.2014.10.015

Duan, X. D. (2021). Isolation and identification of several broad bean root rot pathogens. *Heilongjiang Agric. Sci.* 6, 59–66. doi: 10.11942/j.issn1002-2767.2021.06.0059

Duchene, O., Vian, J. F., and Celette, F. (2017). Intercropping with legume for agroecological cropping systems: complementarity and facilitation processes and the importance of soil microorganisms. a review. *Agriculture Ecosyst. Environment.* 240, 148–161. doi: 10.1016/j.agee.2017.02.019

Ellis, M. L., Broders, K. D., Paul, P. A., and Dorrance, A. E. (2011). Infection of soybean seed by *Fusarium graminearum* and effect of seed treatments on disease under controlled conditions. *Plant Disease.* 95 (4), 401–407. doi: 10.1094/PDIS-05-10-0317

El-Mehy, A. A., El-Gendy, H. M., Aioub, A. A., Mahmoud, S. F., Abdel-Gawad, S., Elesawy, A. E., et al. (2022). Response of faba bean to intercropping, biological and chemical control against broomrape and root rot diseases. *Saudi J. Biol. Sci.* 29 (5), 3482–3493. doi: 10.1016/j.sjbs.2022.02.032

Esker, P. D., and Conley, S. P. (2012). Probability of yield response and breaking even for soybean seed treatments. *Crop Science.* 52 (1), 351–359. doi: 10.2135/cropsci2011.06.0311

FAO (2016). Available at: http://www.fao.org/pulses-2016/en/ (Accessed April 11, 2016).

FAOSTAT (2022) *Statistics database of the food and agriculture organization of the united nations.* Available at: http://www.fao.org/statistics/databases/en/ (Accessed 26 May 2022).

Guo, Y., Lv, J., Dong, Y., and Dong, K. (2021). Exploration of the potential mechanism of faba bean–wheat intercropping to control faba bean fusarium wilt due to allelopathic plant extracts. *ACS omega.* 6 (24), 15590–15600. doi: 10.1021/acsomega.0c06120

He, Z. B. (2019). *Study on the nutrient release pattern and allelopathic mechanism of faba bean green manure in chongqing* (China: Southwest University).

Hou, S. W., Li, M. ,. Q., Yang, X. M., and Yang, F. R. (2011). Identification of fusarium pathogens for root rot of *Vicia faba* l. at seedling stage in the cold and humid regions of gansu. *Hunan Agric. Sci.* 15, 97–100. doi: 10.3969/j.issn.1006-060X.2011.15.030

Hwang, S. F., Ahmed, H., Gossen, B. D., Kutcher, H., Brandt, S., Strelkov, S. E., et al. (2009). Effect of crop rotation on the soil pathogen population dynamics and canola seedling establishment. *Plant Pathol. J.* 8 (3), 106–112. doi: 10.3923/ppj.2009.106.112

Infantino, A., Kharrat, M., Riccioni, L., Coyne, C.J., McPhee, K.E., and Grünwald, N.J. (2006). Screening techniques and sources of resistance to root diseases in cool season food legumes. *Euphytica* 147, 201–221. doi: 10.1007/s10681-006-6963-z

Johnson, J. B., Skylas, D. J., Mani, J. S., Xiang, J., Walsh, K. B., and Naiker, M. (2021). Phenolic profiles of ten Australian faba bean varieties. *Molecules.* 26, 4642. doi: 10.3390/molecules26154642

Kuttibai, T. G. J., Bhagavathi, M. S., and Prakash, V. (2022). Smart farming: future of agriculture. *Res. Highlights Agric. Sci.* 6, 64–72. doi: 10.9734/bpi/rhas/v6/3951E

Lang, L. J., Yu, Z. H., Zheng, Z., Xu, M., and Ying, H. Q. (1993). *Faba bean in China: state-of-the-art review* (Aleppo, Syria: ICARDA), 4–7.

Li, L., Guo, Y. P., and Yang, S. H. (2018). Breeding of spring faba bean cultivar lincan 12 and the cultivation technic. *China Seed Industry.* 9, 88–89. doi: 10.19462/j.cnki.1671-895x.20180829.015

Li, C. J., and Nan, Z. B. (1996). Investigation of the incidence and effect of root rot on spring faba bean in linxia area. *Plant Protection.* 22 (06), 25–26.

Li, C. J., and Nan, Z. B. (2000). Effects of soil moisture contents on root rot and growth of faba bean. *Acta Phytopathologica Sinica.* 30 (3), 245–249. doi: 10.3321/j.issn:0412-0914.2000.03.010

Liebenberg, A. J. (2002) *Dry bean production. printed and published by department of agriculture, resource centre, directorate agricultural information services, private bag X.* Available at: https://archive.org/details/liebenberg-2002-dry-bean-production.

Liu, T., and Wu, G. (2022). Does agricultural cooperative membership help reduce the overuse of chemical fertilizers and pesticides? *Evidence Rural China. Environ. Sci. pollut. Res.* 29 (5), 7972–7983. doi: 10.1007/s11356-021-16277-0

Luo, Y. T., Tang, L., Zheng, Y., and Dong, Y. (2012). Effects of wheat-faba bean intercropping on the yield and rhizosphere pathogen in different n application rates. *Chin. J. Soil Science.* 43 (4), 826–831. doi: 10.19336/j.cnki.trtb.2012.04.011

Lv, J., Dong, Y., Dong, K., Zhao, Q., Yang, Z., and Chen, L. (2020). Intercropping with wheat suppressed fusarium wilt in faba bean and modulated the composition of root exudates. *Plant Soil.* 448, 153–164. doi: 10.1007/s11104-019-04413-2

Mahmoud, A. F., and Abd El-Fatah, B. E. S. (2020). Genetic diversity studies and identification of molecular and biochemical markers associated with fusarium wilt resistance in cultivated faba bean (*Vicia faba*). *Plant Pathol. J.* 36 (1), 11–28. doi: 10.5423/PPJ.OA.04.2019.0119

Marburger, D., Venkateshwaran, M., Conley, S., Esker, P., Lauer, J., and Ane, J.-M. (2014). Crop rotation and management effect on fusarium spp. populations. *Crop Science.* 55, 1–12. doi: 10.2135/cropsci2014.03.0199

Minor Grain Crops (2018). Available at: http://www.mgcic.com/content/4378 (Accessed December 12, 2018).

Mousa, A. M., and El-Sayed, S. A. (2016). Effect of intercropping and phosphorus fertilizer treatments on incidence of *Rhizoctonia* root-rot disease of faba bean. *Int. J. Curr. Microbiol. Appl. Sci.* 5 (4), 850–863. doi: 10.20546/ijcmas.2016.504.097

Munkvold, G. P., and O'Mara, J. K. (2002). Laboratory and growth chamber evaluation of fungicidal seed treatments for maize seedling blight caused by *Fusarium* species. *Plant Disease.* 86 (2), 143–150. doi: 10.1094/PDIS.2002.86.2.143

Nan, Z. B., Ge, G. Z., and Li, C. J. (2002). Effect of pesticides on field-controlling root rot of *Vicia faba.* Chinese journal of applied ecology 13, 8, 943–947. doi: 10.13287/j.1001-9332.2002.0220

Oxford Analytica (2019). World hunger is likely to rise as 2030 UN target nears. *Expert Briefings*. doi: 10.1108/OXAN-DB246018

Paul, S. K., and Gupta, D. R. (2021). Faba bean (*Vicia faba* l.), a promising grain legume crop of Bangladesh: a review. *Agric. Rev.* 42 (3), 292–299. doi: 10.18805/ag.R-203

Ren, H. Y. (2002). *Study on the pathogen of faba bean fusarium wilt and their control in changshu of jiangsu province* (Nanjing, China: Nanjing Agricultural University).

Ren, H. Y., Chen, Z. Y., Xu, Z. G., Lu, J. Y., and Xu, Y. C. (2003). Study on main species and virulence of faba bean fusarium wilt in changshu area. *Plant Protection*. 04, 30–32. doi: 10.3969/j.issn.0529-1542.2003.04.009

Ruan, X. Y., Jiang, Y. C., Luo, W. F., and Wang, J. H. (1982). Two new forms of *Fusarium avenaceum* (FR) sacc. -the pathogens of broad bean stem-end rot. *Acta Phytopathologica Sinica*. 02, 27–34.

Ruan, X. Y., Wang, J. H., Tang, J. Y., and Gu, S. (1986). Analysis on the mycoflora and their dominant species of the pathogen which caused seedling root disease of faba bean. *J. Yunnan Agric. University.* 01, 15–22.

Rubiales, D., and Khazaei, H. (2022). Advances in disease and pest resistance in faba bean. *Theor. Appl. Genet.* 135 (11), 3735–3756. doi: 10.1007/s00122-021-04022-7

Shi, K., Chen, Y., Yu, B., Xu, T., Li, L., Huang, C., et al. (2016). Urban expansion and agricultural land loss in China: a multiscale perspective. *Sustainability*. 8 (8), 790. doi: 10.3390/su8080790

Sillero, J. C., Villegas-Fernández, A. M., Thomas, J., Rojas-Molina, M. M., Emeran, A. A., Fernández-Aparicio, M., et al. (2010). Faba bean breeding for disease resistance. *Field Crops Res.* 115 (3), 297–307. doi: 10.1016/j.fcr.2009.09.012

Singh, A. K., Bharati, R. C., Manibhushan, N. C., and Pedpati, A. (2013). An assessment of faba bean (*Vicia faba* l.) current status and future prospect. *Afr. J. Agric. Res.* 8 (50), 6634–6641. doi: 10.5897/AJAR2013.7335

Singh, S. P., and Schwartz, H. F. (2010). Breeding common bean for resistance to diseases: a review. *Crop Science.* 50 (6), 2199–2223. doi: 10.2135/cropsci2009.03.0163

Šišić, A., Baćanović-Šišić, J., Schmidt, H., and Finckh, M. R. (2020). "Root pathogens occurring on pea (*Pisum sativum*) and faba bean (*Vicia faba*) in Germany," in *30th Scientific-Experts Conference of Agriculture and Food Industry: Answers for Forthcoming Challenges in Modern Agriculture*. 69–75. (Springer International Publishing).

Snowdon, R. J., Wittkop, B., Chen, T. W., and Stahl, A. (2021). Crop adaptation to climate change as a consequence of long-term breeding. *Theor. Appl. Genet.* 134 (6), 1613–1623. doi: 10.1007/s00122-020-03729-3

Sun, S. L., Zhu, Z. D., Duan, C. X., Zhao, P., Sun, F., Deng, D., et al. (2019). First report of charcoal rot caused by *Macrophomina phaseolina* on faba bean in China. *Plant Disease.* 103 (6), 1415. doi: 10.1111/jph.12413

Varshney, R. K., Close, T. J., Singh, N. K., Hoisington, D. A., and Cook, D. R. (2009). Orphan legume crops enter the genomics era! *Curr. Opin. Plant Biol.* 12, 202–210. doi: 10.1016/j.pbi.2008.12.004

Wang, H. Z. (2013). Occurrence and control for stem wilt (*Fusarium avenaceum*) of broad beans. *Fujian Agric. Sci. Technology.* 10, 45–46. doi: 10.3969/j.issn.0253-2301.2013.10.020

Wang, J. H., Nie, Z. L., Xu, Y. Q., and Zheng, Y. (2018). The inoculation effect of rhizobia on *Vicia faba* growth and its disease resistance with root rot. *J. Southwest Forestry University.* 38 (4), 94–99. doi: 10.11929/j.issn.2095-1914.2018.04.015

Wang, Y. Y., Ren, J. B., Zhang, Y., Zheng, Y., and Tang, L. (2020b). Effect of wheat and faba bean intercropping on improving rhizosphere microflora and reducing fusarium wilt of faba bean. *Chin. J. Soil Sci.* 51 (05), 127–1133. doi: 10.19336/j.cnki.trtb.2020.05.16

Wang, J. H., Tang, J. Y., and Ruan, X. Y. (1988). Study on the correlation of root-disease incidence between seedling and adult stage of faba bean. *J. Yunnan Agric. University.* 02, 119–124.

Wang, J. H., and Wang, C. D. (2002a). Outbreak characters of broad bean blight and complex infection by pathogens in yunnan, China. *J. Yunnan Agric. University.* 04, 449. doi: 10.3969/j.issn.1004-390X.2002.04.062

Wang, J. H., Wang, C. D., and Lu, N. (2002b). Toxic effects of *Fusarium oxysporum* extracts on broad bean seed germination and seedling growth. *J. Yunnan Agric. Univ.* 04, 395–396+399. doi: 10.3969/j.issn.1004-390X.2002.04.028

Wang, L. P., Yu, H. T., Lv, M. Y., and He, Y. H. (2020a). *Superior varieties of food legume and cultivation technologies in yunnan* (Yunnan: Yunnan Technology Press).

Wang, X. O., Zhu, Z. D., Leur, J. V., Bretag, T., Bayaa, B., Kumari, S., et al. (2006). "Predictive forecasting and integrated control," in *Proceedings of the 2006 Academic Conference of the Chinese Society of Plant Pathology, Status of disease of faba bean and pea in Qinghai province*. (Changsha, China: Chinese Agricultural Science and Technology Press). 363–368.

Wang, H. F., Zong, X. X., Guan, J. P., Yang, T., Sun, X. L., Ma, Y., et al. (2012). Genetic diversity and relationship of global faba bean (*Vicia faba* l.) germplasm revealed by ISSR markers. *Theor. Appl. Genet.* 124 (5), 789–797. doi: 10.1007/s00122-011-1750-1

Wu, Q., Yang, X., and Qiu, D. (2006). 3% plant activating protein induced antibiotic resistance in broad bean. *Plant Prot.* 06, 149–152. doi: 10.3969/j.issn.0529-1542.2006.06.045

Xiang,, et al. (2022). Available at: http://www.chinawestagr.com/homepage/showcontent.asp?id=50272.

Xiao, J. X. (2013). *Characteristics of root exudates and its reaction to faba bean fusarium wilt in wheat and faba bean intercropping* (China: Yunnan Agricultural University).

Yang, Z. X., Tang, L., Zheng, Y., Dong, K., and Dong, Y. (2014). Effects of different wheat cultivars intercropped with faba bean on faba bean fusarium wilt, root exudates and rhizosphere microbial community functional diversity. *J. Plant Nutr. Fertilizer.* 20 (3), 570–579. doi: 10.11674/zwyf.2014.0307

Ye, Y., Lang, L., Xia, M., and Tu, J. (2003). *Faba bean in China* (Beijing: China Agriculture Press), 1–15.

Yu, H. T., Wang, L. P., Lv, M. Y., Yang, F., Tang, Y. S., Ding, M. L., et al. (2020). Correlation and path analysis of major agronomic traits to fresh yield of early-mature and autumn-sowing faba bean (*Vicia faba* l.). *Southwest China J. Agric. Sci.* 33 (4), 711–717. doi: 10.16213/j.cnki.scjas.2020.4.005

Yu, H. T., Wang, L. P., Lv, M. Y., Yang, F., Yan, H. B., Wang, Q. F., et al. (2019a). Analysis of status and development of food legumes industry in yunnan province. *Southwest China J. Agric. Sci.* 32 (supp.), 80–85.

Yu, H. T., Wang, L. P., Yang, F., He, Y. H., and Lv, M. Y. (2021). Complete mitochondrial genome of the important phytopathogenic fungus *Macrophomina phaseolina* (Botryosphaeriales, ascomycota). *Mitochondrial DNA. Part B Resources.* 6 (10), 2972–2974. doi: 10.1080/23802359.2021.1975505

Yu, H. T., Wang, L. P., Yang, F., Lv, M. Y., Zong, X. X., Yang, T., et al. (2019b). Identification and utilization of short wing petal broad bean (*Vicia faba* l.) germplasm. *J. Plant Genet. Resource* 20 (5), 1334–1339+1348. doi: 10.13430/j.cnki.jpgr.20181212001

Yu, H. T., Yang, F., Wang, L. P., Lv, M. Y., Hu, C. Q., Yang, X., et al. (2018). Highly efficient cultivation model of fresh edible autumn-sown early-maturing faba bean in yunnan-using mulching-film side seeding. *Liaoning Agric. Sci.* 6, 87–88. doi: 10.3969/j.issn.1002-1728.2018.06024

Yuan, T. T., Dong, Y., and Zhao, Q. (2020). Effects of benzoic acid on pathogenicity of *Fusarium oxysporum* f. sp. *fabae* and tissue structure resistance of faba bean root. *Plant Physiol. J.* 56 (3), 441–454. doi: 10.13592/j.cnki.ppj.2019.0411

Zhang, Y., Bai, X. J., Fan, J. X., Guo, Y. P., Liu, Y., and Xia, Z. L. (2020). Effects of different intercropping modes on root rot and crop growth of broad bean. *Agric. Sci. Technol. Communication.* 1, 128–131. doi: 10.3969/j.issn.1000-6400.2020.01.045

Zhang, C., Dong, Y., Tang, L., Zheng, Y., Makowski, D., Yu, Y., et al. (2019). Intercropping cereals with faba bean reduces plant disease incidence regardless of fertilizer input; a meta-analysis. *Eur. J. Plant Pathology.* 154 (4), 931–942. doi: 10.1007/s10658-019-01711-4

Zhang, Y., Li, L., Guo, Y. P., and Shao, Y. (2018). Impact of different planting densities on root rot and crop growth of faba bean in intercropping systems. *Anhui Agric. Sci. Bullet.* 24 (18), 60–61. doi: 10.16377/j.cnki.issn1007-7731.2018.18.028

Zhang, L. Y., Liu, Y., Chen, P. Q., Weng, H., and Ma, Z. Q. (2022). Control efficacy of several biological pesticides on the main diseases and pests of broad bean in qinghai. *Chin. J. Biol. Control.* 38 (6), 1377–1384. doi: 10.16409/j.cnki.2095-039x.2022.01.019

Zhang, Z., Yang, W., Li, Y., Zhao, Q., and Dong, Y. (2023). Wheat-faba bean intercropping can control fusarium wilt in faba bean under *F.commune* and ferulic acid stress as revealed by histopathological analysis. *Physiol. Mol. Plant Pathology.* 124, 101965. doi: 10.1016/j.pmpp.2023.101965

Zhao, Z. Y., Xiao, Y. N., and Zhu, Z. D. (2011). "Identification and biological characteristics of the pathogen *Fusarium proliferatum* isolated from root rot tissue of broad bean," in *Proceedings of the 2011 Academic Conference of the Chinese Society of Plant Pathology*. 1. (Yichang, China: China Agricultural Science and Technology Press).

Zhou, Y., Yao, M. N., Miao, Y. M., Jin, J. H., Gu, C. Y., Zhao, N., et al. (2022). The developmental of fresh broad bean industry in China. *J. Agriculture.* 12 (2), 80–84. doi: 10.11923/j.issn.2095-4050.cjas2021-0137

frontiers | Frontiers in Plant Science

TYPE Original Research
PUBLISHED 28 July 2023
DOI 10.3389/fpls.2023.1120435

OPEN ACCESS

EDITED BY
Marie-Laure Pilet-Nayel,
INRAE Bretagne Normandie, France

REVIEWED BY
Sylvain Jeandroz,
Agrosup Dijon, France
Lyndon Porter,
United States Department of Agriculture (USDA), United States

*CORRESPONDENCE
Luke D. Bainard
luke.bainard@agr.gc.ca

RECEIVED 09 December 2022
ACCEPTED 13 July 2023
PUBLISHED 28 July 2023

CITATION
Hubbard M, Thomson M, Menun A, May WE, Peng G and Bainard LD (2023) Effects of nitrogen fertilization and a commercial arbuscular mycorrhizal fungal inoculant on root rot and agronomic production of pea and lentil crops. *Front. Plant Sci.* 14:1120435. doi: 10.3389/fpls.2023.1120435

Effects of nitrogen fertilization and a commercial arbuscular mycorrhizal fungal inoculant on root rot and agronomic production of pea and lentil crops

Michelle Hubbard[1], Madeleine Thomson[1], Alexander Menun[1], William E. May[2], Gary Peng[3] and Luke D. Bainard[1,4]*

[1]Swift Current Research and Development Center, Agriculture and Agri-Food Canada, Swift Current, SK, Canada, [2]Indian Head Research Farm, Agriculture and Agri-Food Canada, Indian Head, SK, Canada, [3]Saskatoon Research and Development Centre, Agriculture and Agri-Food Canada, Saskatoon, SK, Canada, [4]Agassiz Research and Development Center, Agriculture and Agri-Food Canada, Agassiz, BC, Canada

In the Canadian prairies, pulse crops such as field pea (*Pisum sativum* L.) and lentil (*Lens culinaris* L.) are economically important and widely grown. However, in recent years, root rot, caused by a variety of fungal and oomycete pathogens, including *Aphanomyces euteiches*, has become a limiting factor on yield. In this study, we examined the impacts of nitrogen (N) fertilization and a commercial arbuscular mycorrhizal fungal (AMF) inoculant on pea and lentil plant health and agronomic production at three locations in Saskatchewan: Swift Current, Indian Head and Melfort. The AMF inoculation had no impact on root rot severity, and therefore is not considered a reliable method to manage root rot in pea and lentil. In contrast, N fertilization led to reductions in root rot in Swift Current, but not the other two sites. However, N fertilization did reduce nodulation. When both pea and lentil are considered, the abundance of *A. euteiches* in soil increased from pre-seeding to mid-bloom. A negative correlation between soil pH and disease severity was also observed. The high between-site variability highlights the importance of testing root rot mitigation strategies under multiple soil conditions to develop site-specific recommendations. Use of N fertilizer as a root rot management strategy merits further exploration, including investigation into its interactions with other management strategies, soil properties, and costs and benefits.

KEYWORDS

***Aphanomyces euteiches*, *Fusarium*, nitrogen, commercial arbuscular mycorrhizal fungi (AMF), root rot, Pea, Lentil**

1 Introduction

Field pea (*Pisum sativum* L.) and lentil (*Lens culinaris* L.) are grown extensively across the Canadian prairies (Statistics Canada, 2020) and are valuable cash crops for many farmers. However, both crops are susceptible to root rot which can greatly lower yields. The root rot complex is widespread across the Canadian prairies and consists of several fungal and oomycete pathogens including *Fusarium* spp., *Pythium* spp., *Rhizoctonia solani*, and *Aphanomyces euteiches* (Xu et al., 2012; Gossen et al., 2016; Taheri et al., 2017; Chatterton et al., 2019). Between 2014 and 2017 root rot was considered severe in up to 99% of surveyed pea fields and 34% of surveyed lentil fields (Chatterton et al., 2019). Pea yield losses due to *A. euteiches* can be up to 86% (Wu et al., 2018). The severity and prevalence of root rot in pea and lentil depend on both field conditions and crop management techniques. High soil moisture and compaction favor more severe disease (Van der Plaats-Niterink, 1981; Hall and Phillips, 1992; Tu, 1994; Hossain et al., 2012; Chatterton et al., 2019). Fungal pathogens can also build up over time when pulse crops are grown in short succession (Bainard et al., 2017; Niu et al., 2018).

Seed treatment, cultivar selection, and cultural practices such as crop rotation have been suggested as management strategies for pulse crop-associated root rot (Bailey et al., 2001; Chang et al., 2004; Chang et al., 2013; Gossen et al., 2016). However, none of these strategies are fully effective (Gossen et al., 2016) and all create challenges and limitations for growers. *A. euteiches* is a particularly difficult component of the root rot complex to manage because it produces resting oospores that can survive for 10 to 20 years in soil (Pfender and Hagedorn, 1983; Persson et al., 1999; Hughes and Grau, 2013). The only recommended control measures are to avoid planting in fields with high inoculum levels and 6-8 year breaks between susceptible crops (Hossain et al., 2012; Moussart et al., 2013). These long rotations are highly impractical for producers. Thus, there is an urgent need to further explore alternative options to manage root rot that will benefit both crop and soil health.

Pulse crops, including pea and lentil, produce the majority of their own nitrogen (N) by hosting N-fixing bacteria in their nodules (Herridge et al., 2008). In the Canadian prairies, pea and lentil can fix the equivalent of 37-69 and 23-87 kg of N ha^{-1}, respectively, depending on the year (Hossain et al., 2016). Because of this, most producers do not add N to their pea or lentil crops, which helps reduce input costs (Salvagiotti et al., 2008). N fertilization has been shown to decrease nodulation in pea, altering biological N fixation (Clayton et al., 2004; Achakzai, 2007). However, application of N fertilizer may reduce root rot by inducing roots to harden and become "woodier", potentially impeding pathogen penetration (Nightingale and Farnham, 1936; Smith and Walker, 1941; Papavizas and Lewis, 1971; Hossain et al., 2015). N plays an important, but complex, role in the response of plants to diseases, including *A. euteiches* (Ballini et al., 2013; Gupta et al., 2013; Fagard et al., 2014; Mur et al., 2017; Thalineau et al., 2018). Increased N supply can lead to either increased or decreased susceptibility to disease. Factors such as the plant genotype (Ballini et al., 2013; Thalineau et al., 2018), the lifestyle of the pathogen (biotroph versus necrotroph) (Ballini et al., 2013) and the N form (Gupta et al., 2013) can alter the impact of N on phytopathosystems. Thalineau et al. (2018) suggests that whether N increased or decreased *A. euteiches* root rot in the legume *Medicago truncatula* is independent of how the plant in impacted by low N levels. Gupta et al. (2013) found that NO_3^-, but not NH_4^+, led to enhanced disease resistance in tobacco, potentially due to the conversion of NO_3^- to NO, an important signalling molecule. Given the lack of consensus on the net effects of N fertilization on root rot in pea and lentil, further research is necessary to help producers make informed management decisions.

The application of a commercial arbuscular mycorrhizal fungal (AMF) inoculant is another potential management strategy to help decrease root rot in pulse crops. In natural systems, AMF form symbiotic relationships with plants, increasing nutrient uptake, improving plant health and suppressing disease (Azcón-Aguilar and Barea, 1997; Bødker et al., 1998; Borowicz, 2001; Wehner et al., 2010; Meç et al., 2016). In agriculture, commercial AMF inoculants can be used to promote AMF colonization of crops. However, the effects of AMF inoculation on plant health and root rot in pulse crops are highly variable. Inconsistencies between studies on the effectiveness of AMF inoculation as a root rot management tool, depending on the AMF product used, or field versus greenhouse, (Rosendahl, 1985; Talukdar and Germida, 1994; Bødker et al., 2002; Thygesen et al., 2004; Faye et al., 2013; Jin et al., 2013) point to the need for additional research. In addition, N fertilizer application can interfere with AMF functioning (Ryan and Ash, 1999; Corkidi et al., 2002), making the combined impacts of N and AMF application more interesting for further research.

The current study explores whether and how N fertilization and an AMF commercial inoculant influence root rot and agronomic production in field-grown pea and lentil crops on the Canadian prairies. We used a combination of disease ratings and qPCR to analyze rhizosphere and root samples from three locations in Saskatchewan. The specific objectives of this study were to determine the effects of N fertilization and an AMF commercial inoculant on 1) *A. euteiches* inoculum levels in soil planted to pea or lentil, 2) pea and lentil root health (i.e., root rot severity and association with beneficial symbionts) and 3) pea and lentil crop yield.

2 Materials and methods

2.1 Experimental design

Field experiments were conducted in 2018 at three locations in Saskatchewan: 1) Agriculture and Agri-Food Canada (AAFC) Research Farm in Melfort (soil type: Orthic Black Chernozem silty clay loam), 2) a commercial field located approximately 15 km south of Swift Current (soil type: Orthic Brown Chernozem with a silt loam), and 3) AAFC Research Farm in Indian Head (soil type: Redo Black Chernozem with a heavy clay). All field sites had high levels, sufficient to cause root rot symptoms, of *A. euteiches* as well as other root rot pathogens, including

Fusarium spp. All sites were seeded to field pea (*P. sativum*) in 2016 and 2017 to encourage inoculum build-up for these pathogens.

The impacts of N fertilizer, AMF inoculation, and crop [field pea ('CDC Amarillo') or lentil ('CDC Maxim')] on root rot, nodulation, biomass and yield were examined with a three-factorial experiment using a randomized complete block design. Each block contained three N fertilization rates (0, 60, or 120 kg/ha N; 46-0-0 urea [$CO(NH_2)_2$], side-banded) and two AMF inoculant treatments (no inoculation or a commercial AMF inoculant [AGTIV Field Crops Granular, active ingredient *Glomus intraradices* with 142 viable spores/g] at 5.2 kg/ha, applied in-furrow). The 12 treatments were replicated four times at each location, for a total of 48 plots per site. All plots were fertilized with phosphorus at 17 kg/ha and received 5.2 kg/ha of Cell-Tech single action granular rhizobial inoculant (100 million (1 x 10^8) viable cfu/g *Rhizobium leguminosarum bv. viciae*), applied in-furrow, and the row spacing was 25 cm. The plots were 4 x 8 m in Melfort, 2 x 8 m in Swift Current and 4 x 11 m in Indian Head. Seeding occurred on May 4 (Indian Head), May 16 (Swift Current) and May 23 (Melfort). Pea was seeded at 200 kg/ha and lentil at 67 kg/ha in Melfort and Swift Current, and at 194 and 54 kg/ha, respectively, in Indian Head. In Melfort, in season herbicide application consisted of imazamox (8 g/acre) and bentazon (171.6 g/acre) (June 18) and bentazon (436.8 g/acre) (July 6) applied to pea; 37 g/acre each of imazethapyr and imazamox, 13.4g/acre of tepraloxydim and 0.20 L/acre of the surfactant Merge (June 18) to lentil; and sethoxydim (202.5g/acre) (June 29) on both crops 7.0 g/ac). In Swift Current, glyphosate (270 g/acre) and carfentrazone (7 g/acre) were applied pre-seeding (May 9); imazamox (8.1 g/ac) and quizalofop (19.0 g/ac) were applied for in-crop weed control (June 13) and Diquat (167.9 g/ac) was used for desiccation (August 9). At Indian Head, imazamox and imazethapyr (6.1 g/ac each) with sethoxydim (6750 g/ac) and Merge surfactant (0.5% v/v) were applied for in-crop weed management (June 19).

2.2 Sampling and analysis of soil and plant material

Soil samples were collected before seeding of each trial in early to mid-May (at Indian Head on May 2, Swift Current on May 4, and Melfort on May 16) and again during the growing season at early flowering (at Indian Head on June 27, Swift Current on July 5, and Melfort on July 9). At both sampling times, four soil cores (2.5 cm in diameter and 20 cm deep) were collected from two 1 m sampling locations in each plot. This included collecting two soil cores from the front left corner of each plot (i.e., 1 m in from the front of the plot and between the 3rd and 4th crop row from the left side) and two soil cores from the back right corner of each plot (i.e., 1m in from the back of the plot and between the 3rd and 4th row of crops from right side). The four soil cores were homogenized in the field to form one composite sample per plot. A 10 g subsample was immediately removed and flash frozen in liquid N in the field and then stored at -80°C prior to molecular analysis. In the laboratory, the remaining soil was passed through a 2 mm sieve, and a 20 g subsample of the sieved soil was used to determine soil moisture gravimetrically. Another 200 g of sieved soil from each plot was air-dried for chemical analysis. Crop yield of each plot was collected at harvest.

Soil nitrate N (NO_3-N), phosphate phosphorus (PO_4-P) and potassium were determined using sodium bicarbonate extractions and colorimetric analysis using Technicon Autoanalyzer (Harm et al., 1973; Gendry and Willis, 1988). Soil total carbon was determined using the dry combustion method with a Elementar vario MICRO cube elemental analyser (Schumacher, 2002). Soil organic carbon and total N were determined by acidification with HCl, followed by a dry combustion procedure from Schumacher (2002). Soil pH and electrical conductivity were measured using water saturation paste (Hendershot et al., 2008) and paste extracts (Miller and Curtin, 2008).

Plants used for disease assessment were collected at early flowering, the same time and same locations in each plot as the second soil sampling. From each plot, 10 plants (5 from each sampling location in a plot) were dug up, keeping their roots intact, and stored at 4°C for processing. Roots were subsequently washed and individually rated within two days for 1) shoot symptom severity (SSS), 2) *Fusarium* root rot (Fusarium severity [FS]), 3) *A. euteiches* and *Fusarium* root rot (*Aphanomyces* severity [AS]), and 4) nodulation. The average ratings of the 10 plants from a plot were used for statistical analysis. SSS was rated on a 1-5 scale based on the discoloration and stunting (Pilet-Nayel et al., 2002). A rating of 1 or 5 indicate a healthy or dead plant, respectively. FS was rated using a 1-7 scale from Chatterton et al. (2019), which was modified from Bilgi et al. (2008). This scale incorporates the presence of lesions, percentage of root area with discolouration, and reduction of root mass. A 0-5 scale developed by Willsey et al. (2018) was used to rate AS, and the nodulation was rated on a 0-10 scale (Table 1). Subsamples of roots were preserved in 50% ethanol and used to assess AMF colonization. The level of AMF root colonization was assessed by staining with an ink-vinegar solution (Vierheilig et al., 1998) and using the magnified intersects method (McGonigle et al., 1990). The above-ground plant material was

TABLE 1 Rating scale for nodulation.

Rating	Nodules
0	No nodules
1	<5 total nodules or 1 large nodule
2	<10 total nodules or 2 large nodules
3	<15 total nodules or 3 large nodules
4	<20 total nodules or 4 large nodules
5	<25 total nodules or 5 large nodules
6	>25 total nodules or >5 large nodules
7	>30 total nodules or crown nodulation* started but incomplete
8	Crown nodulation < 1 cm3
9	Crown nodulation >1 cm3
10	2 or more crown nodules >1 cm3

* nodulation near the soil surface.

excised and dried, and then weighed to determine the plant dry weight.

In order to quantify the abundance of *A. euteiches* in the soil, DNA was extracted from each sample (0.25 g x 2 per sample) using a DNeasy PowerSoil Kit (Qiagen) and quantified via qPCR as described in detail by Karppinen et al. (2020) using the methods initially developed by Willsey et al. (2018).

2.3 Statistical analyses

To determine whether there were differences in soil properties prior to seeding at the three field trial locations, we used non-parametric tests (i.e., Kruskal-Wallis test followed by Dunn test for multiple means comparison) due to the data not meeting the assumptions of an analysis of variance (ANOVA). Principal component analysis (PCA) was also used to visualize the differences in composition of the soil properties at the three locations. Linear mixed models were used to test the effects of crop (lentil and pea), N fertilization rate (0, 60, and 120 kg N ha^{-1}), and AMF inoculation (seeded with or without commercial inoculant) on *A. euteiches* abundance, crop disease symptoms (FS, AS, and SSS), root symbioses (nodulation and AMF colonization), and agronomic production (crop biomass and grain yield). Crop, N fertilization rate, and AMF inoculation were included as fixed factors, and replicate was included as a random factor in the models. Initial assessment revealed when all sites were analyzed together the data did not meet the assumptions of the linear mixed model. As a result of this and different soil types at these trial locations (Table 2; Figure 1), we analyzed the experimental treatment data at each location independently. When dependent variables did not meet the assumptions of the linear mixed models, they were transformed (log, square root or arcsine square root) to meet the assumptions, or analyzed with the non-parametric Kruskal-Wallis test. We also used a linear mixed model to test the effect of sampling date (pre-seeding and mid-bloom), crop (lentil and pea), and their interaction on the abundance of *A. euteiches*. Relationships between variables hypothesized to be related, such as *A. euteiches* abundance, soil properties, and disease symptoms, were examined using regression analysis across all three locations. All statistical analyses were completed in R (v.4.2.2).

3 Results

3.1 Soil chemical composition and moisture

All soil properties at the three field trial sites (Swift Current, Indian Head, and Melfort) were significantly different (Table 2), and differences in soil composition were distinguishable using PCA (Figure 2). Soil moisture, pH, potassium (K), electrical conductivity, nitrate-N, phosphate-P, total N, total carbon and organic carbon were important in differentiating the soils. Swift Current was drier, had lower pH, K, total carbon, organic carbon and total N than the other two sites, but higher NO_3-N. Indian Head had the highest mid-bloom % soils moisture, pH, electrical conductivity and K. Melfort had the highest PO4-P, total carbon, organic carbon and total N. Soil moisture levels decreased between pre-seeding and mid-bloom in Indian Head and Melfort, but not Swift Current (Table 2). Because of the strong differences between sites, further statistical analyses were analysed separately by site. The differences in soil texture between the three sites strengthens this argument.

3.2 *A. euteiches* levels in soil and disease symptoms

A. euteiches abundance in the soil significantly increased in Indian Head and Melfort from pre-seeding to mid-bloom where peas were grown, however, there was no significant increase where lentils were grown at all three locations (Table 3). At mid-bloom, soil in which pea crops were grown had significantly higher *A. euteiches* levels compared to lentil at all three locations (Table 4, Figure 1; Supplementary Tables 1.1–1.3). This effect was more evident at the Indian Head and Melfort locations as we observed

TABLE 2 Mean soil properties (± standard error) of the three field trials at each location in Saskatchewan, Canada, prior to seeding.

Site	Soil moisture		pH	EC	K	NO_3-N	PO_4-P	Total C	Organic C	Total N
	(%)	(%)		(mS/cm)	(mg kg^{-1})	(mg kg^{-1})	(mg kg^{-1})	(mg kg^{-1})	(mg kg^{-1})	(mg kg^{-1})
	pre-seeding	mid-bloom	pre-seeding	pre-seeding	pre-seeding	pre-seeding	pre-seeding	pre-seeding	pre-seeding	pre-seeding
	***	***	***	***	***	***	***	***	***	***
Indian Head	35.4 ± 0.4a	29.5 ± 0.3a	7.56 ± 0.01a	0.66 ± 0.01a	572 ± 13a	16.3 ± 0.5b	12.9 ± 0.6b	2.9 ± 0.0b	2.7 ± 0.0b	0.27 ± 0.00b
Melfort	34.4 ± 0.2a	27.0 ± 0.3b	6.63 ± 0.03b	0.46 ± 0.02c	430 ± 15b	13.7 ± 0.4c	32.7 ± 1.0a	4.7 ± 0.1a	4.6 ± 0.1a	0.42 ± 0.01a
Swift Current	18.7 ± 0.1b	19.8 ± 0.1c	6.31 ± 0.04c	0.57 ± 0.02b	222 ± 5c	20.0 ± 1.0a	15.7 ± 0.8b	1.7 ± 0.0c	1.5 ± 0.0c	0.18 ± 0.00c

[1]EC, electrical conductivity.
[2]Different letters within columns represent significant differences at P < 0.001 based on Kruskal-Wallis test. Mean separations based on a Dunn's Test.
***$P < 0.001$ based on Kruskal-Wallis test.

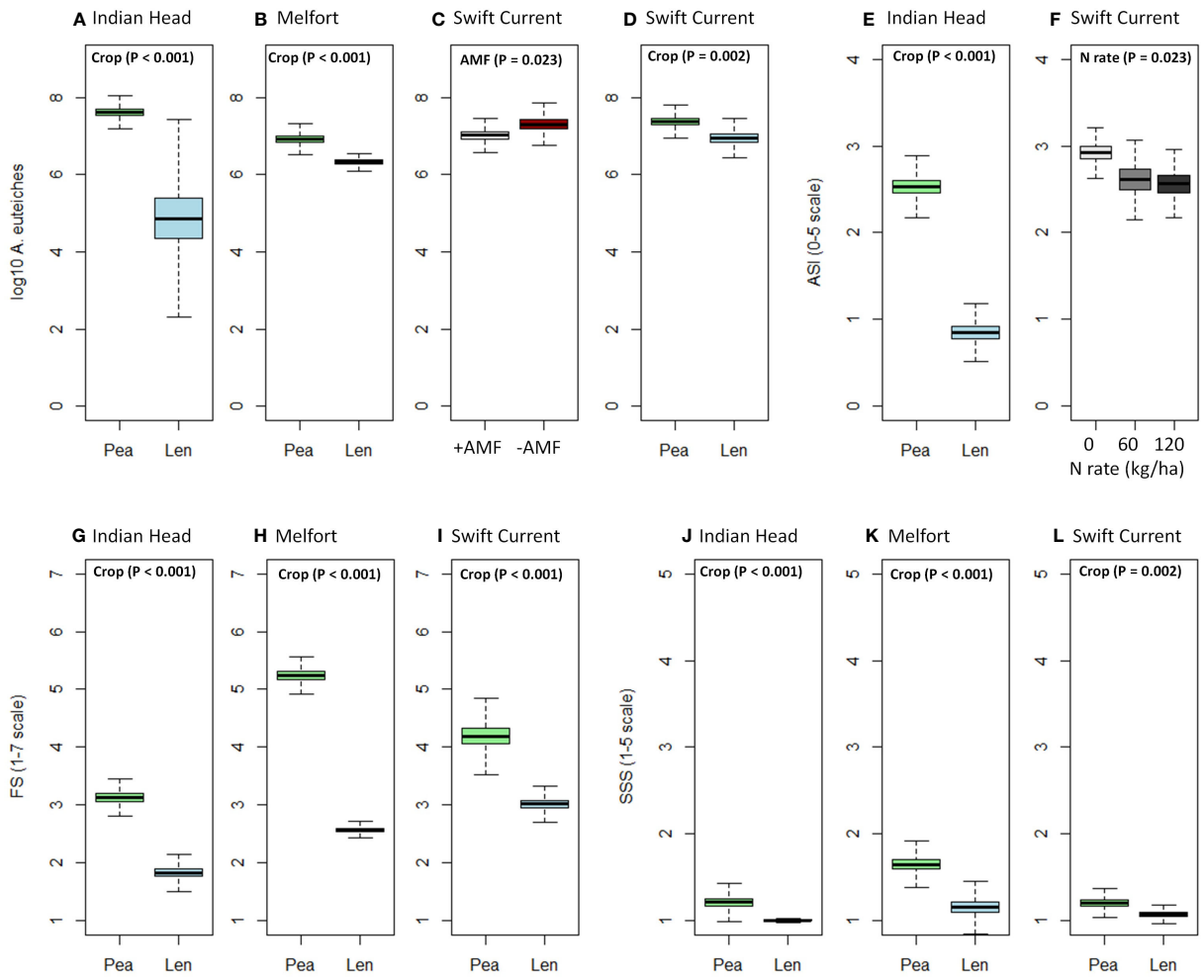

FIGURE 1
Boxplots (mean, standard error, and standard deviation) of the significant effects (based on Table 4) of crop, N fertilizer rate, and AMF inoculation on **(A–D)** *A. euteiches* abundance in soil, **(E, F)** *Aphanomyces* and *Fusarium* symptoms (AS), **(G–I)** *Fusarium spp.* symptoms (FS), **(J–L)** shoot symptom severity (SSS) at each location. P-values of the significant effects are included in each boxplot. All other results (i.e., non-significant) for *A. euteiches* abundance, AS, FS, and SSS can be found in Supplementary Tables 1.1–1.3.

significant sampling date by crop interactions (Table 3). At both Indian Head and Melfort, *A. euteiches* inoculum load was higher in the soil from plots containing pea assessed at mid-bloom than in pre-seeding soil samples from plots that would be seeded to pea or in lentil plots either before seeding or at mid-bloom. There was no interaction between sampling date and crop at Swift Current (Table 3). At Swift Current, but not Indian Head or Melfort, AMF inoculation increased *A. euteiches* abundance in the soil (Table 4; Figure 1).

N fertilization lowered AS at Swift Current, but did not affect disease ratings at any other site (Table 4; Figure 1F). AMF inoculation did not have a significant impact on disease ratings. Overall, pea had more severe disease symptoms than lentil; AS at Indian Head and FS and SSS at all sites were impacted (Table 4; Figure 1).

Several relationships were observed between disease ratings, pre-seeding soil chemical parameters, and *A. euteiches* inoculum levels (Supplementary Figures 1–4). Because pea and lentil were consistently different, the two crops were analysed separately. For pea, there were positive relationships between pre-seeding *A. euteiches* levels and both AS and FS. However, a negative relationship was found between FS and mid-bloom abundance of *A. euteiches* in the soil, and no significant relationship was found between AS and this variable (Supplementary Figure 1). For lentil, both pre-seeding and mid-bloom *A. euteiches* levels were positively correlated with FS and AS (Supplementary Figure 2). Negative linear relationships were observed between soil moisture and FS and AS for lentil, (Supplementary Figure 3). For pea, the relationship between soil moisture and disease were not significant. Inverse linear relationships were found between pre-seeding soil pH and FS and AS for both pea and lentil crops (Supplementary Figure 4).

3.3 Nodulation and AMF colonization

Nodulation was significantly higher in lentil than pea at Indian Head and Melfort, but not Swift Current (Table 4; Figure 3). N fertilization decreased nodulation at Melfort (Figure 3). Inoculation

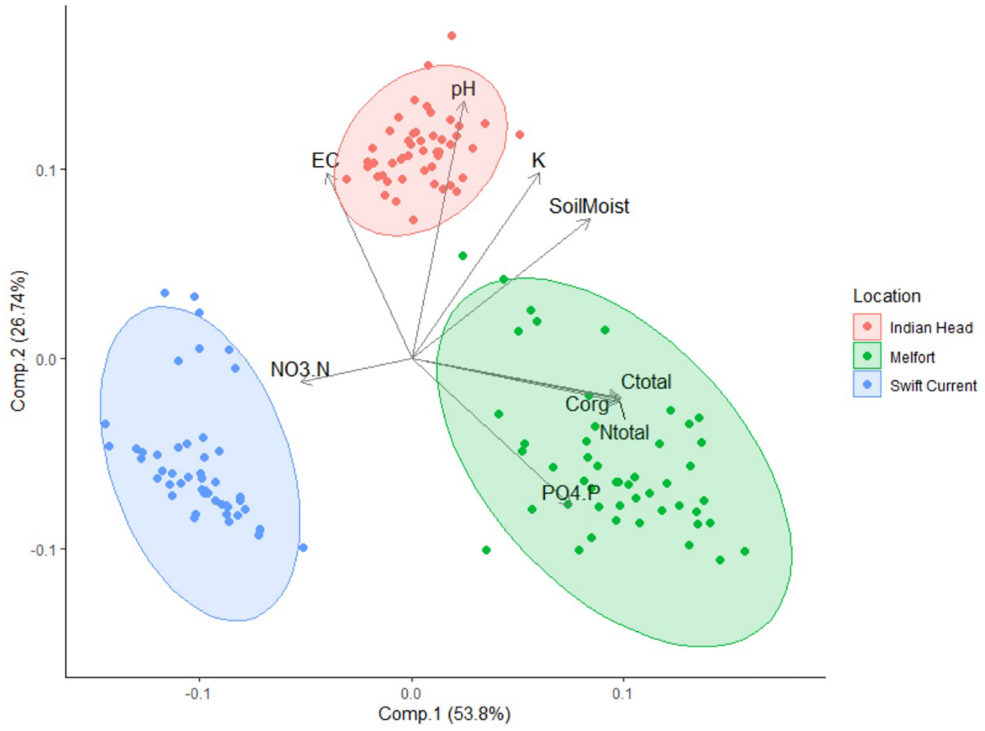

FIGURE 2
Principle component analysis (PCA) ordination showing the variation in pre-seeding soil properties of samples collected at the three field trial locations. EC, electrical conductivity; Soil Moist, soil moisture; NO_3.N, nitrate-N; PO_4.P, phosphate-P; Corg, organic carbon; Ctotal, total carbon; Ntotal, total nitrogen.

with AMF and N fertilization interacted at Swift Current (Table 4, Figure 3; Supplementary Tables 1.1–1.3).

AMF inoculation did not impact percent AMF colonization (Table 4; Supplementary Tables 1.1–1.3). AMF colonization was decreased by N fertilization in Swift Current, but not at both other locations (Figure 3). In Swift Current, lentil had higher AMF colonization than pea (Figure 3).

3.4 Plant dry weight and grain yield

Plant biomass (dry weight) was consistently higher in pea than lentil at all three sites (Table 4, Figure 4; Supplementary Tables 1.1–1.3). Biomass was also significantly increased by N fertilization at all three sites (Figure 4). Grain yield was higher in pea than lentil at Melfort and Swift Current, but not Indian Head (Figure 4). N

TABLE 3 Effect of sampling date and crop on the abundance of *A. euteiches* (log_{10} gene copies g^{-1} soil) at each location in Saskatchewan, Canada.

Factor		Indian Head	Melfort	Swift Current
Date		*p* <0.001	*p* <0.001	*p* <0.001
	Pre-seeding	3.97 ± 0.41b	6.21 ± 0.03b	6.35 ± 0.14b
	Mid-bloom	6.25 ± 0.33a	6.63 ± 0.06a	7.38 ± 0.09a
Crop		*p* <0.001	*p* <0.001	*p* = 0.073
	Lentil	4.30 ± 0.41b	6.25 ± 0.03b	6.61 ± 0.16
	Pea	5.91 ± 0.38a	6.59 ± 0.07a	6.90 ± 0.09
Date : Crop		*p* = 0.011	*p* <0.001	*p* = 0.365
	Pre-seeding:Lentil	3.74 ± 0.61b	6.17 ± 0.04b	6.27 ± 0.28
	Mid-bloom:Lentil	4.87 ± 0.52b	6.33 ± 0.05b	6.95 ± 0.10
	Pre-seeding:Pea	4.20 ± 0.57b	6.24 ± 0.03b	6.42 ± 0.07
	Mid-bloom:Pea	7.63 ± 0.09a	6.93 ± 0.08a	7.38 ± 0.09

P-values are based on linear mixed model analysis of variance. Means with different letters at each location and under each factor are significantly different ($p < 0.05$) based on least squares means test.

TABLE 4 Analysis of variance results (*P*-values) of the effects of crop, N fertilizer rate, arbuscular mycorrhizal fungal (AMF) inoculation, and their respective interactions on *A. euteiches* abundance in soil, crop disease symptoms (AS, Aphanomyces and Fusarium symptoms; FS, Fusarium spp. symptoms; SSS, shoot symptoms), root symbioses (nodulation and AMF colonization), and agronomic production at each location in Saskatchewan, Canada.

Site	Factor	*A. euteiches* abundance	AS	FS[a]	SSS[a]	Nodulation	AMF colonization	Crop biomass	Grain yield
Indian Head	Crop	**<0.001**	**<0.001**	**<0.001**	**<0.001**	**<0.001**	0.821	**<0.001**	0.468
	N rate	0.781	0.126	0.756	0.271	0.250	0.214	**0.023**	<0.001
	AMF	0.893	0.887	0.926	0.498	0.486	0.388	0.543	0.151
	Crop:N rate	0.830	0.053			0.141	0.065	0.781	**<0.001**
	Crop : AMF	0.634	0.480			0.543	0.056	0.653	0.830
	N rate:AMF	0.927	0.811			0.934	0.648	0.868	0.832
	Crop:N rate: AMF	0.667	0.768			0.571	0.660	0.740	0.720
Melfort	Crop	**<0.001**	0.634	**<0.001**	**<0.001**	**<0.001**	0.219	**<0.001**	<0.001
	N rate	0.184	0.842	0.803	0.998	**<0.001**	0.724	**0.046**	0.999
	AMF	0.214	0.185	0.413	0.802	0.280	0.209	0.988	0.582
	Crop:N rate	0.323	0.368			0.372	0.711	0.954	**0.048**
	Crop : AMF	0.973	0.762			0.957	0.662	0.800	0.650
	N rate:AMF	0.998	0.273			0.798	0.410	0.930	**0.035**
	Crop:N rate: AMF	0.938	0.389			0.074	0.743	0.378	0.202
Swift Current	Crop	**0.002**	0.568	**<0.001**	**0.002**	0.326	**<0.001**	<0.001	**<0.001**
	N rate	0.056	**0.023**	0.235	0.445	0.028	**<0.001**	<0.001	**0.039**
	AMF	**0.023**	0.425	0.656	0.889	0.904	0.961	0.098	0.073
	Crop:N rate	0.477	0.288			0.587	0.216	**0.011**	0.410
	Crop : AMF	0.637	0.241			0.203	0.549	0.145	0.613
	N rate:AMF	0.728	0.242			**0.035**	0.493	0.299	0.525
	Crop:N rate: AMF	0.321	0.446			0.705	0.514	0.324	0.879

[a]P-values based on Kruskal-Wallis test.
P-values in bold font represent results that are shown in figure format (Figures 1, 3, and 4), whereas all other results can be found in Supplementary Tables 1.1-3.

fertilization had a significant main effect on grain yield at Indian Head and Swift Current, but not Melfort (Table 4). At Swift Current, yield was highest when 60 kg N ha^{-1} N was applied and 120 kg N ha^{-1} rate produced a greater yield at Indian Head (Figure 4). At Indian Head and Melfort, but not Swift Current, there was an interaction between crop and N fertilizer rate in terms of grain yield. At Indian Head, pea responded to N fertilizer rate, while lentil did not (Figure 4). At Melfort, lentil yield declined in response to N fertilizer rate (Figure 4).

4 Discussion

In this study, N fertilization showed variable effects on root rot for pea and lentil crops. These findings are partially consistent with previous observations that N fertilization can reduce pea root rot (Papavizas and Lewis, 1971) by "hardening" the roots, perhaps increasing the woodiness, toughness and mechanical strength, and preventing pathogen penetration (Nightingale and Farnham, 1936; Smith and Walker, 1941; Hossain et al., 2015). Consistently, pea varieties with genetic resistance to *F. oxysporum* prevent infection, at least in part, by means of barriers of carbohydrates and phenolic acids such as lignin in cell walls (Bani et al., 2018). In contrast, other studies have found that adding N is positively correlated with *Rhizoctonia* root rot in pulses (Liu et al., 2016), as well as root and soil populations of *Fusarium* species (Naseri and Ansari Hamadani, 2017) and *A. euteiches* abundance (Karppinen et al., 2020) in soil. Thus, variation in our results are both consistent with the literature and may be explained by differences in soil chemical properties and *A. euteiches* inoculum levels (Papavizas and Lewis, 1971). It is well documented that finer textured soils favor the development of Aphanomyces root rot due to increased moisture

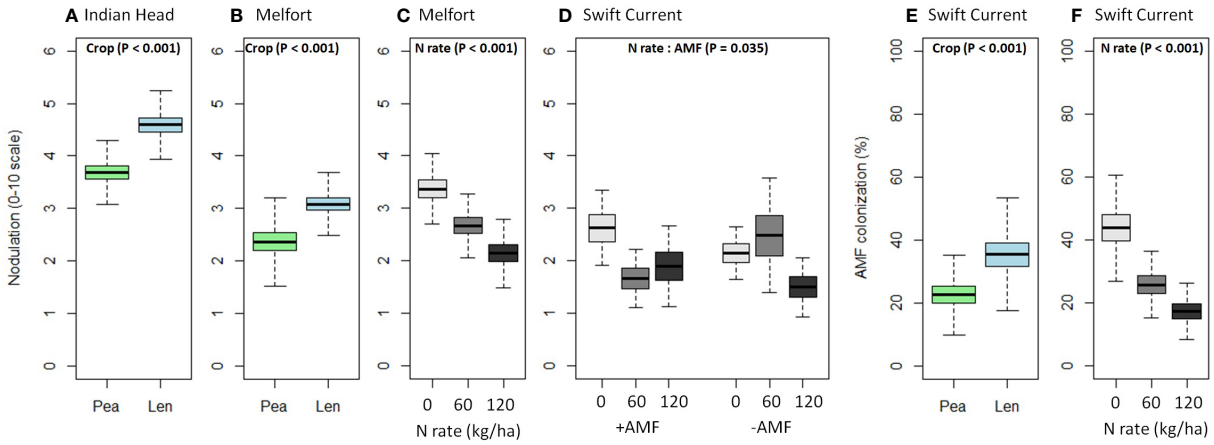

FIGURE 3
Boxplots (mean, standard error, and standard deviation) of the significant main and interaction effects (based on Table 4) of crop, N fertilizer rate, and AMF inoculation on **(A–D)** nodulation and **(E, F)** AMF colonization at each location. P-values of the significant effects are included in each boxplot. All other results (i.e., non-significant) for nodulation and AMF colonization can be found in Supplementary Tables 1.1–1.3.

retention (Kraft et al., 1990; Fritz et al., 1995; Allmaras et al., 2003; Gossen et al., 2016). Thus, it is reasonable that each site would respond to root rot management practices differently. Swift Current was drier than either of the other sites, had lower pre-seeding soil pH, K levels, total carbon, organic carbon and total N. The lower N levels in particular may partially explain the response of AS, crop biomass and grain yield to N fertilization at Swift Current. Although significant, the reductions in AS were minimal and the biological

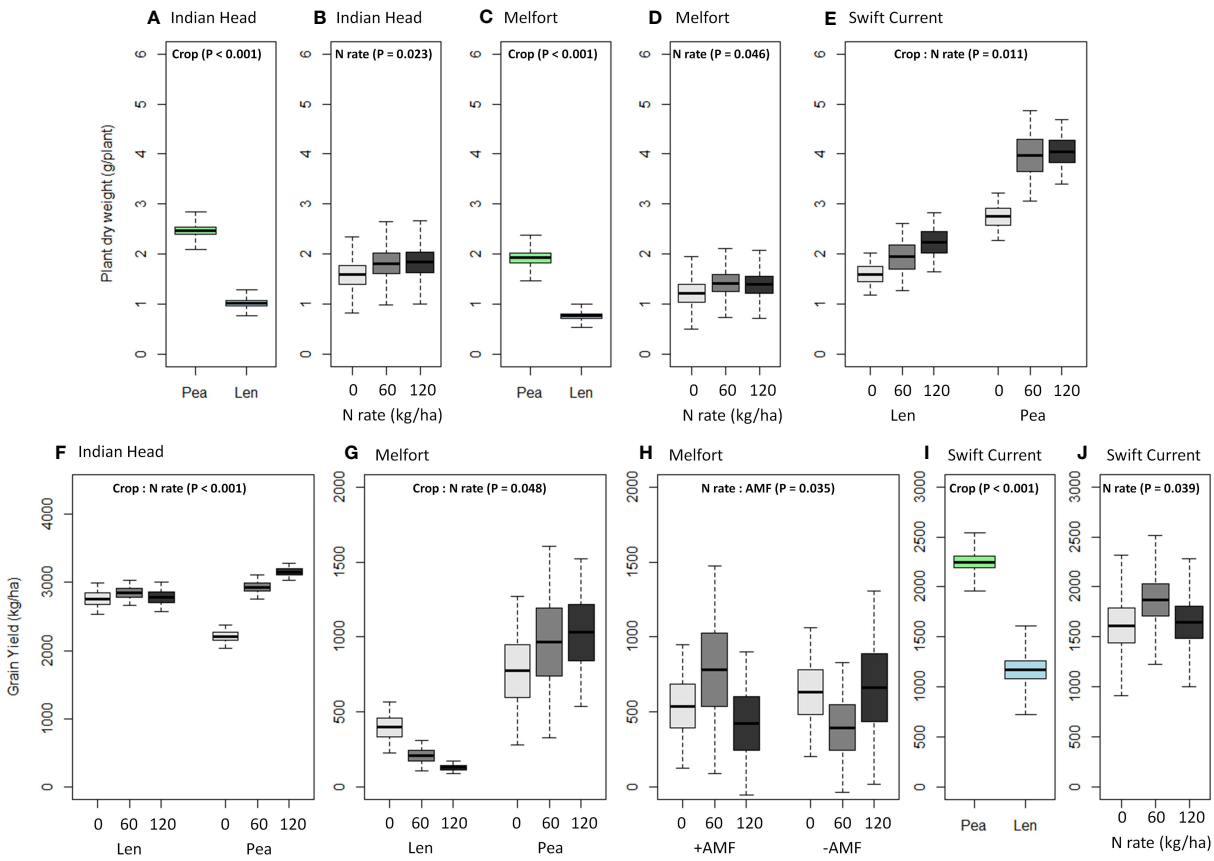

FIGURE 4
Boxplots (mean, standard error, and standard deviation) of the significant main and interaction effects (based on Table 4) of crop, N fertilizer rate, and AMF on **(A–E)** plant dry weight and **(F–J)** grain yield at each location. P-values of the significant effects are included in each boxplot. All other results (i.e., non-significant) for plant dry weight and grain yield can be found in Supplementary Tables 1.1–1.3.

and agricultural relevance is questionable. There remains a need for additional research on the complex links between soil properties and responses of pea and lentil to N fertilization as a root rot management approach.

N application increased plant biomass production (i.e., dry weight) at all sites. Similarly, Nasser et al. (2008) found that N fertilization led to higher lentil biomass. Voisin et al. (2002) found that elevated mineral N availability increased root biomass in pea; this would allow crops to maintain N uptake despite root rot potentially reducing root growth, inhibiting symbiosis with N-fixing bacteria and absorption of soil N. The impact of N fertilization on grain yield was variable depending on the crop, but had a significant impact on yield at all three sites. Voisin et al. (2002) found that pea seed yield was unaffected by soil mineral N availability at moderate N levels, but levels higher than 400 kg N ha^{-1} could slightly decrease seed yield and result in crop lodging. We observed a significant drop in grain yield at high N rates (120 kg ha^{-1}) at the Swift Current site for both crops relative to 60 kg ha^{-1}, and a strong drop in lentil grain yield with increasing N rates at the Melfort site. These results, along with the lack of N fertilization effect on lentil yield at the Indian Head site are not consistent with previous studies that showed N to increase seed yield of lentil (Gan et al., 2005; Nasser et al., 2008). Gan et al. (2005) also found that N increased lentil grain yield only in heavy clay soil, but not silt loam. This indicates that soil properties can affect the impact of N on lentil grain yield, potentially explaining the variation seen in our results.

Inoculation with AMF had no significant impact on shoot or root symptoms in our field study. In contrast, previous studies under controlled, greenhouse conditions have found reduced above and belowground symptoms caused by *A. euteiches* infection when pea plants were inoculated with AMF (Rosendahl, 1985; Thygesen et al., 2004). This may indicate there are additional hurdles to overcome in the field environment for AMF inoculation to provide beneficial effects due to the need for a fully established AMF symbiosis to provide pea plants bio-protection against *A. euteiches* (Slezack et al., 2000). Additionally, the lack of effect in our field study could potentially be due to the lack of success (i.e., colonization of crop roots) by the commercial AMF inoculant or the inoculant could have displaced native AMF species and not altered the overall level of root colonization and/or impacted disease suppressiveness. Differing levels of AMF inoculation success have been reported to be related to variation in local edaphic and environmental conditions (Faye et al., 2013). Different commercial AMF inoculants have shown varying levels of success in pea and lentil (Talukdar and Germida, 1994; Thygesen et al., 2004; Faye et al., 2013; Jin et al., 2013). One reported factor that limits the success or effectiveness of the AMF inoculants is the species composition, with mixed species being more effective than single species inoculants (Jin et al., 2013). Our field trials utilized a single species commercial inoculant (*Rhizophagus irregularis*), which may have limited the effectiveness of this treatment and highlights the need for further research in field-based experiments to better understand the potential of AMF inoculants for controlling root rot pathogens.

The levels of *A. euteiches* present in soil pre-seeding were correlated with AS and FS in both pea and lentil (Supplementary Figures 1, 2). However, the R^2 values were quite low, consistent with Karppinen et al. (2020), pointing to the role of other factors in root rot development, the difficulties of getting complete extraction of *A. eutieches* DNA from soils, and the inability of the current assay to distinguish between living inoculum capable of causing infection and DNA from dead and/or non-virulent material. Mid-bloom *A. euteiches* abundance in soil was only positively correlated with AS and FS in lentil. The inoculum level of *A. euteiches* at mid-bloom may not translate to infection or disease because earlier infection tends to be more important to root rot development (Gaulin et al., 2007; Wu et al., 2018). The qPCR quantification showed the abundance of *A. euteiches* increased between pre-seeding and mid-bloom at Melfort and Indian Head in pea plots only. At Melfort and Indian Head, this occurred only in pea plots. The increase between the two crop stages is likely due to oospores germinating and to forming structures with greater biomass, such as zoosporangia or mycelia during the growing season (Wu et al., 2018). Growing susceptible legumes, such as pea and lentil, can also quickly increase the *A. euteiches* inoculum as the pathogen replicates and completes its life cycle (Moussart et al., 2013; Gossen et al., 2016). It was unclear why the *A. euteiches* population did not increase significantly in lentil plots at Melfort, but at the Indian Head site, it was likely due to the significantly lower disease symptoms observed in these plots compared to pea (i.e., AS rating: lentil = 0.85 and pea = 2.53). The larger root systems that pea plants tend to have compared to lentil may have contributed to this effect by providing more tissue in which *A. euteiches* could potentially reproduce. Other edaphic factors also likely played a role in the varying levels of *A. euteiches* abundance at these locations by influencing the germination and/or further fungal structure formation during the growing season.

There was a positive correlation between pre-seeding abundance of *A. euteiches* and FS for both crops. This is consistent with Willsey et al. (2018) finding of more severe disease when both *Fusarium* and *Aphanomyces* were present. In contrast, a negative relationship was found between these variables for pea at mid-bloom. A possible explanation is that, root rot ratings such as FS may have limitations in determining specific pathogens responsible for the root rot complex (Willsey et al., 2018). Thus, FS may reflect the contribution of multiple pathogens, including those that do not positively reinforce *A. euteiches*.

N application decreased percent nodulation at Swift Current and Melfort in both pea and lentil (Supplementary Tables 1.2, 1.3). Voisin et al. (2002) found that while pea nodulation was inhibited by high N (120 kg ha^{-1}), symbiotic N fixation was replaced by direct absorption from the soil. As a result, N had no significant effect on grain yield. This suggests N fertilization remains a viable option for managing root rot despite its reduction in nodulation. Wu et al. (2018) found root rot may destroy nodules, making mineral N of greater importance for crops grown in the presence of these soil-borne pathogens. Nodulation was largely unaffected by AMF treatment. Xavier and Germida (2003) found the response of lentil to AMF depends on the rhizobium strain and AMF species; indigenous AMF populations can vary in soil of different locations. Incompatible rhizobium and AMF strains do not result in increased nodulation (Xavier and Germida, 2003), and the compatibility is

unknown for the current study. In addition, N fertilization may interfere with AMF functioning (Ryan and Ash, 1999; Corkidi et al., 2002). Consistent with this idea, we observed that for pea and lentil at Swift Current, both N fertilization rates decreased percent AMF colonization (Supplementary Table 1.3). Variation by site, but not crop, may indicate that differences in environmental and soil chemical factors impact the inhibitory effects of N fertilization on AMF colonization.

More acidic pH values were linked to increased AS and FS for both pea and lentil. Soils with high pH, as well as calcium and clay content, can be suppressive to Aphanomyces root rot (Persson and Olsson, 2000; Heyman et al., 2007). Excess calcium can inhibit oospore or zoospore germination (Deacon and Saxena, 1998; Heyman et al., 2007). pH values differed significantly by site, especially between Indian Head and the other sites. However, all sites had pH values between 6 and 7, meaning that nutrient availability should not be inhibited. N fertilization, including urea, can acidify soils, impacting calcium availability (Tian and Niu, 2015), thereby potentially increasing the risk of Aphanomyces root rot. Additional research on the impacts of soil pH across different soil types on pea and lentil crops is merited in conjunction with N fertilization.

The AMF inoculant used in this study is likely not a reliable method of managing *A. euteiches* root rot in pea and lentil. However, N fertilization merits further exploration. However, financial costs, environmental considerations, and potential reduction in biological N fixation may mean that N application is a not a practical approach for root rot management. Based on a price of $623.33 USD/ton for urea (Illinois Production cost report, June 1, 2023, Report-Illinois Production Cost Report (Bi-weekly) (GX_GR210) | MMN (usda.gov)), equating to $49.17 CAD per hectare to apply the 60 kg/ha rate used in this study, $0.34 CAD/kg for yellow pea (5 year average from Farm Credit Canada, 2023 Grains, oilseeds and pulses sector outlook | FCC (fcc-fac.ca)) and the pea yields from Indian Head ($2207 and 2931.7 kg/ha for the 0 and 60 N rates), the 60 N rate would yield $246.40 more for an input cost of $49.17 per hectare. Future research should focus on determining the mechanisms by which the protection against root rot occurs, as the current methods can not confirm the explanation of "woodiness" of roots previously proposed by Hossain et al. (2015). A better understanding of the role of soil pH in *A. euteiches* infection and root rot suppression would also be useful. Variation in our results demonstrate the importance of testing pea and lentil root rot treatments in multiple site-year trials, including different soil types and pre-existing field conditions, for robust conclusions. As shown by this study, both environmental and soil characteristics can affect treatment efficacy substantially.

Data availability statement

The raw data supporting the conclusions of this article will be made available by the authors, without undue reservation.

Author contributions

LB conceived the idea, and developed and conducted the field trials with WM and GP. LB was responsible for conducting the field sampling and laboratory analyses. MH was responsible for assessing plant disease ratings. LB, MT, AM, and MH conducted the statistical analyses and contributed to writing the manuscript. All authors contributed to editing the manuscript and approved the final version.

Funding

The authors declare that this study received funding from Saskatchewan Pulse Growers (grant no. AGR1616). The funder was not involved in the study design, collection, analysis, interpretation of data, and the writing of this article or the decision to submit it for publication.

Acknowledgments

The authors gratefully acknowledge the technical assistance from Bianca Evans, Kelly Seymour, Nick Mateyko, Nicole York, Josephine Payment, Benjamin Kellough, Lee Poppy, Eric Walker, Clint Dyck, Vanessa Healey, and Rebecca Davies.

Conflict of interest

The authors declare that the research was conducted in the absence of any commercial or financial relationships that could be construed as a potential conflict of interest.

Publisher's note

Supplementary material

The Supplementary Material for this article can be found online at: https://www.frontiersin.org/articles/10.3389/fpls.2023.1120435/full#supplementary-material

References

Achakzai, A. K. K. (2007). Effect of various levels of nitrogen fertilizer on nodulation of pea cultivars. *Pakistan J. Bot.* 39, 1673–1680.

Allmaras, R. R., Fritz, V. A., Pfleger, F. L., and Copeland, S. M. (2003). Impaired internal drainage and *Aphanomyces euteiches* root rot of pea caused by soil compaction in a fine-textured soil. *Soil Tillage Res.* 70, 41–52. doi: 10.1016/S0167-1987(02)00117-4

Azcón-Aguilar, C., and Barea, J. M. (1997). Applying mycorrhiza biotechnology to horticulture: significance and potentials. *Scientia Horticulturae* 68 (1–4), 1–24. doi: 10.1016/S0304-4238(96)00954-5

Bailey, K. L., Gossen, B. D., Lafond, G. R., Watson, P. R., and Derksen, D. A. (2001). Effect of tillage and crop rotation on root and foliar diseases of wheat and pea in Saskatchewan from 1991 to 1998: Univariate and multivariate analyses. *Can. J. Plant Sci.* 81, 789–803. doi: 10.4141/p00-152

Bainard, L. D., Navarro-Borrell, A., Hamel, C., Braun, K., Hanson, K., and Gan, Y. (2017). Increasing the frequency of pulses in crop rotations reduces soil fungal diversity and increases the proportion of fungal pathotrophs in a semiarid agroecosystem. *Agriculture Ecosyst. Environ.* 240, 206–214. doi: 10.1016/j.agee.2017.02.020

Ballini, E., Nguyen, T. T. T., and Morel, J.-B. (2013). Diversity and genetics of nitrogen-induced susceptibility to the blast fungus in rice and wheat. *Rice.* 6, 32. doi: 10.1186/1939-8433-6-32

Bani, M., Pérez-De-Luque, A., Rubiales, D., and Rispail, N. (2018). Physical and chemical barriers in root tissues contribute to quantitative resistance to *fusarium oxysporum* f. sp. pisi in pea. *Front. Plant Sci.* 9 (199). doi: 10.3389/fpls.2018.00199

Bilgi, V. N., Bradley, C. A., Khot, S. D., Grafton, K. F., and Rasmussen, J. B. (2008). Response of dry bean genotypes to Fusarium root rot, caused by *Fusarium solani* f. sp. *phaseoli*, under field and controlled conditions. *Plant Dis.* 92 (8), 1197–1200. doi: 10.1094/PDIS-92-8-1197

Bødker, L., Kjøller, R., Kristensen, K., and Rosendahl, S. (2002). Interactions between indigenous arbuscular mycorrhizal fungi and *Aphanomyces euteiches* in field-grown pea. *Mycorrhiza* 12 (1), 7–12. doi: 10.1007/s00572-001-0139-4

Bødker, L., Kjøller, R., and Rosendahl, S. (1998). Effect of phosphate and the arbuscular mycorrhizal fungus *Glomus intraradices* on disease severity of root rot of peas (*Pisum sativum*) caused by *Aphanomyces euteiches*. *Mycorrhiza* 8, 169–174. doi: 10.1007/s005720050230

Borowicz, V. A. (2001). Do arbuscular mycorrhizal fungi alter plant-pathogen relations? *Ecology* 82, 3057–3068. doi: 10.1890/0012-9658(2001)082[3057:DAMFAP]2.0.CO;2

Chang, K. F., Hwang, S. F., Ahmed, H. U., Gossen, B. D., Turnbull, G. D., and Strelkov, S. E. (2013). Management strategies to reduce losses caused by fusarium seedling blight of field pea. *Can. J. Plant Sci.* 93, 619–625. doi: 10.4141/cjps2012-293

Chang, K. F., Hwang, S. F., Gossen, B. D., Turnbull, G. D., Howard, R. J., and Blade, S. F. (2004). Effects of soil temperature, seeding depth, and seeding date on rhizoctonia seedling blight and root rot of chickpea. *Can. J. Plant Sci.* 84, 901–907. doi: 10.4141/p03-024

Chatterton, S., Harding, M. W., Bowness, R., McLaren, D. L., Banniza, S., and Gossen, B. D. (2019). Importance and causal agents of root rot on field pea and lentil on the Canadian prairies 2014–2017. *Can. J. Plant Pathol.* 41 (1), 98–114. doi: 10.1080/07060661.2018.1547792

Clayton, G. W., Rice, W. A., Lupwayi, N. Z., Johnston, A. M., Lafond, G. R., Grant, C. A., et al. (2004). Inoculant formulation and fertilizer nitrogen effects on field pea: Nodulation, N-2 fixation and nitrogen partitioning. *Can. J. Plant Sci.* 84, 79–88. doi: 10.4141/p02-089

Corkidi, L., Rowland, D. L., Johnson, N. C., and Allen, E. B. (2002). Nitrogen fertilization alters the functioning of arbuscular mycorrhizas at two semiarid grasslands. *Plant Soil* 240, 299–310. doi: 10.1023/a:1015792204633

Deacon, J. W., and Saxena, G. (1998). Germination triggers of zoospore cysts of *Aphanomyces euteiches* and *Phytophthora parasitica*. *Mycological Res.* 102, 33–41. doi: 10.1017/S0953756297004358

Fagard, M., Launay, A., Clément, G., Courtial, J., Dellagi, A., Farjad, M., et al. (2014). Nitrogen metabolism meets phytopathology. *J. Exp. Bot.* 65, 5643–5656. doi: 10.1093/jxb/eru323

Faye, A., Dalpe, Y., Ndung'u-Magiroi, K., Jefwa, J., Ndoye, I., Diouf, M., et al. (2013). Evaluation of commercial arbuscular mycorrhizal inoculants. *Can. J. Plant Sci.* 93, 1201–1208. doi: 10.4141/cjps2013-326

Fritz, V. A., Allmaras, R. R., Pfleger, F. L., and Davis, D. W. (1995). Oat residue and soil compaction influences on common root rot (*Aphanomyes euteiches*) of peas in a fine-textured soil. *Plant Soil* 171, 235–244. doi: 10.1007/BF00010277

Gan, Y., Hanson, K. G., Zentner, R. P., Selles, F., and McDonald, C. L. (2005). Response of lentil to microbial inoculation and low rates of fertilization in the semiarid Canadian prairies. *Can. J. Plant Sci.* 85, 847–855. doi: 10.4141/p04-111

Gaulin, E., Jacquet, C., Bottin, A., and Dumas, B. (2007). Root rot disease of legumes caused by *Aphanomyces euteiches*. *Mol. Plant Pathol.* 8, 539–548. doi: 10.1111/j.1364-3703.2007.00413.X

Gendry, C. E., and Willis, R. B. (1988). Improved methods for automated determination of ammonium on soil extracts. *Commun. Soil Sci. Plant Anal.* 19, 721–737. doi: 10.1080/00103628809367970

Gossen, B. D., Conner, R. L., Chang, K., Pasche, J. S., McLaren, D. L., Henriquez, M. A., et al. (2016). Identifying and managing root rot of pulses on the northern Great Plains. *Plant Dis.* 100 (11), 1965–1978. doi: 10.1094/PDIS-02-16-0184-FE

Gupta, K. J., Brotman, Y., Segu, S., Zeier, T., Zeier, J., Persijn, S. T., et al. (2013). The form of nitrogen nutrition affects resistance against *Pseudomonas syringae* pv. *phaseolicola tobacco. J. Exp. Bot.* 64 (2), 553–568. doi: 10.1093/jxb/ers348

Hall, R., and Phillips, L. G. (1992). Effects of crop sequence and rainfall on population dynamics of Fusarium solani f.sp. *phaseoli soil. Can. J. Bot.* 70 (10), 2005–2008. doi: 10.1139/b92-249

Harm, J., Bettany, J., and Halstead, E. (1973). A soil test for sulphur and interpretative criteria for Saskatchewan. *Commun. Soil Sci. Plant Anal.* 4, 219–231. doi: 10.1080/00103627309366440

Hendershot, W. H., Lalande, H., and Duquette, M. (2008). "Soil pH in water," in *Soil Sampling and Methods of Analysis*, *2nd ed*. Eds. M. R. Carter and E. G. Gregorich (Boca Raton, Florida: Canadian Society of Soil Science. CRC Press).

Herridge, D. F., Peoples, M. B., and Boddey, R. M. (2008). Global inputs of biological nitrogen fixation in agricultural systems. *Plant Soil* 311 (1), 1–18. doi: 10.1007/s11104-008-9668-3

Heyman, F., Bjorn, L., Lars, P., Mariann, W., and Jan, S. (2007). Calcium concentrations of soil effect suppressiveness against Aphanomyces root rot of pea. *Soil Biol. Biochem.* 39 (9), 2222–2229. doi: 10.1016/j.soilbio.2007.03.022

Hossain, S., Bergkvist, G., Berglund, K., Mårtensson, A., and Persson, P. (2012). Aphanomyces pea root rot disease and control with special reference to impact of Brassicaceae cover crops. *Acta Agriculturae Scandinavica Section B — Soil Plant Sci.* 62 (6), 477–487. doi: 10.1080/09064710.2012.668218

Hossain, S., Bergkvist, G., Glinwood, R., Berglund, K., Martensson, A., Hallin, S., et al. (2015). Brassicaceae cover crops reduce Aphanomyces pea root rot without suppressing genetic potential of microbial nitrogen cycling. *Plant Soil* 392, 227–238. doi: 10.1007/s11104-015-2456-y

Hossain, Z., Wang, X., Chantel, H., Knight, D., Morrison, M. J., and Gan, Y. (2016). Biological nitrogen fixation by pulse crops on the semiarid Canadian prairies. *Can. J. Plant Sci.* 97 (1), 119–131. doi: 10.1139/cjps-2016-0185

Hughes, T. J., and Grau, C. R. (2013). "Aphanomyces root rot (common root rot) of legumes," (The Plant Health Instructor). Available at: https://www.apsnet.org/edcenter/disandpath/oomycete/pdlessons/Pages/Aphanomyces.aspx.

Jin, H. Y., Germida, J. J., and Walley, F. L. (2013). Impact of arbuscular mycorrhizal fungal inoculants on subsequent arbuscular mycorrhizal fungi colonization in pot-cultured field pea (Pisum sativum L.). *Mycorrhiza* 23, 45–59. doi: 10.1007/s00572-012-0448-9

Karppinen, E. M., Payment, J., Chatterton, S., Bainard, J. D., Hubbard, M., Gan, Y., et al. (2020). Distribution and abundance of *Aphanomyces euteiches* in agricultural soils: effect of land use type, soil properties, and crop management practices. *Appl. Soil Ecol.* 150, 103470. doi: 10.1016/j.apsoil.2019.103470

Kraft, J. M., Marcinkowska, J., and Muehlbauer, J. (1990). Detection of *Aphanomyces euteiches* in field soil from northern Idaho by a wet-sieving/baiting technique. *Plant Dis.* 74, 716–718. doi: 10.1094/PD-74-0716

Liu, B., Shen, W., Wei, H., Smith, H., Louws, F. J., Steadman, J. R., et al. (2016). Rhizoctonia communities in soybean fields and their relation with other microbes and nematode communities. *Eur. J. Plant Pathol.* 144 (3), 671–686. doi: 10.1007/s10658-015-0805-6

McGonigle, T. P., Miller, M. H., Evans, D. G., Fairchild, G. L., and Swan, J. A. (1990). A new method which gives an objective measure of colonization of roots by vesicular-arbuscular mycorrhizal fungi. *New Phytol.* 115, 495–501. doi: 10.1111/j.1469-8137.1990.tb00476.x

Meç, E., Salluku, G., and Balliu, A. (2016). Artificial inoculation of AM fungi improves nutrient uptake efficiency in salt stressed pea (*Pissum Sativum* L) plants. *J. Agric. Stud.* 4, 37–46. doi: 10.5296/jas.v4i3.9585

Miller, J. J., and Curtin, D. (2008). "Chapter 15: electrical conductivity and soluble ions," in *Soil sampling and methods of analysis*, *2nd edn*. Eds. M. R. Carter and E. G. Gregorich (Boca Raton: Canadian Society of Soil Science, CRC Press), 161–171.

Moussart, A., Even, M. N., Lesné, A., and Tivoli, B. (2013). Successive legumes tested in a greenhouse crop rotation experiment modify the inoculum potential of soils naturally infested by *Aphanomyces euteiches*. *Plant Pathol.* 62 (3), 545–551. doi: 10.1111/j.1365-3059.2012.02679.x

Mur, L. A. J., Simpson, C., Kumari, A., Gupta, A. K., and Gupta, K. J. (2017). Moving nitrogen to the centre of plant defence against pathogens. *Ann. Bot.* 119, 703–709. doi: 10.1093/aob/mcw179

Naseri, B., and Ansari Hamadani, S. (2017). Characteristic agro-ecological features of soil populations of bean root rot pathogens. *Rhizosphere* 3, 203–208. doi: 10.1016/j.rhisph.2017.05.005

Nasser, R. R., Fuller, P., and Jellings, J. (2008). Effect of elevated CO2 and nitrogen levels on lentil growth and nodulation. *Agron. Sustain. Dev.* 28, 175–180. doi: 10.1051/agro:2007056

Nightingale, G. T., and Farnham, R. B. (1936). Effects of nutrient concentration on the anatomy, metabolism, and bud abscission of sweet pea. *Bot. Gaz* 97, 477–517. doi: 10.1086/334583

Niu, Y. N., Bainard, L. D., May, W. E., Hossain, Z., Hamel, C., and Gan, Y. T. (2018). Intensified pulse rotations buildup pea rhizosphere pathogens in cereal and pulse based cropping systems. *Front. Microbiol.* 9. doi: 10.3389/fmicb.2018.01909

Papavizas, G. C., and Lewis, J. A. (1971). Effect of amendments and fungicides on Aphanomyces root rot of peas. *Phytopathology* 61, 215–21+. doi: 10.1094/Phyto-61-215

Persson, L., Larsson-Wikstrom, M., and Gerhardson, B. (1999). Assessment of soil suppressiveness to Aphanomyces root rot of pea. *Plant Dis.* 83, 1108–1112. doi: 10.1094/pdis.1999.83.12.1108

Persson, L., and Olsson, S. (2000). Abiotic characteristics of soils suppressive to Aphanomyces root rot. *Soil Biol. Biochem.* 32, 1141–1150. doi: 10.1016/s0038-0717(00)00030-4

Pfender, W. F., and Hagedorn, D. J. (1983). Disease progress and yield losss in Aphanomyces root-rot of peas. *Phytopathology* 73, 1109–1113. doi: 10.1094/Phyto-73-1109

Pilet-Nayel, M., Muehlbauer, F., McGee, R., Kraft, J., Baranger, A., and Coyne, C. (2002). Quantitative trait loci for partial resistance to Aphanomyces root rot in pea. *Theor. Appl. Genet.* 106 (1), 28–39. doi: 10.1007/s00122-002-0985-2

Rosendahl, S. (1985). Interactions between the vesicular-arbuscular mycorrhizal fungus *Glomus fasciculhtum* and *Aphanomyces euteiches* root rot of peas. *J. Phytopathol.* 114 (1), 31–40. doi: 10.1111/j.1439-0434.1985.tb04335.x

Ryan, M., and Ash, J. (1999). Effects of phosphorus and nitrogen on growth of pasture plants and VAM fungi in SE Australian soils with contrasting fertiliser histories (conventional and biodynamic). *Agric. Ecosyst. Environ.* 73, 51–62. doi: 10.1016/s0167-8809(99)00014-6

Salvagiotti, F., Cassman, K. G., Specht, J. E., Walters, D. T., Weiss, A., and Dobermann, A. (2008). Nitrogen uptake, fixation and response to fertilizer N in soybeans: A review. *Field Crops Res.* 108 (1), 1–13. doi: 10.1016/j.fcr.2008.03.001

Schumacher, B. A. (2002). *Methods for the Determination of Total Organic Carbon (TOC) in Soils and Sediments* (United States Environmental Protection Agency Environmental Sciences Division National Exposure Research Laboratory: Ecological Risk Assessment Support Center, US Environmental Protection Agency).

Slezack, S., Dumas-Gaudot, E., Paynot, M., and Gianinazzi, S. (2000). Is a fully established arbuscular mycorrhizal symbiosis required for bioprotection of *Pisum sativum* roots against *Aphanomyces euteiches*? *Mol. Plant-Microbe Interact.* 13, 238–241. doi: 10.1094/mpmi.2000.13.2.238

Smith, P. G., and Walker, J. C. (1941). Certain environmental and nutritional factors affecting Aphanomyces root of garden pea. *J. Agric. Res.* 63, 1–20.

Statistics Canada (2020). Table 32-10-0359-01 Estimated areas, yield, production, average farm price and total farm value of principal field crops, in metric and imperial units. doi: 10.25318/3210035901-eng

Taheri, A. E., Chatterton, S., Foroud, N. A., Gossen, B. D., and McLaren, D. L. (2017). Identification and community dynamics of fungi associated with root, crown, and foot rot of field pea in western Canada. *Eur. J. Plant Pathol.* 147, 489–500. doi: 10.1007/s10658-016-1017-4

Talukdar, N. C., and Germida, J. J. (1994). Growth and yield of lentil and wheat inoculated with 3 glomus isolates from Saskatchewan soils. *Mycorrhiza* 5, 145–152. doi: 10.1007/s005720050052

Thalineau, E., Fournier, C., Gravot, A., Wendehenne, D., Jeandroz, S., and Truong, H.-N. (2018). Nitrogen modulation of *Medicago truncatula* resistance to *Aphanomyces euteiches* depends on plant genotype. *Mol. Plant Pathol.* 19 (3), 644–676. doi: 10.1111/mpp.12550

Thygesen, K., Larsen, J., and Bødker, L. (2004). Arbuscular Mycorrhizal Fungi reduce development of pea root-rot caused by *Aphanomyces euteiches* using oospores as pathogen inoculum. *Eur. J. Plant Pathol.* 110 (4), 411–419. doi: 10.1023/B:EJPP.0000021070.61574.8b

Tian, D., and Niu, S. (2015). A global analysis of soil acidification caused by nitrogen addition. *Environ. Res. Lett.* 10, 024019. doi: 10.1088/1748-9326/10/2/024019

Tu, J. C. (1994). Effects of soil compaction, temperature, and moisture on the development of the Fusarium root rot complex of pea in southwestern Ontario. *Phytoprotection* 75 (3), 125–131. doi: 10.7202/706059ar

Van der Plaats-Niterink, A. J. (1981). Monograph of the genus *Pythium*. *Stud. Mycology* 21, 244 pp. Available at: https://studiesinmycology.org/index.php/issue/23-studies-in-mycology-no-21.

Vierheilig, H., Coughlan, A. P., Wyss, U., and Piché, Y. (1998). Ink and vinegar, a simple staining technique for arbuscular-micorrhizal fungi. *Appl. Environ. Microbiol.* 64 (12), 5004–5007. doi: 10.1128/AEM.64.12.5004-5007.1998

Voisin, A. S., Salon, C., Munier-Jolain, N. G., and Ney, B. (2002). Effect of mineral nitrogen on nitrogen nutrition and biomass partitioning between the shoot and roots of pea (*Pisum sativum L.*). *Plant Soil* 242, 251–262. doi: 10.1023/a:1016214223900

Wehner, J., Antunes, P. M., Powell, J. R., Mazukatow, J., and Rillig, M. C. (2010). Plant pathogen protection by arbuscular mycorrhizas: A role for fungal diversity? *Pedobiologia* 53, 197–201. doi: 10.1016/j.pedobi.2009.10.002

Willsey, T. L., Chatterton, S., Heynen, M., and Erickson, A. (2018). Detection of interactions between the pea root rot pathogens Aphanomyces euteiches and Fusarium spp. *using multiplex qPCR assay. Plant Pathol.* 67 (9), 1912–1923. doi: 10.1111/ppa.12895

Wu, L., Chang, K. F., Conner, R. L., Strelkov, S., Fredua-Agyeman, R., Hwang, S. F., et al. (2018). *Aphanomyces euteiches*: A threat to canadian field pea production. *Engineering* 4 (4), 542–551. doi: 10.1016/j.eng.2018.07.006

Xavier, L. J. C., and Germida, J. J. (2003). Selective interactions between arbuscular mycorrhizal fungi and Rhizobium leguminosarum bv. viceae enhance pea yield and nutrition. *Biol. Fertility Soils* 37, 261–267. doi: 10.1007/s00374-003-0605-6

Xu, L. H., Ravnskov, S., Larsen, J., Nilsson, R. H., and Nicolaisen, M. (2012). Soil fungal community structure along a soil health gradient in pea fields examined using deep amplicon sequencing. *Soil Biol. Biochem.* 46, 26–32. doi: 10.1016/j.soilbio.2011.11.010

frontiers | Frontiers in Plant Science

TYPE Original Research
PUBLISHED 28 September 2023
DOI 10.3389/fpls.2023.1189289

OPEN ACCESS

EDITED BY
Valerio Hoyos-Villegas,
McGill University, Canada

REVIEWED BY
Harsh Raman,
NSW Government, Australia
Brigitte Uwimana,
International Institute of Tropical Agriculture (IITA), Uganda

*CORRESPONDENCE
Marie-Laure Pilet-Nayel
marie-laure.pilet-nayel@inrae.fr

†These authors have contributed equally to this work

RECEIVED 18 March 2023
ACCEPTED 25 July 2023
PUBLISHED 28 September 2023

CITATION
Leprévost T, Boutet G, Lesné A, Rivière J-P, Vetel P, Glory I, Miteul H, Le Rat A, Dufour P, Regnault-Kraut C, Sugio A, Lavaud C and Pilet-Nayel M-L (2023) Advanced backcross QTL analysis and comparative mapping with RIL QTL studies and GWAS provide an overview of QTL and marker haplotype diversity for resistance to Aphanomyces root rot in pea (*Pisum sativum*). *Front. Plant Sci.* 14:1189289. doi: 10.3389/fpls.2023.1189289

Advanced backcross QTL analysis and comparative mapping with RIL QTL studies and GWAS provide an overview of QTL and marker haplotype diversity for resistance to Aphanomyces root rot in pea (*Pisum sativum*)

Théo Leprévost[1], Gilles Boutet[1], Angélique Lesné[1], Jean-Philippe Rivière[1], Pierrick Vetel[1], Isabelle Glory[1], Henri Miteul[1], Anaïs Le Rat[1], Philippe Dufour[2], Catherine Regnault-Kraut[3], Akiko Sugio[1], Clément Lavaud[1,3†] and Marie-Laure Pilet-Nayel[1*†]

[1]IGEPP, INRAE, Institut Agro, University of Rennes, Le Rheu, France, [2]RAGT 2n, Druelle Balsac, France, [3]KWS MOMONT Recherche SARL, Allonnes, France

Aphanomyces euteiches is the most damaging soilborne pea pathogen in France. Breeding of pea resistant varieties combining a diversity of quantitative trait loci (QTL) is a promising strategy considering previous research achievements in dissecting polygenic resistance to *A. euteiches*. The objective of this study was to provide an overview of the diversity of QTL and marker haplotypes for resistance to *A. euteiches*, by integrating a novel QTL mapping study in advanced backcross (AB) populations with previous QTL analyses and genome-wide association study (GWAS) using common markers. QTL analysis was performed in two AB populations derived from the cross between the susceptible spring pea variety "Eden" and the two new sources of partial resistance "E11" and "LISA". The two AB populations were genotyped using 993 and 478 single nucleotide polymorphism (SNP) markers, respectively, and phenotyped for resistance to *A. euteiches* in controlled conditions and in infested fields at two locations. GWAS and QTL mapping previously reported in the pea-Aphanomyces collection and from four recombinant inbred line (RIL) populations, respectively, were updated using a total of 1,850 additional markers, including the markers used in the Eden x E11 and Eden x LISA populations analysis. A total of 29 resistance-associated SNPs and 171 resistance QTL were identified by GWAS and RIL or AB QTL analyses, respectively, which highlighted 10 consistent genetic regions confirming the previously reported QTL. No new consistent resistance QTL was detected from both Eden x E11 and Eden x LISA AB populations. However, a high diversity of resistance haplotypes was identified at

11 linkage disequilibrium (LD) blocks underlying consistent genetic regions, especially in 14 new sources of resistance from the pea-Aphanomyces collection. An accumulation of favorable haplotypes at these 11 blocks was confirmed in the most resistant pea lines of the collection. This study provides new SNP markers and rare haplotypes associated with the diversity of Aphanomyces root rot resistance QTL investigated, which will be useful for QTL pyramiding strategies to increase resistance levels in future pea varieties.

KEYWORDS

Aphanomyces euteiches, sources of resistance, AB populations, integrative study, SNPs

Introduction

Genetic resistance represents a key approach to reduce chemical applications for sustainable crop disease management. Partial resistance, also known as "quantitative resistance", is often governed by multiple QTL and characterized by a compatible interaction between the pathogen and its host plant, typically resulting in a reduction of disease severity and limited progression of the pathogen within the host tissues (Poland et al., 2009). Quantitative resistance has generally lower resistance effect but is considered more durable than monogenic complete resistance. Pyramiding a diversity of resistance QTL showing a broad spectrum of action on pathogen populations and targeting various steps in the pathogen life cycle appears to be a promising approach to increase the level and durability of quantitative resistance in plant breeding programs (Pilet-Nayel et al., 2017). Linkage analysis has been broadly employed to identify resistance QTL in RIL plant populations derived from single biparental crosses between parents showing contrasted level of resistance (Varshney and Dubey, 2009). Balanced allele segregation ratios and high recombination events enable efficient QTL detection in RIL populations but considerably delay the transfer of valuable resistance alleles from wild donor genotypes to elite breeding lines by backcrossing and/or intercrossing (Tanksley and Nelson, 1996). AB populations derived by backcrossing the F_1 hybrid to the elite parent until an advanced generation, *e.g.* BC_2 or BC_3, allow to develop recombinant lines genetically less similar to the donor parental line, accelerating the transfer of wild alleles into agronomic lines. Transfer of disease resistance traits has been successfully achieved through AB-QTL analysis in several major field crops, like barley (Haas et al., 2016), maize (Palanichamy and Smith, 2022), rice (Jiang et al., 2020), sunflower (Talukder et al., 2022), and wheat (Naz et al., 2015). GWAS is a powerful tool to investigate complex genetic determinism and identify exotic or agronomic alleles in plant natural diversity panels. Compared to linkage analysis, GWAS takes advantage of high recombination rates between unrelated individuals to better refine genomic regions associated with trait variation. But, GWAS suffers also from low statistical power to detect low-frequency favorable alleles, *i.e.* carried by only a few genotypes of interest in the plant panel (Tibbs Cortes et al., 2021). Combining linkage analysis and GWAS is a promising approach to better understand polygenic determinisms underlying partial resistance to pathogens in plants.

Pea (*Pisum sativum*) is an important crop with significant nutritional and environmental value. It offers high protein (≈23.5%), vitamin, mineral, and carbohydrate-rich seeds for human and animal consumption. It also contributes to reduce nitrogen fertilization, due to its ability to fix atmospheric nitrogen through its symbiosis with soil bacteria, and to break disease cycles in cereal rotations (Amarakoon et al., 2012; Powers and Thavarajah, 2019). Aphanomyces root rot, caused by the soil-borne oomycete *Aphanomyces euteiches* Drechs., is among the most damaging pulse root rot diseases worldwide, particularly affecting spring pea varieties (Bénézit et al., 2017; Jha et al., 2021). The pathogen has been reported in 21 different countries across all five continents, including major pea-growing nations such as Russia, Canada, China, India, France, Australia, and the USA (Becking et al., 2022). Two main pathotypes of *A. euteiches* were reported, including pathotype I predominant in Europe and main pea-growing regions in Canada, and pathotype III observed in some regions of the USA (Le May et al., 2018; Sivachandra Kumar et al., 2021). Under favorable weather conditions, both pathotypes can cause rotting of roots and epicotyls, resulting in yellow leaves and, in some cases, plant mortality. In addition, the disease can cause yield losses of up to 100% in highly infested fields (Hughes and Grau, 2007). Two main recommended prophylaxis methods are commonly advised: (i) assessing the level of soil infestation to avoid the pea crop in contaminated fields and (ii) implementing crop rotations with non-host or resistant crops to reduce the inoculum potential in the soil (Wu et al., 2019). While chemical and biological strategies have demonstrated limited efficacy in controlling the disease, and complete resistance to *A. euteiches* has not been reported in any pea cultivar, breeding for quantitative resistance is a promising approach to reduce pea yield losses caused by the root rot disease (Wu et al., 2019; Wu et al., 2021).

Since the early-2000s, genetic resistance to *A. euteiches* in pea has been well-explored. Using four pea RIL populations derived from the partially resistant parents PI180693, 552, 90-2131, and 90-2079, linkage mapping studies, mainly based on SSR markers, identified 27 meta-QTL associated with partial resistance to *A.*

euteiches in controlled conditions and/or infested field nurseries in France and the USA. The meta-QTL covered seven main resistance QTL regions (Pilet-Nayel et al., 2002; Pilet-Nayel et al., 2005; Hamon et al., 2011; Hamon et al., 2013). In particular, two major-effect QTL *Ae-Ps4.5* and *Ae-Ps7.6* located on linkage groups (LGs) IV and VII, were associated with a high level of partial resistance to the strains Ae109 (pathotype III) and RB84 (pathotype I), respectively (Hamon et al., 2011; Hamon et al., 2013, Lavaud et al., submitted[1]). The five other main QTL regions, presenting lower effects, were named *Ae-Ps1.2* on LGI genetically close to the *Af* locus (leaf type), *Ae-Ps2.2* on LGII close to the *A* locus (anthocyanin production), *Ae-Ps3.1* on LGIII close to the *Hr* locus (photoperiod high-responsive flowering), *Ae-Ps4.1* on LGIV and *Ae-Ps5.1* on LGV close to the *R* locus (seed type). At *Ae-Ps2.2* and *Ae-Ps3.1*, resistance and late-flowering alleles derived from PI180693 were reported to be linked (Hamon et al., 2013). Resistance to *A. euteiches* in pea was thus suggested to be influenced by pleiotropy or genetic linkage involving plant morphology and phenology genes. In addition, GWAS achieved in a collection of 175 *Pisum sativum* lines, mentioned as the "pea-Aphanomyces collection", detected 52 resistance LD blocks associated with partial resistance to *A. euteiches*, which validated six of the seven main QTL previously reported (Desgroux et al., 2016). A QTL analysis conducted in Canada, from a pea RIL population whose resistant parent (00-2067) shares the same PH14-119 progenitor as 90-2079 (Kraft et al., 1972; Kraft, 1981; Kraft, 1992; Conner et al., 2013), also revealed a major-effect QTL which was identified in both field and greenhouse experiments. This QTL was found to be located near the *Ae-Ps4.5* region (Wu et al., 2021). Finally, using near-isogenic lines (NILs) carrying resistance alleles at different combinations of one to three of the seven main resistance QTL, major-effect and some minor-effect QTL were validated in controlled conditions (Lavaud et al., 2015; Lavaud et al., 2016) and infested French field nurseries (Lavaud et al., unpublished data). However, although the main Aphanomyces resistance QTL are currently used in research and pea private breeding programs, levels of partial resistance are still difficult to increase and the durability of major-effect QTL remains questioned (Quillévéré-Hamard et al., 2021). Thus, the identification of new QTL or alleles conferring resistance to *A. euteiches* would be useful, in order to diversify and cumulate resistance alleles for breeding pea varieties for high level and durable resistance.

From 2002 to 2008, a large germplasm screening program of approximately 1900 *Pisum* accessions was conducted in controlled conditions for resistance to *A. euteiches* and resulted in the selection of 20 partially resistant pea lines as new sources of resistance (Pilet-Nayel et al., 2007; Desgroux et al., 2016). Among the 20 pea lines, two exotic sources of resistance, named E11 and LISA, showed rare resistance haplotypes mostly different from the ones previously reported in the four RIL resistant parents (Desgroux et al., 2016). Therefore, E11 and LISA were crossed with the susceptible pea variety Eden to produce two pea AB populations, in order to simultaneously detect and introgress into an agronomic background new potential resistance QTL or alleles.

The objectives of this study were to (i) identify genetic loci controlling Aphanomyces root rot resistance in two new pea sources of resistance, then (ii) conduct a comparative genetic mapping of QTL identified in this study along with QTL updated from previous reports using common SNP markers. This comprehensive approach aimed to represent the diversity of QTL and haplotypes associated with resistance to *A. euteiches* on a reference consensus marker map. QTL mapping was carried out in the two new AB populations produced from the crosses Eden x E11 and Eden x LISA, using SNP marker genotyping data and Aphanomyces root rot resistance data collected in controlled conditions and infested field nurseries at two locations. Then, genetic analyses of resistance to *A. euteiches* previously conducted by linkage analysis and GWAS in the four RIL populations Baccara x PI180693, Baccara x 552, DSP x 90-2131, and Puget x 90-2079 and in the pea-Aphanomyces collection, respectively, were updated using new genotyping data from SNP markers common to both Eden x E11 and Eden x LISA AB populations. These common SNPs made it possible the comparison of QTL detected from the independent populations. By integrating GWAS, RIL, and AB QTL analyses in pea, this study identified consistent genetic regions and haplotypes of resistance to *A. euteiches*, for future pyramiding strategies of resistance alleles in pea breeding.

Materials and methods

Plant material

Two AB populations of 179 and 180 BC_2F_7 pea lines derived from the crosses Eden x E11 and Eden x LISA, respectively, were used for QTL mapping. Eden is a spring pea cultivar susceptible to *A. euteiches* with white flowers, afila leaves, and wrinkled seeds. E11 and LISA are two pea germplasms partially resistant to *A. euteiches*, showing high plants with purple flowers, normal leaves, and smooth seeds. LISA is a spring fodder cultivar which originates from Germany. The sowing type and end use of the wild Egyptian pea E11 remain unknown (Desgroux et al., 2016). Four pea RIL populations derived from the crosses Baccara x PI180693 (178 RILs), Baccara x 552 (178 RILs), DSP x 90-2131 (111 RILs), and Puget x 90-2079 (127 RILs), were used to update previous QTL mapping studies (Pilet-Nayel et al., 2002; Pilet-Nayel et al., 2005; Hamon et al., 2011; Hamon et al., 2013).

The pea-Aphanomyces collection of 175 lines previously described by Desgroux et al. (2016), was used for updated GWAS. The collection includes about 60% of spring-type germplasm lines, named AeA95xx, AeB97xx, AeD99xx, from an Aphanomyces recurrent breeding program conducted by French breeders in 1995-2005, using PI180693, 552 and 90-2131 as sources of resistance. It includes about 40% of best RILs, parental lines of mapping populations, sources of resistance selected from INRAE and USDA genetics programs for Aphanomyces root rot resistance, and French cultivars, described for different end-uses (food, feed or

1 Lavaud, C., Lesné, A., Leprévost, T., and Pilet-Nayel, M.-L. (submitted). Fine mapping of *Ae-Ps4.5*, a major locus for resistance to pathotype III of *Aphanomyces euteiches* in pea. Theor. Appl. Genet.

fodder peas) and sowing times (spring and winter peas). The pea lines in the collection showed different levels of resistance or susceptibility to *A. euteiches* and variability in agronomic traits (seed type, foliage type and flower color).

Phenotyping

In infested fields, the Eden x E11 and Eden x LISA populations were evaluated for root rot disease resistance in two locations in France, *i.e.* Riec-sur-Belon, Finistère (RI) and Dijon-Epoisses, Côtes d'Or (DI) (Hamon et al., 2011), in 2019 and 2021, respectively. *A. euteiches* isolates of pathotype I were described from these infested fields (Quillévéré-Hamard et al., 2018; Onfroy et al, unpublished data). Field assays were carried out in the spring and sown in double-row plots of 30 plants/row. The plots were distributed according to a randomized complete block design with three replicates, incorporating crossed "assessor" et "gradient" blocks. A susceptible cultivar (Solara) was repeated every four plots to adjust disease severity score of the pea lines relative to that of the adjacent Solara plots, as described by Hamon et al. (2011). Two disease criteria were used to assess root rot resistance for each plot: (i) the root rot index (RRI), as the average disease severity score of 10 plants on a 0 (healthy plant) to 5 (dead plant) scoring scale, evaluated in Riec-sur-Belon, and (ii) the aerial decline index (ADI), as the disease impact score on all the plants in the plot, on a 1 (green plant) to 8 (dead plant) scoring scale, evaluated in Riec-sur-Belon and Dijon-Epoisses, as described by Hamon et al. (2011). The number of calendar days to 50% bloom (Flo1) was also evaluated in Dijon-Epoisses for each plot.

In inoculated controlled conditions, the Eden x E11 and Eden x LISA populations were evaluated for root rot resistance to both pure-culture strains (i) *A. euteiches* Ae109 (pathotype III) and (ii) *A. euteiches* RB84 (pathotype I), respectively. For each strain and population, all the AB lines and parents were evaluated within a single disease test comprising four randomized complete blocks with five plants/block, as described by Moussart et al. (2001). Disease severity was scored on each plant using the same 0 (healthy plant) to 5 (dead plant) scoring scale as used for the field scorings (Hamon et al., 2011).

Phenotyping datasets produced on the RIL populations by Pilet-Nayel et al. (2002; 2005); Hamon et al. (2011; 2013) and Lavaud et al. (submitted[1]), and datasets produced on the pea-Aphanomyces collection by Desgroux et al. (2016), were used in this study.

Statistical analysis of phenotypic data

Phenotypic datasets for plant morphology and resistance to *A. euteiches*, obtained from the Eden x E11 and Eden x LISA populations, were analyzed using the R 4.0.2 software (R Core Team, 2020).

Global statistical analyses were conducted to assess: (i) genotype x environment interactions in field experiments, employing a global linear model [R function lm], and (ii) genotype x strain interactions in controlled conditions tests, utilizing a cumulative link model (R function clm of package ordinal; Christensen, 2019).

In addition, individual statistical analyses of phenotypic data obtained from each field and controlled conditions experiment were computed using (i) a linear mixed model (R function lmer of package lme4; Bates et al., 2019) for field variables, including G (genotype) as fixed factor and replicates with assessor (R_A) and gradient (R_{Gr}) blocks, as random factors, and (ii) a cumulative link mixed model (R function clmm of package ordinal; Christensen, 2019) for controlled conditions variables, including G as fixed factor, and B (block) and GxB interaction as random factors.

Broad-sense heritability (H^2) was assessed for each variable from variance estimates in a global linear model, including only G as fixed factor, and using the formula: $H^2 = \sigma_G^2/[\sigma_G^2 + (\sigma_E^2/r)]$, where σ_G^2 is the genetic variance, σ_E^2 the residual variance and *r* the number of replicates per genotype.

Significance of factor effects in each model was tested (R function Anova of package car and RVAideMemoire; Fox and Weisberg, 2020; Hervé, 2020) and estimated marginal means (EMMs) were computed for all individual variables on each genotype and from each model (R function and package emmeans; Lenth, 2020). Pearson correlation analysis was carried out between EMMs (R function rcorr of package Hmisc; Harrell and Dupont, 2020) and a correlation matrix was drawn using the Pearson coefficient (r; R function rcorr of package corrplot; Wei and Simko, 2017).

Adjusted means datasets produced by Pilet-Nayel et al. (2002; 2005); Hamon et al. (2011; 2013) and Desgroux et al. (2016) were used for updated QTL mapping and GWAS, respectively.

Genotyping

The Eden x E11 AB population was genotyped using a total of 1,850 markers designed in KASP™ assays as described in Boutet et al. (2016). The 1,850 markers were selected from Duarte et al. (2014); Boutet et al. (2016) and Tayeh et al. (2015), based on their genetic positions regularly distributed outside and inside stress resistance QTL. In the Eden x E11 population, 1,010 markers were retained as polymorphic, including 725, 246, and 37 SNP markers named "Ps1" (Boutet et al., 2016), "PsCam" (Tayeh et al., 2015) and "Ps0" or "Ps9" (Duarte et al., 2014), respectively, and two other SNPs located in trypsin inhibitor gene loci. The Eden x LISA AB population was genotyped using a sub-set of 481 polymorphic SNPs among the 1,850 markers, including 117 "Ps1", 127 "PsCam" and 10 "Ps0" or "Ps9" common SNPs to the 1,010 markers selected in the Eden x E11 population. The Eden x E11 and Eden x LISA genotyping datasets were then reduced to 993 and 478 SNPs respectively, based on marker quality (heterozygosity ratio < 15%) and quality of linkage mapping (see next section) in each LG. A total of 160 and 178 Eden x E11 and Eden x LISA pea lines were selected, respectively, based on marker quality (missing data < 15% and heterozygosity ratio < 15%), quality of linkage mapping, and pea line homozygosity for flower color, foliar type, and plant morphology, observed in controlled conditions and greenhouse in

Le Rheu, Ille-et-Vilaine, as well as in infested field nurseries in Riec-sur-Belon and Dijon-Epoisses.

Genotyping datasets produced on RIL populations by Pilet-Nayel et al. (2002; 2005) and Hamon et al. (2011; 2013), and genotyping dataset of 12,067 SNPs previously selected on the pea-Aphanomyces collection by Desgroux et al. (2016), were supplemented with the 1,850 markers which were used as bridges for comparative AB-, RIL- QTL mapping and GWAS. Genotyping matrices consisting of 1,866, 1,082, 950 and 669 SNPs and 176, 178, 111 and 121 RILs were established for Baccara x PI180693, Baccara x 552, DSP x 90-2131 and Puget x 90-2079 populations, respectively, based on quality of linkage mapping in each LG. A genotyping matrix consisting of 10,824 SNPs and 172 pea genotypes from the pea-Aphanomyces collection was retained, based on marker quality (markers with MAF > 5% and missing data < 10%; individuals with heterozygosity ratio < 15% and missing data < 10%). The filtered genotyping matrix, containing 0.94% missing values, was imputed using Beagle 5.1 software (Browning et al., 2018). Imputation parameters were established using a sliding window, length of overlap between adjacent sliding windows, and number of iterations of 15 cM, 5 cM, and 15, respectively.

Linkage mapping and consensus marker map construction

Genetic maps for AB and RIL populations were established using the "sem" and "annealing 100 100 0.1 0.9" commands of CarthaGene software (de Givry et al., 2005), as presented in Boutet et al. (2016). These commands allowed the computation and optimization of the maximum likelihood for the order and position of markers (in cM Haldane) on each LG. For each SNP marker from each AB or RIL genetic map, a χ^2 test (*p-value* < 0.001) was used to analyze adjustments of allelic segregation to the expected Mendelian ratios (1:1 in RIL populations, 1:7 in BC_2F_7 populations).

A consensus marker map, named "DORA" as the project name of this study, including 16,647 markers, was obtained by projecting the positions of the 1,850 markers used as supplemental marker set in this study onto the pea reference consensus genetic map described by Tayeh et al. (2015), using Biomercator 4.2 software (Sosnowski et al., 2012). Pairwise LD (r^2) between markers was explored within LGs using PLINK 1.9 software (Purcell et al., 2007; Chang et al., 2015), as described by Desgroux et al. (2016).

AB and RIL populations QTL analysis

Composite interval mapping models were performed using R/qtl package (Broman et al., 2003) to identify QTL for resistance to *A. euteiches*, flowering, and morphological traits from the RIL and AB populations. For each variable, a forward-backward stepwise selection of QTL covariate (window size = 5cM) was performed using the Haley-Knott regression method. To limit the number of covariables and potential impacts of overparameterization, new LOD score thresholds were estimated for each additional covariable introduced in the composite interval mapping models. These thresholds were computed by conducting 1,000 permutations to determine, with a genome-wide α error risk of 5%, the significance of putative QTL. For each QTL, the percentage of phenotypic (R^2) and genotypic variation, additive and epistatic interaction effects, and one LOD drop-off confidence intervals were computed.

Population structure, individual relatedness, and genome-wide association study

The structure of the collection was investigated using the ADMIXTURE 1.3 software (Alexander et al., 2009) with the whole SNP dataset. Ten groups were determined after 15 cross-validations according to the procedure presented in ADMIXTURE. The structure matrix was represented using pophelper (Francis, 2017). IBD relatedness between individuals was computed using the Astle and Balding (2009) algorithm. Ward's clustering of pea lines was computed according to their estimating IBD relatedness values and was represented with the kinship matrix using GAPIT R packages (Lipka et al., 2012).

GWAS was performed using a modified version of the multi-locus mixed model (MLMM) R package (Segura et al., 2012), as described by Desgroux et al. (2016). For each variable, a forward-backward regression model (maxsteps = 5) was performed to select significant SNP markers as covariates. To declare significant SNPs, a multiple-Bonferroni (mBonf) threshold of 4.44 (*p-value* of 3.6E-05) was calculated using the formula: mBonf = [−log(α/m)] described by Desgroux et al. (2016), with α = 10%, the overall false positive threshold, and m = 2,738, the number of markers selected at non-redundant genetic positions on the DORA consensus marker map. The structure and kinship matrices were also set as covariates in MLMM models. For each model, the *p-value* and allelic effect of significant SNPs, and the partition of variance explained by covariates were scored.

Comparative mapping

Genetic maps, QTL identified in this study from linkage analysis of AB and RIL populations, and QTL recently detected for resistance to the Ae109 and RB84 strains in the Puget x 90-2079 RIL population (Lavaud et al., submitted[1]) were projected onto the consensus marker map DORA using Biomercator 4.2 software. QTL and marker-trait associations identified by linkage analysis and GWAS, respectively, were visualized on the consensus marker map DORA using MapChart 2.1 software (Voorrips, 2002). Consistent genetic regions controlling partial resistance to *A. euteiches* were defined according to the colocalization of at least four partial resistance QTL and/or resistance-associated SNPs identified by linkage analysis and/or GWAS, respectively, based on their genetic positions on the consensus genetic map. Intervals of consistent genetic regions were delimited by the positions of upper and lower resistance QTL or resistance-associated GWAS-SNPs overlapping at least one of the four co-located resistance QTL/SNPs of each region. Main *Ae-Ps* QTL identified by Hamon et al. (2011;

2013) were repositioned using genetic analysis results and DORA marker map positions.

Haplotype analysis

Local LD analysis was performed to define LD block intervals around significant markers detected by GWAS in consistent genetic regions of partial resistance, using PLINK 1.9 software. A LD block was determined as the interval including all markers in LD ($r^2 > 0.7$) with the targeted marker. For each variable associated with a significant marker in a given LD block, EMMs of pea line groups carrying haplotypes that were not considered as rare, *i.e.* comprising more than 8 individuals (> 5% of the total number of accessions), were computed and compared using the Tukey-HSD test ($\alpha = 5\%$; R functions emmeans and cld of package emmeans). For each LD block, haplotypes significantly associated with higher or lower mean phenotypic scores compared to the other haplotypes, were defined as favorable (named a) or unfavorable (named b or c), respectively. At each LD block containing most significant markers, the phenotypic mean and range (adjusted EMMs) of the group of pea lines carrying different rare haplotypes (cumulated frequency > 5%; n ≥ 2 rare haplotypes) was compared to that of the group of pea lines carrying the favorable or unfavorable haplotype, using the Tukey-HSD test ($\alpha = 5\%$). Results of mean comparison tests were shown using box plots (R function ggplot of package ggplot2; Wickham, 2016).

Results

Phenotypic data analysis

In both Eden x E11 and Eden x LISA AB populations, global statistical analyses of disease scores obtained in field and controlled conditions experiments revealed significant genotype x environment (*p-value* < 0.05) and highly significant genotype x strain (*p-value* < 0.001) interaction effects, respectively, except for the first ADI ratings evaluated in Riec-sur-Belon and Dijon-Epoisses in the Eden x E11 population. The analysis of phenotypic and QTL data was therefore carried out for each environment and strain.

Individual statistical analyses of all *A. euteiches* resistance and flowering traits evaluated in both AB populations displayed significant G effects (*p-value* < 0.01), except for the EL_RI21_RRI variable (*p-value* = 0.07). They showed significant R_A or R_{Gr} effect for field variables (*p-value* < 0.01), as well as significant B effects (*p-value* < 0.05) and GxB interactions (*p-value* < 0.001) for controlled conditions variables, except for the E11_Ae109 variable (*p-value* = 0.54 and 0.14, respectively). Broad-sense heritability of ADI variables ranged from very low values for the first ratings performed in both Eden x E11 and Eden x LISA populations in Riec-sur-Belon (H^2 = 0.05 and 0.13, respectively) to high values for the third ratings in Dijon-Epoisses (H^2 = 0.67 and 0.73, respectively). Heritability values for root resistance evaluated in Riec-sur-Belon and in controlled conditions ranged from 0.41 to 0.86 and were especially higher in the Eden x E11 population ($H^2 > 0.81$) compared to those assessed in the Eden x LISA population ($H^2 < 0.61$). Heritabilities of flowering traits were very high in each population ($H^2 > 0.95$). Frequency distributions of EMMs values for each variable tended to fit normal curves except for flowering traits which showed bimodal distribution. Transgressive segregation was observed for all the traits (Supplementary Figure 1; Supplementary Table 1).

In both AB populations, all ADI scores assessed in Riec-sur-Belon and Dijon-Epoisses were highly significantly and positively (r > 0.41, *p-value* < 0.001) correlated within each location, and most of the ADI variables showed significant and positive correlations between locations. RRI scores assessed in Riec-sur-Belon were poorly correlated with other field data except for ADI scores evaluated in the Eden x LISA population in the same environment (r > 0.21, *p-value* < 0.01). In the Eden x E11 population, RB84 and Ae109 strain data were significantly correlated between each other (r = 0.29, *p-value* < 0.001) but poorly correlated with all the other traits, except for the RB84 and RRI data (r = 0.23, *p-value* < 0.01). In the Eden x LISA population, RB84 and Ae109 data were not correlated between each other but were mostly significantly and positively correlated with ADI scores evaluated in Riec-sur-Belon and Dijon-Epoisses, especially for RB84 strain data (r > 0.18, *p-value* < 0.05). Flowering data were significantly (*p-value* < 0.05) and negatively (r < -0.19) correlated with ADI scoring data, and were poorly correlated with field RRI and controlled conditions data in both populations, except for the RB84 strain data (r < -0.26, *p-value* < 0.001) associated with the Eden x LISA population (Figure 1).

Genetic maps construction

The genetic maps, constructed from the Eden x E11, Eden x LISA, Baccara x PI180693, Baccara x 552, DSP x 90-2131, and Puget x 90-2079 populations, comprised 993, 478, 1,866, 1,082, 950, and 669 markers covering 785.0, 449.6, 927.8, 982.3, 854.5, and 644.8 cM Haldane, respectively, over nine to nineteen LGs (Table 1 and Supplementary Table 2). On each genetic map, marker distribution and order were well conserved with the pea reference consensus map presented in Tayeh et al. (2015). Depending on the RIL genetic map, the average marker densities ranged from 1.0 to 2.0 markers/cM and the maximum gaps between two contiguous markers varied from 13.0 to 18.1 cM. Although the AB populations exhibited lower levels of genetic recombination compared to the RIL populations, the quality of linkage mapping remained satisfactory. Specifically, the Eden x E11 and Eden x LISA genetic maps displayed an average marker density of 1.3 and 1.1 markers/cM, respectively, along with a maximum gap of 18.2 and 10.9 cM, respectively. Non-Mendelian allelic segregation ($\alpha = 0.001$) was observed for less than 5.5% of the total number of markers in each RIL and AB population, except for the Eden x E11 AB population showing 214 mapped markers (21.6%) at which alleles did not segregate according to the expected Mendelian ratio. Out of the 214 markers, 158 SNPs (mostly on the LGIII, LGV, and LGVI) and 56 SNPs (on LGI, LGII, and LGVII) showed allelic segregation with a lower (< 3%) and higher (> 15%) frequency of E11 alleles, respectively, than the expected Mendelian allelic frequency of 12.5%.

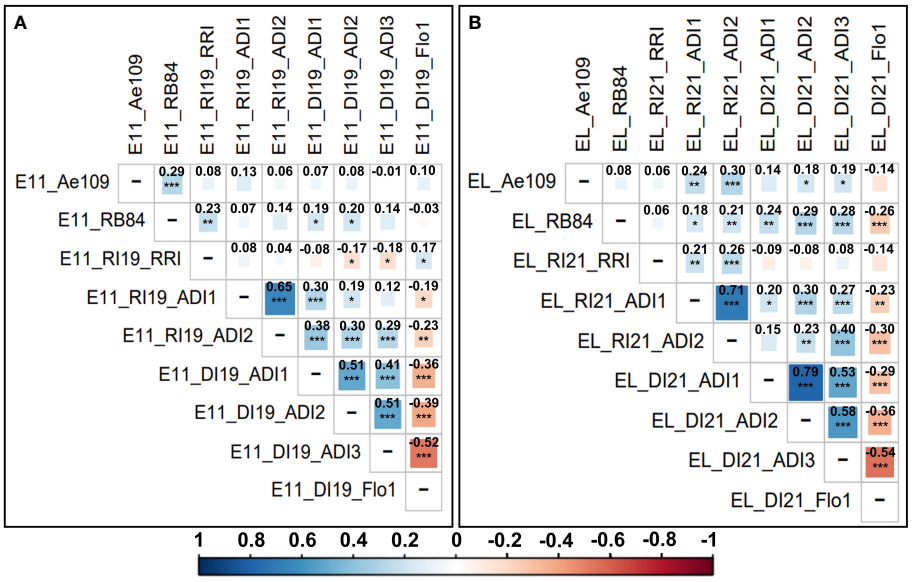

FIGURE 1
Correlogram and Pearson correlation coefficients between the different adjusted mean scoring data variables obtained for resistance to *A. euteiches* and flowering traits in the **(A)** Eden x E11 and **(B)** Eden x LISA AB populations. Scoring variables are coded as follows: population (E11 = Eden x E11 and EL = Eden x LISA); location (DI = Dijon-Epoisses, Côtes d'Or and RI = Riec-sur-Belon, Finistère (France)); experimental year (19 = 2019 and 21 = 2021); criterion (controlled conditions: Ae109 and RB84 = *A euteiches* strains belonging to the pathotype III and I, respectively; field: ADI = Aerial Disease Index, Flo1 = Number of calendar days to 50% bloom, RRI = Root Rot Index). Pearson correlation coefficients are indicated in bold. Level of correlation is coded with a color gradation scale from dark blue or red (r = ± 1) to white (r = 0). Significance *p-value* codes: 0 < '***' ≤ 0.001 < '**' ≤ 0.01 < '*' ≤ 0.05.

Out of the 1,850 supplementary marker set used in this study, 1,832 markers were well projected from individual genetic maps onto the pea reference consensus genetic map (Tayeh et al., 2015), and contributed to densify the final consensus marker map DORA which comprises 16,647 markers and covers 801.2 cM Haldane. The consensus marker map DORA has an average marker density ranging from 19.1 to 22.1 markers/cM, depending on LGs, and includes seven gaps ranging from 1.0 to 5.7 cM between two contiguous markers (Supplementary Table 2).

QTL mapping

A total of 11, 13, 61, 34, 39, and 13 additive-effect QTL were detected for Aphanomyces root rot resistance in the Eden x E11,

TABLE 1 Pea populations and number of markers used in this study.

Collection or population	Number of pea lines	Number of markers used for genotyping						Reference
		Total	PsCam	Ps1	Ps0	Ps9	Other markers[a]	
Pea-Aphanomyces collection	172	10,824	9,549	1,214	21	35	5*	Desgroux et al. (2016)
RIL Baccara x PI180693 population	176	1,866	291	1,292	74	28	181**	Hamon et al. (2011; 2013)
RIL Baccara x 552 population	178	1,082	210	690	61	14	107**	Hamon et al. (2011; 2013)
RIL DSP x 90-2131 population	111	950	203	553	46	11	137**	Hamon et al. (2013)
RIL Puget x 90-2079 population	121	669	190	286	7	17	169**	Pilet-Nayel et al. (2002; 2005); Hamon et al. (2013); Lavaud et al. (submitted[1])
AB Eden x E11 population	160	993	242	712	15	22	2*	This study
AB Eden x LISA population	178	478	317	143	8	9	1*	This study

[a]Other markers including (*) SNP markers and (**) markers from Pilet-Nayel et al. (2002; 2005) and Hamon et al. (2011; 2013).

Eden x LISA, Baccara x PI180693, Baccara x 552, DSP x 90-2131, and Puget x 90-2079 populations, respectively. The characteristics and genetic localizations of these QTL are indicated in Figure 2 and Supplementary Table 3.

In the Eden x E11 population, six genetic regions were significantly associated with resistance. Two of these regions were detected from several variables, including one region on LGIII close to the *Le* (internode length) locus in the *Ae-Ps3.2* QTL region (ADI and RB84, 6.4% < R^2 < 6.7%) and the other one on LGVII in the *Ae-Ps7.6* region (RRI, RB84 and Ae109, 9.1% < R^2 < 53.6%) with a major effect associated with the RB84 variable (R^2 = 53.6%). Four regions were detected from one or several ADI variable(s), on LGII in the *Ae-Ps2.2* region, on LGIII close to the *Hr* (flowering) locus in the *Ae-Ps3.1* region, on LGIV and on LGVII in the *Ae-Ps7.5* region (8.5% < R^2 < 22.3%). In the Eden x LISA population, six genetic regions were also significantly associated with resistance, including (i) the three regions detected from the Eden x E11 population on LGII, LGIII (close to *Le*) and LGVII, the one on LGII showing a consistent and higher effect (ADI and RB84 variables; 7.3% < R^2 < 37.6%) in contrast to that on LGVII (Ae109, R^2 = 7.6%) and (ii) three other minor-effect regions (R^2 < 9.5%), each detected with one or two variables, on LGI in the *Ae-Ps1.3* region, LGIII, and LGIV close to the *Ae-Ps4.1* region. In each population, allelic contribution to the resistance was brought by the resistant parent, E11 or LISA, at all the QTL detected but one showing minor and inconsistent effect. Four additive-effect QTL associated with early flowering were identified, including QTL co-localizing with resistance genetic regions detected on LGII in the *Ae-Ps2.2* region and LGIII close to the *Hr* or *Le* locus, in both populations. In the co-localizing region on LGII, the QTL detected for flowering showed a major additive-effect (46.8% < R^2 < 70.6%, depending on the AB population) and an epistatic effect (R^2 = 3.2%) with another QTL detected for flowering in the Eden x E11 population. In this region, resistance-increasing alleles from E11 or LISA contributed to late flowering.

A total of 50, 31, 37, and 13 resistance additive-effect QTL previously detected in Pilet-Nayel et al. (2002; 2005) and Hamon et al. (2011; 2013), were re-identified in the Baccara x PI180693, Baccara x 552, DSP x 90-2131, and Puget x 90-2079 RIL populations, respectively, using supplemented genotyping datasets and updated linkage analysis studies. In the Puget x 90-2079 population, no additional QTL was identified compared to those previously described in Pilet-Nayel et al. (2002; 2005). In the Baccara x PI180693, Baccara x 552 and DSP x 90-2131 populations, 11, three and two additional resistance QTL were detected, for Ae109, ADI, DW and RRI variables (3.9% < R^2 < 42.0%), ADI variables (6.5% < R^2 < 10.7), and Ae87 and Dead variables (R^2 = 8.3% and 42.2%, respectively), respectively. All additional QTL were detected in genetic regions previously associated with Aphanomyces root rot resistance on LGI (*Ae-Ps1.1*, *Ae-Ps1.2*), LGII (*Ae-Ps2.2*), LGIII (*Ae-Ps3.1*, *Ae-Ps3.2*), LGIV (*Ae-Ps4.5*), LGV (*Ae-Ps5.2*), and LGVII (*Ae-Ps7.5*, *Ae-Ps7.6*). In the Baccara x PI180693 and Baccara x 552 RIL populations, 8 and 4 additional QTL associated with flowering or height traits were identified, respectively, in genetic regions previously detected for these traits (on LGI in *Ae-Ps1.2*, LGII in *Ae-Ps2.1* and *Ae-Ps2.2*, LGIII in *Ae-Ps3.2*, LGVII in *Ae-Ps7.4* and *Ae-Ps7.6* regions) and in a new region on LGVI between the *Ae-Ps6.2* and *Ae-Ps6.4* QTL. Pairwise epistatic interactions associated with flowering traits (R^2 < 9.5%) were identified in the Baccara x PI180693 and DSP x 90-2131 RIL populations.

Genome-wide association mapping

LD, structure and kinship data on the pea-Aphanomyces collection were updated using the genotyping dataset of 10,824 SNPs on 172 pea genotypes, presented in Desgroux et al. (2016). The LD decay value averaged 0.14 cM (Supplementary Figure 2A), which was close to the value (0.12 cM) presented in Desgroux et al. (2016). Ten genetic sub-populations were identified in the collection, according to the optimal likelihood value of K computed by ADMIXTURE (Supplementary Figure 2B). These results completed the PCA analysis conducted in Desgroux et al. (2016), which integrated into GWAS the structure captured by the three first PCA axis. Kinship analysis revealed IBD relatedness coefficients ranging from -0.34 to 1.12 among individuals with an estimated average of -0.006 (Supplementary Figure 2C). The Ward's clustering computed on kinship IBD matrix showed consistent clusters with those described in Desgroux et al. (2016).

Updated GWAS in the collection identified a total of 29 resistance-associated SNPs distributed over the seven LGs, using MLMM with a maximum number of cofactors of 5 and *p-value* < 3.6E-05 (Figure 2 and Supplementary Table 4). This number of significant SNPs was lower compared to the 56 resistance-associated markers described in Desgroux et al. (2016), using MLMM with a maximum number of cofactors of 10 and *p-value* < 2.5E-05. Significant markers were associated with 22 variables, for which a total of 41 marker-trait associations including 14 previously identified (Desgroux et al., 2016), were significantly identified as cofactors in the MLMM model (4.61E-28 < *p-value* < 3.57E-05). Zero to four markers were detected as cofactors for each variable, explaining a total of 0 to 68% of the phenotypic variation. A total of 17 markers significantly associated (9.27E-25 < *p-value* < 2.86E-05) with flowering or morphological variables, and 28 marker-trait associations including five previously detected (Desgroux et al., 2016), were identified on LGII, LGIII, LGV, and LGVII (Figure 2 and Supplementary Table 4).

Consistent genetic regions of resistance

A total of ten consistent genetic regions of partial resistance to *A. euteiches*, numbered from 1 to 10, were identified according to the colocalization of at least four partial resistance QTL and/or resistance-associated SNPs identified by RIL and/or AB linkage analyses and/or GWAS, respectively (Figure 2, Table 2 and Supplementary Table 5). On LGIV, the intervals of two genetic regions named 5 and 7 were slightly extended to include significant resistance QTL or resistance-associated SNPs detected by GWAS flanking the positions of the four co-located QTL/SNPs of each region. The size of each consistent genetic region ranged from 12.1 to 34.0 cM (genetic regions n°7 and n°10, respectively), depending on the region. The number of resistance QTL and resistance-associated GWAS-SNPs comprised in each

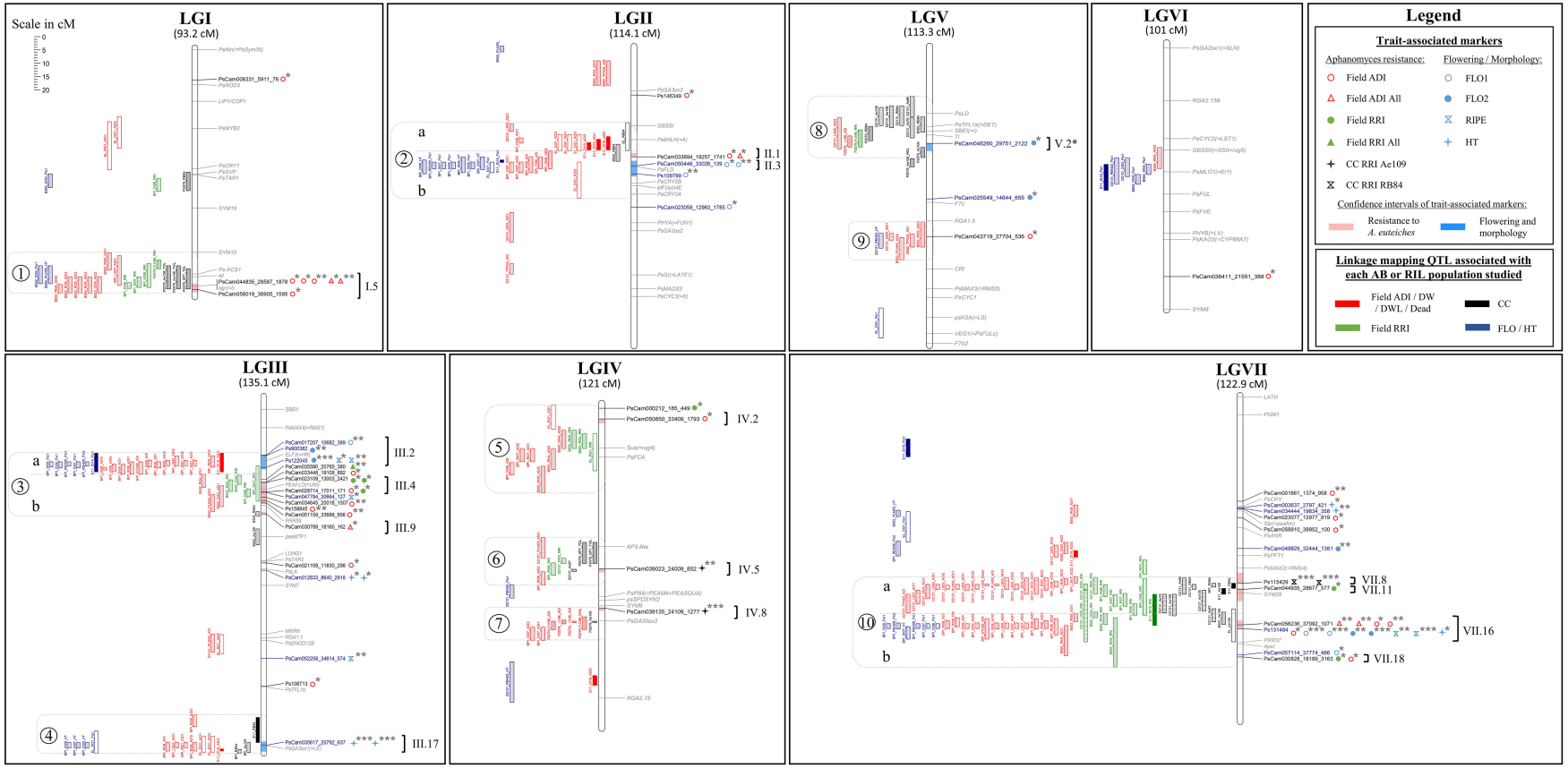

FIGURE 2
Comparative genetic mapping of markers and LD blocks identified by GWAS, and QTL detected by AB and RIL linkage analyses, for resistance to *A. euteiches*. LG names from I to VII and LG sizes in cM Haldane. (i) On the right of each LG: names of significant SNPs identified by GWAS in black and blue with, in red and blue shading in the LG bar, the confidence intervals around the significant SNPs ($r^2 > 0.7$) for resistance and flowering/morphology, respectively; names and genomic positions of cloned pea genes in grey; on the right of each SNP significant marker, symbol(s) for the trait(s) associated markers as described in the legend, and significance of the marker-trait association (*p-value*: '***' ≤ 1.E-12 < '**' ≤ 1.E-6 < '*'); on the far right of each LG, names of the defined LD blocks according to Desgroux et al. (2016), with brackets gathering the markers attributed to the same LD block ($r^2 > 0.7$). (ii) On the left of each LG: QTL detected by linkage mapping for the different variable types studied, as described in the legend; empty and filled rectangles for QTL from Eden x LISA and Eden x E11 AB populations, respectively; diagonal, horizontal, vertical, and crossed bar rectangles for QTL from Baccara x 552, Baccara x PI180693, DSP x 90-2131 and Puget x 90-2079 RIL populations, respectively; rectangle lengths as QTL confidence intervals (one LOD drop-off); on the far left of QTL, numbers from 1 to 10 surrounded by grey dotted rectangles, for consistent genetic regions of partial resistance to *A. euteiches*; sub-regions a and b delimited by grey dotted lines in regions 2, 3 and 10, to separate resistance QTL colocalizing or not with flowering or morphological QTL.

10.3389/fpls.2023.1189289

TABLE 2 Consistent genetic regions, including QTL, SNPs and LD blocks, contributing to partial resistance to *A. euteiches* in pea.

					Linkage analysis in AB and RIL populations						GWAS in the pea-Aphanomyces collection				
LG	Consistent genomic region[a]	Genetic subregion[b]	Position interval [minimum ; maximum][c]	Genes[d]	*Ae-Psxxx QTL*[e]	Nb of population	Nb of QTL	Nb of QTL associated variable	R^2 mean ± sd	Range of R^2 value	LD block	Nb of GWAS-SNP	Nb of GWAS-SNP associated variable	*p-value* mean ± sd	Range of *p-value*
I	**1**	-	[76.6 ; 91.8]	**Af / SGR**	*Ae-Ps1.2*	3	14	7 ADI + 4 RRI + 1 Ae106_TDL + 1 SP7_TDL + 1 Ae106_TWL	11.5 ± 3.8	[5.7 ; 16.6]	I.5	6	6 ADI	1.3E-05 ± 1.3E-05	[3.9E-11 ; 3.0E-05]
II	**2**	**a**	[29.1 ; 39.7]	**A**	*Ae-Ps2.2a*	5	10	8 ADI + 2 RB84	18.7 ± 10.3	[7.2 ; 37.6]	–	–	–	–	–
		b	[39.9 ; 57.9]		*Ae-Ps2.2b*	4	7	6 ADI + 1 RB84	11.3 ± 4.7	[7.2 ; 20.4]	II.1	2	2 ADI	1.6E-05 ± 1.3E-05	[6.6E-06 ; 2.5E-05]
III	**3**	**a**	[21.5 ; 29.5]	**HR**	*Ae-Ps3.1a*	2	14	13 ADI + 1 RRI	17.6 ± 7.0	[7.6 ; 29.4]	–	–	–	–	–
		b	[29.5 ; 45.4]	-	*Ae-Ps3.1b*	2	8	3 ADI + 4 RRI+ 1 RB84	10.5 ± 4.1	[7.6 ; 19.4]	III.4 / III.9	10	6 ADI + 4 RRI	5.8E-06 ± 9.2E-06	[4.0E-09 ; 2.6E-05]
	4	-	[120.4 ; 135.1]	**LE**	*Ae-Ps3.2*	3	11	7 ADI + 1 DW + 1 Ae109 + 2 RB84	11.9 ± 6.6	[5.6 ; 28.5]	–	–	–	–	–
IV	**5**	-	[0.7 ; 33.4]	-	*Ae-Ps4.1*	3	10	7 ADI + 3 RRI	11.5 ± 7	[5.8 ; 26.1]	IV.2	2	ADI + 1 RRI	2.7E-05 ± 1.3E-05	[1.7E-05 ; 3.6E-05]
	6	-	[50.0 ; 67.7]	-	*Ae-Ps4.3*	3	7	2 ADI + 2 RRI + 1 Ae87 + 1 SP7_TDL + 1 SP7_TWL	14.9 ± 14.7	[3.4 ; 46.8]	IV.5	1	1 Ae109	7.8E-07	–
	7	-	[76.1 ; 88.2]	-	*Ae-Ps4.5*	2	7	5 ADI + 1 DWL + 1 Ae109	31.3 ± 30	[3.9 ; 88.9]	IV.8	1	1 Ae109	4.6E-28	–
V	**8**	-	[19.0 ; 42.2]	**r**	*Ae-Ps5.1*	3	11	2 ADI + 1 RRI + 2 Ae109 + 1 Ae106 + 1 Ae85 + 1 Ae78 + 3 RB84	15.8 ± 10.5	[2.2 ; 37.2]	–	–	–	–	–
	9	-	[66.5 ; 80.8]	-	*Ae-Ps5.2*	2	4	4 ADI	12.1 ± 5.8	[6.5 ; 20.3]	–	1	1 ADI	4.1E-06	–
VII	**10**	**a**	[68.3 ; 81.6]	-	*Ae-Ps7.6a*	5	39	17 ADI + 1 Dead + 10 RRI + 4 Ae109 + 1 Ae85 + 1 Ae78 + 1 Ae106 + 1 Ae87 + 3 RB84	27.0 ± 19.5	[7.5 ; 74.8]	VII.8 / VII.11	3	1 RRI + 2 RB84	7.8E-06 ± 1.4E-05	[3.6E-16 ; 2.4E-05]
		b	[81.6 ; 102.3]	-	*Ae-Ps7.6b*	5	25	13 ADI + 1 DW + 7 RRI + 3 Ae109 + 1 Ae87	16.5 ± 10.4	[6.5 ; 44.0]	VII.16 / VII.18	7	6 ADI + 1 RRI	5.8E-06 ± 8.1E-06	[1.6E-07 ; 2.0E-05]

[a]Consistent genetic regions and [b]sub-regions, as described in Figure 2, with their [c]intervals in cM Haldane located on the consensus marker map DORA.
[d]Morphological genes present in consistent genetic regions.
[e]Ae-Psxxx QTL from Hamon et al. (2013) repositioned on the consensus marker map DORA according to updated linkage analyses in RIL populations.
R^2: percentage of phenotypic variation explained by a QTL. LD blocks as described in Figure 2. Variable codes as described in Supplementary Table 1, with field variables on aerial and root plant part written in red and green, respectively, and controlled conditions variables in dark.

10.3389/fpls.2023.1189289

consistent genetic region ranged from 4 to 55 and 0 to 8, respectively (Figure 2). The ten consistent regions cover those of the seven main consistent QTL and three additional less consistent QTL (*Ae-Ps3.2*, *Ae-Ps4.3* and *Ae-Ps5.2*), previously reported (Hamon et al., 2013). Most of the consistent genetic regions comprised resistance QTL and GWAS-SNPs associated with field and controlled conditions variables, except for the fourth and eighth regions including no resistance-associated marker. Both major resistance *Ae-Ps4.5* and *Ae-Ps7.6* QTL were re-identified in QTL mapping and GWAS with a high proportion of phenotypic variation explained by each individual QTL (R^2 = 88.9% and 74.8%, respectively) and a high significance level of resistance-associated GWAS-SNP (*p-value* = 4.6E-28 and 3.6E-16, respectively) (Table 2). Each consistent genetic region colocalized with at least one flowering/morphological QTL or -associated GWAS-SNP, except for genetic regions identified on LGIV (Supplementary Table 5). The *Ae-Ps2.2*, *Ae-Ps3.1* and *Ae-Ps7.6* regions were split into two genetic sub-regions, separating partial resistance QTL colocalizing with flowering and morphological QTL from other partial resistance QTL.

LD blocks

A total of 11 resistance LD blocks, covering 0.1 to 8.1 cM, were identified around significant resistance-associated GWAS-SNPs comprised in the ten consistent genetic regions. Each LD block included 1 to 22 markers in LD (r^2 > 0.7) with each significant marker (Figure 2 and Supplementary Table 6). All disease resistance LD blocks comprised at least one common SNP with the markers composing the LD blocks detected in Desgroux et al. (2016), and were thus named as presented in the previous study. Out of the 11 LD blocks, (i) two were common to field ADI and RRI traits (III.4 and VII.18 in *Ae-Ps3.1* and *Ae-Ps7.6* regions, respectively), (ii) five and one were specific to field ADI (I.5, II.1, III.9, IV.2, and VII.16 in *Ae-Ps1.2*, *Ae-Ps2.2*, *Ae-Ps3.1*, *Ae-Ps4.1*, and *Ae-Ps7.6* regions, respectively) and RRI (VII.11 in the *Ae-Ps7.6* region) variables, respectively, (iii) and two and one were specific to the Ae109 (IV.5 and IV.8 in *Ae-Ps4.3* and *Ae-Ps4.5* regions, respectively) and RB84 (VII.8 in the *Ae-Ps7.6* region) strains evaluated in controlled conditions, respectively.

Five LD blocks, which intervals ranged from 3.0 to 5.9 cM, were defined around significant flowering and morphological-associated SNPs identified in five consistent genetic regions. Among the five LD blocks, two and one LD blocks were specific to flowering (II.3 and V.2* in *Ae-Ps2.2* and *Ae-Ps5.1* regions, respectively) and height (III.17 in the *Ae-Ps3.2* region) variables, respectively. Two were common to flowering, height, or ripening variables (III.2 and VII.16 in *Ae-P3.1* and *Ae-Ps7.6* regions, respectively). Flowering and morphological LD blocks were named according to Desgroux et al. (2016), except for the LD block V.2 (renamed V.2*) which was associated with a different variable compared to the one identified in the previous study. Only the LD block VII.16 associated with flowering and morphological variables was common to *A. euteiches* resistance. At this LD block, opposite allelic effects were found at significant resistance and flowering/morphological-associated SNPs, which suggest that resistance-enhancing alleles contributed to higher plants and later flowering and ripening (Figure 2 and Supplementary Tables 4, 6).

Marker haplotypes

At each of the 11 LD blocks defined around significant resistance-associated GWAS-SNPs, three to twenty-one marker haplotypes showing different genotyping profiles were identified, depending on the LD block (Supplementary Table 6). At each resistance LD block, one favorable haplotype and one unfavorable haplotype, well-represented in the pea-Aphanomyces collection (frequency > 5%), was identified by mean comparison of phenotypic EMMs between each haplotype group (α = 5%). The pea lines AeD99QU-04-4-6-1, AeD99QU-04-15-8-1, and AeD99OSW-49-5-7 cumulated the highest number of favorable haplotypes (n = 8) at the 11 resistance LD blocks and displayed a high level of disease resistance in the pea-Aphanomyces collection (Supplementary Table 7). At each LD block, one to 19 rare haplotypes (frequency ≤ 5%) were detected, depending on the LD block. At five of the 11 LD blocks showing the most significant resistance-associated GWAS-SNPs, the group of pea lines bringing together several rare haplotypes (number of rare haplotypes ≥ 2, cumulated frequencies > 5%) presented a mean resistance level significantly similar (blocks VII.11 and III.4) or lower (blocks I.5, II.1 and VII.8) than the group of pea lines sharing the favorable haplotype (α = 5%) (Figure 3).

Among 14 pea accessions classified as new sources of resistance in the collection and found to carry rare haplotypes in this study, several lines exhibited a higher level of resistance compared to the average resistance level of lines sharing the favorable haplotype. These lines are especially NEPAL A at LD block III.4, and NEPAL A, GAT1259, L2782.1 at LD block VII.11. The AB parental line E11, carrying a rare haplotype at LD block VII.8 in the *Ae-Ps7.6* region, had a lower disease severity in inoculated conditions with the RB84 strain than the group of pea lines sharing the unfavorable haplotype at this LD block (Figure 3). The AB parental line LISA, carrying unfavorable haplotypes at eight of the 11 LD blocks and a rare haplotype at LD block II.1 in the *Ae-Ps2.2* region, displayed lower susceptibility in the field (Supplementary Table 7). Favorable and unfavorable haplotypes were also detected at three of the five LD blocks identified around significant flowering and morphological-associated SNPs (Supplementary Tables 6, 7).

Discussion

This study aimed to identify novel QTL and alleles, as well as QTL-closely linked SNPs, for resistance to Aphanomyces root rot in pea, a complex genetically inherited trait. Indeed, diversifying and efficiently pyramiding resistance QTL and alleles in breeding will be necessary to develop pea varieties with high and durable levels of resistance to Aphanomyces root rot, which remains challenging. This work describes the first AB-QTL mapping approach to investigate the polygenic control of Aphanomyces root rot resistance in new sources of resistance. It describes an update of previous QTL/GWAS studies by incorporating common SNP markers with the AB-QTL mapping approach. This integration was necessary for analyzing the novelty of QTL identified in AB populations based on their genetic locations.

10.3389/fpls.2023.1189289

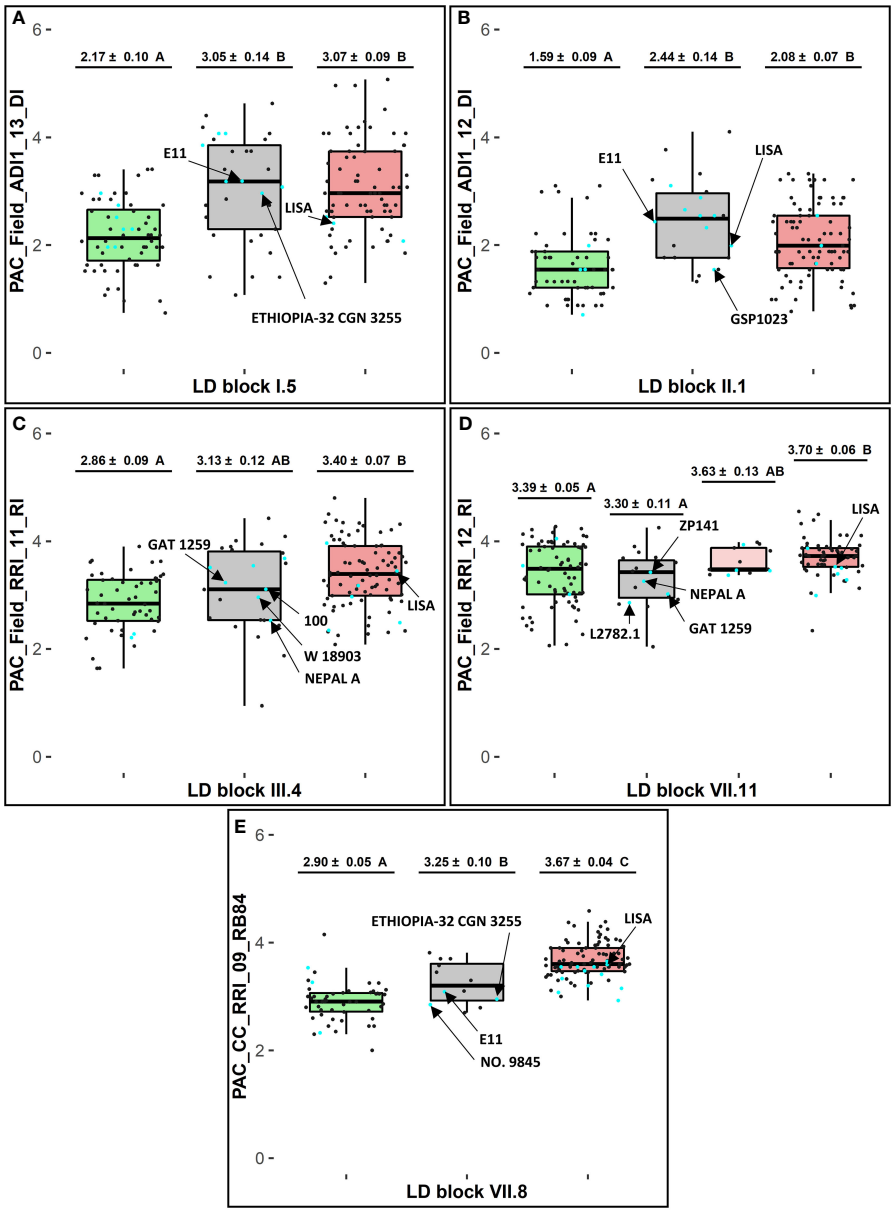

FIGURE 3
Haplotype analysis at selected LD blocks in consistent genetic regions (1, 2b, 3b and 10a) for selected variables of resistance to *A euteiches*. At each LD block **(A)** I.5, **(B)** II.1, **(C)** III.4, **(D)** VII.11, and **(E)** VII.8: adjusted EMMs phenotypic scores ± standard deviation and Tukey-HSD mean comparison groups (α = 5%), for each favorable (in green), rare (in grey), and unfavorable (in red) haplotype box with n = 1 haplotype in each green and red box and n ≥ 2 haplotypes in each grey box; cyan and dark dots showing phenotypic EMMs values of pea lines belonging or not, respectively, to the 20 new sources of resistance defined in the pea-Aphanomyces collection; arrows pointing values for E11 and LISA, or for new sources of resistance carrying rare haplotypes which showed lower values than the average ones of lines sharing the unfavorable haplotype.

AB-QTL mapping in two new sources of resistance confirmed previous resistance QTL

AB mapping is a suitable approach both to detect and advance introgression of exotic alleles originating from germplasms genetically distant from elite varieties. In addition, QTL mapping in AB populations makes it possible to identify rare QTL or alleles in an agronomic background (Tanksley and Nelson, 1996), which would not be detectable in GWAS approach. Among the 20 new sources of resistance selected from the extensive screening program of Aphanomyces resistance accessions previously conducted by Pilet-Nayel et al. (2007), E11 and LISA were identified as two new pea germplasm lines partially resistant to *A. euteiches*. These two lines showed rare marker haplotypes at consistent resistance loci in the pea Aphanomyces collection (Desgroux et al., 2016), which were mostly different from those derived from the reference parents PI180693, 552, 90-2131 and 90-2079. We thus produced AB populations using E11 and LISA as partially resistant parents, to identify new QTL for resistance to *A. euteiches* and advance their introduction into an agronomic genetic background (Eden) previously used for NIL creation at Aphanomyces resistance QTL (Lavaud et al., 2015).

In this study, QTL mapping detected 11 and 13 additive-effect QTL associated with *A. euteiches* resistance in the Eden x E11 and Eden x LISA AB populations, respectively. These QTL were located in the *Ae-Ps1.3*, *Ae-Ps2.2*, *Ae-Ps3.1*, *Ae-Ps3.2*, *Ae-Ps4.1*, *Ae-Ps7.5* and *Ae-Ps7.6* regions, previously reported (Hamon et al., 2011; Hamon et al., 2013; Desgroux et al., 2016). Highest effects of resistance QTL were identified in the *Ae-Ps7.6* region (8.5% < R^2 < 53.6%) from the Eden x E11 population and in the *Ae-Ps2.2* region (7.3% < R^2 < 37.6%) from both AB populations. At QTL *Ae-Ps7.6*, we can hypothesize that the resistance allele with major effect identified in E11 could be identical to those identified with major effects in PI180693 and 90-2131. However, to our knowledge, no pedigree data from the parental line E11 is available to highlight potential genetic relationship with PI180693 and 90-2131. Genome sequencing of the three genotypes at QTL *Ae-Ps7.6* would be helpful to address this issue. At QTL *Ae-Ps2.2*, we can presume that the resistance alleles in E11 and LISA are closely-linked or correspond to late flowering alleles, since co-localizations were observed between resistance and flowering QTL with opposite allelic effects as reported in Hamon et al. (2013). Pleiotropy or linkage between genes controlling plant disease resistance and undesired development traits, *e.g.* late-flowering, were commonly reported in the literature (Poland et al., 2009). In addition, resistance alleles in the *Ae-Ps2.2* region cosegregated with colored flower alleles in pea lines of the two AB populations, suggesting pleiotropy or genetic linkage between the resistance QTL and the *A* morphological gene controlling anthocyanin production (*i.e.* the PsbHLH gene). Updated GWAS refined the localization of the resistance LD block II.1 in the *Ae-Ps2.2* region to a genetic position close to but different from the *A* locus as previously highlighted by Desgroux et al. (2016), which suggests the possibility to break the negative correlation between resistance and colored flowers in pea.

In the Eden x LISA and Eden x E11 populations, AB lines showing highest levels of partial resistance to *A. euteiches* carried resistance alleles at QTL *Ae-Ps2.2* or *Ae-Ps7.6*, individually (lines EL.61, EL.143 and lines E11.87, E11.133, respectively) or in combination with resistance alleles at one or two additional minor-effect QTL (*Ae-Ps2.2* and *Ae-Ps1.3*, *Ae-Ps3.2* or *Ae-Ps7.6* in lines EL.65, EL.186; *Ae-Ps7.6* and *Ae-Ps2.2*, *Ae-Ps3.1*, *Ae-Ps3.2* or *Ae-Ps7.5* in lines E11.9, E11.42, E11.68, E11.79). By advancing backcross generations to the elite background, the frequency of undesirable alleles from the unadapted donor line is reduced in AB populations, favoring the transfer of valuable QTL into established elite inbred lines (Tanksley and Nelson, 1996). In the two AB populations studied, allele frequencies skew towards the recurrent breeding parent Eden (frequency > 87.6%), favoring the future development of NILs by further backcrossing selected AB lines to the agronomic recipient parent Eden.

Integrated linkage and genome-wide association mapping identified ten consistent genetic regions and closely-linked SNP markers associated with resistance

Comparative mapping is a valuable approach to compare QTL identified from different populations and genetic analysis methods, thus providing insight into their organization and diversity across the genome. This approach is based on the use of common "bridge" markers between genetic studies and mapping populations, in sufficiently high density to precisely compare QTL positions between genetic maps. So far, the comparative mapping of Aphanomyces root rot resistance QTL detected by linkage mapping in the RIL populations and by GWAS in the pea-Aphanomyces collection has only been performed previously based on the projection of 144 common markers onto a consensus map (Desgroux et al., 2016). In this study, we used 1,850 markers publicly available (Duarte et al., 2014; Tayeh et al., 2015; Boutet et al., 2016), including 462 SNPs anchored to the pea genome (Kreplak et al., 2019), as bridge markers between AB and RIL studies and GWAS to accurately compare the QTL positions re-detected in the different studies on the consensus marker map DORA. These SNP markers also made possible to localize the most stable major-effect QTL $Ae_{MRCD1}Ps\text{-}4.1/2$ recently reported in Wu et al. (2021) in the region of QTL *Ae-Ps4.5*.

In addition, the QTL detection methods in RIL populations (Pilet-Nayel et al., 2002; Pilet-Nayel et al., 2005; Hamon et al., 2011; Hamon et al., 2013) and the pea-Aphanomyces collection (Desgroux et al., 2016) have been revisited with more stringency, allowing more robust QTL re-detection. In QTL mapping from the four RIL populations, higher minimum LOD score thresholds (2.8 < LOD < 4.8) were estimated in updated composite interval mapping analyses compared to the ones (2.8 < LOD < 2.9) computed in previous studies. This resulted in the detection of more consistent QTL and fewer putative false positives, confirming the seven main *Ae-Ps* meta-QTL and invalidating 15 to 42 minor-effect resistance QTL (R^2 < 27.2%) previously detected, depending on the population. In addition, in the Baccara x PI180693 population, updated analysis identified mismatches between phenotyping and genotyping datasets from Hamon et al. (2011), showing three spurious resistance QTL associated with resistance to the Ae109 and/or RB84 strains that were previously detected on LGII, LGVI, and LGVII (8.7% < R^2 < 49.4%). Updated QTL mapping taking into account these corrections, showed colocalization in the *Ae-Ps7.6* region between PI180693 and 90-2131 alleles contributing to resistance to the RB84 strain, in accordance with the pedigree relationship between these two resistant germplasms (Kraft, 1992). In this study, we observed that major QTL identified in controlled conditions accounted for a higher percentage of phenotypic variation compared to the QTL detected in field environments in AB and RIL populations. This discrepancy in variance could be attributed to the higher level of control over environmental factors in controlled conditions, such as temperature, humidity, light, and nutrient availability, resulting most often in higher heritability values.

In the updated GWAS of the pea-Aphanomyces collection, we confirmed 29 resistance-associated SNPs out of the 56 resistance markers previously reported. This lower number of associated SNPs detected was mostly explained in the MLMM model by (i) a minimum number of cofactors associated with a single variable set at 5 instead of 10 in Desgroux et al. (2016), (ii) a higher *p-value* threshold to declare significant cofactors (*p-value* = 3.6E-05), and (iii) a larger percentage of phenotypic variation explained by the

structure matrix computed with ADMIXTURE. These new parameters used for GWAS resulted in the reduction of the number of low-effect loci (1.0E-07 < *p-value* < 3.6E-05) detected in this study compared to Desgroux et al. (2016).

Integrating bi-parental linkage mapping and GWAS approaches allows to take advantage of both methods while limiting the drawbacks of each of them, which improves the identification of consistent candidate loci in plants (He et al., 2017; Guo et al., 2019; Zhao et al., 2022). In our study, comparative mapping of Aphanomyces resistance QTL and resistance-associated GWAS-SNPs identified 10 consistent genetic regions on the consensus marker map DORA, each of them being identified from at least three of the seven populations studied. It refined, with a high resolution, the positions of the main *Ae-Ps* QTL previously described in Hamon et al. (2011; 2013) and identified novel SNPs flanking the intervals of these regions (12.1 cM ≤ interval ≤ 34.0 cM). A total of 11 LD blocks associated with Aphanomyces root rot resistance were detected in 10 consistent genetic regions, including at least one common SNP with the markers composing the resistance LD blocks previously identified by Desgroux et al. (2016). Three of the 10 consistent genetic regions (2.a, 3.b, and 10.a) associated with partial resistance QTL could be divided into sub-regions, separating resistance QTL from flowering or morphological QTL, which suggests the possibility of breaking undesirable correlations between traits in pea breeding.

Rare and favorable marker haplotypes were identified for QTL pyramiding and diversification in breeding for pea resistant varieties

Haplotype analysis is a powerful tool to reveal rare alleles in LD with molecular markers (Bhat et al., 2021), especially because rare causal variants often determine extreme phenotypes (Wray et al., 2013). In plant collections, new germplasms provide a useful genetic diversity to develop durable disease-resistant cultivars (Thudi et al., 2021). In our study, the new source of resistance E11 showed five rare haplotypes in the *Ae-Ps1.2*, *Ae-Ps2.2*, *Ae-Ps4.5*, and *Ae-Ps7.6* genetic regions and a high rate of missing haplotypes (n = 5/11). Especially, the high level of resistance to RB84 strain was explained in E11 by the rare haplotype VII.8.d. Although LISA combined few haplotypes significantly detected as favorable (n = 2/11), this new source of resistance displayed reduced aerial symptoms in infested field conditions. Partial resistance to *A. euteiches* in LISA was especially associated with the rare haplotype II.1.m identified in the *Ae-Ps2.2* genetic region and the haplotype effect was confirmed by linkage analysis in the Eden x LISA AB population.

Nine other new sources of resistance, clustered into the same kinship group as the winter pea varieties, showed a high number of rare haplotypes (1 ≤ n ≤ 7) at 11 resistance LD blocks. In particular, rare haplotypes in NEPAL A (III.4.e and VII.11.l), NO. 9845 (VII.8.f), GAT 1259 and L2782.1 (VII.11.i and VII.11.k, respectively) were associated with a higher level of resistance than the average level of the pea lines in the collection carrying favorable haplotypes at these LD blocks. Beji et al. (2020) recently revealed colocalization in the *Ae-Ps1.1* and *Ae-Ps7.6* regions between LD blocks detected in GWAS for frost tolerance, and QTL and LD blocks associated with Aphanomyces root rot resistance identified in previous studies (Hamon et al., 2011; Desgroux et al., 2016). This may suggest that rare alleles in this region may contribute to resistance to multiple stresses, which is a major breeding goal in pea (Burstin et al., 2021), and that it may be possible to breed favorably for Aphanomyces resistance and frost tolerance in future pea breeding programs.

Haplotype analysis has been highly relevant to reveal combinations of favorable haplotypes to be used in marker-assisted selection. Pyramiding of QTL for resistance to pathogens is a promising approach to increase levels of resistance and limit QTL erosion in breeding lines (Pilet-Nayel et al., 2017). Lavaud et al. (2016) reported that the combination of resistance alleles at two or three of the main resistance QTL, including the major-effect *Ae-Ps7.6* QTL, increased partial resistance to *A. euteiches* in pea NILs. Additionally, the combination of the *Ae-Ps7.6* QTL with other QTL was recently suggested to preserve the durability of the major QTL, since aggressive isolates on NILs carrying *Ae-Ps7.6* were found in *A. euteiches* natural populations (Quillévéré-Hamard et al., 2021). In our study, haplotype analysis at 11 resistance LD blocks in ten consistent genetic regions confirmed that lines showing the highest level of partial resistance to *A. euteiches* carried mostly favorable haplotypes (3 < n < 7) in combination with the resistance haplotype VII.8.a located in the major-effect *Ae-Ps7.6* genetic region. The most resistant lines in the collection, derived from the AeD99 phenotypic recurrent breeding program, carried a higher number of favorable haplotypes (n = 6) originating from the combination of the three reference resistant parents 90–2131, PI180693 and 552 (Desgroux et al., 2016). However, the best AeD99 breeding lines cumulated also two to three unfavorable haplotypes at three LD blocks (II.3, V.2*, and VII.16) associated with flowering and morphological traits. In particular, negative linkages between haplotypes associated with resistance and developmental traits were identified at the LD block VII.16. The combination of major-effect QTL with multiple small-effect QTL, coupled with the breakage of negative linkages, is a promising approach to enhance resistance levels against *A. euteiches* in future pea varieties. Recent registrations of French tolerant varieties carrying several Aphanomyces resistance QTL further support the effectiveness of this strategy (Moussart, 2022).

Conclusion

This study provides an overview of the diversity of QTL and haplotypes that significantly contribute to Aphanomyces root rot resistance in pea, by integrating AB-, RIL-linkage mapping and GWAS data using 1,850 common SNP markers. Most of the previously identified resistance QTL were confirmed and mapped onto a consensus marker map. No new consistent resistance QTL were identified in both Eden x E11 and Eden x LISA AB populations. However, ten consistent genetic regions comprising resistance QTL with closely linked new SNPs, as well as favorable haplotypes in these regions, were identified and appear to be good

choices for future resistance allele pyramiding in marker-assisted selection strategies. New relevant rare haplotypes identified in new sources of resistance and negative associations between resistance and undesirable alleles in targeted regions will remain to be explored in future pea breeding programs. Another major challenge will consist in identifying and validating candidate genes underlying Aphanomyces resistance QTL in pea.

Data availability statement

The original contributions presented in the study are included in the article/Supplementary Material. Further inquiries can be directed to the corresponding author.

Author contributions

TL participated in phenotypic data acquisition, managed all the statistical and genetic analyses, and drafted the manuscript. GB and CL generated genotypic data and participated in updated linkage analyses in RIL populations. AL, J-PR, PV, IG, HM, ALR, and CL contributed to implementing experimental assays and evaluating plant disease resistance and development traits. CR-K and PD contributed to the setting up and implementation of this study. AS contributed to the drafting of the manuscript. M-LP-N and CL coordinated the overall study and the manuscript drafting. All authors read and approved the final manuscript.

Funding

This study was supported by the pre-doctoral fellowship of TL, provided by the SPECIFICS project and Brittany region (France). It was funded by the French DORA, PEAMAS and PEAPOL projects, which were supported by the FASO (Fonds d'Action Stratégique des Oléoprotéagineux) managed by SOFIPROTEOL, as well as by the SPECIFICS and PeaMUST projects. SPECIFICS (ANR-20-PCPA-0008) was funded by the "Growing and Protecting crops Differently" French Priority Research Program (PPR-CPA), part of the 3rd Program for Future Investments (France 2030) operated by the French National Research Agency (ANR). PeaMUST (ANR-11-BTBR-0002) was funded by the 2nd Program for Future Investments operated by ANR.

Acknowledgments

We greatly thank the Greenhouse-Experimental Facilities platform of IGEPP for its contribution to plant material production and experimentation in controlled conditions, as well as the Bioinformatics GO-GEPP platform for having provided computing and data storage space on servers. We greatly thank the INRAE experimental units of Dijon-Epoisses (U2E) and Le Rheu (UE La Motte), as well as UNILET (Union Nationale Interprofessionnelle des Légumes Transformés, Quimperlé, France) for their contribution to the field experiments. We acknowledge LGC Genomics service lab, UK, and Limagrain Europe, FR, for the genotyping of plant material. We acknowledge GSP (Groupement des Sélectionneurs de Protéagineux, France) for having provided improved breeding lines for Aphanomyces resistance. We are grateful to Jean-François Herbommez, Audrey Courtial, and Isabelle Lejeune-Henaut who contributed to implement this study. We also thank Rémi Ollivier for discussing various parameters to be applied in GWAS.

Conflict of interest

The authors declare that the research was conducted in the absence of any commercial or financial relationships that could be construed as a potential conflict of interest.

Publisher's note

Supplementary material

The Supplementary Material for this article can be found online at: https://www.frontiersin.org/articles/10.3389/fpls.2023.1189289/full#supplementary-material

SUPPLEMENTARY FIGURE 1
Frequency distribution of EMMs obtained for *A. euteiches* resistance and flowering variables in the **(A)** Eden x E11 and **(B)** Eden x LISA AB populations. Scoring variables are coded as presented in Supplementary Table 1. Reference susceptible Eden and partially resistant E11 and LISA parents are indicated in red and green, respectively. n: total number of pea lines assessed; m: mean ± standard deviation; H^2: mean-based heritability.

SUPPLEMENTARY FIGURE 2
(A) LD decay in the pea-Aphanomyces collection. Colored curves represent the estimated LD decay for each LG. Dashed vertical lines represent the LD threshold (maximum $r^2/2$) and arrows the LD decay rate, as the estimated genetic distance (cM) to reach this LD threshold on each LG. **(B)** Population structure in the pea-Aphanomyces collection for 10 subgroups (Q). Each colored horizontal line of individual accession shows the ancestral fraction that was assigned proportionally to the estimated clusters. **(C)** Ward's clustered heatmap of the kinship matrix of the pea-Aphanomyces collection. The color gradient represents the degree of relationship between two lines. Pea lines are gathered in 14 subgroups described in the legend.

SUPPLEMENTARY TABLE 1
Phenotypic data obtained for resistance to *A. euteiches*, flowering and morphological traits in the pea RIL and AB populations. 1st to 4th sheets: adjusted mean datasets for 33, 21, 31, and 12 variables previously evaluated in the Baccara x PI180693, Baccara x 552, DSP x 90-2131 and Puget x 90-2079 RIL populations, respectively. Data associated with Height (Baccara x PI180693 and Baccara x 552 RILs) and Dead (DSP x 90-2131 RILs) variables were not presented in Hamon et al. (2013). 5th to 6th sheets: EMMs for 9

variables evaluated in the Eden x E11 and Eden x LISA AB populations, respectively. 7th sheet: description of resistance, flowering, and morphological variables presented in these phenotyping datasets. N.B. The adjusted means of phenotypic data in the pea-Aphanomyces collection can be found in the Additional file 16 of Desgroux et al. (2016).

SUPPLEMENTARY TABLE 2
Consensus marker map and genotyping data used in this study. 1st sheet: consensus marker map DORA including 16,647 markers used to genotype one or several of the seven populations used in this study, synonymous marker names from Duarte et al. (2014) and Tayeh et al. (2015) are indicated in the second column; Genotyping matrices from: (2nd sheet) the pea-Aphanomyces collection (10,824 filtered markers), (3rd to 6th sheets) RIL populations derived from the crosses Baccara x PI180693, Baccara x 552, DSP x 90-2131, and Puget x 90-2079, respectively (1,866, 1,082, 950, and 669 filtered markers, respectively), and (7th to 8th sheets) AB populations derived from the crosses Eden x E11 and Eden x LISA, respectively (993 and 478 filtered markers, respectively). 9th sheet: coding information of reference parental alleles presented in previous genotyping datasets.

SUPPLEMENTARY TABLE 3
QTL detection results updated from previous phenotypic data in the Baccara x PI180693, Baccara x 552, DSP x 90-2131, Puget x 90-2079 RIL populations, and obtained in this study in the Eden x E11 and Eden x LISA AB populations, for resistance to *A. euteiches*, flowering, and morphological traits in controlled and field conditions. QTL are ordered by position in cM Haldane on the linkage group. [a] Scoring traits are coded as presented in the Supplementary Table 1. [b] Marker from the LOD score peak of the QTL ("-" attributed if no marker is located at the computed LOD score peak). [c] positions of epistatic QTL (interactions are shown as "LG of the first QTL@ Position of the first QTL: LG of the second QTL@Position of the second QTL). [d,e] Mean effects of pea lines carrying allele from the susceptible parent (Baccara, DSP, Puget, or Eden) or the partially resistant parent (PI180693, 552, 90-2131, 90-2079, E11, or LISA) at the peak marker of the QTL. H^2: broad-sense heritability value collected from previous genetic studies conducted on RIL populations and computed based on data obtained from two new AB populations in this study. LOD: log of likelihood ratio peak value at the QTL position for each variable. R^2: percentage of phenotypic variation explained by a QTL.

SUPPLEMENTARY TABLE 4
GWAS detection results updated from previous phenotypic data in the pea-Aphanomyces collection for resistance to *A. euteiches*, flowering, and morphological traits. 1st sheet: [a] genetic position (cM Haldane) of significant marker detected by GWAS on the DORA consensus marker map. [b] Variable name as described in the third table sheet. 2nd sheet: partition of phenotypic variance for each variable. 3rd sheet: description of resistance, flowering, and morphological variables evaluated in the pea-Aphanomyces collection.

SUPPLEMENTARY TABLE 5
Consistent genetic regions associated with partial resistance to *A. euteiches*, flowering, and morphology in pea. The Supplementary Table 5 is an expanded version of the Table 2, including information on QTL and significant SNPs associated with Aphanomyces resistance, flowering and morphology variables, detected in the pea-Aphanomyces collection, and RIL and AB populations. LD blocks associated with resistance to *A. euteiches* and flowering or morphological traits are indicated in dark and blue, respectively. Variable codes as described in Supplementary Tables 1 and 4, with field variables on aerial and root plant part written in red and green, respectively, controlled conditions variables in dark, and flowering and morphology variables in blue.

SUPPLEMENTARY TABLE 6
Markers and haplotypes in the detected LD blocks. For each LD block: (1st column) repositioned *Ae-Psxxx* QTL regions comprising LD blocks. (2nd column) LD block number, as shown in Figure 2. (3rd and 4th columns) LG and genetic position of significant SNPs in the LD block on the DORA consensus marker map; (5th column) SNPs significantly detected by GWAS in the LD block; (6th column) variable coded as described in Supplementary Table 4 from which each significant SNP was detected; (7th column) *p-value* of each significant SNP (*p-value* < 3.6E-05); (following lines and columns) marker ID and genetic position on the DORA consensus marker map for each marker in the LD block, pairwise LD (r^2) values between each marker defined in the LD block and markers detected by GWAS (detected markers in bold font and their markers in LD in plain font, "-" indicates r^2 values ≤ 0.7 between markers); haplotype letter, number and percentage of pea lines from the pea Aphanomyces collection sharing the haplotype; mean phenotypic values ± standard error and significantly different means (Tukey-HSD, α = 5%) for each haplotype carried by more than 5% of lines. Favorable and unfavorable haplotypes are shown in green and orange, respectively. Haplotypes carried by 5% or less than 5% of the pea lines in the pea Aphanomyces collection are considered as rare.

SUPPLEMENTARY TABLE 7
Marker haplotype description in the pea-Aphanomyces collection. [a] Names of the lines from the pea-Aphanomyces collection, as described in Desgroux et al. (2016); **Lines not retained in GWAS based on markers quality. Haplotype content (haplotype names in small letters) of each pea line in the collection at: [b] 11 consistent LD blocks associated with resistance to *A. euteiches* and [e] three consistent LD blocks associated with flowering or morphological traits, comprised in repositioned *Ae-Psxxx* QTL regions; favorable and unfavorable marker resistance haplotypes are indicated in green and red, respectively, rare and missing haplotypes are presented in grey and white, respectively. Adjusted means of each pea line for [c] field resistance synthetic variables and isolate- specific variables in controlled conditions, as well as [g] flowering and morphological synthetic variables in healthy nursery; names of variables are described in Supplementary Table 4. Number of favorable and unfavorable haplotypes for: [d] resistance to *A. euteiches* and [f] flowering or morphological traits, for each pea line.

References

Alexander, D. H., Novembre, J., and Lange, K. (2009). Fast model-based estimation of ancestry in unrelated individuals. *Genome Res.* 19, 1655–1664. doi: 10.1101/gr.094052.109

Amarakoon, D., Thavarajah, D., McPhee, K., and Thavarajah, P. (2012). Iron-, zinc-, and magnesium-rich field peas (*Pisum sativum* L.) with naturally low phytic acid: A potential food-based solution to global micronutrient malnutrition. *J. Food Compos Anal.* 27, 8–13. doi: 10.1016/j.jfca.2012.05.007

Astle, W., and Balding, D. J. (2009). Population structure and cryptic relatedness in genetic association studies. *Stat. Sci.* 24, 451–471. doi: 10.1214/09-STS307

Bates, D., Maechler, M., Bolker, B., Walker, S., Christensen, R. H. B., Singmann, H., et al. (2019). *lme4: linear mixed-effects models using "Eigen" and S4*. Available at: https://cran.r-project.org/web/packages/lme4/index.html.

Becking, T., Kiselev, A., Rossi, V., Street-Jones, D., Grandjean, F., and Gaulin, E. (2022). Pathogenicity of animal and plant parasitic Aphanomyces spp and their economic impact on aquaculture and agriculture. *Fungal Biol. Rev.* 40, 1–18. doi: 10.1016/j.fbr.2021.08.001

Beji, S., Fontaine, V., Devaux, R., Thomas, M., Negro, S. S., Bahrman, N., et al. (2020). Genome-wide association study identifies favorable SNP alleles and candidate genes for frost tolerance in pea. *BMC Genomics* 21, 536. doi: 10.1186/s12864-020-06928-w

Bénézit, M., Biarnès, V., and Jeuffroy, M.-H. (2017). Impact of climate and diseases on pea yields: what perspectives with climate change? *OCL* 24, D103. doi: 10.1051/ocl/2016055

Bhat, J. A., Yu, D., Bohra, A., Ganie, S. A., and Varshney, R. K. (2021). Features and applications of haplotypes in crop breeding. *Commun. Biol.* 4, 1266. doi: 10.1038/s42003-021-02782-y

Boutet, G., Alves Carvalho, S., Falque, M., Peterlongo, P., Lhuillier, E., Bouchez, O., et al. (2016). and genetic mapping using genotyping by sequencing of whole genome genomic DNA from a pea RIL population. *BMC Genomics* 17, 121. doi: 10.1186/s12864-016-2447-2

BrOman, K. W., Wu, H., Sen, S., and Churchill, G. A. (2003). R/qtl: QTL mapping in experimental crosses. *Bioinformatics* 19, 889–890. doi: 10.1093/bioinformatics/btg112

Browning, B. L., Zhou, Y., and Browning, S. R. (2018). A one-penny imputed genome from next-generation reference panels. *Am. J. Hum. Genet.* 103, 338–348. doi: 10.1016/j.ajhg.2018.07.015

Burstin, J., Avia, K., Carillo-Perdomo, E., Lecomte, C., Beji, S., Hanocq, E., et al. (2021). PeaMUST (Pea MultiStress Tolerance), a multidisciplinary French project

uniting researchers, plant breeders, and the food industry. *Legume Sci.* 3, e108. doi: 10.1002/leg3.108

Chang, C. C., Chow, C. C., Tellier, L. C., Vattikuti, S., Purcell, S. M., and Lee, J. J. (2015). Second-generation PLINK: rising to the challenge of larger and richer datasets. *GigaScience* 4, 7. doi: 10.1186/s13742-015-0047-8

Christensen, R. H. B. (2019). *ordinal: regression models for ordinal data*. Available at: http://www.cran.r-project.org/package=ordinal/.

Conner, R. L., Chang, K. F., Hwang, S. F., Warkentin, T. D., and McRae, K. B. (2013). Assessment of tolerance for reducing yield losses in field pea caused by Aphanomyces root rot. *Can. J. Plant Sci.* 93, 473–482. doi: 10.4141/cjps2012-183

de Givry, S., Bouchez, M., Chabrier, P., Milan, D., and Schiex, T. (2005). CAR(H)(T) AGene: multipopulation integrated genetic and radiation hybrid mapping. *Bioinformatics* 21, 1703–1704. doi: 10.1093/bioinformatics/bti222

Desgroux, A., L'Anthoëne, V., Roux-Duparque, M., Rivière, J.-P., Aubert, G., Tayeh, N., et al. (2016). Genome-wide association mapping of partial resistance to *Aphanomyces euteiches* in pea. *BMC Genomics* 17, 124. doi: 10.1186/s12864-016-2429-4

Duarte, J., Rivière, N., Baranger, A., Aubert, G., Burstin, J., Cornet, L., et al. (2014). Transcriptome sequencing for high throughput SNP development and genetic mapping in Pea. *BMC Genomics* 15, 126. doi: 10.1186/1471-2164-15-126

Fox, J., and Weisberg, W. (2020). Available at: https://cran.r-project.org/web/packages/car/index.html.

Francis, R. M. (2017). POPHELPER : an R package and web app to analyse and visualize population structure. *Mol. Ecol. Resour.* 17, 27–32. doi: 10.1111/1755-0998.12509

Guo, T., Yang, J., Li, D., Sun, K., Luo, L., Xiao, W., et al. (2019). Integrating GWAS, QTL, mapping and RNA-seq to identify candidate genes for seed vigor in rice (*Oryza sativa* L.). *Mol. Breed.* 39, 87. doi: 10.1007/s11032-019-0993-4

Haas, M., Menke, J., Chao, S., and Steffenson, B. J. (2016). Mapping quantitative trait loci conferring resistance to a widely virulent isolate of *Cochliobolus sativus* in wild barley accession PI 466423. *Theor. Appl. Genet.* 129, 1831–1842. doi: 10.1007/s00122-016-2742-y

Hamon, C., Baranger, A., Coyne, C. J., McGee, R. J., Le Goff, I., L'Anthoëne, V., et al. (2011). New consistent QTL in pea associated with partial resistance to *Aphanomyces euteiches* in multiple French and American environments. *Theor. Appl. Genet.* 123, 261–281. doi: 10.1007/s00122-011-1582-z

Hamon, C., Coyne, C. J., McGee, R. J., Lesné, A., Esnault, R., Mangin, P., et al. (2013). QTL meta-analysis provides a comprehensive view of loci controlling partial resistance to *Aphanomyces euteiches* in four sources of resistance in pea. *BMC Plant Biol.* 13, 45. doi: 10.1186/1471-2229-13-45

Harrell, F. E., and Dupont, C. (2020). *Hmisc: Harrell miscellaneous*. Available at: https://cran.r-project.org/web/packages/Hmisc/Hmisc.pdf.

He, Y., Wu, D., Wei, D., Fu, Y., Cui, Y., Dong, H., et al. (2017). GWAS, QTL mapping and gene expression analyses in *Brassica napus* reveal genetic control of branching morphogenesis. *Sci. Rep.* 7, 15971. doi: 10.1038/s41598-017-15976-4

Hervé, M. (2020). *RVAideMemoire: testing and plotting procedures for biostatistics*. Available at: https://cran.r-project.org/package=RVAideMemoire.

Hughes, T. J., and Grau, C. R. (2007). Aphanomyces root rot or common root rot of legumes. *Plant Health Instr.* doi: 10.1094/PHI-I-2007-0418-01

Jha, A. B., Gali, K. K., Alam, Z., Lachagari, V. B. R., and Warkentin, T. D. (2021). Potential application of genomic technologies in breeding for fungal and oomycete disease resistance in pea. *Agronomy* 11, 1260. doi: 10.3390/agronomy11061260

Jiang, H., Feng, Y., Qiu, L., Gao, G., Zhang, Q., and He, Y. (2020). Identification of blast resistance QTLs based on two advanced backcross populations in rice. *Rice* 13, 31. doi: 10.1186/s12284-020-00392-6

Kraft, J. M. (1981). Registration of 792022 and 792024 pea germplasm. *Crop Sci.* 21, 352–353.

Kraft, J. M. (1992). Registration of 90-2079, 90-2131, and 90-2322 pea germplasms. *Crop Sci.* 32, 1076.

Kraft, J. M., Silbernagel, M. J., and Muehlbauer, F. J. (1972). Registration of PH-14-119 and PH-91-3 pea germplasm. *Crop Sci.* 12, 399.

Kreplak, J., Madoui, M.-A., Cápal, P., Novák, P., Labadie, K., Aubert, G., et al. (2019). A reference genome for pea provides insight into legume genome evolution. *Nat. Genet.* 51, 1411–1422. doi: 10.1038/s41588-019-0480-1

Lavaud, C., Baviere, M., Le Roy, G., Hervé, M. R., Moussart, A., Delourme, R., et al. (2016). Single and multiple resistance QTL delay symptom appearance and slow down root colonization by *Aphanomyces euteiches* in pea near isogenic lines. *BMC Plant Biol.* 16, 166. doi: 10.1186/s12870-016-0822-4

Lavaud, C., Lesné, A., Piriou, C., Le Roy, G., Boutet, G., Moussart, A., et al. (2015). Validation of QTL for resistance to *Aphanomyces euteiches* in different pea genetic backgrounds using near-isogenic lines. *Theor. Appl. Genet.* 128, 2273–2288. doi: 10.1007/s00122-015-2583-0

Le May, C., Onfroy, C., Moussart, A., Andrivon, D., Baranger, A., Pilet-Nayel, M. L., et al. (2018). Genetic structure of *Aphanomyces euteiches* populations sampled from United States and France pea nurseries. *Eur. J. Plant Pathol.* 150, 275–286. doi: 10.1007/s10658-017-1274-x

Lenth, R. (2020). *emmeans: Estimated Marginal Means, aka Least-Squares Means*. Available at: https://cran.r-project.org/web/packages/emmeans/emmeans.pdf.

Lipka, A. E., Tian, F., Wang, Q., Peiffer, J., Li, M., Bradbury, P. J., et al. (2012). GAPIT: genome association and prediction integrated tool. *Bioinformatics* 28, 2397–2399. doi: 10.1093/bioinformatics/bts444

Moussart, A. (2022). "Management of Aphanomyces root of pea in France," in *International Legume Root Diseases workshop*, *ed 8th* (Rennes, France).

Moussart, A., Wicker, E., Duparque, M., and Rouxel, F. (2001). "Development of an efficient screening test for pea resistance to *Aphanomyces euteiches*," In *AEP (ed) 4th European Conference on Grain Legumes — Towards the sustainable production of healthy food, feed and novel products*, July 8-12th (pp 272–273) (Cracow, Poland).

Naz, A. A., Klaus, M., Pillen, K., and Léon, J. (2015). Genetic analysis and detection of new QTL alleles for *Septoria tritici* blotch resistance using two advanced backcross wheat populations. *Plant Breed.* 134, 514–519. doi: 10.1111/pbr.12301

Palanichamy, D., and Smith, M. (2022). QTL mapping and colocalization analysis reveal novel candidate genes for multiple disease resistance in maize. *Crop Sci.* 62, 624–636. doi: 10.1002/csc2.20681

Pilet-Nayel, M.-L., Coyne, C. J., Hamon, C., Lesne, A., Le Goff, I., Esnault, R., et al. (2007). "Understanding genetics of partial resistance to Aphanomyces root rot in pea for new breeding prospects," in *International Aphanomyces Workshop on Legumes*, *ed 3rd* (Rennes, France).

Pilet-Nayel, M.-L., Moury, B., Caffier, V., Montarry, J., Kerlan, M.-C., Fournet, S., et al. (2017). Quantitative resistance to plant pathogens in pyramiding strategies for durable crop protection. *Front. Plant Sci.* 8. doi: 10.3389/fpls.2017.01838

Pilet-Nayel, M.-L., Muehlbauer, F. J., McGee, R. J., Kraft, J. M., Baranger, A., and Coyne, C. J. (2002). Quantitative trait loci for partial resistance to Aphanomyces root rot in pea. *Theor. Appl. Genet.* 106, 28–39. doi: 10.1007/s00122-002-0985-2

Pilet-Nayel, M.-L., Muehlbauer, F. J., McGee, R. J., Kraft, J. M., Baranger, A., and Coyne, C. J. (2005). Consistent quantitative trait loci in pea for partial resistance to *Aphanomyces euteiches* isolates from the United States and France. *Phytopathology* 95, 1287–1293. doi: 10.1094/PHYTO-95-1287

Poland, J. A., Balint-Kurti, P. J., Wisser, R. J., Pratt, R. C., and Nelson, R. J. (2009). Shades of gray: the world of quantitative disease resistance. *Trends Plant Sci.* 14, 21–29. doi: 10.1016/j.tplants.2008.10.006

Powers, S. E., and Thavarajah, D. (2019). Checking agriculture's pulse: Field pea (*Pisum sativum* L.), sustainability, and phosphorus use efficiency. *Front. Plant Sci.* 10. doi: 10.3389/fpls.2019.01489

Purcell, S., Neale, B., Todd-Brown, K., Thomas, L., Ferreira, M. A. R., Bender, D., et al. (2007). PLINK: a tool set for whole-genome association and population-based linkage analyses. *Am. J. Hum. Genet.* 81, 559–575. doi: 10.1086/519795

Quillévéré-Hamard, A., Le Roy, G., Lesné, A., Le May, C., and Pilet-Nayel, M.-L. (2021). Aggressiveness of diverse French *Aphanomyces euteiches* isolates on pea near isogenic lines differing in resistance quantitative trait loci. *Phytopathology* 111, 695–702. doi: 10.1094/PHYTO-04-20-0147-R

Quillévéré-Hamard, A., Le Roy, G., Moussart, A., Baranger, A., Andrivon, D. , Pilet-Nayel, M.-L., et al. (2018). Genetic and pathogenicity diversity of *Aphanomyces euteiches* populations from pea-growing regions in France. *Front. Plant Sci.* 91673. doi: 10.3389/fpls.2018.01673

R Core Team (2020). *R: a language and environment for statistical computing* (R Foundation for Statistical Computing).

Segura, V., Vilhjálmsson, B. J., Platt, A., Korte, A., Seren, Ü., Long, Q., et al. (2012). An efficient multi-locus mixed-model approach for genome-wide association studies in structured populations. *Nat. Genet.* 44, 825–830. doi: 10.1038/ng.2314

Sivachandra Kumar, N. T., Caudillo-Ruiz, K. B., Chatterton, S., and Banniza, S. (2021). Characterization of *Aphanomyces euteiches* pathotypes infecting peas in Western Canada. *Plant Dis.* 105, 4025–4030. doi: 10.1094/PDIS-04-21-0874-RE

Sosnowski, O., Charcosset, A., and Joets, J. (2012). BioMercator V3: an upgrade of genetic map compilation and quantitative trait loci meta-analysis algorithms. *Bioinformatics* 28, 2082–2083. doi: 10.1093/bioinformatics/bts313

Talukder, Z. I., Underwood, W., Misar, C. G., Seiler, G. J., Cai, X., Li, X., et al. (2022). Genomic insights into sclerotinia basal stalk rot resistance introgressed from wild *Helianthus praecox* into cultivated sunflower (*Helianthus annuus* L.). *Front. Plant Sci.* 13. doi: 10.3389/fpls.2022.840954

Tanksley, S. D., and Nelson, J. C. (1996). Advanced backcross QTL analysis: a method for the simultaneous discovery and transfer of valuable QTLs from unadapted germplasm into elite breeding lines. *TAG Theor. Appl. Genet. Theor. Angew Genet.* 92, 191–203. doi: 10.1007/BF00223376

Tayeh, N., Aluome, C., Falque, M., Jacquin, F., Klein, A., Chauveau, A., et al. (2015). Development of two major resources for pea genomics: the GenoPea 13.2K SNP Array and a high-density, high-resolution consensus genetic map. *Plant J.* 84, 1257–1273. doi: 10.1111/tpj.13070

Thudi, M., Palakurthi, R., Schnable, J. C., Chitikineni, A., Dreisigacker, S., Mace, E., et al. (2021). Genomic resources in plant breeding for sustainable agriculture. *J. Plant Physiol.* 257, 153351. doi: 10.1016/j.jplph.2020.153351

Tibbs Cortes, L., Zhang, Z., and Yu, J. (2021). Status and prospects of genome-wide association studies in plants. *Plant Genome* 14, e20077. doi: 10.1002/tpg2.20077

Varshney, R. K., and Dubey, A. (2009). Novel genomic tools and modern genetic and breeding approaches for crop improvement. *J. Plant Biochem. Biotechnol.* 18, 127–138. doi: 10.1007/BF03263311

Voorrips, R. E. (2002). MapChart: software for the graphical presentation of linkage maps and QTLs. *J. Hered.* 93, 77–78. doi: 10.1093/jhered/93.1.77

Wei, T., and Simko, V. (2017). *corrplot: visualization of a correlation matrix*. Available at: https://cran.r-project.org/web/packages/corrplot/corrplot.pdf.

Wickham, H. (2016). *ggplot2: elegant graphics for data analysis* (Available at: https://ggplot2.tidyverse.org).

Wray, N. R., Yang, J., Hayes, B. J., Price, A. L., Goddard, M. E., and Visscher, P. M. (2013). Pitfalls of predicting complex traits from SNPs. *Nat. Rev. Genet.* 14, 507–515. doi: 10.1038/nrg3457

Wu, L., Chang, K.-F., Hwang, S.-F., Conner, R., Fredua-Agyeman, R., Feindel, D., et al. (2019). Evaluation of host resistance and fungicide application as tools for the management of root rot of field pea caused by *Aphanomyces euteiches*. *Crop J.* 7, 38–48. doi: 10.1016/j.cj.2018.07.005

Wu, L., Fredua-Agyeman, R., Hwang, S.-F., Chang, K.-F., Conner, R. L., McLaren, D. L., et al. (2021). Mapping QTL associated with partial resistance to Aphanomyces root rot in pea (*Pisum sativum* L.) using a 13.2 K SNP array and SSR markers. *Theor. Appl. Genet.* 134, 2965–2990. doi: 10.1007/s00122-021-03871-6

Zhao, M., Liu, S., Pei, Y., Jiang, X., Jaqueth, J. S., Li, B., et al. (2022). Identification of genetic loci associated with rough dwarf disease resistance in maize by integrating GWAS and linkage mapping. *Plant Sci.* 315, 111100. doi: 10.1016/j.plantsci.2021.111100

frontiers | Frontiers in Plant Science

TYPE Original Research
PUBLISHED 20 October 2023
DOI 10.3389/fpls.2023.1156733

OPEN ACCESS

EDITED BY
Marie-Laure Pilet-Nayel,
INRAE Bretagne Normandie, France

REVIEWED BY
Mukesh Dubey,
Swedish University of Agricultural Sciences, Sweden
Timothy Paulitz,
United States Department of Agriculture, United States

*CORRESPONDENCE
Thomas Rey
reyt@desangosse.com
Bernard Dumas
bernard.dumas@univ-tlse3.fr

†These authors have contributed equally to this work and share last authorship

RECEIVED 01 February 2023
ACCEPTED 02 October 2023
PUBLISHED 20 October 2023

CITATION
Hashemi M, Amiel A, Zouaoui M, Adam K, Clemente HS, Aguilar M, Pendaries R, Couzigou J-M, Marti G, Gaulin E, Roy S, Rey T and Dumas B (2023) The mycoparasite *Pythium oligandrum* induces legume pathogen resistance and shapes rhizosphere microbiota without impacting mutualistic interactions.
Front. Plant Sci. 14:1156733.
doi: 10.3389/fpls.2023.1156733

The mycoparasite *Pythium oligandrum* induces legume pathogen resistance and shapes rhizosphere microbiota without impacting mutualistic interactions

Maryam Hashemi[1], Aurélien Amiel[1,2], Mohamed Zouaoui[1], Kévin Adam[1], Hélène San Clemente[1], Marielle Aguilar[1], Rémi Pendaries[1,2], Jean-Malo Couzigou[1], Guillaume Marti[1,3], Elodie Gaulin[1], Sébastien Roy[1,4], Thomas Rey[1,2*†] and Bernard Dumas[1*†]

[1]Laboratoire de Recherche en Sciences Végétales, Université de Toulouse, Centre National de la Recherche Scientifique (CNRS), Université Toulouse III, Toulouse Institut National Polytechnique (INP), Auzeville-Tolosane, France, [2]DE SANGOSSE, Pont-Du-Casse, France, [3]Metatoul-AgromiX Platform, MetaboHUB, National Infrastructure of Metabolomics and Fluxomics, Toulouse, France, [4]AGRONUTRITION, Carbonne, France

Pythium oligandrum is a soil-borne oomycete associated with rhizosphere and root tissues. Its ability to enhance plant growth, stimulate plant immunity and parasitize fungal and oomycete preys has led to the development of agricultural biocontrol products. Meanwhile, the effect of *P. oligandrum* on mutualistic interactions and more generally on root microbial communities has not been investigated. Here, we developed a biological system comprising *P. oligandrum* interacting with two legume plants, *Medicago truncatula* and *Pisum sativum*. *P. oligandrum* activity was investigated at the transcriptomics level through an RNAseq approach, metabolomics and finally metagenomics to investigate the impact of *P. oligandrum* on root microbiota. We found that *P. oligandrum* promotes plant growth in these two species and protects them against infection by the oomycete *Aphanomyces euteiches*, a devastating legume root pathogen. In addition, *P. oligandrum* up-regulated more than 1000 genes in *M. truncatula* roots including genes involved in plant defense and notably in the biosynthesis of antimicrobial compounds and validated the enhanced production of *M. truncatula* phytoalexins, medicarpin and formononetin. Despite this activation of plant immunity, we found that root colonization by *P. oligandrum* did not impaired symbiotic interactions, promoting the formation of large and multilobed symbiotic nodules with *Ensifer meliloti* and did not negatively affect the formation of arbuscular mycorrhizal symbiosis. Finally, metagenomic analyses showed the oomycete modifies the composition of fungal and bacterial communities. Together, our results provide novel insights regarding the involvement of *P. oligandrum* in the functioning of plant root microbiota.

KEYWORDS

***Pythium oligandrum*, microbiota, symbiotic interaction, plant defense, legumes, isoflavonoid**

Introduction

Biological control agents (BCAs) are the products based on living organisms, which address biotic stress including disease, pests, and weeds in crops (Ehlers, 2011; Shoham, 2020). BCAs can protect crops from pathogens through different mechanisms, including niche competition, production of antimicrobial compounds, or mycoparasitism (Upadhyay et al., 2021). Today, together with a heightened public awareness toward integrated pest management and sustainable agriculture, alternative disease control strategies, notably biological control, have become a rapidly growing area especially when the application of abusive chemical products threatens human health and harms the environment (Baker et al., 2020; Hashemi et al., 2021).

Among the BCAs, soil mycoparasites, such as *P. oligandrum*, gained a particular interest through their ability to parasitize fungal pathogens (Benhamou et al., 2012). *Pythium oligandrum* is a soil-borne oomycete associated with rhizosphere and root tissues and has been used in different plant systems to control various soil-borne pathogens, including Ascomycetes, Basidiomycetes, and pathogenic Oomycetes, notably, *Aphanomyces euteiches* (Daraignes et al., 2018; Bělonožníková et al., 2020; Yacoub et al., 2020; del Pilar Martínez-Diz et al., 2021). The root colonization by *P. oligandrum* is associated with induced plant growth promotion (via the production of tryptamine, an auxin precursor (Le Floch et al., 2003). *P. oligandrum* can also trigger plant immunity by releasing two major glycoproteins with elicitin activity, namely, POD-1 and POD-2, and by interplaying with iron homeostasis in roots (Takenaka et al., 2011; Bělonožníková et al., 2020; Cheng et al., 2022).

These biological activities prompted the development of *P. oligandrum* as an active ingredient of agricultural products, notably, the strain ATCC 38472. *Pythium oligandrum* ATCC 38472 was first isolated from sugar beet as an indigenous wild type strain by Dáša Veselý in 1972 in the former Czechoslovakia (now the Czech Republic) (Vesely, 1977). Then, in the 1980s, it was first applied against damping-off of sugar beet by the Slušovice cooperative as an agricultural product. Finally, in the 1990s, Dáša Veselý licensed it exclusively to the Biopreparáty company with the aim of producing Polyversum, the registered biological fungicide (Faure et al., 2020).

While the benefits of *P. oligandrum* on plant fitness and defense have been widely investigated, the impact of this mycoparasite on other types of plant–microbe interactions, notably, the mutualistic ones as well as its overall impact on microbial community in rhizosphere, was not clear. The rhizosphere is a favorable niche for the development of a wide variety of organisms, including parasitic, saprophytic, neutral, and beneficial microorganisms which can have a huge impact on plant growth and health as well as soil fertility (Compant et al., 2019; Hamid et al., 2021). Plant roots can also physically and chemically affect the rhizosphere by changing the microbial composition through providing organic carbon from the tissues or root-secreted nutrients and antimicrobials (Lemanceau et al., 2017). While the microbial community that plants recruit depends on plant genotype and agricultural management, the goal would be to optimize this microbiota to sustain plant growth and health (Lemanceau et al., 2017; Compant et al., 2019). In particular, plants establish mutualistic interactions with arbuscular mycorrhizal fungi (AMF), symbiotic fungi of almost 80% of land plants, which provide water and minerals (phosphate and nitrogen) in exchange of carbohydrates (Ho-Plágaro et al., 2020). Besides AMFs, some plant families, notably, legumes, establish symbiotic interactions with nitrogen-fixing bacteria (Bagyaraj, 1991; Ramasamy and Muthukumar, 2019). This property is of tremendous importance in the objective to reduce chemical fertilizers and reach sustainable agriculture (Ramasamy and Muthukumar, 2019).

However, the effect on the mutualistic interactions of the introduction in the rhizosphere of *P. oligandrum* and, more generally, of BCAs on the functioning of the root microbiota remained poorly understood. A study focusing on a fungal and oomycete population after the introduction of *P. oligandrum* into the rhizosphere of tomato plants concluded that *P. oligandrum* did not modify the microbial ecosystem (Vallance et al., 2009). More recently, it was found that wheat seed dressing with the fungal mycoparasite *Trichoderma atroviride* significantly modified the composition and structure of the fungal community (Sui et al., 2022). However, the specific effect of these BCAs on mutualistic interactions was not investigated.

In this context, our research aims at studying the potential impact of BCAs such as *P. oligandrum* on root–microbe interactions and the composition of the root microbiota. To address these points, we report here the establishment of a biological system involving *P. oligandrum* and two legume plants, namely, the model legume *Medicago truncatula* and the agronomic relevant legume, *Pisum sativum* (garden pea). We first dissected the effects of root inoculation with *P. oligandrum* on plant growth and immunity to evaluate the impact of *P. oligandrum* on protection against pathogenic attack, establishment of mutualistic interactions, and, more globally, on root microbiota.

Materials and methods

Microbial strains and culture conditions

The M1 (ATCC384722) strain of *P. oligandrum* was cultured and grown on V8 juice (Campbell's, USA) 10% (v/v) supplemented with 2 g L^{-1} of $CaCO_3$ and agar in 90-mm Petri dishes. Oospore collection was obtained through a culture of 7- to 14-days-old of *P. oligandrum* on solid V8 and by washing with 8–10 mL of distilled water, followed by filtration through 100-µm filters. The final concentration of oospores was adjusted so that each seedling received around 10,000 oospores per milliliter.

Mycelium production was carried out through a liquid culture of *P. oligandrum* obtained from adding 10 plugs of *P. oligandrum* to 100 mL of liquid V8 medium and maintaining the mixture in the dark at 28°C for 3 days in Roux flasks. The *P. oligandrum* mycelium was then washed with distilled water and filtered through 100-µm fiber filters. Finally, around 15 g of mycelium was then blended in 100 mL of distilled water for the inoculation solution.

Aphanomyces euteiches Drechsler isolates MF1, an alfalfa-infecting strain, and RB84, a pea-infecting strain, were grown and maintained on corn meal agar plates in the dark at 22°C (Malvick and Grau, 2001; Moussart et al., 2008). Zoospores were obtained based on the previously described protocol (Badreddine et al., 2008).

A rifampicin-resistant isolate of *Ensifer meliloti* CCMM B554 strain (Nagymihály et al., 2017) was transformed with the pHC60-GFP plasmid (Cheng and Walker, 1998; Cheng and Yao, 2004) by tri-parental mating. The resulting pHC60-GFP *E. meliloti* CCMM B554 strain was grown on tryptone yeast (TY) medium (Beringer, 1974) with the following modifications: pH was adjusted to 6.8, and TY medium was supplemented by adding $CaCl_2$ at a final concentration of 20 mM after autoclaving. The strain and the plasmid were selected using rifampicin (100 µg mL^{-1}) and tetracycline (5 µg mL^{-1}), respectively. A pre-culture was inoculated by adding a loop of bacteria to 100 mL of liquid TY medium (pH = 6.8; $CaCl_2$, 20 mM; rifampicin, 50 µg mL^{-1}; tetracycline, 2 µg mL^{-1}) and was grown at 28°C for 2 days in a shaker incubator (220 rpm). The cultures were then centrifuged at 5,000 rpm for 10 min, followed by two successive washes with 10 mL of sterile distilled water. The final OD used for plant inoculation was adjusted to 0.05 (10^8 CFU mL^{-1}). The GFP-transformed *E. meliloti* strain CCMM B554, also known as FSM-MA, was maintained on TY medium (for 1 L, 5 g of Difco Bacto tryptone and 3 g of Difco Bacto yeast extract, with the pH adjusted to 6.8), supplemented by 1 mL of $CaCl_2$ (20 mM), and selected with rifampicin (100 µg mL^{-1}) (Gage et al., 1996; Fox et al., 2011; Nagymihály et al., 2017). A pre-culture was done by adding a loop of bacteria to 100 mL of liquid TY media supplemented with liquid $CaCO_3$ at 20 mM and antibiotics, including tetracycline 2 µg mL^{-1} and rifampicin 50 µg mL^{-1}, and was kept at 28°C for 2 days in a shaker incubator. The cultures were then centrifuged at maximum speed for 10 min and followed by two successive washes with 10 mL of distilled water. The final OD for the applied solution was adjusted to 0.05 (10^8 CFU mL^{-1}).

Rhizophagus irregularis DAOM 197198 inoculum was a suspension of spores derived from CONNECTIS™ (Connectis AMM no. 150007, Agronutrition, Carbonne, France). The base solution was at 1,000 spores per milliliter, which was finally diluted to 500 spores per milliliter in the applied solution.

Plant material, growth condition, and inoculation procedures

A17 and F83005.5 accessions of *M. truncatula* [Gaertn.] seeds were scarified in sulphuric acid for 5 min, washed three times in water, and then sterilized in 2.4% active chlorine bleach for 3 min before three washes in sterile water. To induce germination, seeds were soaked in water for 1 h for imbibition and then placed on 1% agarose in Petri dishes incubated at 22°C for 2 or 3 days in the dark.

The Cv. Precovil cultivar (Vilmorin, France) of *Pisum sativum* [L.] seeds were surface-sterilized and scarified by immersion in 70% ethanol (v/v) for 1 min, followed by 10 min of immersion in 2.4% active chlorine bleach. Subsequently, the seeds were washed with sterile water and left for pre-germination on water–agar 1% at 28°C for 5 days in the dark.

For plant growth stimulation assays with *P. oligandrum*, germinated *M. truncatula* A17 or *P. sativum* cv. Cv. Precovil seedlings were cultivated in each pot containing 1:1 v/v mixture of soil and sand. Then, 10 mL of *P. oligandrum* mycelium was added to pots of 300-mL capacity, while for 2-L round pots, 66.6 mL of mycelium containing 15 mg of mycelium in 100 mL of water was added (the amount of soil in the pots was approximately 300 mL and 2 L, respectively). The *Pythium* solution was added directly to the pots after planting the seedlings. The plants were then kept under controlled conditions in greenhouse (22°C, 14-h light photoperiod) or in phytotron (22°C, 80%, 16:8-h light/dark photoperiod). The nutrition solution was given to plants by watering every 5 weeks according to the manufacturer's recommendation ("Engrais Universel Toute Plante", Algoflash, France). For pea growth stimulation, a total of 10 plants with five replications per condition were tested, while for *M. truncatula* growth promotion test the total number of tested plants were 20, with 10 replications per condition. For plant protection assays with *P. oligandrum*, for *M. truncatula* 10 mL of MF1 and for *P. sativum* 10 mL of RB84 *A. euteiches* zoospore solution, with a final concentration of 25,000 zoospores per pot, were added directly to the seedlings using the same setup in the plant growth stimulation assays. The total number of *M. truncatula* plants in this experiment was 14, with seven biological replications per modality, while a total number of 10 plants with five replications per condition were considered for the pea protection assay.

For *in vitro* inoculation with *E. meliloti*, five A17 *M. truncatula* seedlings were placed on Fahraeus media (0.132 g L^{-1} $CaCl_2$, 0.12 g L^{-1} $MgSO_4{\cdot}7H_2O$, 0.1 g L^{-1} KH_2PO_4, 0.075 g L^{-1} $Na_2HPO_4{\cdot}2H_2O$, 5 mg L^{-1} NaFe EDTA, and 0.07 mg L^{-1} each of $MnCl_2{\cdot}4H_2O$, $CuSO_4{\cdot}5H_2O$, $ZnCl_2$, H_3BO_3, and $Na_2MoO_4{\cdot}2H_2O$, adjusted to pH 7.5 before autoclaving, supplemented with 1.5% agar) on 12-cm^2 petri dishes. In addition, 20 mL of *E. meliloti* mixture at OD of 0.05 (10^8 CFU mL^{-1}) was added to each Fahraeus plate with gentle stirring and was removed after 1 h. Around 10,000 *P. oligandrum* oospores were added to each seedling in each square petri dish. Seven biological replications were considered for each condition. The plates were kept at 22°C under 16-h light and 8-h dark photoperiod for 35 days.

For the experiments carried out in pots, we used sterilized vermiculite as substrate. Pregerminated A17 seedlings were placed in each pot, and then 10 mL of *E. meliloti* mixture with 0.05 OD (10^8 CFU mL^{-1}) was added to the pots near the seedlings. *P. oligandrum* mycelium solution containing 15 g of fresh mycelium in 100 mL of water was also added near the seedlings at the same time. Seven biological replications per condition were considered. Watering was carried out with both water and nutrient solution without nitrogen (N/P/K = 0/15/40, supplied by PlantProd®, ref. 211.00, Fertil S.A.S., Boulogne Billancourt, France), alternating two waterings with deionized water and one watering with Plant Prod solution (1 g L^{-1}, pH 7).

Mycorrhization assays with *R. irregularis* were carried out by adding one A17 *M. truncatula* seedling to each pot filled with around 300 mL of a mixture consisting of 20% vermiculite and 80%

zeolite (fine and coarse, 1:1 v/v). Before filling the pots, the fine zeolite was passed through a 300-µm sieve, while a 630-µm one was used for the coarse zeolite. Together with vermiculite, they were put in the oven for 5 h at 180°C. They were then mixed with 20% osmotic water. The *R. irregularis* spore solution concentration was adjusted to 500 spores mL^{-1}, and 1 mL was added near the seedling in the substrate, while the *P. oligandrum* mycelium solution constituted 15 g of mycelium in 100 mL of water, which was likewise added near the seedling at the same time. For each condition, seven biological replications were considered.

Transcriptomics

P. oligandrum-inoculated and non-inoculated A17 *M. truncatula* seedlings were grown on M medium prepared based on Becard and Fortin (1988). In the *P. oligandrum* treatments, each seedling received 10,000 oospores per milliliter. Petri dishes were then placed in a phytotron at 22°C under 16-h light and 8-h dark photoperiod. Total RNA comprised of a pool of five seedlings in each replication of different conditions, at 3, 5, 7, and 14 dpi, was then extracted by using RNeasy plant mini kit (Qiagen) according to the manufacturer's instruction, and rough RNA purity was checked using NanoDrop (Thermo Fisher). The quality control, library preparation, and sequencing were based on the kit Illumina TruSeq Stranded mRNA, sequenced with high-throughput Illumina Novaseq (2×150 pb). The quality of the obtained sequence was verified by using FastQC. HTseq-counts files were analyzed with the R software, using also EdgeR package version 3.24.3 (McCarthy et al., 2012).

Genes which did not have at least one read after a count per million normalization in at least one half of the samples were discarded. Raw counts were normalized using TMM method, and count distribution was modeled with a negative binomial generalized linear model where the treatment, the time, and the double interaction between treatment and time were considered and where the dispersion is estimated by the EdgeR method (Robinson et al., 2009). A likelihood ratio test was performed to evaluate an infection effect at a given time point. Raw *p*-values were adjusted with the Benjamini–Hochberg procedure to control the false discovery rate (FDR). The raw files were imported to R software for data analysis (http://www.r-project.org/). After that, principal component analysis was done on normalized data. Differentially expressed genes (DEGs) were then selected based on FC>1 or FC<-1 (log2). Clustering took place by HCE3.0 software with DEGs average linkage (UPGMA) Euclidean distance. After that, gene ontology was done through ShinyGo visualization (Ge et al., 2020) and with Mapman analysis.

Metagenomics

F83005.5 accession of *M. truncatula* seedlings was grown in pots containing a 1:1 v/v mixture of soil and sand and kept under controlled conditions in phytotron (22°C, 80%, 16:8-h light/dark photoperiod). Seven replications per condition were considered. At 56 days post-inoculation (dpi) (or 2 months after inoculation), the plants were uprooted and the rhizosphere was separated by reversing the pots, the whole plant was brought out of the pot. By a gentle shake, the loosened soil (bulk) was removed. The root was then cut from the aerial part and put in a 50-mL Falcon tube filled with 30 mL of sterile water. To separate the roots from the soil, a vortex at maximum speed was applied for about 2 min. The roots were then removed from the tube with the help of forceps. The Falcon tube was centrifuged for 30 min at maximum speed. The supernatant was then removed, and the pellet was put in Eppendorf tubes and kept at 20°C. The DNA was then extracted with a quick DNA fecal/soil microbe miniprep kit (Zymo Research Europe GmbH, Freiburg, Germany).

Libraries were generated using the Illumina two-step PCR protocol and normalized using SequalPrep plates (ThermoFischer™). The bacteria- and fungi-specific primer sets targeting the V3–V4 region of the small ribosomal RNA gene (16S rDNA) and ITS2 are presented in Table 1. Paired-end sequencing with a 2 × 250-bp read length was performed at the Bio-Environment platform (University of Perpignan Via Domitia Perpignan, France) on a MiSeq system (Illumina) using v2 chemistry according to the manufacturer's protocol. The amplicon sequencing paired-end service on the Illumina MiSeq platform (2 × 250 bp) was performed by the Bio-Environment platform of Perpignan, France (plateformes.univ-perp.fr). Illumina sequence reads in the FastQ format were processed using QIIME2 (version 2021.4) (Bolyen et al., 2019). The DADA2 workflow (Callahan et al., 2016) was used to merge paired-end reads, perform filtering, dereplication, chimera removal, and identify representative sequences of amplicon sequence variants (ASVs). The taxonomic affiliations for the rRNA gene sequences 16S and ITS2 were, respectively, assigned using a pre-trained naive Bayes classifier on the basis of the SILVA 138 database (Quast et al., 2013) and the UNITE v8 database (Nilsson et al., 2019).

The sequencing data were processed under R v3.4 (www.r-project.org) using the R-Studio (http://www.rstudio.com/) Phyloseq

TABLE 1 Primers used in this study for 16S rDNA and ITS2 amplicon sequencing.

Application	Primers	Sequence (5′–>3′)	Annealing temperature (°C)	Reference
16S rDNA gene amplicon	Bact_341F	CCTACGGGNGGCWGCAG	65°C (30 cycles)	Herlemann et al., 2011
	Bact_805R	GACTACHVGGGTATCTAATCC		
ITS2 gene amplicon	ITS86F	GTGAATCATCGAATCTTTGAA	62°C (30 cycles)	(Op De Beeck et al., 2014)
	ITS4	TCCTCCGCTTATTGATATGC		

package (McMurdie and Holmes, 2012). Beta diversity for all conditions was calculated using the Bray–Curtis dissimilarity and compared using analysis of similarities (ADONIS) on normalized data (999 permutations) through Vegan R packages (Oksanen et al., 2020). Kruskal–Wallis tests were performed to compare diversity and richness indices between the conditions. Determination of statistically significant differences (p-value < 0.01) in ASV abundance was performed using the DESeq2 package to compare the impact of *P. oligandrum* on the rhizosphere (Love et al., 2014).

Metabolomics

The impact of *P. oligandrum* on medium-polar metabolites was tested within an *in vitro* system with five replications and three time points (3, 5, and 7 dpi) for inoculated and non-inoculated A17 *M. truncatula*. Five A17 *M. truncatula* seedlings were placed on M medium into 12-cm^2 Petri dishes for each condition with six replications. Each seedling was inoculated with around 10,000 oospores per milliliter. They were then kept in a phytotron at 22° C under 16-h light and 8-h dark photoperiod. At the designated time points, medium-polar metabolites were extracted from the pool of five seedings for each replication of each condition based on Salem et al. (2016). The roots were put in 2-mL Eppendorf tubes accompanied with two steel beads of 4 mm in size and were ground with a Mixer Mill MM 400 grinder through two cycles of 30 s at 30 Hz (Retsch, Eragny sur Oise, France). Moreover, 2-mL FastPrep tubes (MP Biomedicals Lysing Matrix D, Illkirch, France) were filled with 80 mg of tissue powder containing 1.4-mm ceramic spheres and 700 µL of M1 solution (methyl tert-butyl ether/methanol, 3:1). After two cycles of 20 s at 6 m/s in FastPrep-24™ (MP Biomedicals™), 700 µL of M2 solution (MeOH/H_2O, 1:3) was added, followed by 30 s of vortexing at maximum level. The tubes were then centrifuged at 4°C and 10,000 rpm for 20 min. All supernatants were then collected separately. Among the three observed phases, the lower phase containing medium-polar metabolites were used for ultra-high-pressure liquid chromatography–high-resolution mass spectrometry (UHPLC–HRMS). The non-polar phase was then evaporated overnight with SpeedVac™ SPD111V (ThermoFisher Scientific™), and then the normalized amount of MeOH/H_2O (2 mg mL^{-1}), based on the tubes' weight before and after SpeedVac™, was added to each tube. Then, 0.2-µm PTFE filters (Thermo Scientific™) were then used to filter the extracts, and they were finally transferred into vials. The extraction blanks and quality control were also provided for extraction and analytical validation.

UHPLC–HRMS analyses were performed on a Q Exactive Plus quadrupole mass spectrometer, equipped with a heated electrospray probe (HESI II) coupled to an U-HPLC Vanquish system (ThermoFisher™ Scientific, Hemel Hempstead, UK). The samples were separated on a Luna Omega Polar C18 column (150 × 2.1 mm i.d., 1.6 µm, Phenomenex, Sartrouville, France) equipped with a guard column. Mobile phase A (MPA) was water with 0.05% formic acid (FA), and mobile phase B (MPB) was acetonitrile with 0.05% FA. The solvent gradient was as follows: 0 min, 98% MPA; 0.5 min, 98% MPA; 10.5 min, 70% MPB; 10.6 min, 98% MPB, 12.6 min, 98% MPB; 12.7 min, 98% MPA; and 14 min, 98% MPA. The flow rate was 0.4 mL/min, and the column temperature was adjusted to 40°C, while the autosampler temperature was fixed to 10°C. The injection volume was adjusted to 5 µL for root extracts. The mass parameters were used based on Fraisier-Vannier et al. (2020) and Chervin et al. (2022).

LC–MS data were processed by MS-DIAL 4.80 for mass signal extraction between 100 and 1,500 Da from 0.5 to 12 min (Tsugawa et al., 2015). MS1 and MS2 tolerance were set to 0.01 and 0.05 Da, respectively, in the centroid mode. The optimized detection threshold concerning MS1 for positive and negative mode was set to 1.5.10^6 and 2.10^6, respectively. Peak alignment was done according to Fraisier-Vannier et al. (2020). MS-DIAL data were then cleaned by using MS-CleanR based on Fraisier-Vannier et al. (2020). An in-house database constructed on MS-FINDER version 3.52 model was used for peak annotation (Tsugawa et al., 2016; Chervin et al., 2022). C, H, O, N, P, and S atoms were utilized principally in Formula finder. Databases based on *Medicago* (genus) and *Fabaceae* (family) and dictionary of natural product were constituted and used (DNP-CRC press, DNP on DVD v. 28.2). Through a successive ranking based on a genus database, then family database, and finally generic database, annotation prioritization was performed using the final MS-CleanR output. The generic databases were KNApSAcK, PlantCyc, and PubChem available within MS-FINDER.

Normalized LC–MS dataset created by using MS-CleanR was imported in R for multivariate data analysis. The mixOmics package (Rohart et al., 2017) was used to perform principal component analysis (PCA) as a first exploratory step before discriminant modeling. All data were centered and scaled to unit variance. To consider the effect of dpi, data were sloped between 3 to 7 dpi and 3 to 14 dpi. Partial Least-squares Determinant Analysis (PLS-DA) model was applied on this transformed dataset to extract features correlated to each sample class. The loading weights of each variable were extracted from the two first components to rank the top 50 loadings of the discriminant model. Finally, these 50 features (m/z × RT pairs) were used to construct a clustered image map by using euclidian distance and ward agglomeration for both rows (features) and columns (samples).

Microscopy

For visualization and counting of vesicular and arbuscular structures formed by *R. irregularis* colonization, coloration with ink and vinegar was carried out (Vierheilig et al., 1998), and the grid intersect method was used to assess the frequency of mycorrhizal colonization events (Giovannetti and Mosse, 1980). For experiments using the *E. meliloti* GFP strain, all observations were done using a green fluorescent protein (Nikon P2-EFL, GFP-L) filter with an excitation filter of 460–500 nm, dichroic mirror of 505, and barrier filter of 510, resulting in a fluorescent green color. The microscopical observations were done by using a dissecting microscope, Nikon SMZ18, using BF, GFP-L, and RFP-B filters depending on the experiment.

Statistics and data analysis

The general statistical analysis was done using SAS 9.4 software, and graphs were made by using Graphpad prism 8.0.2 software (San Diego, CA, USA). Transcriptomic and metagenomic data were analyzed using R software as well as EdgeR package versions 3.24.3 and R v3.4 (http://www.r-project.org/) using the R-Studio (http://www.rstudio.com/), respectively.

Statistical analyses for metabolomics were done using SIMCA (version 14.1, Umerics, Umea, Sweden). All data were scaled by unit variance scaling before the multivariate analysis. The partial least squares-discriminant analysis (PLS-DA) and orthogonal projection to latent structure using discriminant analysis was used to separate data according to *M. truncatula* growing conditions. The general statistics was performed using SAS 9.4 software.

Results

Pythium oligandrum promotes the growth and seed production of *M. truncatula* and *P. sativum* and protect against the root pathogen *A. euteiches*

Pythium oligandrum was previously reported to promote plant growth and protect them from diseases in several plant species. Here we investigated the effects on legume plant development and on protection against the legume root pathogen *A. euteiches*. To do so, we developed a soil inoculation assay with the ground mycelium of *P. oligandrum* in which seeds of A17 *M. truncatula* and *P. sativum* Cv. Precovil line were sown (Figure 1A). A significant positive effect of *P. oligandrum* was observed both on plant height at 42 days post-inoculation and on the number of seeds formed by plants (Figure 1B). *M. truncatula* did not show a significantly enhanced growth but developed more pods and seeds at 90 days post-inoculation with *P. oligandrum* (Figure 1B), whereas *P. oligandrum* increased the size of pea plants and the number of seeds produced but not the number of pods.

We then assessed whether *P. oligandrum* may protect *P. sativum* and *M. truncatula* against the root rot caused by the legume pathogen *A. euteiches*. We first inoculated the highly susceptible line *M. truncatula* F83005.5 line with the alfalfa isolate MF1 of *A. euteiches*. As shown in Figures 2A, B, all plants treated with *A. euteiches* showed a clear reduction of disease symptoms and displayed a statistically inferior mass of aerial part and whole plants as compared to control plants. Plants treated with *P. oligandrum* again showed enhanced growth as compared to the control.

Inoculation with *A. euteiches* pea isolate RB84 on *P. sativum* cv. Precovil resulted in a severe reduction of plant aerial size and total plant weight (Figures 2C, D) as compared to the control plant. Similar to *M. truncatula*, *P. oligandrum* plants showed enhanced biomass, and inoculation with both *P. oligandrum* and RB84 slightly reduced the detrimental effect on shoot length and plant weight as observed following *A. euteiches* inoculation.

Pythium oligandrum strongly activates *M. truncatula* defense responses and isoflavonoid metabolism

In order to better understand the molecular basis of plant growth promotion and protection caused by *P. oligandrum*, we probed A17 *M. truncatula* responses to *P. oligandrum* oospores with transcriptome and metabolome analyses within an *in vitro* culture system at 3, 5, 7, and 14 dpi. These time points were chosen to observe the early responses of root colonization by *P. oligandrum*. For transcriptomic studies, after RNA sequencing and mapping on model genes (Supplementary Material S1), we performed a principal component analysis (Figure 3A). The difference between mock and *P. oligandrum* datasets could be observed as soon as day 3 post-inoculation but was more noticeable at 5 and 7 days post-inoculation, and then it tends to decrease at 14 days. The fold changes of each individual gene were calculated relatively to the control plants for each time point. In total, 2,236 differentially expressed genes ($\log_2$ FC > 1 or FC < -1; FDR < 0.01 in at least one condition) were obtained and subjected to further analysis. The number of induced and repressed genes are presented in Figure 3B. The strongest transcriptional response was observed at 7 dpi, where 1,182 genes were induced by the oomycete (Figures 3B, C). Clustering analysis allowed the definition of four well-defined clusters among the 2,236 DEGs (Figure 3D). Cluster 1 represented genes strongly induced at all time points of the kinetic, cluster 2 was the group of genes being repressed at one or several time points, cluster 3 represented genes induced in later time points of the kinetic (5, 7, and 14 dpi), and cluster 4 was the group of genes mostly induced at 5 and 7 dpi (Figure 3C).

We subjected the induced genes (clusters 1, 3, and 4) to gene ontology GO terms enrichment analysis using ShinyGO (Ge et al., 2020). Several GO terms related to the synthesis of isoflavonoids, a major class of antimicrobial compounds in *Medicago* species (Gholami et al., 2014), were found (Figure 4A). Downregulated genes fall mainly in GO categories belonging to primary metabolism such as the reductive pentose-phosphate cycle (Figure 4B). Strikingly, enzymes involved in the metabolism of isoflavonoids were strongly upregulated notably at 7 dpi (Figure 4C).

To confirm the induction of isoflavonoid biosynthesis by *M. truncatula* in response to *P. oligandrum*, we performed an analysis of *M. truncatula* root metabolome upon *in vitro* inoculation with the oomycete *P. oligandrum* oospore M1 strain through 3, 7, and 14 days post-inoculation kinetics. Based on retention time and mass spectra, major peaks were annotated and assigned through a comparison with standards and data from the literature sources. Mass spectrometry was carried out in positive and negative ionization modes. The total number of ions retained following MS-CleanR sorting was 474 (Supplementary Material S2). A global metabolomic analysis based on PCA validated our dataset by regrouping the samples according to their group of origin (Figure 5A). Then, a supervised PLS-DA resulted in the clear separation of control and *P. oligandrum*-treated plants at 7 and 14 dpi (Figure 5A). We then plotted the 46 most significant variables which supported the PLS-DA separation of the groups (Figure 5B) (Supplementary Material S2). The annotation of these

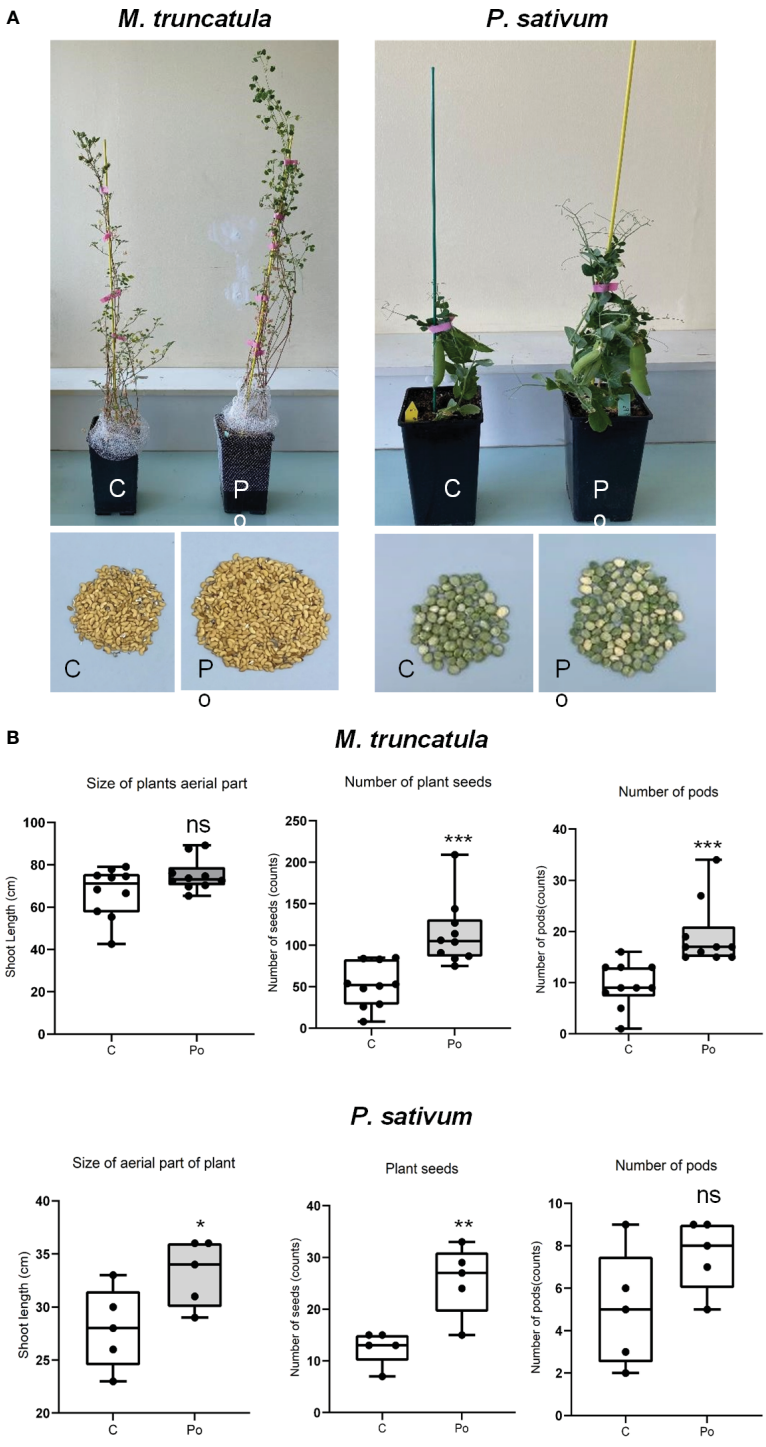

FIGURE 1
Comparison of different treatments on *M. truncatula* and *P. sativum* development and yield in soil. **(A)** A17 *M. truncatula* and *P. sativum* cv. Precovil plants at 90 and 42 days post-inoculation, respectively. **(B)** Box plots of shoot length, number of seeds, and number of pods in control and *P. oligandrum* M1 strain mycelium (Po) conditions; $n = 10$ for *M. truncatula* and $n = 5$ for *P. sativum*. *, **, and *** mean significance at 0.05, 0.01, and 0.001 probability level, respectively, and n.s. means not statistically significant based on Student's *t*-test.

variables revealed that salicylic acid 2-beta-D-glucoside (variable neg_226) was the most strongly accumulated in *M. truncatula* roots at 7 and 14 days post-inoculation with *P. oligandrum* (Figure 5C); a similar trend was observed for the phenylpropanoids pterosupin (neg_420) and 3-hydroxy-8,9-dimethoxycoumestan (neg_245). Consistently with transcriptomic data, we found that *P. oligandrum*-inoculated plants strongly induced the accumulation of isoflavonoids such as medicarpin and formononetin at 7 and 14 dpi in the presence of the oomycete (Figure 5C). These transcriptomic and metabolomics data together support the role

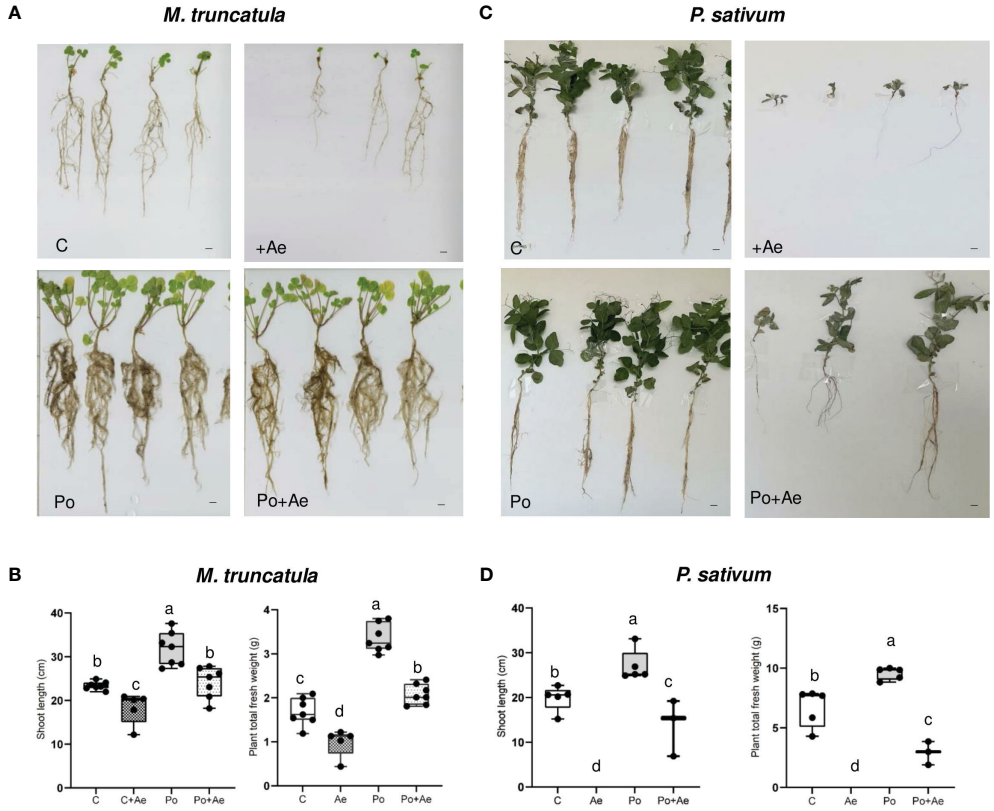

FIGURE 2
Effect of *P. oligandrum* on pea and *M. truncatula* growth and protection against root rot causal agent *A. euteiches*. **(A)** Images of representative *M. truncatula* F83005.5 seedlings at 40 days post-inoculation (scale bars = 2 cm). **(B)** Shoot length and plant fresh weight of *M. truncatula* F83005.5 in control non-inoculated **(C)**, *A. euteiches* (Ae), *P. oligandrum* M1 strain mycelium (Po), and *P. oligandrum* + *A. euteiches* (Po + Ae) conditions. **(C)** Images of representative *Pisum sativum* cv. Precovil plants at 28 days post-inoculation (scale bars = 2 cm). **(D)** Shoot length and plant fresh weight of *Pisum sativum* cv. Precovil in control non-inoculated **(C)**, *A. euteiches* (Ae), *P. oligandrum* M1 strain mycelium (Po), and *P. oligandrum* + *A. euteiches* (Po + Ae) conditions. The mean of each trait for each condition is compared with a Duncan test, and means labeled with the same letter are not statistically significant.

of *P. oligandrum* in root defense stimulation and notably the synthesis of antimicrobial isoflavonoids and phenylpropanoids.

Root colonization by *P. oligandrum* does not hamper symbiotic interactions

As we documented a strong induction of plant defense mechanisms by *P. oligandrum*, we wondered whether root colonization by *P. oligandrum* could have a negative impact on the formation of symbiotic interactions such as nitrogen-fixing symbiosis and arbuscular mycorrhizal symbiosis. To study the nitrogen-fixing symbiosis, a biological system has been devised to study a possible interplay between *P. oligandrum* and GFP-tagged *E. meliloti* on A17 *M. truncatula*, during both early-stage and fully formed symbiosis.

Microscopic inspections of seedlings grown *in vitro* at 35 days post-inoculation showed that *P. oligandrum* did not affect the early stage of nodule establishment (Figure 6A). Relatively, we observed a brighter GFP signal all around the roots in the *P. oligandrum* conditions (Figure 6A). To confirm the stronger bacterial development around roots colonized by the oomycete, we collected the bacteria from each individual plate and performed a colony-forming unit count. This analysis confirmed that *E. meliloti* developed 10 times more (2.247×10^9 CFU mL^{-1} in Po + Em condition *versus* 0.208×10^9 CFU mL^{-1} in Em condition) around A17 roots when they were colonized by *P. oligandrum* (Figure 6B). Finally, in this *in vitro* assay, a similar amount of nodule formation was observed in the presence or absence of *P. oligandrum* (Figure 6C).

To assess the effect of *P. oligandrum* on the later stages of symbiosis, we performed experiments in pots. The mean number of nodules formed per centimeter of roots was similar in the two conditions (Figure 6D). However, while 11% of the nodules formed in the control situation displayed a multi-lobed morphology, this frequency increased to 29% in the *P. oligandrum*-treated situation (Figures 6E, F). This suggests that the *M. truncatula* responses to *P. oligandrum* may increase the development of multi-lobed nodules.

Regarding the effect of *P. oligandrum* on the establishment of arbuscular mycorrhizal (AM) symbiosis, we devised a co-inoculation assay in pots filled with A17 *M. truncatula*. Our results demonstrated that *P. oligandrum* does not inhibit mycorrhization in *M. truncatula* roots, as mycorrhizal structures including vesicles and arbuscular were detected in inoculated roots

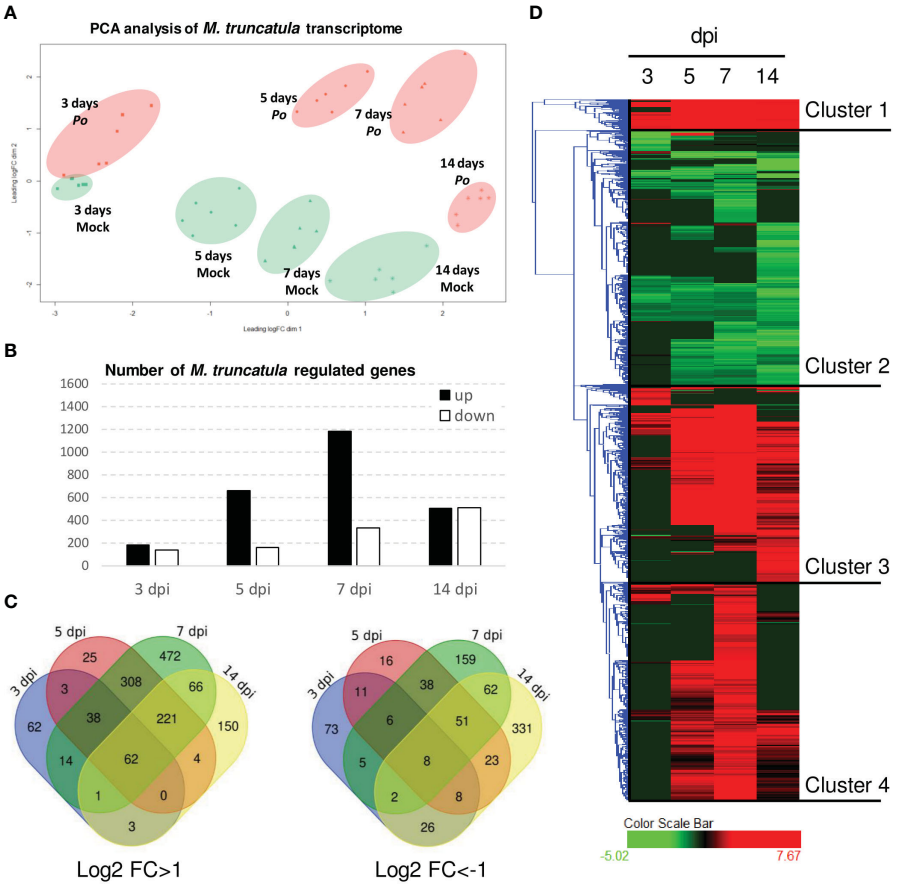

FIGURE 3
Transcriptomic analysis of *Pythium oligandrum*-inoculated roots. RNAseq experiments were performed on RNA extracted from *in vitro* grown plants inoculated with *P. oligandrum* oospores at different time points. **(A)** Principal component analysis of data obtained from the RNA sequencing of *P. oligandrum* and A17 *M. truncatula* at 3, 5, 7, and 14 days post-inoculation. Orange dots show data belonging to *M. truncatula* plants inoculated with *P. oligandrum*, and green dots show data belonging to mock plants. **(B)** Number of differentially expressed genes (DEGs) at each time point. **(C)** Venn diagrams representing the DEGs for each condition. **(D)** Hierarchical clustering on DEGs; clustering was obtained using Hierachical Clustering Explorer version 3.5 with default parameters.

visualized by coloration and microscopy (Figure 6G). The rate of mycorrhization in the presence of *P. oligandrum* was indistinguishable from the control mycorrhizal inoculation (Figure 6H). Thus, the plant defense-stimulating and mycoparasitic *P. oligandrum* oomycete M1 strain does not affect the AM symbiotic interaction.

Pythium oligandrum influences the composition of the rhizosphere microbiota

We then investigated the effect of root colonization by *P. oligandrum* on the rhizosphere of *M. truncatula* (F83005.5) plants sown in potting soil. A total of 14 samples comprising seven controls and seven *P. oligandrum*-inoculated plants were harvested at day 56 post-sowing, and DNA from their rhizosphere was extracted and subjected to PCR. The 16S rRNA dataset retained 194,708 reads, and the Internal Transcribed Spacer dataset retained 422,171 reads, which were assigned respectively to 1,413 bacterial amplicon single variants and 374 fungal ASVs (Supplementary Materials S3, S4). The data were normalized to account for unequal sequencing depth, resulting in a minimum sampling depth of 3,834 for 16S and 10,556 sequences per sample for ITS.

The analysis of alpha diversity of bacteria and fungi (observed and Shannon diversity) in the rhizosphere of *M. truncatula* inoculated with *P. oligandrum* showed no significant difference *versus* the uninoculated control (Figure 7A). Conversely, the addition of *P. oligandrum* had a tremendous impact on the community structure (beta diversity) in both bacteria and fungi (Figure 7B). A principal component analysis (PCoA) based on Bray–Curtis dissimilarities revealed that the introduction of *P. oligandrum* is a large source of variation capturing 44.5% (PCoA, axis 1) of the variation of bacterial community composition and 45.1% (PCoA, axis 1) of the variation of fungal community composition (Figure 7B). The PERMANOVA tests confirmed a significant clustering of the inoculated sample and the uninoculated control in both bacteria (df = 1, $F = 4.09$, $r^2 = 0.25$, $P = 0.01^{**}$) and fungi (df = 1, $F = 2.8$, $r^2 = 0.19$, $P = 0.043^{*}$). The taxonomic assignment of ASVs suggested that four bacterial phyla,

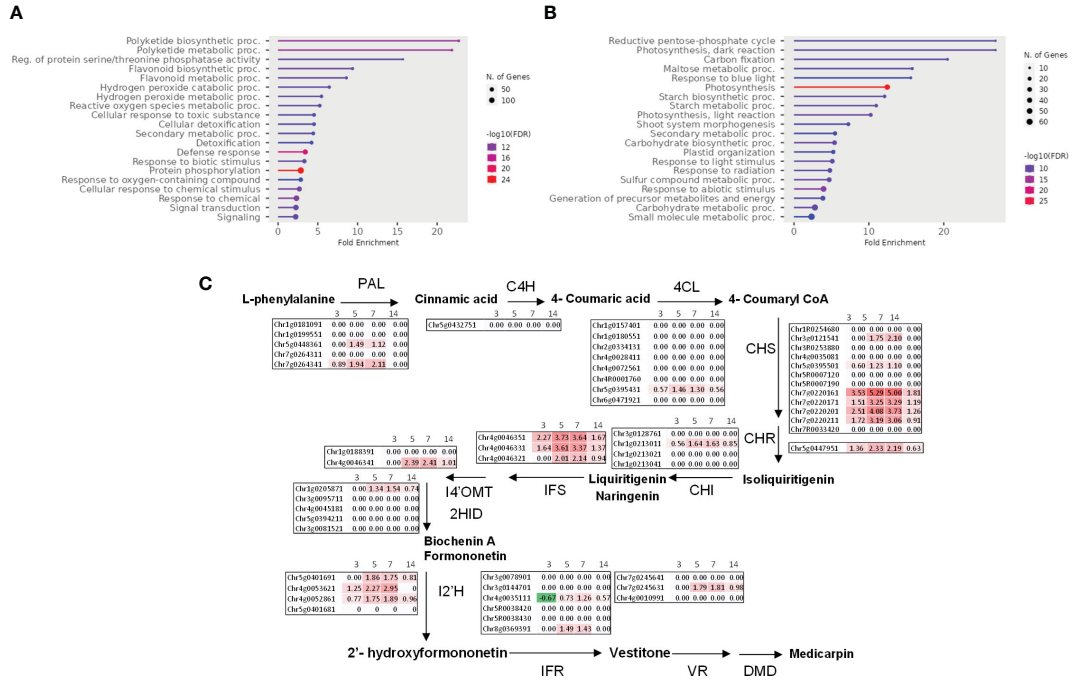

FIGURE 4
Pythium oligandrum root colonization induces *M. truncatula* defense genes and the expression of the isoflavonoid pathway. **(A)** Upregulated genes (clusters 1, 3, and 4) and **(B)** downregulated genes (cluster 2) were analyzed using ShinyGO with the GO parameter "Biological Process". **(C)** Log_2 fold change of the expression of genes coding the biosynthetic enzymes of medicarpin at 3 to 14 dpi with *P. oligandrum*. The biosynthetic pathway for medicarpin and related isoflavonoids is shown (Naoumkina et al., 2006) for each time point as indicated. PAL, L-phenylalanine ammonia-lyase; C4H, cinnamate 4-hydroxylase; 4CL, 4-coumarate:CoA ligase; CHS, chalcone synthase; CHI, chalcone isomerase; IFS, isoflavone synthase; I4'OMT, 2-hydroxyisoflavanone 4'-O-methyltransferase; 2HID, 2-hydroxyisoflavanone dehydratase; I2'H, isoflavone 2'-hydroxylase; IFR, isoflavone reductase; VR, vestitone reductase; DMID, 7,2'-dihydroxy-4'-methoxy-isoflavonol dehydratase.

including Planctomycetota, Proteobacteria, Bacteroidota, and Actinobacteriota, dominated the rhizosphere regardless of the treatment. The pairwise comparison of relative abundances for each bacterial phylum showed that there was a significant drop in the phylum Actinobacteria (Wilcoxon: $p > 0.05$) among the bacterial community in the presence of *P. oligandrum*. The fungal taxonomic assignment showed the dominance of Ascomycota and Basidiomycota phyla in the non-inoculated control, whereas a third dominant phyla was detected in the rhizosphere of *P. oligandrum*-treated plants (Chytridiomycota; Figure 7B). Consistently, the pairwise comparison of relative abundances of fungal phyla showed that there was a significant increase in the phylum Chytridiomycota (Wilcoxon: $p > 0.05$) among the fungal community upon *P. oligandrum* treatment.

In order to determine more precisely whether particular bacterial or fungal genera are affected by *P. oligandrum* in their rhizospheric abundance, we performed a DEseq2 analysis on the individual ASVs of the dataset. A total of 17 bacterial ASVs and 20 fungal ASVs were differentially occurring upon *P. oligandrum* inoculation. We confirmed that *P. oligandrum* largely reduced rhizosphere colonization by the *Streptomyces*-related ASV219 belonging to Actinobacteria and found out that it impacts either positively or negatively 10 ASVs belonging to Planctomycota and four ASVs affected to Alphaproteobacteria (Supplementary Material S5). In addition, the oomycete inoculation increased the abundance of nine fungal ASVs related to Basidiomycota, among which six were belonging to the *Clitopilus* genus. Similarly, five Ascomycota-related ASVs were more abundant in the presence of the oomycete, and two showed the opposite behavior (Supplementary Material S6). Consistently with the PCoA, the Chytridiomycota ASV117 was enriched in *P. oligandrum* conditions by a fold change of 12.12. Taken together, these data illustrate how *P. oligandrum* can shape the host plant microbiota in addition to its impact on pathogenic interactions.

Discussion

While *P. oligandrum* potential in crop protection has been largely documented, in the present study we aimed to describe the effect of oomycete on symbiotic interactions and microbial community. To do so, we devised biological systems with the model legume *M. truncatula* or pea and the oomycete.

Firstly, we validated that treatment of soil with *P. oligandrum* mycelium resulted in a higher yield and enhanced the growth in both *M. truncatula* and *P. sativum*. These findings are in line with previous reports which reported the same effect on cucumber (Kratka et al., 1994; Wulff et al., 1998). It is proposed that improved nutrient uptake by plant in the presence of *P. oligandrum*, notably phosphorus, gives rise to boosted plant growth (Kratka et al., 1994; Lugtenberg and Kamilova, 2009; Backer et al., 2018).

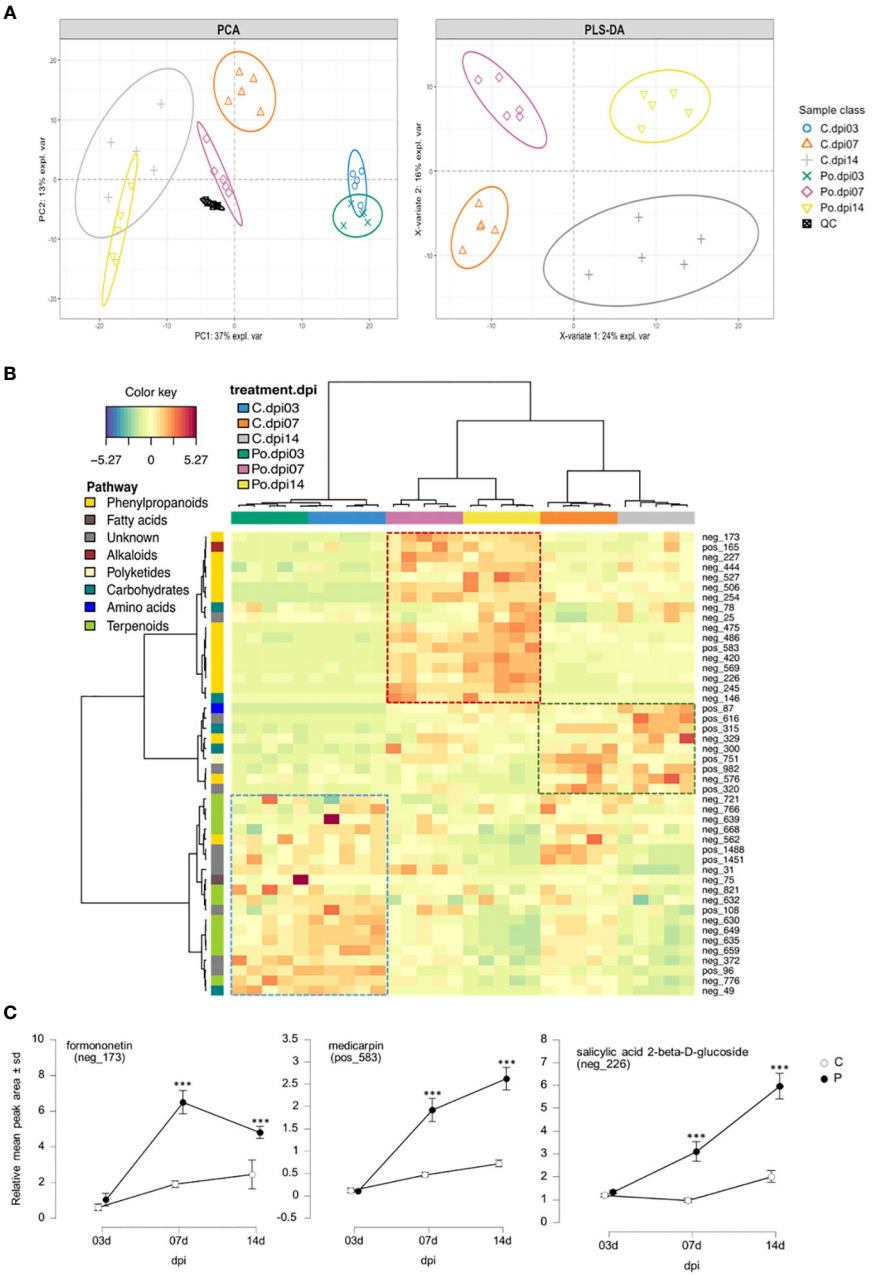

FIGURE 5
Medicarpin and formononetin are two major components of *Medicago truncatula* metabolic response to *Pythium oligandrum*. **(A)** Principal component analysis score plot of LC–MS dataset from PC1 and PC2, and PLS-DA score plot from the two first latent variables after slope-based transformation. Data were centered and unit scaled. **(B)** Clustered Image Map from the most important variables selected by PLS-DA model. Rows display the LC–MS features numbered according to Supplementary Material S2. Each feature is color-coded along the vertical axis according to the pathway of origin deciphered by NPclassifier. Column display samples. Each sample is color-coded according to its class (3, 7, or 14 dpi). Both rows and columns were clustered using Euclidian distance and ward agglomeration. The dotted line square displays the most representative cluster of each group. **(C)** Line plots of selected features from the top 50 PLS-DA loading weights. The data represent the relative mean peak area (Y) of each sample class along the dpi (X). The plotted features were selected for their high confidence annotation level from level 2 to level 3 in the genus or family. *** means significance at 0.001 probability level based on Student's T-test.

Secondly, we observed the efficacy of *P. oligandrum* treatment on legume plants' protection against *A. euteiches*, an oomycete causing damping off and root rot, in *M. truncatula* and *P. sativum*. The ability of *P. oligandrum* to promote plant growth and nutrition may account for this improved resistance to the disease. In addition, the production of elicitors such as POD1 and POD2 cell wall proteins or of oligandrin by *P. oligandrum* can activate jasmonate and ethylene signaling; the oomycete can trigger host plant ferroptosis as well (Picard et al., 2000; Takenaka et al., 2003; Hase et al., 2006; Hase et al., 2008; Takenaka, 2015; Cheng et al., 2022).

10.3389/fpls.2023.1156733

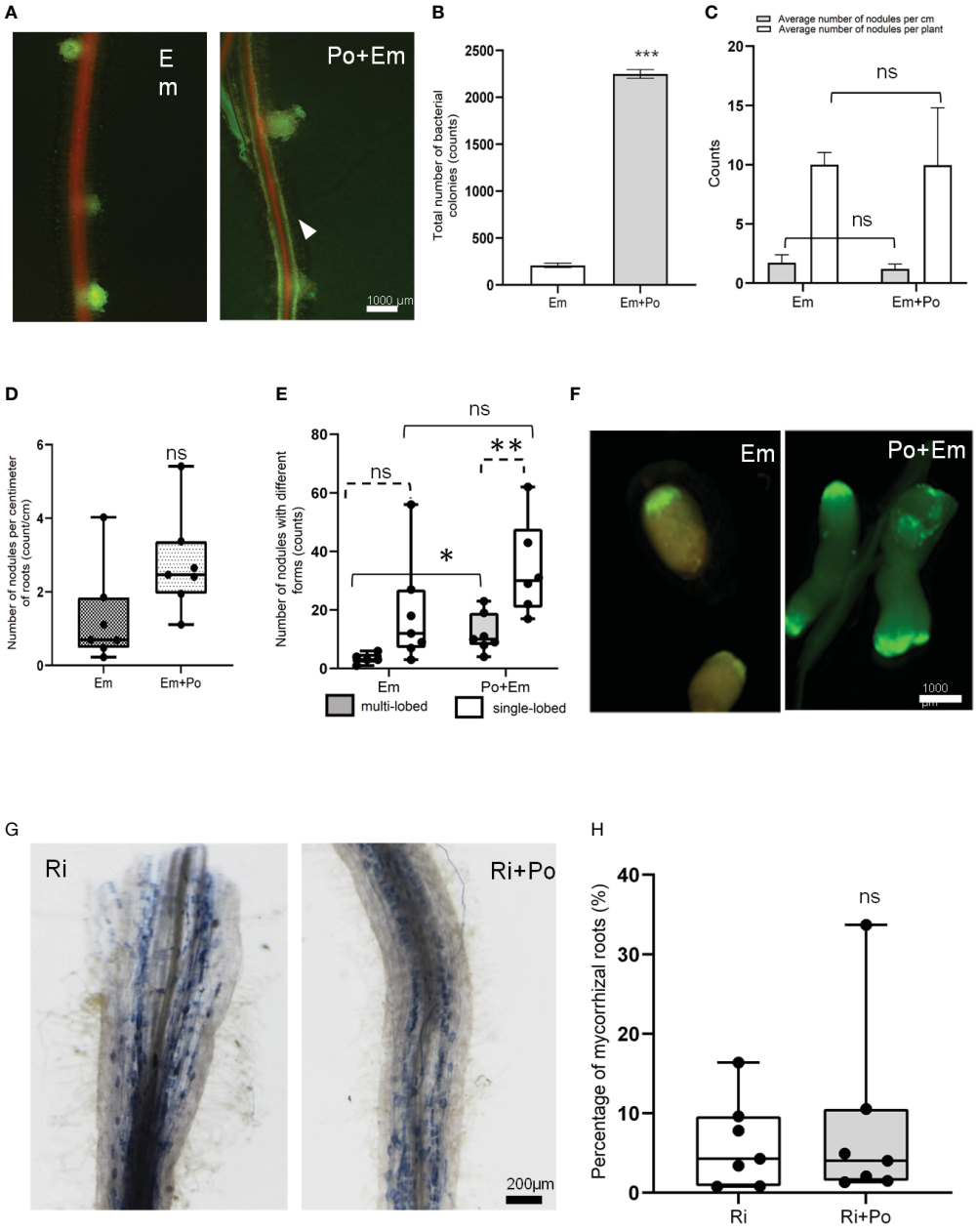

FIGURE 6
Effect of *P. oligandrum* on nitrogen fixing and arbuscular mycorrhizal symbiosis in *M. truncatula*. **(A)** Representative *M. truncatula* A17 nodules with or without *P. oligandrum* inoculum. The arrowhead points to GFP-tagged *E. meliloti* biofilm formation around the *M. truncatula* A17 root in *P. oligandrum* M1 strain mycelium + *E. meliloti* (Po + Em) condition. **(B)** Counting of colony-forming units of *E. meliloti* inoculated alone on *M. truncatula* A17 (Em) or co-inoculated with *P. oligandrum* M1 strain mycelium + (Po + Em) at 35 days post-inoculation (dpi). **(C)** Counting of *M. truncatula* A17 nodules in Em and Po + Em at 35 dpi. **(D)** Box plots of the number of nodules per centimeter of *M. truncatula* A17 roots and **(E)** number of nodules with single- or multi-lobed shape upon inoculation with a GFP-tagged *E. meliloti strain* (Em) or *P. oligandrum* M1 strain mycelium + *E. meliloti* (Po + Em). **(F)** Images of representative nodules at 42 dpi. **(G)** Images of representative mycorrhizal roots inoculated or not with *P. oligandrum* M1 mycelium (Ri or Ri + Po). **(H)** Histograms of percentage of mycorrhized root in different conditions including *R. irregularis* (Ri) and *P. oligandrum* M1 strain mycelium + *R. irregularis* (Po + Ri) at 42 dpi. *** means significance at 0.001 probability, and n.s. means not statistically significant based on Student's *t*-test. * and ** mean significance at 0.05 and 0.01, probability level, respectively, and n.s. means not statistically significant based on Student's T-test.

Collectively, these different mechanisms may account for the plant protection against *A. euteiches*. In line with this hypothesis, our transcriptomic data showed induction of defense genes, including secondary metabolites—notably, flavonoids. Several lines of evidence display the inhibitory potential of isoflavonoids against some pathogens within an *in planta* system (Stevenson et al., 1997). Previous work showed that rapid root colonization by *P. oligandrum* ends up with the activation of defense reactions through the phenylpropanoid pathway, which results in the production of secondary metabolites and formation of cell wall appositions (Benhamou et al., 1997; Benhamou et al., 2012; Bělonožníková et al., 2022). Our metabolomic data likewise

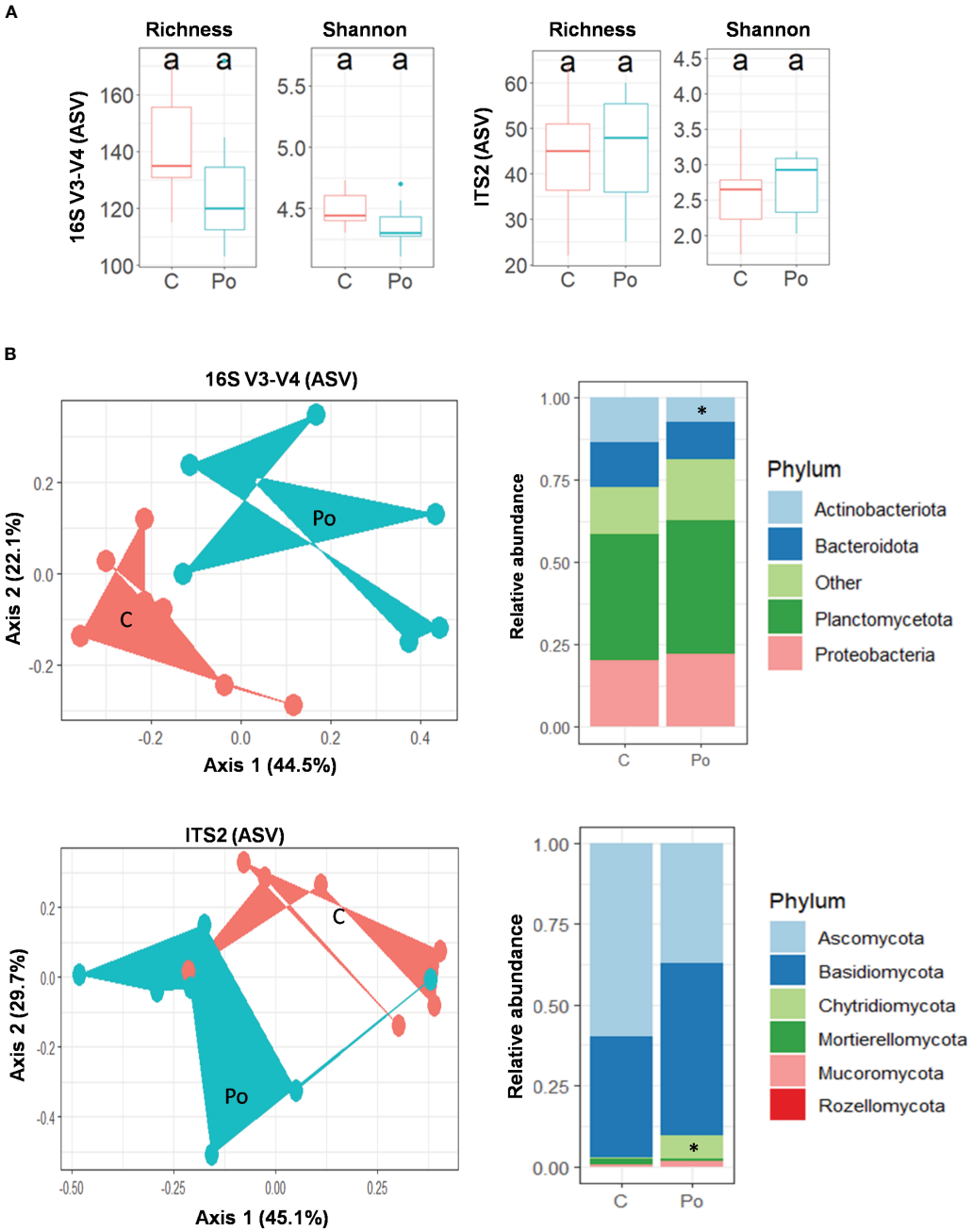

FIGURE 7
Pythium oligandrum shapes the bacterial and fungal communities associated to the rhizosphere of *Medicago truncatula* F83005.5 rhizosphere. **(A)** Alpha diversity measurements are based on observed ASVs and Shannon index for the bacterial and fungal microbiome. **(B)** Principal component analysis for beta diversity using Bray–Curtis distances in bacterial and fungal communities. C stands for control and Po for *P. oligandrum* M1 mycelium-inoculated plants. Relative bacterial and fungal abundances at phylum level. Statistical data analyses were performed using non-parametric Wilcoxon test (*$p < 0.05$).

proved the induction of flavonoid-like medicarpin and formononetin, two isoflavonoids with proven antifungal activity (Blount et al., 1992; Gupta et al., 2022). Accordingly, we have previously shown that this pathway is an essential component of the resistance of *M. truncatula* to *A. euteiches* (Badis et al., 2015).

Once we validated the effect of *P. oligandrum* on legume plants' growth and protection, we decided to investigate its effect on mutualistic interactions, including the legume-specific nitrogen-fixing symbiosis. Interestingly, our results regarding the co-inoculation of *P. oligandrum* and *E. meliloti* showed that the number of *E. meliloti* colonies forming around the roots increased with the presence of *P. oligandrum*. This effect can be due to the stimulation by *P. oligandrum* of the flavonoid metabolism which has been shown to have a positive chemotaxis effect on rhizobia (Aguilar et al., 1988). In addition, the number of nodules formed in the presence of *P. oligandrum*

was similar to that of the control, suggesting that the oomycetes do not compromise the symbiosis.

Regarding AMFs, a similar rate of mycorrhization was obtained between the control plants and *P. oligandrum*-treated plants. This suggests that the strong stimulation by *P. oligandrum* of various defense reactions (PR proteins and secondary metabolism) does not impair the interaction between plant roots and AMFs and that, in some way, AMFs are resistant to the mycoparasitic activity. Consistently, the isoflavonoids formononetin and biochanin A were formerly reported to improve the root colonization and hyphal growth of vesicular–arbuscular mycorrhizal bacteria ending in the stimulated growth of clover (Elias and Safir, 1987; Nair et al., 1991; Siqueira et al., 1991). Thus, stimulation of isoflavonoid biosynthesis by *P. oligandrum* may not hamper *M. truncatula* mycorrhization. Regarding arbuscular mycorrhizal symbiosis, a similar rate of mycorrhization was obtained between the control plants and the *P. oligandrum*-treated plants. This suggests that the strong stimulation by *P. oligandrum* of various defense reactions (PR proteins and secondary metabolism) did not impair the interaction between the plant roots and AMFs and that, in some ways, AMFs are resistant to the mycoparasitic activity. Consistently, the isoflavonoid formononetin and biochanin A were formerly reported to improve the root colonization and hyphal growth of vesicular–arbuscular mycorrhizal bacteria ending in the stimulated growth of clover (Elias and Safir, 1987; Nair et al., 1991; Siqueira et al., 1991). Thus, stimulation of isoflavonoid biosynthesis by *P. oligandrum* may not hamper *M. truncatula* mycorrhization.

Finally, we investigated whether *P. oligandrum* could have a wider impact on the microbial community of the rhizosphere. The analysis of alpha diversity showed no significant differences with the untreated control. However, the introduction of oomycete did change the community structure of both fungi and bacteria. These shifts in fungal and bacterial beta diversity has been documented previously and associated with beneficial outcomes (Vallance et al., 2012; Gerbore et al., 2014; Cernava et al., 2019; Uhlig et al., 2021).

In line with the drop of Actinobacteria abundance at the genera level in the presence of *P. oligandrum*, we observed a reduction in *Streptomyces* sp. ASV219. *Streptomyces* are major producers of antibiotics and antifungal, hence capable of inhibiting the growth of plant pathogens (Lee et al., 2018). Furthermore, they are considered as plant growth-promoting rhizobacteria involved in various activities such as phosphate solubilization, siderophore production, and nitrogen fixation (Bhatti et al., 2017; Rey and Dumas, 2017; Boubekri et al., 2022). Thus, the fact that *P. oligandrum* can modulate *Streptomyces* population in the rhizosphere may have important consequences on the microbiota functions. Regarding fungal communities, the result suggests that the mycoparasite *P. oligandrum* has a predation preference for Ascomycota-related ASVs rather than Basidiomycota. The *Trichoderma*-related ASV505 was still enhanced in the presence of the oomycete. *Trichoderma* are the most widely used fungal biocontrol agents against fungal diseases of pulses, grapes, cotton, onion, carrot, peas, plums, maize, apple, etc. (Kumar and Ashraf, 2017). From *in vitro* interaction assays of *P. oligandrum* and *T. harzianum*, it was concluded that the fungus can kill the oomycete (Floch et al., 2009). Thus, *Trichoderma*-related fungi may be enriched in the rhizosphere and use the oomycete as a prey. Their enrichment in presence of *P. oligandrum* may still participate in the protection against soil pathogens. Similarly, we noticed an enrichment of six ASVs belonging to *Clitopilus*, having some species considered as mycoparasitic basidiomycetes (Jatuwong et al., 2017). Finally, the enrichment of Chytridiomycota in response to *P. oligandrum* may participate in the control of insect populations since these fungi are often entomopathogenic (Kaczmarek and Bogus, 2021). Taken together, our data provide novel insights regarding the effect of *P. oligandrum* on the microbial communities of the rhizosphere and suggest that the oomycete may favor the recruitment of plant-beneficial microorganisms.

Conclusion

The present study concluded that *P. oligandrum* is a potential biocontrol agent for legume crops, which could be used to promote plant growth and protect them from pathogenic attacks. We also revealed that *P. oligandrum* does not inhibit symbiotic interactions with other mutualistic microorganisms, including *E. meliloti* and *R. irregularis*. This beneficial mycoparasite likewise modifies the microbial community of the soil, and the functional outcome of these perturbations still needs to be investigated to address whether it benefits the plant by reducing or eliminating plant bacterial and fungal pathogens or by activating other mycoparasitic organisms that can fight against pathogens. Finally, the relative contribution in the protection against pests of *P. oligandrum* mycoparasitic *versus* plant defense-stimulating activities still has to be disentangled. The proven advantages of *P. oligandrum* still make it a great candidate for further studies in biocontrol industry and sustainable agriculture.

Data availability statement

The sequence data were deposited at the Sequence Read Archive of the National Center for Biotechnology Information (NCBI) and are available under accession numbers PRJNA787426 and PRJNA787434 for 16S rDNA and ITS metagenomic data respectively. The RNA sequencing data of *M. truncatula* can be uploaded from the NCBI BioProject PRJNA806852.

Author contributions

BD, EG, TR, and MH conceived this study. J-MC provided *E. meliloti* strain and information regarding nitrogen-fixing symbiosis assays. SR provided Connectis™ and information regarding mycorrhization assays. MH and RP coordinated the experiments and analyzed phenotypic data. GM and AA performed the metabolomics analysis. HS and MA analyzed the transcriptomic data, and KA and MZ analyzed the metagenomic data. MH along with BD, TR, and EG drafted the manuscript. All authors contributed to the article and approved the submitted version.

Funding

This research was funded by the European Union's Horizon 2020 Research and Innovation Program [grant agreement numbers 766048 (MSCA-ITN PROTECTA) and 774340 (Organic-PLUS)]. The metabolomics studies were carried out at MetaToul-AgromiX platform with financial support from the French National Infrastructure for Metabolomics and Fluxomics (grant MetaboHUB-ANR-11-INBS-0010). The bioenvironment platform is funded by the platform (UPVD, Région Occitanie, CPER 2007-2013 Technoviv, CPER 2015-2020 Technoviv2). The Laboratoire de Recherche en Sciences Végétales belongs to TULIP Laboratoire d'Excellence (ANR-10-LABX-41; ANR- 18-EURE-0019) and was also supported by the Agence Nationale de la Recherche (LabCom BioPlantProtec ANR-14-LAB7-0001) and the Région Occitanie (projet GRAINE-BioPlantProducts).

Acknowledgments

We warmly thank Joshua Bougon-Ronin and Valérie Arnal from the R&D staff of DE SANGOSSE company (Agen, France) for support within the BioPlantProducts projects and in the frame of industrial secondment during the ITN-PROTECTA. We are grateful to Eve Toulza, Jean-François Allienne, Margot Doberva, and Michèle Laudié from the Bio-Environment platform (Université de Perpignan Via Domitia, France) for their technical support in library preparation and sequencing.

Conflict of interest

The authors declare that the research was conducted in the absence of any commercial or financial relationships that could be construed as a potential conflict of interest.

Publisher's note

Supplementary material

The Supplementary Material for this article can be found online at: https://www.frontiersin.org/articles/10.3389/fpls.2023.1156733/full#supplementary-material

References

Aguilar, J. M. M., Ashby, A. M., Richards, A. J. M., Loake, G. J., Watson, M. D., and Shaw, C. H. (1988). Chemotaxis of *Rhizobium leguminosarum* biovar phaseoli towards flavonoid inducers of the symbiotic nodulation genes. *Microbiology* 134, 2741–2746. doi: 10.1099/00221287-134-10-2741

Backer, R., Rokem, J. S., Ilangumaran, G., Lamont, J., Praslickova, D., Ricci, E., et al. (2018). Plant growth-promoting rhizobacteria: context, mechanisms of action, and roadmap to commercialization of biostimulants for sustainable agriculture. *Front. Plant Sci.* 871. doi: 10.3389/fpls.2018.01473

Badis, Y., Bonhomme, M., Lafitte, C., Huguet, S., Balzergue, S., Dumas, B., et al. (2015). Transcriptome analysis highlights preformed defences and signalling pathways controlled by the *prAe1* quantitative trait locus (QTL), conferring partial resistance to *Aphanomyces euteiches* in Medicago truncatula. *Mol. Plant Pathol.* 16, 973–986. doi: 10.1111/mpp.12253

Badreddine, I., Lafitte, C., Heux, L., Skandalis, N., Spanou, Z., Martinez, Y., et al. (2008). Cell wall chitosaccharides are essential components and exposed patterns of the phytopathogenic oomycete *Aphanomyces euteiches*. *Eukaryot. Cell* 7, 1980–1993. doi: 10.1128/EC.00091-08

Bagyaraj, D. J. (1991). Ecology of vesicular arbuscular mycorrhizae. *Handb. Appl. Mycol.* 1, 1–34.

Baker, B. P., Green, T. A., and Loker, A. J. (2020). Biological control and integrated pest management in organic and conventional systems. *Biol. Control* 140, 104095. doi: 10.1016/j.biocontrol.2019.104095

Becard, G., and Fortin, J. A. (1988). Early events of vesicular–arbuscular mycorrhiza formation on Ri T-DNA transformed roots. *New Phytol.* 108, 211–218. doi: 10.1111/j.1469-8137.1988.tb03698.x

Bělonožníková, K., Hýsková, V., Chmelík, J., Kavan, D., Čeřovská, N., and Ryšlavá, H. (2022). *Pythium oligandrum* in plant protection and growth promotion: Secretion of hydrolytic enzymes, elicitors and tryptamine as auxin precursor. *Microbiol. Res.* 258. doi: 10.1016/j.micres.2022.126976

Bělonožníková, K., Vaverová, K., Vaněk, T., Kolařík, M., Hýsková, V., Vaňková, R., et al. (2020). Novel insights into the effect of *Pythium* strains on rapeseed metabolism. *Microorganisms* 8, 1–24. doi: 10.3390/microorganisms8101472

Benhamou, N., le Floch, G., Vallance, J., Gerbore, J., Grizard, D., and Rey, P. (2012). *Pythium oligandrum*: An example of opportunistic success. *Microbiol. (United Kingdom)* 158, 2679–2694. doi: 10.1099/mic.0.061457-0

Benhamou, N., Rey, P., Chérif, M., Hockenhull, J., and Tirilly, Y. (1997). Treatment with the mycoparasite *Pythium oligandrum* triggers induction of defense-related reactions in tomato roots when challenged with *Fusarium oxysporum* f. sp. *radicis-lycopersici*. *Phytopathology* 87, 108–122. doi: 10.1094/PHYTO.1997.87.1.108

Beringer, J. E. (1974). R factor transfer in *Rhizobium leguminosarum*. *J. Gen. Microbiol.* 84, 188–198. doi: 10.1099/00221287-84-1-188

Bhatti, A. A., Haq, S., and Bhat, R. A. (2017). Microbial Pathogenesis Actinomycetes benefaction role in soil and plant health. *Microb. Pathog.* 111, 458–467. doi: 10.1016/j.micpath.2017.09.036

Blount, J. W., Dixon, R. A., and Paiva, N. L. (1992). Stress responses in alfalfa (*Medicago sativa* L.) XVI. Antifungal activity of medicarpin and its biosynthetic precursors; implications for the genetic manipulation of stress metabolites. *Physiol. Mol. Plant Pathol.* 41, 333–349. doi: 10.1016/0885-5765(92)90020-V

Bolyen, E., Rideout, J. R., Dillon, M. R., Bokulich, N. A., Abnet, C. C., Al-Ghalith, G. A., et al. (2019). Reproducible, interactive, scalable and extensible microbiome data science using QIIME 2. *Nat. Biotechnol.* 37, 852–857. doi: 10.1038/s41587-019-0209-9

Boubekri, K., Soumare, A., Mardad, I., Lyamlouli, K., Ouhdouch, Y., Hafidi, M., et al. (2022). Multifunctional role of Actinobacteria in agricultural production sustainability: a review. *Microbiol. Res.* 127059. doi: 10.1016/j.micres.2022.127059

Callahan, B. J., McMurdie, P. J., Rosen, M. J., Han, A. W., Johnson, A. J. A., and Holmes, S. P. (2016). DADA2: High-resolution sample inference from Illumina amplicon data. *Nat. Methods* 13, 581–583. doi: 10.1038/nmeth.3869

Cernava, T., Chen, X., Krug, L., Li, H., Yang, M., and Berg, G. (2019). The tea leaf microbiome shows specific responses to chemical pesticides and biocontrol applications. *Sci. Total Environ.* 667, 33–40. doi: 10.1016/j.scitotenv.2019.02.319

Cheng, H. P., and Walker, G. C. (1998). Succinoglycan is required for initiation and elongation of infection threads during nodulation of alfalfa by *Rhizobium meliloti*. *J. Bacteriol.* 180, 5183–5191. doi: 10.1128/jb.180.19.5183-5191.1998

Cheng, H. P., and Yao, S. Y. (2004). The key Sinorhizobium meliloti succinoglycan biosynthesis gene exoY is expressed from two promoters. *FEMS Microbiol. Lett.* 231, 131–136. doi: 10.1016/S0378-1097(03)00952-2

Cheng, Y., Zhang, H., Zhu, W., Li, Q., and Meng, R. (2022). Ferroptosis induced by the biocontrol agent *Pythium oligandrum* enhances soybean resistance to Phytophthora sojae. *Environ. Microbiol.* 24 (12), 6267–6278. doi: 10.1111/1462-2920.16248

Chervin, J., Romeo-Oliván, A., Fournier, S., Puech-Pages, V., Dumas, B., Jacques, A., et al. (2022). Modification of early response of *Vitis vinifera* to pathogens relating to Esca Disease and biocontrol agent Vintec® revealed by untargeted metabolomics on woody tissues. *Front. Microbiol.* 13. doi: 10.3389/fmicb.2022.835463

Compant, S., Samad, A., Faist, H., and Sessitsch, A. (2019). A review on the plant microbiome: Ecology, functions, and emerging trends in microbial application. *J. Adv. Res.* 19, 29–37. doi: 10.1016/j.jare.2019.03.004

Daraignes, L., Gerbore, J., Yacoub, A., Dubois, L., Romand, C., Zekri, O., et al. (2018). Efficacy of *P. oligandrum* affected by its association with bacterial BCAs and rootstock effect in controlling grapevine trunk diseases. *Biol. Control* 119, 59–67. doi: 10.1016/j.biocontrol.2018.01.008

del Pilar Martínez-Diz, M., Díaz-Losada, E., Andrés-Sodupe, M., Bujanda, R., Maldonado-González, M. M., Ojeda, S., et al. (2021). Field evaluation of biocontrol agents against black-foot and Petri diseases of grapevine. *Pest Manage. Sci.* 77, 697–708. doi: 10.1002/ps.6064

Ehlers, R. U. (2011). Regulation of biological control agents. *Regul. Biol. Control Agents*, 1–416. doi: 10.1007/978-90-481-3664-3

Elias, K. S., and Safir, G. R. (1987). Hyphal elongation of *Glomus fasciculatus* in response to root exudates. *Appl. Environ. Microbiol.* 53, 1928–1933. doi: 10.1128/aem.53.8.1928-1933.1987

Faure, C., Veyssière, M., Boëlle, B., Clemente, H. S., Bouchez, O., Lopez-Roques, C., et al. (2020). Long-read genome sequence of the sugar beet rhizosphere mycoparasite *Pythium oligandrum*. *G3 Genes Genomes Genet.* 10, 431–436. doi: 10.1534/g3.119.400746

Floch, G., Vallance, J., Benhamou, N., and Rey, P. (2009). Combining the oomycete *Pythium oligandrum* with two other antagonistic fungi: Root relationships and tomato grey mold biocontrol. *Biol. Control* 50, 288–298. doi: 10.1016/j.biocontrol.2009.04.013

Fox, S. L., O'Hara, G. W., and Bräu, L. (2011). Enhanced nodulation and symbiotic effectiveness of Medicago truncatula when co-inoculated with *Pseudomonas fluorescens* WSM3457 and *Ensifer (Sinorhizobium) medicae* WSM419. *Plant Soil* 348, 245–254. doi: 10.1007/s11104-011-0959-8

Fraisier-Vannier, O., Chervin, J., Cabanac, G., Puech-Pages, V., Fournier, S., Durand, V., et al. (2020). MS-CleanR: A feature-filtering approach to improve annotation rate in untargeted LC-MS based metabolomics. *Anal. Chem.* 92, 9971–9981. doi: 10.1101/2020.04.09.033308

Gage, D. J., Bobo, T., and Long, S. R. (1996). Use of green fluorescent protein to visualize the early events of symbiosis between *Rhizobium meliloti* and alfalfa (*Medicago sativa*). *J. Bacteriol.* 178, 7159–7166. doi: 10.1128/jb.178.24.7159-7166.1996

Ge, S. X., Jung, D., Jung, D., and Yao, R. (2020). ShinyGO: A graphical gene-set enrichment tool for animals and plants. *Bioinformatics* 36, 2628–2629. doi: 10.1093/bioinformatics/btz931

Gerbore, J., Vallance, J., Yacoub, A., Grizard, D., Regnault-roger, C., and Rey, P. (2014). Characterization of *Pythium oligandrum* populations that colonize the rhizosphere of vines from the Bordeaux region. *FEMS Microbiol. Ecology.* 90, 153–167. doi: 10.1111/1574-6941.12380

Gholami, A., De Geyter, N., Pollier, J., Goormachtig, S., and Goossens, A. (2014). Natural product biosynthesis in *Medicago* species. *Nat. Prod. Rep.* 31, 356–380. doi: 10.1039/c3np70104b

Giovannetti, M., and Mosse, B. (1980). An evaluation of techniques for measuring vesicular arbuscular mycorrhizal infection in roots. *Mosse Source: New Phytol.* 84, 489–500. doi: 10.1111/j.1469-8137.1980.tb04556.x

Gupta, A., Awasthi, P., Sharma, N., Parveen, S., Vats, R. P., Singh, N., et al. (2022). Medicarpin confers powdery mildew resistance in *Medicago truncatula* and activates the salicylic acid signalling pathway. *Mol. Plant Pathol.* 23(7), 966–983. doi: 10.1111/mpp.13202

Hamid, S., Lone, R., and Mohamed, H. I. (2021). "Production of Antibiotics from PGPR and Their Role in Biocontrol of Plant Diseases," in *Plant Growth-Promoting Microbes for Sustainable Biotic and Abiotic Stress Management*, Heba I. Mohamed, Hossam El-Din Saad El-Beltagi and Kamel A. Abd-Elsalam eds., (Springer). doi: 10.1007/978-3-030-66587-6

Hase, S., Shimizu, A., Nakaho, K., Takenaka, S., and Takahashi, H. (2006). Induction of transient ethylene and reduction in severity of tomato bacterial wilt by *Pythium oligandrum*. *Plant Pathol.* 55, 537–543. doi: 10.1111/j.1365-3059.2006.01396.x

Hase, S., Takahashi, S., Takenaka, S., Nakaho, K., Arie, T., Seo, S., et al. (2008). Involvement of jasmonic acid signalling in bacterial wilt disease resistance induced by biocontrol agent *Pythium oligandrum* in tomato. *Plant Pathol.* 57, 870–876. doi: 10.1111/j.1365-3059.2008.01858.x

Hashemi, M., Tabet, D., Sandroni, M., Benavent-Celma, C., Seematti, J., Andersen, C. B., et al. (2021). The hunt for sustainable biocontrol of oomycete plant pathogens, a case study of *Phytophthora infestans*. *Fungal Biol. Rev.* 40, 1–17. doi: 10.1016/j.fbr.2021.11.003

Herlemann, D. P. R., Labrenz, M., Jürgens, K., Bertilsson, S., Waniek, J. J., and Andersson, A. F. (2011). Transitions in bacterial communities along the 2000 km salinity gradient of the Baltic Sea. *ISME J.* 5, 1571–1579. doi: 10.1038/ismej.2011.41

Ho-Plágaro, T., Tamayo-Navarrete, M. I., and García-Garrido, J. M. (2020). Histochemical staining and quantification of arbuscular mycorrhizal fungal colonization. *Methods Mol. Biol.* 2146, 43–52. doi: 10.1007/978-1-0716-0603-2_4

Jatuwong, K., Hyde, K. D., Karunarathna, S. C., Chamyoung, S., and Kakumyan, P. (2017). Two species of Clitopilus (entolomataceae, agaricales) from Northern Thailand. *Chiang Mai J. Sci.* 44, 115–124.

Kaczmarek, A., and Bogus, M. I. (2021). Fungi of entomopathogenic potential in Chytridiomycota and Blastocladiomycota , and in fungal allies of the Oomycota and Microsporidia. *IMA Fungus* 12, 29. doi: 10.1186/s43008-021-00074-y

Kratka, J., Bergmanova, Ev., and Kudelova, A. (1994). Effect of Pythium oligandrum and *Pythium ultimum* on biochemical changes in cucumber (*Cucumis sativus* L .) / Wirkung von *Pythium oligandrum* und *Pythium ultimum* auf biochemische Veränderungen in Gurkenpflanzen (*Cucumis sativus* L .). *J. Plant Dis. Protec.* 101, 406–413. Jirina Kr.

Kumar, M., and Ashraf, S. (2017). Role of *Trichoderma* spp. as a biocontrol agent of fungal plant pathogens. *Probiotics Plant Heal.* 497, 497–506.

Lee, L., Chan, K., Stach, J., Wellington, E. M. H., Lee, L., and Chan, K. (2018). Editorial: the search for biological active agent (s) from actinobacteria. *Front. Microbiol.* 9. doi: 10.3389/fmicb.2018.00824

Le Floch, G., Rey, P., Benizri, E., Benhamou, N., and Tirilly, Y. (2003). Impact of auxin-compounds produced by the antagonistic fungus *Pythium oligandrum* or the minor pathogen *Pythium* group F on plant growth. *Plant Soil* 257, 459–470. doi: 10.1023/A:1027330024834

Lemanceau, P., Blouin, M., Muller, D., and Moënne-Loccoz, Y. (2017). Let the core microbiota be functional. *Trends Plant Sci.* 22, 583–595. doi: 10.1016/j.tplants.2017.04.008

Love, M. I., Huber, W., and Anders, S. (2014). Moderated estimation of fold change and dispersion for RNA-seq data with DESeq2. *Genome Biol.* 15, 1–21. doi: 10.1186/s13059-014-0550-8

Lugtenberg, B., and Kamilova, F. (2009). Plant-growth-promoting rhizobacteria. *Annu. Rev. Microbiol.* 63, 541–556. doi: 10.1146/annurev.micro.62.081307.162918

Malvick, D. K., and Grau, C. R. (2001). Characteristics and frequency of *Aphanomyces euteiches* races 1 and 2 associated with alfalfa in the midwestern United States. *Plant Dis.* 85, 740–744. doi: 10.1094/PDIS.2001.85.7.740

McCarthy, D. J., Chen, Y., and Smyth, G. K. (2012). Differential expression analysis of multifactor RNA-Seq experiments with respect to biological variation. *Nucleic Acids Res.* 40, 4288–4297. doi: 10.1093/nar/gks042

McMurdie, P. J., and Holmes, S. (2012). Phyloseq: A bioconductor package for handling and analysis of high-throughput phylogenetic sequence data. *Pacific Symp. Biocomput.* 235–246. doi: 10.1142/9789814366496_0023

Moussart, A., Even, M. N., and Tivoli, B. (2008). Reaction of genotypes from several species of grain and forage legumes to infection with a French pea isolate of the oomycete *Aphanomyces euteiches*. *Eur. J. Plant Pathol.* 122, 321–333. doi: 10.1007/s10658-008-9297-y

Nagymihály, M., Vásarhelyi, B. M., Barrière, Q., Chong, T. M., Bálint, B., Bihari, P., et al. (2017). The complete genome sequence of Ensifer meliloti strain CCMM B554 (FSM-MA), a highly effective nitrogen-fixing microsymbiont of *Medicago truncatula* Gaertn. *Stand. Genomic Sci.* 12, 1–9. doi: 10.1186/s40793-017-0298-3

Nair, M. G., Safir, G. R., and Siqueira, J. O. (1991). Isolation and identification of vesicular-arbuscular mycorrhiza-stimulatory compounds from clover (*Trifolium repens*) roots. *Appl. Environ. Microbiol.* 57, 434–439. doi: 10.1128/aem.57.2.434-439.1991

Naoumkina, N., Farag, M. A., Sumner, L. W., Tang, Y., Liu, C. J., and Dixon, R. A. (2006). Different mechanisms for phytoalexin induction by pathogen and wound signals in *Medicago truncatula*. *Proc. Natl. Acad. Sci.* 104, (46) 17909–17915. doi: 10.1073/pnas.07086971

Nilsson, R. H., Larsson, K. H., Taylor, A. F. S., Bengtsson-Palme, J., Jeppesen, T. S., Schigel, D., et al. (2019). The UNITE database for molecular identification of fungi: Handling dark taxa and parallel taxonomic classifications. *Nucleic Acids Res.* 47, D259–D264. doi: 10.1093/nar/gky1022

Oksanen, J., Blanchet, F. G., Kindt, R., Legendre, P., Minchin, P. R., O'Hara, R. B., et al. (2014). Vegan: Community Ecology Package. R Package Version 2.2-0. http://CRAN.Rproject.org/package=vegan

Op De Beeck, M., Lievens, B., Busschaert, P., Declerck, S., Vangronsveld, J., and Colpaert, J. V. (2014). Comparison and validation of some ITS primer pairs useful for fungal metabarcoding studies. *PloS One* 9. doi: 10.1371/journal.pone.0097629

Picard, K., Ponchet, M., Blein, J.-P., Rey, P., Tirilly, Y., and Benhamou, N. (2000). Oligandrin. A Proteinaceous Molecule Produced by the MycoparasitePythium oligandrum Induces Resistance to Phytophthora parasitica Infection in Tomato Plants. *Plant Physiol.* 124, 379–396. doi: 10.1104/pp.124.1.379

Quast, C., Pruesse, E., Yilmaz, P., Gerken, J., Schweer, T., Yarza, P., et al. (2013). The SILVA ribosomal RNA gene database project: Improved data processing and web-based tools. *Nucleic Acids Res.* 41, 590–596. doi: 10.1093/nar/gks1219

Ramasamy, N., and Muthukumar, A. (2019). "Arbuscular mycorrhizal fungi and their effectiveness against soil borne diseases," in *Bio-intensive approaches: Application and effectiveness in plant diseases management* (Delhi, India: Today & Tomorrow's Printers and Publishers), 183–199.

Rey, T., and Dumas, B. (2017). Plenty is no plague: *Streptomyces* symbiosis with crops. *Trends Plant Sci.* 22, 30–37. doi: 10.1016/j.tplants.2016.10.008

Robinson, M. D., McCarthy, D. J., and Smyth, G. K. (2009). edgeR: A Bioconductor package for differential expression analysis of digital gene expression data. *Bioinformatics* 26, 139–140. doi: 10.1093/bioinformatics/btp616

Rohart, F., Gautier, B., Singh, A., and Lê Cao, K. A. (2016). mixOmics: An R package for 'omics feature selection and multiple data integration. *PLoS Comp. Biol.* 13 (11), e1005752. doi: 10.1371/journal.pcbi.1005752

Salem, M. A., Jüppner, J., Bajdzienko, K., and Giavalisco, P. (2016). Afast , comprehensive and reproducible one – step extraction method for the rapid preparation of polar and semi – polar metabolites , lipids , proteins , starch and cell wall polymers from a single sample. *Plant Methods* 12, 1–15. doi: 10.1186/s13007-016-0146-2

Shoham, J. (2020). The rise of biological products in the crop protection and plant nutrition markets. *Outlooks Pest Manage.* 31, 129–131. doi: 10.1564/v31_jun_09

Siqueira, J. O., Safir, G. R., and Nair, M. G. (1991). Stimulation of vesicular-arbuscular mycorrhiza formation and growth of white clover by flavonoid compounds. *New Phytol.* 118, 87–93. doi: 10.1111/j.1469-8137.1991.tb00568.x

Stevenson, P. C., Turner, H. C., and Haware, M. P. (1997). Phytoalexin accumulation in the roots of chickpea (*Cicer arietinum* L.) seedlings associated with resistance to fusarium wilt (*Fusarium oxysporum* f.sp. *ciceri*). *Physiol. Mol. Plant Pathol.* 50, 167–178. doi: 10.1006/pmpp.1997.0082

Sui, L., Li, J., Philp, J., Yang, K., Wei, Y., Li, H., et al. (2022). *Trichoderma atroviride* seed dressing influenced the fungal community and pathogenic fungi in the wheat rhizosphere. *Sci. Rep.* 12, 1–12. doi: 10.1038/s41598-022-13669-1

Takenaka, S. (2015). Studies on biological control mechanisms of *Pythium oligandrum*. *J. Gen. Plant Pathol.* 81, 466–469. doi: 10.1007/s10327-015-0620-0

Takenaka, S., Nishio, Z., and Nakamura, Y. (2003). Induction of defense reactions in sugar beet and wheat by treatment with cell wall protein fractions from the mycoparasite *Pythium oligandrum*. *Phytopathology* 93, 1228–1232. doi: 10.1094/PHYTO.2003.93.10.1228

Takenaka, S., Yamaguchi, K., Masunaka, A., Hase, S., Inoue, T., and Takahashi, H. (2011). Implications of oligomeric forms of POD-1 and POD-2 proteins isolated from cell walls of the biocontrol agent *Pythium oligandrum* in relation to their ability to induce defense reactions in tomato. *J. Plant Physiol.* 168, 1972–1979. doi: 10.1016/j.jplph.2011.05.011

Tsugawa, H., Cajka, T., Kind, T., Ma, Y., Higgins, B., Ikeda, K., et al. (2015). MS-DIAL: Data-independent MS/MS deconvolution for comprehensive metabolome analysis. *Nat. Methods* 12, 523–526. doi: 10.1038/nmeth.3393

Tsugawa, H., Kind, T., Nakabayashi, R., Yukihira, D., Tanaka, W., Cajka, T., et al. (2016). Hydrogen rearrangement rules: computational MS/MS fragmentation and structure elucidation using MS-FINDER Software. *Anal. Chem.* 88, 7946–7958. doi: 10.1021/acs.analchem.6b00770

Uhlig, E., Kjellstrom, A., Nurminen, N., Olsson, C., Oscarsson, E., and Canaviri-paz, P. (2021). Use of bacterial strains antagonistic to *Escherichia coli* for biocontrol of spinach: A field trial. *Innov. Food Sci. Emerg. Techno* 74. doi: 10.1016/j.ifset.2021.102862

Upadhyay, A. K., Bandi, S. R., and Maruthi, P. D. (2021). BioControl agents -antagonistic magicians against soil borne pathogens: A review. *Biol. Forum Int. J.* 13, (1) 232–242.

Vallance, J., Déniel, F., Barbier, G., Guerin-Dubrana, L., Benhamou, N., and Rey, P. (2012). Influence of *Pythium oligandrum* on the bacterial communities that colonize the nutrient solutions and the rhizosphere of tomato plants. *Can. J. Microbiol.* 58, 1124–1134. doi: 10.1139/w2012-092

Vallance, J., Le Floch, G., Déniel, F., Barbier, G., Lévesque, C. A., and Rey, P. (2009). Influence of *Pythium oligandrum* biocontrol on fungal and oomycete population dynamics in the rhizosphere. *Appl. Environ. Microbiol.* 75, 4790–4800. doi: 10.1128/AEM.02643-08

Vesely, D. (1977). Potential biological control of damping-off pathogens in emerging sugar beet by *Pythium oligandrum* Dreschsler Phytopathologische Zeitschrift (Germany, FR). *J. Phytopathology* 90, 113–115. doi: 10.1111/j.1439-0434.1977.tb03225.x

Vierheilig, H., Coughlan, A. P., Wyss, U., and Piché, Y. (1998). Ink and vinegar, a simple staining technique for arbuscular-mycorrhizal fungi. *Appl. Environ. Microbiol.* 64, 5004–5007. doi: 10.1128/aem.64.12.5004-5007.1998

Wulff, E. G., Pham, A. T. H., Chérif, M., Rey, P., Tirilly, Y., and Hockenhull, J. (1998). Inoculation of cucumber roots with zoospores of mycoparasitic and plant pathogenic *Pythium* species: Differential zoospore accumulation, colonization ability and plant growth response. *Eur. J. Plant Pathol.* 104, 69–76. doi: 10.1023/A:1008662927507

Yacoub, A., Haidar, R., Gerbore, J., Masson, C., Dufour, M. C., Guyoneaud, R., et al. (2020). *Pythium oligandrum* induces grapevine defence mechanisms against the trunk pathogen *Neofusicoccum parvum*. *Phytopathol. Mediterr.* 59, 565–580. doi: 10.14601/Phyto-11270

frontiers | Frontiers in Plant Science

TYPE Original Research
PUBLISHED 28 March 2024
DOI 10.3389/fpls.2024.1332976

OPEN ACCESS

EDITED BY
Filipa Monteiro,
University of Lisbon, Portugal

REVIEWED BY
Guillermo A. Galvan,
Universidad de la República, Uruguay
Mihir Kumar Mandal,
University of California, Davis, United States

*CORRESPONDENCE
Christophe Le May
christophe.lemay@agrocampus-ouest.fr
Marie-Laure Pilet-Nayel
marie-laure.pilet-nayel@inrae.fr

†These authors have contributed equally to this work and share first authorship

‡These authors have contributed equally to this work and share last authorship

RECEIVED 04 November 2023
ACCEPTED 01 March 2024
PUBLISHED 28 March 2024

CITATION
Moussart A, Lavaud C, Onfroy C, Leprévost T, Pilet-Nayel M-L and Le May C (2024) Pathotype characterization of *Aphanomyces euteiches* isolates collected from pea breeding nurseries.
Front. Plant Sci. 15:1332976.
doi: 10.3389/fpls.2024.1332976

Pathotype characterization of *Aphanomyces euteiches* isolates collected from pea breeding nurseries

Anne Moussart[1†], Clément Lavaud[2†], Caroline Onfroy[1], Théo Leprévost[2], Marie-Laure Pilet-Nayel[2*‡] and Christophe Le May[3*‡]

[1]Terres Inovia, Le Rheu, France, [2]IGEPP, INRAE, Institut Agro, Univ Rennes, Le Rheu, France, [3]IGEPP, INRAE, Institut Agro, Univ Rennes, Rennes, France

Introduction: *Aphanomyces euteiches* Drechsler is an oomycete pathogen that affects legume crops, causing root rot, a severe disease of peas (*Pisum sativum* L.) worldwide. While significant research progress has been made in breeding pea-resistant varieties, there is still a need for a deeper understanding of the diversity of pathogen populations present in breeding nurseries located in various legume-growing regions around the world.

Methods: We analysed the diversity of 51 pea-infecting isolates of *A. euteiches*, which were recovered from four American (Athena, OR; Le Sueur, MN; Mount Vernon, WA; Pullman, WA) and three French (Riec-sur-Belon, Templeux-le-Guérard, Dijon) resistance screening nurseries. Our study focused on evaluating their aggressiveness on two sets of differential hosts, comprising six pea lines and five *Medicago truncatula* accessions.

Results: The isolates clustered into three groups based on their aggressiveness on the whole pea set, confirming the presence of pathotypes I and III. Pathotype I was exclusive to French isolates and American isolates from Athena and Pullman, while all isolates from Le Sueur belonged to pathotype III. Isolates from both pathotypes were found in Mount Vernon. The *M. truncatula* set clustered the isolates into three groups based on their aggressiveness on different genotypes within the set, revealing the presence of five pathotypes. All the isolates from the French nurseries shared the same Fr pathotype, showing higher aggressiveness on one particular genotype. In contrast, nearly all-American isolates were assigned to four other pathotypes (Us1, Us2, Us3, Us4), differing in their higher aggressiveness on two to five genotypes. Most of American isolates exhibited higher aggressiveness than French isolates within the *M. truncatula* set, but showed lower aggressiveness than French isolates within the *P. sativum* set.

Discussion: These results provide valuable insights into *A. euteiches* pathotypes, against which the QTL and sources of resistance identified in these nurseries displayed effectiveness. They also suggest a greater adaptation of American isolates to alfalfa, a more widely cultivated host in the United States.

KEYWORDS

Aphanomyces root rot, virulence, aggressiveness, differential genotypes, *Pisum sativum*, *Medicago truncatula*

Introduction

Aphanomyces euteiches Drechsler is an oomycete pathogen affecting various legume species and causing the devastating root rot of peas (*Pisum sativum* L.) worldwide (Harveson et al., 2021). In Europe, *A. euteiches* was first observed in Norway in 1925 (Sundheim, 1972), and was reported a few years later in France (Labrousse, 1933), where it has been considered as the most important pathogen of peas since 1993 (Didelot and Chaillet, 1995). The pathogen causes root rots, which develop depending on high soil moisture and are optimal between 16°C and 28°C (Papavizas and Ayers, 1974). In favourable conditions, Cunningham and Hagedorn (1962) observed the rapid invasion of the root cortex, as well as the appearance of the sexual stage (oospores), a few days after the infection. The disease often appears early in the spring, affecting young pea plants, and yield losses may be considerable. Oospores were reported to resist adverse conditions, such as alternate freezing and thawing, dry conditions (Sherwood and Hagedorn, 1962), and to survive in soils for 10 to 20 years in the absence of susceptible crops (Pfender and Hagedorn, 1983). *A. euteiches* displays a broad host range within the legume family (Levenfors et al., 2003; Moussart et al., 2008). Initially regarded as exclusively infecting peas (Scott, 1961), *A. euteiches* was later reported as a pathogen that can also attack other legume species, including common bean, broad bean, faba bean, clover, and alfalfa (Pfender and Hagedorn, 1982; Greenhalgh and Merriman, 1985; Lamari and Bernier, 1985; Burnett et al., 1994; Tivoli et al., 2006; Moussart et al., 2008).

Understanding the diversity of pathogenicity within pathogen populations is crucial for optimizing effective strategies for plant disease management. The diversity of pathogenicity within *A. euteiches* populations infecting peas has been documented in grower fields across multiple countries. However, there have been only a few studies that have compared *A. euteiches* populations between countries. No study has yet provided a description of *A. euteiches* populations from contaminated nurseries used for pea resistance screenings. However, such knowledge is essential for understanding the pathogen populations that interact with the resistance sources, loci or breeding lines during the creation and deployment of pea resistant varieties. In addition, there is a lack of knowledge about the diversity of *A. euteiches* populations that infect peas and their adaptation to other commonly grown legume hosts, such as alfalfa (*Medicago sativa*). Better understanding whether populations are adapted to multiple legume hosts could potentially facilitate the transfer of genetic knowledge regarding resistance from one host to another.

In pea, Wicker and Rouxel (2001) initially identified two main pathotypes within a collection of 109 pea-infecting isolates, based on their differential reactions on a set of six pea genotypes (Wicker et al., 2003). Among these isolates, 88 isolates were from France, and 21 originated from Denmark, Sweden, Norway, the USA, Canada and New Zealand. All French isolates were classified as pathotype I and showed a wide range of aggressiveness. In contrast, a distinct pathotype, named pathotype III, was identified among American isolates and characterized by reduced aggressiveness towards the pea genotype MN313. Regardless of their pathotype, all American isolates displayed lower aggressiveness towards peas compared to French isolates. In an additional study including 34 *A. euteiches* isolates of pathotype I collected from the main pea-growing regions in France, Quillévéré-Hamard et al. (2018) detected a moderate level of pathogenicity diversity across various legume hosts. However, some isolates from fields with a history of diversified legume cultivation exhibited specific genetic patterns. More recently, Sivachandra et al. (2021) identified primarily pathotype I among 32 Canadian isolates collected from fields in Saskatchewan and Alberta, and only three isolates of pathotype III. In Europe, Kälin et al. (2022) showed varying levels of disease severity on pea genotypes, caused by ten *A. euteiches* isolates collected from pea fields in four countries (Sweden, Finland, Italy, France) and representing three genetic clusters, but no specific pathotype was identified.

In alfalfa, Malvick and Grau (2001) and Fitzpatrick et al. (1998) described two pathotypes (race 1 and race 2), based on the reaction of *A. euteiches* isolates on three differential lines (Saranac, Waph-1 and Waph-5). In a survey of 30 fields across 18 counties in Illinois, Malvick et al. (2009) highlighted the diversity of *A. euteiches* populations in alfalfa fields. These populations frequently consisted of both races 1 and 2. In addition, Holub et al. (1991) showed that 97% of isolates collected from pea fields in Wisconsin (USA) had the capacity to infect alfalfa. In contrast, only a limited number of isolates from alfalfa fields displayed pathogenicity towards peas. Wicker et al. (2001) also demonstrated that among

91 pea-infecting isolates from France, the majority were pathogenic on alfalfa. The wide host range of pea-infecting isolates of *A. euteiches* has led several authors to hypothesize that crop rotations involving peas and other legumes such as alfalfa, could potentially facilitate the emergence of complex pathogen populations consisting of multiple pathotypes, promoting population adaptation to different legume hosts (Malvick et al., 1998; Wicker and Rouxel, 2001; Wicker et al., 2001; Levenfors and Fatehi, 2004). The model legume *M. truncatula* is also susceptible to *A. euteiches* infection. Moussart et al. (2007) identified a continuum of variation, ranging from resistance to susceptibility, among different accessions of *M. truncatula* when exposed to a single pea isolate of *A. euteiches*. A similar variation was also observed in *M. truncatula* accessions evaluated for resistance to alfalfa race 2 isolates of *A. euteiches* (Vandemark and Grunwald, 2004). Resistance was shown to be either controlled by a major locus (Pilet-Nayel et al., 2009; Bonhomme et al., 2014), or by a complex genetic network of minor QTL (Hamon et al., 2010), depending on the *A. euteiches* pea or alfalfa pathotype considered. These observations led to hypothesize that the model species *M. truncatula* may constitute an efficient bridge for comparing the expression and genetic control of resistance to *A. euteiches* between grain and forage legumes (Tivoli et al., 2006).

Thus, various studies have characterized pathotypes of pea- or alfalfa- infecting isolates of *A. euteiches* isolated from commercial pea fields. However, the characterization of *A. euteiches* isolates found in breeding nurseries has remained unreported, despite its significance in the development of resistant varieties effective against *A. euteiches* populations within commercial legume fields. To address this gap, a transatlantic collection of 51 A. *euteiches* isolates collected from French and American breeding nurseries was established. These nurseries were grown with pea research genetic material employed to detect Quantitative Trait Loci (QTL) for resistance to *A. euteiches* (Hamon et al., 2013; Desgroux et al., 2016). Genetic structure analysis of this collection using Sequence-Related Amplified Polymorphism (SRAP) (Le May et al., 2018) or Simple Sequence Repeat (SSR) (Mieuzet et al., 2016) markers clustered the French and American isolates in two different groups, showing higher genetic diversity between countries than within them. However, this collection has not yet been characterized for its pathogenicity diversity.

The objective of this study was to characterize the pathotypes of *A. euteiches* isolates from the transatlantic collection, focusing on their aggressiveness and virulence towards both pea and *M. truncatula*. Two questions were addressed: (i) are the pathotypes found in French and American nurseries consistent with those employed in genetics and breeding programs? (ii) are American isolates better adapted to *Medicago* spp., a legume species more extensively cultivated in the USA than in France? In this study, we evaluated the aggressiveness and virulence of the 51 A. *euteiches* isolates from the transatlantic collection established by Le May et al. (2018) on a set of pea differential genotypes, as defined by Wicker et al. (2001), and on a new set of *M. truncatula* accessions specifically curated for this work.

Materials and methods

Pathogen material

The 51 isolates of *A. euteiches* employed in this study were collected from contaminated nurseries in 2005 and subsequently baited following the protocol presented in Le May et al. (2018). The set included 25 isolates originating from three French nurseries, *i.e.* ten isolates from Dijon (isolates Di1 to Di10), ten isolates from Templeux-le-Guérard (Tpx1 to Tpx10) and five isolates from Riec-sur-Belon (Ri2, Ri4, Ri7, Ri8 and Ri10). In addition, this study included 26 isolates from four nurseries in the United States (US), *i.e.* seven isolates from Athena (Ath1 to Ath7), nine isolates from Le Sueur (LS1 to LS3, LS5 to LS10), five isolates from Mount-Vernon (MV1, MV3 to MV5 and MV7) and five isolates from Pullman (Plm1 to Plm4 and Plm7). The nurseries were characterized based on distinct growing seasons and climatic conditions (Additional File 1). All 51 isolates were single-spored, grown, and maintained on Corn Meal Agar (CMA) at a temperature of 10°C. Two isolates were employed as standards in this study: RB84, originating from a pea field in Riec-sur-Belon, France, selected as the reference isolate for pathotype I (Moussart et al., 2007); and Ae109, also known as synonym 467, collected in Wisconsin, USA, used as the reference isolate for pathotype III (Malvick et al., 1998; Wicker and Rouxel, 2001).

Plant material

The pea differential set previously established by Wicker et al. (2003), was used in this study to distinguish the two main pathotypes I and III, according to the differential reaction of the MN313 genotype. The pea set consisted of a total of six genotypes, including (i) the spring-sown field pea cultivars Baccara (Ets Florimond Desprez) and Capella (Svalöf Weïbull AB), (ii) the garden pea breeding lines MN313 (Davis et al., 1995), 552 (Gritton, 1995) and 90-2131 (Kraft, 1992), and (iii) the germplasm accession PI180693 (USDA Plant Introduction Pullman).

The *M. truncatula* differential set consisted of a total of five genotypes, including A17 (Australia), DZA045.5 (Algeria), F83005.5 (France), DZA241.2.2 (Algeria) and F83005.9 (France) (Moussart et al., 2007). The establishment of the *M. truncatula* differential set involved a two-step process. Initially, a screening of 112 *M. truncatula* pure lines (obtained from Dr Prosperi, INRAE Montpellier, UMR AGAP, Mauguio, France) using the reference isolate RB84 (Pilet-Nayel et al., 2005) led to the selection of a subset of 15 accessions based on their differential responses. Then, these 15 *M. truncatula* accessions were screened using both reference isolates RB84 and Ae109, according to the procedure presented in Moussart et al. (2007), resulting in the selection of five genotypes. Notably, Ae109 was more aggressive on all the five genotypes than RB84. DZA045.5 and F83005.5 were partially resistant and susceptible to both isolates, respectively. DZA241.2, A17 and F83005.9 showed differential reactions to both isolates (unpublished results).

Pathogenicity tests

Pathogenicity experiments were conducted at INRAE, IGEPP (Le Rheu, France). In these experiments, all isolates were tested on both the pea and *M. truncatula* differential sets within the same growth chamber.

For the pea differential sets comprising both pea and *M. truncatula* genotypes, the methods described by Moussart et al. (2001) and Moussart et al. (2007), were followed, respectively. Zoospores were produced following the method described by Wicker et al. (2001) for the French isolates. However, for the American isolates that did not yield sufficient zoospores under these conditions, we made adjustment to the culture process. Specifically, we transferred six agar discs from four-day-old cultures on CMA to glucose-peptone broth. These discs were then incubated at 22°C (instead of 25°C) for a period of three days before being rinsed with sterilized Volvic® water, following the same rinsing procedure as described above.

Pea and *M. truncatula* seeds were planted in 500 ml plastic pots (5 plants/pot) filled with vermiculite (VERMEX, M, Soprema, France). Each pot was considered as an experimental unit and there were three replicates per isolate x host combination in each independent experiment. Two independent experiments were performed for each isolate. A total of 30 plants (5 plants * 3 replicates * 2 independent experiments) was evaluated per isolate x host combination. Pots were arranged in a completely randomised design within a growth-chamber under controlled conditions, maintaining temperatures ranging within 23-25°C and a photoperiod of 14 h. Seven days after sowing, seedlings were inoculated by applying 5 ml of inoculum suspension at the base of each plant (10^3 zoospores per plant on pea; 10^4 zoospores per plant on *M. truncatula*) using a pipette. After inoculation, the vermiculite was saturated with water to favour disease development. Pea and *M. truncatula* plants were removed 7 and 14 days after inoculation, respectively, and disease severity was visually evaluated on infected roots using a scoring scale ranging from 0 to 5 scoring, as previously described by Moussart et al. (2007): 0 = no symptoms; 1 = traces of discoloration on the roots (<25%); 2 = discoloration of 25 to 50% of the roots; 3 = discoloration of 50 to 75% of the roots; 4 = discoloration of more than 75% of the roots; 5 = dead plant.

Data analysis

Statistical analyses of variance were conducted using R software (R version 4.3.1; R Core Team, 2023). Disease severity data obtained from the pea and *M. truncatula* differential sets were analysed separately, using a linear mixed model [LMM; 'lmer' function (Bates et al., 2015)], considering the disease severity as the explanatory variable, the genotype, the isolate, and the genotype x isolate interaction as fixed factors, and the experiment effect as random factor. Estimated Marginal Mean (EMMean) values were estimated for each genotype and isolate combination using the 'emmeans' function (Lenth, 2023). Multiple comparisons of EMMean values were performed (i) between pea or *M. truncatula* genotypes for each isolate, and (ii) between isolates for each nursery based on the mean response of each set of pea or *M. truncatula* genotypes, with the Tukey test (α=5%), using the 'cld' function (Graves et al., 2019). For each isolate, phenotypes of pathogenicity were defined based on significant differences of disease severity values between the six pea genotypes or between the five *M. truncatula* lines. The effect of the country of origin of the isolates on the mean disease severity observed on each set of pea or *M. truncatula* genotypes was tested using a general linear model [LM; 'lm' function (Chambers, 1992)], with the disease severity as the explanatory variable and the country as fixed factor.

Principal component analysis (PCA) and hierarchical clustering analysis (HCA) were performed based on EMMean values obtained separately from pea and *M. truncatula* genotypes, using R software. PCA was conducted to analyse similarities of i=53 or 52 isolates of *A. euteiches* (the analysis included Ae109 and RB84 reference isolates; the LS9 isolate was not tested with the *M. truncatula* differential set of genotypes), for pea or *M. truncatula* data, respectively. The 'PCA' function implemented in the 'FactoMineR' package was used for this analysis (Lê et al., 2008). HCA was performed to define different clusters of isolates using the Ward D method aiming to minimize the variance within each defined cluster (Murtagh and Legendre, 2014). HCA was implemented using the 'dist' and 'hclust' functions from R.

Results

Aggressiveness and virulence of the *A. euteiches* isolates on the pea differential set

The pea differential set allowed the identification of the two distinct pathotypes I and III within the collection of 51 isolates of *A. euteiches*. This identification was based on the varying responses observed in the pea genotype MN313. Isolates belonging to the pathotype I displayed aggressiveness across the entire set of genotypes. In contrast, isolates belonging to the pathotype III showed lower aggressiveness when interacting with the genotype MN313 (Additional File 2A). Disease severity on MN313 was significantly lower ($P < 0.001$) compared to that on Baccara and Capella, the most susceptible genotypes. In addition, it was either equal to or lower than the disease severity observed on PI180693, the most resistant genotype among the set.

Among the 25 isolates obtained from French nurseries, 22 isolates belonged to the pathotype I (Table 1). Three isolates (Di6, Di7 and Di9) were not assigned to a pathotype group since they displayed intermediate behaviours that fell between the characteristics of pathotypes I and III. For two of the three isolates, disease severity values on MN313 (2.8 and 2.1 for Di6 and Di7, respectively) were higher than what is typically observed for isolates belonging to pathotype III. For Di9 isolate, disease severity on Capella (1.8) was lower than generally observed for isolates belonging to pathotype III. In addition, these values were significantly lower than those recorded on Baccara and Capella, and matched the disease severity observed on PI180693, as observed for isolates belonging to pathotype I. Significant variability in the mean

10.3389/fpls.2024.1332976

TABLE 1 Disease severity on six pea differential host genotypes, for 51 *A. euteiches* isolates and two *A. euteiches* reference isolates (RB84 and Ae109), from French and American nurseries.

Nursery	Isolate	Genotype [a]						Pathotype [b]	EMMeans Disease Severity [c]	HAC groups [d]
		Baccara	Capella	MN313	552	90-2131	PI180693			
Dijon (FR)	Di1	3.4 a	3.3 ab	3.0 bc	3.1 ab	2.5 d	2.7 cd	I	3.0 CDE	2
	Di2	3.7 a	3.3 b	3.0 bc	2.7 c	2.8 c	2.7 c	I	3.0 CDE	2
	Di3	3.8 a	3.3 b	3.1 bc	2.9 c	2.9 c	2.9 c	I	3.1 E	2
	Di4	3.5 a	3.0 b	2.8 bc	2.6 c	2.7 bc	2.6 c	I	2.9 C	2
	Di5	3.4 a	3.4 a	3.3 a	2.7 b	2.8 b	2.9 b	I	3.1 DE	2
	Di6	3.5 a	3.3 a	2.8 b	2.5 c	2.8 bc	2.8 bc	NA	3.0 CD	2
	Di7	3.0 a	2.5 b	2.1 cd	2.2 bc	1.8 d	2.1 cd	NA	2.3 B	1
	Di8	3.6 a	3.1 b	3.0 bc	2.8 c	2.8 bc	2.7 c	I	3.0 CDE	2
	Di9	2.8 a	1.8 b	1.4 c	1.5 bc	1.7 bc	1.6 bc	NA	1.8 A	1
	Di10	3.5 a	3.1 b	3.1 b	2.9 b	2.9 b	2.9 b	I	3.1 DE	2
Riec-sur-Belon (FR)	Ri2	3.8 a	3.2 bc	3.3 b	3.2 bc	2.9 c	2.9 c	I	3.2 BC	2
	Ri4	3.8 a	3.3 b	3.7 a	3.0 b	3.0 b	3.0 b	I	3.3 C	2
	Ri7	3.8 a	3.4 b	3.5 ab	3.1 bc	2.9 c	2.8 c	I	3.3 C	2
	Ri8	3.6 a	3.3 ab	3.3 ab	3.1 b	2.9 b	2.5 c	I	3.1 AB	2
	Ri10	3.5 a	3.2 a	3.3 a	2.7 b	2.5 b	2.8 b	I	3.0 A	2
Templeux-Le-Guérard (FR)	Tpx1	3.6 a	3.2 b	2.7 c	1.9 d	1.6 d	1.8 d	I	2.5 A	2
	Tpx2	3.3 a	3.0 ab	2.9 b	2.7 b	2.2 c	2.1 c	I	2.7 BC	2
	Tpx3	3.6 a	3.2 ab	3.2 bc	2.9 c	2.9 bc	2.9 c	I	3.1 EF	2
	Tpx4	3.5 a	3.0 b	2.7 bc	2.4 cd	2.4 d	2.5 cd	I	2.8 CD	2
	Tpx5	3.7 a	3.2 b	3.3 b	3.0 b	2.7 c	2.7 c	I	3.1 E	2
	Tpx6	3.3 a	2.8 b	3.2 a	2.5 b	1.6 c	1.7 c	I	2.5 AB	2
	Tpx7	3.6 a	3.4 a	3.4 a	2.8 b	2.0 c	2.1 c	I	2.9 D	2
	Tpx8	3.7 a	3.8 a	3.5 a	2.4 b	2.3 b	1.6 c	I	2.9 D	2
	Tpx9	3.7 a	3.6 a	3.5 a	3.1 b	3.1 b	2.7 c	I	3.3 F	2
	Tpx10	3.8 a	3.3 b	3.3 b	2.5 c	2.2 cd	1.8 d	I	2.8 CD	2
Athena (US)	Ath1	3.3 a	2.9 bc	3.1 ab	2.9 bc	2.7 cd	2.3 d	I	2.9 E	2
	Ath2	2.9 a	3.0 a	2.8 a	2.8 a	1.8 b	1.4 b	I	2.4 C	2
	Ath3	3.8 a	3.3 b	3.2 bc	3.1 bc	2.9 c	2.8 c	I	3.2 F	2
	Ath4	3.0 a	3.0 a	2.7 ab	2.5 bc	2.3 c	2.3 c	I	2.7 D	2
	Ath5	3.1 a	3.0 ab	2.8 b	2.2 c	1.9 d	1.7 d	I	2.4 C	2
	Ath6	3.1 a	2.9 a	2.1 b	1.9 bc	1.6 cd	1.4 d	I	2.2 B	1
	Ath7	2.8 a	2.1 b	1.8 bc	1.6 cd	1.3 de	1.0 e	I	1.8 A	1
Le Sueur (US)	LS1	2.7 a	2.2 b	0.9 d	1.9 b	1.4 c	1.4 c	III	1.8 C	1
	LS2	3.2 a	3.0 a	1.5 c	2.2 b	1.6 c	1.5 c	III	2.1 DE	1
	LS3	3.1 a	2.8 a	1.1 d	2.2 b	1.8 c	1.5 c	III	2.1 D	1
	LS5	3.3 a	3.0 a	1.7 cd	2.5 b	1.9 c	1.4 d	III	2.3 EF	1

(Continued)

10.3389/fpls.2024.1332976

TABLE 1 Continued

Nursery	Isolate	Genotype [a]						Pathotype [b]	EMMeans Disease Severity [c]	HAC groups [d]
		Baccara	Capella	MN313	552	90-2131	PI180693			
	LS6	1.6 a	1.5 ab	1.0 c	1.0 c	1.2 bc	1.0 c	NA	1.2 A	1
	LS7	3.4 a	2.9 b	1.5 d	2.3 c	1.6 d	1.3 d	III	2.1 DE	1
	LS8	3.1 a	2.8 a	1.3 c	1.9 b	1.9 b	1.5 c	III	2.1 D	1
	LS9	2.4 a	2.4 a	0.4 d	1.8 b	1.0 c	1.3 bc	III	1.6 B	1
	LS10	3.1 a	3.0 ab	1.5 d	2.6 b	2.3 c	2.2 c	III	2.5 F	1
Mount Vernon (US)	MV1	2.9 a	2.0 b	1.8 bc	1.5 c	1.5 c	1.5 c	I	1.8 A	1
	MV3	3.2 a	2.8 a	0.9 c	2.2 b	2.0 b	2.2 b	III	2.2 B	1
	MV4	2.9 a	3.0 a	1.1 c	2.3 b	2.3 b	2.0 b	III	2.3 B	1
	MV5	3.0 a	2.8 a	2.3 b	1.9 c	1.8 c	2.0 c	I	2.3 B	1
	MV7	3.7 a	3.3 b	3.0 bc	2.7 cd	2.6 d	2.9 cd	I	3.0 C	2
Pullman (US)	Plm1	3.0 a	2.7 a	2.2 b	2.0 b	1.1 c	1.1 c	I	2.0 A	1
	Plm2	3.4 a	3.2 a	3.1 a	2.3 b	1.5 c	1.3 c	I	2.5 B	2
	Plm3	3.3 a	3.1 a	2.7 b	2.7 b	2.3 c	1.6 d	I	2.6 C	2
	Plm4	3.4 a	3.1 ab	2.8 bc	2.6 c	1.6 d	1.5 d	I	2.5 BC	2
	Plm7	3.2 a	3.1 a	2.9 a	3.0 a	2.4 b	2.2 b	I	2.8 D	2
Standard isolates	RB84	3.7 a	3.4 b	3.3 b	3.0 c	2.7 d	2.4 e	I	3.1	2
	Ae109	3.3 a	2.9 b	1.2 d	2.1 c	2.1 c	1.8 c	III	2.2	1

Disease severity was recorded on a scale from 0 (no symptoms) to 5 (dead plant). [a] For each isolate (*i.e.* each row), EMMean values on the different pea genotypes followed by the same lower case letter are not significantly different (Tukey test, α=5%). [b] Pathotypes identified according to Wicker et al. (2003) and Wicker and Rouxel (2001); NA: isolates with undefined pathotypes. [c] Between isolates for each nursery, EMMean values on all pea genotypes followed by the same upper-case letter are not significantly different (Tukey test, α=5%). [d] Hierarchical Ascending Classification groups obtained from the Ward D method in this study.

disease severity across the entire set of pea genotypes was observed among the French isolates ($P < 0.001$). For each isolate, the range of disease severity observed across the six pea genotypes was low ($0.6 < Range_{DS} < 1.2$) but significant ($P < 0.001$), except for five isolates from Templeux-le-Guérard (Tpx1, Tpx6, Tpx7, Tpx8 and Tpx10; $1.5 < Range_{DS} < 2.2$) and one isolate from Dijon (Di9; $Range_{DS} = 1.4$), exhibiting larger range of disease severity but lower mean level of aggressiveness.

Among the 26 isolates obtained from American nurseries, 15 were classified as belonging to pathotype I (Table 1). One isolate (LS6) was not assigned to a pathotype group since it displayed intermediate behaviour between the characteristics of pathotype I and III. For LS6 isolate, the disease severity on Capella (1.5) was lower than that usually observed for pathotype III isolates. The remaining ten isolates belonged to pathotype III, showing significantly lower disease severity on MN313 than those observed on Baccara and Capella. Additionally, their disease severity matched or was even lower than that on PI180693, as displayed by the reference isolate Ae109. All the isolates from Athena and Pullman nurseries belonged to pathotype I. All the isolates from Le Sueur (except LS6) belonged to pathotype III. However, in the case of Mount-Vernon isolates, there was a split: some were categorized as pathotype I (MV1, MV5, and MV7), while others fell into pathotype III (MV3 and MV4). The majority of American isolates distinguished between susceptible and partially resistant genotypes within the differential set. Significant variability for mean disease severity across the entire set of pea genotypes was observed within isolates from the United States. Four American isolates, including Ath7 and MV1 from pathotype I, as well as LS1 and LS9 from pathotype III, showed low mean disease severity values (≤1.8) over the whole set of pea genotypes. Conversely, isolates Ath3 and MV7 showed high mean disease severity values (≥3) across the entire set. Overall, the American isolates showed a lower level of aggressiveness compared to the French isolates when tested on the set of pea genotypes (Figure 1).

PCA mainly distinguished the 51 isolates based on their level of aggressiveness across the entire set of pea genotypes, as shown by the high percentage of total variation explained by the first principal component (PCA.Dim1: 78.78%) (Figure 2A). Isolates classified as pathotype I exhibited a higher level of aggressiveness when evaluated on the differential set of pea genotypes in comparison to isolates belonging to pathotype III. The second (PCA.Dim2: 9.76%) and third (PCA.Dim3: 5.06%) principal components of the analysis separated isolates based on their aggressiveness towards susceptible versus partially resistant pea genotypes and the MN313 genotype, respectively. Variability in aggressiveness was observed among pathotypes I and III for susceptible and partially resistant

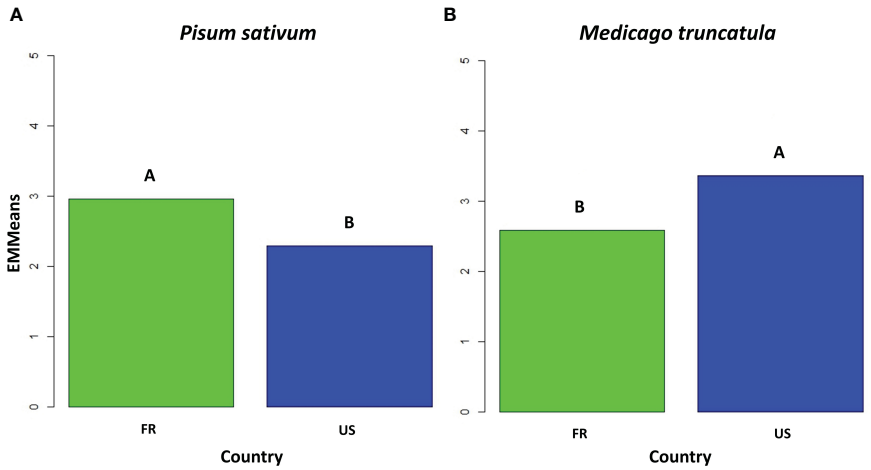

FIGURE 1
Bar plot of disease severity adjusted means for the French (FR) and American (US) isolates of the transatlantic collection of *A. euteiches* and two *A. euteiches* reference isolates (n=52), **(A)** on the six pea differential genotypes, and **(B)** the five *Medicago truncatula* differential genotypes. Significantly different means are indicated by letters (Tukey test, α = 1%).

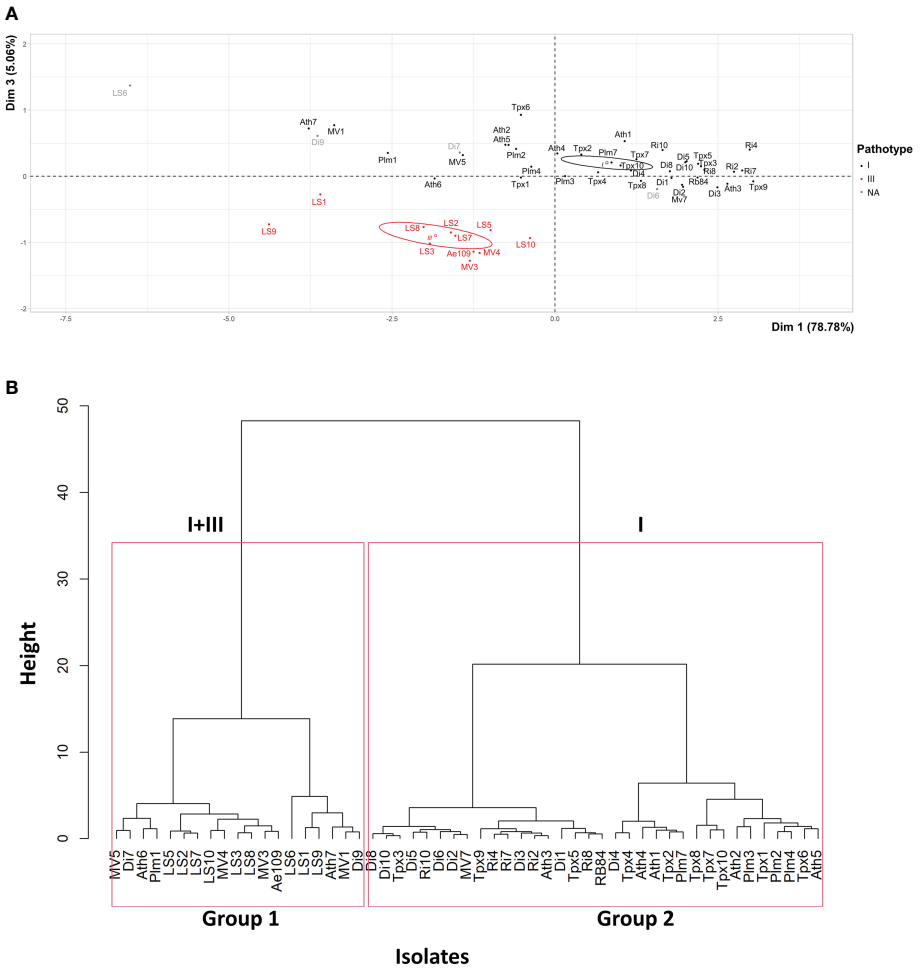

FIGURE 2
(A) Principal Component Analysis and **(B)** Hierarchical Ascending Classification, of 51 *A. euteiches* isolates from the US-FR transatlantic collection and two *A. euteiches* reference isolates (RB84 and Ae109), based on disease severity data on six pea differential genotypes. I, III: pathotypes I and III of *A. euteiches*. NA, isolates with undefined pathotype. Confidence ellipses, calculated at the confidence level of 95%, are overlaid to visualize the grouping patterns.

10.3389/fpls.2024.1332976

genotypes (Dim2, not shown). Isolates from pathotype III clustered based on aggressiveness towards MN313 (Dim3, Figure 2A).

HAC identified two groups among the 51 isolates, according to their mean level of aggressiveness across the set of pea genotypes, which aligns with the results from the PCA (Figure 2B). Group 1 comprised 18 isolates, along with the standard Ae109 isolate. This group encompassed 16 isolates from American nurseries and two isolates from French nurseries. This group also included six isolates, mostly collected from American nurseries, displaying lower levels of aggressiveness. Among these isolates, two were from pathotype I (Ath7, MV1), two were from pathotype III (LS1, LS9), and two isolates from French nurseries (LS6, Di9) were unassigned to a pathotype. Group 2 included 33 isolates, along with the standard RB84 isolate. All isolates were categorized as belonging to pathotype I. This group encompassed 23 isolates from French nurseries and 10 isolates from American nurseries.

Aggressiveness and virulence of the *A. euteiches* isolates on the *M. truncatula* differential set

All the 25 isolates from the French nurseries, as well as the reference isolate RB84, belonged to the same pathotype, named Fr, characterized by significantly higher disease severity on F83005.5 compared to the other four genotypes within the *M. truncatula* differential set (Table 2; Additional File 2B). Significant variability ($P<0.001$) was observed among the isolates in terms of mean disease severity across the five genotypes. For each isolate, the range of disease severity across the five *M. truncatula* genotypes varied from low to high ($0.1 < Range_{DS} < 2.3$), with all French isolates compared to only half of the American isolates showing higher ranges ($Range_{DS} \geq 1.4$).

The *M. truncatula* differential set was not challenged by the American isolate LS9 due to the inability to produce a sufficient quantity of zoospores from this isolate for inoculation at the

TABLE 2 Disease severity on five *M. truncatula* differential host accessions, for 50 *A. euteiches* isolates and two *A. euteiches* reference isolates (RB84 and Ae109), from French and American nurseries.

Nursery	Isolate	Accession [a]					Pathotype [b]	EMMeans disease severity [c]	HAC group [d]
		F83005.5	F83005.9	A17	DZA241.2	DZA045.5			
Dijon (FR)	Di1	3.9 a	2.7 b	2.7 b	1.8 c	1.8 c	Fr	2.6 BCDE	3
	Di2	3.6 a	2.4 b	1.9 c	1.9 c	1.9 c	Fr	2.3 A	3
	Di3	3.5 a	2.2 c	2.9 b	2.0 c	2.0 c	Fr	2.5 BCD	3
	Di4	3.8 a	2.8 b	2.0 c	1.9 c	1.9 c	Fr	2.5 ABC	3
	Di5	3.8 a	3.0 b	1.9 c	1.8 c	1.8 c	Fr	2.4 AB	3
	Di6	4.0 a	2.9 b	2.4 c	2.3 c	1.9 d	Fr	2.7 DE	3
	Di7	3.6 a	3.1 b	2.7 c	2.2 d	2.0 d	Fr	2.7 E	3
	Di8	3.4 a	2.5 b	2.6 b	2.6 b	2.0 c	Fr	2.6 BCDE	3
	Di9	3.4 a	3.0 b	2.7 b	2.0 c	2.0 c	Fr	2.6 CDE	3
	Di10	3.7 a	3.0 b	3.0 b	2.2 c	1.9 c	Fr	2.7 E	3
Riec-sur-Belon (FR)	Ri2	4.0 a	3.1 c	3.5 b	2.0 d	1.9 d	Fr	2.9 D	3
	Ri4	3.9 a	2.9 b	2.8 b	1.9 c	1.9 c	Fr	2.7 C	3
	Ri7	3.8 a	2.3 c	2.8 b	1.9 d	1.9 d	Fr	2.6 B	3
	Ri8	3.5 a	2.0 b	2.0 b	1.8 b	2.0 b	Fr	2.3 A	3
	Ri10	4.0 a	2.3 b	2.1 bc	1.9 c	1.9 c	Fr	2.5 B	3
Templeux-Le-Guérard (FR)	Tpx1	4.0 a	2.5 b	2.6 b	1.9 c	1.9 c	Fr	2.6 BC	3
	Tpx2	3.9 a	2.7 b	2.4 c	1.7 e	2.0 d	Fr	2.6 ABC	3
	Tpx3	4.0 a	3.0 b	2.2 c	1.8 d	1.9 cd	Fr	2.6 BC	3
	Tpx4	3.8 a	2.3 b	2.1 bc	1.9 c	2.0 bc	Fr	2.4 A	3
	Tpx5	4.0 a	2.8 b	1.9 c	1.8 c	1.7 c	Fr	2.4 AB	3
	Tpx6	3.5 a	2.9 b	2.2 c	1.8 d	1.7 d	Fr	2.4 AB	3
	Tpx7	3.6 a	3.1 b	2.2 c	1.7 d	1.8 d	Fr	2.5 ABC	3
	Tpx8	3.9 a	3.1 b	2.2 c	1.9 d	2.0 cd	Fr	2.6 C	3

(Continued)

10.3389/fpls.2024.1332976

TABLE 2 Continued

Nursery	Isolate	Accession [a]					Pathotype [b]	EMMeans disease severity [c]	HAC group [d]
		F83005.5	F83005.9	A17	DZA241.2	DZA045.5			
	Tpx9	4.0 a	2.9 b	2.4 c	1.8 d	2.1 c	Fr	2.6 C	3
	Tpx10	4.0 a	3.2 b	2.8 c	1.9 d	2.2 d	Fr	2.8 D	3
Athena (US)	Ath1	3.7 ab	3.6 b	4.0 a	4.0 a	3.1 c	Us2	3.7 D	1
	Ath2	3.2 b	3.3 b	4.0 a	4.0 a	2.4 c	Us3	3.4 C	1
	Ath3	2.9 a	2.6 a	2.3 b	1.9 c	1.9 bc	NA	2.3 A	2
	Ath4	3.9 a	3.5 b	4.0 a	4.0 a	2.8 c	Us2	3.6 D	1
	Ath5	3.7 b	3.1 c	4.0 a	3.9 ab	2.5 d	Us2	3.4 C	1
	Ath6	3.2 b	3.0 b	4.0 a	3.8 a	2.4 c	Us3	3.3 C	1
	Ath7	2.4 b	2.5 b	4.0 a	3.7 a	2.2 b	Us4	3.0 B	2
Le Sueur (US)	LS1	3.9 a	3.5 b	4.0 a	3.8 a	2.4 c	Us2	3.5 B	1
	LS2	4.0 a	3.9 a	4.0 a	3.8 ab	3.6 b	Us1	3.9 DE	1
	LS3	4.0 a	3.9 a	3.9 a	3.9 a	2.8 b	Us2	3.7 C	1
	LS5	4.0 a	3.8 ab	4.0 a	3.9 ab	3.6 b	Us1	3.9 DE	1
	LS6	2.5 b	2.1 c	3.6 a	3.8 a	1.9 c	Us4	2.8 A	2
	LS7	4.2 a	4.0 a	4.0 a	4.0 a	2.7 b	Us2	3.8 CD	1
	LS8	4.0 a	3.9 a	4.0 a	4.0 a	2.7 b	Us2	3.7 C	1
	LS10	4.0 a	4.0 a	4.0 a	4.0 a	3.9 a	Us1	4.0 E	1
Mount Vernon (US)	MV1	2.8 a	2.0 b	2.0 b	1.9 b	2.0 b	Fr	2.1 A	2
	MV3	3.9 a	3.5 b	3.9 a	3.8 ab	3.0c	Us2	3.6 C	1
	MV4	4.0 a	3.8 a	4.0 a	4.0 a	3.1 b	Us2	3.8 C	1
	MV5	2.3 a	2.3 ab	2.0 bc	1.9c	2.2 abc	NA	2.1 A	2
	MV7	3.3 a	2.8 b	2.5 b	2.0 c	2.0 c	Fr	2.5 B	3
Pullman (US)	Plm1	3.5 b	3.1 c	4.0 a	3.9 a	2.2 d	Us3	3.3 A	1
	Plm2	3.1 c	3.4 b	4.0 a	4.0 a	2.3 d	Us3	3.4 A	1
	Plm3	3.6 b	3.5 b	4.0 a	4.0 a	2.9 c	Us3	3.6 B	1
	Plm4	4.0 a	3.9 a	4.0 a	4.0 a	2.7 b	Us2	3.7 C	1
	Plm7	4.0 a	3.4 b	4.0 a	3.9 a	2.2 c	Us2	3.5 B	1
Standard isolates	RB84	4.0 a	2.8 b	2.7 c	2.0 d	1.8 e	Fr	2.7	3
	Ae109	4.1 a	3.9 ab	3.7 b	3.8 b	2.8 c	Us2	3.6	1

Disease severity was recorded on a scale from 0 (no symptoms) to 5 (dead plant). [a] For each isolate (*i.e.* each row), EMMean values on the different *M. truncatula* genotypes followed by the same lower case letter are not significantly different (Tukey test, α=5%). [b] Pathotypes identified according to this study; NA: isolates with undefined pathotypes. [c] Between isolates for each nursery, EMMean values on all *M. truncatula* genotypes followed by the same upper-case letter are not significantly different (Tukey test, α=5%). [d] Hierarchical Ascending Classification groups obtained from the Ward D method in this study.

required concentration. The 25 isolates from the American nurseries were classified into five distinct pathotypes, named Fr, Us1, Us2, Us3, and Us4, according to their aggressiveness towards the *M. truncatula* differential set (Table 2; Additional File 2B). (i) Isolates from pathotype Us1 (3 isolates: LS2, LS5 and LS10) exhibited high aggressiveness across the entire set, with no significant differences observed in disease severity between the most resistant genotype DZA045.5, and at least one of the four other genotypes. (ii) Pathotype Us2 (11 isolates: Ath1, Ath4, Ath5, LS1, LS3, LS7, LS8, MV3, MV4, Plm4, Plm7) was characterized by disease severity on DZA045.5 significantly lower than on the four other genotypes, and at least one genotype between F83005.5 and F83005.9 (intermediate behavior) that was not significantly different to at least one genotype between A17 and DZA241.2 (susceptible). (iii) Pathotype Us3 (5 isolates: Ath2, Ath6, Plm1, Plm2, Plm3) was characterized by disease severity on DZA045.5 significantly lower

than on the four other genotypes, and both genotypes F83005.5 and F83005.9 that were significantly different to both genotypes A17 and DZA241.2. (iv) Pathotype Us4 (2 isolates: Ath7 and LS6) was characterized by disease severity on DZA045.5, not significantly lower than at least one genotype between F83005.5 and F83005.9, but significantly lower than both genotypes DZA241.2 and A17 (*p-value* < 0,001). Two isolates, MV1 and MV7, were assigned to pathotype Fr. The last two isolates, Ath3 and MV5, could not be classified, but their behaviour closely resembled the pattern exhibited by isolates from pathotype Fr.

Isolates from pathotypes Us1, Us2 and Us3 were significantly more aggressive ($P < 0.001$) on the *M. truncatula* differential set compared to isolates from pathotypes Fr and Us4. Mean disease severity among American isolates was higher (2.8 < MeanDS < 4) than that observed among French isolates (2.3 < MeanDS < 2.9), except for MV1, MV5, MV7, and Ath3 isolates. The level of partial resistance of DZA045.5 was lower for the American isolates (1.9 < DS < 3.9) than for the French isolates (1.7 < DS < 2.2). Significant variations in mean disease severity were observed among isolates from each of the Athena (US), Le Sueur (US), Mount Vernont (US) and Riec-sur-belon (FR) nurseries. However, such variations were not observed among isolates from Dijon (FR), Templeux-le-Guérard (FR), or Pullman (US) nurseries.

PCA mainly separated the 50 isolates based on their aggressiveness towards the four *M. truncatula* genotypes: DZA045.5, F83005.9, A17 and DZA241.2, as shown by the high percentage of total variation explained by the first principal component (PCA.Dim1: 67.65%) (Figure 3A). The isolates belonging to the American pathotypes (except Us4) differed from the French isolates by their high level of aggressiveness on the four genotypes. The second and third principal components of the analysis separated the isolates based on their aggressiveness on the F83005.5 and DZA045.5 genotypes, respectively (PCA.Dim2: 22.46%; PCA.Dim3: 5.59%). The isolates belonging to the Us3 and Us4 pathotypes differ from those belonging to the Fr, Us1 and Us2 pathotypes by their lower aggressiveness on F83005.5 (Dim2, Figure 3A). The isolates from the Us1 pathotype differ from the others based on their higher aggressiveness on DZA045.5 (Dim3, not shown).

HAC identified three groups among the 50 isolates, according to their average aggressiveness towards the set of *M. truncatula* genotypes (Figure 3B). Group 1 clustered all the 19 American isolates from the Us1, Us2 and Us3 pathotypes, as well as the standard Ae109 isolate, which were more aggressive on the *M. truncatula* set of genotypes than the other isolates. Group 2 clustered five American isolates with low to moderate aggressiveness, including two isolates from the Us4 pathotype (LS6 and Ath7), one isolate from the Fr pathotype (MV1), and two isolates with undefined pathotype (MV5 and Ath3). Group 3 consisted of 25 French isolates, one American isolate (MV7) belonging to the Fr pathotype, and the RB84 standard isolate. Isolates from this group showed lower aggressiveness on the *M. truncatula* genotypes. Overall, the mean disease severity observed with all the French isolates was significantly lower than that observed with all the US isolates on the set of *M. truncatula* genotypes (Figure 1).

Discussion

This study investigated the aggressiveness and virulence diversity among pea-infecting *A. euteiches* isolates collected from French and American nurseries. To our knowledge, this study represents the first comprehensive investigation comparing the aggressiveness of *A. euteiches* populations obtained from breeding nurseries across different countries. Results are highly valuable for breeding, particularly because both countries have selected shared sources of resistance (Kraft, 1992; Gritton, 1995) to enhance partial resistance levels in pea varieties.

Distribution of pathotypes I and III over French and American breeding nurseries

The pea differential set of genotypes employed in this study demonstrated its effectiveness in classifying the sampled isolates into the two main pathotypes, I and III, previously described by Wicker and Rouxel (2001). Other pathotypes were also previously described by these authors, including the avirulent pathotype II on PI1806903 and the avirulent pathotypes IV to XI on at least two of the six pea genotypes, corresponding to generally less aggressive isolates. However, these pathotypes, which often exhibit lower variations between genotypes, were difficult to demonstrate in this study. Our results offer a comprehensive analysis of the prevalence of pathotypes I and III across French and American nurseries. While pathotype III was exclusively found in some American nurseries, pathotype I was detected in both French and American sites. Interestingly, some American nurseries were infested by only one pathotype (pathotype I at Athena and Pullman, pathotype III at Le Sueur), whereas both pathotypes coexisted in the Mount Vernon nursery. At the continent scale, our data show pathogenic variation between American sites, and a much more uniform population structure in France, as described by Wicker and Rouxel (2001). Especially, it is remarkable that pathotype I was found in the three American nurseries located closer to each other (Athena, Mount Vernon and Pullman), but not in the more distant site (Le Sueur).

These results provide valuable insights into the interpretation of previous QTL studies on resistance to *A. euteiches* (Pilet-Nayel et al., 2002; Hamon et al., 2013; Desgroux et al., 2016; Leprévost et al., 2023). These studies identified QTL from pea Recombinant Inbred Line (RIL) and Advanced Backcross (AB) populations, as well as from a pea-Aphanomyces collection, evaluated in six of the seven nurseries sampled in this study (Riec-sur-Belon, Dijon, and Templeux-le-Guérard, FR; Pullman, Athena, and Le Sueur, US). Results of these studies indicated that the resistance QTL showed little specificity across nurseries, which is in line with the predominance of pathotype I in most of them. Indeed, most of the 10 consistent genetic regions identified for resistance to *A. euteiches* in Leprévost et al. (2023) were detected from disease scorings in both the French and US nurseries studied. Particularly, the main *Ae-Ps7.6* QTL was highly consistently detected from disease scores in all FR-US nurseries, except at Mount-Vernon which was not used in QTL mapping studies, on the populations

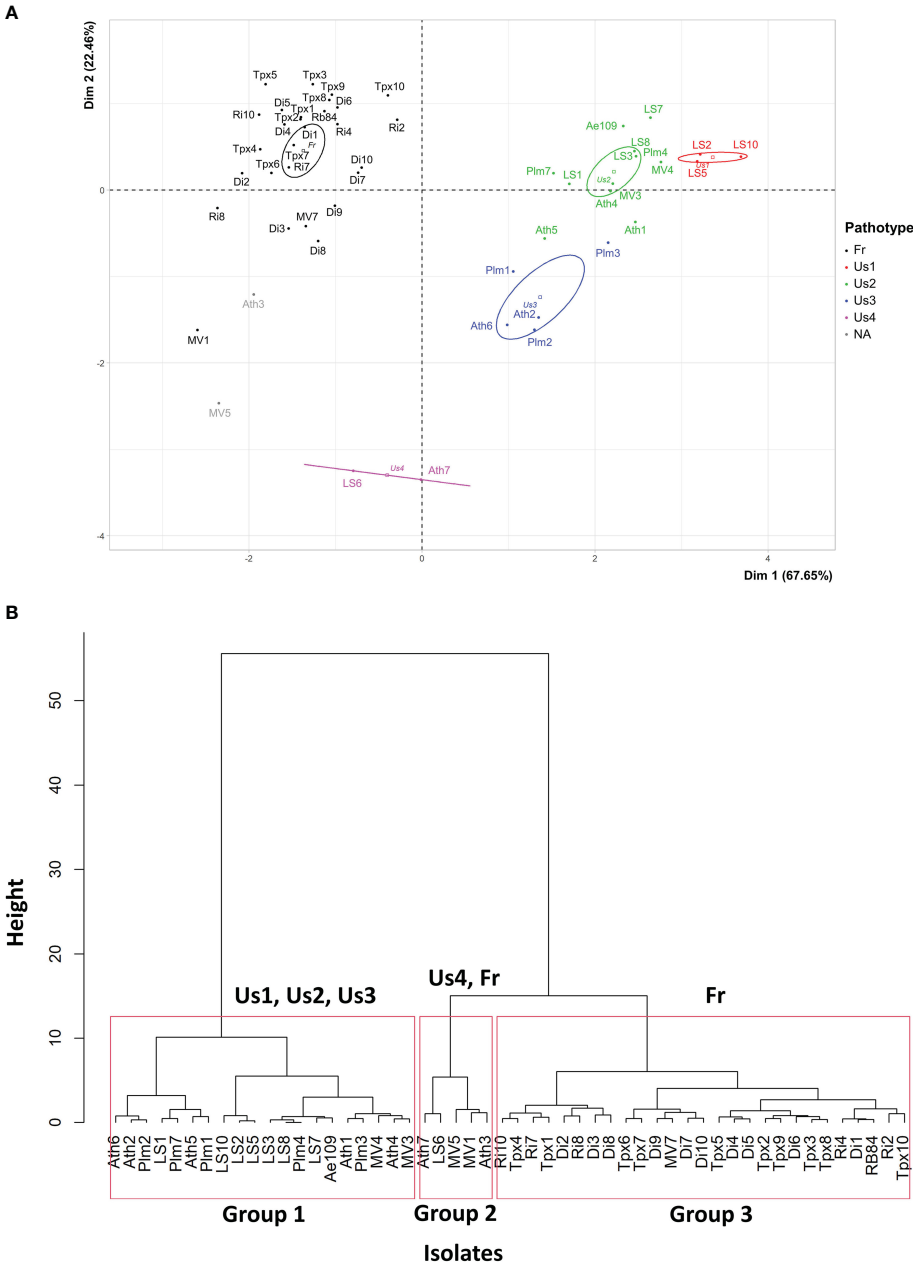

FIGURE 3
(A) Principal Component Analysis and **(B)** Hierarchical Ascending Classification, of 50 *A. euteiches* isolates from the US-FR transatlantic collection and two *A. euteiches* reference isolates (RB84 and Ae109), based on disease severity data on five *Medicago truncatula* differential genotypes. Us1, Us2, Us3, Us4, Fr: pathotypes Us1, Us2, Us3, Us4 and Fr of *A. euteiches*. NA: isolates with undefined pathotype. Confidence ellipses, calculated at the confidence level of 95%, are overlaid to visualize the grouping patterns.

DSP x 90-2131, Baccara x PI180693 and Baccara x 552 RIL. Nevertheless, from disease scoring data in the Le Sueur nursery in which we identified only pathotype III isolates in the present study, another major QTL named *Ae-Ps4.5* (or *Aph1)*, was detected from the Puget x 90-2079 mapping population (Pilet-Nayel et al., 2002). The source of resistance 90-2079 was derived from the MN313 genotype. MN313 was selected by Davis et al. (1995), from a breeding program that employed screening of progenies in a disease nursery infested with *A. euteiches* in Minnesota, US. The specificity of the major-effect *Ae-Ps4.5* QTL for pathotype III was recently confirmed (Lavaud et al., 2024). The identification of *A. euteiches* isolates within breeding nurseries is essential for understanding the effectiveness of detected QTL and the suitability of selected breeding lines regarding the diversity of pathogen populations. This information is crucial for making informed decisions about their deployment in various pea-growing regions. In France, the presence of a single pathotype simplifies resistance breeding efforts but requires vigilance and precautionary measures against any change in the pathogen population. In contrast, American pea breeders have to consider the presence of both pathotypes of *A. euteiches*, even though pathotype I is predominant, when evaluating their breeding lines.

Similarly, in Canada, it is advisable to consider both pathotypes in breeding programs, given that Sivachandra et al. (2021) highlighted the co-occurrence of the two pathotypes, with pathotype I being the predominant one.

Several hypotheses could explain the observed distribution of *A. euteiches* pathotypes in the French and American nurseries studied. Firstly, variations in climatic conditions and sowing dates between the nurseries may account for a part of the pathogen diversity observed. Variation in climate (rainfall, temperature) and growing seasons between the nurseries located in the Pacific Northwest (Pullman, Athena, and Mount-Vernon) and in Minnesota (Le Sueur) regions of the United States may have impacted the dispersion and multiplication of different *A. euteiches* pathogen populations, thus affecting population diversity. In France, fewer climatic and cultural variations were recorded between the three breeding nurseries studied. Secondly, the cultivation of other leguminous crops susceptible to *A. euteiches* in the regions of the nurseries studied might also explain the diversity of *A. euteiches* isolates observed. The large pathogenicity diversity of *A. euteiches* on several legumes including pea, alfalfa, vetch, faba bean, bean and lentil (Malvick and Percich, 1998; Levenfors et al., 2003; Moussart et al., 2008; van Leur et al., 2008) and the genetic variation found even within fields (Grünwald and Hoheisel, 2006) suggest that this pathogen has the ability to adapt to different cropping systems and rotations. Our pathogenicity characterization results for French and American isolates on *M. truncatula* genotypes provide further support for this last hypothesis.

Aggressiveness of French and American isolates on *M. truncatula*

The set of differential genotypes of *M. truncatula* especially curated for this study made it possible to highlight the level of adaptation of isolates from French and American nurseries to a host model legume genetically close to cultivated alfalfa. Our results revealed that isolates from French nurseries were less aggressive on *M. truncatula* but more aggressive on pea compared to most isolates from American nurseries. The set of *M. truncatula* genotypes grouped isolates by geographical origin, with lower variability in aggressiveness observed among the French isolates compared to the American isolates. These results suggest that *A. euteiches* isolates from American nurseries display greater adaptation to *Medicago* spp., while isolates from French nurseries are stronger adapted to pea. The greatest adaptation of American isolates to *Medicago* spp. could be attributed to the extensive and longstanding cultivation of this crop in the north-central regions of the United States, which is the world's leading producer of *Medicago* spp. In contrast, *Medicago* spp. cultivation is relatively recent and limited to specific regions in France. Even if *Medicago* spp. are native to Europe, no species of the genus *Medicago* were cultivated in any of the three French nurseries studied, whereas alfalfa has been grown in rotation with pea in the United States over the past few decades, particularly in areas such as the Midwest region, including states like Minnesota. Historical literature reveals that alfalfa was the earliest forage crop cultivated in the USA, while France focused on its production in the 1950s, mainly for dehydrated alfalfa (Goplen et al., 1987). Thus, the localized selection of *A. euteiches* populations by pea in France may have resulted in an increased specialization of isolates on this host. In contrast, the more diverse legume rotation practices in America may have facilitated the presence of isolates with markedly different host pathogenicity. The reduced pathogenicity diversity observed in French isolates in comparison to American ones can likely be attributed to a more uniform selection pressure resulting from the predominant cultivation of pea as the main leguminous crop in France. Since the 1980s, the prevalence of pea crops and the susceptibility of the pea cultivars used by growers in France may account for the high aggressiveness and limited variation in pathogenicity observed among the French isolates, as suggested by Quillévéré-Hamard et al. (2018).

Our results suggest that the plant host plays a key role in driving the evolution of *A. euteiches* populations, offering promising perspectives for exploiting the host as a means to manage pathogen populations. The cultivation of diversified legume hosts in rotation with peas or alfalfa could potentially help limit the adaptation or even the size of *A. euteiches* populations. In France, the growing of faba bean, resistant to *A. euteiches* (Moussart et al., 2008), in alternation with pea, has been recommended for several years as an effective strategy to improve the management of Aphanomyces root rot.

Data availability statement

The original contributions presented in the study are included in the article/Supplementary Material. Further inquiries can be directed to the corresponding authors.

Author contributions

AM: Conceptualization, Data curation, Formal analysis, Investigation, Methodology, Writing – original draft. CLa: Data curation, Formal analysis, Methodology, Validation, Visualization, Writing – review & editing. CO: Data curation, Formal analysis, Methodology, Writing – review & editing. TL: Formal analysis, Methodology, Software, Writing – review & editing. M-LP-N: Conceptualization, Formal analysis, Investigation, Supervision, Validation, Writing – review & editing. CLM: Conceptualization, Formal analysis, Investigation, Supervision, Validation, Writing – review & editing.

Funding

The author(s) declare financial support was received for the research, authorship, and/or publication of this article. This work was supported by INRAE and Terres Inovia, as well as the FP6 EU Grain Legumes project (FOOD-CT-2004-506223) (GLIP) which enabled the development of the *M. truncatula* differential set.

Acknowledgments

The authors acknowledge Dr N. Grünwald and Dr B. Tivoli for their advices in the conception of the study. They thank Dr A. Baranger, and Dr D. Andrivon for their advices in the data analysis. They are grateful to Dr C. Coyne and Dr L. Porter for providing soils from the USA. They extend their gratitude to Dr J-M Prospéri for generously providing *Medicago truncatula* genotypes used in the differential set. They thank the Greenhouse-Experimental Facilities platform of IGEPP for providing and managing the equipment necessary for conducting the experiments.

Conflict of interest

The authors declare that the research was conducted in the absence of any commercial or financial relationships that could be construed as a potential conflict of interest.

Publisher's note

All claims expressed in this article are solely those of the authors and do not necessarily represent those of their affiliated organizations, or those of the publisher, the editors and the reviewers. Any product that may be evaluated in this article, or claim that may be made by its manufacturer, is not guaranteed or endorsed by the publisher.

Supplementary material

The Supplementary Material for this article can be found online at: https://www.frontiersin.org/articles/10.3389/fpls.2024.1332976/full#supplementary-material

ADDITIONAL FILE 1

Mean weather conditions (mean temperature and rainfall) recorded in the different French (Templeux-Le-Guérard, Dijon, and Riec-sur-Belon) and American (Athena, OR; Mount Vernon, WA; Le Sueur, MN; and Pullman, WA) nurseries during the last twenty years (http://www.infoclimat.fr.html and http://www.prism.oregonstate.edu for French and American nurseries, respectively).

ADDITIONAL FILE 2

Bar plot of disease severity (EMMeans) **(A)** on the six differential pea genotypes, for the 51 *A. euteiches* isolates and two *A. euteiches* reference isolates (RB84 and Ae109) classified into pathotypes I and III according to Wicker and Rouxel (2001), and **(B)** on the five differential *M. truncatula* genotypes, for 50 *A. euteiches* isolates and two *A. euteiches* reference isolates (RB84 and Ae109) classified into pathotypes Fr, Us1, Us2, Us3 and Us4 in this study. NA: isolates with undefined pathotype.

References

Bates, D., Mächler, M., Bolker, B., and Walker, S. (2015). Fitting linear mixed-effects models using lme4. *J. Stat. Softw.* 67, 1–48. doi: 10.18637/jss.v067.i01

Bonhomme, M., André, O., Badis, Y., Ronfort, J., Burgarella, C., Chantret, N., et al. (2014). High-density genome-wide association mapping implicates an F-box encoding gene in *Medicago truncatula* resistance to *Aphanomyces euteiches*. *New Phytol.* 201, 1328–1342. doi: 10.1111/nph.12611

Burnett, V. F., Coventry, D. R., Hirth, J. R., and Greenhalgh, F. C. (1994). Subterranean clover decline in permanent pastures in north-eastern victoria. *Plant Soil* 164, 231–241. doi: 10.1007/BF00010075

Chambers, J. M. (1992). Linear models. *Chapter 4 of Statistical Models*. Eds. J. M. Chambers and T. J. Hastie (Wadsworth & Brooks/Cole). doi: 10.1177/096228029200100208

Cunningham, J. L., and Hagedorn, D. J. (1962). Penetration and infection of pea roots by zoopores of Aphanomyces euteiches. *Phytopathol* 52, 827–834.

Davis, D. W., Fritz, V. A., Pfleger, F. L., Percich, J. A., and Malvick, D. K. (1995). MN144, MN313 and MN314: Garden pea lines resistant to root-rot caused by *Aphanomyces euteiches* Drechs. *Hortscience* 30, 639–640. doi: 10.21273/HORTSCI.30.3.639

Desgroux, A., L'Anthoëne, V., Roux-Duparque, M., Rivière, J. P., Aubert, G., Tayeh, N., et al. (2016). Genome-wide association mapping of partial resistance to *Aphanomyces euteiches* in pea. *BMC Genom.* 17, 124. doi: 10.1186/s12864-016-2429-4

Didelot, D., and Chaillet, I. (1995). "Relevance and interest of root disease prediction tests for pea crop in France," in *AEP (ed) 2nd European Conference of Grain Legumes*, Copenhagen, Denmark, July 9-13th.

Fitzpatrick, S., Brummer, J., Hudelson, B., Malvick, D., and Grau, C. (1998). "Aphanomyces root rot resistance (races 1 and 2)," in *Page D-2 in: Standard Tests Bull. N. Am. Alfalfa Improvement Conf.*

Goplen, B. P., Baenziger, H., Bailey, L. D., Gross, A. T. H., Hanna, M. R., Michaud, R., et al. (1987). *Growing and Managing Alfalfa in Canada*. Publication 1705/E, Communications Branch, Agriculture Canada, Ottawa, 52 p.

Graves, S., Piepho, H.-P., Selzer, L., and Dorai-Raj, S. (2019) *multcompView: Visualizations of paired comparisons. R package version 0.1-8*. Available online at: https://CRAN.R-project.org/package=multcompView.

Greenhalgh, F. C., and Merriman, P. R. (1985). *Aphanomyces euteiches*, a cause of root rot of subterranean clover in Victoria. *Aust. Plant Pathol.* 14, 34–37. doi: 10.1071/APP9850034

Gritton, E. T. (1995). Offer of seed from the Earl Gritton pea improvement program at Madison. *Pisum Genet.* 27, 29–30.

Grünwald, N. J., and Hoheisel, G. A. (2006). Hierarchical analysis of diversity, selfing, and genetic differentiation in populations of the oomycete *Aphanomyces euteiches*. *Phytopathol* 96, 1134–1141. doi: 10.1094/PHYTO-96-1134

Hamon, C., Baranger, A., Miteul, H., Lecointe, R., Le Goff, I., Deniot, G., et al. (2010). A complex genetic network involving a broad-spectrum locus and strain-specific loci controls resistance to different pathotypes of *Aphanomyces euteiches* in *Medicago truncatula*. *Theor. Appl. Genet.* 120, 955–970. doi: 10.1007/s00122-009-1224-x

Hamon, C., Coyne, C. J., McGee, R. J., Lesné, A., Esnault, R., Mangin, P., et al. (2013). QTL meta-analysis provides a comprehensive view of loci controlling partial resistance to *Aphanomyces euteiches* in four sources of resistance in pea. *BMC Plant Biol.* 13, 45. doi: 10.1186/1471-2229-13-45

Harveson, B., Pasche, J., Burrows, M., Porter, L., and Chen, W. E. (2021). Compendium of pea diseases and pests, 3rd edition. *Am. Phytopathol. Soc. St-Paul Minnesota U.S.A.*, 130pp.

Holub, E. B., Grau, C. R., and Parke, J. L. (1991). Evaluation of the forma specialis concept in *Aphanomyces euteiches*. *Mycol. Res.* 95, 147–157. doi: 10.1016/S0953-7562(09)81004-6

Kälin, C., Berlin, A., Brantestam, A. K., Dubey, M., Arvidsson, A. K., Riesinger, P., et al. (2022). Genetic diversity of the pea root pathogen *Aphanomyces euteiches* in Europe. *Plant Pathol.* 71, 1570–1578. doi: 10.1111/ppa.13598

Kraft, J. (1992). Registration of 90-2079, 90-2131 and 90-2322 pea germplasms. *Crop Sci.* 32, 1076. doi: 10.2135/cropsci1992.0011183X003200040063x

Labrousse, F. (1933). Notes de pathologie végétale. *Rev. pathol. végétale d'Entomol. agricole* 19, 71–84.

Lamari, L., and Bernier, C. C. (1985). Etiology of seedling blight and root rot of faba bean (*Vicia faba*) in Manitoba. *Can. J. Plant Pathol.* 7, 139–145. doi: 10.1080/07060668509501490

Lavaud, C., Lesné, A., Leprévost, T., and Pilet-Nayel, M.-L. (2024). Fine mapping of *Ae-Ps4.5*, a major locus for resistance to pathotype III of *Aphanomyces euteiches* in pea. *Theor. Appl. Genet.* 137, 47. doi: 10.1007/s00122-024-04548-6

Lê, S., Josse, J., and Husson, F. (2008). FactoMineR: An R package for multivariate analysis. *J. Stat. Software* 25, 1–18. doi: 10.18637/jss.v025.i01

Le May, C., Onfroy, C., Moussart, A., Andrivon, D., Baranger, A., Pilet-Nayel, M. L., et al. (2018). Genetic structure of *Aphanomyces euteiches* populations sampled from

United States and France pea nurseries. *Eur. J. Plant Pathol.* 150, 275–286. doi: 10.1007/s10658-017-1274-x

Lenth, R. (2023) *emmeans: Estimated Marginal Means, aka Least-Squares Means. R package version 1.8.9*. Available online at: https://CRAN.R-project.org/package=emmeans.

Leprévost, T., Boutet, G., Lesné, A., Rivière, J. P., Vetel, P., Glory, I., et al. (2023). Advanced backcross QTL analysis and comparative mapping with RIL QTL studies and GWAS provide an overview of QTL and marker haplotype diversity for resistance to Aphanomyces root rot in pea (*Pisum sativum*). *Front. Plant Sci.* 14. doi: 10.3389/fpls.2023.1189289

Levenfors, J. P., and Fatehi, J. (2004). Molecular characterization of *Aphanomyces* species associated with legumes. *Mycol. Res.* 108, 682–689. doi: 10.1017/S0953756204009931

Levenfors, J. P., Wikström, M., Persson, L., and Gerhardson, B. (2003). Pathogenicity of *Aphanomyces* spp. from different leguminous crops in Sweden. *Eur. J. Plant Pathol.* 109, 535–543. doi: 10.1023/A:1024711428760

Malvick, D. K., and Grau, C. R. (2001). Characteristics and frequency of *Aphanomyces euteiches* races 1 and 2 associated with alfalfa in the midwestern United States. *Plant Dis.* 85, 740–744. doi: 10.1094/PDIS.2001.85.7.740

Malvick, D. K., Grau, C. R., and Percich, J. A. (1998). Characterization of *Aphanomyces euteiches* strains based on pathogenicity tests and random amplified polymorphic DNA analyses. *Mycol. Res.* 102, 465–475. doi: 10.1017/S0953756297005029

Malvick, D., Grunwald, N., and Dyer, A. (2009). Population structure, races, and host range of *Aphanomyces euteiches* from alfalfa production fields in the central USA. *Eur. J. Plant Pathol.* 123, 171–182. doi: 10.1007/s10658-008-9354-6

Malvick, D. K., and Percich, J. A. (1998). Genotypic and pathogenic diversity among pea-infecting strains of *Aphanomyces euteiches* from the central and western United States. *Phytopathol* 88, 915–921. doi: 10.1094/PHYTO.1998.88.9.915

Mieuzet, L., Quillévéré, A., Pilet, M. L., and Le May, C. (2016). Development and characterization of microsatellite markers for the oomyceta *Aphanomyces euteiches*. *Fung. Genet. Biol.* 91, 1–5. doi: 10.1016/j.fgb.2016.03.001

Moussart, A., Even, M. N., and Tivoli, B. (2008). Reaction of genotypes from several species of grain and forage legumes to infection with a French pea isolate of the oomycete *Aphanomyces euteiches*. *Eur. J. Plant Pathol.* 122, 321–333. doi: 10.1007/s10658-008-9297-y

Moussart, A., Onfroy, C., Lesné, A., Esquibet, M., Grenier, E., and Tivoli, B. (2007). Host status and reaction of *Medicago truncatula* accessions to infection by three major pathogens of pea (*Pisum sativum*) and alfalfa (*Medicago sativa*). *Eur. J. Plant Pathol.* 117, 57–69. doi: 10.1007/s10658-006-9071-y

Moussart, A., Wicker, E., Duparque, M., and Rouxel, F. (2001). "Development of an efficient screening test for pea resistance to *Aphanomyces euteiches*.," in *Proc 4th Eur Conf Grain Legumes*, Cracow, Pologne, 8-12 Juillet, Vol. 272-273.

Murtagh, F., and Legendre, P. (2014). Ward's hierarchical agglomerative clustering method: which algorithms implement ward's criterion? *J. Classif.* 31, 274–295. doi: 10.1007/s00357-014-9161-z

Papavizas, G. C., and Ayers, W. A. (1974). Aphanomyces species and their root diseases on pea and sugarbeet. *U.S. Dept. Agric. Res. Tech. Bull.* 1485, 1–157.

Pfender, W. F., and Hagedorn, D. J. (1982). *Aphanomyces euteiches* f. sp. *phaseoli*, a causal agent of bean root and hypocotyl rot. *Phytopathol* 72, 306–310.

Pfender, W. F., and Hagedorn, D. J. (1983). Disease progress and yield loss in aphanomyces root rot of peas. *Phytopathol* 73, 1109–1113. doi: 10.1094/Phyto-73-1109

Pilet-Nayel, M.-L., Lesné, A., Prospéri, J.-M., Delalande, M., Lecointe, R., and Baranger, A. (2005). "Resistance to *Aphanomyces euteiches* in *Medicago truncatula*.," in *Model Legume Congress, Asilomar Conference Grounds*, Pacific Grove, California.

Pilet-Nayel, M. L., Muehlbauer, F. J., McGee, R. J., Kraft, J. M., Baranger, A., and Coyne, C. J. (2002). Quantitative trait loci for partial resistance to Aphanomyces root rot in pea. *Theor. Appl. Genet.* 106, 28–39. doi: 10.1007/s00122-002-0985-2

Pilet-Nayel, M. L., Prospéri, J. M., Hamon, C., Lesné, A., Lecointe, R., Le Goff, I., et al. (2009). *AER1*, a major gene conferring resistance to *Aphanomyces euteiches* in *Medicago truncatula*. *Phytopathol* 99, 203–208. doi: 10.1094/PHYTO-99-2-0203

Quillévéré-Hamard, A., Le Roy, G., Moussart, A., Baranger, A., Andrivon, D., Pilet-Nayel, M. L., et al. (2018). Genetic and pathogenicity diversity of *Aphanomyces euteiches* populations from pea-growing regions in France. *Front. Plant Sci.* 9. doi: 10.3389/fpls.2018.01673

R Core Team (2023). *R: a language and environment for statistical computing* (Vienna, Austria: R Foundation for Statistical Computing). Available at: https://www.R-project.org/.

Scott, W. W. (1961). *A Monograph of the Genus Aphanomyces. Technical Bulletin (Virginia Agricultural Experiment Station).* 151, 1–95.

Sherwood, R. T., and Hagedorn, D. J. (1962). Studies on the biology of. *Aphanomyces euteiches. Phytopathol.* 52, 150–154.

Sivachandra Kumar, N. T., Caudillo-Ruiz, K. B., Chatterton, S., and Banniza, S. (2021). Characterization of Aphanomyces euteiches pathotypes infecting peas in Western Canada. *Plant Dis.* 105, 4025–4030. doi: 10.1094/PDIS-04-21-0874-RE

Sundheim, L. (1972). Physiologic specialization in *Aphanomyces euteiches*. *Physiol. Plant Pathol.* 2, 301. doi: 10.1016/0048-4059(72)90013-6

Tivoli, B., Baranger, A., Sivasithamparam, K., and Barbetti, M. J. (2006). Annual *Medicago*:: From a model crop challenged by a spectrum of necrotrophic pathogens to a model plant to explore the nature of disease resistance. *Ann. Bot.* 98, 1117–1128. doi: 10.1093/aob/mcl132

Vandemark, G. J., and Grunwald, N. J. (2004). Reaction of *Medicago truncatula* to *Aphanomyces euteiches* race 2. *Arch. Phytopathol. Plant Protec.* 37, 59–67. doi: 10.1080/03235400410001662148

van Leur, J. A. G., Southwell, R. J., and Mackie, J. M. (2008). Aphanomyces root rot on faba bean in northern NSW. *Aust. Plant Dis. Notes* 3, 8–9. doi: 10.1071/DN08004

Wicker, E., Hullé, M., and Rouxel, F. (2001). Pathogenic characteristics of isolates of *Aphanomyces euteiches* from pea in France. *Plant Pathol.* 50, 433–442. doi: 10.1046/j.1365-3059.2001.00590.x

Wicker, E., Moussart, A., Duparque, M., and Rouxel, F. (2003). Further contributions to the development of a differential set of pea cultivars (*Pisum sativum*) to investigate the virulence of isolates of *Aphanomyces euteiches*. *Eur. J. Plant Pathol.* 109, 47–60. doi: 10.1023/A:1022020312157

Wicker, E., and Rouxel, F. (2001). Specific behaviour of French *Aphanomyces euteiches* Drechs.: populations for virulence and aggressiveness on pea, related to isolates from Europe, America and New Zealand. *Eur. J. Plant Pathol.* 107, 919–929. doi: 10.1023/A:1013171217610

Frontiers in Plant Science

Cultivates the science of plant biology and its applications

The most cited plant science journal, which advances our understanding of plant biology for sustainable food security, functional ecosystems and human health.

Discover the latest Research Topics

See more →

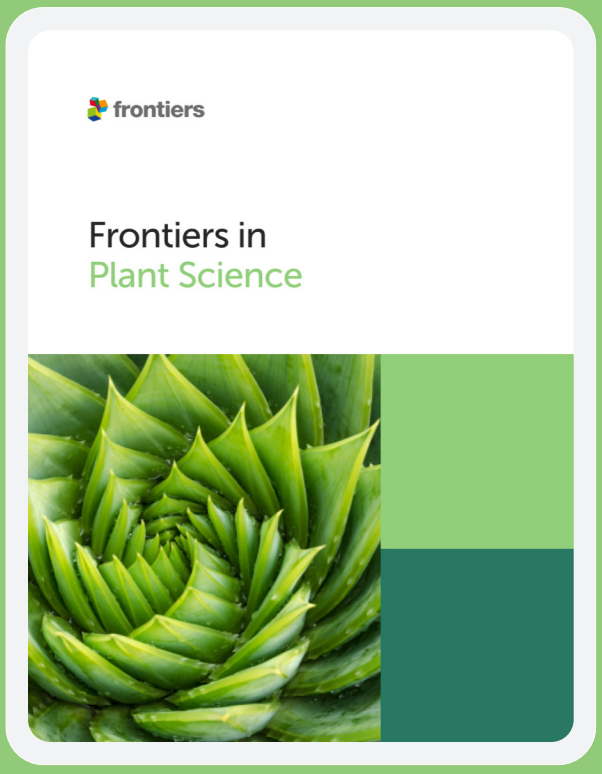

Frontiers

Avenue du Tribunal-Fédéral 34
1005 Lausanne, Switzerland
frontiersin.org

Contact us

+41 (0)21 510 17 00
frontiersin.org/about/contact